# RELATIONSHIP BETWEEN FERROMAGNETIC PARTICLES AND AIRBORNE CHRYSOTILE FIBRES IN THE ASBESTOS MINES AND MILLS OF QUEBEC

By

© Okay Tewfik DJAMGOUZ, P.Eng.,
Associate Professor of Mining Engineering
M.Sc. (Mining) Istanbul, M.Eng. (Mining) McGill

A thesis submitted to the Faculty of Graduate Studies and Research in partial fulfilment of the requirements for the degree of Ph.D.

Department of Mining and Metallurgical Engineering
McGILL UNIVERSITY
MONTREAL, P.Q., CANADA

May, 1982

## ABSTRACT

RELATIONSHIPS BETWEEN FERROMAGNETIC PARTICLES AND AIRBORNE CHRYSOTILE FIBRES IN THE ASBESTOS MINES AND MILLS OF QUEBEC

O.T. Djamgouz

Department of Mining and Metallurgical Engineering

McGill University

Candidate of Ph.D. Degree

Examination of Chrysotile Asbestos from the Eastern Townships of Quebec using optical and electron microscopic methods has shown that Chrysotile fibres are intimately associated with minute particles of magnetite.

Measurements were made using a fluxgate magnetometer of the remanent magnetic fields of bulk commercial fibres and of airborne total dust and of the respirable fraction of airborne dust collected in Quebec asbestos mines and mills using a Hexhlet horizontal eleutriator. The validity of the Hexhlet horizontal eleutriator for respirable fibre collection in the mill environment was determined. It was observed that the remanent magnetic field intensities of airborne dust in laboratory generated dust clouds, and in the work places were related in a meaningful way to the magnetite content of the dust and to the total mass and respirable mass fractions of airborne dust, and also, to the concentrations of fibre greater than 5 micrometre length (aspect ratio > 3:1) measured using phase contrast

microscopy. Calibration curves were developed for each of 9 Quebec mills. Repeat calibrations showed the lines to be reproducible within ± 10 percent. The accuracy of the method for mass dust determination was dependent on sample size with errors as low as ± 7.5 percent for samples larger than 3 milligrams, and as large as ± 40 percent for samples of mass smaller than 0.5 milligrams. The relationships between fibre concentrations and remanent magnetic fields were less reproducible and the lower detection limit was limited by the sensitivity of the fluxgate magnetometer. Although the measured remanent magnetic field varied as the magnetite content varied between different mills and commercial fibre products, magnetite to chrysotile ratio remained constant for a given mill and commercial product. Measurements of the remanent magnetic fields of airborne dusts collected in mill environments can thus provide the possibility of the rapid determination of airborne chrysotile fibre concentrations both in terms of mass and number of fibres per litre of air sampled as well as their iron content.

Measurement of the magnetic content of specimens of autopsied lung tissue from asbestos exposed workers indicated that the residual estimated fibre content measured by electron microscopy was less than estimated using magnetic field measurements. As the distribution of magnetic particles has been measured in living persons using magnetic chest scans, our

results suggests that such measurements subject to consideration of particle removal rates may provide an estimate of magnitude of original asbestos dust exposure.

## Résumé

LES RELATIONS ENTRE LES PARTICULES FERROMAGNETIQUES ET LES FIBRES DE CHRYSOTILE AEROPORTEES DANS LES MINES ET LES CONCENTRATEURS D'AMIANTE DU QUEBEC



O.T. Djamgouz

Département de Genie Minier et Metallurgique

Université McGill

Candidat au Diplôme de Docteur en Philosophie



L'examen de l'amiante chrysotile, prélevé dans les Cantons de l'Est du Queébec, utilisant des méthodes de microscopie optiques et électronique a révelé que les fibres de chrysotile étaient intimement associées à des minuscules particules de magnétite.

Des mesures de champs magnétiques traces furent effectuées utilisant un magnétomètre "fluxgate" sur trois types d'échantillons des fibres commerciales en vrac, la poussière totale aéroportée et la partie respirable des Jaoussieras aéroportées. Ces échantillons furent prélevés dans les mines et concentrateur d'amiante du Québec utlisant un "eleutriator" horizontal Hexlet. Il fut déterminé que l'"eleutriator" horizontal Hexlet était un appareil valide pour le prélèvement de la fibre respirable dans le milieu du concentrateur. Il fut observé que les intensités du champ magnétique trace de la poussière aéroportée, dans des nuages de poussière générés en laboratoire et dans la poussière dans les lieux de travail, étaient reliées de façon significative au contenu en magnétite de la poussière, la masse totale et la masse de la partie respi-

rable de la poussière aéroportée et également à la concentration de fibre de plus de 5 micromètres de longueur (rapport d'aspect > 3:1) mesurée par microscopie à phase contrastée. Des courbes de calibration furent développées pour chacun des 9 concentrateurs du Québec. Des calibrations répétées demontrèrent que les lignes étaient reporductibles à l'intérieur d'une marge de ± 10 pourcent. La précision de la méthode pour déterminer le poids de la poussière est fonction de la grandeur de l'échantillon avec des erreurs aussi faibles que ± 7,5 pourcent pour des échantillons de plus de 3 milligrammes et aussi grandes que ± 40 pourcent pour des échantillons dont le poids est inférieur à 0,5 milligrammes. Les relations entre les concentrations de fibre et les champs magnétiques traces étaient moins reporductibles et la limite de détection inférieure était bornée par la sensibilité du magnétomètre "fluxgate".

Malgré que le champ magnétique trace variait en fonction du contenu en magnétique, qui variait entre différents concentrateurs et produits commerciaux de fibre, la rapport entre la magnétite et la chrysotile demeurait constant pour un concentrateur donné et un produit donné. Les mesures de champs magnétiques traces des poussières aéroportées prélevées dans les environnements de concentrateurs peuvent alors fournir la possibilité de déterminer rapidément les concentrations de fibre chrysotile aéroportée, tout en termes de poids et nombre de fibres par litre d'air échantillonné, et également leur contenu en fer.

Les mesures du contenu magnétique de tissus de poumons prélevés de travailleurs exposés à l'amiante indiquèrent que le contenu résiduel de fibre estimé par microscopie électronique était moins que le contenu estimé par des mesures du champ magnétique. Puisque la distribution des particules magnétiques a été mesuré chez des êtres vivants utilisant des balayages magnétique de la poitrine, les résultats suggèrent que de telles mesures, sujet à des considérations tant qu'aux taux d'évacuation des particules, peuvent fournir un estimé de la grandeur de l'exposition originale à la poussière d'amiante.

TO MY WIFE YILDIZ,

AND CHILDREN

TEVFIK, HATICE & CIGDEM

## ACKNOWLEDGEMENTS

The author takes pleasure in expressing his gratitude to Dr. G.W. Gibbs, the supervisor of this research, whose guidance and advice, were invaluable in carrying out this work. The author is indebted to Dr. W. Williams, former chairman of the Department of Mining and Metallurgical Engineering at McGill University, who has made this research work possible through the award of a departmental research grant to purchase the Fluxgate Magnetometer. Thanks are also extended to Dr. J. Gruzleski, present chairman of the Department of Mining and Metallurgical Engineering and Dr. J.E. Udd, Director of Mining Program for their sincere interest and encouragement.

Appreciation and thanks are extended to Dr. D. Cohen of M.I.T. who helped the author in learning and gaining experience in the measurement of remnant magnetic fields of magnetite, design of the magnetic shielding box and his interest in this research work. Further thanks are extended to Drs. C. Fengler and O. Jensen and to Mr. K.L. Frazer who helped the author in expanding his knowledge in magnetism, improving the sensitivity and calibration of the fluxgate magnetometer.

Special thanks and appreciation are extended to Dr. N. Rowlands who provided the expertise in electron microscopy and electron probe microanalysis of the chrysotile asbestos samples. Further thanks and appreciation are extended to Mr. M. Harrigan, technician at the Institute of Occupational Health and Safety

of McGill University, for assistance in conscientious counting of chrysotile fibres and other particles in hundreds of optical microscope slides and for his excellent photomicrography.

The author also wishes to thank Messers. R. Robb, Chief technician, M. Ross, technician and other technicians at the Institute of Occupational Health and Safety for providing excellent service and maintaining and calibration of the environmental chamber and other instruments. Further thanks are due to Mr. D. Leashman, technician in the Department of Mining and Metallurgical Engineering for building the magnetic shielding box.

Also the author would like to take this opportunity and thank those asbestos mining companies of Quebec who supplied the required bulk chrysotile asbestos samples, offerred their help and allowed the author to visit their plants to take actual field samples. Furthermore the author wishes to thank Dr. M.I. Arhririi, Director of Graduate Studies, Institute of Occupational Health and Safety for his assistance in the author's understanding of the physiology of the human lungs and occupational diseases, Dr. A. Farah, of Laurentian University for assisting in statistical analysis of the data.

Also the author is indebted and thanks are due to Mr. L. Rudd, senior technologist in the School of Engineering of Laurentian University for drafting all the figures in this thesis and to Mrs. F. DiMaio for typing this manuscript.

Part of this research work was made possible by the Energy Mines and Resources, Department of Mines grants in the years of 1977-78 and 1978-79.

Very special thanks goes to my wife Yildiz for her moral support, understanding and encouragement throughout the research and writing of the thesis.

TABLE OF CONTENT


| | | |
|---|---|---|
| ABSTRACT | | ii |
| RESUME | | v |
| AKNOWLEDGEMENT | | viii |
| TABLE OF CONTENT | | xi |
| LIST OF FIGURES | | xx |
| LIST OF TABLES | | xxxi |
| PROJECT OVERVIEW | | xxxiv |
| LIST OF TERMS | | xxxviii |
| NOTATIONS | | xxxxi |
| I | ASBESTOS | |
| 1.1 | General Definition | 1 |
| 1.2 | History | 1 |
| 1.3 | Classification of the Asbestos Minerals and their Crystal Structures | 5 |
| 1.3.1 | Inosilicates: Amphibole Group | 6 |
| 1.3.2 | Phyllosilicates: Serpentine Group | 9 |
| 1.4 | The Chemical and Physical Properties of Asbestos | 13 |
| 1.4.1 | Chemical Composition of Asbestos | 13 |
| 1.4.2 | Chemical Composition of Chrysotile | 14 |
| 1.4.3 | Chemical Properties of Chrysotile | 17 |
| 1.4.4 | Physical Properties of Chrysotile | 19 |
| 1.4.4.1 | Tensile Strength of Chrysotile | 19 |
| 1.4.4.2 | Thermal Decomposition of Chrysotile | 20 |

List of References for Chapter I 22

II GEOLOGY

2.1 General 26

2.2 Serpentinization and Formation of Chrysotile 26

2.3 General Geology of the Asbestos Mining District of South-Eastern Quebec: 30

2.3.1 Ultrabasic and Basic Intrusives 31

2.3.2 Acid Intrusives 33

2.3.3 Alteration 34

2.3.4 Structure 36

2.3.5 Genesis of Asbestos Veins 38

2.4 Pennington Dyke 39

2.5 Thetford Mines Deposits 42

2.6 The British-Canadian Mine 45

2.7 Lake Asbestos of Quebec Mine 47

2.8 The Vimy, Normandie, and Penhale Deposits 49

2.9 The Jeffrey Mine Regional and Local Geology 52

2.10 Conclusion 59

List of References for Chapter II 60

III THE MINING AND MILLING OF CHRYSOTILE ASBESTOS IN QUEBEC

3.1 General Review 61

3.2 Conclusion 65

List of References for Chapter III 66

IV CANADA'S SHARE IN WORLD PRODUCTION AND THE USES OF ASBESTOS, AND ENVIRONMENTAL PROBLEMS

4.1 General 67

4.2 World Asbestos Industry 68

4.3 World Asbestos Market; Production and Consumption 69

4.4 Asbestos Fibre Groups and the Uses 74

4.5 Environmental Problems of Asbestos and Substitution 77

4.6 Conclusion 81

List of References for Chapter IV 82

V HEALTH EFFECTS OF CHRYSOTILE ASBESTOS

5.1 General 84

5.2 Anatomy and the Normal Functioning of the Respiratory Tract 85

5.2.1 The Lung Volumes and Capacities 86

5.2.2 Diffusion of the Oxygen Molecules from Alveolar Gas to Pulmonary Capillary Blood 90

5.3 Inhalation and Deposition of Aerosols and Chrysotile Fibres 92

5.3.1 Inhaled Aerosols and Physical Laws of Depositions 94

5.3.1.1 Impaction 94

5.3.1.2 Sedimentation 95

5.3.1.3 Diffusion 97

5.3.1.4 Interception 100

5.3.2 Aerosol and Chrysotile Fibre Deposition in the Respiratory Tract 101

5.3.2.1 Nasopharyngeal Deposition 104

5.3.2.2 Tracheobronchial Deposition 105

5.3.2.3 Pulmonary Deposition 108

5.3.2.4 Deposition of Chrysotile Fibre 112

5.4 Elimination of Aerosols and Chrysotile Fibres from Lungs 117

5.4.1 Nasopharyngeal Clearance (NP) 119

5.4.2 Tracheobronchial Clearance (TB) 120

5.4.3 Pulmonary Clearance 122

5.4.4 Clearance of the Chrysotile Fibres from the Lungs 127

5.5 Inhaled Chrysotile Fibres and Asbestos Related Diseases 130

5.5.1 Asbestosis (Diffuse Interstital Fibrosis) 133

5.5.2 Pleural Thickening and Pleural Plaques 135

5.5.3 Carcinoma of the Lung and its Association with Chrysotile Asbestos Exposure 137

5.5.4 Mesothelioma and its Association with Chrysotile Asbestos Exposure 138

5.5.5 Gastrointestinal Cancer and its Association with Chrysotile Asbestos Exposure 140

5.5.6 Pulmonary Function in Asbestos Related Diseases 141

5.6 Conclusion 143

List of References for Chapter V 145

VI STATE OF KNOWLEDGE: EXAMINATION AND MEASUREMENT OF AIRBORNE CHRYSOTILE ASBESTOS FIBRES

6.1 General 154

6.2 Chrysotile Asbestos Dust Sampling and Instrumentation 155

6.2.1 Konimeters 156

6.2.2 Midget Impingers 156

6.2.3 Thermal Precipitation 158

6.2.4 Electrostatic Precipitation 159

6.2.5 Light Scattering Techniques: Tyndallometers 159

6.2.6 The Membrane Filter Technique 160

6.2.7 Gravimetric Size Selective Sampling of Respirable Chrysotile ASbestos Dust 164

6.2.7.1 The Hexhlet Size-Selective Gravimetric Sampler 167

6.2.7.2 Other Gravimetric Sampler with Cyclone Size Selector Attachment 176

6.2.8 Royco and Airborne Asbestos Dust Sampling 179

6.3 Chrysotile Asbestos Dust Indentification and Measurements by Electron Microscopy and Microprobe Analysis 180

6.3.1 Scanning Electron Microscopy and Fibre Identification 180

6.3.2 Transmission Electron Microscopy and Fibre Identification 182

6.4 Analytical Methods to Determine or Elemental Composition of Chrysotile Asbestos Dust 186

6.2 Conclusion 190

List of References for Chapter VI 192

VII MAGNETISM AND MAGNETIC PROPERTIES OF MAGNETITE AND CHRYSOTILE ASBESTOS

7.1 General 199

7.2 Basic Principles of Magnetism and Magnetic Properties of Magnetite 199

7.2.1 Induction of Magnetization and Hysteresis Curve of Ferromagnetic Materials, and Demagnetization Process 203

| | | |
|---|---|---|
| | 7.2.2 Magnetization Curves of Magnetite and Magnetocrystalline Anisotropy | 205 |
| | 7.2.3 Magnetostriction of Magnetite | 206 |
| | 7.2.4 Magnetic Domains of Magnetite | 206 |
| | 7.2.5 Magnetization Process of Fine Magnetite Particles and Their Magnetic Behaviour | 207 |
| 7.3 | Detection of the Distribution of Ferromagnetic and Magnetite Particles in Human Lungs by Remanent Field Measurements | 212 |
| 7.4 | Biological Effects of Magnetic Field | 215 |
| 7.5 | Low Magnetic Field Measuring Device: The Fluxgate Magnetometer (Model MF-5000) and the Principle of its operation | 218 |
| 7.6 | High Magnetic Field Measuring Device: Gaussmeter (Model D-855) and the Principle of its Operation | 220 |
| 7.7 | New Developments in the Field of Instrumentation for Measurement of Magnetic Lung Contaminants, Airborne Asbestos Fibres and Other Magnetic Materials | 221 |
| 7.8 | Conclusion | 224 |
| | List of References for Chapter VII | 225 |
| VIII | RESEARCH WORK: DETERMINATION OF THE RELATIONSHIP BETWEEN FERROMAGNETIC PARTICLES AND AIRBORNE CHRYSOTILE FIBRES IN THE ASBESTOS MINES AND MILLS OF QUEBEC | |
| 8.1 | General Purpose | 229 |
| 8.2 | Materials and Methods | 230a |
| | 8.2.1 Materials | 231 |
| | 8.2.2 Methodology and Instrumentation | 232 |
| | 8.2.2.1 Environmental Chamber | 232 |
| | 8.2.2.2 Chrysotile Asbestos Dust Cloud Generation | 234 |

8.2.2.3 Chrysotile Dust Sampling, Equipment and Methodology 237

8.2.2.4 Mass Determination of the Gravimetric Samples 240

8.2.2.5 Sample Analysis by Fibre Counting with Phase Contrast Optical Microscopy 242

8.2.2.6 Sample Analysis by Using Transmission and Scanning Electron Microscope 246

8.2.3 Calibration of the Dust Sampling Instruments 250

8.2.3.1 Calibration of the Battery Operated MSA Pumps 250

8.2.3.2 Calibration of the Hexhlet Horizontal Eleutriators 251

8.2.4 Remanent Magnetic Field Measurements, Magnetic Shielding and Magnetometers 253

8.2.4.1 Magnetization of the Samples 253

8.2.4.2 Magnetic Shielding 255

8.2.4.3 The Fluxgate Magnetometer, Model MF-5000 259

8.2.4.4 Remanent Magnetic Field Measurements 264

8.3 Field Studies 266

List of References for Chapter VIII 271

IX STATISTICAL ANALYSIS AND INTERPRETATION OF RESULTS

9.1 General 273

9.2 Calibration Curves for Mass Determination of Airborne, Respirable Size Pure Magnetite 274

9.3 Calibration Curves for Mass Determination of the Airborne, Respirable Size Chrysotile Asbestos for Various Mills of Quebec 277

9.4 Calibration Curves for Number Determination of Chrysotile Fibre Content of the Airborne Respirable Size Dust for Various Mills of Quebec 282

9.5 Correlation of the Remanent Magnetic Fields with the Mass and Number of the Airborne Fibres in Various Locations of the Visited Mills and their Interpretation 285

9.6 Correlation of the Remanent Magnetic Field Measurements of Lung Specimens from Autopsy of Asbestos Workers with the Determined Mass and Counts of Chrysotile 289

9.7 Recommendations for Further Research 292

CONCLUSIONS 295

References for Chapter IX 298

APPENDICES

Appendix "A" 299

A.1 Carey-Canadian Mine, Quebec 300

A.1.1 Mining 300

A.1.2 Ore Processing 301

A.2 National Asbestos Mines Limited, Quebec 303

A.2.1 Mining 303

A.2.2 Ore Processing 304

A.3 Bell Asbestos Mine, Quebec 305

A.3.1 Mining 305

A.3.2 Ore Processing 306

A.4 King-Beaver, Quebec 307

A.4.1 Mining 307

A.4.2 Ore Processing 311

A.5 British-Canadian Mine, Quebec 311

A.5.1 Mining 311

A.6 Lake Asbestos of Quebec Limited 313

A.6.1 Mining 313

A.6.2 Ore Processing 314

A.7 Normandie Mine, Quebec 315

A.7.1 Mining 315

A.7.2 Ore Processing 316

A.8 The Jeffrey Mine, Quebec 318

A.8.1 Mining 318

A.8.2 Ore Processing 321

Appendix "B"

Calibration Curves for Various Mills of Quebec for Chrysotile Mass Determination 325

BIBLIOGRAPHY 339

## LIST OF FIGURES


| Fig. No. | | Page |
|---|---|---|
| 1.1 | The Basic Structural Unit: Silicone-Oxygen Tetrahedron | 8a |
| 1.2 | (a) The Single Silicate (Pyroxene) Chain<br>(b) The Double Silicate (Amphibole) | 8a |
| 1.3 | Two Stages in Building up an Amphibole I-Beam | 8b |
| 1.4 | The Thedrahedral Sheet of Serpentine | 9 |
| 1.5 | The Octahedral Sheet | 11 |
| 1.6 | Fundamental Structure of Chrysotile Fibrils | 11a |
| 1.7 | Varieties of Asbestos | 12 |
| 1.8 | Variations in the Composition of Asbestos | 13a |
| 1.9 | Hollow Tubuler Structure of Chrysotile Asbestos | 13a |
| 1.10 | Decomposition of Asbestiform Fibres in Boiling 4N Hydrochloric Acid | 19a |
| 2.1 | General Map of South-Eastern Quebec | 31a |
| 2.2 | The Ultramafic Belt of Southeastern Quebec | 31b |
| 2.3 | Geological Map of the Quebec Asbestos Belt | 32a |
| 2.4 | Geological Map of the Thetford Mines-Black Lake Area | 33a |
| 2.5 | Mine Geology Plans Thetford Mines-Black Lake, Quebec | 43a |
| 2.6 | Map of Asbestos Deposits in Thetford Mines | 43b |
| 2.7 | Vertical Cross Section A - A Through King Deposit | 43c |
| 2.8 | Vertical Cross-Section B - B'Through the Bell-Johnson Deposit | 43d |

| Fig. No. | | Page |
|---|---|---|
| 2.9 | Vertical Cross-Section C - C' Through No.1 and Beaver No. 2 Deposits | 43e |
| 2.10 | Vertical Cross-Section D - D' Through Bennett-Martin Deposit | 43f |
| 2.11 | British Canadian Orebody | 46a |
| 2.12 | Geological Map of Vimy Ridge and Normandie Deposits | 51a |
| 2.13 | Vertical Cross-Section A - A Through the Vimy Ridge and Normandie Deposites | 52a |
| 2.14 | Normandie Plant Asbestos Corporation Limited | 52b |
| 2.15 | Section Through Jeffrey Mine Overburden | 57a |
| 3.1 | Typical Milling Circuit in a Canadian Asbestos Mill | 63a |
| 4.1 | World Production of Asbestos | 68a |
| 4.2 | Major International Asbestos Mining Groups | 69a |
| 4.3 | Apparent World Consumption of Asbestos | 70b |
| 4.4 | Apparent National Asbestos Comsumption and Trends | 70c |
| 4.5 | Quebec Production Trends; from Analysis of 1951-70 Data | 73 |
| 4.6 | Actual World Versus Canadian Asbestos Production for Last 20 Years | 81a |
| 5.1 | Respiratory System | 86a |
| 5.2 | Breakdown of Respiratory Tracts in the Lung | |
| 5.3 | Processes Involved in Pulmonary Gas Exchange | 87b |
| 5.4 | Lung Volumes | 88a |
| 5.5 | Mechanisms Responsible for Non-Uniform Distribution of Inspired Air | 91a |

| Fig. No. | | Page |
|---|---|---|
| 5.6 | Schematic Representation of Passage of $O_2$ Molecules from Alveolar Gas to Pulmonary Capillary Blood | 91b |
| 5.7 | Theoretical and experimental determinations of the Total Deposition Fractions of Inhaled Particles | 104a |
| 5.8 | Theoretical and Experimental Determinations of Pulmonary Deposition Fractions of Inhaled Particles | 104b |
| 5.9 | Deposition as a Function of Particle Size for 15 Respirations/min. | 106a |
| 5.10 | Aerosol Deposition in Respiratory Tract | 106b |
| 5.11 | Equivalent Diameters of Chrysotile Fibre of Different Lengths | 114a |
| 5.12 | Fraction of Inhaled Particles Deposited in the Lower Respiratory Tract Versus Volume-Equivalent Sphere Diameter (microns), for Aspect Ratio Values of 1 (sphere) 10 and 100 | 115a |
| 5.13 | Fraction of Inhaled Particles Deposited in the Lower (alveolated) Region of the Respiratory Tract, vs Equatorial Diameter of the Particle, for Various Values of Aspect Ratio | 115b |
| 5.14 | Fractions of Rods of Selected Lengths Which are Predicted to Deposit in Each Respiratory Compartment | 116a |
| 5.15 | Fractions of Rods of Selected Lengths Which are Predicted to Deposit in Each Respiratory Compartment | 116b |
| 5.16 | Fractions of Rods of Selected Lengths Which are Predicted to Deposit in Each Respiratory Compartment | 116c |
| 5.17 | Nasopharynx, Predicted Deposition by $D_e$ and Length | 117a |
| 5.18 | Tracheobronchial, Predicted Deposition by $D_e$ and Length | 117b |

| Fig. No. | | Page |
|---|---|---|
| 5.19 | Pulmonary Spaces, Predicted Deposition by $D_e$ and Length | 117c |
| 5.20 | Predicted Deposition of Slender Rods | 117d |
| 5.21 | Schematic Representation of Deposition and Clearance Pathways for Inhaled Aerosols | 120a |
| 5.22 | Simplified diagram of a Macrosphage Ingesting a Particle | 124a |
| 6.1 | Ray Diagram of Phase Contrast Optical Microscope | 162a |
| 6.2 | Medical Research Council/Johannesbury and U.S.A.E.C. Selection Curves for Respirable Dust in Comparison with the Alveolar Deposition Curve of Brown et al. | 166a |
| 6.3 | Diagram of Hexhlet Sampler | 168a |
| 6.4 | Diagram of a Cyclone Sampler | 177a |
| 6.6 | Determination of Equivalent Dust Concentrations | 179a |
| 6.7 | Schematic Diagram of a Scanning Electron Microscope with Energy Dispersive X-Ray Analyser | 182a |
| 6.8 | Ray Diagram Showing Operation of Transmission Electron Microscope in Both Microscopy and Selected Area Electron Diffraction Modes | 184a |
| 6.9 | Atomic Absorption Spectrometer Light Path | 189a |
| 7.1 | Specific Susceptibility of Natural Magnetite as Dependent on Grain Size | 203a |
| 7.2 | Schematic Illustration of Distribution of Magnetization Vectors in Crystals | 204a |
| 7.3 | Inverse Spinel Structure (magnetite). | 204a |
| 7.4 | Induction and Hysteresis Curve for a Ferromagnetic Body | 205a |
| 7.5 | Graded Cyclic Magnetization of Iron | 205a |

| Fig. No. | | Page |
|---|---|---|
| 7.6 | Magnetization Curves of Magnetite (after Weiss) | 208a |
| 7.7 | Distribution of Magnetization Vectors in Polycrystals | 208a |
| 7.8 | Types of Simple Domain Arrangements in a Small Sphere | 211a |
| 7.9 | Coercive Force of Magnetite as Dependent on Particle Size | 211a |
| 7.10 | The Range of Magnetic Field at the Chest, due to $Fe_3O_4$ in the Lung, of Persons in various Groups | 214a |
| 7.11 | Block Diagram of Fluxgate Magnetometer | 219a |
| 7.12 | (a) Haul Generator of the Gaussmeter<br>(b) Block Diagram of the Gaussmeter | 221a |
| 8.1 | Environmental Chamber | 234a |
| 8.2 | Dust Feed Mechanism | 235a |
| 8.3 | Fiber Dust Dispersing Chamber | 235b |
| 8.4 | Fibre Diameter Distribution of Chrysotile Dust Clouds in Environmental Chamber in Terms of Unit Density Spheres | 245c |
| 8.5 | Length Distribution of Chrysotile Fibres in Dust Clouds in Environmental Chamber | 245d |
| 8.6 | Picture (a): Settled Nonrespirable Fibres and Dust at the Entrance of the Hexhlet's Eleutriator Plate . . . (a)(b)<br>(c)(d) | 253a<br>253b |
| 8.7 | Picture (a): Settled Nonrespirable Dust and Fibres at the Entrance of the Hexhlet's Eleutriator Plate . . . (a)(b)<br>. . . (c)(d)<br>. . . (e)(f) | 253c<br>253d<br>253e |
| 8.8 | Picture (a): Total Airborne Silica Dust . . . (a)(b)<br>. . . (c) | 253f<br>253g |

| Fig. No. | | Page |
|---|---|---|
| 8.9 | Respirable and Nonrespirable Fibres and Particles in the Air Monitor Filter | 253g |
| 8.10 | Selection Curve of Hexhlet for Respirable Chrysotile Asbestos Dust | 253i |
| 8.11 | Picture (a): Electromagnet Powered by 12 Volts Car Battery and a Millipore Filter in a Petry Dish in the Gap of the Electromagnets Being Magnetized ...(b) | 255a |
| 8.12 | Section Through Magnetic Shielding Box | 258a |
| 8.12A | Probe Arrangement | 258b |
| 8.13 | Tests to Measure the Capacity & the Accuracy of Fluxgate Magnetometer | 261a |
| 8.14 | Low Pass Filter for - 3db cut off | 261a |
| 8.15 | Linear Relationship Between Magnetic Field Readings and Mass of Chrysotile | 270c |
| 8.16 | Linear Relationship Between Magnetic Field Readings and Mass of Total Iron Present in Quebec Chrysotile | 270d |
| 9.1 | Correlation of the Remanent Magnetic Field with the Mass of Pure Magnetite Hexhlet Samples | 275a |
| 9.2 | Calibration Line for Pure Magnetite Mass Determination | 275b |
| 9.3 | Correlation of the Remanent Magnetic Field with the Mass of Pure Magnetite Hexhlet Samples | 275c |
| 9.4 | Correlation of the Remanent Magnetic Field with the Mass of Pure Magnetite Cyclone Samples | 275d |
| 9.5 | Correlation of the Remanent Magnetic Field with the Mass of Pure Magnetite Cyclone Samples | 275e |
| 9.6 | Calibration Line for Mill # VI Chrysotile Mass Determination | |
| 9.7 | Correlation of the Remanent Magnetic Field with the Mass of Mill # VI Chrysotile Cyclone Samples | 279a |

| Fig. No. | | Page |
|---|---|---|
| 9.8 | Correlation of the Remanent Magnetic Field with the Mass of Mill # VI Chrysotile Cyclone Samples | 279b |
| 9.9 | Calibration Line for Mill # VII Chrysotile Mass Determination | 280a |
| 9.10 | Correlation of the Remanent Magnetic Field with the Mass of Mill # VII Chrysotile Cyclone Samples | 280b |
| 9.11 | Correlation of the Remanent Magnetic Field with the Mass of Mill # VII Chrysotile Cyclone Samples | 280c |
| 9.12 | Correlation of Magnetic Fields | 283a |
| 9.13 | Correlation of Magnetic Fields | 283b |
| 9.14 | Correlation of Magnetic Fields | 283c |
| 9.15 | Calibration Line for Fibre Number Determination for Mill # 1 Chrysotile | 284a |
| 9.16 | Calibration Line for fibre Number Determination for Mill # II Chrysotile | 284b |
| 9.17 | Calibration Line for Fibre Number Determination for Mill # IV Chrysotile | 284c |
| 9.18 | Calibration Line for Fibre Number Determination for Mill # V Chrysotile | 284d |
| 9.19 | Calibration Line for Fibre Number Determination for Mill # VI Chrysotile | 284e |
| 9.20 | Calibration Line for Fibre Number Determination for Mill # VII Chrysotile | 284f |
| 9.21 | Calibration Line for Fibre Number Determination for Mill # VIII Chrysotile | 284g |
| 9.22 | Calibration Line for Fibre Number Determination for Mill # IX Chrysotile | 284h |
| 9.23 | Calibration Line for Fibre Number Determination for Rhodesian Chrysotile U.I.C.C. Samples | 284i |

| Fig. No. | | Page |
|---|---|---|
| 9.24 | Picture (a) is Showing a Magnetite Particle Associated with Short Fibres. Picture (b) is Showing a magnetite Particle Associated with Submicroscopic Fibres. | 285a |
| | Picture (c) is Showing a Magnetite Particle and Some Iron Associated with a Small Fibre Bundle. Picture (d) is Showing Magnetite Associated with Submicroscopic Chrysotile Fibres. | 285b |
| 9.25 | Magnetic Particle Associated with Antigorite (at the bottom of Picture "a" and in Picture (b) magnified 15,000 times) | 285c |
| 9.26 | Picture (a) is Showing a Brucite Particle Containing Iron and Nickel. | 285d |
| 9.27 | Picture (a) is Showing a Large Antigorite Particle Containing Some Iron and Surrounded by Chrysotile Fibres. | 285e |
| 9.28 | Picture (a) is Showing a Typical Chrysotile Fibre Bundle and X-ray Elemental Mapping for Iron. Picture (b) is Showing the EDXA Analysis of the Bundle. | 285f |
| | Picture (c) is Showing the same Chrysotile Fibre Bundle Magnified 10,000 times and (d) Fibre Bundle Magnified 50,000 Times and Showing a Minute Magnetite particle surrounded by Fibres in the Centre of the Picture. | 285g |
| 9.29 | Pictures (a) and (b) are Showing a magnetite particle Intimately Attached to the Chrysotile Fibre. Picture (b) is Showing the Identification of the Magnetite Particle with X-ray elemental mapping. | 285h |
| 9.30 | Correlation of the Remanent Magnetic Field with the Mass of Airborne Dust at Dry Rock Storage Area of Chrysotile Mill # VII | 286a |

| Fig. No. | | Page |
|---|---|---|
| 9.31 | Correlation of the Remanent Magnetic Field with the Mass of Airborne Dust at Milling and Screening Area of Chrysotile Mill # VII | 286b |
| 9.32 | Correlation of the Remanent Magnetic Field with the Mass of Airborne Dust at Above Bagging Area of Chrysotile Mill # VII | 286c |
| 9.33 | Correlation of the Remanent Magnetic Field with the Number of Airborne Respirable Chrysotile Fibre per Microscopic Field at Dry Rock Storage, Mill # VII | 286d |
| 9.34 | Correlation of the Remanent Magnetic Field with the Number of Airborne Respirable Chrysotile Fibres per Microscopic Field at Milling and Screening Area, Mill # VII | 286e |
| 9.35 | Correlation of the Remanent Magnetic Field With the Number of Airborne Respirable Chrysotile Fibre per Microscopic Field at Above Bagging Area, Mill # VII | 286f |
| 9.36 | Airborne Respirable Dust at Dry Rock Storage Area of Mill # VI and it's correlation with Remanent Magnetic field | 290a |
| 9.37 | Airborne Respirable Dust at Milling and Screening Area of Mill #VI and It's correlation with Remanent Magnetic Field | 290b |
| 9.38 | Airborne Respirable Dust at Above Bagging Area of Mill # VI and it's Correlation with Remanent Magnetic Field | 290c |
| 9.39 | Correlation of the Remanent Magnetic Field with the Number of Airborne Respirable Chrysotile Fibre per Microscopic Field at Dry Rock Storage Area of Mill # VI | 290d |
| 9.40 | Correlation of the Remanent Magnetic Field with the Number of Airborne Respirable Chrysotile Fibres per Microscopic Field at Milling & Screening Area of Mill # VI | 290e |

| Fig. No. | | Page |
|---|---|---|
| 9.41 | Correlation of the Remanent Magnetic Field with the Number of Airborne Respirable Chrysotile Fibres per Microscopic Field of Above Bagging Area of Mill # VI | 290f |
| 9.42 | Determination of the mass of Chrysotile Content of the Dry Lung Tissue by Magnetic Measurements | 291a |
| 9.43 | Correlation of the Number of Chrysotile Fibre Content of the Dry Lung Tissue with the $Fe_3O_4$ Content | 291b |
| 9.44 | Correlation of the Number of Chrysotile Fibre Content of the Dry Lung Tissue with $Fe_3O_4$ Content as Determined by Remanent Magnetic Field Measurement Method | 291c |
| B.1 | Calibration Line for Mill # 1 Chrysotile Mass Determination with Confidence Limits of 90% | 325 |
| B.2 | Calibration Line for Mill # II Chrysotile Mass Determination with Confidence Limits of 90% | 326 |
| B.3 | Calibration Line for Mill # III Chrysotile Mass Determination with Confidence Limits of 90% | 327 |
| B.4 | Calibration Line for Mill # IV Chrysotile Mass Determination with Confidence Limits of 90% | 328 |
| B.5 | Calibration Line for Mill # V Chrysotile Mass Determination with Confidence Limits of 90% | 329 |
| B.6 | Calibration Line for Mill VIII Chrysotile Mass Determination with Confidence Limits of 90% | 330 |
| B.7 | Calibration Line for Mill # IX Chrysotile Mass Determination with Confidence limits of 90% | 331 |
| B.8 | Calibration Line for Rhodesian UICC Chrysotile Mass Determination with Confidence Limits of 90% | 332 |

| Fig. No. | | Page |
|---|---|---|
| B.9 | Correlation of the Remanent Magnetic Field with the Mass of Mill # 1 Chrysotile | 333 |
| B.10 | Correlation of the Remanent Magnetic Field with the Mass of Mill # II Chrysotile | 334 |
| B.11 | Correlation of the Remanent Magnetic Field with the Mass of Mill # III Chrysotile | 335 |
| B.12 | Correlation of the Remanent Magnetic Field with the Mass of Mill # V Chrysotile | 336 |
| B.13 | Correlation of the Remanent Magnetic Field with the Mass of Mill # VI Chrysotile | 337 |
| B.14 | Correlation of the Remanent Magnetic Field with the Mass of Mill # VII Chrysotile | 338 |

# LIST OF TABLES


| Table No. | | Page |
|---|---|---|
| 1.1 | The Principle Properties of the Important Asbestos Varieties | 14a |
| 1.2 | Typical Chemical Composition of Chrysotile and Asbestiform Amphiboles | 15a |
| 1.3 | Chemical Composition of Some Typical Chrysotile Asbestos | 15b |
| 1.4 | Physical Properties of Chrysotile Asbestos | 20a |
| 4.1 | World Asbestos Production, 1978, and Capacity, 1978 and 1980 | 70a |
| 4.2 | Summary of Forecasts of U.S. and Rest-of World Asbestos Demand, 1977-2000 | 75a |
| 4.3 | World and Canadian Asbestos Production (1961-1980) | 75b |
| 5.1 | Dimensions of the Human Airway | 87a |
| 5.2 | Lung Volumes in Healthy Recumbent Subjects | 89 |
| 5.3 | Rates of Fall in Air at 760 mm Hg Pressure and 20°C of Spherical Particles of unit Density as Given by Stokes' Law and as Modified by Cunningham Correction Factor and Root-Mean-Square Brownian Displacement | 99 |
| 5.4 | Pathologic Effects of Asbestos Exposure in Man | 133a |
| 5.5 | Studies of Mortality in Chrysotile Mines 1910-75 | 138a |
| 5.6 | Relative Risk of Cancer for Male Chrysotile Asbestos Workers | 139a |
| 6.1 | Five General Categories for Asbestos Dust Sampling Instruments and Techniques | 157a |

| Table No. | | Page |
|---|---|---|
| 7.1 | Magnetic Units | 202a |
| 7.2 | Biological Effects of Magnetic Field on Man | 218a |
| 7.3 | Recommended Exposure Limits to Stationary Magnetic Fields | 218b |
| 8.1 | Average Diameters of Chrysotile Dust Clouds in Environmental Chambers, in Terms of Equivalent Unit Density Spheres and Actual Fibre Diameters | 245a |
| 8.2 | Chrysotile Asbestos Fibre Length Distribution of Chrysotile Dust Clouds in Environmental Chamber: (Optical Observations) | 245b |
| 8.3 | The Average Ratios of the Surface Areas of Magnetite to Chrysotile and Calculated Magnetite Content | 249a |
| 8.4 | Size Selection Curve of Hexhlet Horizontal Eleutriator for Respirable Chrysotile Asbestos Dust in Terms of Equivalent Unit Density Spheres | 253h |
| 8.5 | Magnetite Content as Determined by Electron Microscope Observations | 269a |
| 8.6 | Total Chrysotile and/or Serpentine and iron Content of Airborne Chrysotile Samples from Mills # VI and VII | 270a |
| 8.7 | Iron Content of Quebec Chrysotile Asbestos | 270b |
| 8.8 | Chrysotile Contnet of Grade # 6 Asbestos of Quebec, Determined by Magnesium Analysis with Atomic Absorption Method, and Iron Content | 270e |
| 9.1 | Statistical Data for Hexhlet Samples of Pure Magnetite | 276a |
| 9.2 | Statistical Data for Hexhlet Samples of Grade # 6 Chrysotile from Mill # VI | 278a |
| 9.3 | Statistical Data for Hexhlet Samples of Grade # 6 Chrysotile from Mill # VII | 278b |

| Table No. | | Page |
|---|---|---|
| 9.4 | Statistical Data for Hexhlet Samples of Rhodesian Chrysotile U.I.C.C. Samples | 278c |
| 9.5 | Statistical Data for Hexhlet Samples, Chrysotile from Various Mills | 278d |
| 9.6 | Actual Dust Counts and Magnetically Determined Magnetite and Chrysotile Content of the Dry Lung Tissues of Asbestos Workers | 292a |

## PROJECT OVERVIEW

In recent years a considerable increase in asbestos production and the industrial uses of chrysotile asbestos fibre has widened the range of exposure to fibrous dust. Since 1961 the production rate has increased from 2.8 million tonnes to 5.1 million tonnes in 1980. Ninety five percent of the total production is chrysotile and Canada produces approximately 30 percent of the total free world chrysotile asbestos. In addition to those directly exposed in asbestos mining and milling operations, many other industrial workers who are involved in manufacturing of products containing asbestos, e.g. textile workers; insulation and construction workers, are also exposed to airborne chrysotile asbestos fibre inhalation. Exposure to asbestos dust, above the threshold limit values, may cause the development of asbestosis within a period of 25 to 30 years. Lung cancer is commonly associated with advanced cases of asbestosis.

In order to maintain exposure levels below the recommended threshold limit values and to maintain a healthy environment at the work place, it is necessary to monitor the exposure levels to chrysotile fibres regularly, and accordingly, take the appropriate measures to control or suppress dust. Presently available dust monitoring techniques are either too slow or expensive to accurately determine the number and concentration of chrysotile fibres in airborne respirable dust. In the case of membrane filtering and fibre counting by phase contrast

optical microscopy, the reproducibility of the results may vary considerably from one person to another or from one laboratory to another. No other physical or chemical technique for determination of the mass of airborne chrysotile fibres, has previously been established. Therefore it was necessary to develop a practical and economical method to monitor the airborne chrysotile fibre levels in the work environment.

In the medical field, even an early detection of asbestosis does not help to prevent the advancement of the disease. Chest X-rays indicate only the pulmonary changes and not the amount of dust inhalation which causes the pulmonary complications. Therefore, monitoring of chrysotile fibre exposure or inhalation could assist in the development of maximum cumulative exposure guidelines. The overall objective of this doctoral researchwas to determine the relationship between the measured remanent magnetic field and airborne magnetite, and association of these with the respirable mass and fibre number of the chrysotile component in the total dust.

In order to achieve this objective the following investigations have been conducted to determine;

1. The extent and manner in which magnetite and other ferromagnetic particles such as iron are attached to chrysotile asbestos fibres.

2. The ratio of magnetite to chrysotile asbestos fibre in airborne dust present in the work environment at different stages of asbestos production.

3. The correlation between the respirable mass or number concentrations of chrysotile asbestos fibre in air and the remanent magnetic field intensities of the airborne dust.

4. Correlation of results with the remanent magnetic field intensities of lung tissues obtained at autopsy and their fibre counts.

From extensive chemical, microscopic and magnetic investigations of airborne samples of chrysotile, magnetite and total dust, generated in the laboratory and taken from the asbestos milling industry of Quebec, the following results have been obtained which contribute to original knowledge:

1. The measured remanent magnetic field of chrysotile is linearly related to the mass of total iron; and therefore, the iron content of chrysotile asbestos or asbestos ore can be determined via its remanent magnetic field.

2. The majority of microscopic magnetite particles are intimately attached to chrysotile fibres, or are entrapped among the fibres or fibre bundles. The ratio of magnetite to chrysotile fibre in airborne dust is thus constant for a given product and hence the mass of

chrysotile and fibre number can be determined by remanent magnetic field measurement.

3. The distribution of inhaled and retained chrysotile asbestos fibres can also be measured with the magnetic chest scans. Thus magnetic chest scans might provide an estimate of the order of magnitude of asbestos originally present in the lung if removal mechanism and rates are taken into account.

## LIST OF TERMS

| | |
|---|---|
| Acinus: | a respiratory unit made up of bronchiole, alveolar ducts and alveoli. |
| Alveolus: | Terminal air-sac of lung in which exchange of gases between lung and blood takes place. |
| Anoxemia: | Lack of oxygen, caused by asphyxiation or by various diseases which render the blood incapable of conveying enough oxygen to the tissues. |
| Bronchi: | The two main divisions of windpipe. |
| Bifurcation: | Branching off. |
| Cilia: | A motile extension of a cell surface, containing nine longitudinal double filaments or microtubules arranged in a peripherial ring together with a central pair. |
| Collagen: | White fibrous tissue consisting of bundles of uniform diameter fibres. |
| Dyspnoea: | Subjective difficulty or distress in breathing, frequently rapid breathing. |
| Endothelium: | Layers of cells lining blood-vessels. |
| Epithelium: | Layers of cells which covers the body surface or lines a cavity. |
| Erythrocytes: | Red blood cells. |
| Fibroblast: | An elongated cell with cytoplasmic processes present in the connective tissue capable of forming collagen fibres. |
| Fibromata: | Nodule or mass derived from fibrous connective tissue, not neoplastic. |
| Fibrosis: | Collagenous fibrosis, poliferation of collagen fibres, development of fibrous tissue in organ characterized by formation or inflamation of connective tissue. |
| Gastrointestinal Tract: | Stomach and bowl system of the body |

| | |
|---|---|
| Globulin: | Protein found usually associated with albumen in lung tissue. |
| Haemolysis: | Loss of hemoglobin from red blood cell. |
| Hilum: | Point of attachment of the lungs to the body. |
| Larynx: | Cavity in upper part of windpipe. |
| Lymph: | Clear, transparent slightly opalecent fluid that is collected from tissues through out the body, flows in lymphatic vessels (through the nodes) and is eventually added to the venous blood circulation. |
| Lysis: | Disintegration of cells. |
| Lysosome: | They are organelles that produce enzymes in macrophages. |
| Mesothelioma: | Type of cancer of pleura or peritoneum, malignant tumour. |
| Nasopharynx: | Pasage between nose and larynx. |
| Neoplasms: | Abnormal tissue that grows by cellular proliferation, tumour. If malignant, called cancer. |
| Parietal pleura: | The wall of the membrane enveloping the lungs. |
| Peritonea: | Seros sacs of mesothelium and a thin layer of irregular connective tissue that lines the abdominal cavity and covers most of the viscera contained therein. |
| Phagocyte: | Type of colourless blood cell capable of ingesting and destroying dead or foreing material |
| Pharynx: | Cavity, with enclosing muscles and mucous membrane, behind and communicating with nose, mouth, and larynx. |
| Pleura: | Serous membrane enveloping the lungs and lining the walls of the thoratic cavity. |
| Purulent: | Containing or forming pus. |
| Reticulin: | Delicate randomly arranged fibers of |

| | |
|---|---|
| | varying thickness. |
| Sarcoma: | Tumour, usually highly malignant, malignant connective tissue neplasm. |
| Tachycardia: | Abnormally rapid action of hart. |
| Trachea: | Tube from larynx to bronchial tubes, conveying air to lungs. |
| Trauma: | Wound inflicted suddenly. |
| Turbinate: | One of scroll-like bones of the nose. |

## NOTATIONS

| | | |
|---|---|---|
| $A$ | = | Cross sectional area of the duct. |
| $A_c$ | = | Constant used in Cunningham correction (approximately 0.9). |
| $A_f$ | = | Floor area of the horizontal eleutriator. |
| $B$ | = | Density of magnetic flux or the strength of magnetic induction. |
| $B_c$ | = | Diameter or width of the cyclone inlet. |
| $C$ | = | Cunningham correction. |
| $c$ | = | Velocity of light. |
| $C_f$ | = | Concentration of fibres. |
| $D$ | = | Actual diameter of the particle. |
| $D_a$ | = | Aerodynamic diameter of the particle. |
| $D_c$ | = | Diffusion coefficient. |
| $D_e$ | = | The diameter of an equivalent unit density sphere. |
| $d$ | = | Diameter of the tube or air passage. |
| $d$ | = | Distance from magnetic pole. |
| $d_a$ | = | Diameter of airway at generation "a" in centimetres. |
| $d_{av}$ | = | Average diameter. |
| di | = | Inner diameter. |
| do | = | Outer diameter. |
| $F$ | = | Flow rate in litres per minute. |
| $E$ | = | Expected deposition at bronchial bifurcations by impaction. |
| $e$ | = | The charge of electron. |
| $g$ | = | Gravitational constant. |
| $\vec{H}$ | = | Magnetic field. |
| $h$ | = | Vertical hight of the dust above the duct floor. |

$h_p$ = Plank's constant = $6.63 \times 10^{-34}$ joule-sec.

I = Probability of Inertial Impaction.

J = Intensity of magnetization or the magnetic moment of the material per unit volume caused by the magnetic field.

K = Coefficient of friction.

k = Magnetic susceptibility.

L = Horizontal traverse distance or length of the duct.

l = Lenght of the airway.

$M_o$ = Statical mass of electron.

m = Magnetic unit pole.

N = Avogadro's constant = $6.02 \times 10^{23}$ atoms is contained in one gram atom.

$N_d$ = Nasal deposition.

$N_t$ = The effective number of turns made by the air stream in the cyclone.

O = Perimeter of the duct.

$O_e$ = Oersted.

Q = Air volume in litres per minute.

R = Gas constant = 1.987 cal./mole K.

$R_e$ = Reynoldsnumber - a dimensionless number.

$R_{in}$ = Input resistance of the chart recorder.

r = Radius of the airway.

$r_p$ = Radius of the particle.

S = Shielding factor.

S = Fractional deposition by sedimentation.

$S_{(a-1)}$ = Total cross section of all airways of generation (a-1) in cm square.

SP = Static pressure.

| | | |
|---|---|---|
| $T$ | = | Absolute temperature in K. |
| $t$ | = | Residence time of the particle. |
| $t$ | = | Thickness of the shielding material. |
| $V$ | = | Velocity of the flow in the tube. |
| $V_a$ | = | Average air stream velocity. |
| $V_c$ | = | The average inlet velocity of the air and particles in cyclones. |
| $V_t$ | = | Terminal settling velocity. |
| $V_l$ | = | Velocity of the laminarly flowing air or horizontal velocity of the airborne particles. |
| $w$ | = | Width of the rectangular duct. |
| $X$ | = | Deposition parameter. |
| $\gamma$ | = | Viscosity of the air or fluid. |
| $\bar{\Delta}$ | = | Root-mean-square Brownian displacement. |
| $\Theta$ | = | Angle of the bifurcation. |
| $\epsilon_o$ | = | Permittivity. |
| $\lambda$ | = | Mean free path of the fluid molecules. |
| $\mu$ | = | Magnetic permeability. |
| $\mu_B$ | = | Bohr Magneton = $0.9274 \times 10^{-20}$ emu. |
| $\nu$ | = | Airflow rate or volume |
| $\rho$ | = | Density of the aerosol. |
| $\rho_a$ | = | Density of the air. |
| $\rho_p$ | = | Density of the particle. |
| $\omega$ | = | Probability of deposition by diffusion |
| $\Psi$ | = | Angle of the airway to horizontal |

# CHAPTER I

## ASBESTOS

### 1.1 General Definition:

The word asbestos does not refer to any one particular mineral but rather to a group of naturally fibrous minerals with a variety of hydrated silicate compositions. It does not include fibrous forms of other minerals such as wollastonite, nemolite (fibrous brucite), or the fibrous forms of calcite or gypsum. According to Speil and Leineweber[1] the term "asbestiform minerals" is perhaps most descriptive of the asbestos group.

Asbestos is incombustible and can be separated into relatively soft, silky fibres of various lengths and diameters. Because of the variety of these characteristics, Badollet[2] mentions that asbestos is often referred to as a "mineral of unparalleled properties".

### 1.2 History:

The peculiar property of incombustibility combined with a fibrous structure attracted attention to asbestos over 2,000 year ago. Small amounts were used by the Romans for winding sheets to preserve the ashes of the dead when bodies were cremated[2][6]. Pausanias, a Greek writer who lived in the second

century, referred to golden lamps used in some of the Greek temples and mentions the wick being made of Carpasian flax, which alone of all other things is incomsumable by fire(6).

The name "Carpasian" in Greek meaning "cotton-like" is the earliest known fiber; and at the same time Carpasia is the name of a location in the north eastern part of Cyprus island. The ancient and still operating "Amiantos" mine is farther southwest and in Soli district.

The name "Amiantos" meaning "Undefiled" was given to it by the Greeks and Romans. This referred to the fact that cloth made from it was cleansed when thrown into the fire.

The word "asbestos" was derived from a Greek word meaning "unquenchable" or "inextinguishable". However, since asbestos was used in lamp wicks, the term came to mean "incombustible".

Sinclair(3) claims that the first use of asbestos was among stone-age man in Finland, who was thought to have used a variety called "anthophyllite" as a cementing agent in the preparation of clay pottery.

Very little mention of asbestos was made throughout the Middle Ages. Charlemagne, who reigned from 768 to 814 A.D., was supposed to have had an asbestos tablecloth which he would throw into the fire for cleansing to mystify his guests. Apparently, this was the only reason for its use.(2)

Marco Polo, in writing his travels to the Far East in the thirteenth century, related that:(4)

> "A substance is likewise found of the nature of the salamander, for when woven into cloth, and thrown into the fire, it remains incumbustible".

He continues on to say that: "this fossil substance, is prepared, spun and woven into cloth". Furthermore:

> "...in order to render the texture white, they put it in the fire and suffer it to remain there about an hour, when they draw it out uninjured by the flame, and as white as snow. And so again whenever it becomes dirty, it is bleached by being put into the fire".

The next reference to asbestos is in 1678 when, at a meeting of the Royal Society of London, a Chinese merchant exhibited a handkerchief of "Salamander's wool". An asbestos napkin belonging to Ferdinand III was exhibited in Vienna in 1679.(5) One of the earliest discoveries of an asbestos deposit was in the Ural Mountains of Russia between 1710 and 1720. The

first factory for making asbestos products operated for a short time near the end of the reign of Peter the Great. However, because of limited demand for the product, it was not successful.

The utilization of asbestos on a commercial scale originated in Italy. Several companies were founded between 1860 and 1875. It was used in the manufacture of rope packings and heat-insulating board.

Exhibits at the Universal Exhibition in Paris in 1878 gave wider publicity to the products then manufactured.

In 1860, asbestos was discovered near St. Joseph, Quebec, and a specimen of fine silky fiber from this region, later known as "chrysotile" asbestos, was exhibited in London in 1862. However, the deposits were few and small in the area, and attempts to work them profitably failed.

A new era in the asbestos industry began with the discovery of the deposits near Danville, Quebec in 1877. Mining began in 1878. The fibre could be worked more easily than Italian asbestos and its popularity in London, together with the easy availability of a growing market in the United States, led

to rapid development in the Danville and Thetford Mines area.

An occurrence of "blue" asbestos on the Orange River, South Africa was discovered in 1815. The name "Crocidolite", meaning "a stone with a woolly appearance", was given to it. The mining of this variety began with the establishment of the Cape Asbestos Co. Ltd., in 1893.

This brief review of asbestos history explains the historical development of the basic use and production of the mineral which gave rise to the major asbestos producing areas of today. These asbestos producing countries are: Canada, South Africa, U.S.S.R., People's Republic of China, Italy, U.S.A., and Cyprus. The detailes of production and the uses of asbestos will be covered in Chapter IV.

## 1.3 Classification of the Asbestos Minerals and Their Crystal Structure:

In general, asbestos is a particular form of serpentine (chrysotile) or of the amphibole group of minerals. Both are silicates but their crystal structure and chemical formulae are different. The atomic structure of the amphibole group consists

of silicate chains whereas the atomic structure of chrysotile is comprised of sheets.

According to Wicks[7] serpentine may have the same chemical composition as chrysotile and may give the same X-ray diffraction pattern as the chrysotile asbestos. When serpentine is crushed the end product is not fibres but irregularly shaped rock fragments and splinters. These features may be used to distinguish chrysotile asbestos from other serpentine minerals under the electron microscope.

The chemical composition, of the serpentine group of asbestos minerals, generally is less complex than the amphiboles but structurally it is more complex. In general, asbestos minerals, according to their crystal atomic structures, can be divided into two major groups:

a) Inosilicates (Amphibole Group)

b) Phyllosilicates (Serpentine Group)

### 1.3.1 Inosilicates: Amphibole Group

The inosilicates or chain structural group of asbestos minerals belonging to the inosilicate structural group have relatively simple structures but complex chemical formulae.

that is why their name, taken from the Greek word amphibolos, meaning ambiguous, is a very apt choice[1][8].

In order to understand the composition of amphiboles it is essential to know the basic crystal structure. The basic structural unit for the construction of the amphibole double silicate chain is the silicon-oxygen tetrahedron[8][9] (see Fig. 1.1). In this structure one silicon atom is surrounded by four oxygen atoms. These $SiO_4$ groups are arranged in a row by sharing two of their oxygens with their neighbours, and they form a single silicate (pyroxene) chain (see Fig. 1.2a)[8]. Two of these single chains are linked by the sharing of more oxygen atoms and create double chains; these are the basic structure of the amphiboles (see Fig. 1.2b). The Hydroxyl (OH) groups are placed in the centers of the upper tetrahedra, with the hydrogen atom below (see Fig. 1.3a); metal cations are placed on this band as shown in Fig. 1.3b. Now if a second double chain with hydroxyl groups is inverted and placed on top of the first double chain, the metal cations act to bond the two double chains rigidly and this creates the amphibole I-Beam structure. The two basal tedrahedral groups create the horizontal portion of the I-beam and the oxygen and metal atoms that bond them together create the vertical portion of the I-Beam.

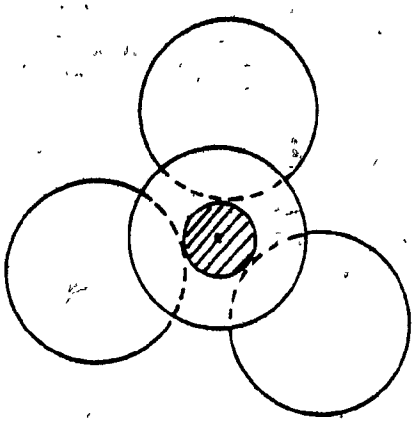

Fig. 1.1 The basic structural unit: Silicon-Oxygen tetrahedron ($SiO_4$). Open circles represent oxygen atoms and small filled circle represent silicon. The open circle concentric with the silicon atom represents an oxygen atom vertically above the silicon.

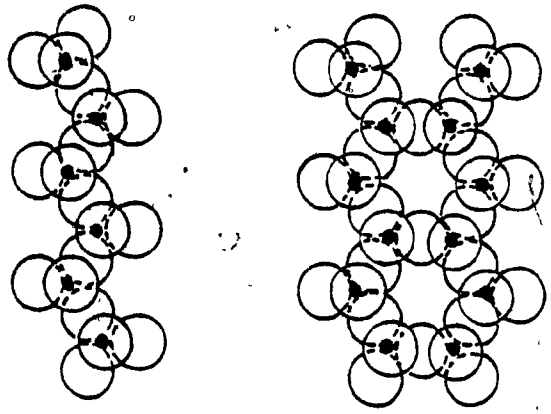

(a) (b)

Fig. 1.2 (a) The single silicate (pyroxene) chain.
(b) The double silicate (amphibole) chain. (8)

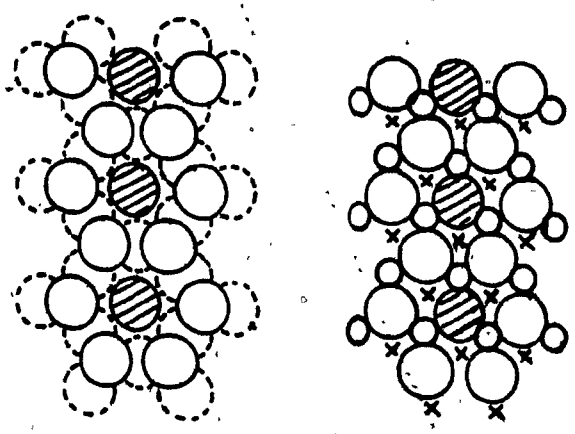

(a) (b)

Fig. 1.3 Two stages in building up an amphibole I-beam.[8] (a) Shaded circles are representing the OH groups and broken circles are representing the oxygen atoms at the lower level. (b) Cations are represented by the small circles and crosses indicates the positions occupied by O, OH atoms of the next chain.

### 1.3.2 Phyllosilicates: Serpentine Group :

The structure of the serpentine minerals is also made of silicon-oxygen tetrahedrons built up in a sheet like structure. That is why the Greek word "Phyllo", meaning "sheet", is added to the name of this group of silicates. In this sheet structure each tetrahedron shares 3 oxygen atoms of the neighbouring tetrahedrons; therefore the $Si_2O_5$ part of the formula is realized[9]. The sheet structure of chrysotile is related to the amphibole double chain and the triple silicate chain. However the difference is that the crystal structure growth is not restricted to one direction but could elongate in either or both of the two horizontal directions[7]. These types of sheets are arranged in 6-membered rings with hexagonal symmetry (see Fig. 1.4). There is also an octahedral sheet structure

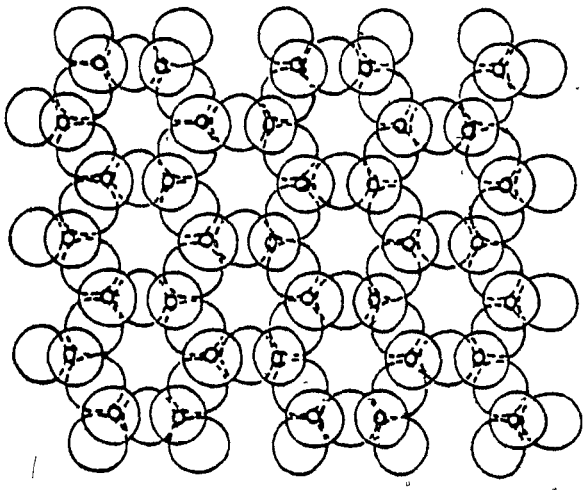

Fig. 1.4 - The tetrahedral sheet of Serpentine Crystal Structure.[7]

composed of magnesium octahedra with trigonal symetry, (brucite structure). The structural formula of this type of structure is $Mg_6Si_4O_{10}(OH)_8$ (see Fig. 1.5). This formula represents chrysotile and lizardite but not antigorite. The antigorite is slightly different[7] and the idealized version of the antigorite formula is $Mg_{5.65}Si_4O_{10}(OH)_{7.29}$.

In the basic structure a silicon layer is sandwiched between two layers of oxygen. A hydroxyl layer then becomes attached to the oxygen atoms and additional hydroxyl and magnesium layers are piled on top of the original structure. This entire structure is then repeated. This is how the sheets of the fundamental fibrills are formed[1] (see Fig. 1.6) Once the layers are formed, they tend to curve or coil into a hollow turbular structure in order to relieve the misfit between two layers of different sizes[7]. This is quite common in chrysotile structure as shown by Bates et al.[10], Zussman et al.[11], Turkevitch and Hellier[12] and Yada[13] with electron microscopy (see Fig. 1.9). Therefore chrysotile is a fibrous variety of the mineral serpentine. It is a hydrous magnesium silicate represented by the formula $Mg_3Si_2O_5(OH)_4$. Occasionally there is some replacement of the magnesium by other ions such as $Fe^{2++}$, Ni, Co[14].

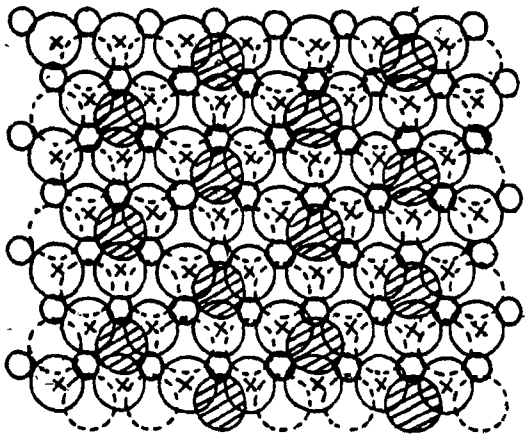

Fig. 1.5 The Octahedral Sheet.[7] Large dashed circles represent the apical oxygens of the underlying tetrahedral sheet. Shaded circles with crosses represent hydroxyls at the top of the octahedral sheet. Small circles represent magnesium cations.

Chrysotile, according to its crystallographic symmetry can be classified as: Orthochrysotile, Parachrysotile and Clinochrysotile.[2] The first two are orthorombic and last one is monoclinic.

To classify the serpentine minerals on their structural properties it is observed that chrysotile has a

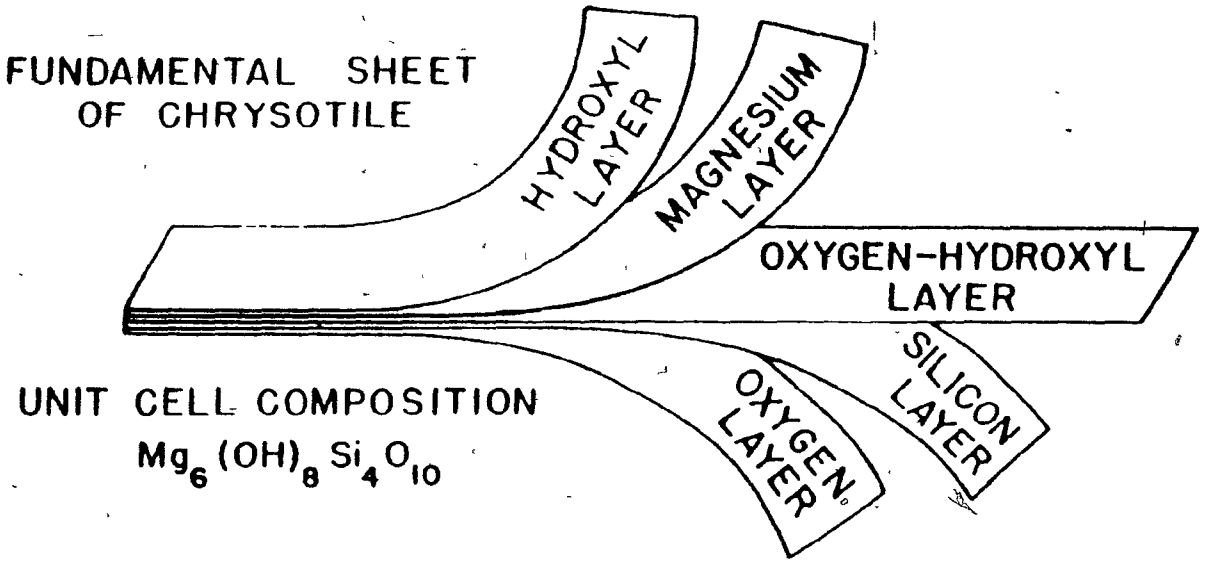


BUILD-UP OF SHEETS INTO FUNDAMENTAL FIBRILS

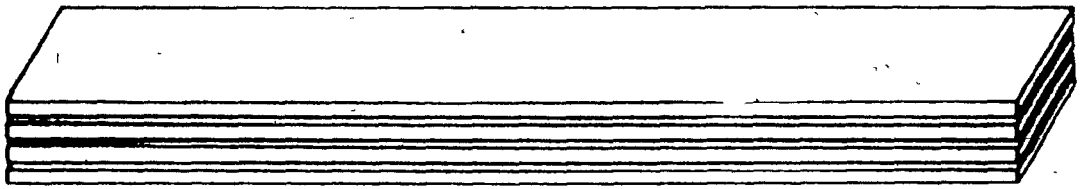

Fig. 1.6 Fundamental structure of chrysotile Fibrils[1]

tabular or cylindro-spiral structure. Lizardite has a planar structure and antigorite has an alternating wave or corrugated structure[7].

Another clan of phyllosilicates, that does not belong to the asbestos family, has an integral part of its structure sheets of OH ions coordinated by magnesium ions, forming the brucite $Mg_3(OH)_6$ structure; it is often mistaken for Lizardite or Antigorite under the electron microscope.

The general classification of asbestos minerals are summarized and shown in Figs. 1.7 and 1.8.

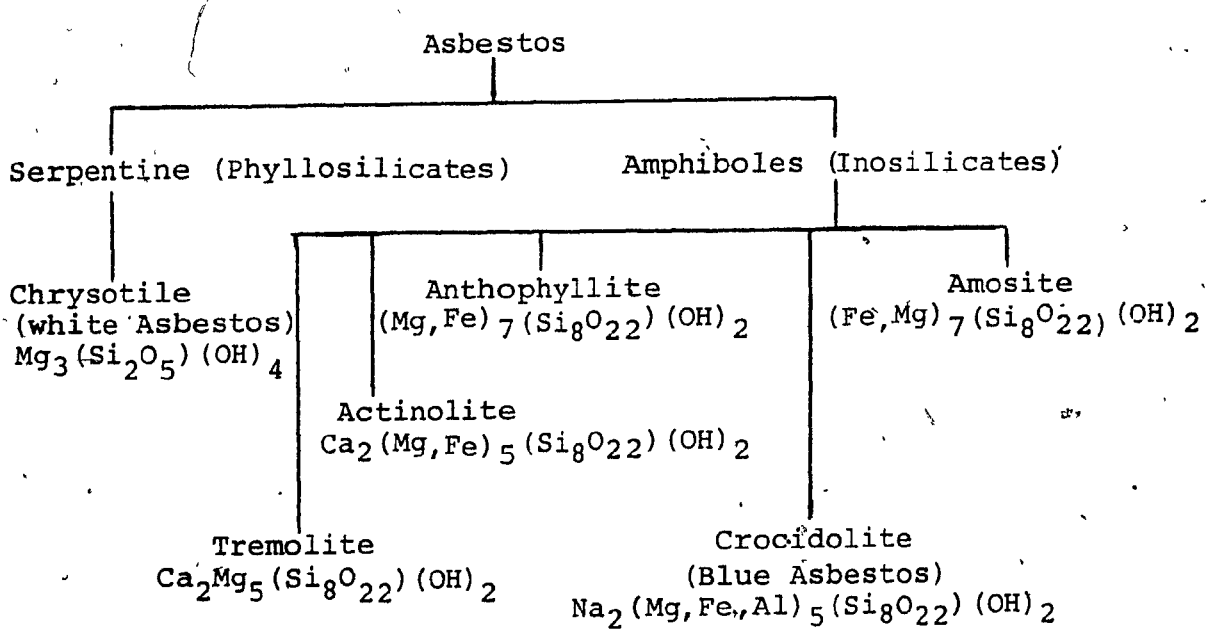


Fig. 1.7 Varieties of Asbestos[14]

## 1.4 The Chemical and Physical Properties of Asbestos:

The chemical composition of asbestos is directly related to its physical and mechanical properties. However the chemical properties and their ability to subdivide into finer fibres varies within the same or different groups of asbestos as a function of the geological, geochemical, petrographic and mineralogic conditions that prevailed during the formation period; whereas the physical and mechanical properties are governed by the fine-fibre structure[15].

Table 1.1 presents in convenient form for easy comparison data on the principle properties of the important asbestos varieties[16].

### 1.4.1 Chemical Composition of Asbestos:

Typical chemical analyses of the asbestos group of minerals are shown in table 1.2[1][2][17]. The difference between the chemical compositions shown in the table 1.2 and the chemical compositions of the given formulae in Fig 1.7 are quite significant. The impurities present in the minerals can be either part of the structure or might be due to occasional or accessory minerals occuring with chrysotile, or other amphibole group asbestos[1][2][7][8][17].

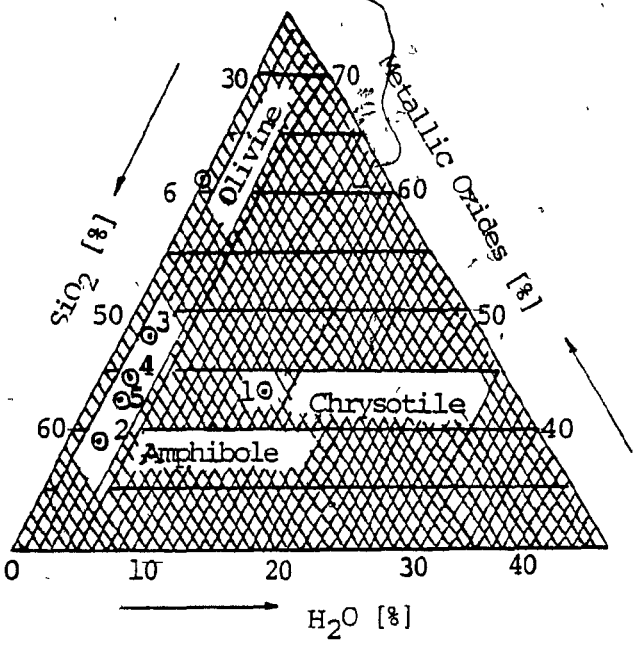


1) Chrysotile, Serpentine, Antigorite
2) Tremolite
3) Crocidolite
4) Amosite
5) Anthophyllite
6) Olivine*

Fig. 1.8 Variations in the Composition of Asbestos[15]. (*Olivine is shown to illustrate absorption of water in formation of chrysotile).

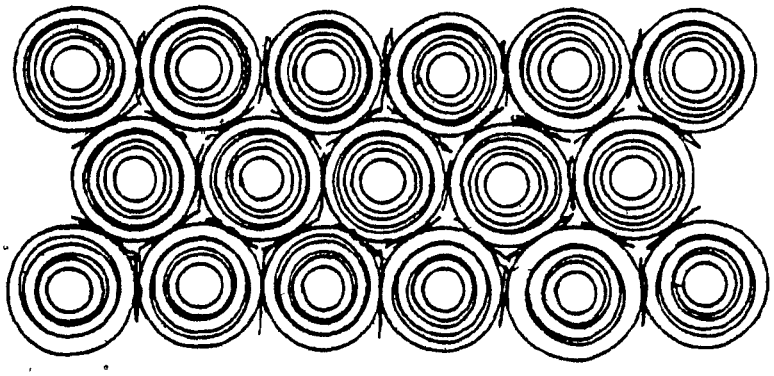

Fig. 1.9 Hollow Tubuler Structure of Chrysotile Asbestos[13].

1.4.2 Chemical Composition of Chrysotile:

Table 1.3 indicates the chemical composition of some typical chrysotile asbestos of Canada and the world. Usually the most common impurity is iron, present in the form of $Fe^{++}$ (ferric) ions[7][8]. Harrington and other researchers[18][19][26] indicate that ferric ions can be substituted for silicon in the silica sheets while the ferrous ions would be substituted for the magnesium in the brucite layer[27]. There are other impurities in lesser amounts as indicated in table 1.3 as part of the crystal structure. Some of these minerals are associated with massive serpentine and commercial chrysotile as occasional minerals (gangue minerals)[17]. These are: Magnetite, brucite, chromite, calcite, magnesite, olivine, pyroxene, tremolite, actinolite, clorite, talc, chalcedony, lizardite and antigorite. The proportion of each mineral will vary considerably with the nature and location of the deposit. Reimchussel's[28] research work has also shown that some of the above mentioned minerals are present in the crystal structure of massive serpentine and chrysotile asbestos as trace minerals, and some of them as gangue minerals. He has also indicated that the chance of iron contamination from crushing and

TABLE 1.1 - THE PRINCIPLE PROPERTIES OF THE IMPORTANT ASBESTOS VARIETIES[16].

| | ACTINOLITE | AMOSITE (FERRO ANTHOPHYLLITE) | ANTHOPHYLLITE | CHRYSOTILE | CROCIDOLITE | TREMOLITE |
|---|---|---|---|---|---|---|
| STRUCTURE | Reticulated long prismatic crystals and fibres | Lamellar. Coarse to fine fibrous and asbestiform | Lamellar. Fibrous Asbestiform | In veins of Serpentine. Etc | Fibrous in ironstones | Long. Prismatic and fibrous aggregates |
| MINERAL ASSOCIATION | In limestone and in crystalline schists | In crystalline schists etc. | In crystalline schists and gneisses | In altered peridotite adjacent to serpentine & limestone near contact with basic igneous rocks | Iron rich siliceous argillite in quartzone schists | In Mg limestones as alteration prod. of highly magnesian rocks. Metamorphic and igneous rocks |
| ORIGIN | Results of contact metamorphism | Metamorphic | Metamorphic. Usually from olivine | Alteration & Metamorphism of basic igneous rocks rich in magresian silicates | Regional Metamorphism | Metamorphic |
| VEINING | Slip or mass fibre | Cross fibre | Slip. Mass fibre unoriented and interlacing | Cross and slip fibres | Cross fibre | Slip or mass fibre |
| ESSENTIAL COMPOSITION | Ca. Mg. Fe. Silicate water up to 5% | Silicate of Fe and Mg higher iron than anthophyllite | Mg Silicate with iron | Hydrous silicates of magnesia | Silicate of Na and Fe with some water | Ca & Mg silicate with some water |
| THEORETICAL FORMULA | $Ca(Mg\ Fe)_3(SiO_3)_4$ x $H_2O$ | $(Fe\ Mg)SiO_3$ 1.5% $H_2O$ | $(Mg.Fe)_7Si_8O_{22}(OH)_2$ | $3MgO\ 2SiO_2 2H_2O$ | $Na\ Fe\ (SiO_3)_2$ $FeSiO_3$ x $H_2O$ | $Ca_2Mg_5Si_8O_{22}(OH)_2$ |
| CRYSTAL STRUCTURE | Long & Thin columnar to fibrous | Prismatic lamellar to fibrous | Prismatic. Lamellar to fibrous | Fibrous and asbestiform | Fibrous | Long & Thin Columnar to fibrous |
| CRYSTAL SYSTEM | Monoclinic | Orthorhombic | Orthorhombic | Monoclinic (Pseudo-Orthorhombicy) | Monoclinic | Monoclinic |

## Continuation of Table 1.1

| | | | | | | |
|---|---|---|---|---|---|---|
| COLOR | Greenish | Ash gray, grenish, or brown | Grayish white Brown. Gray or Green | White. Gray, Green. Yellowish | Lavender, Blue Greenish | Gray-white. Greenish. Yellowish. Bluish |
| LUSTRE | Silky | Vitreous. Somewhat Pearly | Vitreous to pearly | Silky | Silky to dull | Silky |
| HARDNESS | 6± | 5.5 - 6.0 | 5.5 - 6.0 | 2.5 - 4.0 | 4 | 5.5 |
| SPECIFIC GRAVITY | 3.0 - 3.2 | 3.0 - 3.25 | 2.85 - 3.0 | 2.4 - 2 6 | 3.2 - 3.3 | 2.9 - 3.2 |
| CLEAVAGE | 110 Perfect | 110 Perfect | 110 Perfect | 010 Perfect | 110 Perfect | 110 Perfect |
| OPTICAL PROPERTIES | Biaxial negative extinction inclined | Biaxial & Positive extinction parallel | Biaxial Positive extenction parallel | Biaxial Positive extinction parallel | Biaxial I extincion inclined | Biaxial negative extinction inclined |
| REFRACTIVE INDEX | 1.63± weakly pleochroic | 1.64± | 1.64± | 1 50 - 1 55 | 1 7 pleochroic | 1.61± |
| FUSIBILITY | Fusible at 4 | Fusible at 6. Losses water at moderate Temperatures | Infusible or difficult. Fusible. | Fusible at 6 | Fusible at 3 | Fusible at 4 |
| FLEXIBILITY | Brittle and Nonflexible | Good Less than Crysotile | Very Brittle. Nonflexible | Ver flexible | Fair to good | Generally brittle. Sometimes flexible |
| LENGTH | Short to long | 2 to 11 varies | short | short to long | short to long | short to long |
| TEXTURE | Harsh | Coarse but somewhat pliable | Harsh | Soft to harsh. Also silky | soft to harsh | Generally harsh. Sometimes soft. |

## Continuation of Table 1.1

| | | | | | | |
|---|---|---|---|---|---|---|
| TENSILE STRENGTH | Very weak | Fair. Less than chrysotile | Very weak | Very good | Very good. Highest of all varieties | Weak |
| ACID RESISTANCE | Relatively insoluble in in HCl | Fairly resistant to acids | Fairly resistant to acids | Soluble up to approximately 5% | Fairly resistant to acids | Fairly resistant to acids |
| SPINNABILITY | Poor | Fair | Poor | Best | Fair | Generally poor. Some are spinnable |

milling operations is very low or remote. The iron content of chrysotile fibre structure is estimated to be very low, varying between 0.5 and 1.5% Fe[28]. The remainder of iron is in the form of Magnetite ($Fe_3O_4$) and associated with asbestos as a gangue mineral in the amounts of 0.5% to 5%[15][28][29]. According to Laurent[35] the magnetite is distributed along the contact between the fibres and the selvages of the veins during the first episode of serpentinization:

Olivine ($Fo_{90}$) + Enstatite ($En_{93}$) + $H_2O$ → Lizardite + Magnetite + $H_2$ ± Awaruite

Awaruite ($FeNi_2$ or $FeNi_3$) is present mainly in the non-chrysotile component of the dust[28][30][35][39]. Laurent[35] states that magnetite which is distributed within the fibre bundles, is formed as follows:

Lizardite + $H_2O$ + $O_2$ → Clinochrysotile + Brucite + Magnetite

During the growth of chrysotile fibres, large amounts of magnetite formation take place as well[30][35]. Lamarche and Wicks[36] observed that the magnetite content of the ultramafic rocks increase with their degree of serpentinization. Allen and Smith[37] have observed under the electron microscope that even after the fibres are reduced in size to -325 mesh, magnetite particles and chrysotile fibres remain interlocked.

Table 1.2 - Typical Chemical Composition of Chrysotile and Asbestiform amphiboles[1] [2] [17]
(Typical Ranges in Percent)

| | Chrysotile | Crocidolite | Amosite | Anthophyllite | Actinolite | Tremolite |
|---|---|---|---|---|---|---|
| $SiO_2$ | 38-44.5 | 49-53 | 49-53 | 56-58 | 51-56 | 55-60 |
| MgO | 40-43 | 0-3 | 1-7 | 28-34 | 15-20 | 21-26 |
| FeO | 0.14-2 | 13-20 | 34-44 | 3-12 | 5-15 | 0-4 |
| $Fe_2O_3$ | 0.2-1.6 | 17-20 | trace | -- | 0-3 | 0-0.5 |
| $Al_2O_3$ | 0.3-3 | 0-0.2 | 0-0.4 | 0.5-1.5 | 1.5-3 | 0-2.5 |
| MnO | 0-0.1 | 0-0.1 | 0-0.7 | -- | 0-0.1 | 0-0.1 |
| CaO | trace-1 | 0.3-2.7 | 0-1 | 0-0.2 | 9-12 | 11-13 |
| $K_2O$ | trace-0.2 | 0-0.4 | 0-0.6 | trace-0.1 | 0-0.5 | 0-0.6 |
| $Na_2O$ | 0-0.06 | 4-8.5 | trace-0.2 | 0-0.1 | 0.2-1.5 | 0-1.5 |
| $CO_2$ | 0.2-0.5 | 0.2-0.4 | 0-0.2 | -- | -- | 0-0.1 |
| $H_2O$ | 12-14 | 1.9-4.5 | 1.9-4.5 | 1-6 | 1.5-2.5 | 0.5-3.6 |

Table 1.3 - Chemical Composition of Some Typical Chrysotile Asbestos[1][2]
(Typical Ranges in Per Cent)

| | Asbestos, P.Q. Jeffrey Mines | Thetford, P.Q. King Beaver | British Columbia Cassiar | California New Idria | Arizona | S. Africa Transvaal | S. Africa Swaziland | Rodesia Shakoni | Russia |
|---|---|---|---|---|---|---|---|---|---|
| $SiO_2$ | 44.1 | 38.75 | 40.75 | 38.4 | 41.07 | 41.83 | 39.93 | 39.70 | 39.00 |
| MgO | 41.6 | 39.78 | 41.28 | 39.9 | 42.35 | 41.39 | 40.25 | 40.30 | 38.22 |
| $Fe_2O_3$ | 0.92 | 1.59 | 0.44 | 1.1 | 0.42 | 1.29 | 0.10 | 0.27 | 0.54 |
| FeO | 0.80 | 2.03 | 0.28 | 2.4 | 0.14 | 0.08 | 0.45 | 0.70 | 1.53 |
| $Al_2O_3$ | 0.34 | 3.09 | 3.37 | 0.44 | 0.55 | 0.30 | 3.92 | 3.17 | 4.66 |
| $Cr_2O_3$ | 0.019 | trace | 0.13 | 0.31 | 0.03 | ---- | ---- | ---- | ----- |
| NiO | 0.010 | trace | 0.18 | 0.18 | trace | ---- | ---- | ---- | ----- |
| MnO | 0.03 | 0.08 | 0.03 | 0.10 | 0.07 | 0.04 | 0.05 | 0.26 | 0.11 |
| CaO | 0.04 | 0.89 | 0.35 | 0.96 | 1.02 | trace | 1.02 | 1.08 | 2.03 |
| $TiO_2$ | 0.01 | ---- | ---- | 0.05 | 0.01 | 0.02 | ---- | ---- | ----- |
| $Na_2O$ | 0.06 | 0.10 | 0.07 | 0.04 | trace | ---- | 0.09 | 0.04 | 0.07 |
| $K_2O$ | 0.04 | 0.18 | 0.04 | 0.04 | 0.03 | ---- | 0.09 | 0.05 | 0.07 |
| $CO_2$ | ---- | 0.48 | 0.44 | ---- | ---- | ---- | 1.04 | 2.13 | 1.83 |
| $H_2O$ | 13.2 | 12.82 | 13.64 | 14.00 | 13.97 | 13.66 | 13.28 | 12.81 | 12.14 |
| TOTAL | 101.17 | 99.79 | 101.00 | 97.92 | 99.66 | 98.61 | 100.22 | 100.51 | 100.20 |

Hahn-Weinheimer and Hirner[38] stated that in majority of the cases the separation of chrysotile fibres from intergrown magnetite with tweezers or by a magnet was impossible. Choi and Smith[39] stated that magnetite and brucite is commonly associated with chrysotile and are often found intergrown with the fibres.

Monkman[30] states that the accessory mineral content of chrysotile asbestos is dependent on the conditions under which the chrysotile was formed or to which it was later subjected. Therefore the initial composition of the magnesium rich ultrabasic rock and hydrothermal solutions' composition play an important role in the forming of new accessory minerals with the chrysotile fibres. Monkman has also shown that if the dust fraction of the commercial chrysotile is removed the chemical composition of the original sample is modified, indicating that accessory minerals are not part of the crystal structure of chrysotile. Harrington[19] states that these minerals are intergrown with the fibre bundles, but during the processing stage the majority of the associated minerals are separated from the chrysotile fibre. However magnetite, brucite and magnesite are commonly found even in the purer grades of chrysotile[19]. Large portions of the magnetite content can be freed by grinding and removed with magnetic separation. But this is a costly process and is done only when there

is a commercial demand for such a product. This type of chrysotile product is commonly used in the electrical insulation industry. Harrington[26] reported that the associated organic matter, and some of the primary oils are contaminants due to the bagging of the chrysotile in jute bags. Later, Commins and Gibbs[31] found that storing chrysotile asbestos in polythene bags results in contaminating it with hydrocarbons and possibly stabilizers present in the plastic. Further studies by Gibbs[24] and Gibbs and Hui[25] has shown that Canadian Chrysotile contains organic material in the range of 0.5 to 20.0 mg per 100 mg of chrysotile. However, it is indicated that this organic content is largely the result of contamination by mining or milling processes, although virgin fibre from the Thetford area does contain minute quantities of organic material.

1.4.3 Chemical Properties of Chrysotile :

There was a time when chrysotile asbestos was considered as being almost indestructible. However, at present with the new techniques such as electron microscopy, electron diffraction, and X-ray diffraction analysis it is possible to show that chrysotile is not as resistant to the attack of acids as it was expected to be. In reality, in comparison to other asbestos minerals, chrysotile is the least stable. When chrysotile and antigorite were subjected

to 1N HCl acid for one hour at 100°C the diffraction pattern of chrysotile completely disappeared while the antigorite pattern was not too much affected(1). Examination with the electron microscope indicated that the chrysotile was very severely attacked by the acid and its tubular morphology destroyed. In 1965, Hodgson(15) studied the stability and rate of decomposition of asbestos minerals in boiling 4N HCl acid. The results indicated that after half hour the chrysotile had lost almost the 60% of its weight, while tremolite, Anthophyllite, Crocidolite, Actinolite and Amostite had lost only between 4 and 8% of their weight (see Fig. 1.10).

### 1.4.4 Physical Properties of Chrysotile:

A summary of the physical properties of chrysotile asbestos is shown in Table 1.4. The two most important physical properties, tensile strength and thermal decomposition are discussed in next two sections of this thesis.

#### 1.4.4.1 Tensile Strength of Chrysotile:

One of the most important characteristic of chrysotile asbestos fibres is their tensile strength. This property is particularly important in the construction industry where asbestos is used as a reinforcing material. However, due to non-uniformity of the fibre lengths and diameters, it is very difficult to find a precise value for the tensile strength of fibres. Zukowski and Gaze[33] showed maximum tensile strength of 58,000 Kg/cm$^2$ for chrysotile fibres having a length of 2 millimeters. It is also stated that the failure does occur at the weak interfibrillar bonds and does not show a true tensile failure of a fibre. Badolet[2] has stated that average chrysotile fibre tensile strength is 31,000 Kg/cm$^2$ as indicated in table 1.4. The published data in Speil and Leineweber's[1] report corresponds with that of Badolet and they indicate that the average tensile strength of Arizona, U.S.A. chrysotile is 38,500 Kg/cm$^2$ and the tensile

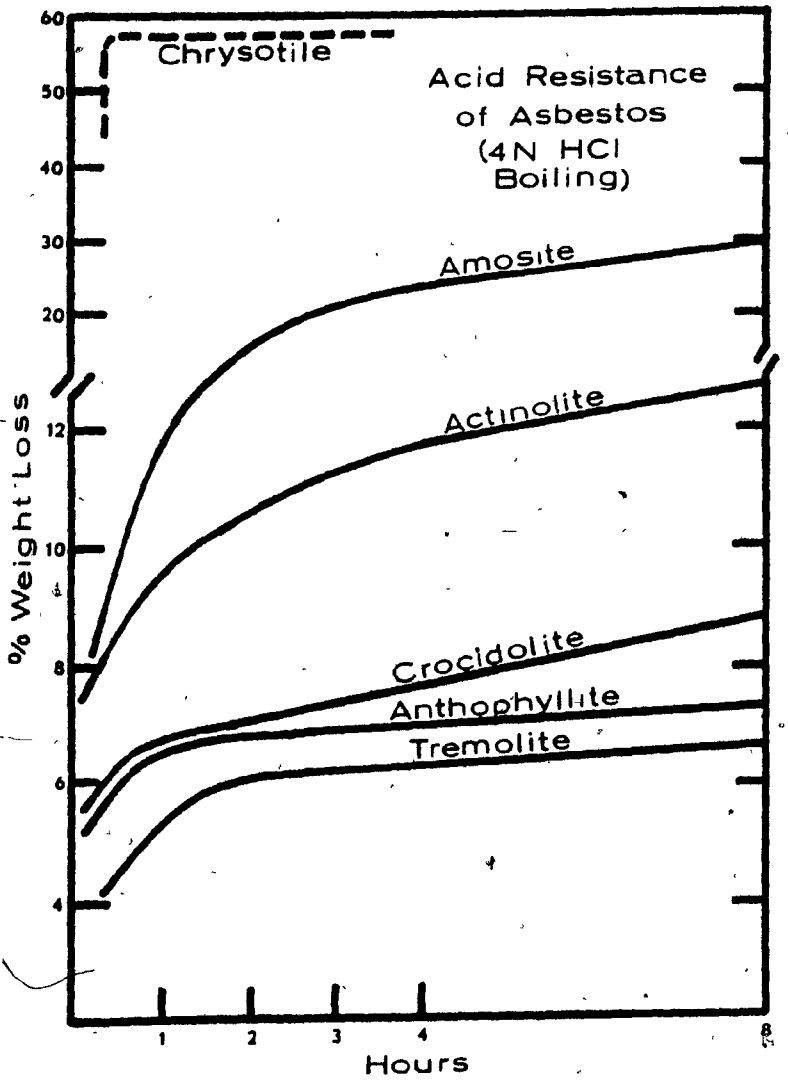


Fig. 1.10 Decomposition of Asbestiform Fibres in Boiling 4N Hydrochloric Acid. (1)

strength of Thetford, Canada chrysotile is 37,100 Kg/$cm^2$. Average cross sectional area of fibres tested were $2.07 \times 10^{-6}$ $cm^2$ and $2.13 \times 10^{-6}$ $cm^2$ respectively. According to theoretical calculations[34] the silicate chain structures should have tensile strengths over 100,000 Kg/$cm^2$. Whittaker[34] suggests that this discrepancy is due to crystal imperfections which have occured during the fibre formation and therefore the measured strength is not purely dependent on atomic structure of the fibre.

1.4.4.2 Thermal Decomposition of Chrysotile:

Chrysotile asbestos like other asbestiform minerals does not fuse even at a temperature of 1000°C but at lower temperatures completely decomposes or breaks down. Typical thermal analysis of chrysotile would indicate that up to 500°C the decomposition is neglegible[1], however, some scientists suggest that dehydration starts at low temperatures such as 200°C to 250°C[19]. Actual dehydroxylation occurs at temperatures between 600° - 720°C[2]. At 800°C the chrysotile fibres completely lose their crystal structure and become amorphous. Further heating up to 825°C causes recrystalization and forsterite ($Mg_2SiO_4$) is formed[1][2][19]. During the process the loss of weight ranges from 12.7 to 13.1%[2].

Table 1.4 - Physical Properties of Chrysotile Asbestos[2]

| Property | Values & Remarks |
|---|---|
| Tensile Strength $Kg/cm^2$ | 31,000 |
| Young's Modules $Kg/cm^2$ | $1.65 \times 10^6$ |
| Flexibility | Good |
| Specific Gravity | 2.55 |
| Hardness, Mohs | 2.5 to 4.0 |
| Specific Heat kcal/g/°C | 0.266 |
| Volume Resistivity megohm-cm | 0.003 - 0.15 |
| Colour | Colourless |
| Refractive Index $n_\alpha$ | 1.493 - 1.553 |
| Refractive Index $n_\gamma$ | 1.517 - 1.557 |
| Pleochroism | NIL |
| Birefringence | Moderate (first order) |
| Orientation | Length slow |
| Extinction | Parallel |

$$2H_4Mg_3Si_2O_9 \xrightarrow[\text{Temp.}]{\text{High}} 3Mg_2SiO_4 + 4H_2O + SiO_2$$

Chrysotile Forsterite Water Cristobalite

Above the temperatures of 1100°C enstatite ($MgSiO_3$) is formed. The actual process of course is more complicated than the explanations above; in reality before complete dehydroxylation is observed, forsterite could be detected by infrared spectroscopy(19).

During the grinding of chrysotile asbestos and other asbestos minerals, the temperature rise due to mechanical energy can cause structural changes in the outside layers of chrysotile bundles(1)(19). If this temperature rise is not controlled by adding water, the crystal structure and even the fibrous morphology is destroyed. Therefore the future thermal characteristics of chrysotile fibres can be affected at the mineral processing stage.

## LIST OF REFERENCES FOR CHAPTER I


1. Speil, S., and Leineweber, J.P.: Asbestos Minerals in Modern Technology Environmental Technology, Vol. 2, No. 3, April 1969. Reprint Academic Press Inc., pp. 2-29.

2. Badollet, M.S.: "Asbestos" A Remarkable Mineral Fibre, 1975, pp. 1-4.

3. Sinclair, W.E.: Asbestos, Its Origin, Production and Utilization, Mining Publications Ltd., Second Edition, 1959.

4. Polo, Marco: Travels, Book 1, Chapter XLII of the Province of Chingintalas, John Murry, 3rd Edition, London, 1903, pp. 212-213.

5. Currens, W.W.: Asbestos Mines and Minerals, Pub. Scranton, Pa. 1912-13, Vol. 33, pp. 229-230.

6. Report No. ARB-TDA-01-75: Asbestos as a Hazardous Contaminant II, Ministry of the Environment, Air Resources Branch, Toronto, Ont. January 1975, pp. 9-10.

7. Wicks, F.J.: Mineralogical Association of Canada, "Short Course in Mineralogical Techniques of Asbestos Determination", Quebec, May 1979, pp. 35-72.

8. Whittaker, E.J.W.: Mineralogical Association of Canada, "Short Course in Mineralogical Techniques of Asbestos Determination", Quebec, May 1979, pp. 1-34.

9. VanDers, I., Kerr, P.F.: Mineral Recognition, John Wiley & Sons Inc., New York, 1967.

10. Bates, T.F., Sands, L.B., and Mink, J.F.: Tabular Crystals of Chrysotile Asbestos, Science, Vol. III, 1950, pp. 512-514.

11. Zussman, J., Brindley, G.W.: Electron Diffraction Studies of Serpentine Minerals, American Mineralogist, Vol. 42, pp. 133-157, 1957.

12. Turkevitch, J., Hiller, J.: Electron Microscopy of Collodial Systems, Analytical Chemistry, Vol. 21, pp. 475-485, 1949.

13. Yada, K.: Study of Chrysotile Asbestos by High Resolution Electron Microscopy, Acta Crystallographica, Vol. 23, pp. 703-708, 1967.

14. Berry, L.G., Mason, B.: Mineralogy, Freeman and Co., San Francisco, 1959.

15. Berger, H.: Asbestos Fundamentals, Chemical Publishing Co., New York, 1963.

16. Badollet, M.S.: "Asbestos a Mineral of Unparalleled Properties", Transactions CIMM, Vol. 54, pp. 151-161, 1951.

17. Gaze, R.: "The Physical and Molecular Structure of Asbestos", Annals of the New York Academy of Sciences, Vol. 132, Art. 1, pp. 23-30, New York, 1965.

18. Harrington, J.S.: "Chemical Studies of Asbestos", Annals of the New York Academy of Sciences, Vol. 132, Art. 1, pp. 31-47, New York, 1965.

19. Harrington, J.S., Allison, A.C. and Badami, D.V.: "Mineral Fibres: Chemical, Physicochemical and Biological Properties", pp. 291-402, 1975.

20. Lockwood, T.H.: "The Analysis of Asbestos for Trace Metals", American Industrial Hygiene Association Journal, Vol. 35, No. 5, May 1974.

21. Cralley, L.J., Keenan, R.G., Kupel, R.E., Kinser, R.E. and Lynch, J.R.: "Characterization and Solubility of Metals Associated with Asbestos Fibres", American Industrial Hygiene Conference, May 13-17, 1968.

22. Holmes, A., Morgan, A., Sandalls, F.J.: "Determination of Chromium, Cobalt, Iron, Nickel and Scandium in the International Union Against Cancer (UICC) Asbestos Reference Samples by Newtron-Activation", AERE-R5910, Harwell, Berkshire, 1968.

23. Morgan, A., Lally, A.E., and Holmes, A.: "Some Observations on the Distribution of Trace Metals in Chrysotile Asbestos", AERE-R7188, Harwell, Berkshire, 1972.

24. Gibbs, G.W.: "The Organic Geochemistry of Chrysotile Asbestos from the Eastern Townships, Quebec", Geochemica et Cosmochimica Acta, 1971, Vol. 35, pp. 485-502, Pergamon Press, Northern Ireland, Dec. 1970.

25. Gibbs, G.W., Hui, H.Y.: "The Organic Content of Canadian Chrysotile", American Industrial Hygiene Association Journal, August 1971.

26. Harrington, J.S., Roe, F.J.C.: "Studies of Carcinogenesis of Asbestos Fibres and their Natural Oils" Annals of the New York Academy of Sciences, Vol. 132, Art. 1, pp. 439-450, New York, 1965.

27. Roy, J.C., Barbeau, C., and Dupuis, M.: "Characterization of Chrysotile and Asbestos Ore by Substitution Ions", Third International Conference on Asbestos, University Laval, Quebec, August 17-21, 1975.

28. Reimschussel, G.: "The Association of Trace Minerals with Chrysotile Asbestos", Third International Conference on Asbestos, University Laval, Quebec, August 17-21, 1975.

29. Assad, J.R., et Associes: "Etude Mineralogique de L'Amiante Au Quebec en Relation Avec Son Exploitation, Extraction et Utilisation", Comite D'Etude Sur La Salubrite Dans L'Industrie De L'Amiante. Document I, Universite Laval, Quebec, 1976.

30. Monkman, L.J.: "Mineralogical and Chemical Contaminants in Graded Milled Chrysotile". Third International Conference on Asbestos, University Laval, Quebec, August 17-21, 1975.

31. Commins, B.T., Gibbs, G.W.: "Contaminating Organic Material in Asbestos", British Journal of Cancer 23, pp. 358-362, 1969.

32. Hodgson, A.A.: "Fibrous Silicates" Royal Institute of Chem., Lecture Series, No. 4, 1965.

33. Zukowski, R., and Gaze, R.: "Tensile Strength of Asbestos", Nature 183, 35 London, 1959.

34. Whittaker, E.J.W.: Oxford Conference on the Physics and Chemistry of Asbestos Minerals, Ppaer No. 1-1, 1967.

35. Laurent, R.: "Petrology of The Asbestos Serpentinites of South Quebec", In: Third International Conference on the Physics and Chemistry of Asbestos Minerals, August 1975, pp. 5-12.

36. Lamarche, R.Y. and Wicks, F.J.: "Where To Look For New Asbestos Deposits", In: Third International Conference on the Physics and Chemistry of Asbestos Minerals, August 1975, pp. 1-2, 5-6.

37. Allen, M.P. and Smith, R.W.: "Dissolution of Asbestos Minerals in Acid and Buffered Salt Solutions", In: Third International Conference on the Physics and Chemistry of Asbestos Minerals, August 1975, p. 2.

38. Hahn-Weinheimer, P., and Hirner, A.: "Major and Trace Elements in Canadian Asbestos Ore Bodies - Analytical Results and Statistical Interpretation", In: Third International Conference on the Physics and Chemistry of Asbestos Minerals, August 1975, p. 2.

39. Choi, I. and Smith, R.W.: "Identification of the Transition Elements Associated with Asbestos Minerals and Their Behaviour In Aqueous Solution", In: Third International Conference on the Physics and Chemistry of Asbestos Minerals, August 1975, p. 2-3.

# CHAPTER II

## GEOLOGY

### 2.1 General:

Canada is one of the world's major producers of chrysotile. The bulk of Canadian chrysotile production comes from a fairly large region of south-eastern Quebec. The two other important regions are northern British Columbia and the Yukon Territory. These two regions produce a much smaller amount of asbestos fibre, but the fibre quality, notably that at Cassiar, B.C., is better than the Quebec fibre.

This chapter describes serpentinization and formation of chrysotile, general geology of the asbestos-mining district of the province of Quebec and the history and geology of each deposit.

### 2.2 Serpentinization and Formation of Chrysotile:

Chrysotile asbestos, a hydrous magnesium silicate, is a fibrous form of serpentine. The host rock is a serpentinized ultramafic rock, usually a serpentinized peridotite or in some cases a dolomite. Peridotite is an ultrabasic rock containing over 30 percent olivine and more than 10 percent leucocratic minerals(9). In certain extensive areas the peridotite was acted on, under high pressures, by hydrothermal solutions, carrying dissolved salts and carbon dioxide. The high temperatures were due to the increase in temperature with depth (i.e. thermal gradient) combined

with heat given off by intrusive rocks. These hydrothermal solutions gradually changed the olivine in the original rock to serpentine.

$$3(Mg,Fe)_2\,SiO_4 + SiO_2 + 4H_2O \rightarrow 2(Mg,Fe)_3[(OH)_4Si_2O_5]$$

Olivine — Hydrothermal Solution of Silicic Acid — Serpentine

This process, known as serpentinization, is believed to have led to the formation of the Quebec Serpentine-Asbestos deposits.

A variation of the serpentinization process, requiring the presence of polymineralic peridotites, results in the formation of serpentinites (serpentines and oxides) as follows:

$$3(Mg,Fe)_2\,SiO_4 + (Mg,Fe)SiO_4 + 4H_2O \rightarrow 2(Mg,Fe)[(OH)_4Si_2O5]$$

Olivine — Pyroxene — Serpentine

+ $(Mg,Fe)O$

Oxide

Serpentine can also be produced by the alteration of dolomite as follows:

$$3CaMg(CO_3)_2 + 2SiO_2 + 2H_2O \rightarrow Mg_3[(OH)_4Si_2O_5] +$$

Dolomite — Hydrothermal Solutions of Silicic Acid — Iron free Serpentine

$$+ 3CaCO_3 + 3CO_2$$

Calcite

This last process led to the formation of iron free serpentine-asbestos deposits in Arizona and in the Transvaal.

The serpentinization process result in an increase in volume and this produces innumerable cracks and slips, which provided channels for hydrothermal solutions. These hydrothermal solutions circulated through the cracks in the rock, descending slowly through the smaller openings in the rocks and ascending through the larger openings and cracks. The high temperature water, containing carbon dioxide under pressure, is a good rock solvent. The rising water eventually loses pressure and slowly cools, resulting in a decrease in solvent power and the deposition of a small amount of dissolved rock. This material accumulates on the sides of the cracked areas in the rocks through which the water is flowing. This deposit tends to form regular growth of fibrous magnesium silicate fibres from the walls toward the centre, the width of the fracture controlling the length of the fibre.

Chrysotile occurs mainly as cross fibre and, to a lesser extent, as slip fibre and mass fibre. Cross fibre occurs in veins with fibres occupying a position somewhere between a normal and a sharply oblique angle to the vein walls, whereas slip fibre is a stress mineral occuring as a coating on slip planes

and orientated parallel to the direction of slip. Mass fibre is present in the ore of a few mines as aggregates of unoriented or semi-oriented leaves or bundles of chrysotile. The mass fibre recrystallization is within the serpentine and at some locations the rocks have been completely or nearly converted into mass fibre.

The most common minerals associated with chrysotile are carbonates, brucite, nemalite, picrolite, magnetite and talc. The amount and mode of occurance of these minerals is an important factor in determining the quality of the final fibre product.

The formation of chrysotile is a complex process involving a combination of extremely high pressures and temperatures, a particular chemical composition of the host rock and intensive faulting of the rock. This process was not, however, exactly the same for every deposit and thus a more detailed explanation must be made for each major deposit in order to describe more accurately the geological occurance of chrysotile asbestos in the Province of Quebec.

## 2.3 General Geology of the Asbestos Mining District of South-Eastern Quebec: (1,7)

The asbestos-mining district of South-Eastern Quebec is one of the chief sources of the world's estimated 6.6 million ton annual production of chrysotile asbestos. This district lies in a belt of ultra-basic rocks running northeastward through the hilly country south of the St. Lawrence River (see Fig. 2.1). Referring to Fig. 2.2 the productive portion of this belt, which represents the boundaries of the asbestos-mining district, extends from the town of Asbestos in the South, for a distance of some 60 miles north-eastward to beyond the village of East-Broughton.

Throughout southeastern Quebec the host rock to the asbestos deposits is primarily a peridotite which originally contained 10% to 15% pyroxene. The peridotite, associated with dunite, pyroxenite, and gabbro was introduced into sedimentary and volcanic rocks of paleozoic and possibly pre-cambrian age. The oldest rocks consist of a thick series of schists, quartzites, slates, and metabasalt. These were folded, faulted, and metamorphosed prior to the accumulation of the younger group made up of pyroclastics and flows, and a predominant series of slates accompanied by minor beds of arkose. Prior to the accumulation of the devonian, these later ordovician rocks were subjected to folding. The Acadian disturbance was the last period

of mountain building which affected the region, and produced open folds as opposed to the isoclinal folds in the ordovican and older rocks. (Fig. 2.2)

The emplacement of the ultrabasic, basic and acidic rocks of the belt occurred during either the Taconic (ordovician) or Acadian disturbances. The major bodies of these rocks have been intruded along a zone which follows the contact between the Caldwell and Beauceville rocks.

In the central part of the asbestos belt, three intrusive complexes may be distinguished, although they probably followed one another with only a minor time interval between each. The first of these complexes is composed of peridotite and dunite, the second of dunite, pyroxenite, and gabbro, and the third of granite and syenite. Wherever the first two complexes are both present, the asbestos deposits are always associated with the earliest, or peridotite-dunite complex (Fig. 2.3)

2.3.1 Ultrabasic and Basic Intrusives:

Peridotite, which is the host rock of the asbestos deposits, constitutes a large portion of the ultrabasic rocks of the belt. In the Thetford area the main body is 15 miles long, and up to 3 miles wide. The thin sill that constitutes the northeast part of the belt is composed of peridotite with only minor amounts of dunite. Peridotite is the prelevent rock

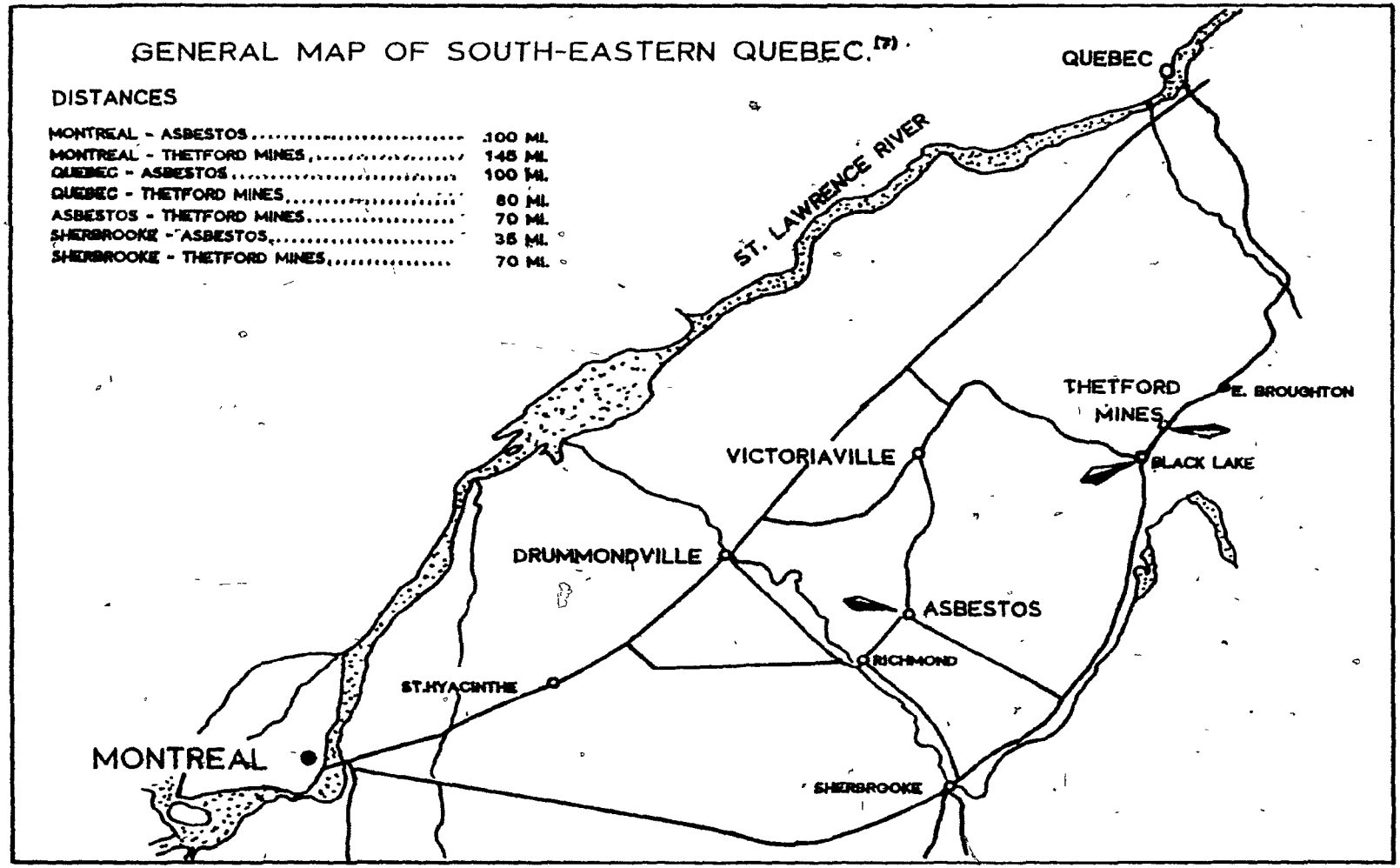
GENERAL MAP OF SOUTH-EASTERN QUEBEC.[7]
DISTANCES
MONTREAL - ASBESTOS ..... 100 MI.
MONTREAL - THETFORD MINES ..... 145 MI.
QUEBEC - ASBESTOS ..... 100 MI.
QUEBEC - THETFORD MINES ..... 80 MI.
ASBESTOS - THETFORD MINES ..... 70 MI.
SHERBROOKE - ASBESTOS ..... 35 MI.
SHERBROOKE - THETFORD MINES ..... 70 MI.
ST. LAWRENCE RIVER
QUEBEC
THETFORD MINES
E. BROUGHTON
BLACK LAKE
VICTORIAVILLE
DRUMMONDVILLE
ASBESTOS
RICHMOND
ST.HYACINTHE
MONTREAL
SHERBROOKE

FIGURE 2.1.

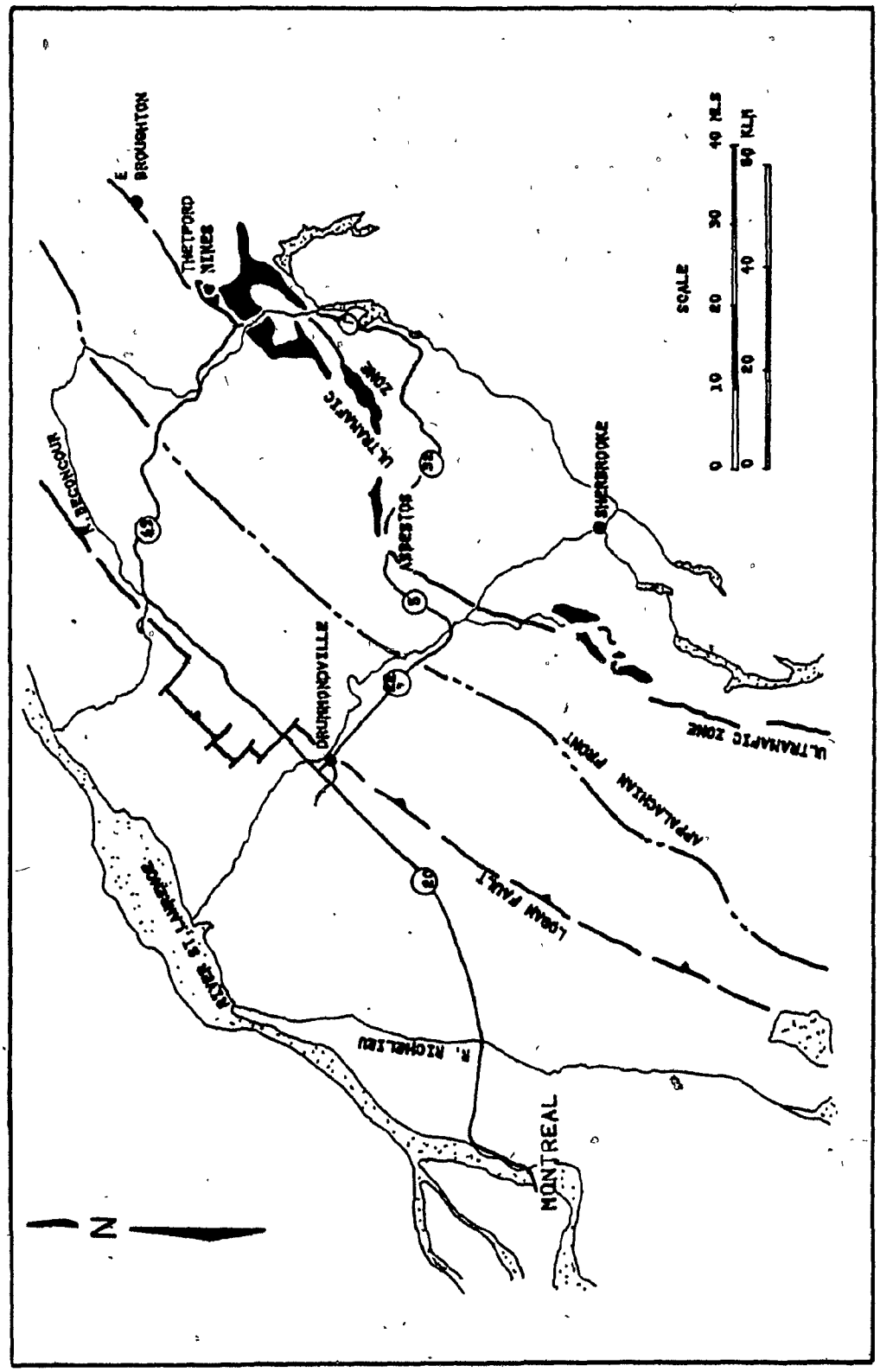


THE ULTRAMAFIC BELT OF SOUTHEASTERN QUEBEC[7]

FIGURE 2.2

type at the Asbestos end of the belt, and only in the vicinity of Breeches Lake and Nicolet Lake is less abundant than the other intrusive types, (Fig. 2.3). It is essentially a harzburgite containning 10% to 15% enstatite. Small bodies of dunite are scattered through the peridotite as local segragations. In addition, a belt of dunite is exposed over a length of 4 miles along the southeast side of the Thetford peridotite mass and appears to be the result of gravitational differentiation.

In the Thetford area, (Fig. 2.4), the dunite-pyroxenite-gabbro complex is the result of gravitational differentiation. The contacts between different rock types are gradational, and there are a number of places where a layered sequence is well displayed, with dunite at the base and gabbro at the top. The ultrabasic members of this complex have intruded the peridotite-dunite sequence. The earliest injection of ultrabasic magma had cooled rapidly giving rise to an even-grained, olivine-rich harzburgite with only minor amounts of dunite. The amphibolite, which occurs at several places adjacent to the peridotite contact was derived from the Caldwell rocks largely as a result of lime-metasomatism. Immediately following the consolidation of the earlier injection, another upsurge of ultrabasic magma into rocks that were already hot, gave rise, through slower cooling, to a more complete segration of its crystallizing constituents, and resulted in the formation of a

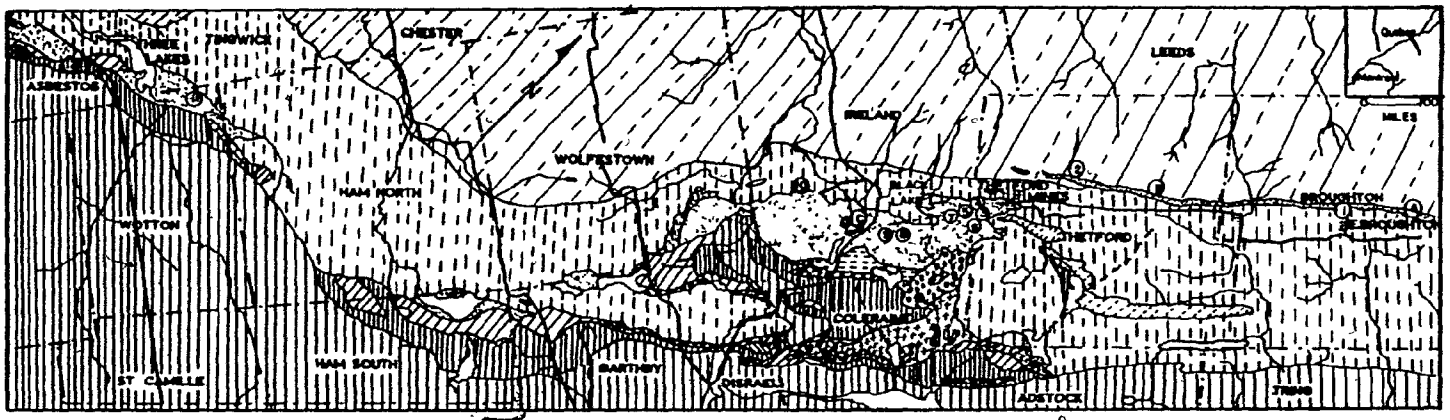


ORDOVICIAN(OR LATER)

INTRUSIVE ROCKS

- GRANITE
- GABBRO
- PYROXENITE
- DUNITE
- PERIDOTITE
- DUNITE

LATE COMPLEX

EARLY COMPLEX

METAMORPHIC ROCKS

- AMPHIBOLITE

ORDOVICIAN

BEAUCEVILLE GROUP

- SLATE
- VOLCANICS,BRACCIA

(MAJOR UNCONFORMITY)

CAMBRIAN

CALDWELL GROUP

- VOLCANICS
- QUARTZITE,SLATE
- SCHISTS

SCALE

0 8

MILES

- FAULT
- TOWNSHIP LINE
- MAIN ROADS

PRODUCING MINES

1 QUEBEC ASBESTOS
2 PLINTKOTE
3 KING(ASB.CORP)
4 BELL ASBESTOS
5 JOHNSONS CO.
6 BENNET-MARTIN (ASB.CORP)
7 BEAVER(ASB.CORP)
8 MEGANTIC(JOHNSONS)
9 BRITISH CANADIAN(ASB.CORP)
10 NORMANDIE(ASB.CORP)
11 NICOLET ASBESTOS
12 JEFFREY(CAN.JOHNS-MANSVILLE)

MINES UNDER DEVELOPMENT

A CAREY(QUE.ASB)
B NATIONAL GYPSUM
C LAKE ASBESTOS

GEOLOGICAL MAP OF THE QUEBEC ASBESTOS BELT[1]

FIGURE 2.3

large portion of dunite, rather coarse-grained diallagite, and large amounts of gabbro. The peridotite-dunite complex is confined, for the most part, to the Caldwell quartzite and schist, whereas much of the dunite-pyroxenite-gabbro complex is associated with volcanic rocks.

The ultrabasic and basic intrusive are generally concordant. The large bodies were introduced along the major unconformity between the Beauceville and Caldwell formations and moved upward along fold axis, thrusting aside the overlying rocks and locally spreading out laterally. The smaller bodies are generally in the form of sills, such as the Pennington "dyke" that extends 20 miles northeastward from Thetford Mines.

2.3.2 Acid Intrusives:

The sequence of acidic rocks, in the form of relatively small bodies of granite and even smaller bodies of syenite, has been intruded, almost exclusively into the ultrabasic and basic rocks. The distribution of these rocks displays no particular pattern. They are tabular in form and often flat lying. The smaller bodies, and those which are a common associate of asbestos deposits, are normally

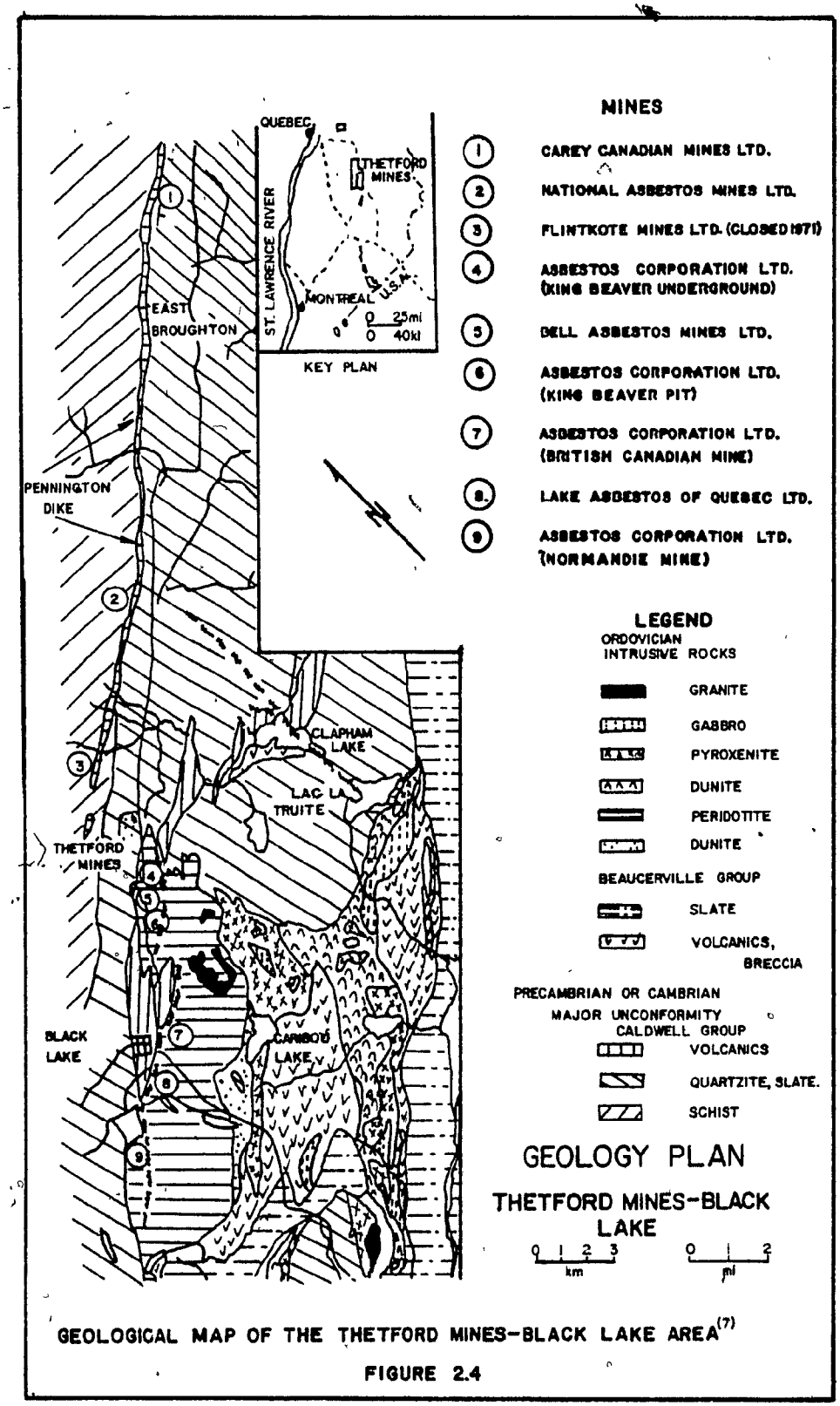


GEOLOGICAL MAP OF THE THETFORD MINES-BLACK LAKE AREA[7]

FIGURE 2.4

syenitic in composition and composed predominantly of albite with a variable content of orthoclase and biotite. They are frequently highly altered. Contacts between the acidic intrusives and ultrabasic rocks are commonly sharp.

The acidic rocks do not appear to be associated with any of the major persistent shear zones, but had a tendency to localise shearing in the host rocks in their immediate vicinity. The acidic rocks were intruded soon after the emplacement of the ultrabasic to basic rocks.

The granite and syenite do not intrude one another. The larger bodies are granitic, and the syenitic dykes were derived from them. Loss of unsaturated silica through reaction with partially serpentinized ultrabasic rocks produced the completely serpentinized aureoles surrounding these acid intrusives. Talc and tremolite are often associated with the margins of these dykes.

2.3.3 Alteration:

The peridotite, which is host to the asbestos deposits, was subjected to a pervasive type of serpentinization that affected the whole body of rock in a fairly uniform manner to the extent that

it contains on the average, from 30% to 40% serpentine. Complete serpentinization of this rock is to be found in association with aureoles that surround the acidic intrusives, and the shatter zones, faults, and joints.

The small dunite segregations, and most of the belt along the southeast side of the peridotite are completely serpentinized. The dunite associated with the pyroxenite is completely serpentinized, but in the pyroxenite serpentinization has been largely confined to the minor olivine and rhombic pyroxenes.

Following the intrusion of granite and syenite, which effectively serpentinized the adjacent wall-rock, major adjustements provided an abundance of openings through which solutions gained access to broad zones of shearing and shattering, and thus caused widespread serpentinization.

The magnetite which is a by-product of serpentinization, tended to concentrate along the larger fractures and is thus a common constituent of asbestos veins and the immediate wallrock.

A final stage of hydrothermal alteration resulted in the formation of steatite and a mixture of

carbonate and quartz. This type of alteration has been confined for the most part to major shear zones, and to some extent has given rise to the replacement of asbestos or other types of serpentine veins.

2.3.4 Structure:

Adjustments which followed the emplacement of the intrusive rocks resulted in considerable fracturing and shearing of the ultrabasic rocks, mainly along margins, and sometimes as oblique and cross-faults. Brecciation occurred under certain favourable conditions and provided the channels through which solutions rising along these zones might spread out into the surrounding rocks. These structural conditions were necessary to the formation of the stockwork of veins which constitute an asbestos deposit.

The aureoles of serpentinized rock which surrounded syenitic bodies behaved as incompetent masses within which considerable shearing occurred and around which fracturing of the more competent peridotite took place. Bodies of serpentinized dunite had a similar influence, and had a tendency to fail by shearing or flowage, whereas a complex network of fractures developed in the surrounding peridotite. The contact zones of the syenite are normally barren, and dunite

bodies are commonly barren or carry only small amounts of asbestos, although some dunite may be found to contain good quantities of asbestos, and where the serpentinized aureole enveloping the syenite intrusive is thin, asbestos veins may lie close to the contact.

The faults in the peridotite appear to take the form of shatter zones. Within the zone, the rock is composed of slickenside fragments from the size of small scales up to blocks of several feet in length.

Structural conditions have played an important role in localizing the asbestos deposits, which occur adjacent to major shatter zones beyond immediate areas within which fracturing has been intense. Those deposits that lie adjacent to the contact of the peridotite and the country rocks are commonly associated with pronounced rolls in the contact. Those which lie within the narrow, sill-like bodies of peridotite, occur where there is a local pronounced widening of the intrusive. Most of these bodies are heavily sheared. The other contributing factors are the presence of syenitic and sometimes granitic intrusives, or bodies of dunite.

Most of the deposits that occur within an intrusive whose breadth is appreciably greater than that of the deposit, lie close to the country rock contact. On the other hand, in the orebodies at Black Lake the presence of a strong persistent fault zone is the most important structural requsite. The orebody on the east side of Black Lake lies on the hanging wall side of a strong transverse fault zone.

A relatively impervious cover that tends to hold back the rising solutions may be an important condition.

2.3.5 Genesis of Asbestos Veins:

Most of the asbestos veins are of the cross-fibre variety, and range up to 4 inches in width, although the majority are under 1/2 inch. The veins are in the form of minute lenses or up to several tens of feet in length, and often intersect or branch. Their colour is normally that of the wall-rock serpentine or some lighter shade. The fibres are parallel and occupy any position between normal and parallel to the vein. They may be straight, curved, or crenellated. One or more partings may be present in the vein. Abundant magnetite often occurs along the partings, as well as along the vein margins. At the intersection of veins the fibre directions of both veins

may coalesce or there may be a mixture of magnetite, serpentine, and asbestos. Cross-cutting veins are extremely rare. Asbestos veins may grade into picrolite veins or terminate abruptly.

The origin of the cross-fibre asbestos has been attributed to either growth of fibres in open fractures, growth from one or both walls of a fracture as these drew apart, or to a process of crystallization within one or both walls of the fracture. There seems to be good evidence, however, that both fissure-filling and wall-rock replacement has occurred.

Final stages of stress relief produced some slip fibre.

## 2.4 Pennington Dyke[6][7]:

Two deposits are presently being mined along the Dyke. The deposit owned by Lake Asbestos Mines Limited is located 4 miles northeast of the city of Thetford Mines. The deposit mined by Carey-Canadian comprises at least four miles of the northeast end of the Dyke.

The Pennington Dyke is on the southeast limb of an anticline in the Caldwell series at or near the

contact between the Bennett schist and L'Islet formation. It has a lenticular structure with thickness varying from 10 feet to several hundred and is generally conformable with the enclosing Bennett schists which are crumpled and dragfolded. It exhibits wide variation in dip from place to place. The average dip is 60 degrees near Thetford, 40 degrees at Quebec Asbestos, and 30 degrees at Carey-Canadian. All dips are to the southeast. The structure varies from massive to schistose and appears to be a function of the average dip and thickness.

The massive serpentine composing it varies in colour from light to dark green and has an irregular to conchoidal fracture. The schistose material varies from light yellowish green to brown, with a greasy or soapy appearance.

Near Thetford, wide portions of the dyke are predominantly massive with only a narrow zone of schistose material on the footwall side. Near East Broughton, the wide portions are predominantly schistose with a zone of massive material on the hanging wall and intervening narrow sections of schist or gauge. At Carey-Canadian, the wide portions are schistose with a zone of gauge up to 25 feet thick on the footwall.

The dyke was probably peridotite, but all traces of the original minerals have been obliterated, and their places taken by serpentine talc, picrolite, brucite, chrysotile, carbonate, and magnetite.

The asbestos is generally classed as slip fibre, but it also occurs in cross-fibre veins and as mass fibre. Slip fibre occurs along slip planes in the serpentine schist, and varies in length from a fraction of an inch to several inches. The cross-fibre veins are found in fractures in the massive serpentine. The mass fibre occurs in the interior of lenses of the fish-scale material.

Picrolite occurs along the hanging wall and footwall contacts. White fibrous brucite in sheaves of resilient fibres occasionally occurs along slip planes along with chrysotile. The talc content of the dyke is variable.

The magnetite occurs in granular form disseminated through the serpentine of the asbestos zones, along partings in cross-fibre veins, and in fibrous forms parallel with and disseminated through masses of slip fibre.

The carbonate occurs in massive form and as fibrous intergrowths with chrysotile.

The formation of asbestos in the Pennington dyke is attributed to dynamic metamorphism (Figs. 2.3, 2.4).

## 2.5 Thetford Mines Deposits[2][7]:

Thetford Mines is situated near the northeast extremity of a large peridotite mass which extends southwestward for some 15 miles (Figs. 2.3, 2.4).

The peridotite host rock is almost completely serpentinized. It orginally contained about 15% enstatite which has been altered to bastite or antigorite. Segregations of dunite occur throughout the ore zone, and are completely serpentinized, and are of irregular shape with no apparent pattern of distribution. Within the orebodies, the dunite bodies are usually small, whereas large bodies are often encountered on the fringes (Figs. 2.5 through 2.10).

There are numerous syenitic bodies associated with the deposits. These are distributed throughout the area, but are usually confined to those portions of the ultrabasic rock mass which have undergone complete serpentinization. They occur both within and outside of the orebody, and are more numerous within the ore zone.

The only granite in the vicinity lies just outside the ore zone to the southeast of the Beaver No.1 orebody.

The near-surface rock and much of the rock mass lying between the ore zone and the country rock contact to the northeast is only partially serpentinized.

The intrusion of small syenitic bodies caused complete serpentinization of the enclosing peridotite in their immediate vicinity. A later, more intensive stage of alteration which worked outward from the existing fractures resulted in much of the rock being completely serpentinized and gave rise to the formation of asbestos veins.

Subsequent to this last stage of serpentinization, there was another period of metasomatism. This talc-carbonate alteration is confined to the ground lying along the southeast side of the deposit, and has affected a zone ranging in width from 50 feet up to 700 feet. This alteration zone has been traced for more than 2 1/2 miles. The zone as a whole dips northwest at from 55 to 60 degrees (Fig. 2.6).

The talc-carbonate zone marks the presence of a pronounced zone of thrust faulting. To the southeast of the zone and between it and the ore zone, the peridotite is heavily sheared. The Thetford deposits lie along the northwest or hanging wall side of the zone. The other zones of shearing or shattering are subsidiary to the major thrust zone, and either dip

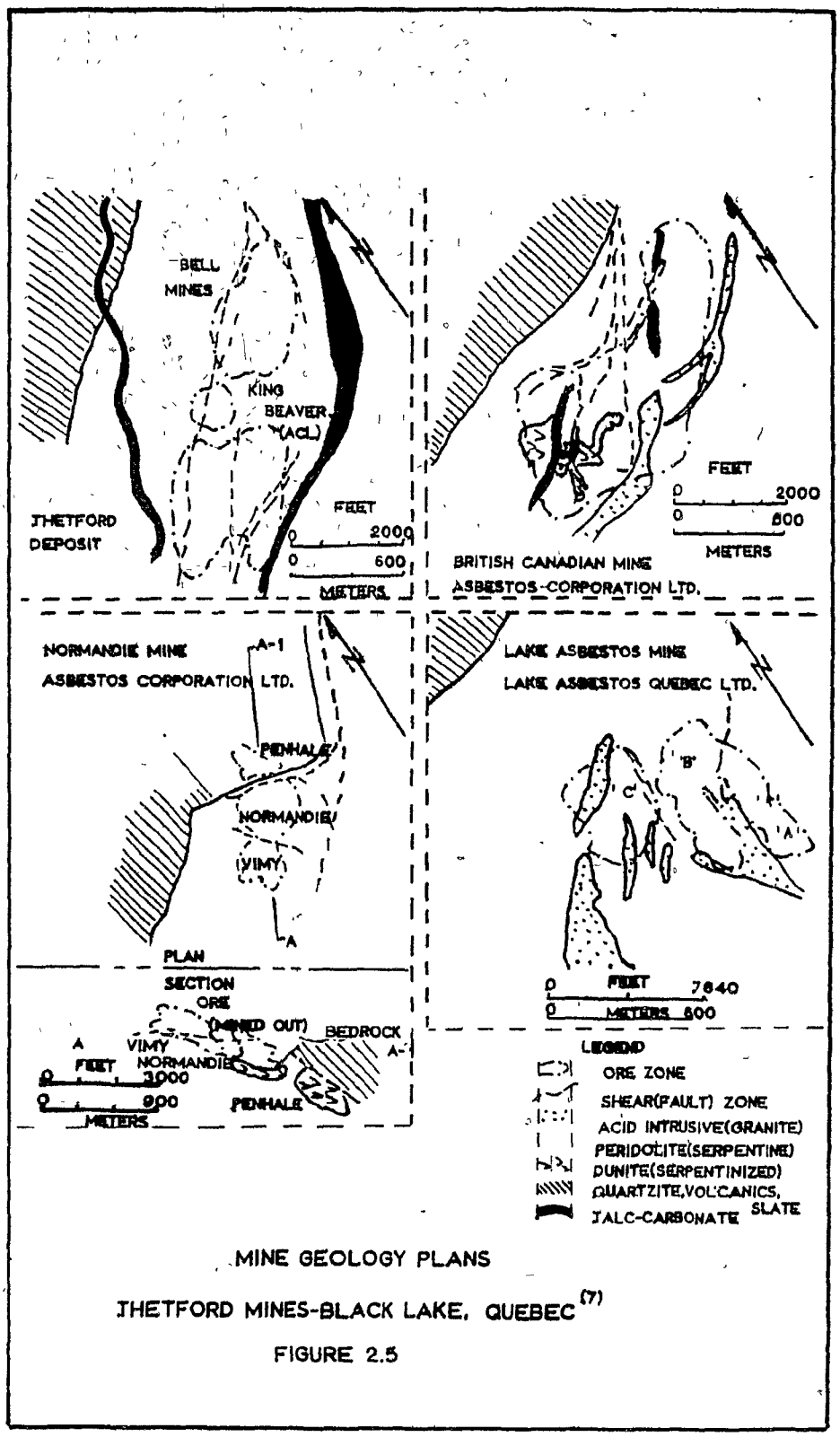


MINE GEOLOGY PLANS

THETFORD MINES-BLACK LAKE, QUEBEC [7]

FIGURE 2.5

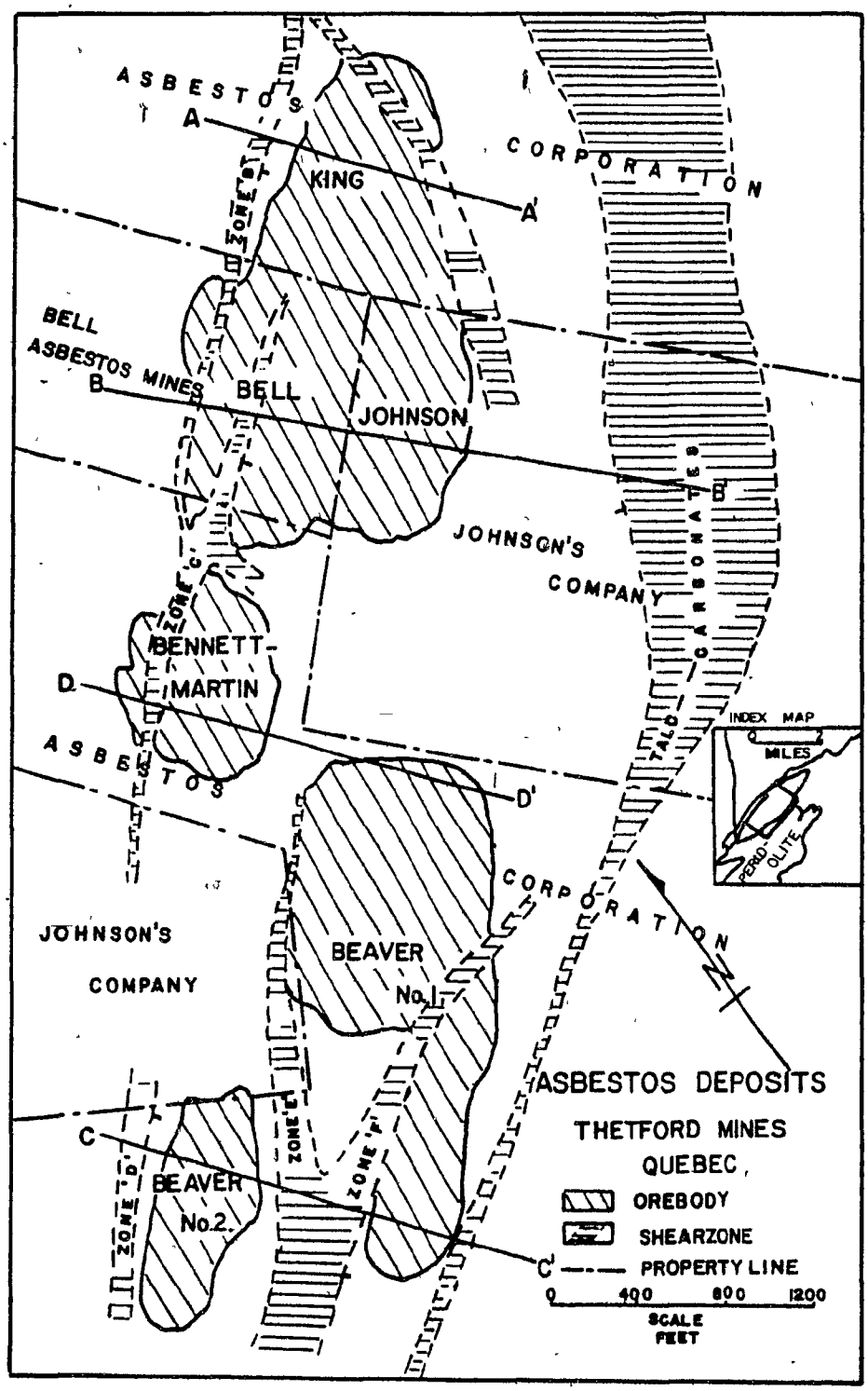


MAP OF ASBESTOS DEPOSITS IN THETFORD MINES, QUEBEC SHOWING THE RELATIONSHIP OF SHEAR ZONES AND TALC-CARBONATE OR THETFORD FAULT ZONE, TO THE DEPOSITS(2)

FIGURE 2.6

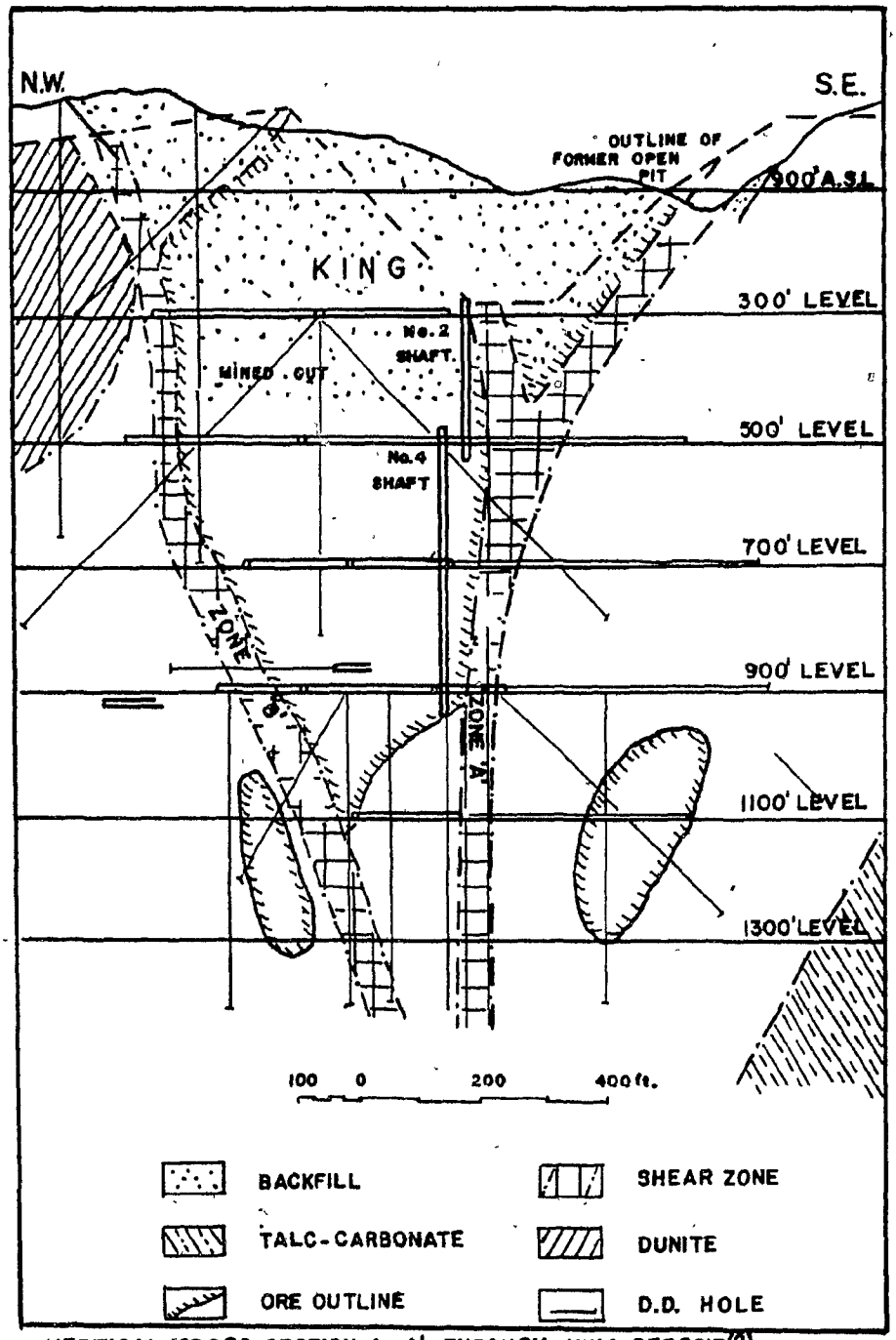


VERTICAL CROSS SECTION A-A' THROUGH KING DEPOSIT(2)

FIGURE 2.7

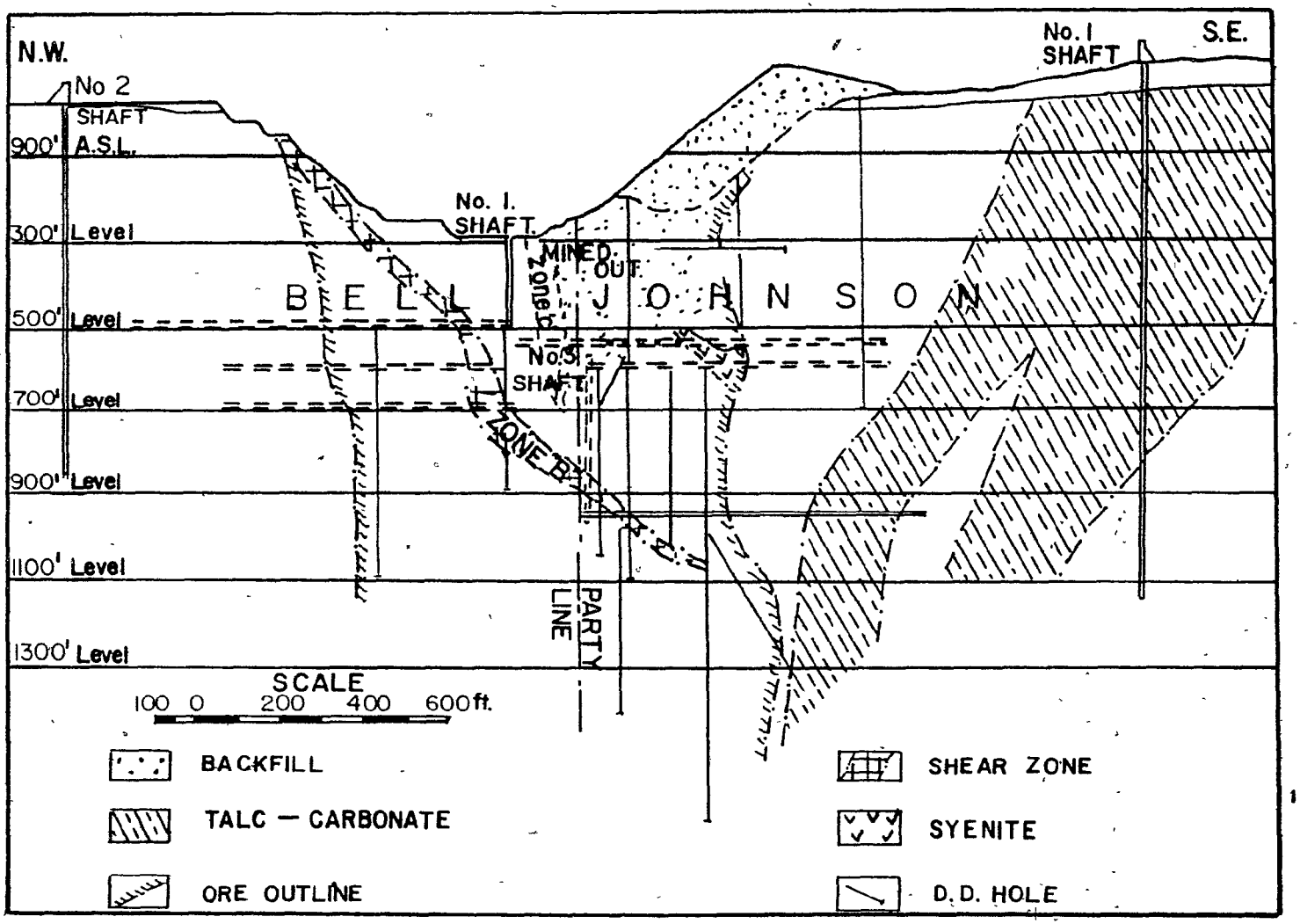


VERTICAL CROSS-SECTION B–B' THROUGH THE BELL-JOHNSON DEPOSIT(2)

FIGURE 2.8

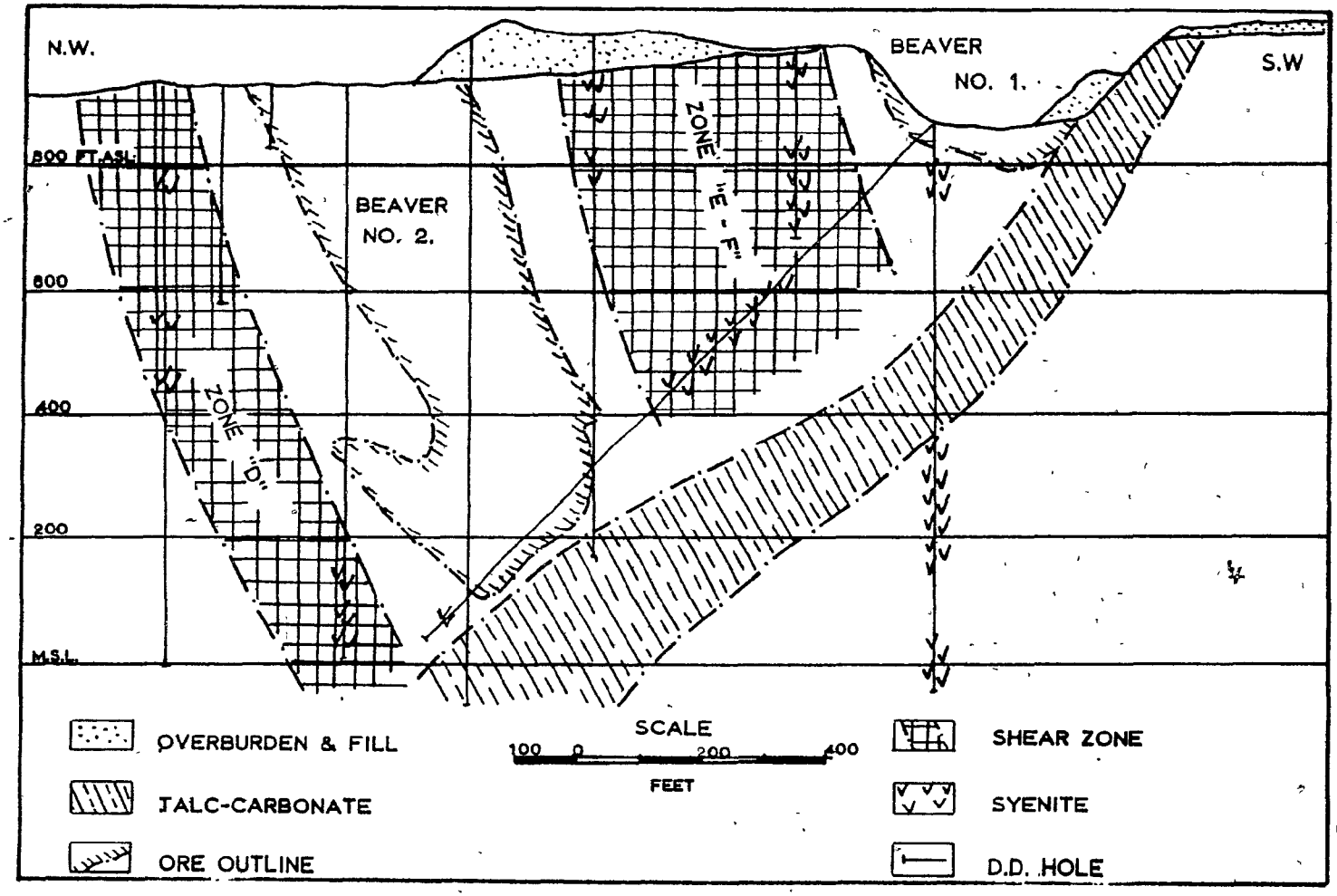


VERTICAL CROSS-SECTION C-C'. THROUGH BEAVER NO.1 AND BEAVER. NO.2. DEPOSITS.[2]

FIGURE 2.9

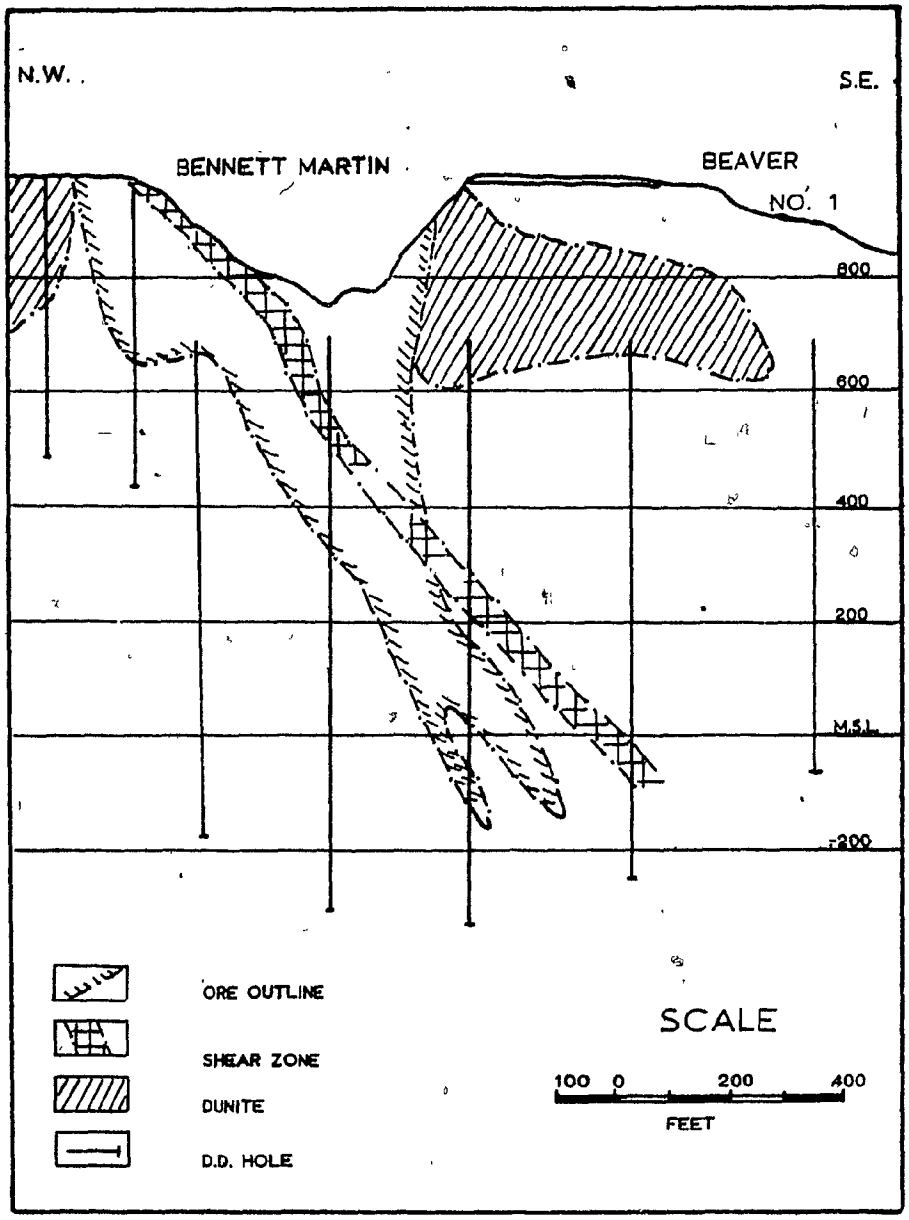


VERTICAL CROSS-SECTION D-D' THROUGH BENNETT-MARTIN DEPOSIT[2]

FIGURE 2.10

toward the southeast or are nearly vertical. Syenite bodies tended to localize shearing to their immediate vicinity, and their distribution and form are irregular, the shatter zones likewise display irregularity. Some parts of these shear zones lie along the margins of orebodies and tend to roughly define their limits, while some cut across orebodies and tend to produce barren belts (Figs. 2.5 through 2.10).

The Thetford orebodies are oblong in plan, with long axis roughly parallel to the axis of the ore zone proper. Their sides have steep dips and generally tend to converge downward. The asbestos ore is concentrated along a strike length of some 6000 feet, a width of 1500 feet, and in certain areas a depth exceeding 1000 feet (Figs. 2.5 through 2.10).

All of the Thetford orebodies are made up of stockwork of cross-fibre asbestos veins ranging in width from a hairline to 4 inches. Appreciable amounts of slip-fibre are recovered and in some portions of the deposit this variety may predominate. The majority of the asbestos veins is under 3/8 inch wide.

The content of asbestos within the deposit is highly variable, locally as high as 25%, but on average around 5 to 7%.

## 2.6 The British-Canadian Mine[3][7]:

This deposit is one of the largest in the Thetford-Black Lake area, and it lies immediately northeast of the town of Black Lake. The orebody occupies an area about a mile in length, by a half a mile in width, and has vertical depth of 1000 feet.

The deposit, as a whole, has a major axis which strikes roughly parallel to the peridotite-country rock contact which lies some 500 to 1000 feet to the northwest of the outcrop of the ore zone (Figs. 2.3, 2.4, 2.11).

The host rock is a harzburgite containing 10% to 15% enstatite. It has been uniformly altered as a result of autometasomatism and contains 30% to 40% serpentine. In shear zones and adjacent to these and acidic intrusives, the rock has been completely serpentinized. Adjacent to asbestos veins serpentinization is complete to distances several times the width of the vein.

Numerous irregularly shaped bodies of dunite are present and the largest of these has a length of 1600 feet and a maximum width of 800 feet. The dunite bodies, which are for the most part completely serpentinized, trend roughly transverse to

the major axis of the ore zone (Fig. 2.11).

Syenite dykes are also numerous. The largest of these may be traced for nearly a mile and reaches widths of 400 feet. All the major dykes strike roughly northeast and have dips from nearly vertical to flat (Fig. 2.11).

A pronounced fault is believed to lie along the contact between the country rocks and the peridotite. Within the orebody itself the numerous shear zones and dykes strike southwest and either fade out in this direction or continue in a more westerly trend. The close proximity of the ore zone to the contact has had a major controlling influence.

Faulting has occurred at almost all of the syenite dykes contacts, and the dykes themselves are often shattered or even sheared, particularly where they are narrow or small. The ultrabasic rock mass is broken into blocks by numerous faults and joints, and some of these fractures extend into the dykes.

The orebody is broad in plan and relatively shallow in depth. The various shear zones and syenite dykes have resulted in the main body of ore being split up into series of lenticular shoots. The overall grade runs between 2% and 3%, but there is a wide range within the deposit. The "fresh" peridotite

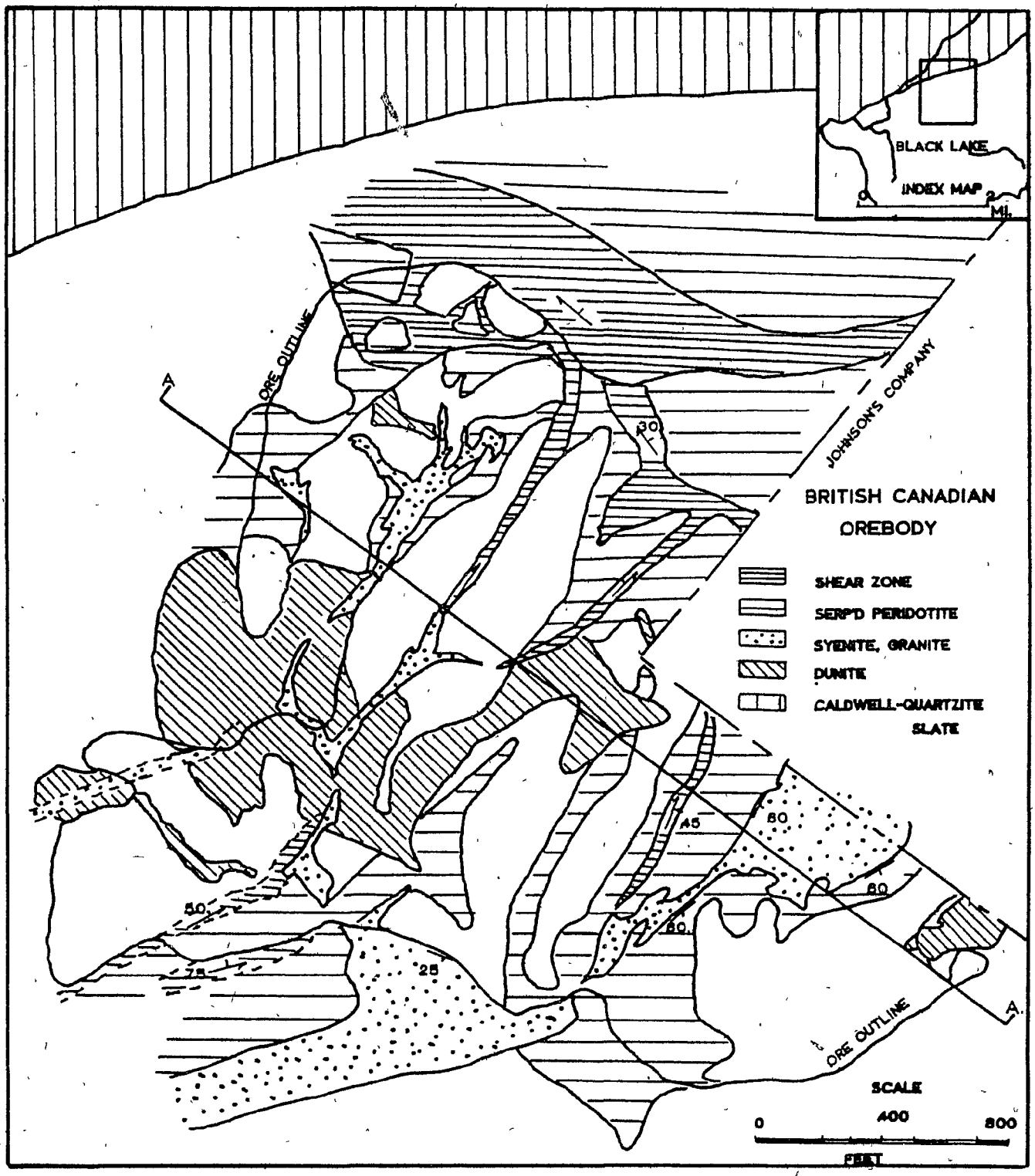
BLACK LAKE
INDEX MAP
0
2
Mi.
ORE OUTLINE
A
30
JOHNSON'S COMPANY
BRITISH CANADIAN
OREBODY
SHEAR ZONE
SERP'D PERIDOTITE
SYENITE, GRANITE
DUNITE
CALDWELL-QUARTZITE
SLATE
45
60
60
60
50
75
25
ORE OUTLINE
A
SCALE
0
400
800
FEET

FIGURE 2.11[3]

normally carries the high-grade ore shoots, which not only contain a higher percentage of fibre, but also larger veins. The serpentinized peridotite is generally low grade or barren, and carries, for the most part, only small lenticular veins and a certain amount of slip fibre. The shear zones are generally barren or contain only modest amounts of short cross-fibre and some slip fibre.

## 2.7 Lake Asbestos of Quebec Mine[7]:

The Lake Asbestos orebodies lie under the area formerly occupied by Black Lake, about a half mile south of the main peridotite-quartzite contact (Figs. 2.3, 2.4).

The host rock consists mainly of serpentinized peridotite still containing remnants of the original pyroxene. This results in a coarse-grained, mottled texture. At the western zone, the rock is more serpentinized. In the "c" pit, where generally shorter fibre occurs, the rock has been altered by granite dykes and sills. It consists mostly of dark green or black serpentine, glassy in texture.

The most prominent structural feature within this property is the talc-carbonate zone separating the "A" and "B" pits. The footwall of the mining

operations on the southwest limit of "B" pit could be a subsidiary of the main faulted talc-carbonate zone. The talc-carbonate is commonly highly foliated with intercalated bands of acidic material. The second most prominent structure is the series of granite and syenite dykes located on the west side and north side of the property. They have a predominant 30 to 60 degree northeastern strike, and dip to the northwest.

Within the present open pit limits at Lake Asbestos, there are three major ore zones, referred to as "A", "B", and "C". The main orebody is the "B", or central deposit. It is over 2000 feet long, up to 900 feet wide, and reaches a depth exceeding 1000 feet. It strikes north-northeast and plunges at 30 degrees in the same direction while dipping to the east. The bulk of the ore lies at depth, resulting in high waste-to-ore ratio.

Asbestos occurs predominantly as cross-fibre in joints and fractures within zones of moderate fracturing. A small amount of slip fibre is found in highly sheared areas. The ore averages approximately 4% chrysotile asbestos, varying in length from veinlets 1 1/4 inches, with most fibres in the 1/8 to 3/8 inch range.

## 2.8 The Vimy, Normandie, and Penhale Deposits[4][7]:

These deposits are located close to the village of Vimy Ridge and 2 miles west of Black Lake, and lie immediately adjacent to or below the peridotite-quartzite contact. The Vimy deposit is now mined out. The Normandie is presently being mined while mining has not been accomplished to date from the Penhale deposit. The Normandie deposit contains about 40 million tons of ore (Figs. 2.3, 2.4).

The host rock is peridotite containing 10 to 15% pyroxene, uniformly replaced by 30 to 40% serpentine. A few lenticular bodies of completely serpentinized dunite are scattered through the ore zone.

A granite dyke, having the composition of an alaskite, lies a few hundred feet southwest of the deposits. Numerous small lenticular bodies of syenite occur within the ore zone but are confined to the margins of the ore bodies.

Serpentinization of the peridotite is complete adjacent to the acidic intrusives and to the various shear zones with which the deposits are associated. Complete serpentinization of the rock adjacent to asbestos veins has occured to distances equivalent to 2 or 3 times the width of any one vein. Wherever

veins are numerous and sufficiently closely spaced, the entire rock has been converted to serpentine.

Talc is a common alteration product in the contact zones of the syenitic intrusives, with termolite and chlorite occasionally present immediately adjacent to the contact.

The deposits are situated at a pronounced roll in the ultrabasic intrusive-caldwell rock contact (Fig. 2.12).

The roof of the peridotite intrusive immediately northeast of the deposit dips at about 30 degrees and elsewhere the contact is probably relatively steeply dipping. The sharp bends in the contact may be due either to the presence of an anticlinal fold in the country rocks, with its axis striking northeast and plunging flatly in the same direction or to a flat northeast dipping fault. A fault zone, The Vimy Ridge fault, is present along the south-east side of the ore zone (Fig. 2.12). Two other major shear zones are present, both of which trend northwestwards the contact shear zone dipping flatly to the north between the country rocks and the Normandie deposit, and the intermediate shear zone forming a thick, nearly vertical wall of separation

between the Vimy and the Normandie deposits (Fig. 2.13).

The orebodies lie in a zone whose axis strikes northeast with a rake of about 25 degrees. A unique feature of the deposits is the occurence of ribbon-veins, in which a larger vein is frequently paralleled by numerous asbestos veins of smaller size. The veins commonly dip flatly to the north or northeast and give the orebodies a laminated structure.

The prevalent vein attitude throughout the orebodies has northerly dips close to 20 degrees and strikes which range from east-west to south of east. The rake of the ore zone (25 degrees) conforms very closely to the dip (20 degrees) of the prevalent vein system, and is only slightly flatter than the observed dip of the Caldwell contact.

The ore deposits lie immediately adjacent to the northwest contact of the intrusive, and at the junction of several major fault zones. The adjacent and intervening ground was broken up by a system of minor subsidiary faults, and all of these contributed to the circulation of the siliceous hydrothermal solutions which gave rise to serpentinization and

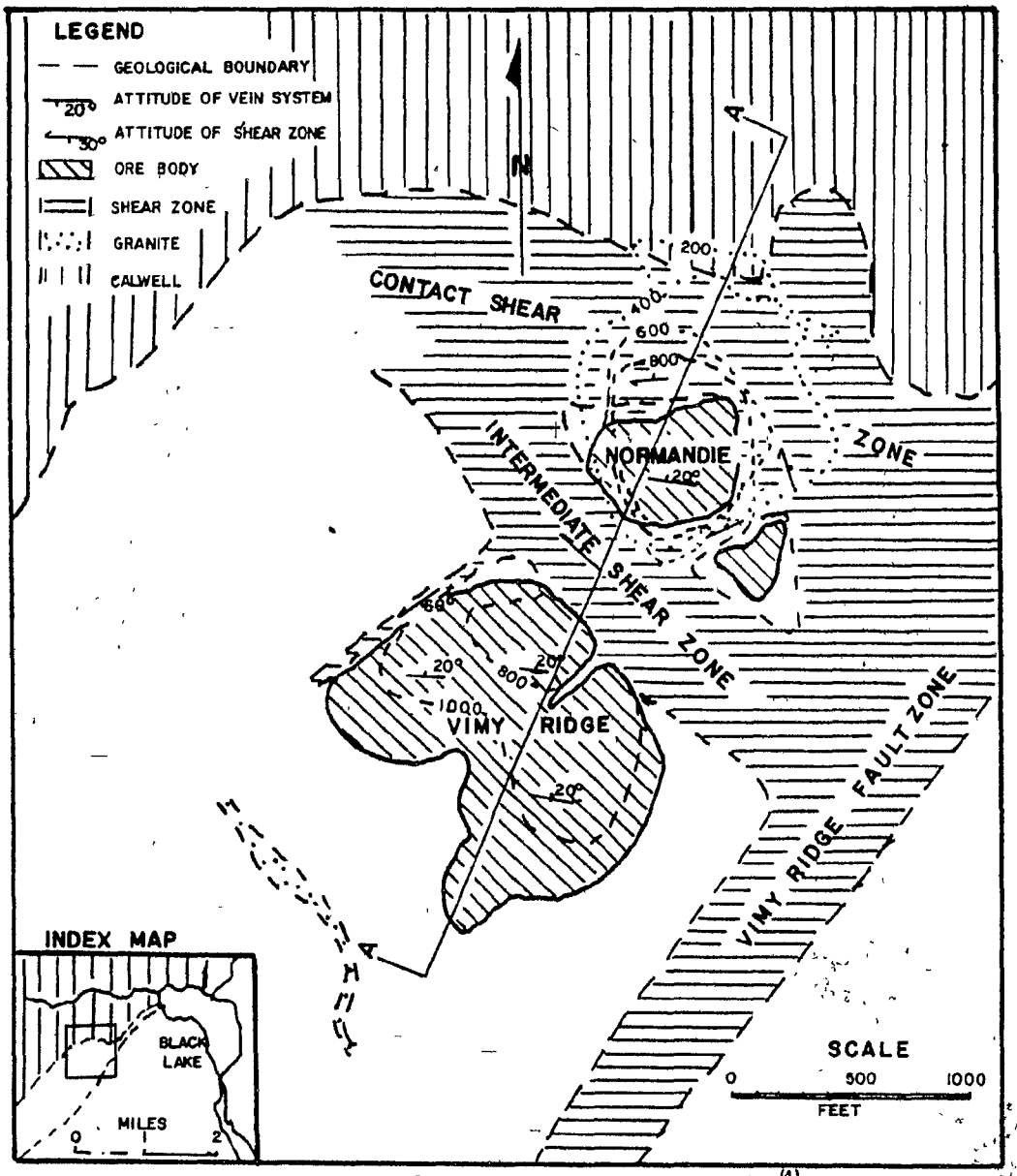


GEOLOGICAL MAP OF VIMY RIDGE AND NORMANDIE DEPOSITS[4]

FIGURE 2.12

the accompanying vein formation.

The chief distinction between the three deposits is in the quality of the fibre. The Vimy fibre is the harshest variety recovered anywhere in the belt, whereas the Normandie fibre, though harsher than Thetford fibre, is noticeably less harsh than in Vimy. The Penhale fibre is even softer than that in the Normandie.

## 2.9 The Jeffrey Mine Regional and Local Geology[5][7][8]:

The igneous complex in the vicinity of the Jeffrey Mine is composed of ultramafic and gabbroic rocks, intrusive dykes of granitic to dioritic composition and a suite of andesitic to mafic volcanic rocks. These igneous rocks are part of a giant ophiolitic complex of lower ordovician age (Fig. 2.3).

The ultramafic rocks of this ophiolitic complex rest uncomformably on metasedimentary rocks of the Caldwell group of Cambro-lower Ordovician age.

The Jeffrey orebody occurs in highly serpentinized peridotite, adjacent to the Caldwell metasediments. This peridotite is followed to the southeast by a wide zone of barren dunite, also highly serpentinized, inwhich lenses or concentrations of pyroxenite have been formed by differentiation. Pyroxenite is also

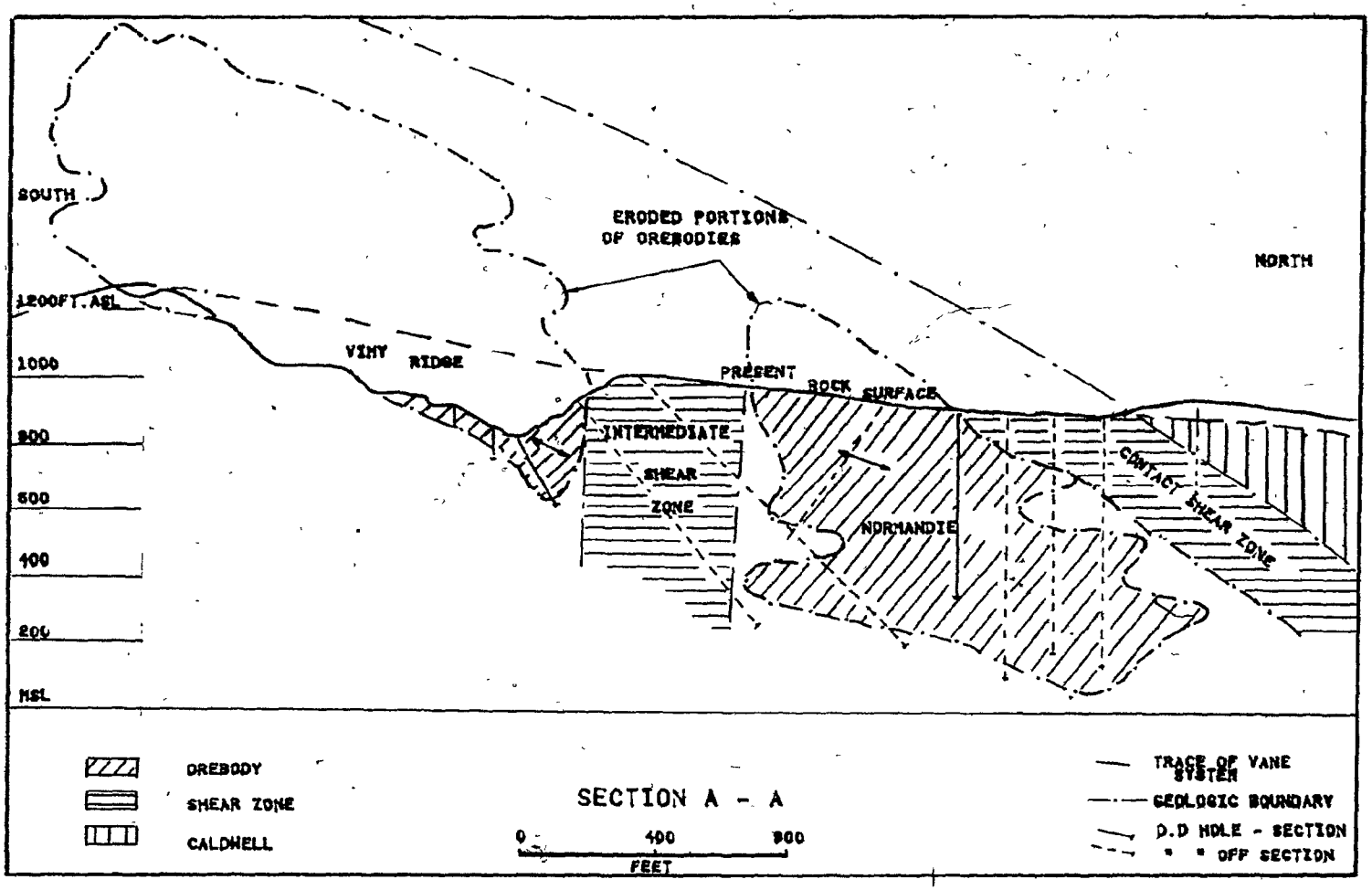


VERTICAL CROSS-SECTION A-A THROUGH THE VIMY RIDGE AND NORMANDIE DEPOSITES[4]

FIGURE 2.13

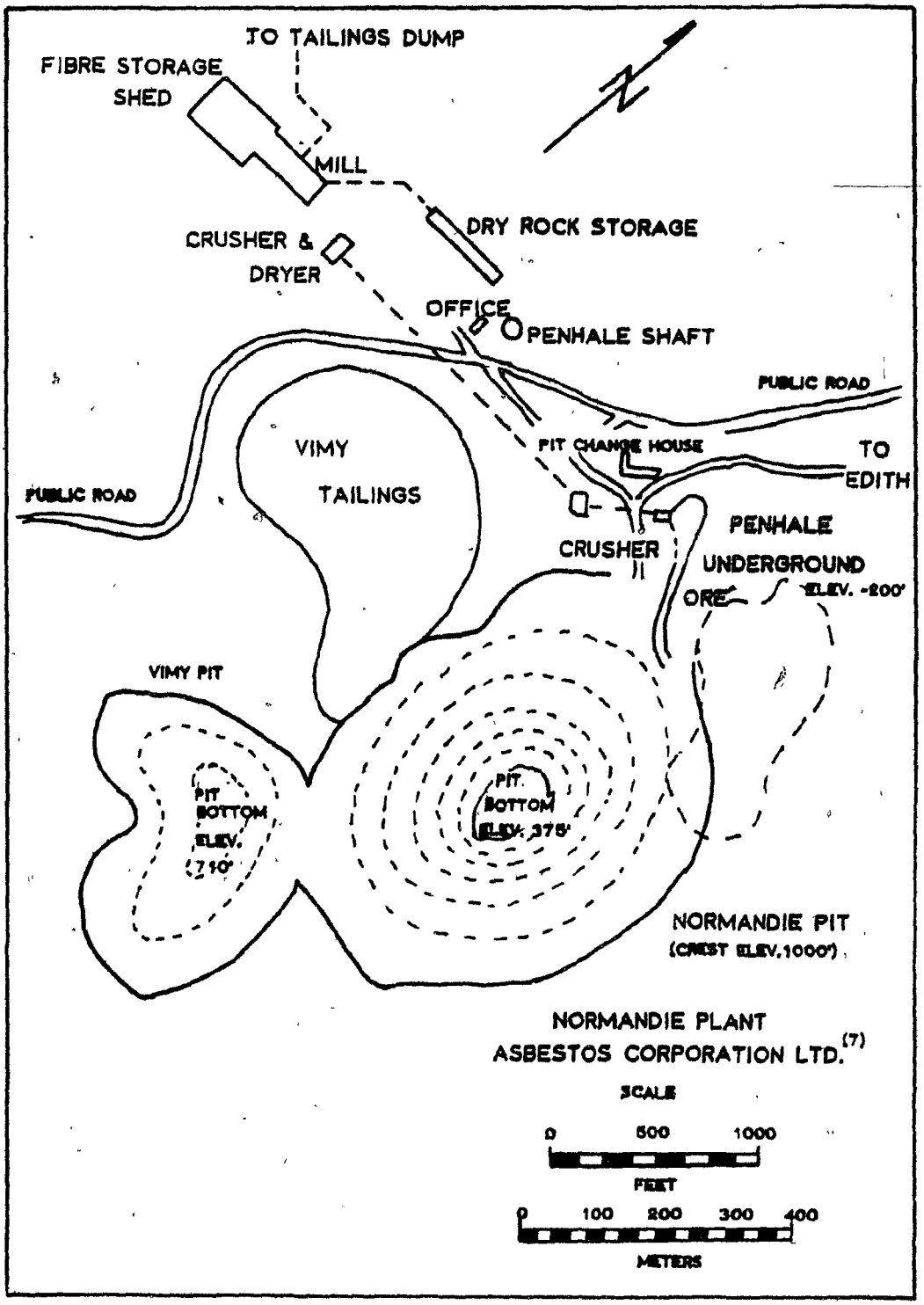
TO TAILINGS DUMP
FIBRE STORAGE SHED
MILL
DRY ROCK STORAGE
CRUSHER & DRYER
OFFICE
PENHALE SHAFT
PUBLIC ROAD
VIMY TAILINGS
PIT CHANGE HOUSE
TO EDITH
PUBLIC ROAD
CRUSHER
PENHALE UNDERGROUND ORE
ELEV. -200'
VIMY PIT
PIT BOTTOM ELEV. 710'
PIT BOTTOM ELEV. 378'
NORMANDIE PIT
(CREST ELEV. 1000')
NORMANDIE PLANT
ASBESTOS CORPORATION LTD.(7)
SCALE
0 500 1000
FEET
0 100 200 300 400
METERS

FIGURE 2.14(7)

present in the upper part of the ultramafic section of this complex and grades into gabbro.

The roof of the ophiolitic complex is formed by brecciated and pillowed volcanics, conformably overlain by the St. Daniel sedimentary rocks, mainly a wildflysch-type shale of pre-normanskill age. Resting on the St. Daniel formation is a thick sedimentary sequence belonging to the middle Ordovician Beauceville formation.

The Caldwell group comprises sedimentary rocks and some amphibolite, and occurs on the northwest side of the ophiolitic complex. Northward from the contact, the succession is black and greenish slate and phyllite, impure quartz and metagreywacke. The beds strike about 60 degrees east of north with an average dip of 55 degrees southeast.

All the igneous rocks in the Jeffrey Mine area belong to the ophiolitic complex.

Serpentinized peridotite is the host rock for the Jeffrey orebody and now occupies the footwall section of the ultramafic rock. It is approximately 2000 feet wide and terminated at the southeast and southwest by a zone of intense shearing. It is normally green to greyish in colour, acquiring a brownish

tint in the central portion of the orebody. It is commonly flecked with small, irregular black patches of fine-grained magnetite. The original peridotite probably contained 10% pyroxene as suggested by the number of bastite crystals and pyroxene remnants.

The second major ultramafic rock type in the Jeffrey Mine area is a highly serpentinized dunite. It is located to the southeast of the peridotite, and occupies a width of some 2400 feet. The contact between the peridotite and dunite is gradational over a distance of several hundred feet on both sides of a major shear zone. The dunite is dense, medium to fine-grained, and dark green to olive green in colour. Two other types of dunite occur in the Jeffrey pit. One is fine-grained, grayish in colour, contains lenses of chromite, and occurs in association with sheared rock. The other is highly serpentinized, brownish in colour, and is found near the northwest contact.

Pyroxenite is found in irregular lenses within the serpentinized dunite and also as a band which extends more or less continuously along its southeastern limit. It is coarse-grained, with unoriented subhedral crystals of augite and some chlorite alteration. The degree of serpentinization varies mainly with

the location with respect to dunite. Fresh surfaces are light or gray-green, but weather rapidly to a dark brown or gray. The contacts of the pyroxenite and dunite are gradational over a few inches.

Masses of gabbro occur across a width of 100 to 500 feet along the southeast side of the pyroxenite. The gabbro is medium to coarse-grained and is composed of greenish pyroxene with feldspar and, locally, coarse black hornblende.

Numerous highly irregular dyke-like masses of granitic to dioritic rocks are found within the serpentinized peridotite and dunite. Rodingite, a rock composed predominantly of grossular garnet with diopside is also present. The most common variety of dyke rock is a medium to coarse-grained, reddish diorite composed of 60% heavily garnetized and saussuritized plagioclase, and 40% relatively unaltered reddish brown biotite. These dyke-like intrusions are extremely irregular and are generally associated with shear zones.

The upper part of the ophiolitic complex is composed of volcanic rocks consisting of intermediate to basic lava flows and breccia, striking 60 degrees east of north with steep dip to the southeast.

The ophiolitic complex is overlain conformably by a sedimentary sequence of the St. Daniel formation. These sediments are essentially black slates, more fissile than the Caldwell and the Beauceville equivalents. The schistosity is vertical and appears to parallel the bedding.

The Beauceville formation outcrops in the Asbestos area as a slate with vertical cleavage and a bedding dipping 75 degrees to the northwest.

Clayey silt and sandy silt of marine origin are the two major types of unconsolidated sediments in the Asbestos area. (Fig. 2.15)

The shape of the Jeffrey orebody resembles an elliptical cylinder raking 60 degrees southeast on the average, and plunging steeply to southwest. In plan the orebody averages 3000 feet long, 2000 feet wide, and strikes 30 degrees east of north. A major shear zone paralleling the slate-phyllite contact, forms the footwall boundary of the ore. A similar structure runs along the southeast and southwest perimeter and seems to wrap the orebody completely on the northwest side. Within the orebody many other structural features, such as shear zones, faults, and slips are present; their shape, size, and dip vary considerably. The direction of these

features generally follows the strike of one of the two main shear zones. Many zones of shattering contain irregular masses of rock of granitic to dioritic composition.

The Jeffrey orebody has been divided into five ore zones, each having its petrological particularities and different grade characteristics. The two zones paralleling the footwall and hanging wall contacts contain the best of the ore in the mine. The most favourable host rock is a highly serpentinized, moderatly to highly fractured peridotite. Shear zones are either barren or poor grade.

The chrysotile occurs normally as a stockwork of cross-fibre veins, although locally it may occur as slip fibre or mass fibre.

Cross-fibre veins consist of tightly packed fibre oriented approximately at right angles to the walls. The majority of veins are narrower than 1/4 mesh and are 3 to 5 feet long, with occasional veins an inch or more wide and up to 30 feet long. Vein intersections are usually indefinite. Many of the veins are composite, and contain a highly irregular central parting composed of serpentine and clusters and veinlets of magnetite. The cross-fibre is commonly of the silky type.

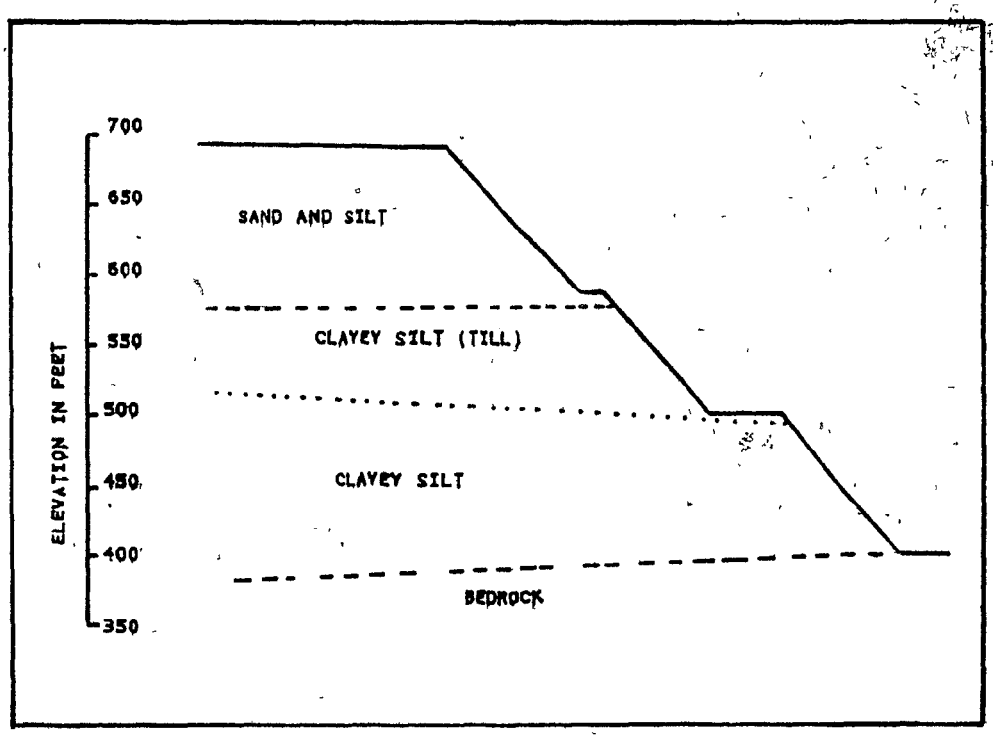


SECTION THROUGH JEFFREY MINE
OVERBURDEN[4]

FIGURE 2.15

Slip fibre is oriented parallel to the vein walls and is more variable in strength than cross-fibre. It is usually accompanied by fibrous brucite.

Mass fibre consists of relatively small, unoriented to semi-oriented bundles of fibre, sparsely disseminated through most of the rock. The largest concentration occurs along the southeast side of the orebody. Some occurences may contain up to 50% chrysotile. Mass fibre is accompanied in places by brucite in small disseminated flakes.

## 2.10 Conclusion:

The formation of chrysotile was a result of two separate metamorphic changes in ultrabasic rock of volcanic origin. The first stage involved the formation of serpentine by the hydrothermal alteration of the original rock. The second stage was the formation of the chrysotile in cracks and fissures in the rock by recrystallization of the serpentine.

The geology of asbestos deposits is relatively well understood, and the structure is similar from deposit to deposit. On the other hand, the actual fibre properties, and the amount and nature of other minerals or "impurities" is very characteristic of a particular deposit. The fibre quality can vary between two orebodies as close as 1,000 feet apart, as exemplified by the Vimy-Normandie-Penhale deposits.

The same statement is true for the magnetite content of Quebec's chrysotile deposits. Because of the variation of magnetite content of a particular deposit from the other, the ferromagnetic characteristic of all Quebec chrysotile asbestos was tested and determined. The detailed ferromagnetic characteristics of Quebec chrysotile are discussed in the future chapters.

## LIST OF REFERENCES FOR CHAPTER II

1. Riordon, P.H., "The Asbestos Belt of Southeastern Quebec". The Geology of Canadian Industrial Mineral Deposits, 6th Comonwealth Mining and Metallurgical Congress, 1957.

2. Riordon, P.H., "The Asbestos Deposits of Thetford Mines, Quebec", 6th., Commonwealth Mining and Metallurgical Congress, 1957.

3. Riordon, P.H., "The British-Canadian Mine", 6th., Commonwealth Mining and Metallurgical Congress, 1957.

4. Riordon, P.H., "Normandie and Vimy Ridge Mines", 6th., Commonwealth Mining and Metallurgical Congress, 1957.

5. Allen, C.C., Gill, J.S., Koski, J.S. et al., "The Jeffrey Mine of Canadian Johns-Manville Co. Ltd.", 6th., Commonwealth Mining and Metallurgical Congress, 1957.

6. Merrill, R.J., "The Carey-Canadian Asbestos Deposit", 6th., Commonwealth Mining and Metallurgical Congress, 1957.

7. Quebec Asbestos Mining Association: "Geological Guide to Asbestos Mining Region of South Eastern Quebec". August, 1972.

8. Trauffer, W.E., "Canadian Johns-Manville's Jeffrey Mine at Asbestos, Quebec", Pit & Quary, pp. 58-64, March, 1974.

9. Moorhouse, W.W., "The Study of Rocks in Thin Section", Harper & Row Publishers, New York and Evanston, 1959, p. 313.

# CHAPTER III

## THE MINING AND MILLING OF CHRYSOTILE ASBESTOS IN QUEBEC

### 3.1 General Review:

As described in the preceeding chapter, the geology of chrysotile asbestos deposits across the province of Quebec shows marked differences, though on the whole, the geological setting is quite similar. The differences present affect the product quality, such as fibre length and impurity content.

The mining and milling processes employed at the various deposits exhibit even less contrast.

Most of the mining operations employ open pit methods. Differences between sites are largely limited to equipment size and number. There is a trend towards the use of larger equipment. Underground mining of chrysotile asbestos is relatively rare, both in Canada and throughout the world. The only fully underground mine in Canada is the Bell Asbestos Mine. In general, as at Bell Asbestos, the mining method used is block caving. Underground mining of chrysotile has the disadvantages of high cost, fibre degradation in handling, difficult environmental control, limited production, and difficult ground support.

The processing of asbestos ore is very similar throughout the industry, or at least it appears to be so. The specific processes used by a particular company are not usually published. This "secrecy" has two reasons. The first is that the basic processes are usually modified to suit the particular type of fibre found in the deposit. Since no two fibre deposits are the same, the processes are not interchangeable. The second reason is competition within the industry. A typical Canadian asbestos milling circuit is shown on figure 3.1.

Primary concentration (all steps before ore enters a dry rock storage bin) is done either at the mine or at the plantsite. It involves crushing down to a size that can be handled by the mill which involves the processing technique of screening and then drying. Some hand sorting can be done at this stage for high grade, long fibre ore.

The run-of-mine ore first passes a large primary crusher, either jaw or gyratory. The gyratory is usually used at larger operations. Then comes a series of three or four secondary cone or gyratory crushers, progressively decreasing in size and setting, and a series of four or five vibrating screens. The "overs" of each screen go to the next crusher, while "throughs"

continue to the next screen. The "overs" of the last screen are usually discarded to the waste dump. These contain little fibre, and it is advantageous to reduce the load on the mill, even if some fibre is lost. The "throughs" of the last screen go to the dryer (rotary or vertical tower). They are then stockpiled. The stockpiles are usually large enough so that smooth feed flow to the mill can be maintained, and sometimes grade blending is done at this stage.

In the mill proper, the first step is to separate the fibres from the rock. This is also done in a series of stages. The feed is crushed, usually in hammer mills. This releases the fibre from rock, and at the same time teases it out or "fluffs" it. Thus the fibre acquires an effectively lower specific gravity than the rock. The fibre is then aspirated out of the rock stream, while the stream passes over a screen. The fines and rejected rock continue to the succeeding stage, and the rejected rock eventually goes to the tailing dump. Thus the long fibres are relased first, and successive stages release shorter and shorter fibre. The fibre released by this process contains much rock and dust, and is only crudely separated according to length. It then enters a multiple series of grading and cleaning operations. This is accomplished with a combination of suction and screens, usually trommels

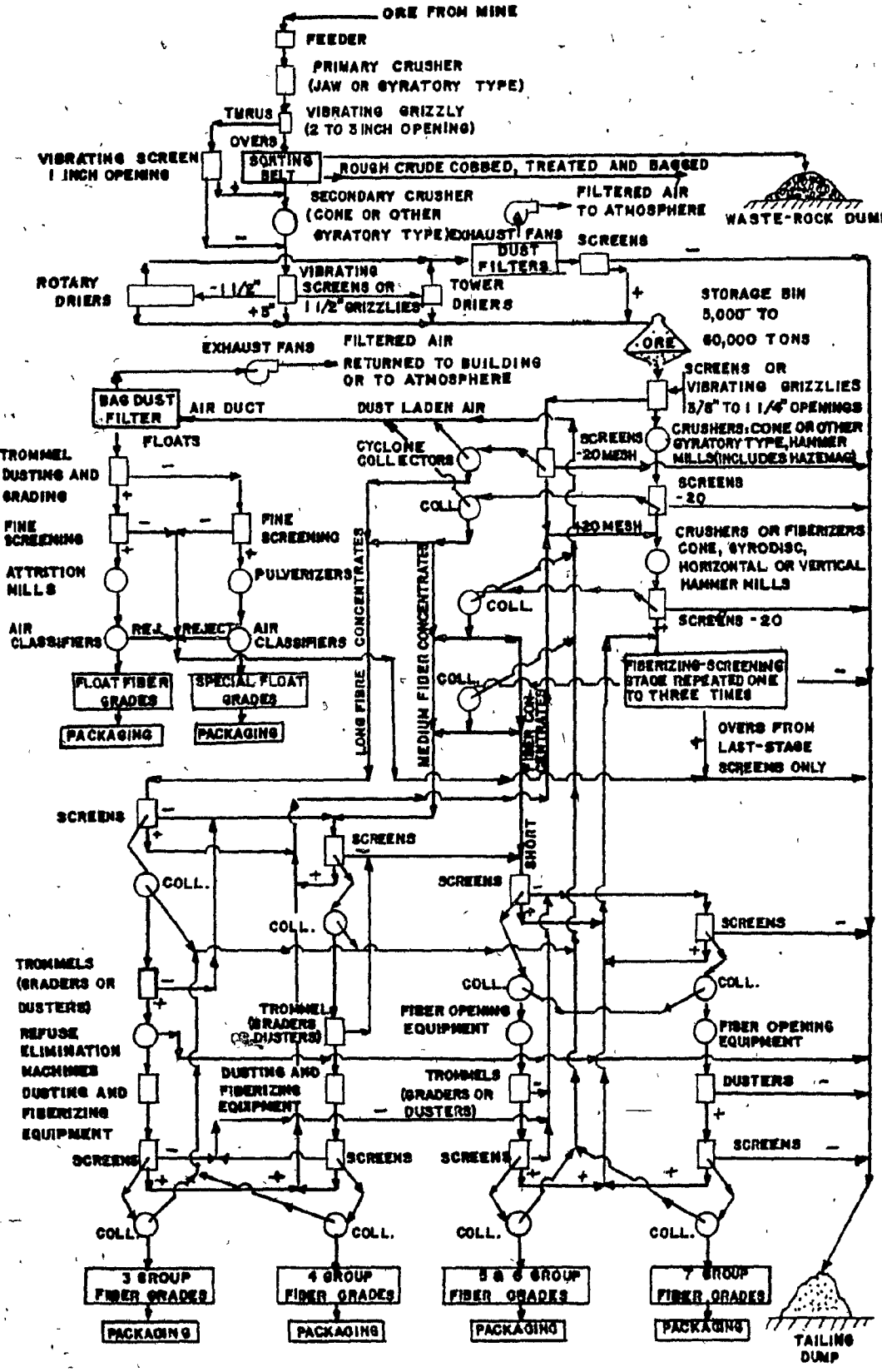


TYPICAL MILLING CIRCUIT IN A CANADIAN ASBESTOS MILL[1]

FIGURE 3,1

or dusters, and graders. Air cyclones are used throughout to remove dust and fibre from air streams. The exhaust air is bag filtered to reduce dust emission.

The finished grades are pressure packed in paper, jute, or nylon bags.

Quebec mine and mill operations are described in the appendix A. A fairly thorough description of the mill at the Jeffrey Mine was available, only partial information was available about most of the other mills, but the basic pattern is the same throughout the industry.

## 3.2 Conclusion:

The mining of asbestos in Quebec is generally open pit method although there are some important differences from one mine to the next due to location and orebody characteristics. Recently, in the mining and milling industry of chrysotile asbestos, there is a general trend towards larger equipment and automation.

The release of the fibre from its host rock is accomplished by successive stages of crushing and screening with air aspiration. A rigid quality control program is essential in every mill to ensure the fibre quality required. The Quebec screen test is the most common method of fibre grading.

There is also a great concern over the environmental and health aspects within the industry. Waste dumps are being revegetated, tailings wetted to suppress particle emission, and, in the mill, larger air volume used and better air filtration are reducing the amount of airborne fibre. Automation is reducing the actual amount of man-hours spent in close association with the dangerous fibre.

At the present production rates, the amount of ore reserves, and the growing demand for asbestos products the chrysotile industry should play a major role in the future of the Canadian economy, as it does in the present.

## LIST OF REFERENCES FOR CHAPTER III

1. The American Institute of Mining, Metallurgical and Petroleum Engineers, "Industrial Minerals and rocks", Third Edition, 1971.

2. Quebec Asbestos Mining Association, "Geological Guide to Asbestos Mining Region of South Eastern Quebec", August, 1972.

3. Carey-Canadian Mines Limited, "Various Pamphlets and Information Brochures".

4. Bell Asbestos Mine, Quebec, "Mining in Canada", October 1967.

5. Trauffer, W.E., "Canadian Johns-Manville's Jeffrey Mine at Asbestos, Quebec". Pit & Quary, pp. 58-64, March, 1974.

## CHAPTER IV

## CANADA'S SHARE IN WORLD PRODUCTION AND THE USES OF ASBESTOS, AND ENVIRONMENTAL PROBLEMS:

### 4.1 General:

According to U.S. Bureau of Mines 1979 statistics 95 per cent of the world asbestos fibre production is Chrysotile. The remaining 5 per cent consisting of about 3.5 per cent Crocidolite, 1.2 per cent Amosite, and 0.3 per cent of other types of asbestos, such as anthophyllite and tremolite. Actinolite is not economically important[1].

As indicated by the world production statistics, chrysotile is the most important variety in demand and therefore most of the data in this chapter relates to chrysotile.

In the free world market, Canada is the leader in chrysotile asbestos fibre production. In 1978 Canada had 58 per cent of the western world market; the Republic of South Africa, 14 per cent; Italy, 6 per cent; and United States, 3 per cent [1]. However, when the total world market production is considered, the U.S.S.R. is the major asbestos producer of the world. Also, the People's Republic of China and Rhodesia have an important contribution to the world asbestos market. U.S.S.R., Canada and the Republic of South Africa combined produce over 82 per cent of the world asbestos output[2] (see Fig. 4.1).

4.2 World Asbestos Industry:

As mentioned above, Canada, with major activity in the Province of Quebec, leads the West in both total quantity produced and the size of individual mines and mills. For example: Canadian Johns-Manville's Jeffery Mine at Asbestos, P. Q. is the largest asbestos producing open pit mine in the world. The asbestos industry of the free-world is largely controlled by American and British corporations. Although Canada is one of the world's major producers of chrysotile asbestos, the industry is largely controlled by the international corporations as indicated by the following examples.

a) At present the Quebec Provincial Government is trying to nationalize the Asbestos Corp. Ltd. (ACL) by purchasing the 54.6 per cent of ACL shares held by General Dynamics Corp. of U.S.A.

b) Canadian Johns-Manville is wholly owned by Johns-Manville Corp of U.S.A. which has many manufacturing plants in the United States and uses large quantities of Canadian chrysotile asbestos as raw material.

c) Turner and Newell, Ltd. of England has mines in the epublic of South Africa and Rhodesia. In Canada it formerly owned Bell Asbestos Mines Ltd. which has a mine at Thetford, P.Q. and a large minority holding in Cassiar

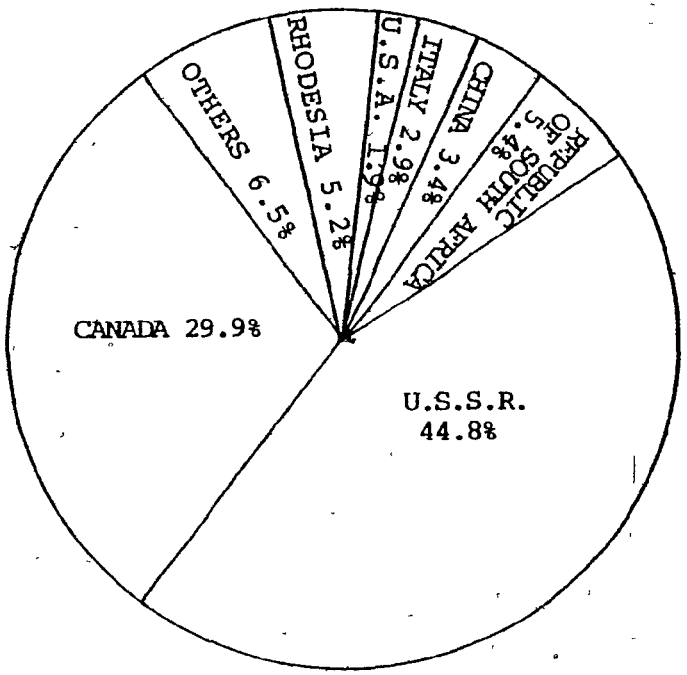


PRODUCTION 4 760 000 m.t.

Fig. 4.1 - World Production of Asbestos(2)

Asbestos Corp. Ltd., and also acts as selling agent for Cassiar Asbestos. Recently the Quebec government purchased Bell Asbestos and its affiliated companies in Canada[20] [21]. The other examples are very well depicted in Fig. 4.2[1].

4.3 World Asbestos Market; Production and Consumption:

The total World's asbestos production of 1978 is estimated to be 5.6 million tons of all grades and varieties (see table 4.1)[1]. The estimated share of the U.S.S.R. was 46 per cent; Canada produced an estimated 29 per cent; South Africa, 7 per cent; Rodesia, 4 per cent; People's Republic of China, 4 per cent; Italy, 3 per cent; United States, 2 per cent; and others, 5 per cent[1]. The lower grades of U.S.S.R. production are not used as fibres and are not included in the above figures.

The world consumption of asbestos for 1978 can be summarized as follow: U.S.S.R. is the leader with 31.9 per cent consumption, and the U.S.A. follows with 13.3 per cent; Europian Economic Community Countries, 13.9 per cent; Japan, 5.1 per cent; Canada, 1.3 per cent; and others 34.5 per cent (see Fig. 4.3)[18]. Until 1974 the apparent world consumption trends were linear (see Fig. 4.4)[15]. A drastic non-linear decrease in the world-wide asbestos consumption (Canada excepted) has

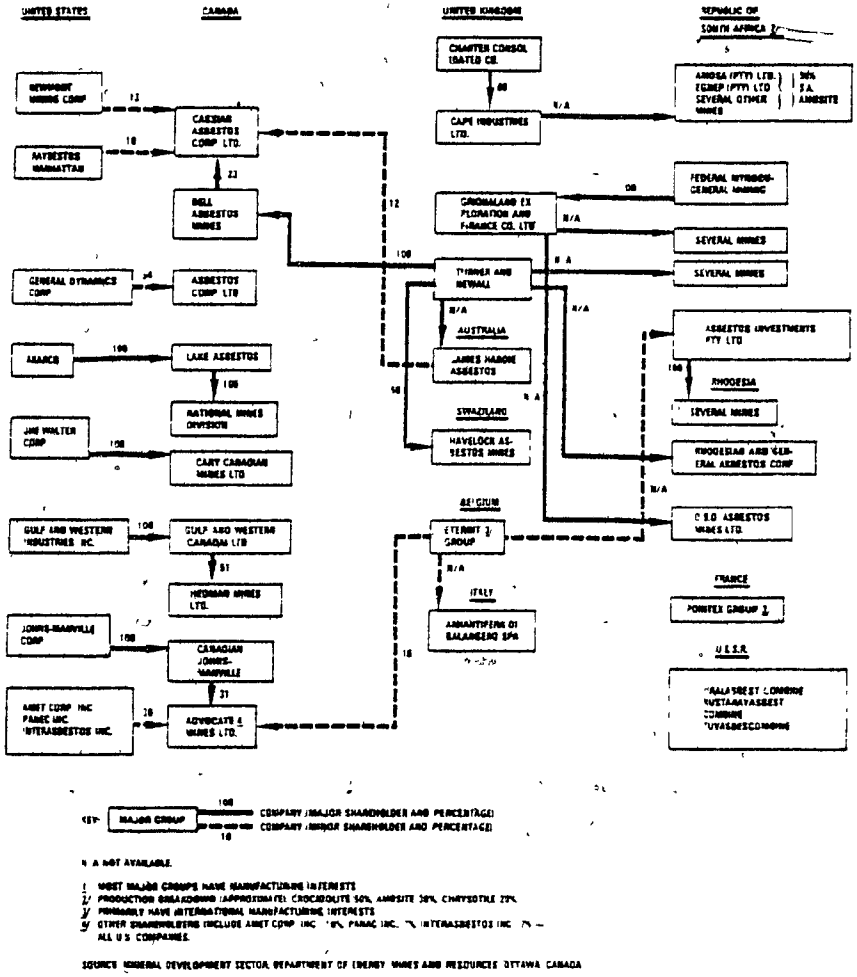


Fig. 4.2 - Major International Asbestos Mining Groups (1)

occured since 1975 (see Fig. 4.4). This was due to a world wide recession coupled with production difficulties in the Canadian asbestos industry such as a lengthy strike and a major fire at King-Beaver Mill of Asbestos Corporation(5). For the United States, this downward trend started in 1972. The major factors for this change were: a recession, the realization and concerns of the seriousness of the Occupational Health problems which are associated with the asbestos industry; and the adoption of stricter government legislation in order to prevent workers being exposed to high-levels of asbestos dust.

Since 1975, the production and consumption of asbestos in U.S.S.R. increased by 39 and 37.5 percent, respectively. This drastic change can be explained by new mine developments in the Southern Urals (by COMECON countries jointly working with U.S.S.R.)(15,16) and the establishment of new markets in the free world. Although the U.S.S.R. is the largest asbestos producer of the world, most of the Soviet asbestos is used domestically or in other COMECON countries. Similarly, the People's Republic of China is consuming its asbestos domestically. Therefore the asbestos production of the communist block countries does not affect the free world market substantially.

Table 4.1 - World asbestos production, 1978, and capacity, 1978 and 1980[1]

(Thousand metric tons)

| | Production 1978 | Capacity 1978 | Capacity 1980 |
|---|---|---|---|
| Chrysotile: | | | |
| North America: | | | |
| Canada | 1,620 | 1,814 | 2,360 |
| Mexico | ..... | ..... | 50 |
| United States | 93 | 113 | 120 |
| Total | 1,713 | 1,927 | 2,530 |
| South America: | | | |
| Argentina | 1 | 1 | 1 |
| Brazil | 100 | 100 | 110 |
| Total | 101 | 101 | 111 |
| Europe: | | | |
| Bulgaria | 21 | 23 | 30 |
| Italy | 162 | 172 | 180 |
| U.S.S.R. | 2,582 | 2,600 | 2,800 |
| Yugoslavia | 10 | 17 | 40 |
| Other | ..... | 4 | 5 |
| Total | 2,775 | 2,816 | 3,055 |
| Africa: | | | |
| Rhodesia | 210 | 210 | 230 |
| South Africa, Republic of | 118 | 120 | 140 |
| Swaziland | 48 | 54 | 60 |
| Other | 1 | 1 | 1 |
| Total | 377 | 385 | 431 |
| Asia: | | | |
| China, People's Republic of | 210 | 210 | 230 |
| Cyprus | 37 | 38 | 40 |
| India | 21 | 23 | 30 |
| Japan | 7 | 22 | 25 |
| Korea, Republic of | 7 | 6 | 6 |
| Taiwan | 1 | 4 | 4 |
| Turkey | 10 | 16 | 23 |
| Total | 293 | 319 | 358 |
| Oceania: Australia | 58 | 65 | 90 |
| World Chrysotile total | 5,317 | 5,613 | 6,575 |
| Crocidolite: | | | |
| South Africa, Republic | 210 | 215 | 230 |
| Australia | ..... | 19 | 19 |
| World Crocidolite total | 210 | 234 | 249 |
| Amosite: South Africa, Republic of | 71 | 110 | 120 |

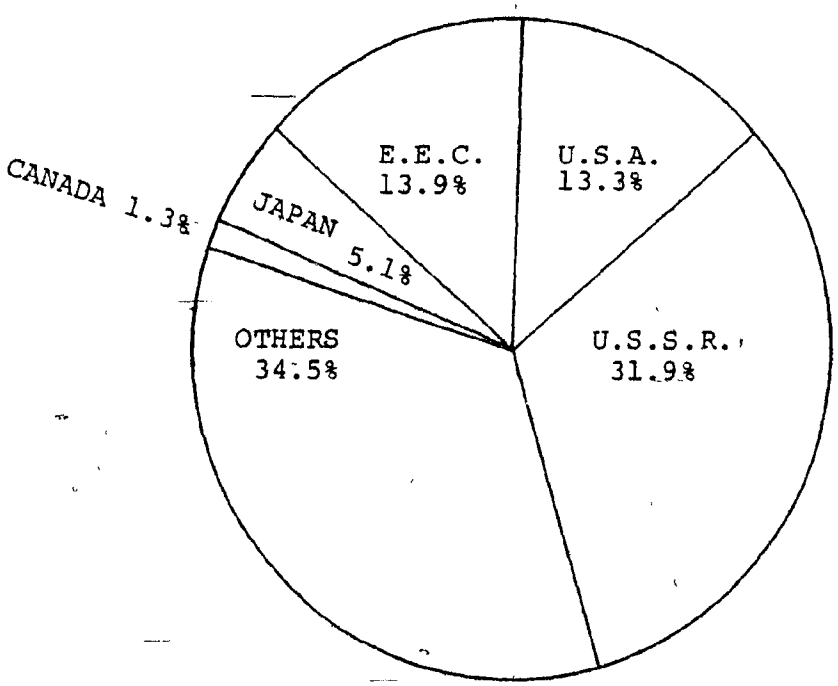


APPARENT CONSUMPTION 4 596 000 m.t.

Fig. 4.3 - Apparent World Consumption of Asbestos[2]

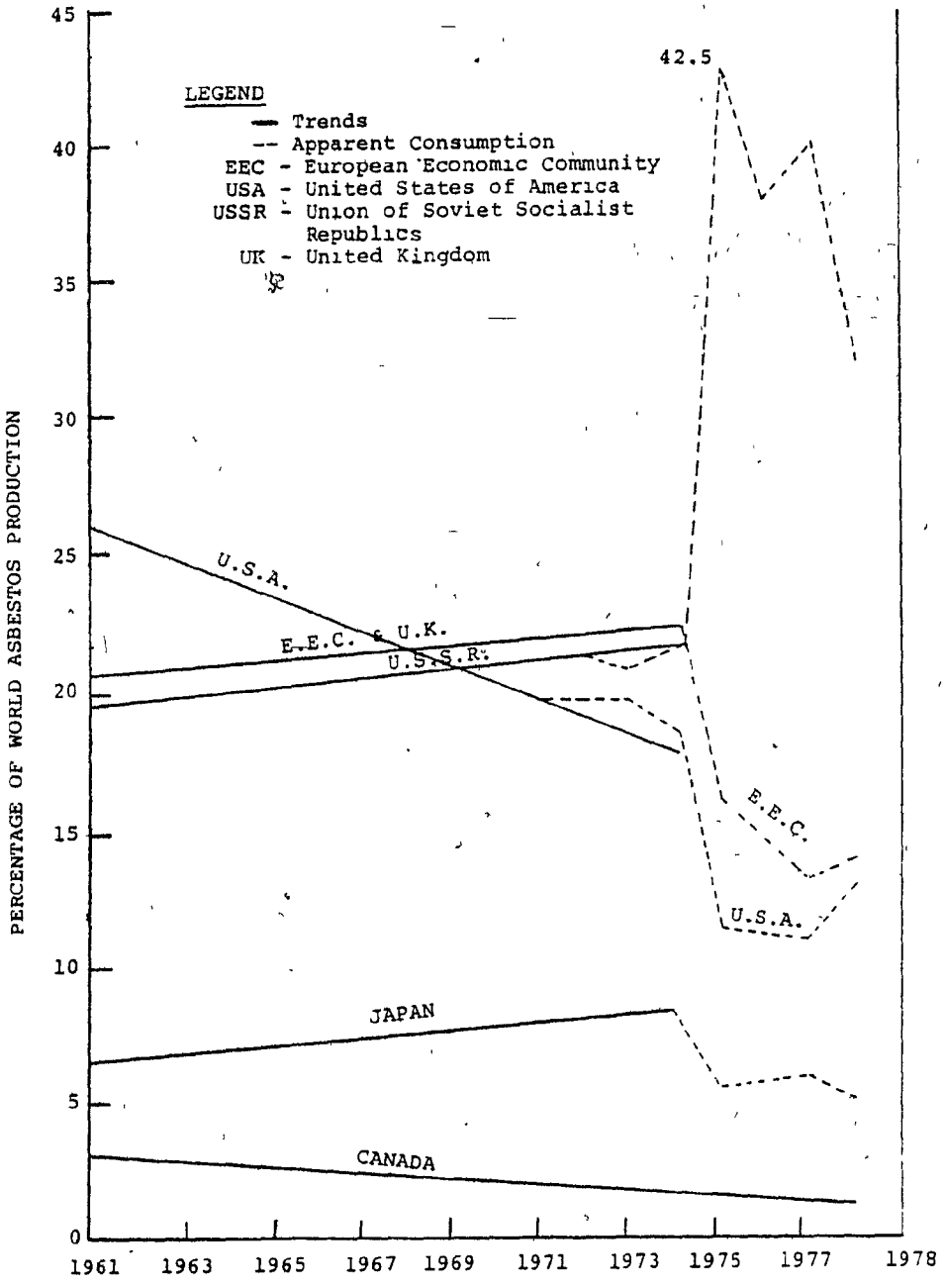


Fig. 4.4 - Apparent National Asbestos Consumption and Trends (18) (15) (3,4,5,6)

Since Rhodesia unilaterally declared its independence in November 1965 and subsequently, in 1967, the United Nations imposed an embargo on Rhodesian products, official figures for Rhodesian asbestos output are not available. However, undoubtedly Rhodesia remains the third largest Western world producer of asbestos after Canada and South Africa with its estimated output of 4 per cent of the world production.

Thirty per cent of the total asbestos production of the Republic of South Africa is chrysotile, 52 per cent is crocidolite and 18 per cent is amosite. At present South Africa is the only major crocidolite and amosite producer in the world. All of the U.S.A. demand for crocidolite and amosite is met by South Africa.

The United States produces 17 per cent and imports 83 per cent of its asbestos needs. Canada plays an important role in supplying the needed chrysotile for the U.S.A. asbestos industry, namely 95 per cent of the U.S.A.'s total asbestos imports. South Africa is another important supplier for the U.S.A. and meets the total demand for the amosite and crocidolite type of asbestos. In 1978 there was some anthophyllite produced in North Carolina[1].

Canada produces approximately 30 per cent of the world's total chrysotile asbestos and exports

nearly 97 per cent of its production to more than 80 countries. The 75.5 per cent of its exports are distributed among the following countries: United States, 38.6 per cent; West Germany, 10.8; Japan, 8.4; United Kingdom, 6.3; Mexico, 3.1; France, 2.7; Brazil, 2.2; Spain, 1.8 and Belgium - Luxembourg 1.6 per cent (2). The importance of these statistical data is more obvious when they are evaluated as per cent of total asbestos imports of these countries: United States, 95 per cent, European Economic Community, 63; Japan, 40; Eastern Europe, 6 and others, 42 per cent.

As mentioned before the major chrysotile asbestos producing province in Canada is Quebec and its total production amounts to approximately 89 per cent of the Canada's total; British Columbia produces 6 per cent and Newfoundland 5 per cent (18).

The estimated energy requirement of a large asbestos mine and mill is equivalent to 3,112 kilowatt-hours per ton produced; the energy cost is $26.41 per ton (1). The average U.S. Producer, because of the ease and size of the mining and milling operations, requires 1500 Kilowatt-hours per ton; the energy cost is $12.73 per ton (1). Like any other industry of today, the asbestos industry is also facing the problem of escalating costs. This is not only because of the higher cost of energy

but also because the open pits are becoming larger and deeper and ore grades are decreasing and finally, the total tons of rock mined are increasing. As only a small portion of this mined rock is asbestos ore, the fibre recovery and the amount of fibre produced is decreasing while the energy consumption and cost of mining and milling is increasing. The Quebec production trends, as seen in Fig. 4.5, are a good example of this statement.

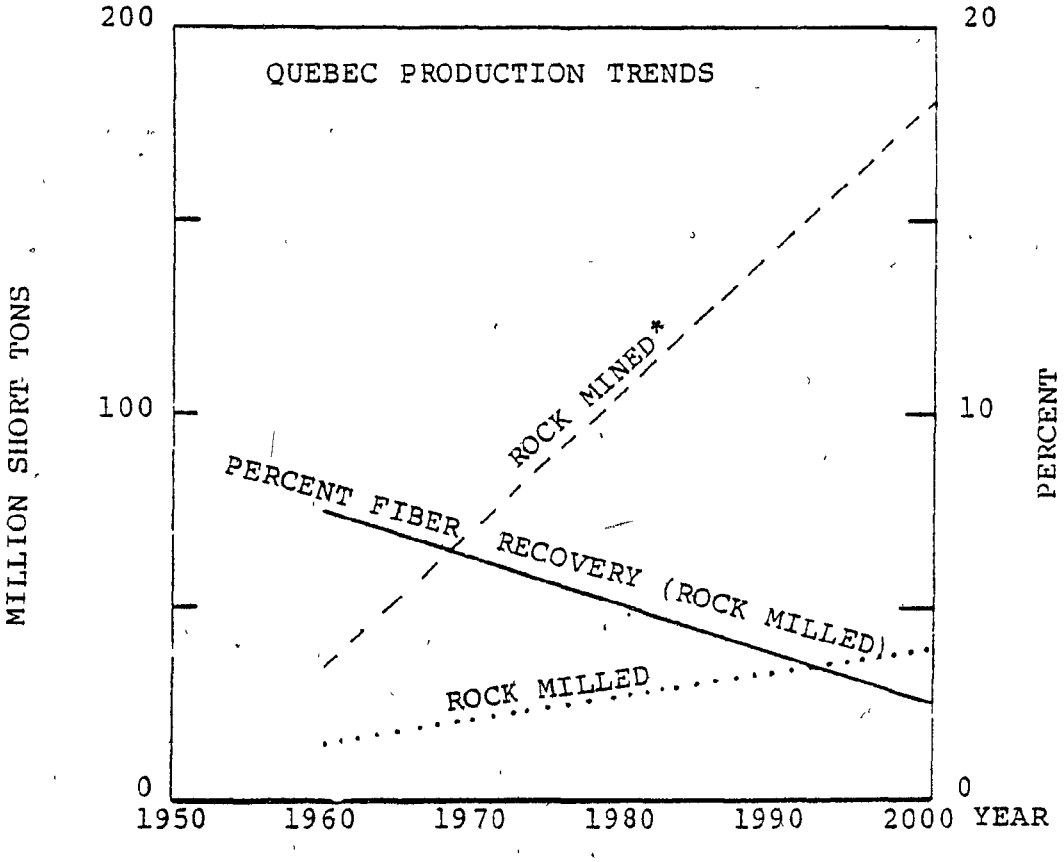


*Ore and waste rock exclusive of overburden

Fig. 4.5 (1) Quebec Production Trends; from analysis of 1951-70 data.

Regardless of the technical or financial problems, the future outlook for the asbestos industry is good, and a 2 percent growth rate per year is expected. The summary of forecasts of asbestos demand for the U.S.A. and the rest of the world, between the years 1977 and 2000, is shown in table 4.2.

4.4 Asbestos Fibre Groups and the Uses:

The grouping of chrysotile asbestos fibre is based upon the length of the fibre and it is priced accordingly. This grouping standard was developed by the Quebec asbestos industry and it is now the world standard. Asbestos is reported to have over 3000 uses; accordingly, each group is sub-divided into major categories based on uses. This classification is described below.

The long fibre groups are crude No. 1, 2 and 3. Any crude fibre which has a length greater than 19 mm. is classified as crude No. 1; if the length is in between 9 and 19 mm. it is crude No. 2; and between 6 and 9 mm. it is classified as crude No. 3. The most important uses of long fibre groups are: (a) Textile Industry: long fibre chrysotile is mainly used to manufacture fire proof clothing, theater curtains, different types of packings and other fire proof textile products. (b) Friction materials such as woven brake linings and clutch facings.

(c) Electrical insulation materials. (d) Filtration medium, and (e) Reinforcing fillers in asbestos-cement products where great strength is required such as high pressure marine insulation[6][15].

The medium length fibre groups are: No. 4, 5 and 6; the lengths vary from slightly less than 3 mm to 6 mm. Group 4 fibres are also used as friction materials; however, in the United States they are mainly used in asbestos cement pipes for transporting water. Group No. 5 products are: (a) Asbestos cement sheets (flat and corrugated). (b) Low pressure asbestos-cement pipes. (c) Molded products. (d) Paper products such as pipe insulation, wrappings and (e) Brake linings and gaskets. The major uses for group No. 6 are: asbestos-cement products, brake linings, gaskets, vinyl sheet backing and mill board.

The short fibre groups are No. 7, 8 and 9. This type is mainly used as reinforcing fillers in plastics, in floor tiles, asphalt compounds, in paints as roof coatings, joint and insulation cements, plastics and caulking compounds, and in oil-well muds.

There are certain uses for amphibole asbestos as well. Amosite asbestos in woven form is used as felted insulation blanket for temperatures up to 480°C; in loosely compacted form it is used for covering marine

Table 4.2 - Summary of forecasts of U.S. and rest-of-world asbestos demand, 1977-2000[1]

(Thousand metric tons)

| | 1977 | Forecast range | | Probable | | Probable average annual growth rate 1977-2000, percent |
|---|---|---|---|---|---|---|
| | | Low | High | 1985 | 2000 | |
| United States: | | | | | | |
| Total: | 610 | 357 | 919 | 610 | 610 | 0.0 |
| Cumulative[1] | .... | 10,739 | 17,501 | 4,880 | 14,030 | ..... |
| Rest of world. | | | | | | |
| Total: | 4,723 | 10,190 | 15,035 | 6,961 | 13,472 | 4.5 |
| Cumulative[2] | .... | 166,272 | 212,942 | 47,981 | 199,174 | ..... |
| World: | | | | | | |
| Total: | 5,333 | 10,547 | 15,954 | 7,571 | 14,082 | 4.1 |
| Cumulative. | .... | 177,011 | 230,443 | 52,861 | 213,204 | ..... |

Table 4.3 - World and Canadian Asbestos Production (1961-1980) (12) (18) (20)

(Thousand metric tons)

| YEAR | WORLD | CANADIAN |
|---|---|---|
| 1961 | 2,827 | 1,065 |
| 1962 | 2,928 | 1,103 |
| 1963 | 3,067 | 1,158 |
| 1964 | 3,212 | 1,288 |
| 1965 | 3,239 | 1,259 |
| 1966 | 3,660 | 1,351 |
| 1967 | 3,053 | 1,318 |
| 1968 | 3,208 | 1,448 |
| 1969 | 3,418 | 1,462 |
| 1970 | 3,610 | 1,508 |
| 1971 | 3,695 | 1,483 |
| 1972 | 3,789 | 1,530 |
| 1973 | 4,370 | 1,690 |
| 1974 | 4,270 | 1,644 |
| 1975 | 4,240 | 1,056 |
| 1976 | 5,340 | 1,536 |
| 1977 | 5,320 | 1,542 |
| 1978 | 4,760 | 1,422 |
| 1979 | 5,278 | 1,501 |
| 1980 | 5,057 | 1,300 (Estimated) |
| 1995 | 6,806 | 1,750 (Estimated) |

turbines and jet engines. Another application is in the field of fire-resistant marine partition board.

The long-fibre crocidolite has a special application for locomotive boiler lagging (in woven fabric form) and is also used as an acid resistant packings and for gaskets. The shorter crocidolite fibre is mainly used in making asbestos-cement pipe.

The tremolite and anthophyllite asbestos has a good resistance to chemicals and therefore they are used for chemical resistant filters, as welding rod coatings and as fillers in plastic products.

According to Energy, Mines and Resources,(2) 70 per cent of the world asbestos consumption is used in construction-related materials. Since the United States is Canada's major export market it is important to study their total apparent consumption of asbestos. The total apparent asbestos consumption of United States is as follows: asbestos-cement pipe, 25 per cent; flooring products, 21 per cent; friction products, 14 per cent; roofing products, 10 per cent; asbestos-paper, 5 per cent; asbestos-cement sheet, 5 per cent; coatings and compounds, 5 per cent; packing and gaskets, 4 per cent; insulation (thermal and electrical), 3 per cent; textiles, 1 per cent; plastics, 1 per cent; and others, 6 per cent.

Prices of each group of chrysotile asbestos fibre varies and the range of Canadian chrysotile asbestos fibre prices are as follows: 1978 prices, f.o.b. mines in Quebec for No. 7, $118 per metric ton; No. 3, $1,655 per ton; crude No. 2, $2,386 per ton; f.o.b. British Columbia, Cassiar mine group CZ or No. 6, $364 per ton; and Crude No. 1, $3,595 per ton [1][12]. U.S. domestic prices are comparable with Canadian; Arizona fibres ranged in price from $110 for group No. 7 to $3,307 american dollars per ton for Crude No. 1, f.o.b. Globe, Arizona. Of course if the transportation cost is added on top of the Canadian prices, it could become a costly process to ship it to the market at competitive price ranges. However, as long as a strong demand for Canadian Chrysotile is in existance this will not be a marketing problem.

## 4.5 Environmental Problems of Asbestos and Substitution:

On March 31, 1971, for the first time in the United States, asbestos was listed as a "harzardous air pollutant" by the Environmental Protection Agency (EPA). Following that, in May 1971, an emergency standard was accepted and issued by the Occupational Safety and Helath Administration (OSHA), Department of Labour that "The 8 hour time-weighted average airborne concentration of asbestos dust to which employees are exposed shall not exceed 5 fibres per millilitre of air greater than 5 microns in length"[17].

Before this the accepted TLV for asbestos was 12 fibres per millilitre of air greater than 5 micron in length. According to U.S. Bureau of Mines (15) there is no consensus between EPA and OSHA on a threshold limit value and that an acceptable concentration would minimize danger from exposure. EPA goes beyond this and states that there is no acceptable way to measure asbestos in the ambient air. The Mine Safety and Health Administration (MSHA) agrees with the OSHA standard and uses a membrane filter and optical microscope counting method with a TLV of 2 fibres per millilitre of air greater than 5 micron in length; this standard was accepted in July 1, 1976 by the OSHA of the Labour Department. However it is the general consensus that prolonged occupational exposure to heavy concentrations of asbestos dust, without adequate protection, could cause the type of pneumoconiosis called asbestosis. This could lead to a dangerous lung cancer disease. The chances of contracting such a disease is increased with cigarette smoking. Also excessive exposure to asbestos, especially crocidolite, could increase the chances of contracting a rare type of cancer called mesothelioma.

The public awareness of these occupational diseases was influenced by the sensational reporting of the news media and even OSHA was pressured to propose to reduce the asbestos TLV to 0.5 fibre per millilitre (in late 1975) and the

proposal in 1976 by the National Institute for Occupational Safety and Health (NIOSH) to reduce the TLV down to 0.1 fibres per millilitre of air. The economic implication of this type of legislation on asbestos producers and asbestos product manufacturers is very serious and detrimental to their survival. The cost of more efficient dust control systems would make the operation uneconomical. When in 1976 the province of Ontario introduced the new TLV standards for the asbestos industry and reduced the fibre counts down to 2 fibres per cubic centimetre of air, practically all of the asbestos producers of Ontario were forced to shut-down their operations by 1978. In Quebec stricter legislation than the existing one was imposed in January 1979 and asbestos TLV was reduced to 5 fibres per cubic centimetre of air. It was expected to be reduced down to 2 fibres per cubic centimetre of air by January 1981.

Stricter environmental legislations and public concern has influenced the apparent consumption trends of the world (see Fig. 4.4). In the state of New York asbestos is forbidden to be used in the construction industry completely, in Sweden all asbestos mining, manufacturing and consumption is forbidden.

The substitution of synthetic fibres for asbestos is physically possible; however, economically competitive substitutes are not available or are rare. At present

commercially available glass-fibre synthetic substitutes are mainly used in thermal insulation; this represents only a small portion of the market. Also glass-reinforced cement is commercially available in United States and Europe. This could affect the asbestos consumption in the future. Glass fibers may not be a competitive substitute for asbestos for the following reasons: glass fibers have inferior drainage characteristics; their strength decreases gradually with time; and they cost four times more than asbestos fibers. At present no substitutes are availabe for friction materials. In spite of the environmental problems, the demand for asbestos in third world countries is increasing alarmingly. If such strong market demands persist, it is believed that by the beginning of the year 2000 present asbestos producing reserves will be largely depleated. Therefore it is important that economically feasible substitutes be sought.

## 4.6 Conclusion:

In the past few years, the depressed world economic conditions together with health and environmental concerns for asbestos and its products has caused a temporary alarm or pessimism in the asbestos market. However, a strong demand for asbestos in third world countries has helped the asbestos market in remaining stable. In the next few years a steady growth of 1.5 to 2 percent is expected.

In the industrialized countries, continuous research efforts in the fields of health and the environment is expected to produce positive results for better environmental controls in the asbestos industry. Although substitutes for asbestos in some asbestos-cement products are commercially available, they are not yet economically competitive with asbestos and possible health problems of the substitutes have to be investigated. In some states and countries, partial or complete banning of the asbestos and its products may speed up the development of competitive good-quality substitutes. However, this should not be looked upon as a threat to the potential growth and development of the asbestos industry. The present rate of growth in demand may deplete most of the presently existing asbestos reserves by the year 2000.

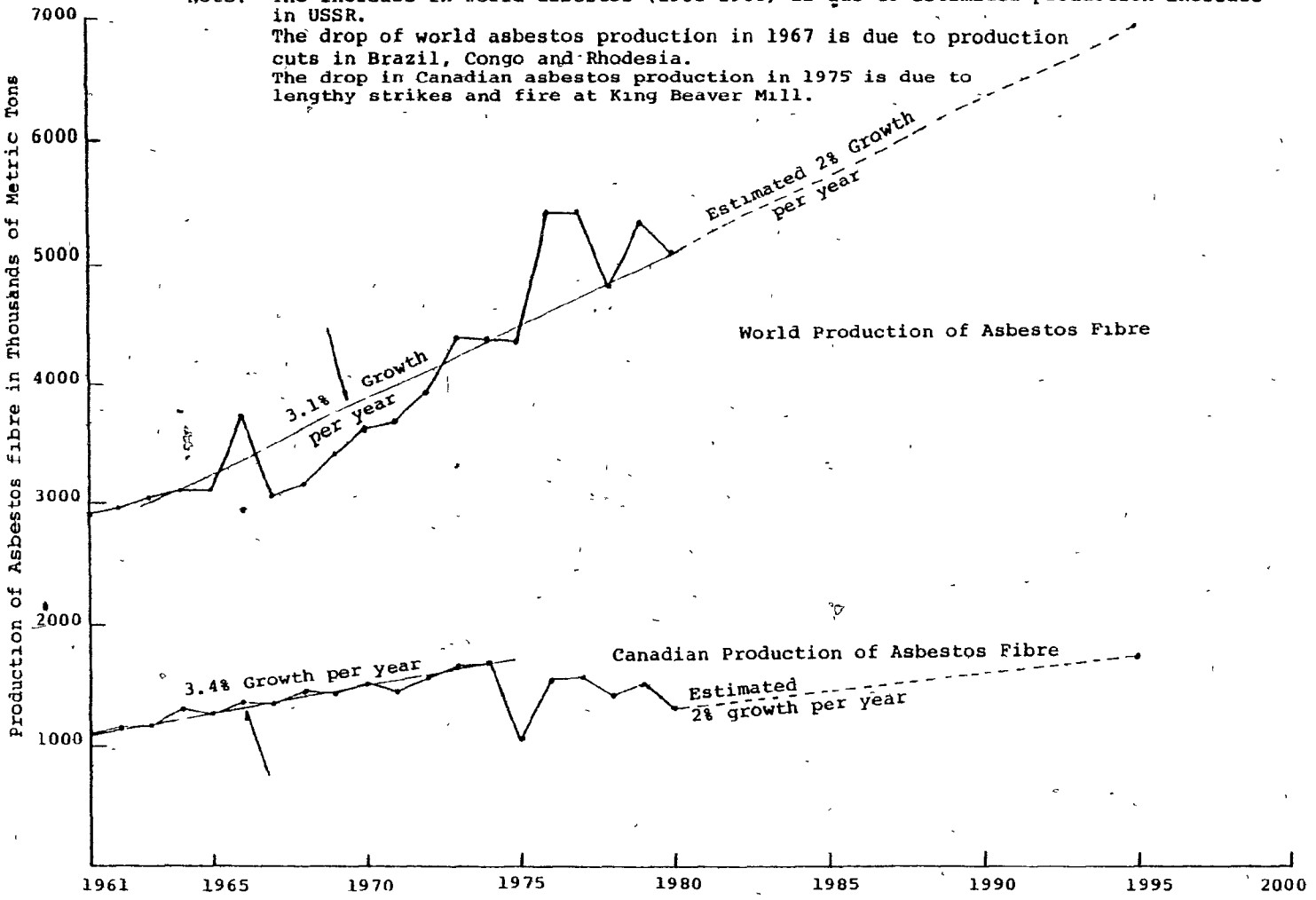


Fig. 4.6 - Actual World Versus Canadian Asbestos Production For Last 20 years (12) (18) (20)

## LIST OF REFERENCES FOR CHAPTER IV


1. Clifton, R.A., "Asbestos", Mineral Commodity Profiles, Bureau of Mines, United States Department of the Interior, July 1979, Washington, D.C., pp. 1-19.

2. Vagt., G.O., "Asbestos", Canadian Minerals Yearbook 1978, Editor: R.B. Abbott, Energy, Mines and Resources, Canada, pp. 1-9.

3. Vagt, G.O., "Asbestos", Canadian Minerals Yearbook 1977, Editor: R.B. Abbott, Energy, Mines and Resources, Canada, pp. 25-34.

4. Vagt, G.O., "Asbestos", Canadian Minerals Yearbook 1976, Editor: R.B. Abbott, Energy, Mines and Resources, Canada, pp. 51-60.

5. Vagt, G.O., "Asbestos", Canadian Minerals Yearbook 1975, Editor: G.H. Meldrum, Energy, Mines and Resources, Canada, pp. 49-58.

6. Hanes, F.E., "Asbestos", Canadian Minerals Yearbook 1974, Editor: G.H. Meldrum, Energy, Mines and Resources, Canada, pp. 47-55.

7. Vagt, G.O., "Asbestos", Canadian Minerals Yearbook 1972, Editor: G.H. Meldrum, Energy, Mines and Resources, Canada, pp. 39-45.

8. Boucher, M.A., "Asbestos", Canadian Minerals Yearbook 1971, Editor: V. Donnelly, Energy, Mines and Resources, Canada, pp. 30-38.

9. Killin, A.F., "Asbestos", Canadian Minerals Yearbook 1970, Editor: G.E. Thompson, Energy, Mines and Resources, Canada, pp. 109-116.

10. Jeffery, W.G., "Asbestos", Canadian Minerals Yearbook 1969, Editor: G.E. Thompson, Energy, Mines and Resources, Canada, pp. 107-114.

11. Jeffery, W.G., "Asbestos" Canadian Minerals Yearbook 1968, Editor: G.E. Thompson, Energy, Mines and Resources, Canada, pp. 99-107.

12. 1970 Standard Industrial Classification Manual, Asbestos Mines S.I.C. 071, Catalogue 12-501.
    a) Revised copy 1971, pp. 4-10
    b) Revised copy 1972, pp. 4-10
    c) Revised copy 1973, pp. 4-10
    d) Revised copy 1974, pp. 4-10
    e) Revised copy 1975, pp. 4-10
    f) Revised copy 1976, pp. 4-10
    g) Revised copy 1977, pp. 4-10

Energy and Minerals section of the Manufacturing and Primary Indsutries Division, Ottawa, Canada.

13. Mining Association of Canada, "Facts & Figures, Mining in Canada, 1980, Ottawa, Canada, pp. 9, 32-35.

14. Argal, Jr. G.O., "World Production Leaders", World Mining Yearbook, July, 1980, pp. 118-119.

15. Clifton, R.A., "Asbestos" Mineral Commodity Profiles", Bureau of Mines, United States Department of the Interior, MCP-6, Sept. 1977, Washington, D.C., pp. 1-17.

16. U.N. Statistical Yearbook, "Asbestos", Mining and Quarrying 1978, New York, N.Y., pp. 216-217.

17. OSHA, "Emergency Standard for Exposure to Asbestos Dust", Federal Digest, U.S. Department of Labour, May 29, 1971. Washington, D.C. Vol. 36, No. 105, Part II.

18. Vagt, G.O., "Asbestos" Preprint from Canadian Minerals Yearbook 1979, Energy, Mines and Resources Canada, pp. 1-11.

19. Clifton, R.A., "Asbestos" U.S. Mineral Commodity Summaries for 1979, Jan. 1980, pp. 14-15.

20. Clifton, R.A., "Asbestos", U.S. Mineral Commodity Summaries for 1980, Jan. 1981, pp. 12-13.

21. Vagt, G.O., "Asbestos" Canadian Mining Journal, Vol. 102, No. 2, February 1981, pp. 129-130.

## CHAPTER V

## HEALTH EFFECTS OF CHRYSOTILE ASBESTOS

### 5.1 General:

In order to understand the health effects of the inhaled and retained chrysotile asbestos dust in the lungs, it is necessary to have an understanding of the breathing mechanism or the functional anatomy of the lung. During breathing, lungs are exposed to air which may contain dust and other noxious agents. However, the lungs possess a complex of protective mechanisms for defense against these potentially harmful materials. This overwhelming onslaught from without results in disrupting of these mechanisms and thus results in complicated pulmonary diseases.

In general terms the respiratory tract is divided into two main zones; the conducting zone with cilia, and the respiratory zone with alveoli[1][2]. The function of the conducting zone as a physiologic unit is directed toward the cleansing, warming and humidification of ventilated air; and the function of the respiratory zone is to provide a surface area for gaseous exchange and also to resist and protect the respiratory system from the damaging activities of aerosols, dust and other bacteria which may be deposited or located in this zone. The Task Group on Lung Dynamics has included the nasopharynx as a first zone or part of the respiratory tract[3]. In reality, however, there are many gross and microscopic changes in

the structure of the respiratory tract from the nasopharynx to the alveoli, which reflect the different physiologic functions.

## 5.2 Anatomy and the Normal Functioning of the Respiratory Tract:

The anatomy and the functions (physiology) of the whole respiratory tract (including the nasopharynx and the lung) can be summarized as follows: the inhaled air enters the body either through the nostrils or through the mouth. Air entering through the nose is filtered, warmed and moistened. Dust particles are deposited on the mucus blanket that flows towards the pharynx (see Fig. 5.1). The air then passes through the pharynx and larynx into the trachea. The larynx at the upper end of the trachea is the voice box that enables a person to speak. Air flow then proceeds through the trachea. The trachea of an ordinary man is a pipe about twelve centimeters in length (see table 5.1 for the dimensions of airways). It is lined with ciliated mucus membrane, the mucus being produced by glandular cells (goblet cells and circulatory glands) within the membrane. Air passing through the trachea splits into two pipes called the main bronchi. Each bronchus leads to a lung. But, as they enter the lungs they further subdivide into small passageways until they are about 0.1 cm in diameter.

Now the airways are called bronchioles. The bronchioles are also lined with mucus membrane but there are no mucus secreting cells. The bronchioles subdivide as well until they are known as the respiratory bronchioles which are differentiated from the bronchioles by the fact that the epithelial lining of these bronchioles are not ciliated and have small air sacs, alveoli, attached to their walls. From the respiratory bronchioles, alveolar ducts arise which in turn lead to large numbers of thin walled air sacs, the alveoli (see Fig. 5.2). The walls of the alveolus are very thin and permeable thus allowing oxygen to diffuse readily into the capillaries of blood and the pulmonary blood vessels (see Fig. 5.3). According to Stuart[4], in a man's lungs there are an estimated 100 million alveoli, and according to Muir[1], 300 million with a total surface area of 30 to 100 metre square for gas exchange (see table 5.1).

5.2.1 The Lung Volumes and Capacities:

Depending upon the amount of work being done, the flow rate of air entering the respiratory tract varies from zero to a maximum of 60-120 litres per minute[4]. These values are a function of the frequency of breathing per minute and the tidal volume, or when work is done it is the function of vital capacity. As indicated, in order to provide the required oxygen for the body, the lung has different volumes and capacities. According to Comroe et al. (6), the lung has four primary volumes

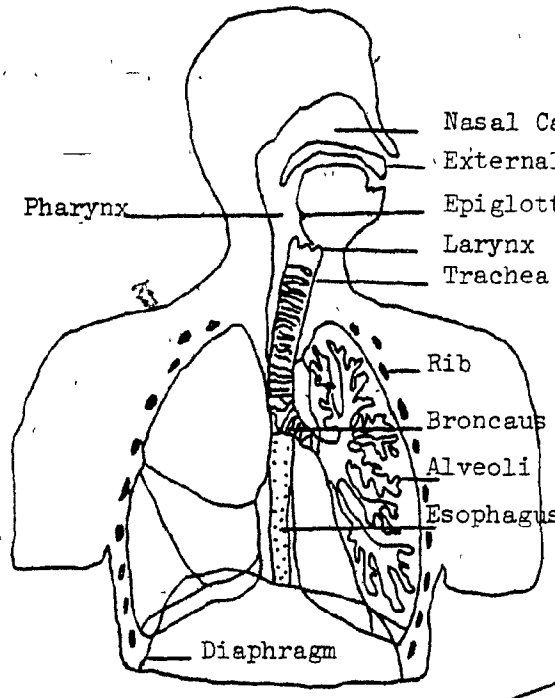


Figure 5.1 Respiratory System (1)

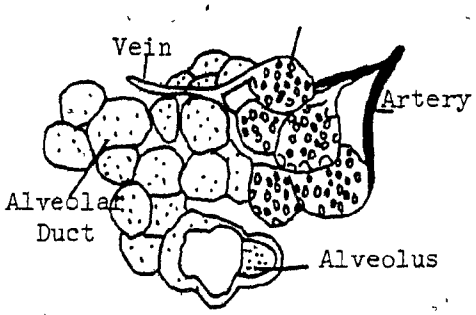


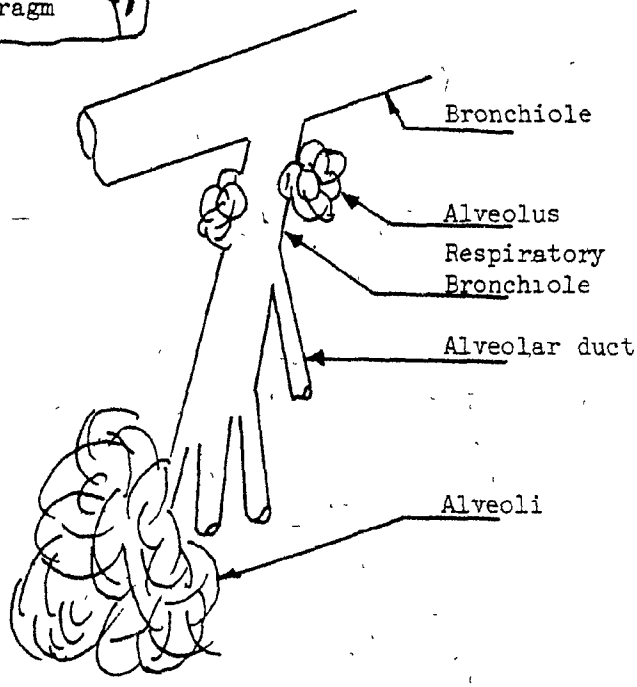


Figure 5.2 Breakdown of Respiratory Tracts in the Lung(5)

which do not overlap with each other[6] (see Fig. 5.4). These volumes are[5][6][7]: (a) Tidal Volume or the depth of breathing, which can be defined as the volume of gas inspired or expired during each respiratory cycle[6]. In this case no extra effort is made to increase the inspiratory or expiratory levels; actually it is the end result of normal breathing cycle. (b) Inspiratory Reserve Volume is defined as the maximal amount of gas that can be inspired from the end or normal inspiratory position; formerly it was known as complimentary air minus tidal volume[6]. (c) Expiratory Reserve Volume is defined as the volume of gas that can be expired from the end or resting expiratory level[6]. Formerly, it was known as supplemental air. (d) Residual Volume is defined as the volume of gas remaining in the lungs at the end of maximal expiration[6]. Formerly, it was named as residual capacity or residual air[6][7].

In a similar manner the lung capacities can be classified into four major categories, each of which includes two or more of the above described primary volumes[5][6][7]. (a) Total Lung Capacity is defined as the amount of gas contained in the lung at the end of maximal inspiration[6]. Formerly it was known as total lung volume. (b) Vital Capacity is defined as the maximal volume of gas that can be expelled from the lungs by forceful effort following a maximal inspiration[6].

Table 5.1 Dimensions of the Human Airways[1]

| | Generation | Name | Number per generation | Length (cm) | Diameter (cm) | Total cross section ($cm^2$) |
|---|---|---|---|---|---|---|
| Conducting zone (with cilia) | 0 | Trachea | 1 | 12.0 | 1.8 | 2.54 |
| | 1 | Main bronchi | 2 | 4.76 | 1.22 | 2.33 |
| | 2 | Lobar bronchi | 4 | 1.90 | 0.83 | 2.13 |
| | 3 | Segmental bronchi | 8 | 0.76 | 0.56 | 2.00 |
| | 4 | Intrasegmental bronchi | 16 | 1.27 | 0.45 | 2.48 |
| | 5 | " | 32 | 1.07 | 0.35 | 3.11 |
| | 6 | " | 64 | 0.90 | 0.28 | 3.96 |
| | 7 | " | 128 | 0.76 | 0.23 | 5.10 |
| | 8 | " | 256 | 0.64 | 0.186 | 6.95 |
| | 9 | " | 512 | 0.54 | 0.154 | 9.56 |
| | 10 | " | 1,024 | 0.46 | 0.130 | 13.4 |
| | 11 | " | 2,048 | 0.39 | 0.109 | 19.6 |
| | 12 | Bronchioles | 4,096 | 0.33 | 0.095 | 28.8 |
| | 13 | " | 8,192 | 0.27 | 0.082 | 44.5 |
| | 14 | " | 16,384 | 0.23 | 0.074 | 69.4 |
| | 15 | " | 32,768 | 0.20 | 0.066 | 113.0 |
| | 16 | Terminal bronchioles | 65,536 | 0.165 | 0.060 | 180.0 |
| Respiratory zone (with alveoli) | 17 | Respiratory bronchioles | 131,072 | 0.141 | 0.054 | 300.0 |
| | 18 | " | 262,144 | 0.117 | 0.050 | 534.0 |
| | 19 | " | 524,288 | 0.099 | 0.047 | 944.0 |
| | 20 | Alveolar ducts | 1,048,576 | 0.083 | 0.045 | 1,600.0 |
| | 21 | " | 2,097,152 | 0.070 | 0.043 | 3,222.0 |
| | 22 | " | 4,194,304 | 0.059 | 0.041 | 5,880.0 |
| | 23 | Alveolar sacs | 8,388,608 | 0.050 | 0.041 | 11,800.0 |

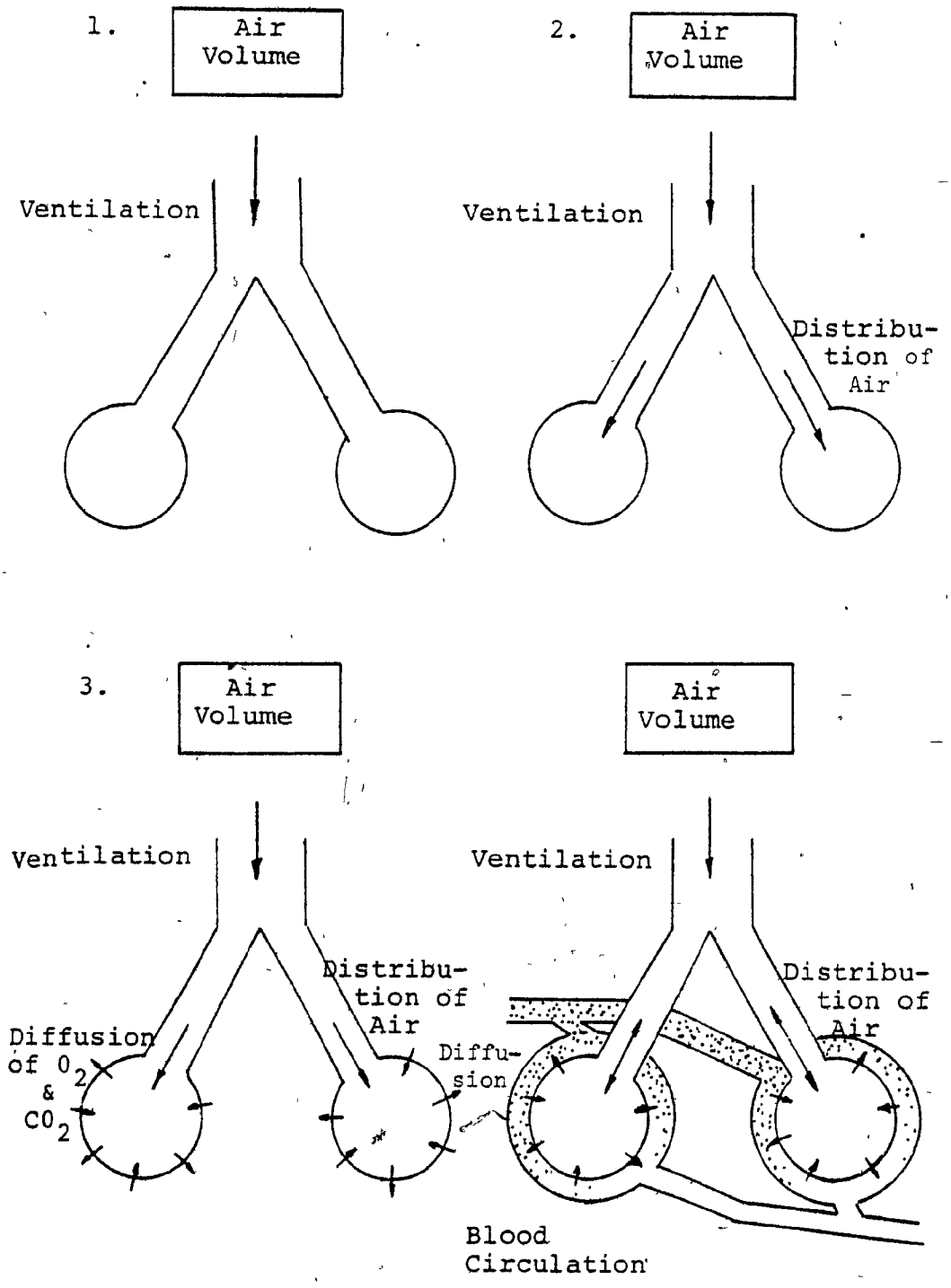


Fig.5.3 --Processes Involved in Pulmonary Gas Exchange.[6]

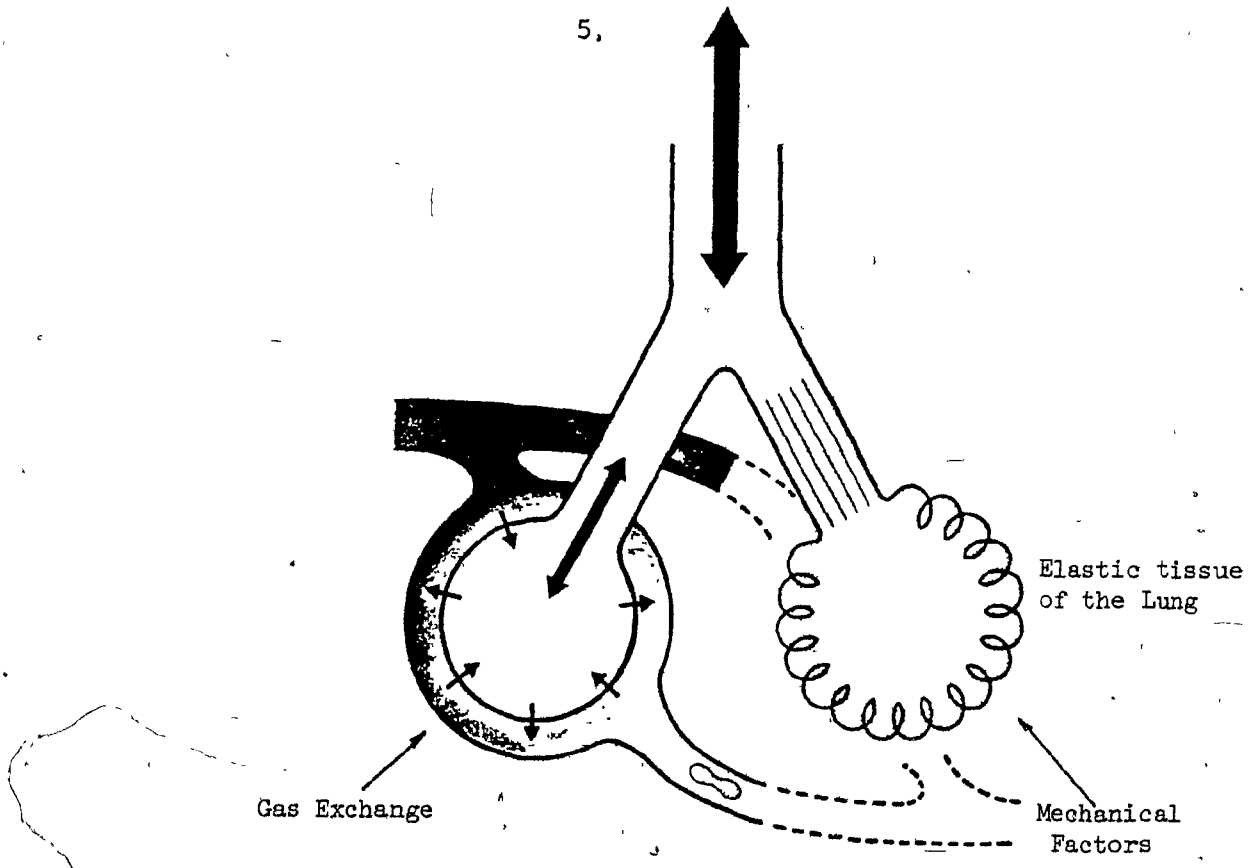


Fig. 5.3 - Continued... Process Involved in Pulmonary Gas Exchange (6)

(c) Inspiratory capacity is defined as the maximal volume of gas that can be inspired from the resting expiratory level[6]. Formerly it was known as complementary air. (d) Functional Residual Capacity is defined as the volume of gas remaining in the lungs at the resting expiratory level; or mathematically, it is equal to the summation of the residual and the expiratory reserve volumes. Formerly it was known as functional residual air[6][7].

The vital lung capacity and the volumes can be measured directly by using a simple instrument called a spirometer, with the exception of residual volume. The residual volume and functional residual capacity can be measured by either an open or closed circuit method which is Nitrogen wash-out method or helium method respectively. In table 5.2 average lung volumes of healthy recumbent subjects are shown. These figures are averages and it is difficult to match and compare another healthy person's lung volumes with these. The reason is that, lung volumes are dependent on the sex, age, weight and the height of a person. The vital capacity of a healthy person who has the same sex, age, weight and height may differ as much as $\pm$ 20 percent from these average figures. In some cases, although the same measuring method is repeated with the same individual, the vital capacity may vary $\pm$ 200 ml. However, the following two useful and practical formulae

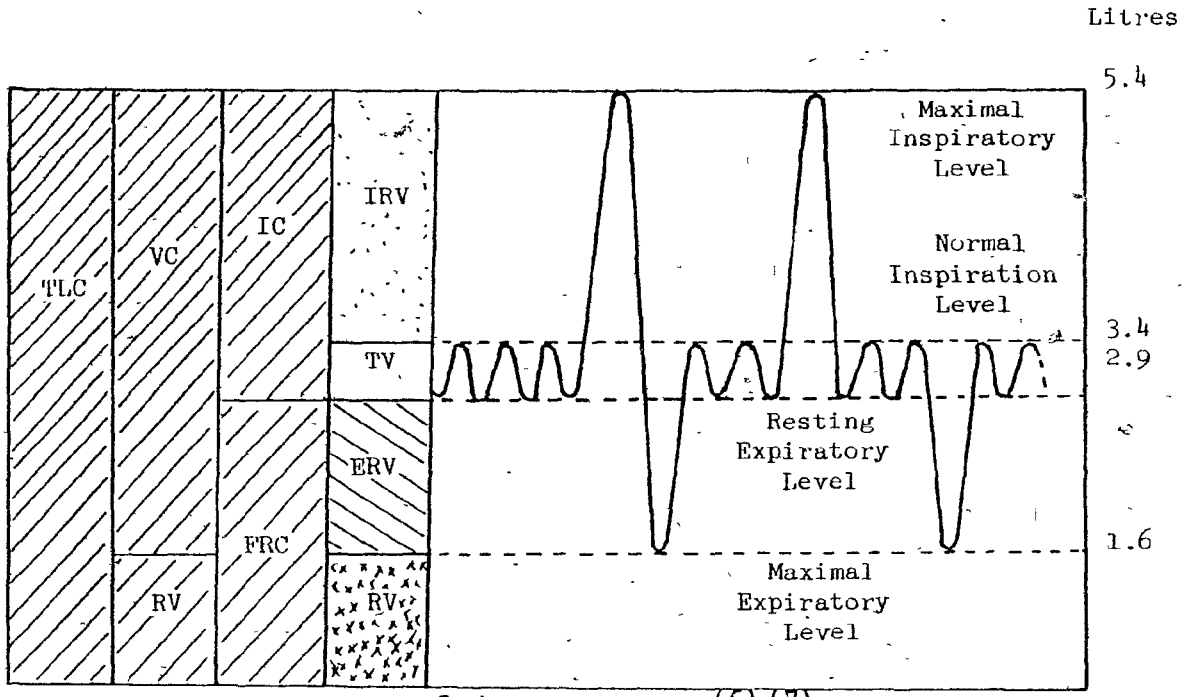


Fig. 5.4--Lung Volumes (6) (7)

Note: TLC = Total Lung Capacity, VC = Vital Capacity, RV = Residual Volume, IC = Inspiratory Capacity, FRC = Functional Residual Capacity, IRV = Inspiratory Reserve Volume, TV = Tidal Volume, ERV = Expiratory Reserve Volume

can be used for calculating comparable vital capacities for males and females. In each case surface area, height, weight and age are taken into consideration[6].

For Males: Vital Capacity = [27.63 - (0.112 x age)] x height in cm.

For Females: Vital Capacity = [21.78 - (0.101 x age)] x height in cm.

Table 5.2 LUNG VOLUMES IN HEALTHY RECUMBENT SUBJECTS[6]

(Approximate values, in ml.)

| Total Body Surface Area | Male Aged 20-30 $1.7m^2$ | Male Aged 50-60 $1.7m^2$ | Female Aged 20-30 $1.6m^2$ |
|---|---|---|---|
| Inspiratory Capacity | 3600 | 2600 | 2400 |
| Expiratory Reserve Capacity | 1200 | 1000 | 800 |
| Vital Capacity | 4800 | 3600 | 3200 |
| Residual Volume | 1200 | 2400 | 1000 |
| Functional Residual Capacity | 2400 | 3400 | 1800 |
| Total Lung Capacity | 6000 | 6000 | 4200 |
| RV/TLC* x 100 | 20% | 40% | 24% |

* RV = Residual Volume, and TLC = Total Lung Capacity.

As it is indicated in Table 5.2 as the person gets older, although the total Lung Capacity stays the same, the Vital capacity decreases and Residual Volume increases.

Usually this is due to loss of elasticity of the alveolar membrane, respiratory muscles, or other pulmonary tissues. In the case of emphysema or other occupational pulmonary disease, in addition to regional changes in elasticity, also the occurance of regional check valves, bronchial obstractions, and regional disturbances in expansion are common. All these are the causes of uneven ventilation (see Fig. 5.5) of the lung. Effects of uneven ventilation are anoxemia (lack of oxygen which renders the blood incapable of conveying enough oxygen to the body tissues), and in severe cases carbon-dioxide retention and respiratory acidosis. In order to prevent the above causes of uneven ventilation, the defence mechanism of the body may develop hyper ventilation and this forces the heart to beat faster and pump the blood through the operating portions of the lung more frequently to compensate the causes of ineffective ventilation.

5.2.2 Diffusion of the Oxygen Molecules From Alveolar Gas to Pulmonary Capillary Blood:

The oxygen molecules move from alveoli through the alveolar membrane and interstital fluid into capillaries under the gas concentration gradient, by changing from a gaseous state to a state of solution on the surface of alveoli tissues (see Fig. 5.6)[6]. The oxygen solutions then pass through capillary membranes and reach the plasma, cross the red blood cell membrane and enter the red blood cell by a diffusion process. At this point

oxygen associates itself with hemoglobin with a chemical reaction and then it is pumped to the different parts of the body by heart. This is a simple description of a complex process which takes place across a short distance of 0.1 micron. However, it is understood that the efficiency and speed of diffusion is effected by the following conditions: (a) availability of a surface area in the alveoli for diffusion; (b) solubility of the gas under the partial gradient pressure; (c) thickness of the alveolar and capillary membranes which may be thickened because of the existence of a pulmonary disease, such as asbestosis; (d) existence and condition of the interstital fluid. In some cases, specially when harmful dust particles are present, it could be replaced by a fibrous tissue or excessive amount of edema fluid may separate the membrane apart and increase the diffusion path, (e) capillary paths could be increased if capillaries are enlarged or widened by containing more than one red blood cell abreast, (f) availability of the red blood cells in the capillary and the speed of chemical reaction between the oxygen and the hemoglobin.

When these conditions and factors exist in a person's pulmonary system, his health and well being would be affected severely.

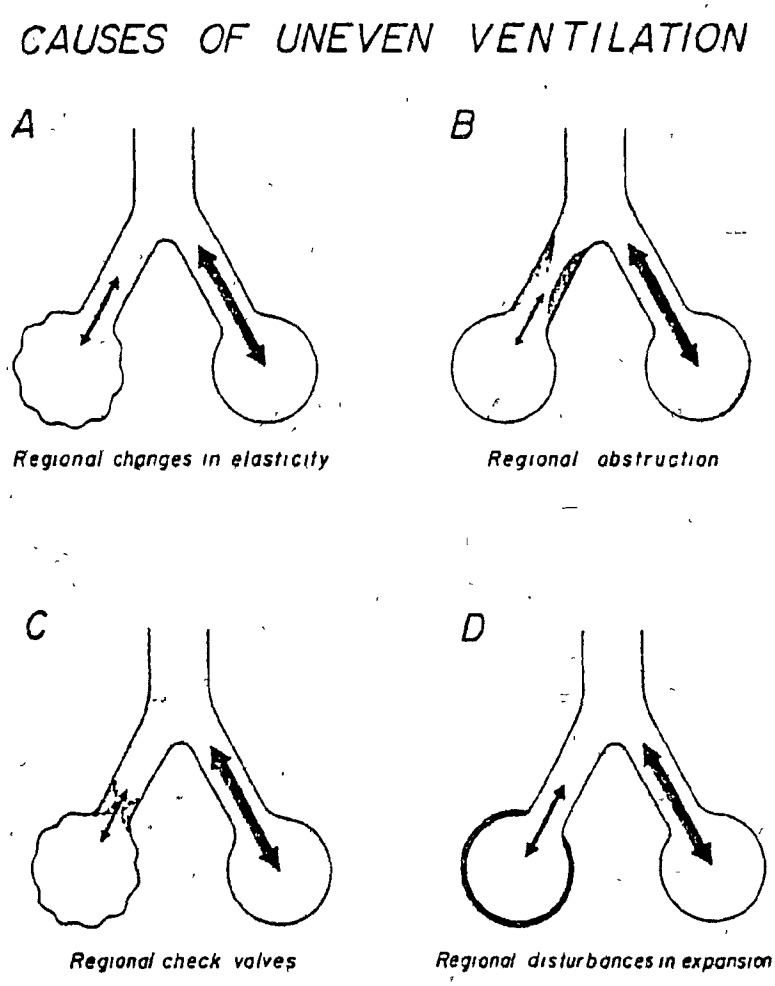


Fig. 5.5--Mechanisms Responsible for Non-Uniform Distribution of Inspired Air[6]

Circular areas represent the alveoli. Wavy lines in A and C represent alveoli that have lost their normal elastic recoil. Thick line in D signifies alveoli that expand less than normally, although their elastic tissue is normal and there is no airway obstruction. Size of arrows indicates the volume of gas ventilating each region.

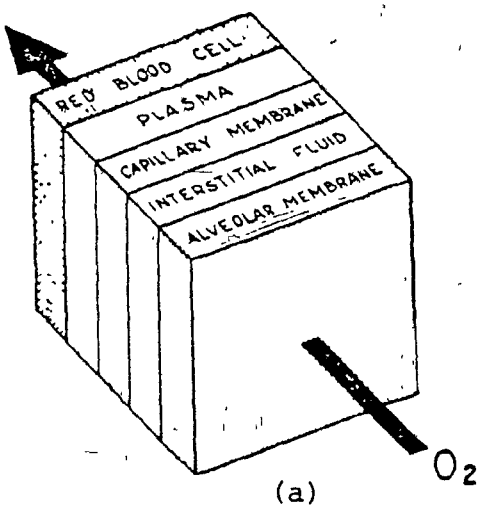


(a)

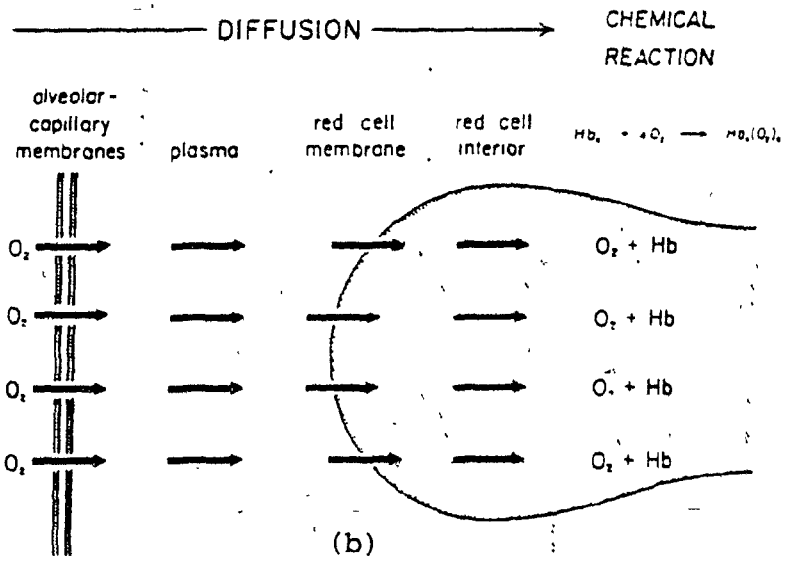


(b)

Fig.5.6 --Schematic Representation of Passage of $O_2$ Molecules from Alveolar Gas to Pulmonary Capillary Blood[6].

## 5.3 Inhalation and Deposition of Aerosols and Chrysotile Fibres in Lungs:

The human respiratory tract is designed to allow air to pass to regions of the lung where oxygen can be taken up into the blood stream. However, so called inhaled fresh air, carries a large number of suspended particles or aerosols. The aerosols have very small size, and depending on their size range they have extremely low settling velocities as described by Stoke's Law, Cunningham correction and Brownian motion(11)(12); therefore they are very much influenced by air movement and are thus likely to enter the breathing system during the breathing cycle. The inhaled dust, in the respiratory tract will follow the three principal physical laws of deposition. These are inertial impaction, gravitational sedimentation, and diffusion. Deposition by interception should be considered also. These principal laws of deposition are influenced by the physical and chemical characteristics of the particles, dimensions of the respiratory tract, the pattern of breathing, and by the pathological condition of the respiratory tract. One of the most important physical characteristics of the aerosols is the aerodynamic behaviour of the individual particles. This behaviour is influenced by the shape, size, diameter and the density of the particles. Particles could have the same density and

size, however because of their shape, such as flaky or fibrous shapes, they may not have the same settling velocities or aerodynamic behaviour. In more complex situations the particle density could be different as well. Therefore, the terminal settling velocities of airborne particles are, for convenience, compared to the diameters of equivalent unit density spheres having the same settling velocity. This can be expressed as follows (8):

$$De = \sqrt{\rho D^2}$$

where De = the diameter of an equivalent unit density sphere

$\rho$ = the density of the particle

D = actual diameter of the particle

The aerodynamic diameter can be defined as the diameter of a sphere of unit density having the same terminal settling velocity as the particle. Therefore, when the aerodynamic diameters of the particles are the same, and the forces which are acting on them are related to their mass, regardless of their shape, size and density, they will have the same aerodynamic behaviour.

The hygroscopic characteristics of airborne particles can affect the aerodynamic properties of an aerosol containing them. Airborne particles, depending on their affinity for water and the relative humidity of the air, will absorb some moisture. However, absorption of the moisture will not affect the particle size, if the particles are insoluble or the relative humidity is below the critical value for soluble particles (3) (8) (9). Also the aerodynamic particle

size change will not be significant for particles which have large densities. Because, as they absorb moisture there will be a decrease in their densities which will tend to offset the effect of increasing particle size[3]. However, when the relative humidity is above the critical value, the size of soluble hygroscopic particles will grow to reach an equilibrium diameter. The effect of electric charges on deposition of inhaled particles is compatible. However, the quantitative experimental evidence to support this opinion is very sparse[8].

5.3.1 Inhaled Aerosols and Physical Laws of Depositions

Inhaled particles will settle in different parts of the respiratory tract not only according to their aerodynamic size and terminal velocity but also according to the travelling velocity or nature of the flow pattern of the airflow. The air flow is greatly influenced by the frequency of the breathing cycle which affects the residence time of the particles in the different parts of the respiratory tract. If the ventilation rate is 200 ml/sec., the velocity of air flow may range from 180 cm/sec in the main bronchi to only 1/25,000 cm/sec., in the alveolar ducts[10]. Therefore it is important to understand the physical laws of deposition at different stages of the travelling velocities.

5.3.1.1 Impaction:

Some airborne particles, because of their high inertia, will tend to follow the path of their inertia instead of following the sudden changes in the path of

supporting air stream and will impact upon obstructions. This type of deposition of large particle sizes which are from few micrometres to 100 micrometres diameter is observed at the entrance of the nose, and the turbinates of the nasal passage where the flow velocity is high and direction changes are sudden, and at the branching (bifurcation) of the airways where the airflow divides into different directions. The probability of inertial impaction "I", of a particle is directly proportional to the particle's terminal settling velocity "$V_t$" times the average air stream velocity "Va" and inversly proportional to the radius "r" of the airway(4):

$$I \alpha V_t \cdot V_a \text{ Sin } (\theta/rg)$$

where "g" is the gravitational constant and "Θ" is the angle of the bifurcation. It can be seen that, when the particle size is large its settling velocity will be high, and if the air velocity and the bend angle are higher and the radius of the air way smaller, the probability of the inertial impaction will be higher as well.

5.3.1.2 Sedimentation:

Sedimentation under the force of gravity is another important physical law of deposition. Any particle in still air will fall and accelerate under the influence of gravitational pull, until the gravitational force acting on the particle will be equal to the sum of the air resistance and the buoyancy of the particle. From

this point on the particle will fall at a constant velocity which is called terminal settling velocity[11][12]. Terminal settling velocity of the particles within the 1 to 50 micrometre size range follows Stokes' law[8][11][12]:

$$V_t = (\rho - \rho_a) \frac{D^2 g}{18 \gamma}$$

where $V_t$ = terminal settling velocity

$\rho$ = density of the particle

$\rho_a$ = density of the air

$D$ = diameter of the particle

$g$ = gravitational constant

$\gamma$ = viscosity of the air

The calculated terminal settling velocity using Stokes' law equation assumes the fluid medium is continuous and that viscous drag is the only restraining force on a particle. However for particles smaller than 1 micrometre this continuity does not exist, and they fall more rapidly than calculated with Stokes' equation. The reason is, as the size of the particles approaches the size of the mean free path of the molecules of the suspending fluid, it is considered that particles tend to slip between the molecules of the fluid and thus acheive a higher terminal velocity. Therefore Cunningham's correction factor must be applied to correct the terminal settling velocities of particles less than 1 micrometres[11][12].

$$C = 1 + \frac{A_C \lambda}{r}$$

where: C = Cunningham Correction

$A_C$ = Constant (approximately 0.9)

$\lambda$ = mean free path of the fluid molecules

r = radius of the particle

the value of A in general will be near unity and only becomes significant for particles approaching the mean free path, less than 1 micrometre.

In table 5.3 a comparison of uncorrected and corrected terminal settling velocities and the Brownian displacement in the air of unit density spherical particles of size range 0.02 to 20 micrometre are shown. As it is seen, the effects of the correction factor decreases when the particle size is greater than 1 micrometre. Particles larger than 50 micrometres have slower terminal velocities, because of the generated turbulance while falling freely[8].

5.3.1.3 Diffusion:

Deposition by diffusion is due to Brownian motion of particles which are 0.2 micrometre or less in diameter. The Brownian motion is created by the bombardments of the particles by the gas molecules which are randomly in motion in the air. The root-mean-square Brownian displacement per second and the terminal settling velocity of a 0.5 micrometre particle is approximately the same. Therefore the diffusion process will dominate

the deposition of particles which have diameters and settling velocities smaller than 0.5 micrometre particles. The root-mean-square Brownian displacement is inversly proportional to the viscosity of the air and to the diameter of the particle and is directly proportional to the residence time of the particle:[4][11][12]

$$\bar{\Delta}^2 = \frac{RTC}{N3\pi\gamma D} t$$

where $\bar{\Delta}$ = Root-mean-square Brownian displacement

$R$ = Gas constant = 1.987 cal./mole °K

$T$ = Absolute Temperature in degrees Kelvin

$C$ = Cunningham Correction factor

$N$ = Avogadro's Constant = $6.02 \times 10^{23}$ atoms is contained in one gram-atom

$\gamma$ = Viscosity of the air

$D$ = Diameter of the particle

$t$ = Residence time of the particle

Table 5.3 Rates of Fall in Air at 760 mm Hg pressure and 20°C of Spherical Particles of Unit Density as Given by Stokes' Law and as Modified by Cunningham Correction Factor and Root-Mean-Square Brownian Displacement[8] [11]

| Diameter of Particle (μm) | Uncorrected terminal Velocity cm. $sec^{-1}$ | Corrected terminal Velocity cm. $sec^{-1}$ | Brownian Displacement cm |
|---|---|---|---|
| 0.02 | $1.2 \times 10^{-6}$ | $1.39 \times 10^{-5}$ | $9.04 \times 10^{-3}$ |
| 0.1 | $3.0 \times 10^{-5}$ | $8.60 \times 10^{-5}$ | $3.70 \times 10^{-3}$ |
| 0.2 | $1.2 \times 10^{-4}$ | $2.20 \times 10^{-4}$ | $2.01 \times 10^{-3}$ |
| 0.4 | $4.8 \times 10^{-4}$ | $6.85 \times 10^{-4}$ | $1.30 \times 10^{-3}$ |
| 1.0 | $3.0 \times 10^{-4}$ | $3.48 \times 10^{-3}$ | $7.43 \times 10^{-4}$ |
| 2.0 | $1.2 \times 10^{-2}$ | $1.30 \times 10^{-2}$ | $5.06 \times 10^{-4}$ |
| 10.0 | $3.0 \times 10^{-1}$ | $3.07 \times 10^{-1}$ | ----- |
| 20.0 | 1.2 | 1.2 | ----- |

As the confining space is decreased and the displacement motion increased, the probability of deposition by diffusion would increase also. With this type of deposition as the size of the particle decreases the Brownian motion increases and therefore deposition increases as well. However, in the case of sedimentation, as the size of a particle decreases the rate of deposition also decreases. Therefore, there is a point at which deposition is minimal since the terminal settling velocity as well as the Brownian displacement velocity is very low. This point coincides with the aerodynamic particle diameters of 0.5 to 0.2 micrometre range.

5.3.1.4 Interception:

Interception is an important parameter when the size of the particle approaches the size of the airway through which it is passing. According to Timbrell[13] when a particle is travelling through the centre line of an airway, interception will take place only when the distance from the surface of the particle to the airway walls is less than the diameter of the particle. However, the size of the terminal bronchiole is approximately 0.6 to 0.7 mm and the largest particle that could penetrate into this region has only a diameter of 10 micrometres; similarly the size of a respiratory bronchiole is in the range of 200 micrometre and the average particle size is 3 micrometres. Thus interception will not take place in these regions while the particle is travelling through the centre line of these airways. On the other hand, the interception and deposition of irregular shaped particles, specially particles with high aspect ratios such as asbestos fibres, is important; particularly in small airway bifurcations. Although very fine or small diameter symmetric shape fibres tend to align themselves with the axis of the laminar air flow, the majority of the asbestos fibres, more specifically chrysotile fibres, are not symmetric. Furthermore, other foreign particles are usually attached to the chrysotile fibres which eliminates the symmetry balance. Therefore, they are accepted to be unsymmetric and randomly aligned in the

air stream and the deposition by interseption is a highly possible process[3].

5.3.2 Aerosol and Chrysotile Fibre Deposition in the Respiratory Tract:

Another important parameter, besides the physiochemical characteristics of particle size and density, which affects deposition of the inhaled particles, is the characteristic of the airflow or the breathing pattern which affects the nature of the air flow. When the breathing pattern or cycle frequency is high, the air velocity is high and accordingly the residence time of the airborne particles in the respiratory tract is low, therefore, the deposition rate of the inhaled particles is low. Also when the tidal volumes are small, smaller quantities of particles are inhaled and fractional deposition values which affect the total deposition, are decreased as well. However, if the tidal volumes are large and the breathing cycle frequency is low, a larger amount of particles is inhaled and longer residence time is allowed, therefore, the deposition rate of inhaled particles is substantially increased[18]. For mathematical modelling of particle deposition in the respiratory tract, the Task Group on Lung Dynamics[3], adopted the respiratory cycle frequency as 15 respirations per minute and tidal volumes of 750, 1450 and 2150 cubic centimetre. For the normal breathing of a person, who is undertaking a mild or moderate activity, the tidal

volume of 750 cubic centimetre is accpeted to be adequate. The other two higher tidal volumes were accepted to be adequate for the following conditions: a relatively sustained work state 1450 cubic centimetre, and a state of greater activity, but not capable of sustaining it too long, 2150 cubic centimetre. The type of airflow in the respiratory tract, with the exception of the nasal passage, is laminar. Because of the narrowness and curvature of the airways, and the high velocities attained by the air in the nasal passage turbulent type of airflow is created. By using a dimensionless parameter called Reynolds number, it is possible to determine the type of flow in tubes or pipes.

$$R_e = \frac{\rho_a d V}{\gamma}$$

where: $R_e$ = Reynolds parameter.

$\rho_a$ = Density of the fluid (air)

$d$ = Diameter of the tube or passage

$V$ = Velocity of the flow in the tube

$\gamma$ = Viscosity of the fluid

In long and cylindrical tubes when the Reynolds number is below the critical value 2000, the flow normally is laminar, and when it exceeds 3000 the flow is usually turbulent. In laminar flow the suspended

particles are distributed nearly uniformly across the cross section of the airway and the velocity profile is parabolic which indicates that the velocities of the air and particles in the axis of the airway is highest and it decreases towards the boundaries of the airway and reaches zero at the walls of the airway. When the flow velocity approaches zero, the settling velocity of the particles attains the terminal settling velocity and rapid deposition takes palce.

Findeisen (1935) developed a theoretical mathematical model of inhalation and deposition of dust particles in a simulated lung. The model assumed a constant rate of inspiration and expiration 200 millilitres per second at 14 cycles per minute. The principle deposition criterion was that in the upper respiratory tract, deposition of the dust was due to impaction, in the bronchiolar lung sedimentation, and in the respiratory lung the primary deposition process was diffusion. Later in 1950 Landahl improved this mathematical model by calculating the probabilities for the three particle deposition processes and combined these probabilities for each region of the respiratory tract[18][4]. These and other theoretical and experimental results of other researchers for total respiratory tract deposition fraction and pulmonary deposition fractions of inhaled dust are

illustrated in figures 5.7 and 5.8 respectively.[18]

5.3.2.1 Nasopharyngeal Deposition:

The nose is a good filter for particles greater than 5 micrometre diameter and is very efficient for particles larger than 8 micrometres. In this size range deposition is according to the inertial impaction principles. However, very small particles which are less than 0.01 micrometre are filtered by the nose according to the diffusion principle. The Task Group on Lung Dynamics [3][4][8] has accepted the work of Pattle and used his formula for calculating the nasal deposition of particles. With this empirical formula, the nasal deposition for a given particle size is expressed as follows:

$$N_d = -0.62 + 0.475 \log D_a^2 F$$

where; $N_d$ = Nasal deposition

$D_a$ = Aerodynamic diameter of the particle in μm

$F$ = Flow rate in litres per minute

Later Hounam et al.[19] indicated that when the flow rate is varied for the same particle diameters there is considerable scatter in deposition rates. To correct this Hounam et al. expressed nasal deposition as a function of the pressure differential between nose and mouth and calculated the probability of deposition of particles in the nasopharynx as follows:

$$\text{Nasal Deposition Probability} = -1.66 + 0.66 \log D_a^2 F^{1.52}$$

However, the pressure difference between mouth and nose is considerably variable from person to person and even

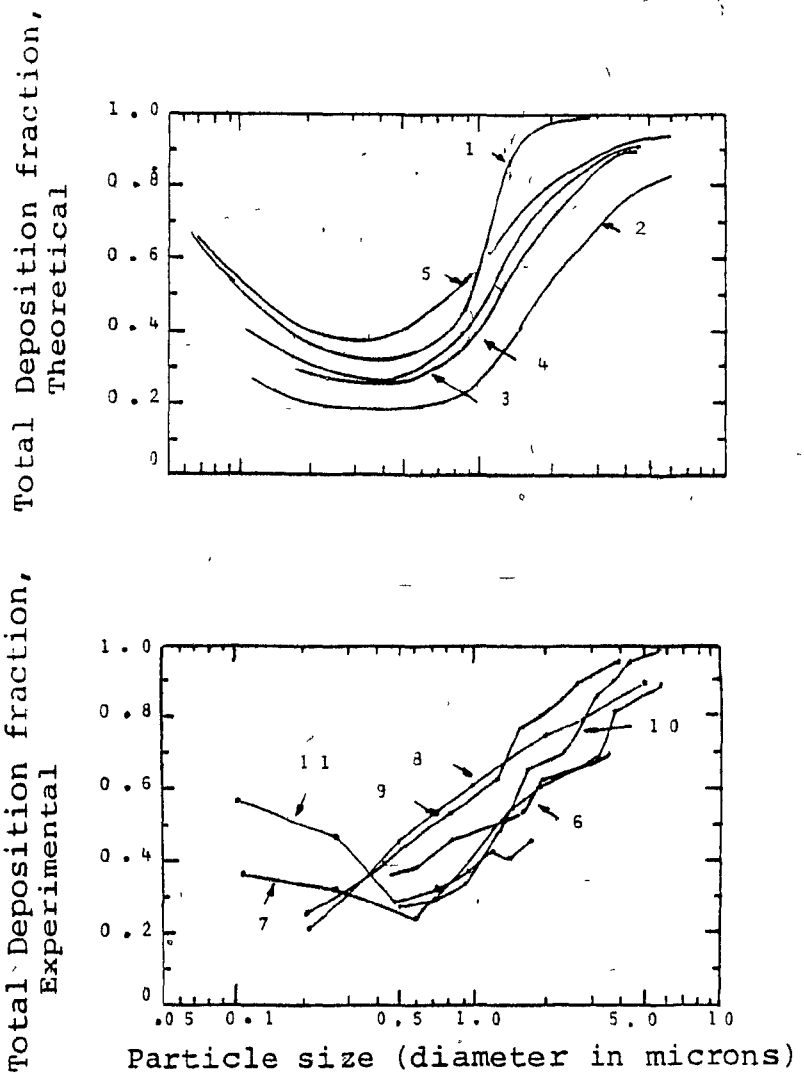


Fig. 5.7[18] - Theoretical and experimental determinations of the total deposition fractions of inhaled particles. Theoretical results: curve 1, Findeisen, 200 ml/sec, 14 respirations/min. Curves 2 to 4 Landahl, using 300 ml/sec, 5 respirations/min, tidal volume 450 ml; 300 ml/sec. 7 1/2 respirations/min, tidal volume 900 ml; 1000 ml/sec. 15 respirations/min, tidal volume 1,500 ml. Curve 5, Beeckmans, 5 respirations/min, tidal volume 1,350 ml. Experimental results: curve 6, Wilson and La Mer, 5 1/2 respirations/min. Curve 7, Landahl et al, 7 1/2 respirations/min, tidal volume 900 ml. Curve 8, Gessner et al, 15 respirations/min. tidal volume 700 ml. Curve 9, Van Wijk and Patterson, 19 respirations/min, tidal volume 700 ml. Curve 10, 13.3 respirations/min. tidal volume 720 ml. Curve 11, Dautreband and Walkenhorst, 10 respirations/min, tidal volume 990 ml.

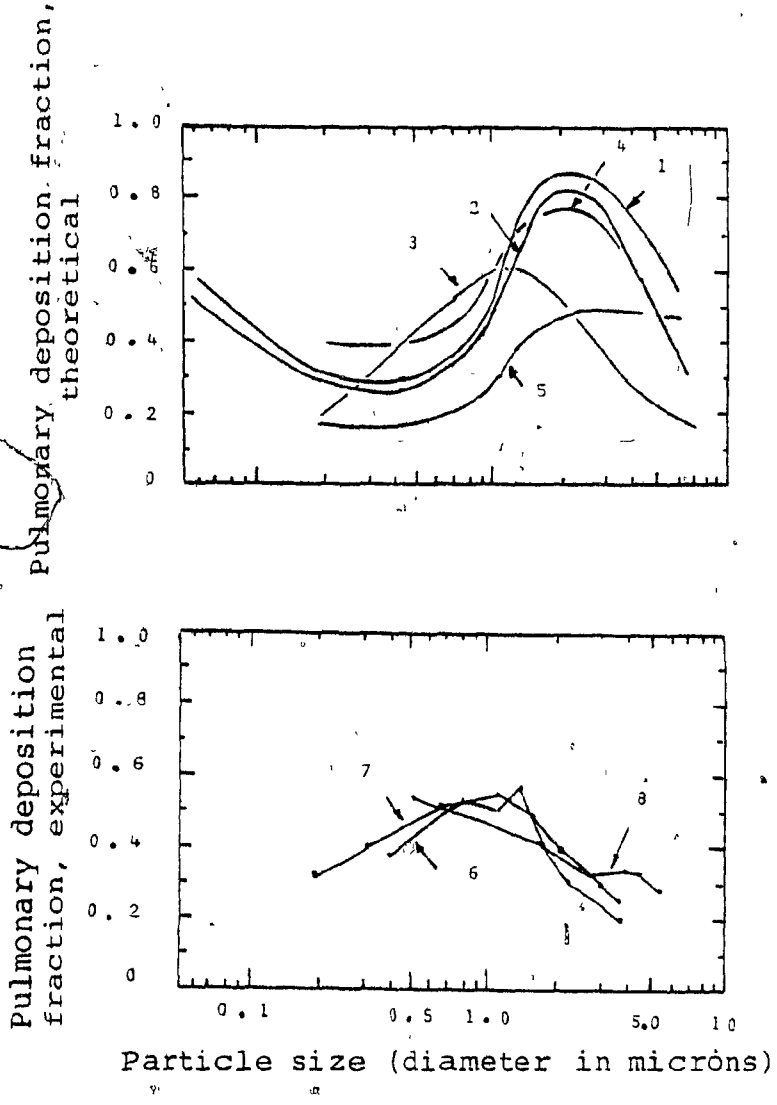


Fig. 5.8[18] - Theoretical and experimental determinations of pulmonary deposition fractions of inhaled particles. Theoretical results: Curve 1, Findeisen, 14 respirations/min. deposition in respiratory bronchioles and below; Curve 2, Findeisen as in curve 1, deposition in alveolar ducts and sacs Curve 3, Hatch and Hemeon. Curve 4, Landahl 300 ml/sec, 5 respirations/min. tidal volume 1,350 ml, deposition in bronchiole and smaller airway. Curve 5, Landahl, 15 respirations/min, tidal volume 450 ml, deposition in respiratory bronchioles and below. Experimental results: curve 6 Wilson and La Mer, 5 1/2 respirations/min. Curve 7, Brown et al., 15 respirations/min, tidal volume 700 ml. Curve 8, Gessner et al.

it is variable for the same person at different times. The major parameter that affects this difference is the size changes of the cross section of the nasal passages from one person to another. Also the cross section size of a nasal passage varies with the flow rate for the same individual.

The rate of deposition of particles in the Nasopharyngeal region according to their aerodynamic size is shown in Figs. 5.9 and 5.10 as adopted from the Task Group on Lung Dyhamics. In real life the variation of deposition in Fig. 5.10 is related to the heterogeneous distribution of aeresols. Therefore, in practice it is accepted that all aerosols have lognormal skewed size distribution and are named as polydispersed aerosols and geometric standard deviation of size ranges from 1.2 to 4.5 micrometre at a tidal volume of 1450 cubic centimetre.

5.3.2.2. Tracheobronchial Deposition:

Tracheobronchial deposition constitutes a maximum of 10 percent for all inhaled particle sizes through nose breathing[3][4][8], (see Figs. 5.9 and 5.10). The deposited dust particles rapidly and efficiently are removed from this region, particularly from the larger airways by mucociliary action. Experimental work by Lippmann et al[25][26] has shown that, for mouth breathing, deposition in the tracheabronhial tree is mainly due to inertial impaction at least for particles greater than 4 micrometres of unit density. The experimental work and

calculations have also indicated that inertial impaction is the main mechanism of deposition for the first 10-12 airway generations. However beyond the 12th generation a transition from deposition by impaction to sedimentation starts to take place and sedimentation governs the deposition for the bronchiolar region. In the bronchial tree where the deposition mechanism is due to impaction, deposition primarily occurs on the bifurcations of the airways[25][30]. As the particle size becomes smaller than 4 micrometres deposition by impaction decreases and deposition by sedimentation increases; and sedimentaion practically dominates the deposition mechanism when the particle size is 2 or less than 2 micrometres[26][30][31]. Similarly deposition by impaction increases as the particle size becomes greater than 4 micrometres. Deposition efficiency of the tracheobronchial region by impaction is less than the head deposition efficiency. However, in the tracheobronchial tree deposition by impaction is more efficient than by sedimentation. For a given particle size, tracheobronchial deposition varies from person to person due to the size difference of the airways of each individual person[26][3]. Therefore since the deposition characteristic alters with the physiological change, it is correct to state that the deposition characteristics do change with the alterations of pathological factors. Lippmann et al.[26] has indicated that tracheobronchial deposition of particles,

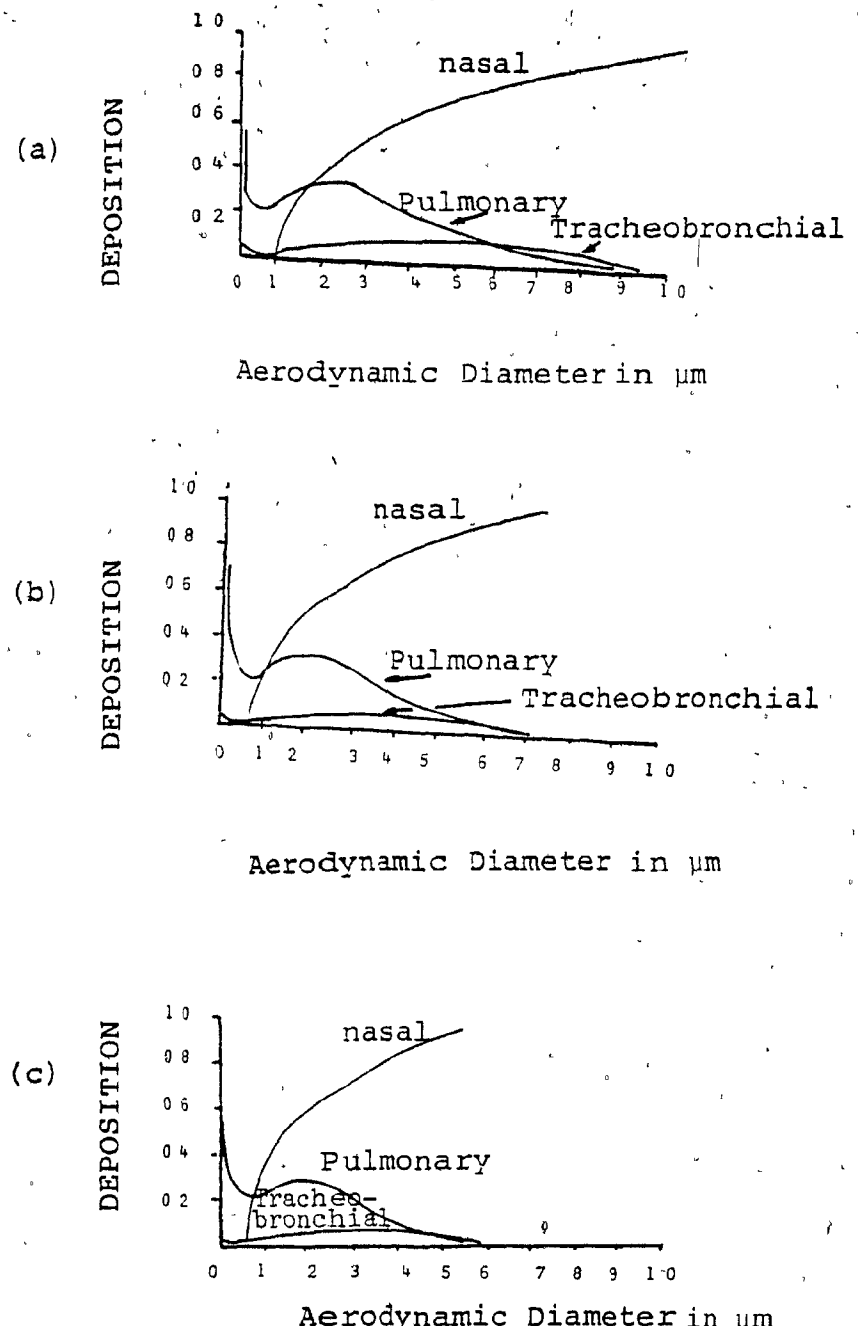


Figure 5.9 (a)(b)(c)[18] Deposition as a function of particle size for 15 respirations/min
(a) 750 $cm^3$ tidal volume.
(b) 1450 $cm^3$ tidal volume.
(c) 2150 $cm^3$ tidal volume.

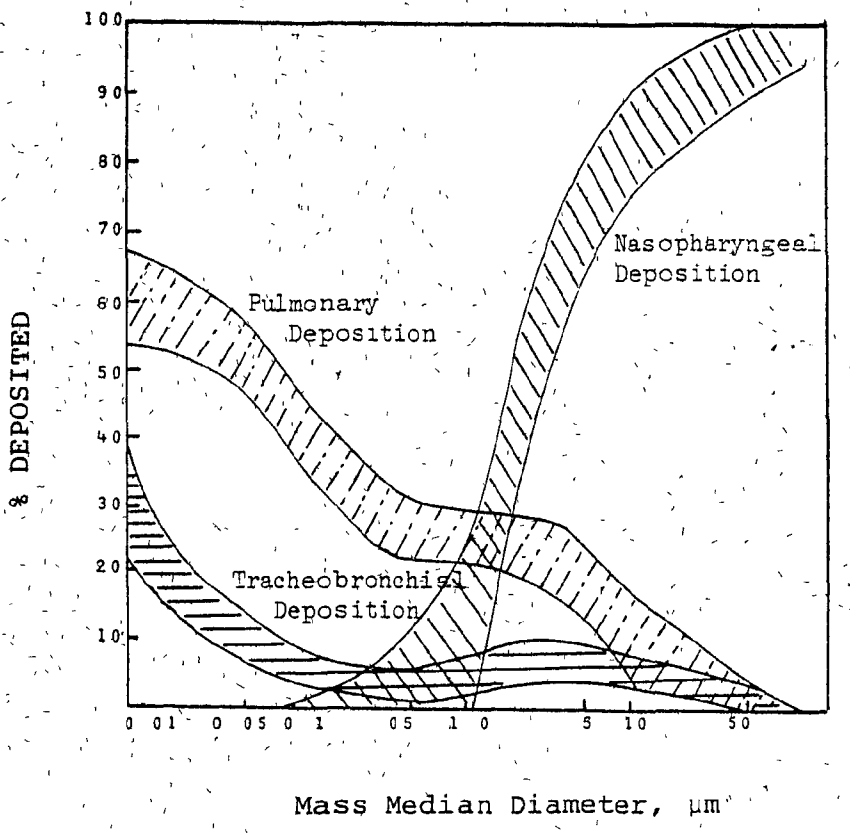


Figure 5.10[20] Aerosol deposition in respiratory tract. Tidal volume is 1,450 ml; frequency, 15 breaths per minute. Variability introduced by change of sigma, geometric standard deviation, from 1.2 to 4.5. Particle size equals diameter of mass median size. (Adapted from Task Group on Lung Dynamics )

between 1-5 micrometre size range, is substantially increased for the persons who have asthmatic and bronchitic lungs in comparison to healthy persons. Among the smokers, deposition of particles in the tracheo-bronchial region has also shown some increase with comparison to non-smokers. However, for persons who have stopped smoking for the last 15 to 20 years the deposition was at the upper normal limits of healthy persons.

Lippmann et al. have used Landahl's formulas for the calculation of regional deposition in the lung, by impaction and sedimentation[34]. For impaction the expected deposition "E" at bronchial bifurcations is equal to:

$$D_e = \frac{X}{1 + X}$$

where $X$ = Deposition Parameter = $5 \times 10^{-5} \frac{\rho D_e^2 Q}{d_a S_{(a-1)}}$

where $\rho$ = particle density in $g/cm^3$

$D_e$ = particle diameter in micrometres

$Q$ = air volume in litres/minute

$d_a$ = diameter of airway at generation "a" in centimeters

$S_{(a-1)}$ = total cross section of all airways of generation (a-1) in cm. square.

For this genralized formula air viscosity at 37°C is accepted to be $189 \times 10^{-6}$ g/cm sec. and the branching

angle of the airways is 30° and the sine of the angle is equal to 0.5.

The fractional deposition "S" by sedimentation is equal to: $S = 1 - E\ (-0.8\ V_t.t.\text{Cos}\ \psi)/r$

where: $V_t$ = terminal settling velocity

$t$ = time of travel along the airway

$\psi$ = angle of the airway to horizontal

$r$ = radius of the airway

Regardless of the deposition mechanism by which inhaled aerosols are deposited, most of the particles in the tracheobronchial tree are cleared out by mucocilliary action within 24 hours. However, those particles which have penetrated into deeper parts and settled at nonciliated regions are retained for much longer times.

5.3.2.3. Pulmonary Deposition:

The majority of the large size inhaled aerosols are filtered by nose or mouth and tracheobronchial tree. Therefore, when aerosols reach to the pulmonary region of the respiratory tract particles larger than 5 micrometres are not inexistent with the aerosols. However, experimental work has indicated that when the subject is breathing through the mouth 30 to 50% of 5 micrometre particles are being deposited beyond the ciliated airways. This rate dropped substantially when breathing was through the nose. The main reason is that the nasopharyngeal compartment has a high filtering efficiency for the

particles of this size and larger[7][8][26][32]. In the pulmonary region, particles within the size range of 0.5 to 5 micrometres will be deposited by sedimentation as described earlier, and by diffusion for the sizes smaller than 0.2 micrometres. The Task Group on Lung Dynamics has used the theory of Gormley and Kennedy[33][35] to predict the probability of deposition "ω" by diffusion in laminar airflow.

$$\omega = 1 - 0.819e^{-7.314h} - 0.0975e^{-44.6h} - 0.0325e^{-114h}$$

for $h > 0.0156$, and

$$\omega = 4.07h^{2/3} - 2.4h - 0.446h^{4/3}$$

for $h < 0.0156$ with $h = \frac{\pi \ell D_c}{2\upsilon}$

where: $\ell$ = length of the airway in cm,

$\upsilon$ = volumetric flow rate in litres/minute

$D_c$ = diffusion coefficient $= \frac{RTC}{N3\pi\gamma d}$

where: R = gas constant

T = absolute temperature in degrees Kelvin

C = Cunningham correction

N = Avagadro's constant

$\gamma$ = viscosity of the air

d = diameter of the airway in cm.

When the figures 5.9 and 5.10 are studied carefully, scarcely any particles above 4 micrometres diameter are exhaled. In the pulmonary region, maximal particle deposition occurs between 3 and 0.8 micrometre diameter range, and approximately 80 percent of the particles

in the 0.5 to 0.2 micrometre size range are exhaled with the air. As explained earlier at this size range deposition by sedimentation and diffusion process is minimum. Due to the small aerodynamic diameter of the particles sedimentation is not an effective mechanism. Deposition by diffusion is also not effective because the particle size is too large for Brownian motion. However as the particle size gets smaller than 0.2 micrometre deposition efficiency increases substantially. The main reason is that Brownian motion is independent of density and reaches a maximum when the particle size is smaller than the free path of the gas molecules in which they are suspended. Experimental studies of the total deposition of aerosol particles in the human respiratory tract by Heyder et al[30] have indicated that the deposition rate of particles of 0.2 to 1.0 micrometre range is much lower than the earlier researchers'results, as well as the Task Group on Lung Dynamics theoretically calculated results. For the above mentioned particle size range, the deposition rate for 750 cubic centimetre tidal volume was calculated to be 20 percent by the Task Group. Heyder et al.'s results indicated 10 percent deposition for a 500 cubic centimetre tidal volume. At first glance, the difference in deposition could be attributed to the lower tidal volume used by Heyder et al. However Davies[31] explains that the diffusion rate of particles of 0.5

micrometre size is 1/50,000 of the diffusion rate of gases. Therefore, during steady breathing only 10 to 15 percent of 0.5 micrometre particles are lost in the reserve air due to mechanical mixing. All the rest are breathed out again. Although sedimentation rates of 0.5 and 1.0 micrometre particles are, respectively, 0.001 and 0.0035 cm/sec. experimental results have shown that practically there is no difference in their deposition rate during steady breathing. This observation indicated that although the deposition of particles of this size range; in the alveolar region is due to sedimentation, the deposition rate determining factor is the mechanical mixing of tidal and reserve air in the 200 centimetre cube of dead space. The mechanical mixing was proven by Heyder et al. when some 0.5 micrometre particles were recovered by deep exhalation of the reserve air after nine breaths of clean air, following a single breath of aerosol[31].

A comparison with recent experimental data and the deposition model of the Task Group on Lung Dynamics was done by Mercer[32]. Mercer states that the experimental results of total deposition during the nasal breathing, correspond very well with the deposition model of the Task Group. However, the experimental results of deposition for mouth breathing are scattered and indicate that the Task Group's model underestimates

the deposition by the impaction mechanism in the Tracheo-bronchial region. Because of this, deposition in the pulmonary region is over estimated by the Task Group's model. However, as a general comparison tool it is adequate at present. Mercer[32] states that "to provide the same degree of protection for all individuals subject to an inhalation exposure, it would be necessary to determine the deposition characteristics of each individual". This statement indicates that from one person to another deposition efficiency changes substantially.

5.3.2.4 Deposition of Chrysotile Fibre:

Deposition of chrysotile fibres in the respiratory tract is effected by the same principal deposition mechanisms, such as: Inertial impaction, sedimentation and diffusion, as described for compact particles. However, the interception mechanism for fibre deposition plays an important role in addition to the above mechanisms. Timbrell[13] has shown that deposition by interception increases with increasing length of fibres and decreasing size of the respiratory tract. Although the size of compact particles found in the pulmonary region is 10 micrometres or less, the chrysotile fibres found in alveoli are usually 50 micrometres long. However, fibres longer than 200 micrometres have also been found in alveoli [15] [16]. This is an indication that the length of the fibres, in deposition, is secondary in importance. Timbrell [13] demonstrated that the rate of deposition of fibres,

measured in terms of their free-falling speed, is a function of their aerodynamic diameters. In Fig. 5.11 the reationship of actual chrysotile fibre diameter to the equivalent aerodynamic diameter is shown[13]. These results indicate that, for practical purposes, the equivalent chrysotile fibre diameter can be estimated by multiplying the actual fibre diameter by 2.5, this shows that a 4 micrometre diameter chrysotile fibre has same settling rate as a 10 micrometre sphere of density 1.1 g/cc. Later studies of Timbrell[14][15][16] concluded that because of the limiting effects of the gravitational settlement and inertial impaction, asbestos fibres with actual diameters of less than about 3 micrometres can reach the pulmonary air spaces. Note that, the length of inhaled fibres is shorter than that of the fibres in dust clouds, and longer fibres are deposited mainly in the narrow air ducts and particularly at bifurcations [15][16][17]. Very long, slender and straight fibres could align themselves with the air stream and could penetrate into the deepest parts of the pulmonary region of the lungs. However, chrysotile fibres are usually in bundles and their orientation is influenced by the other aggregates which are attached to them. Furthermore, chrysotile fibres are curly, this curvature decreases the efficiency of penetration[15][17], and therefore they settle in the upper parts of the respiratory tract[36].

Beeckmans' theoretical study of the deposition of unit density ellipsoidal particles in the human respiratory tract[37] has also concluded that the aspect ratio of the fibres practically has no effect on the settling rate of fibres in the respiratory tract. However, when the aspect ratio is large, such as 100 (see Fig. 5.12) and 64 (see Fig. 5.13) the maximal deposition points have been shifted towards the right to over 5 micrometres equivalent aerodynamic diameter. On the other hand, spherical particles while deposited maximally have approximately 2.5 micrometre size. Similarly, the minimal deposition range for elongated fibres shifted towards the left from 0.3 μm to 0.07 (see Fig. 5.13)[38]. The reason for both cases is that the mass of ellipsoidal particles is much higher than that of the spheres for the same actual diamters. Therefore, it is correct to state that for long fibres in the particle size range at and above 0.2 micrometres, sedimentation and impaction are more important deposition mechanisms than diffusion; since the diffusion coefficient of a particle is proportional to its mobility, and the mobility of heavy particles is low.

Studies on the deposition of inhaled fibrous material (crocidolite) in the respiratory tract of rats and its subsequent clearance using radioactive tracer techniques have been done by Evans et al[39] and it was found that 50 $\pm$ 5 percent of the deposited crocidolite was in the lower respiratory tract. After 30

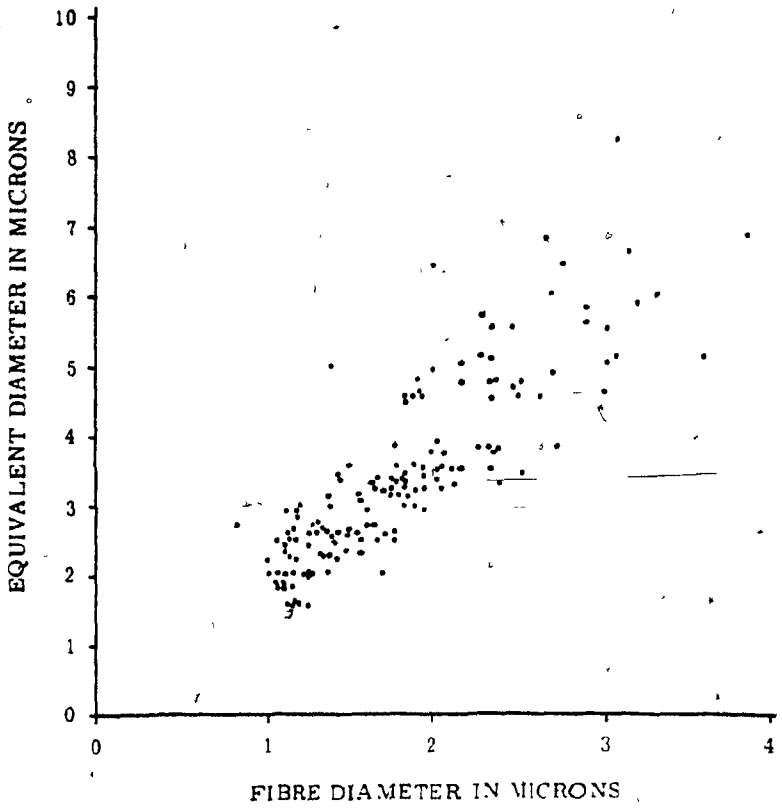


Figure 5.11[13] Equivalent diameters of chrysotile fibre of different lengths

days, 27 percent of the retained dust was found to be cleared out from the rat's lungs. As a continuation of this research project, Morgan et al.[40] reported that similar results were achieved and fibres were present in airways, particularly at bifurcations and in the alveoli. Because of the efficient mucociliary clearance action of the main bronchi, little fibre was found in this region. Compared to amphibole asbestos, chrysotile deposition was much less. This could be explained by stating that the curly or coil shaped chrysotile fibres do not have the same penetration ability or efficiency of amphiboles.

Recently Haris and Fraser[41] have developed a mathematical model for the deposition of fibres in the human respiratory system for thin straight rods of various equivalent aerodynamic diameters and lengths, for each of three tidal volumes. Results are shown in figures 5.14, 5.15 and 5.16. The drawn curves for each region of the respiratory system have the general configuration of those developed by the Task Group on Lung Dynamics model for compact particles. The curves for rod deposition are shifted towards the right in comparison to curves for compact particles of the same falling speed; the size of the displacement increases with increase in rod length. One of the important indication of this work is the efficiency of nasopharyngeal filtering ability which increases, with increase

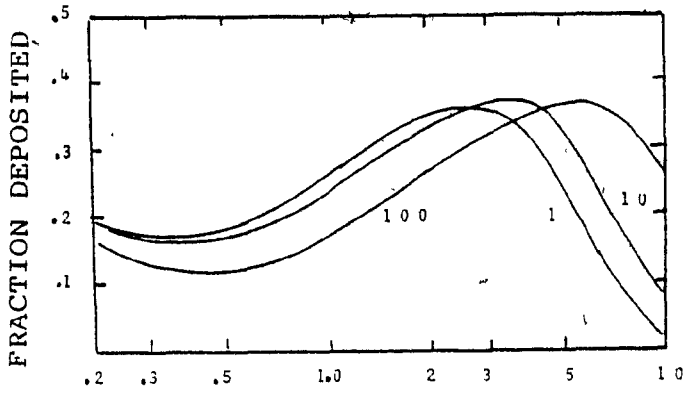


Figure 5.12a (37) Fraction of inhaled particles deposited in the lower respiratory tract versus volume-equivalent sphere diameter (microns), for aspect ratio values of 1 (sphere) 10 and 100.

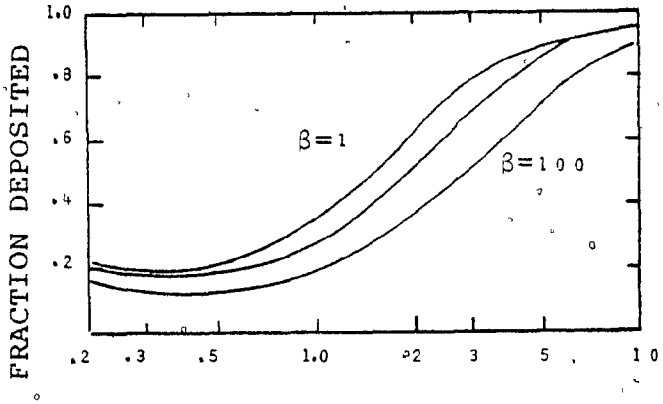


Figure 5.12b (37) Fraction of inhaled particles deposited in all regions of the respiratory tract versus volume-equivalent sphere diameter (microns), for β values of 1, 10, and 100.

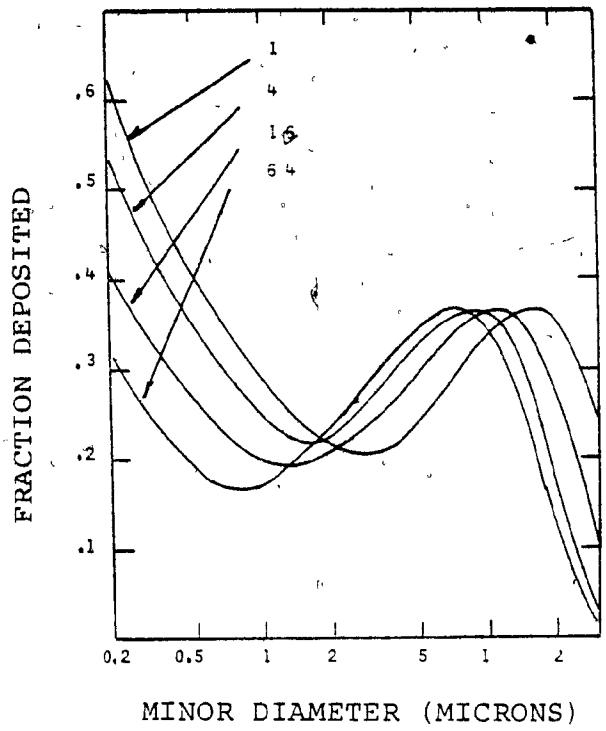


Figure 5.13[38] Fraction of inhaled particles deposited in the lower (alveolated) region of the respiratory tract, vs equatorial diameter of the particle, for various values of aspect ratio.

length of the rods at a greater rate than the size increase for compact particles. This is due to the interception of long particles which have small equivalent diameters of 0.5 to 1 micrometre by the nasal hair. Normally, such small size compact particles do not deposit in the nose. Since as the length of the rod increases the deposition in the nose increases, the number of the rods remaining to be deposited in the tracheobronchial and pulmonary regions decreases. Although 90 percent of the 200 micrometre rods are deposited in the nose one percent of the one micrometre diameter rods appear to be deposited in the pulmonary region. This result is consistent with the reported findings of similar size fibres in the human pulmonary spaces. Later, Harris and Timbrell[14] have improved the mathematical model and applied it to UICC* asbestos chamber aerosols which contained single fibres at ordered orientation, and single, double and triple fibres at random orientations. The results are shown in figures 5.17, 5.18, 5.19 and 5.20. The same conclusions can be drawn for this model as for the previous mathematical model. The only difference is that random doublets and triplets are cleared more efficiently in the nose because of the increase in their aerodynamic diameter. However, the percent of deposition of triplets in the pulmonary region is lowest, since a great number of them is deposited earlier.

---

*UICC asbestos is standard reference samples of asbestos, which is initiated by the International Union Against Cancer (UICC)

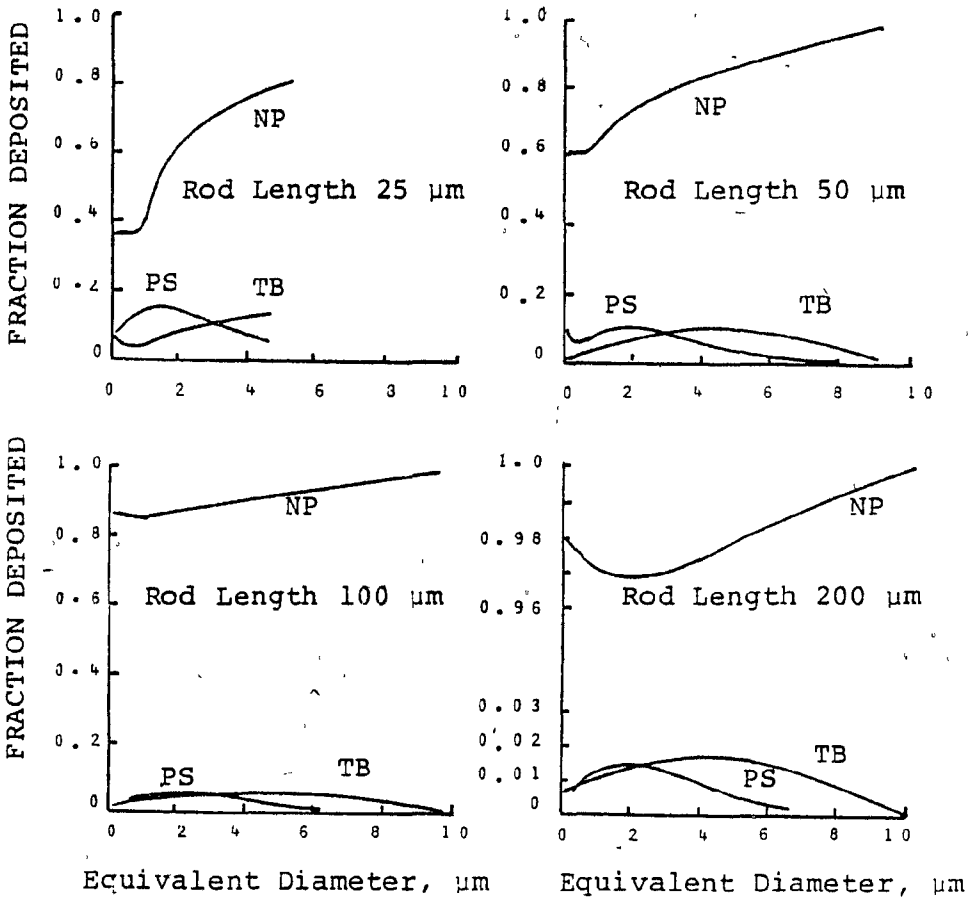


Figure 5.14 [41] Fractions of rods of selected lengths which are predicted to deposit in each respiratory compartment. (tidal volume 750cm$^3$.)
NP = nasopharynx, TB = tracheobronchial,
PS = pulmonary spaces

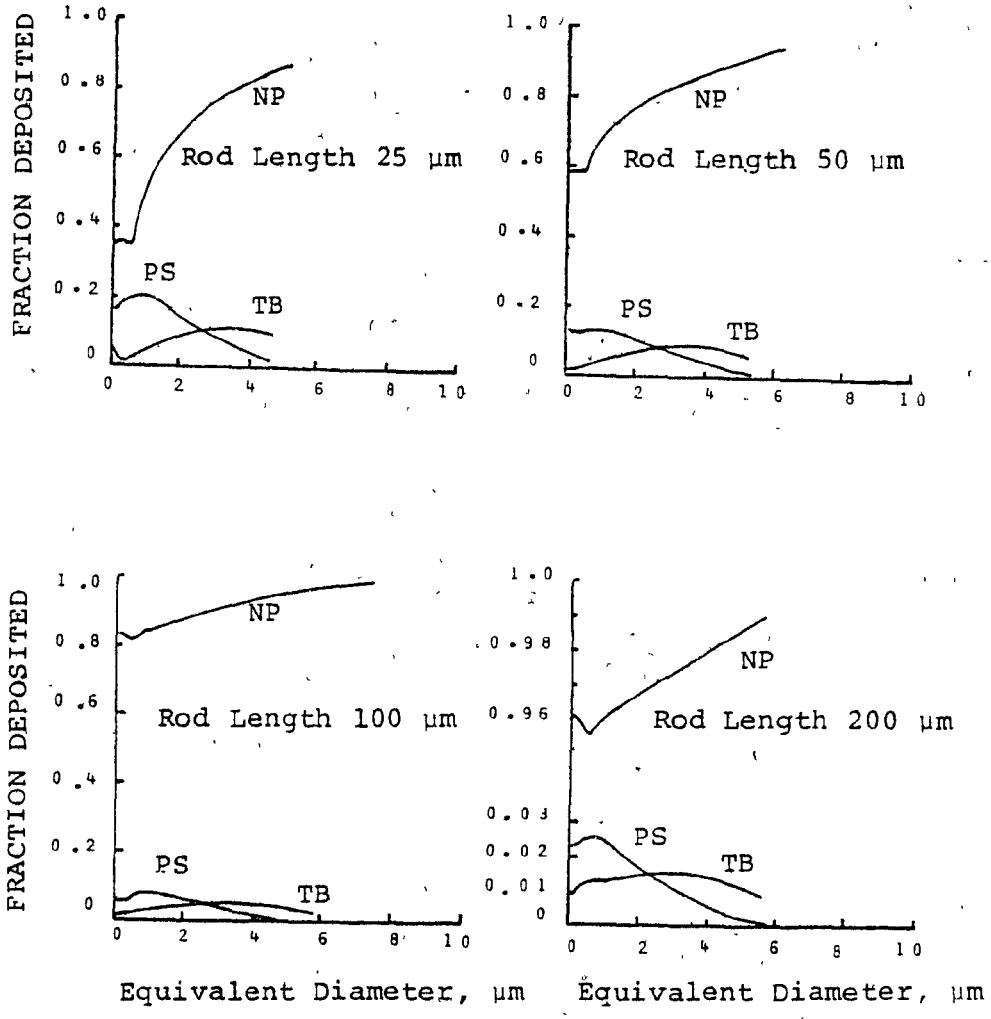


Figure 5.15[41] Fractions of rods of selected lengths which are predicted to deposit in each respiratory compartment. (tidal volume 1450 $cm^3$.)
NP = nasopharynx, TB = tracheobronchial,
PS = pulmonary spaces

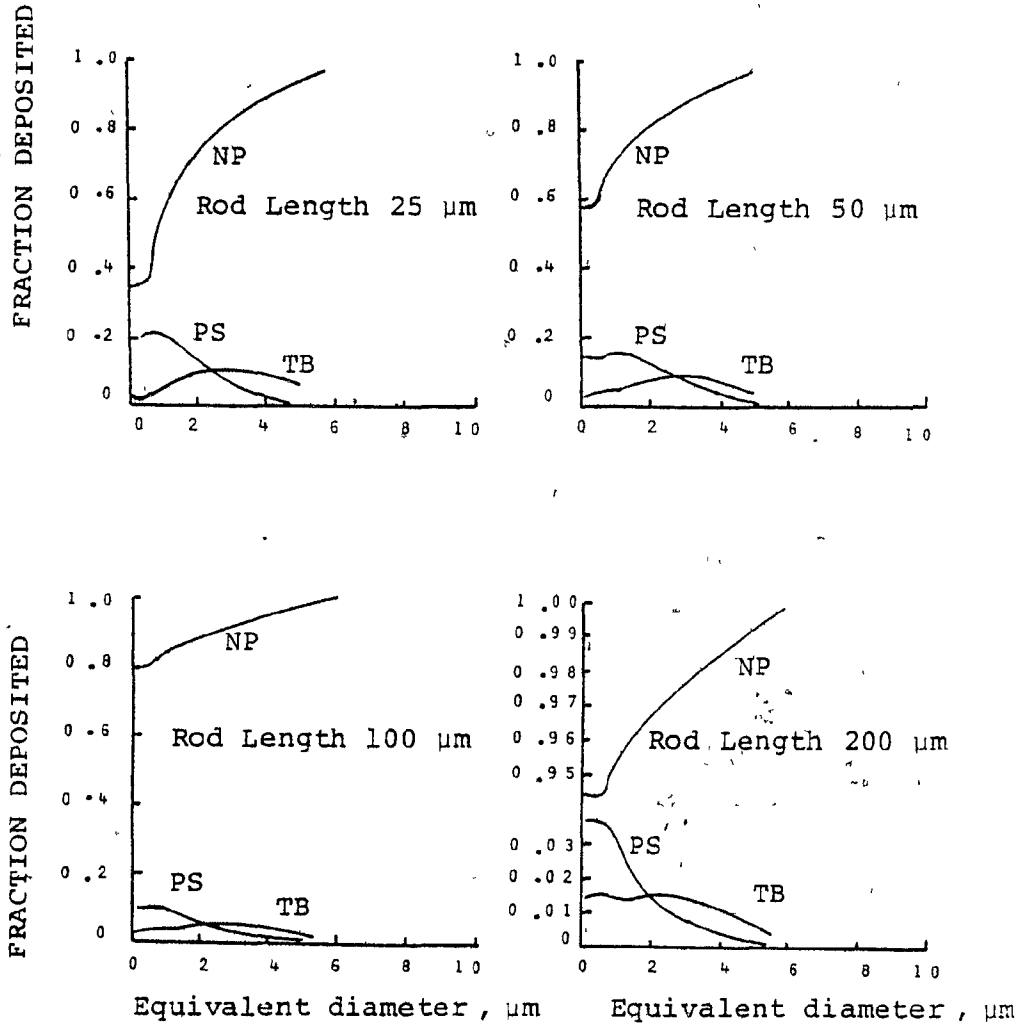


Figure 5.16[41] Fractions of rods of selected lengths which are predicted to deposit in each respiratory compartment. (tidal volume 2150 $cm^3$.)
NP = nasopharynx, TB = tracheobronchial,
PS = pulmonary spaces

Single random fibres escape from being deposited early, and penetrate into pulmonary space in greater number. Because of their slender shape it could be possible for them to align themselves with the air stream axis and avoid earlier interception. Also, the mathematical model has predicted the pulmonary deposition for the single straight fibres in ordered orientation about twice as great as for irregular fibres in random orientation[14].

Therefore, the deposition of fibres is influenced by their aerodynamic size, shape or length and their orientation in the air stream.

5.4 Elimination of Aerosols and Chrysotile Fibres From Lungs:

Although the deposition of inhaled particles is a continuous process, the lungs are exceptionally clean and sterile[42]. According to Gross et al.[43] 99 percent of the inert, insoluble particles are efficiently cleared from the lung. The autopsy results of black lungs of coal mine workers have indicated that they contain less than 5 percent of the estimated coal dust[42]. Similarly, the lungs of asbestos workers who had severe asbestosis did not contain the expected large number of fibres[19]. This indicates that the clearance mechanism of the lung is very efficient. The efficiency of the clearance rate of particles from the respiratory tract is dependent on the following factors:

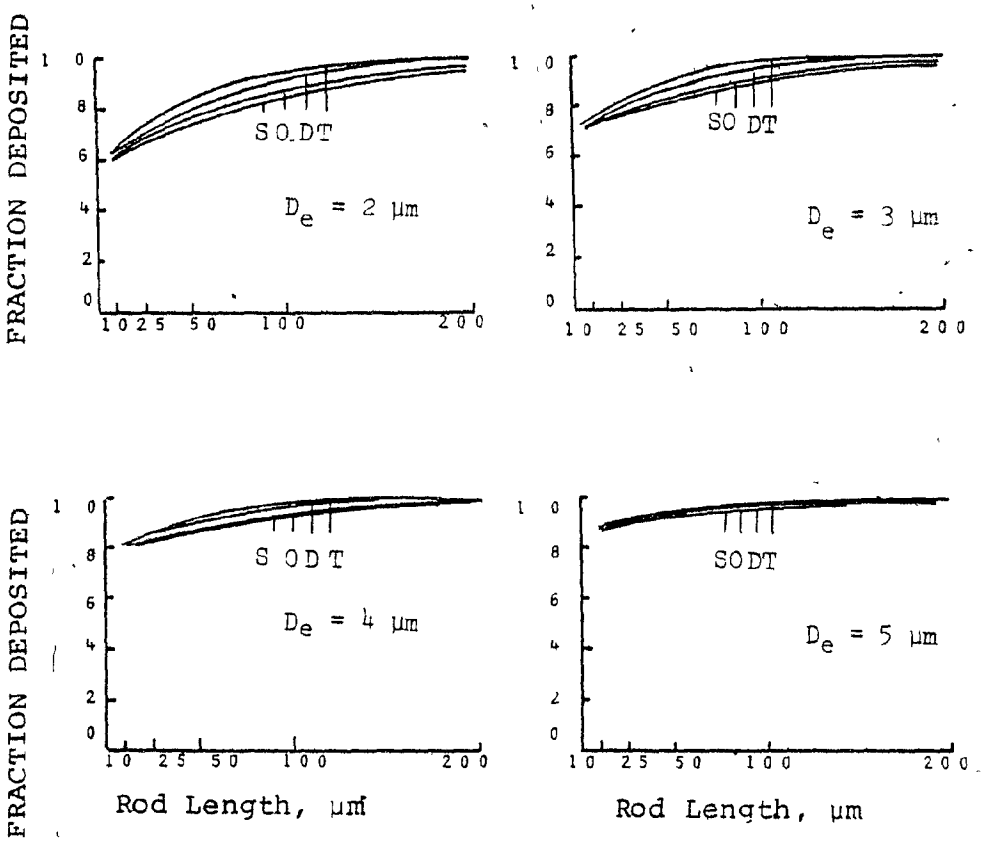


Figure 5.17[14] Nasopharynx, predicted deposition by $D_e$ and length (O: ordered single; S: random single; D: random doublets; T: random triplets)

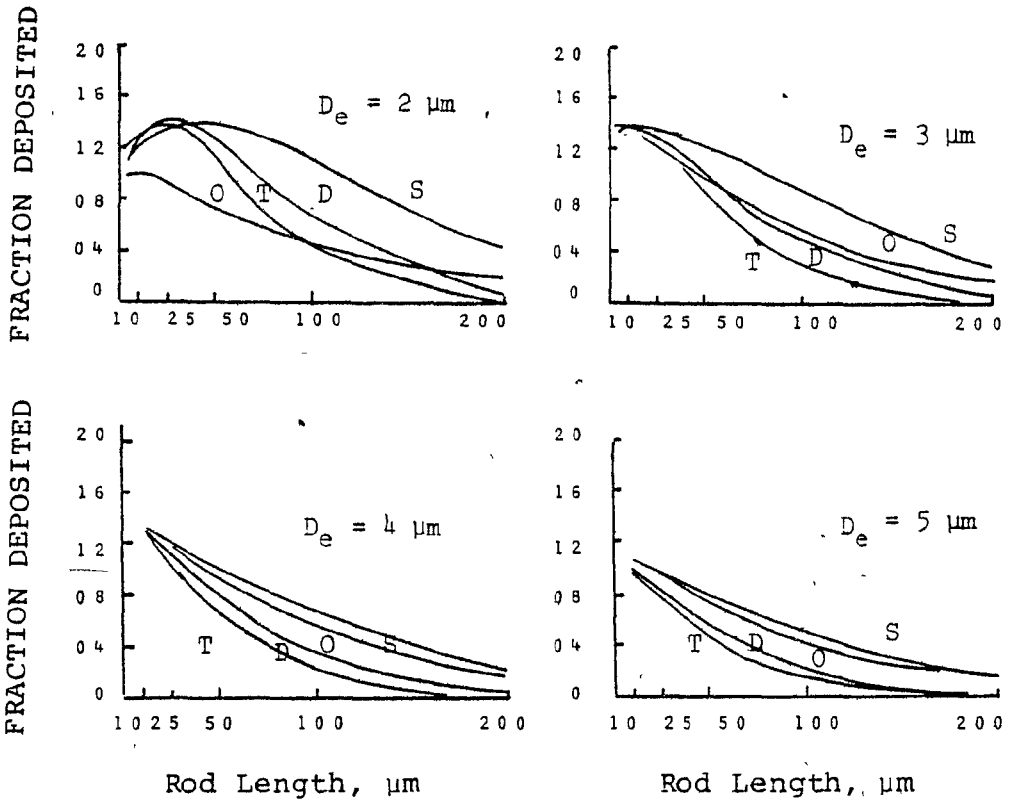


Figure 5.18[14] Tracheobronchial, predicted deposition by $D_e$ and length

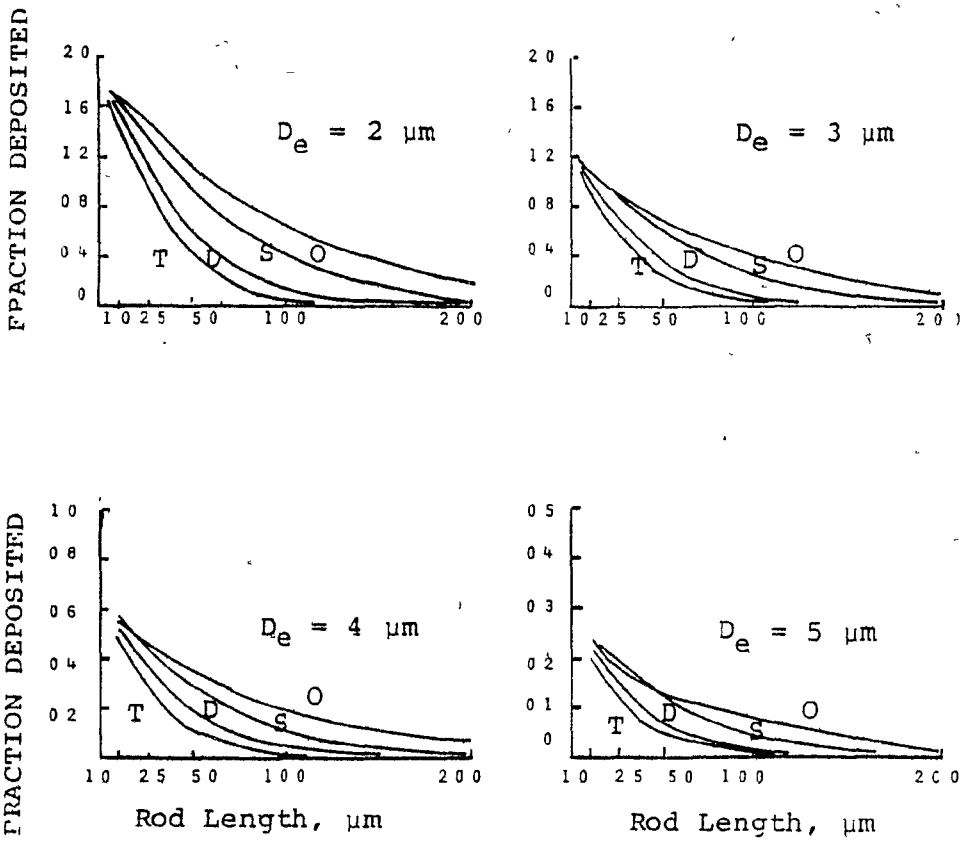


Figure 5.19[14] Pulmonary spaces, predicted deposition by $D_e$ and length.

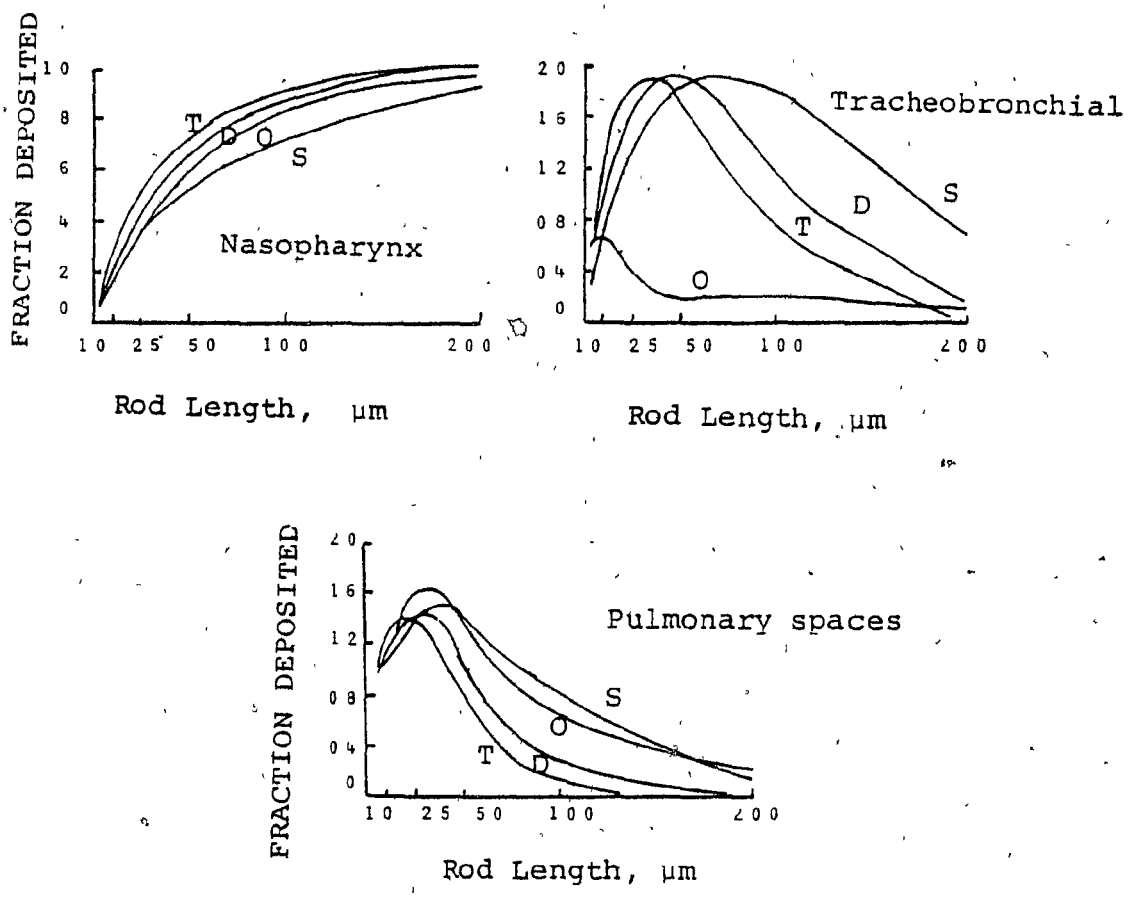


Figure 5.20[14] Predicted deposition of slender rods ($D_e$ = 0.15µm) by respiratory compartment and rod length.

(a) Size and shape of the particles,

(b) Solubility of the particles, and

(c) Site or location of the initial deposition.

The particulate clearance from the respiratory tract can be categorized in three general mechanisms: absorptive transport mechanism, nonabsorptive transport, and a combination of the two[3][42]. Usually, absorption occurs throughout the respiratory tract; however often the effectiveness of the absorption of the nasal mucosa is overlooked. Clear evidence of the absorption mechanism is the appearance of a material in the blood stream after a short time of its inhalation. The two major nonabsorptive transport mechanisms for clearing particles from the respiratory tract are mucociliary transport which serves the conducting airways, and endocytosis with combination of mucociliary transport serving the alveolar region. Another important but minor clearance mechanism is the lymphatic removal of particulates from the pulmonary region[3][4][42].

The lung model used by the International Commission on Radiological Protection (ICRP) assumes that 50 percent of the deposited and readily soluble dust rapidly passes into the gastrointestinal tract and 25 percent is absorbed and promptly enters the blood circulation. In the case of deposited insoluble dust, again 50 percent passes into the gastrointestinal tract, 12.5 percent is assumed to be transported to

the gastrointestinal tract in a period of 24 hours, and 12.5 percent is retained for a long time with a 120 day biological half time[3]. However, this lung clearance model did not receive a general acceptance because it was using two-compartmental respiratory tract system, and dust deposition estimates were arbitrary. Also terms "soluble" and "insoluble" particles were not defined properly and the role of lymphatic removal in the clearance model was not recognized. Later ICRP created the Task Group on Lung Dynamics and in 1965 the revised model for particulate clearance from the human respiratory system was published by the Task Group (Fig. 5.21)

5.4.1 Nasopharyngeal Clearance(NP):

The clearance model of the Task Group on Lung Dynamics consists of two clearance mechanisms for the clearance of the Nasopharyngeal region (NP). One of these mechanisms is absorbtive transport and the other is nonabsorbtive transport system which are shown as pathways "a" and "b" respectively in Fig. 5.21. Pathway "a" indicates a rapid clearance of particles from NP to the blood stream, and pathway "b" indicates clearance with mucociliary movement or drainage from this region to the gastrointestinal tract. Depending on the location of deposition, the particles also could be cleared by sneezing, blowing the nose or wiping them off. However, if the particles have settled in the non-ciliated areas, such as turbinates, they could be trapped for long periods of time.

5.4.2 Tracheobronchial Clearance (TB):

As shown in Fig. 5.21 clearance of particles from the tracheobronchial compartment follows two parallel pathways "c" and "d" representing clearance to the blood stream and gastrointestinal tract respectively. The research work of Camner and Philipson [46] and Camner et al. [47] has supported the effectiveness of mucociliary clearance as indicated by the Task Group on Lung Dynamics. Camner et al. [47] state that in 24 hours, more than 90 percent of the deposited dust in tracheobronchial compartment is cleared by the mucociliary action to gastrointestinal tract. In some cases clearance time is so short that it is measured in minutes. Therefore, Stuart [4] states that even those particles that are relatively more soluble and dissolve in the mucus will be moved rapidly to the esophagus rather than absorbed and transferred to the blood. However, Dayson and Beach [48] consider that absorption of soluble particles and their transfer to the blood takes place in the tracheobronchial tract. But the transfer to the blood, of the moderately soluble particles takes place in the gastro-intestinal tract when the particles are moved there by mucociliary action. Therefore, this process should not be overlooked. The other important finding of Camner and Philipson [46] is that the tracheobronchial clearance rate in man is dependent on the air flow rate during inhalation of the aerosols, and the particle size. Therefore, as the flow rate increases the clearance rate increases as well. Usually, large

## CLEARENCE MODEL

| COMPARTMENT | | CLASS D T | D F | W T | W F | Y T | Y F |
|---|---|---|---|---|---|---|---|
| NP | a | 0.01 | 0.5 | 0.01 | 0.1 | 0.01 | 0.01 |
| ($D_3$= 0.30) | b | 0.01 | 0.5 | 0.4 | 0.0 | 0.4 | 0.00 |
| TB | c | 0.01 | 0.95 | 0.01 | 0.5 | 0.2 | 0.99 |
| ($D_4$= 0.08) | d | 0.2 | 0.05 | 0.2 | 0.5 | 0.2 | 0.99 |
| | e | 0.5 | 0.8 | 50 | 0.15 | 500 | 0.05 |
| P | f | n.a. | n.a. | 1.0 | 0.4 | 1.0 | 0.4 |
| ($D_5$= 0.25) | g | n.a. | n.a. | 50 | 0.4 | 500 | 0.4 |
| | h | 0.5 | 0.2 | 50 | 0.05 | 500 | 0.15 |
| L | i | 0.5 | 1.0 | 50 | 1.0 | 1000 | 0.9 |

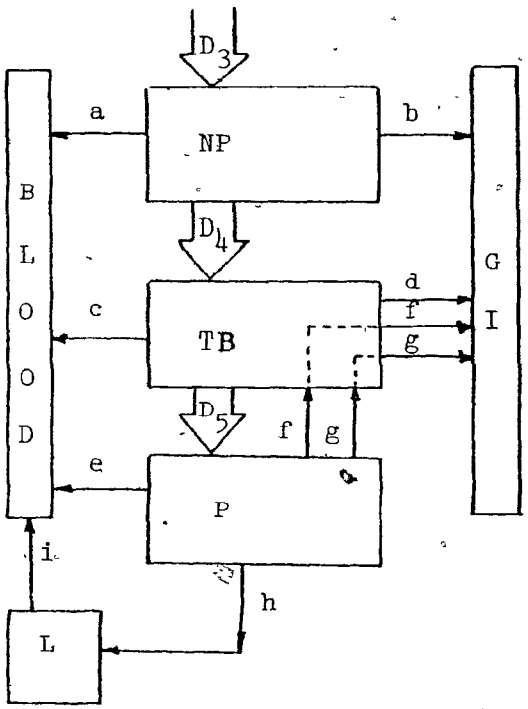


Fig. 5.21 Schematic representation of deposition and clearance pathways for inhaled aerosols, derived from the model of the Task Group on Lung Dynamics for ICRP. Nasal passages depicted by NP, tracheobronchial airways by TB, and Pulmonary Region by P and their clearence pathways from "a" to "h". Lymph nodes are portrayed as compartment L with clearence pathway "i". The tabular portion of the figure indicates the biological half-times (in days), T and compartmental fractions, F, for each pathway and for materials in either of three classifications, D: Minimal retention and rapid clearence, W: Moderate retention and intermediate clearence (half-times varies from few days to few months), and Y: Avid Retention, cleared slowly (half-times varies from few months to years). $D_3$, $D_4$ and $D_5$ indicates the deposition fractions of each compartment. n.a. indicates not applicable (3)(4)(42)

particles settle sooner than the small ones and for this reason they are cleared out from the tracheobronchial region faster than the smaller ones. Further to these studies Camner and Philipson have also conducted some tests with tobacco smokers and to their surprise they found that the tracheobronchial clearance rate was faster among the smokers than the normal non-smokers. However, the clearance rate of smokers decreased when they stopped smoking for 7 to 14 days. This can be explained by the fact that heavy smokers have obstructed airways and a large portion of the dust settles at the upper portion of the tracheobronchial tree where the mucociliary clearance is most effective and the distance to the larynx and esophagus is very short. Somehow, when the smokers stopped smoking, the obstructions in the airways were reduced or airways were enlarged and particles managed to penetrate into lower pulmonary sections in larger quantities. Therefore the amount of deposited particles in the tracheobronchial region was small in comparison to the total deposition. This explanation is supported by Thomson et al.[44] who found that particle clearance from healthy people lungs as compared to that of the group with chronic bronchities, which creates obstructions in the airways, is much slower.

Recently, Van As [49] in the editorial of the American Review of Respiratory Disease states that mucus is not a continuous blanket or sheet in human pulmonary airways

which was an accepted concept for years and occurs as a standard statement in many textbooks. He states that mucus is discontinuous and occurs as large flakes or small droplets depending on the size of the airway. However, the fact remains that mucociliary transport is the most efficient clearance mechanism in the respiratory tract system.

5.4.3 Pulmonary Clearance:

According to the clearance model of the Task Group on Lung Dynamics[3], the clearance of the deposited particles in this region is possible through four pathways. Pathway "f" represents rapid clearance while pathway "g" represents prolonged clearance of materials first being engulfed by macrophages and then translocated through the tracheobronchial region via mucociliary mechanism and reach to the gastrointestinal tract. Pathway "e" represents clearance to the blood and pathway "h" represents clearance into the lymphatic chanels and lymph nodes. Some of the particles move from lymph nodes via pathway "i" to the blood stream.

Brian et al.[58] indicates that there are three types of pulmonary macrophages and these are alveolar macrophage, airway macrophage and interstital magrophage. The alveolar macrophages are fairly large phagocytic cells with a mononucleus and are found on the alveolar surface and they are not part of the epithelial layer of the alveolar membrane. Airway macrophage has

a cell structure similar to that of the alveolar macrophage. They are present in conducting airways in small or large sizes. The interstital macrophages are found in the various connective tissue compartments of the lungs[50][58].

The phagocytic response is a protective mechanism for the pulmonary region and it is believed that alveolar walls cannot be easily penetrated by the dust if the particles are engulfed by the macrophage cells[57]. The basic action of the macrophage can be explained in a simple manner by analogy with the digestive system. Deposited foreign material attracts macrophages by irritating the alveolar surfaces. The attracted macrophages ingest the foreign particles at their boundary membrane, which is called phagocytosis and the vesicule thus formed is called phagosome. Primary lysosomes which are organelles that produce enzymes in a macrophage, move to the phagosome and discharge their enzymes into it. The phagosome is now known as a secondary lysosome and the foreign body is digested by the secondary lysosome. The residue is then ejected from the macrophage. However, the digestion of some particles is not complete and the secondary lysosome may remain in the macrophage as a residual body (see Fig. 5.22). Particle bearing macrophages migrate towards the ciliated region of the broncioles through the nonciliated

alveolar ducts and respiratory bronchioles[43][57][58]. The migration mechanism of macrophages through the nonciliated regions is not very well understood[57]. In order to explain the migration some theories have been developed. However, these theories have not received a general acceptance. Two of these theories are explained by Gross et al.[43] as follows: The alveolar surface is covered by a film of fluid which moves proximally towards ciliated bronchioles as the respiration is taking place. However, in order to accomplish this movement, duration of respiration must be longer than the duration of inspiration period. The second theory states that as the mucus is cleared out by the ciliary movements, created voids are filled by the alveolar fluid due to suction created by the cilia's pumping action or movements. Regardless which ever is the case, based on observations made by Gross et al. [43], the dust removal from rat's lungs is evidence of the proximal transport of the dust from alveoli through the non-ciliated regions, such as the alveolar ducts and respiratory bronchioles. The amount of dust found in the proximal portion of the recemus of the rat's lungs was greater on the fourth day than immediately after the inhalation of the dust burden and there was a reduction in the amount of dust remained in the peripherial portions of the racemus on the fourth day with comparison to immediately after inhalation and deposition of the dust burden. This variation in dust burdens

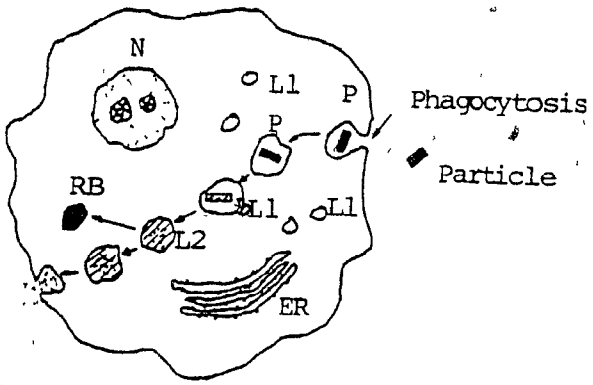


(1)
Figure 5.22 Simplified diagram of a macrophage ingesting a particle. A primary lysosome ($L_1$) is attached to phagosome (P) and is discharging its enzymes into it. The secondary lysosome ($L_2$) either forms a residual body (RB) or discharges its contents outside the cell. (ER, endoplasmic reticulum with ribosomes; N, nucleus)

is a clear evidence of effective dust removal through non-ciliated regions. Further evidence is that there was a considerable amount of dust in the tracheobronchial region of the rats' lungs four days after the exposure. Normally, the deposited dust in the tracheobronchial region is cleared in 24 hours by mucociliary action at a rate of 15 to 18 millimetres per minute[3][4][43]. LaBelle et al.[45] have proven that the dust clearance rate is related to the disappearance of phagocytes from the alveolar regions of the rats' lungs and concluded that transport and clearance of deposited particles by phagocytes is the primary clearance mechanism for the lungs. Camner et al.[47] investigated the lung clearance of 4 micrometre particles coated with silver, carbon, and beryllium from rabbits lungs. Their results indicated that, the alveolar macrophages did not play an active role in removing intact particles from the lung one week after inhalation.

Although it is proven that macrophages are effective in clearing the foreign material from the pulmonary region of the respiratory tract, when the engulfed particle is cytotoxic, such as quartz particles, the membrane structure of the secondary lysosome is damaged and ruptured. The released enzymes destroy the cytoplasm of the macrophage and kill the cell. Once again, after the death of the cell, the freed particle is engulfed by another macrophage and this cycle is

repeated. Bowden[50] states that this continuous killing of macrophages is a critical step in the sequential development of silicotic fibrosis of the lung.

The failure of containing the cytotoxic particles in macrophages leads to their penetration into interstital sites of the lung, where they may provoke a collagenous response,[4][50][57] or once particles gain access into interstital sides, they may move further and reach to the lymphatic or blood capillaries. According to Morrow[57] lymphatic capillaries are permeable to dust particles which are below 10 micrometre diameter and have a reasonable probability of penetrating a lymph node. Particles at lymph nodes may retain and accumulate or gradually may pass on into circulation via a lymph duct. Thomas[56] has experimentally demonstrated and mathematically calculated the transport of relatively insoluble materials from lung to lymph nodes. Taskinen et al.[54] have hypothesised that the lymphatic transport of inspired dust to the parietal pleura is possible and tried to prove this hypothesis with an autopsy result of a welder who had heavy mixed dust pneumoconiosis. The observation was made that in the parietal pleura there were black linear streaks following the course of intercostal arteries. Green[59] states that macrophages containing particles may migrate to certain lung tissues or to peribronchial positions where they

are accumulated for long periods of time and eventually may cause the long-term pulmonary diseases. Another important clearance mechanism is solubility of the particles which may result in material appearing in the lymphatic or blood circulatory systems. Mercer[55] has developed a mathematical model which successfully estimates the solubility of materials which are deposited in the lung. The role of particle size in the dissolution of lung burdens was built in the mathematical model as a function of the surface area of the particle. The mathematical results compared favourably with experimental data.

5.4.4 Clearance of the Chrysotile Fibres From the Lungs:

In the case of asbestos fibres, the above mentioned clearance mechanisms often do not operate efficiently. The only exception is that, short fibres with lengths less than 5 micrometres are easily ingested by the macrophages as described above[53]. However, fibres of 20 micrometres or longer cannot be completely engulfed by the macrophage cells. A group of cells may instead gather around each end of the fibre with some cells around the middle which would make the fibre look like a Q-tip in shape[2][63]. These bulbous ended fibres are known as asbestos bodies[9][63]. Asbestos bodies can be found in human lungs with as little as two months exposure to asbestos. These structures can

be quite long, up to 80 micrometre fibres have been found in human lungs[2]. Asbestos bodies are partly covered with layers of iron containing protein due to the action of alveolar macrophages[9]. However, according to Pooley[60] and Langer et al[61] asbestos bodies present in the lung do not indicate presence of chrysotile fibres. It seems that the chrysotile fibres split into submicroscopic fibrils and the magnesium is then leached out. Therefore, asbestos bodies may have little relation to the amount of chrysotile fibres inhaled[62]. Sometimes intermediate size fibres between 5 and 20 micrometres were completely ingested and at other times they were not.

Local cell fusions are related to those fibres which could not be engulfed by the macrophages. During phagocytosis and macrophage action, there is a period of fibroblast production and collagenous fibrosis development in the walls of the terminal bronchioles which spreads diffusely in the alveolar walls. It is not as yet quite known why this takes place as asbestos fibres do not seem to be cytotoxic, and all this takes place without any damage being done to the macrophage. To this effect, Smith and Davis[52] have shown that chrysotile asbestos fibres are not cytotoxic and in dust containing macrophages the presence of primary lysosomes was less than 50 percent and as few as 10 percent of dust containing phagosomes showed evidence of lysosome

enzyme release. Contrary to the above findings Miller and Harrington[51] state that chrysotile asbestos fibres are as toxic as silica dust but there has hitherto been no evidence that chrysotile damages phagosomes in the way silica does. However, Miller and Harrington are hypothesising that magnesium ions of chrysotile could damage the membrane of the phagosomes as they are active agents in inducing haemolysis of erythrocytes[9][51]. Taskinen et al.[54] state that a current hypothesis of the lymphatic transport of inspired dust to the parietal pleura does apply to asbestos particles as well. Wagner and Skidmore[36] state that the elimination rate of Rhodesian chrysotile fibres from rat lungs have been found to be three times greater than that of the amosite and crocidolite and suggest that fibrogenicity of chrysotile fibres is less than other types of asbestos fibres. Other observations of Wagner and Skidmore were, in the rats killed 24 hours after exposure to chrysotile fibres, only small fragments of fibre were present in phagocyte cells and in the rats killed 29 days after exposure these phagocytes had become large, foamy and vacuolated and very occasional fragments of fibre were seen. On the 58th day no evidence of chrysotile was observed[36]. Evans et al.[39] showed that 30 days after the exposure 27 percent of the inhaled crocidolite fibres were cleared by the macrophage and mucociliary clearance mechanisms of the rat lungs. Morgan et al.[40] have confirmed the findings of Evans et al.

and concluded that mucociliary action is one of the effective clearance mechanisms in clearing the crocidolite from rats lungs. However, some long fibres were found in the interstital septa of the lungs, suggesting that it is difficult to clear the long fibres through the winding, small diameter airways. Becklake[9] states that quite a few submicroscopic and uncoated asbestos fibres are detected in the lung substances of the exposed workers. The proportion of uncoated to coated fibres is 75 to 25 percent respectively. It is suggested that these submicroscopic particles are due to the breakdown products of larger fibres.

5.5 Inhaled Chrysotile Fibres and Asbestos Related Diseases:

The manner in which asbestos dust causes the different diseases associated with the mineral is not precisely known, but it is the object of much research. According to Gross[53] short fibred asbestos dust, with fibre lengths less than 5 micrometres, is not a biological hazard and is incapable of causing fibrosis or cancer. Becklake[9] states that fibrogenic effects of asbestos fibres and particles are neither due to physical irritation nor due to solubility which implies that leached out metal ions and silicic acid affect the lung tissue. Becklake hypothesised that the fibrogenic effect of asbestos fibres is either because of the production or localization of abnormal globulins in alveolar phagocytes and fibroblasts, or because of

autoantibodies developing in response to lysis of phagocytes. Stanton[64] and Stanton et al.[66] showed that the carcinogenicity of asbestos fibres, glass and aluminum oxide fibres is primarily related to their structure rather than to physicochemical properties. Pott et al.[65] results correspond with Stanton's findings. Newball et al.[67] also indicated that fibrous glass has a potential of being carcinogen. On this matter, however, there are conflicting reports. In order to clarify the situation on behalf of the National Institute for Occupational Safety and Health (NIOSH), Bayliss et al.[68] investigated the problem and reported that fibrous glass causes nonmalignant respiratory disease such as chronic bronchitis. However, small diameter glass fibres could create a danger of carcinogenicity. Hill[69] classified the man-made mineral fibres as nuisance dust and stated that it has no excess risk of cancer. The committee on Environmental Health of the American College of Chest Physicians [70] states that fibreglass dust is a nuisance-dust and at present there is no evidence of its being carcinogen. Gross[71] indicated that generated tumors in rats have no relevance to man and biologically categorized the fiber-glass dust as nuisance-dust. Nasr[72] states that glass fibre dust is inert and is not carcinogen. This brief review corroborates the previous statement that the present knowledge of the mechanism of fibrogenic effect

of fibres in man is not precise or complete. However, the association of the cancerous and other diseases with asbestos exposure is well established. Important factors which affect the development of lung disorders, due to inhalation of asbestos dust, are: individual susceptibility, presence of other pulmonary conditions, physical fitness and age at first exposure, particle size, intensity of exposure, length or duration of exposure and content of the fibrogenic substance in the dust.

The summary of pathologic effects of asbestos exposure in man are shown in table 5.4[9].

Minor disorders such as formation of asbestos corns develop as a result of small fibres entering the skin and irritating the tissue. Another minor but serious disorder is laryngeal carcinoma. Shettigra and Morgan's[73] study showed that there is a substantial association between asbestos exposure and laryngeal cancer, and smoking combined with asbestos exposure increase the chance of development of this disease. McDonald et al.[92] report a clear association with smoking.

5.5.1 Asbestosis (Diffuse Interstital Fibrosis):

The general term asbestosis usually refers to asbestotic fibrosis which is the most common disease of asbestos workers. As an occupational disease, asbestosis was first encountered in 1907, however its importance was not realized until 1930[74][75].

The external appearance of a lung with asbestosis depends mostly on the degree of severity of the disease. During the early stages of asbestosis the lung would look quite normal[1][2][9][63]. However, in the advanced cases of asbestosis, the lung would be pale with a firm rubbery texture and tend to be small[2][9]. The pulmonary pleura is usually thickened and fibrosis is most prominent in the lower lobes of the lungs during the early stages of the disease, and eventually the middle and upper lobes may be affected[9]. Often the fibrotic areas contain cysts which may be 3 micrometres or less in diameter. Severe cases of asbestosis may lead to massive fibrosis and large fibrotic masses develop in the lower parts of the lungs[2]. Usually, fibrosing of the lung starts in the alveoli of the respiratory bronchioles with the fibroblast formation by the aggregation of fibre containing macrophages. From this a thin reticulin network gradually evolves and envelopes cells and fibres. Collagenous fibrosis then replaces the network of fibres until these respiratory bronchiolar alveoli are oblitereated. Later, the fibrosis spread from the respiratory bronchioles to the alveolar ducts and into

Table 5.4 Pathologic Effects of Asbestos Exposure in Man[9]

| Organ | Effect | Associated with Asbestos Exposure |
|---|---|---|
| Skin | Asbestos Corns | Established |
| Larynx | Carcinoma | Possible |
| Lungs | Asbestos Bodies/fibres | Established |
| | Asbestosis (Diffuse Interstital Fibrosis) | Established |
| | Carcinoma (Bronchial) | Cofactor with Cigarettes |
| Pleura | Hyaline Plaques and Calcification | Established |
| | Malignant Mesothelioma | Established |
| | Pleural Effusion | Possible |
| Peritoneum | Malignant Mesothelioma | Established |
| Gastrointestinal Tract | Neoplasia | Established |
| Ovary | Carcinoma | Remotely Possible |
| Breast | Carcinoma | Remotely Possible |

the alveolar walls destroying the alveoli in the process by thickening the inner walls of the alveolar respiratory tract[1]. However, inspite of all these changes, the elastic network of alveolar walls is often seen to be intact indicating that much of the fibrosis is inter-alveolar[63]. Where the fibrosis is solid the alveolar structure is completely replaced by a mass of collagen.

Basal asbestosis is essentially the same as asbestotic fibrosis except it occurs in people who have had no industrial exposure to asbestos or who have had a very limited industrial exposure. Most people who contract this type of asbestosis live or have lived for a period of time in an area whereby asbestos is mined, milled or used in some manufacturing process[76]. However, it must be stressed that their overall exposure is low. In this type of asbestosis, asbestos fibres move downwards and accumulate at the base of the lungs where they are coated with the iron protein complex to form asbestos bodies[83][84]. Asbestos bodies are usually inert but their concentration in the lung bases initiates the fibrosing[9][76]. Basal asbestosis is often associated with pleural changes and has also been noted in cases of malignant mesothelioma[74][80]. Asbestosis is a chronic progressive disease, and does not stop after exposure ceases[78][79]. Generally, it takes 20 to 40 years to develop and usually patients suffer from dry cough and breathlesness, and their vital capacity is depressed[75][77].

According to Pelnar[86] the distribution of asbestosis cases among different industries is as follows:

| Years of Exposure | Quebec Mining Industries | British Textile Industries | U.S.A. Insulation Industry |
|---|---|---|---|
| 10 to 30 | 6% | 17% | 49% |
| over 30 | 17% | 60% | 90% |

From the above statistical data, it can be seen that the percentage of the asbestosis cases in asbestos mining industry is not as high as in the insulation or textile industries. The reason is, the intensity of exposure and the asbestos fibre content of the airborne dust in Quebec mines and mills is not as high as in other industries.

5.5.2 Pleural Thickening and Pleural Plaques:

The thickening of the pleura is often found in the pathological examination of asbestos workers. It is most common in the lower parts of the lungs and in the interlobular fissures. Usually, the pleura shows an increase in the thickness of fibrous tissue outside of the elastic membrane and a fibrosis between the elastic membrane and the alveoli immediately below the pleura. These alveoli are destroyed by collagenous tissue in the alveolar air spaces[1][2][9][63].

Pleural plaque formation does not seem to be harmful to health and is not classified as a disease. According

to McDonald[74] pleural plaques do not or have little effect on the respiratory function and there is no proof of their association in the development of malignant mesothelioma.

Pleural plaque is a yellow white patchy thickening of the pleura which projects slightly above the surrounding tissue. There is a wide range of shapes and sizes of plaques up to 1 cm. thick. Plaques are generally found on the parietal pleura and the diaphragm[9][75]. These plaques tend to follow the lines of the lower ribs. The origin of plaques is not yet known for certain but Thomson et al.[82] suggest that plaque formation may be due to a sensitivity reaction from asbestos fibres protruding through the tissue. The location of the plaques in the deep part of the lung would be due to the gravitational migration of the asbestos fibres downward.

Pleural calcification is usually seen among the persons who have occupational exposure to asbestos, and in some cases it also occurs among the population of certain geographic locations. Gibbs[81] has shown that pleural calcification often occured in Thetford Mines workers of Quebec but did not occur or was very rare in those living in Asbestos, Quebec, which is only 50 miles away. Gibbs concluded that it could be due to minerals associated with chrysotile such as, mica, talc and breunnerite that are encountered during mining in Thetford Mines but not

in other mining areas of Quebec.

Development of pleural plaques and calcification takes place at least 20 years after exposure to asbestos dust[85]. The occurance of pleural plaques and calcification does not always mean that there has been heavy or lengthy exposure to asbestos dust but only indicates a past exposure to the mineral.

5.5.3 Carcinoma of the Lung and Its Association with Chrysotile Asbestos Exposure

In early 1930's the association of lung cancer with asbestosis was suspected[74]. This suspicion was confirmed by late 1940's and early 1950 by two British reports[9][87][75] McDonald [88] and McDonald et al's,[89][90][91][92] work entitled "Cancer in Chrysotile Mines and Mills"; and "Dust Exposure, Health and Mortality in Chrysotile Mining Industry of Quebec", confirmed the association of malignant tumors with chrysotile. Results of McDonald et al's. [92] latest study are shown in table 5.5, where exposure to dust and mortality in chrysotile mining for the period of 1910-1975 are given.

The total number of dead, 4463; constitutes 40.8 percent of the male cohort. The significant findings were: lung cancer deaths occured in non-smokers and the incidence of cancer increased with increasing exposure to chrysotile while it decreased in smokers. However, the risk of lung cancer increased with increasing exposure to chrysotile dust for both groups. The overall excess mortality during 1926-75 was 2

percent at Asbestos City and 10 percent at Thetford Mines which is a dustier region.

A similar study was carried out by Peto et al.[93] among workers in an asbestos textile factory in England for the period of 1933 to 1974. The percent of death due to cancer was 30 which is much higher than the 19.5 percent cancer deaths among chrysotile mine workers of Quebec. However, the highest death rate of cancer was among insulation workers in Belfast at 54 percent for the period of 1940-75[94]. Forty percent was due to respiratory cancer and the remaining 14 percent due to other type cancers. Table 5.6 indicates that lung cancer, among other chrysotile exposure related cancers, has the highest relative risk.

### 5.5.4 Mesothelioma and its Association with Chrysotile Asbestos Exposure

Mesothelioma is a malignant tumour often associated with asbestos exposure. Until recent years it was believed that mesothelioma was mainly associated with crocidolite type asbestos of Northwest Cape, South Africa[9][31][53][74][75]. Malignant mesothelioma tumour can grow on the pleura or the peritonia but the pleural site is by far the most common of the two[96]. The macroscopic look of a mesothelioma can vary from a hard sheet 0.5 to 1.0 centimetre thick which covers a limited part of the lung, to a thick rubbery mass which might encase the entire lung. In addition to covering the lung, this tumour has a tendency to spread into the interlobular fissures of the lung. Since the

Table 5.5 Studies of Mortality in Chrysotile Mines, 1910-75[92]

| Cause of Death | Number of Deaths | | Percentage of all deaths | |
|---|---|---|---|---|
| Pneumoconiosis | 46 | | 1.03 | |
| Malignant neoplasms: | | | | |
| Lung | 250 | | 5.60 | |
| Oesophagus and Stomach | 154 | | 3.45 | |
| Colon and Rectum | 88 | | 1.97 | |
| Other Abdominal | 80 | 869 | 1.80 | 19.5% |
| Larynx | 21 | | 0.47 | |
| Other | 276 | | 6.18 | |
| Heart Disease | 1543 | | 34.57 | |
| Respiratory Tuberculosis | 248 | | 5.56 | |
| Other Respiratory | 234 | | 5.24 | |
| Cerebrovascular | 268 | | 6.00 | |
| Accidents | 461 | | 10.33 | |
| All other known causes | 669 | | 15.00 | |
| Causes not known | 125 | | 2.80 | |
| All causes (Total) | 4463 | | 100 | |

growth surrounds the lung and the lobes in the lung, the lobes become compressed and eventually obliterated. The tumour can spread very quickly as compared to other asbestos diseases and unlike the other diseases it can move to parts of the body such as the liver. According to cellular characteristics, mesothelioma can be divided into three types: spindle cell type, epithelial cell type and mixed cell type[1][2].

The spindle cell type may be localized or diffused. When it is localized it looks like a fibromata of the pleura, while the diffused form resembles spindle cell sarcoma. The epithelial cell type consists of masses of cells bunched together, and the mixed cell type of mesothelioma is the most common type of the disease. It consists of bundles of mature collagen with clefts lined or filled with cells resembling the cells that line the pleura. In some places the mature collagen bundles are replaced by a more cellular connective tissue[1][2][63].

It seems possible that mesothelioma of the pleura could develop in a pleural plaque but not in a calcified plaque[74]. Pathological studies have indicated that mesothelioma of the peritoneum may be associated with diffuse fibrosis. However, mesothelioma of the pleura is usually related to basal asbestosis which indicates that it is more common with light exposures to asbestos dust[2][9][75]. McDonald et al.[95][96][97] state that the association of

Table 5.6 Relative Risk of Cancer for Male Chrysotile Asbestos Workers[9]

| Occupation and Country | Population Studies: Number | Minimal Exposure | Years of Follow-up | Deaths: Total No. | No. Due to Lung Cancer | Relative Risk of Cancer: All Others | Lung | G.I.* |
|---|---|---|---|---|---|---|---|---|
| Mining & Milling | 5,958 | 5 years | 6 | 187 | 12 | -- | 1.5 | -- |
| Canada | 9,692 | 1 month | ave. 25 | 3,270 | 134 | 1.4 | 3.1 | -- |
| Secondary Use: | | | | | | | | |
| U.K. Textile | 113 | 20 years (pre 1933) | 20 | 39 | 11 | 4.8 | 13.7 | 1.7 |
| Textile | 674 | 10 years (post 1933) | ave. 17 | 69 | 8 | 0.6 | 1.0 | -- |
| Insulation Production | 1,024 | 6 months | 15 | 133 | 7 | 1.1 | 2.3 | -- |
| Insulation Pipe Coverers | 165 | Not stated | 26 | 98 | 28 | 6.7 | 17.6 | -- |
| Insulation Workers, USA | 623 | 20 years | 28 | 421 | 84 | 4.0 | 8.3 | 3.1 |
| Insulation Workers, USA | 5,118 | 20 years | 4 | 881 | 191 | 3.5 | 5.1 | 2.1 |

* G.I. = Gastrointestinal

mesothelioma with chrysotile exposure is rare, and only 30 percent of the mesothelioma cases in Canada were related to occupational asbestos exposure. Davies[31] and Gross[53] hypothesised that, mesotheliomas of the pleura and peritoneum arise by the transmigration of fibres to the pleura and periotoneum and because of physical characteristics of the chrysotile fibres, specially their curliness, do not permit them to transmigrate in large quantities to the pleura and peritoneum. Therefore, mesothelioma among workers of chrysotile mining industry is very low. McDonald et al.[99] suggest a gradient in mesothelioma inducing potential, by type of fibre, from crocidolite down to chrysotile and anthophyllite. Among the large work force of the chrysotile asbestos industry, Selikoff et al.[38] reported only 20 cases of mesothelioma among insulation workers in the New York area, and McDonald et al.[92] reported 11 cases (10 men and 1 woman) of pleural mesothelioma among the workers of the chrysotile mining industry. Peto et al.[93] indicate 11 mesothelioma cases among textile workers of England, and Elmes et al.[94] listed 19 mesothelioma cases among insulation workers in Belfast.

5.5.5. Gastrointestinal Cancer and Its Association with Chrysotile Asbestos Exposure:

As it is indicated in table 5.6 gastrointestinal cancers represent the next highest relative risk after lung cancer for male chrysotile asbestos workers. Haley[100] states that: "at this point in time, it has not been established, either experimentally or in humans, that ingestion of asbestos fibres causes cancer of the GI tract".

McDonald et al.[92] indicates that although it is difficult to interpret the patterns of gastrointestinal cancer in the Quebec cohort, there is unquestionably a substantial excess in mortality from cancer of the upper gastrointestinal tract in men who have worked in Thetford Mines where the exposure was heavy (see table 5.5). Also for cancer of the lower gastrointestinal tract, there was some evidence to the effect that heavy exposure had some role in its occurence.

5.5.6 Pulmonary Function in Asbestos Related Diseases:

The first stages of asbestosis goes unnoticed, followed by a dry cough and a modest loss of exercise tolerance[74][75]. Since the disease does not appear until 20 or more years after the first exposure to the asbestos dust, the person may believe that this loss of breath is due to advancing age. As the disease progresses dyspnoea becomes marked with mucoid sputum production. Later this changes to prulent sputum. The person does not have a continuous pain but may experience short periods of sharp pain in the pleural regions.

Physiologically, the change in the lung function occurs from the thickening of the alveolar wall. The vital capacity in the initial stages will remain fairly normal but by the time the disease is in the advanced stage this may be greatly reduced. The ratio of forced expiratory volume to vital capacity stays approximately the same throughout the disease until a very late stage. The

residual volume increases slightly as the disease advances. Early diagnosis of asbestosis does not depend on physiological tests of lung function as it can be seen that the early stages of the disease do not change these characteristics much. The physician's stethescope and the radiograph are the best methods of early detection.

With mesothelioma, the first symptoms are a tightness of the chest and pain which may become quite intense if the tumour erodes the ribs. The function of the lung steadily and quickly deteriorates with the growth of the tumor. Eventually the lung ceases to function altogether.

Pleural thickening and calcification are not classified as diseases and have little or no effect on lung function whatsoever(81).

## 5.6 Conclusion:

Chrysotile asbestos is undoubtedly an important industrial mineral, however it presents a very real health hazard for the workers. Prolonged exposure to chrysotile asbestos dust can result in respiratory diseases and sometimes cancer. Even a short exposure to the mineral can lead to malignant mesotheliomal tumors. The solution to these health problems lies not only in medicine but in the proper engineering control of asbestos production and utilization processes. At present there is no cure for asbestosis or cancers which are associated with chrysotile exposure. Therefore, by eliminating the source of dust or preventing human exposure, and thereby eliminating the inhalation and retention of chrysotile fibres in the lungs of workers, can result in overcoming the development of these occupational diseases. This is not an easy task. The technical difficulties in trying to completely eliminate dust of the order of 1 micrometre diameter would be enormous and the price would be prohibitive, making asbestos production uneconomical. New products may soom become substitutes for asbestos and may eventually replace it; however, the health effects of man-made fibres are also a controversial issue. But for the time being isolation of the dust source or a suitable dust control system design would provide the required protection for the workers. However, are the present day TLV's and dust control systems adequate?

What dust levels can be considered to be safe and how effectively can it be determined? What proportion of the airborne dust could be inhaled and retained? What type of instrumentation could give reliable and practical results for the determination of airborne dust and its retained portion in workers lungs?

The research work in the following pages attempts to answer two of the above questions by determining the chrysotile dust quantities and masses by measuring the remanent magnetic fields of airborne total and respirable size dust samples, and dry lung tissues of men who have worked in the chrysotile asbestos mining industry.

## LIST OF REFERENCES FOR CHAPTER V


1. Muir, D.C.F., "Medicine in the Mining Industries", Editor: J.M. Rogan, F.A. Davis Company, Philadelphia, 1972, pp. 56-69.

2. Parkes, W.R., "Occupational Lung Disorders", Butterworth & Co., (Canada) Ltd., Toronto, 1974, pp. 4-14, 71-73, 276-323.

3. Task Group on Lung Dynamics, "Deposition and Retention Models for Internal Dosimetry of the Human Respiratory Tract", Health Physics, Pergamon Press, Northern Ireland, 1966, Vol. 12, pp. 173-207.

4. Stuart, B., "Deposition and Clearance of Inhaled Particles", Environmental Health Perspectives, August 1976, Vol. 16, pp. 41-53.

5. Winston, F.R., Bayliss, L.E., "Human Physiology" fifth edition, J.A. Churchill Ltd., London, 1962.

6. Comroe, J.H., Foster, R.E., Dubois, A.B., Briscoe, W.A., and Carlsen, E., "The Lung", Clinical Physiology and Pulmonary Function Tests, second edition, Yearbook Medical Publishers Inc., Chicago, 1971, pp. 1-9, 72-73, 112-114.

7. Davies, C.N., "Inhalation Risk and Particle Size in Dust and Mist", British Journal of Industrial Medicine, June 1949, Vol. 6, pp. 245-253.

8. Hounam, R.F., Morgan, A., "Particle Deposition", Respiratory Defence Mechanism part I, Lung Biology in Health and Disease, Editors: Brian, Proctor, Reid, Vol. 5, pp. 125-156.

9. Becklake, M.R.,: State of Art: "Asbestos-Related Diseases of the Lung and Other Organs: Their Epidemiology and Implications for Clinical Practice", American Review of Respiratory Disease, Vol. 114, 1976, pp. 187-227.

10. Silverman, L., and Billings, C.E., "Pattern of Airflow in the Respiratory Tract", in: Inhaled Particles and Vapour, Editor: C.N. Davies, Pergamon Press, London, 1961, p. 9.

11. Green, H.L. and Lane, W.R., "Particulate Clouds" Dusts, Smokes and Mists", Their Physics and Physical Chemistry and Industrial and Evnironmental Aspects, Second Edition, E & F N. Spon Ltd., London, 1964, pp. 63-75.

12. Cadle, R.D., "Particle Size" Theory and Industrial Application. Reinhold Publishing Corp., New York, 1965, pp. 65-94.

13. Timbrell, V., "The inhalation of Fibrous Dust" Annals of the New York Academy of Sciences, Vol. 132, Art. 1, New York, 1965, pp. 255-273.

14. Harris, Jr. R.L., and Timbrell, V., "The Influence of Fibre Shape in Lung Deposition-Mathematical Estimates", Inhaled Particles IV, 1976, pp. 75-89.

15. Timbrell, V., "The Inhalation of Fibres" In: Pneumoconiosis, Editor: H.A. Shapiro, Proceedings of the International Conference 1969, Johannesburg, Cope Town, Oxford University Press, 1970, pp. 3-9.

16. Timbrell, V., Pooley, F., and Wagner, J.C., "Characteristics of Respirable Asbestos Fibres", In: International Conference on Pneumoconiosis, Dept. of Mines, Republic of South Africa, 1969, pp. 120-125.

17. Timbrell, V., Skidmore, J.W., "The Effect of Shape on Particle Penetration and Retention in Animal Lungs", In: Inhaled Particles III, W.H. Walton, Unwin Bros. Ltd., Surrey, U.K., 1970, pp. 49-56.

18. Stuart, B.O., Wash, R., "Deposition of Inhaled Aerosols", Arch. Intern. Med., Vol. 131, Jan. 1973, pp. 60-73.

19. Hounam, R.F., Block, A., and Walsh, M., "The Deposition of Aerosol Particles in the Nasopharyngeal Region of the Human Respiratory Tract", Aerosol Science, Pergamon Press, 1971, Vol. 2, pp. 47-61.

20. Brian, J.D., and Valberg, P.A., "Models of Lung Retention Based on ICRP Task Group Report", Arch. Environ. Health, Vol. 28, Jan. 1974, pp. 1-11.

21. Taulbee, D.B., and Yu, C.P., "A Theory of Aerosol Deposition in the Human Respiratory Tract", Journal of Applied Physiology, Vol. 38, No. 1, January 1975, pp. 77-85.

22. Heyder, J., Gebhart, J., and Stahlhofen, W., "Diameters of Airborne Particles", Water, Air and Soil Pollution 3, D. Reidel Publishing Company, Dordrecht Holland 1974, pp. 567-572.

23. Moss, O.R., "Shape Factors for Airborne Particles", American Industrial Hygiene Association Journal, April 1971, pp. 221-229.

24. Brown, J.H., Cook, K.M., Ney, F.G., and Hatch, T., "Influence of Particle Size Upon the Retention of Particulate Matter in the Human Lung", American Journal of Public Health, Vol. 40, April 1950, pp. 450-458.

25. Lippman, M., Albert., R.E., "The Effect of Particle Size on the Regional Deposition of Inhaled Aerosols in the Human Respiratory Tract", American Industrial Hygiene Association Journal, May-June 1969, pp. 257-275.

26. Lippmann, M., Albert, R.E., and Peterson, Jr. H.T., "The Regional Deposition of Inhaled Aerosols in Man", In: Inhaled Particles III, Editor: W.H. Walton, Unwin Bros. Ltd., Surrey, 1970, 1: 105-122.

27. Schlesinger, R.B., Lippmann, M., "Particle Deposition is Costs of the Human Upper Tracheobronchial Tree", American Industrial Hygiene Association Journal, April 1972, pp. 237-251.

28. Morrown, P.E., "Aerosol Characterization and Deposition", American Review of Respiratory Disease, Vol. 110 (b) Dec. 1974, pp. 88-99.

29. Maltoni, G.G., Melardi, C., Prodi, V., and Tarroni, G., "Deposition Efficiency of Monodisperse Particles in Human Respiratory Tract", American Industrial Hygiene Association Journal, Sept. 1972, pp. 603-610.

30. Heyder, J., Gebhart, J., Heigwer, G., Roth, C., and Stahlhofen, W., "Experimental Studies of the Total Deposition of Aerosol Particles in the Human Respiratory Tract", Aerosol Science, Pergamon Press, 1973, Vol. 4, pp. 191-208.

31. Davies, C.N., "Deposition of Inhaled Particles in Man", Chemistry and Industry, June 1974, pp. 441-444.

32. Mercer, T., "The Deposition Model of the Task Group on Lung Dynamics" A Comparison with Recent Experimental Data", Health Physics, Pergamon Press, Northern Ireland, Nov. 1975, Vol. 29, pp. 673-680.

33. Martin, D., and Jacobi, W., "Diffusion Deposition of Small Sized Particles in the Bronchial Tree", Health Physics, Pergamon Press, Northern Ireland, July 1972, Vol. 23, pp. 23-29.

34. Landahl, H.D., "On the Removal of Airborne Droplets by the Human Respiratory Tract: I. The Lung", Bulletin Math. Biophys., 1950, Vol. 12, p. 43.

35. Gormley, P.G., and Kennedy, M., Proc. Roy. Irish Academy, 52A, 1949, p. 163.

36. Wagner, J.C., and Skidmore, J.W., "Asbestos Dust Deposition and Retention in Rats", In: Annals of the New York Academy of Sciences, Vol. 132, Art. 1, New York, 1965, pp. 77-86.

37. Beeckman, J.M., "Deposition of Ellipsoidal Particles in the Human Respiratory Tract", Assessment of Airborne Particles, Editors: T.T. Mercer, P. Morrow, W. Stober, Charles and Thomas Publishers, Spring Field, Ill., 1970, Chap. 17, pp. 361-370.

38. Beakman, J.M., "The Deposition of Asbestos Particles in the Human Respiratory Tract", International Journal of Environmental Studies, Gordon and Breach Science Publishers Ltd., Exeter, England, 1970, Vol. 1, pp. 31-34.

39. Evans, J.C., Evans, R.J., Holmes, A., Hounam, R.F., Jones, D.M., Morgan, A., and Walsh, M., "Studies on the Deposition of Inhaled Fibrous Material in the Respiratory Tract of the Rat and Its Subsequent Clearance Using Radioactive Tracer Techniques, 1. UICC Crosidolite Asbestos", Environmental Research 6, Academic Press Inc., 1973, pp. 180-201.

40. Morgan, A., Evan, J.C., Evans, R.J., Hounam, R.F., Holms, A., and Doyle, S.G., "Studies on the Deposition of Inhaled Fibrous Material in the Respiratory Tract of the Rate and Its Subsequent Clearance Using Radioactive Tracer Techniques, II. Deposition of the UICC Standard Reference Samples of Asbestos", Environmental Research 10, Academic Press Inc., 1975, pp. 196-207.

41. Haris, Jr., R.L., Fraser, D.A., "A Model for Deposition of Fibres in the Human Respiratory System", American Respiratory System", American Industrial Hygiene Association Journal, Feb. 1976, pp. 73-89.

42. Morrow, P.E., "Clearance Kinetics of Inhaled Particles", In: Respiratory Defence Mechanism Part I, Editors: Brian, Proctor, Reid, Vol. 5, pp. 489-543.

43. Gross, P., Pfeitzer, A.E., and Hatch, T.F., "Alveolar Clearance: Its Relation to Lesions of the Respiratory Bronchiole", Amer. Rev. Resp. Dis., 1966, Vol. 94, pp. 10-19.

44. Thomson, M.L., and Pavia, D., "Particle Penetration and Clearance in the Human Lung", Arch. Environ. Health, Oct. 1974, Vol. 29, pp. 214-219.

45. LaBelle, C.W., and Brieger, H., "Patterns and Mechanisms in the Elimination of Dust From the Lung", In: Inhaled Particles and Vapours, Editor: C.N. Davies, Pergamon Press, London, 1961, Vol. I, pp. 356-368.

46. Camner, P., and Philipson, K., "Intra-individual Studies of Tracheobronchial Clearence in Man Using Fluorocarbon Resin Particles Tagged with 18F and 99TC, In: Inhaled Particles III, Editor: W.H. Walton, Unwin Bros., Ltd., Surrey, England, 1971, Vol. 1, pp. 157-163.

47. Camner, P., Hollstrom, P.A., Lundborg, M., Philipson, K., "Lung Clearance of 4 μm Particles Coated with Silver, Carbon or Beryllium", Arch., Environ. Health, 1977, Vol. 32, pp. 58-61.

48. Dyson, E.D., and Beach, S.A., "The Movement of Inhaled Material From the Respiratory Tract to Blood. An Analogue Investigation of the New Lung Model", Health Physics, Pergamon Press, Northern Ireland, 1968, Vol. 15, pp. 385-397.

49. Van As, A., "Pulmonary Airway Clearance Mechanisms: A Reappraisal", Amer. Rev. Resp. Dis., 1977, Vol. 115, pp. 721-726.

50. Bowden, D.H., "The Pulmonary Mocrophage", Environ. Health Presp., 1976, Vol. 16, pp. 55-60.

51. Miller, K., and Harrington, J.S., "Some Biochemical Effects of Asbestos on Macrophages", Br. J. Exp. Path., 1972, Vol. 53, pp. 397-405.

52. Smith, B.A., and Davis, M.G., "The Association of Phagocytosed Asbestos Dust with Lysosome Enzymes", The Journal of Pathology, 1971, Vol. 105, No. 3, pp. 153-157.

53. Gross, P., Charleston, S.C., "Is Short-Fibered Asbestos Dust a Biological Hazard?" Arch. Environ. Health, Aug. 1974, Vol. 29, pp. 115-117.

54. Taskinen, E., Ahlman, K., and Wiikeri, M., "A Current Hypothesis of the Lymphatic Transport of Inspired Dust to the Parietal Pleura", Chest, Aug. 1973, Vol. 64, No. 2, pp. 193-196.

55. Mercer, T.T., "On the Role of Particle Size in the Dissolution of Lung Burdens", Health Physics, Pergamon Press, Northern Ireland, 1967, Vol. 13, pp. 1211-1221.

56. Thomas, R.G., "Transport of Relatively Insoluable Materials From Lung to Lymph Nodes", Health Physics, Pergamon Press, Northern Ireland, 1968, Vol. 14, pp. 111-117.

57. Morrow, P.E., "Alveolar Clearance of Aerosols", Arch. Intern. Med,, Jan. 1973, Vol. 131, pp. 101-108.

58. Brain, J.D., Sorokin, S.P., and Godleski, J.J., "Quantification, Origin, and Fate of Pulmonary Macrophages", In: Respiratory Defense Mechanism, Part I, Editors: Brian, Proctor and Reid, Vol. 5, pp. 849-892.

59. Green, G.M., "Alveolobronchiolar Transport Mechanisms", Arch. Intern. Med., 1973, Vol. 131, p. 109.

60. Pooley, F.D., "Electron Microscope Characteristics of Inhaled Chrysotile Asbestos Fibre", British Journal of Ind. Medicine, 1972, Vol. 29, pp. 146-153.

61. Langer, A.M., Rubin, I and Selikoff, I.J., "Electron Microprobe Analysis of Asbestos Bodies", In: Pneumoconiosis. Proceedings of the International Conference Johhannesburg, Editor: H.A. Shapiro, Oxford University Press, Cape Town, 1969, pp. 57-69.

62. Davis, J.M.G., and Gross, P., "Are Ferruginous Bodies an Indication of Atmospheric Pollution by Asbestos", Archives of Pathology, 1971, Vol. 90, pp. 238-242.

63. Seaton, A., "Asbestosis" in Occupational Lung Diseases, Editors: W.M.K.C. Morgan and A. Seaton, W.B. Saunders Company, Toronto, 1975, pp. 124-148.

64. Stanton, M.F., "Some Aetiologic Considerations of Fibre Carcinogenesis" Biological Effects of Asbestos, Lyon, Oct. 1972, paper 43A, pp. 43A-1-14.

65. Pott, F., Huth, F., and Friederichs, K.H., "Tumorigenic Effect of Fibrous Dusts in Experimental Animals" Environmental Health Perspectives, 1974, Vol. 9, pp. 313-315.

66. Stanton, M.F. and Wrench, C., "Mechanism of Mesothelioma Induction with Asbestos and Fibrous Glass", Journal of National Cancer Institute, 1972, Vol. 48, pp. 297-821.

67. Newball, H.H., and Brahim, S.A., "Respiratory Responses to Domestic Fibrous Glass Explosure", Environmental Research, 1976, Vol. 12, pp. 201-207.

68. Bayliss, D.L., Dement, J.M., Wagoner, J.K., and Blejer, H.P., "Mortality Patterns Among Fibrous Glass Production Workers", Annals New York Academy of Sciences, 1975, pp. 324-335.

69. Hill, J.W., "Man-made Mineral Fres", J. Soc. Occup. Med., Great Britain, 1978, Vol. 28, pp. 134-141.

70. The Committee on Environmental Health, American College Chest Physicians, "The Pulmonary Response to Fibreglass Dust", Chest, Feb. 1976, Vol. 69, pp. 216-219.

71. Gross, P., "The Biologic Categorization of Inhaled Fibre Glass Dust". Archives of Enviornmental Health, Mar./Apr. 1976, pp. 101-106.

72. Nasr, A.N.M., "Pulmonary Hazard From Exposure to Glass Fibres", Journal Occup. Med. 1967, Vol. 9, pp. 345-348.

73. Shetigra, P.T., Morgan, R.W., "Asbestos, Smoking and Laryngeol Carcinoma", Archives of Environmental Health, 1975, Vol. 30, pp. 317-519.

74. McDonald, J.C., "Asbestos and Public Health", For Discussion by CMA Sub-Committee on Environmental Air Pollution and Health (Not Published).

75. Ostiguy, G., "Health Hazards of Asbestos Exposure", Hotel Dieu de Montreal, Faculte de Medecine, Universite de Montreal, Aug. 1976.

76. Selikoff, I.J., Nicholson, W.J., and Langer, A.M., "Asbestos Air Pollution", Archives Environmental Health, July 1972, Vol. 25, pp. 1-13.

77. McDonald, J.C., "Asbestosis in Chrysotile Mines and Mills", In: Biological Effects of Asbestos, Switzerland, 1977, pp. 155-159.

78. Liddel, D., Eyssen, G., Thomas, D., and McDonald, C., "Radiological Changes over 20 Years in Relation to Chrysotile Exposure in Quebec", Inhaled Particles IV, Edited by W.H. Walton, Pergamon Press, Oxford & New York, 1977, pp. 799-811.

79. Becklake, M.R., Liddell, F.D.K., Manfreda, J., and McDonald, J.C., "Radiological Changes after Withdrawal from Asbestos Exposure, British Journal of Industrial Medicine. 1979, Vol. 36, pp. 23-28.

80. Pelnar, P.V., "Diagnosis, Evaluation of Working Capability and Compensation in Asbestosis and Its Complications", XVI. International Congress on Occupational Health, Sept. 1969, Tokyo, pp- 199-202.

81. Gibbs, G.W., "Etiology of Pleural Calcification: A Study of Quebec Chrysotile Asbestos Miners and Millers", Archives of Environmental Health, Mar/Apr. 1979, pp. 76-83.

82. Thomson, M.L., Short, M.D., "Mucocilliary Function in Health, Chronic Obstructive Airway Disease and Asbestos", Journal of Applied Physiology, 1969, Vol. 26, p. 535.

83. Golstein, B., Rendal, R.E.G., "Ferruginous Bodies", In: International Conference on Pneumoconiosis, Johannesburg Apr/May 1969, pp. 40-46.

84. Selikoff, I.J., Hummond, E.C., "Asbestos Bodies in The New York City Population in Two Periods of Time", In: International Conference on Pneumoconiosis, Johannesburg Apr/May 1969, pp. 47-53.

85. Selikoff, I.J., Hammond, E.C., "Mortality Experiences of Asbestos Insulation Workers", In: International Conference on Pneumoconiosis, Johannesburg, Apr/May 1969, pp. 97-103.

86. Pelnar, P.V., "Asbestos in Quebec Mining Industry", Lecture notes, 1972.

87. Becklake, M.R., "Environmental Exposure to Asbestos", Chest, Sept. 1979, Vol. 76, pp. 245-247.

88. McDonald, J.C., "Cancer in Chrysotile Mines and Mills", Biological Effects of Asbestos, International Agency for Research on Cancer, Lyon, 1973, pp. 189-194.

89. McDonald, J.C., Rossiter, C.E., Eyssen, G., McDonald, A.D., "Mortality in the Chrysotile Producing Industry of Quebec: A Progress Report, IVth. International Pneumoconiosis Conference, Apimodia Publishing House, Bucharest, Romania, 1973, pp. 232-237.

90. McDonald, J.C., McDonald, R.D., Gibbs, G.W., Siemiatycki, J., Rossiter, C.E., "Mortality in the Chrysotile Asbestos Mines and Mills of Quebec", Archives of Environmental Health, June 1971, Vol. 22, pp. 677-686.

91. McDonald, J.C., Becklake, M.R., Gibbs, G.W., McDonald, A.D., and Rossiter, C.E., "The Health of Chrysotile Asbestos Mine and Mill Workers of Quebec", Archives of Environmental Health, Feb. 1974, Vol. 28, pp. 61-68.

92. McDonald, J.C., Liddell, F.D.K., Gibbs, G.W., Eyssen, G.E., and McDonald, A.D., "Dust Exposure and Mortality in Chrysotile Mining 1910-75", British Journal of Industrial Medicine, 1980, Vol. 37, pp. 11-24.

93. Peto, J., Doll, R., Howard, S.V., Kinlen, L.J., and Lewinsohn, H.C., "A Mortality Study Among Workers in an English Asbestos Factory", British Journal of Industrial Medicine, 1977, Vol. 34, pp. 169-173.

94. Elmes, P.C., Simpson, M.J.C., "Insulation Workers in Belfast; A Further Study of Mortality Due to Asbestos Exposure (1940-75)", British Journal of Industrial Medicine, 1977, Vol. 34, pp. 174-180.

95. McDonald, A.D., Harper, A., El Attar, O.A., and McDonald, J.C., "Epidemiology of Primary Malignant Mesothelial Tumors in Canada", Cancer, Oct. 1970, Vol. 26, No. 4, pp. 914-919.

96. McDonald, A.D., and McDonald, J.C., "Epidemiologic Surveillance of Mesothelioma in Canada", CMA Journal, Sept. 1973, Vol. 109, pp. 359-362.

97. McDonald, A.D., Magner, D., and Ayssen, G., "Primary Malignant Mesothelial Tumors in Canada, 1960-1968", Cancer, Apr. 1973, Vol. 31, No. 4, pp. 869-876.

98. McDonald, J.C., and Becklake, M.P., "Asbestos Related Diseases in Canada", Hefte zur Unfallheilkunde, Heft 126, 1975, pp. 521-535.

99. McDonald, J.C., and McDonald, A.D., "Epidemiology of Mesothelioma from Estimated Incidence", Prevention Medicine, 1977, Vol. 6, pp. 426-446.

100. Haley, T.J., "Asbestosis: A Reassesment of the Overall Problem", Journal of Pharmaceutical Sciences, Sept. 1975, Vol. 64, pp. 1435-1447.

CHAPTER VI

## STATE OF KNOWLEDGE: EXAMINATION AND MEASUREMENT OF AIRBORNE CHRYSOTILE ASBESTOS FIBRES

### 6.1 GENERAL

At present technically and economically it is not possible to reduce the dust level concentrations down to zero at the work environment. According to the American Conference of Governmental Industrial Hygienists, [71] threshold limit values (TLV's) refer to airborne concentrations of substances and represent conditions under which it is believed that nearly all workers may be repeatedly exposed day after day without adverse effect. In order to achieve the safe health conditions at the work place, effective dust control strategies are required. Therefore, a proper instrumentation, and a knowledge of the measurement and assessment methods for dustiness at the work environment are essential parts of the strategies to achieve the required goal and objectives. It is equally important to know how to use the gathered data and assess the potential danger to health in the work environment. However, the main drawback in assessing the potential danger of asbestos dust is the lack of precise knowledge in answering the following questions: What level of chrysotile fibre concentration would be considered acceptable without causing health problems? What sizes of asbestos fibres are hazardous? How do the fibres cause the lung diseases? These have yet to be satisfactorily determined.

At present, the level of dust concentrations is determined by measuring one or more of the following parameters: size and number of the dust particles, surface area, and mass of the dust particles, in a measured volume of air. Furthermore, the chemical composition of the dust is also an important parameter.

6.2 Chrysotile Asbestos Dust Sampling and Instrumentation:

Although the main objective is to assess and provide a healthy workplace for workers, the instrumentaion requirement changes with the strategies. According to Trudeau(1) the main objective "health at the workplace" can be subdivided into three strategic categories: (a) engineering dust control, (b) compliance with the law and regulations, (c) medical reasons and records.

An engineer at a workplace usually with spot-checking locates the dust source, evaluates the dust concentration and designs a dust control or dust collecting system accordingly. The next step is to measure the efficiency of the dust control system by continous monitoring. However, engineers are also interested in the job habits of workers and may use the personal sampling methods that are used in the field of industrial hygiene to develop dust exposure indices. These are determined based on the job classification, the level of exposure and the duration of employment in the asbestos industry.

The five general categories for chrysotile asbestos dust measuring instruments and techniques are summarized in

in table 6.1. At present some of these instruments and techniques are obsolete and are not used by the asbestos industry.

6.2.1 Konimeters:

Until recently, konimeters were very commonly used instruments for the evaluation of dust counts in the mining industry in South Africa. The reason was that it is a practical instrument and it is possible to collect 42 different samples on one glass slide. Only a small volume of air (5 cc) is sampled each time, in a very short period, almost instantaneously. Later, the dust content of the specially prepared glass slide is counted under the dark field optical microscope. However, since the Konimeter sampling is done in a fraction of a second, it does not represent the varying concentrations in the measured environment for the total work-shift(4). Furthermore, airborne respirable asbestos dust longer than 100 micrometres cannot be sampled with this instrument(2)(3). Although it was a popular instrument for daily silica and coal dust surveys, it was not used in the Canadian asbestos industry, with the exception of Ontario and British Columbia asbestos industries.

6.2.2 Midget Impingers:

The impinger is another practical instrument for measuring asbestos dust concentrations and until recently it was widely used by the asbestos industry of North America(4)(5)(6)(7). However, recent developments in dust sampling

techniques have shown that the determination of hygiene criteria based on impinger asbestos dust counts could be misleading[2][3][5][7]. Roach[7] compared the impinger results of chrysotile asbestos dust surveys with data from four other survey methods. These were membrane filter, thermal precipitator, royco counter and horizontal eleutriator results. The difference is due to dust counting under the optical microscope using small magnification and low counting efficiency. The tendency of the chrysotile fibres to curl up while suspended in water makes it difficult to differentiate them from the other ordinary particles[2][3][7]. Also small diameter fibres have longer settling time and cannot be sampled efficiently by an impinger. The reason being that the alloted sampling time is too short relative to the settling time, and therefore it should not be considered a good instrument for asbestos sampling[3]. The advantage of the impinger over the konimeter is that samples may be taken over a longer period of time and better results may be obtained under average atmospheric working conditions.

In North America, the majority of the past chrysotile asbestos dust evaluations were based on the impinger sampling technique. Several researchers have attempted to correlate these results with those obtained from the recently most accepted membrane filter technique[5][8][27]. However, these efforts and attempts proved to be unsatis-

Table 6.1 FIVE GENERAL CATEGORIES FOR ASBESTOS DUST SAMPLING INSTRUMENTS AND TECHNIQUES:

| General Category | Physical Principle of Collection | Name of the Instrument | Collection Efficiency and Remarks |
|---|---|---|---|
| 1. Inertial Force | a) Suction & Impaction | Konimeters | 40 to 60%. Practical instrument but not used in asbestos industry anymore. |
| | b) Suction & Impingement | Midget-Impinger | 40%. Practical spot checking instrument but not used anymore. |
| | c) Suction & Centrifugal | Cyclones | 95 to 100%. Good instrument for gravimetric sampling and sizing. |
| 2. Filtration | Suction & Milipore filtering media | Gravimetric and Personal Samplers | 95 to 100%. Good instrument for mass measurement, chemical analysis and size distribution by Microscope counting. |
| 3. Precipitation | a) Eleutriator | Horizontal Eleutriator, Hexhlet-Eleutriator | 75-100%. Practical instruments for respirable, gravimetric dust sampling. |
| | b) Thermal Precipitation | Thermal Precipitator & DISA in Combination | 98-100%. It is a good loaboratory instrument. |

Table 6.1 - continued

| General Category | Physical Principle of Collection | Name of the Instrument | Collection Efficiency and Remarks |
|---|---|---|---|
| | c) Electrostatic Precipitation | Electrostatic Precipitators | 98-100%. Good for Bulk Gravimetric Laboratory Sampling. |
| 4. Light Scattering | Light beam deflection by dust | (a) Leitz Tyndallascope | 40%. Practical instrument. |
| | | (b) Royco. | 98-100%. Not practical, good as lab. Instrument. |
| 5. Others | β radiation attenuation | (a) Ambient Pollution Monitor (APM) | 95-98%. Sturdy and practical Instrument. |
| | | (b) Respirable Dust Monitor (RDM 101-4) | 95-98%. Practical Instrument. |

factory and inconclusive. Jacobson and Tomb[9], have shown that there is better correlation between the gravimetric respirable dust concentration and the midget impinger number concentration. However, due to the limited number of experiments the established relationship is not reliable and cannot be generalized.

6.2.3 Thermal Precipitation:

The sampling efficiency of thermal precipitators approaches 100% for particles up to 10 micrometres[3][10]. "The long-running thermal precipitator" (LRTP) is a very useful instrument for chrysotile asbestos fibre sampling, because it uses the principles of both settlement and thermal precipitation. With LRTP, fibres of up to 300 micrometres in length may be observed[2][7]. The fibre sampling with LRTP is dry and large magnification can be used for counting fibres. As a result of better magnification the thermal precipitator counts are higher than other counts[2][7][10].

The main disadvantage of LRTP is that the sampling process is very time consuming (30 minutes or more) since it is effective only at a slow rate of sampling, 2 cubic centimetre per minute. However, this same factor can be considered as an advantage because the longer sampling time provides better representation of the environmental conditions that exist for the period of the working shift.

6.2.4 Electrostatic Precipitation:

The electrostatic precipitator is a good instrument when the collection of a large sample of airborne dust is required. It is also ideal for collecting samples for chemical analysis, and collection efficiency for any size of particle is very high(10).

Electrostatic precipitators have two advantages over the filtration samplers: the sampling rate is not affected by mass loading and the sample is in an easily recoverable form. The main disadvantages of electrostatic precipitators are: the number-concentration or size frequency distribution cannot be determined and therefore nonrespirable particulates cannot be differentiated from the harmful respirable sized ones.

6.2.5 Light Scattering Techniques: Tyndallometers:

The TM Digital Tyndallometer and Leitz Tyndalloscope are two of the most common instruments which work on the light scattering principle. These instruments are widely used in Europe, specially in Germany, and also to some extent in Quebec and New Brunswick. The advantages are that they are simple to operate, provide instantaneous readings and some models of the tyndallometer give size distribution and assess the suspended particulates as they occur in the atmosphere. However, one serious disadvantage is that they do not differentiate the inert dust from the harmful dust, and therefore values from a tyndallometer do not indicate the fibre

portion of the total dust. According to Trudeau[1], in the Quebec Asbestos Mining Industry, the Tyndallometer is used as a spot-checking instrument to monitor the variations of dust concentrations around bag houses and detection of leakage of bag filters.

6.2.6 The Membrane Filter Technique:

Since 1973, the membrane filter technique has been most commonly used for sampling, mounting and determining the index concentration of respirable chrysotile asbestos fibres, for strategies of fixed station sampling and for personal sampling. The index concentration is the number of fibres of a certain dimension per cubic centimetre of air. The dimensional limits are: an aspect ratio (length to diameter) of at least 3:1; a fibre length greater than 5 micrometres; and a fibre diameter no greater than 3 micrometres. The lower size limit of the fibre diameter is dictated by the resolving power of the phase contrast optical microscope of 400 to 500 mangification[1] (11 to 20). Authors of referenced documentation, reference #11 to 19, all agree on the following basic principles of the membrane filter method: the sample is collected on a membrane filter with pore size 0.8 micrometre by drawing a predetermined quantity of air by means of a battery operated sampling pump. Later, by using aceton vapour and/or glycerol triacetate (triacetin), an opaque membrane filter is rendered transparent and optically homogeneous specimen. It is then mounted. Then,

the fibres are counted under the phase contrast optical microscope and the airborne fibre concentration is reported as "fibres per cubic centimetre or millilitre of air". Since the duration of the sampling time and the total volume of sampled air is measured and known, calculation of the airborne fibre concentration is simple. However, if the same sample is studied under the transmission electron microscope, it is observed that the calculated airborne fibre concentration is substantially higher than the optical microscope concentration results. According to Gibbs[22] only between 1.9% and 10.6% of the airborne chrysotile fibres of the textile industry would be observed by optical microscopy when the actual counts were based on transmission electron microscope observations. Therefore, when fibre dust count results are reported it is important to specify the counting method and magnification. Gibbs et al.[23] and Walton et al.[24] have carried out international comparisons of counts of airborne asbestos fibres sampled on membrane filters and their findings indicate that different counting techniques have substantial influence on concentration results. Filters cleared by acetone vapour gave significantly higher counts when compared with triacetin results. Gibbs and du Toit[25] state that, because of the variation in sampling techniques such as: different sampling rates and the sizes of membrane filters used, the air entry velocity into the filter is varied and this may also influence the recorded concentrations.

According to Trudeau[1] even within the same laboratory, significant count differences could occur if two different microscopes have been used. Trudeau also states that "the coefficient of variation of the counting step within one group of laboratories is ± 15 percent when all technicians are using the same microscope fields".

The causes of errors which influence the concentration results of the membrane filter method are summarized in tables 6.2 and 6.3

Table 6.2 - Variations in Dust Counts Due to Differences in Techniques Within the Membrane Filter Method[1].

| | |
|---|---|
| Sampling: | The Flowrate |
| | The Velocity at the Input of Filter |
| | The Diameter of Filters |
| Mounting: | The Mounting Liquids |
| Counting: | The Counting Criteria |
| | The Counting Objectives |
| | The Phase Contrast System |
| | The Graticules |
| | The Magnification |

Table 6.3 - Causes of Variation in Dust Counts Due to Errors Inherent in the Method[1].

| | |
|---|---|
| Sampling: | Variation in the flowrate of one pump during the same sampling period |
| | Non-Uniform distribution of fibres on the filter |
| | Recording of Sampling time |
| | Contamination |

Table 6.2 continue...

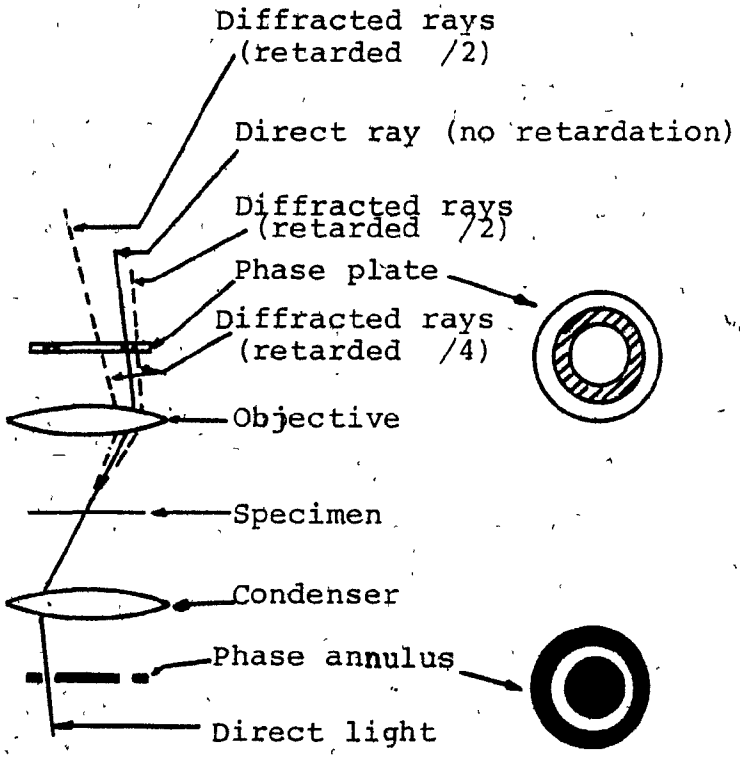


(52)
Fig. 6.1 - Ray diagram of phase contrast optical microscope

Table 6.2 - continued

Mounting: The quantity of mounting liquid may create the condition of migration of the particles

Counting: The different comprehension of the same criteria of counting by two technicians. The state of mind of one technician.

In order to eliminate the variations in the evaluation techniques of the membrane filter method, and provide a single and precise technique, the Dust Measurement Advisory Panel of the Asbestos International Association [26] has proposed a uniform membrane filter method which mainly follows the Australian membrane filter method [18] and contains good parts of all the other existing methods. Knight [21] has studied the "fibre overlap problems in counting fibres" and justified a simple rule of counting a pair of fibres as a fibre bundle and count them as one if all four ends cannot be resolved; and states that this would minimize the differences between microscopists, and would get better agreement among them. Knight [28], futhermore, investigated the reproducibility of chrysotile abestos fibre counting for the QAMA (Quebed Asbestos Mining Association) and concluded that reproducibility is higher for aspect ratios greater than 5:1 as compared to 3:1 and for lengths greater than 10 micrometres as compared to 5 micrometres.

Some of the advantages of membrane filter sampling are: a) the dust collecting efficiency is very close to 100 percent and dust particles as small as 0.01 micrometre in diameter may be collected. b) in the case of chrysotile asbestos, since the fibres are collected on the

surface of the filter they can be distinguished very easily from the other dust particles and examined directly with an incident light phase contrast microscope, or the particles may be transfered to an electron microscope grid and examined by electron microscopy. c) the samples may be taken in short or long periods at rates between 10 to 500 millilitres or 2 to 50 litres per minute. The high rate of sampling is used for mass determination and chemical analysis. d) personal sampling can be used for the assessment of the respirable chrysotile asbestos fibre to which an operator is exposed for the duration of the shift work, since the filter holder is small enough to be mounted on the lapel of a coat.

The two major disadvantages of membrane filter sampling are: a) in the case of microscopic observation the inefficiency of the counting technique, and b) in the case of mass determination, the respirable chrysotile asbestos fibre content of total dust is not known. The sampled dust is representing the total airborne dust and it is not possible to determine the respirable dust portion of the sample. This disadvantage can be eliminated by using a size selective sampling instrument.

6.2.7 Gravimetric Size Selective Sampling of Respirable Chrysotile Asbestos Dust:

Since 1940[30] the importance of gravimetric assessment of dust has been a controversial issue. However, the recent trends in the increasing use of mass measuring dust sampling instrumentation in the asbestos industry

is a result of good correlations between the mass concentration of respirable dust and the progression of disease among the exposed population[30]. The most important parameter in gravimetric size selective sampling is to differentiate and sample airborne respirable size dust from non-respirable dust by using size selective devices as the integral part of the main dust sampling instrument, simulating the dust settling action of filtration of the human nose and upper respiratory passages, while respirable dust being collected on filters.

Today, there are quite a few gravimetric, respirable dust size selective instruments on the market. However, the basic principle of size selection is either dependent on horizontal elutriation or cyclonic centrifugal separation. In 1952, the British Medical Research Council panels recommended the use of a horizontal eleutriator which had a specified selection curve for respirable dust, and later in 1959, Johannesburg International Conference on Pneumoconiosis endorsed the British Medical Research Council panels' recommendations[35][30][32][34]. In 1962, the United States Atomic Energy Commission adopted somewhat a different selection curve, based on using a cyclone as a size selector. Both of these selection curves are shown in Fig. 6.2 superimposed on the alveolar deposition curve of Brown et al.[31].

The selection curve of the horizontal eleutriator does not allow the penetration of any particles with falling speeds greater than 1.5 millimetre per second which corresponds

with the terminal velocity of particles of 7.1 micrometre spheres of unit density, and allows 50 percent penetration of particles of falling speed equal to 0.75 millimetre per second which corresponds to a terminal velocity of particles of 5 micrometre spheres of unit density(7)(30)(32)(33)(34)(35)(36).

In the case of cyclone, 100 percent of 1 micrometre unit density spheres are allowed to be collected with 50 percent of 3.5 micrometres, and complete rejection for all particles of falling speed, or terminal velocity, greater than 10 micrometre unit density spheres(30)(37).

The size selection curve of the cyclone corresponds better with the alveolar deposition curve in comparison to the selection curve of horizontal eleutriator. However, the cut off diameter of 7.1 micrometres for horizontal eleutriator is sharp and effective, but 10 micrometres cut off diameter for the cyclone is a gradual one, therefore, allowing the non-respirable size particles to penetrate and be collected(30). Furthermore, according to the Task Group on Lung Dynamics and Morrow(38), the airborne dust size distribution is a log-normal distribution and generally more than 85 percent of the airborne dust is smaller than 2.5 micrometres. When Fig. 6.2 is carefully studied, at this size range, it is noted that all curves pass through the same point allowing 92 percent penetration(7)(30)(38). Therefore the discrepancy in cut of curve of horizontal eleutriator does not affect the end result of collecting the specified respirable size dust(7)(32)(34)(35)(39).

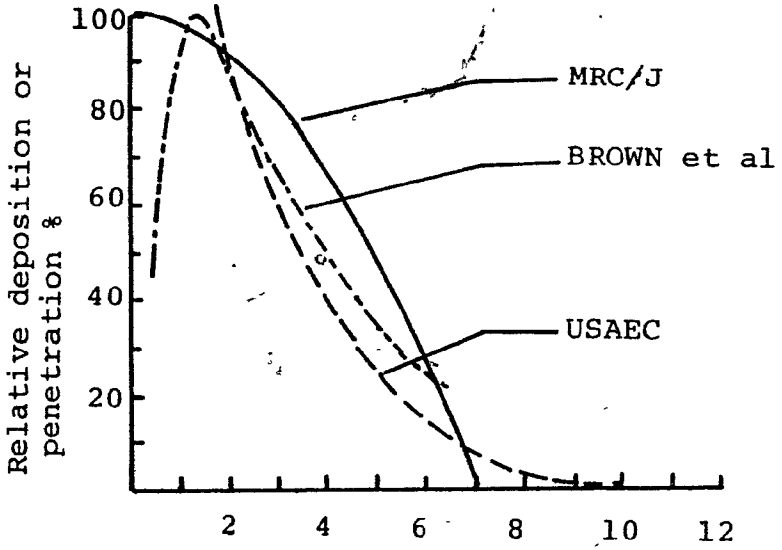


Fig. 6.2 (30) - Medical Research Council/Johannesbury and U.S.A.E.C. selection curves for respirable dust in comparison with the alveolar deposition curve of Brown et al. (1950)

6.2.7.1 The Hexhlet Size-Selective Gravimetric Sampler:

The Hexhlet sampler was designed by B.M. Wright[32] in 1954, using the horizontal eleutriator as size selector which is designed according to the British Medical Research Council specifications[30][34][35][39] (see Fig. 6.3). The name "Hexhlet" is a portmanteau name, incorporated from the four components that make up the instrument [34] [36]; the horizontal eleutriator to capture the nonrespirable portion of the airborne dust, a critical orfice to control the air flow, a "Soxhlet" thimble for collecting the respirable portion of dust, which is interchangeable with a screw-on filter holder, and a compressed air ejector to provide the suction or an electrically operated oil-less vacuum pump. Hexhlet samples the air at 50 litres per minute. However, originally it was designed to sample at 100 litres per minute. The reason for reducing the flow rate down to 50 litres per minute was to avoid the possibility of some settled, nonrespirable particles being removed from the eleutriator plates and collected on the back filter with respirable size dust, by the high velocity air[30][35] [36][38][39]. Before the sampling rate was reduced it was also suggested that the eleutriator plates should be coated with a sticky substance[36] to prevent the dislodging of the nonrespirable particles from the eleutriator plates; and Hamilton and Walton[35] suggested that the separation of the selector plates should be increased which would reduce the air flow velocity and prevent the reentraining of the large

particles. The basic principle of horizontal eleutriator is that as the airborne dust passes through a horizontal duct in a laminar flow regime at such velocity that nonrespirable particles which are desired to be captured and separated, will settle on the floor of the duct, according to their terminal settling velocity, before they reach the end. The respirable size dust particles which have lower terminal settling velocities will pass through the duct in different proportions. This proportionality is dependent on the height of the path of the dust particle within the duct. If initially the dust particles were high in the duct, they would pass through and those which were near the floor would be captured, because the sedimentation time is a function of height and the terminal settling velocity.[35] [38]

$$t = \frac{h}{V_t} \text{ , and } L = V_1 . t$$

where: $t$ = The sedimentation time

$h$ = Height of the dust above the duct floor

$V_t$ = Terminal Settling Velocity

$L$ = Horizontal traverse distance

$V_1$ = Velocity of the laminarly flowing air or horizontal velocity of the airborne particles

Therefore, other than the height of the particles above the floor of the plates, the proportion of capture varies inversely as their settling rate (or terminal settling velocity) and in turn the terminal settling velocity varies as the square of the particle's aerodynamic diameter[32] [35]. Accordingly, the length of traverse

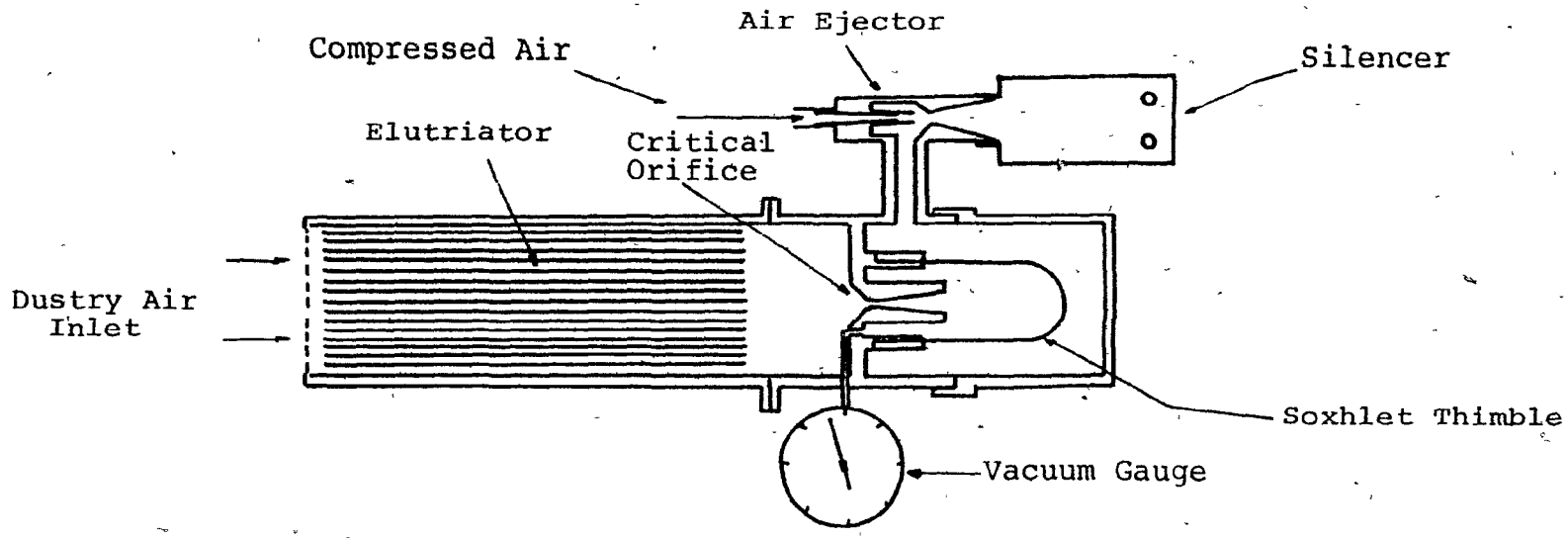


(30)
Fig. 6.3 - Diagram of Hexhlet Sampler

(until depositon) is directly proportional to the mean airflow velocity within the eleutriator duct, as long as the flow regime is laminar flow and not turbulent[32]. Similarly the air flow velocity is directly proportional to the volume of flowing air and inversely proportional to the cross sectional area of the duct, which can be expressed as follows[32][35]:

$$Q = V.A \text{ or } V = \frac{Q}{A}$$

where: Q = Volumetric flow rate

V = Air flow velocity

A = Cross Sectional Area of the duct

From these simple relationships it can be deduced that if the height of the duct is increased but the width kept constant, the falling time of a dust particle, from the top of the duct to the bottom, will be increased, however the air velocity will be decreased proportionately and therefore the traversed horizontal distance will remain unchanged, and the chance of a particle passing right through will not be affected. Thus, it can be stated that for a known volumetric flow rate, the eleutriator performance of a horizontal eleutriator is independent of its height and is dependent on its width and length, or in other words it is dependent on its floor area. This floor area can be calculated as follows: if the volume of air "Q" is known and the terminal settling velocity of the largest particle to be captured at a rate of 100%, is "$V_t$", the required floor area "$A_f$" is[32]: $A_f = \frac{Q}{V_t}$

According to Wright[32] the floor area of a horizontal eleutriator can be arranged either as a single long wide duct or as a stack of shorter and narrower ones so that it will be a compact instrument to carry around easily and take dust samples conveniently. Therefore, when Wright designed the eleutriator portion of the Hexhlet, he used a stack of plates to divide the duct into multiple horizontal ducts. However, from the basic ventilation formula it is known that the air flow through a duct at a given pressure is dependent on the cube of its height; and, therefore, care must be excercised during the construction in order to prevent height variations within the compartments of the eleutriator,

$$SP = \frac{KLO}{5.2A^3} Q^2$$

where: SP = Static pressure of the system

K = Coefficient of friction

L = Length of the duct

O = Perimeter of the duct

Q = Air Volume

A = Cross ectional area = h x w, "h" is the height and "w" is the width of the duct.

As stated earlier, the Hexhlet is a practical instrument for gravimetric sampling of respirable size dust in large quantities and in a relatively short period of time. Respirable size dust is defined by the British Medical Research Council (BMRC) as that "reaching the alveoli and is applicable to the pneumoconiosis producing dust", and selected the horizontal eleutriator cut-off curve to provide the best match to experimental lung deposition

data[30][39]. The U.S. Atomic Energy Commission (AEC) defined respirable dust as that "portion of the inhaled dust which penetrates to the non-ciliated portions of the lung". According to Lippman[39] if the Hexhlet penetration rate is compared with the International Commission of Radiological Protection Task Group Deposition Model for a tidal volume of 1450 cubic centimetres it is estimated that Hexhlet over samples only by 10 percent. Futhermore, it is known that the penetration rates of dust in humans drastically vary from one person to another (see Chapter V). Therefore, the Hexhlet is an adequate instrument for sampling pneumoconiosis producing dusts where the hazards and concentration standards are based entirely on the respirable fraction[39]. However, when there is a need for information about the non-respirable fraction of the dust, cyclones should be preferred, because it is too difficult to recover the non-respirable fraction from the eleutriator plates. In 1964, Davies[40] criticized the design of the Hexhlet as having a wide and square front, a partition in the middle which would create turbulent flow in the centre adjacent to the partition, and at the rectangular corners when the instrument is facing into a wind of minimum 8 miles/hour, in spite of the control of sampling flow by the critical orfice. This was corrected by increasing the duct height of each horizontal partition by decreasing the number of plates from 58 down to 27, and eliminating the middle partition and decreasing the horizontal duct number from 118 down to 28. The width of the entry was also reduced[35][36].

Ashford and Jones[41] have compared performances of Hexhlet, cyclones, and thermal precipitators at different flow rates. Their results indicated that cyclones over sampled the respirable dust. However, between the Hexhlet and thermal precipitation gravimetric samples there were consistent relationships among the mass concentrations. Also with cyclone sampling there is a considerable degree of aggregation in the airborne dust, which would increase the respirable dust sizes, which may be separated and collected as part of the non-respirabel fraction. Ashford and Jones [41] stated that Hexhlet eleutriator was unsatisfactory for prolonged underground use because the soxhlet thimble clogs up, the pressure of the instrument drops below 100 millimetres of mercury and the critical orfice could not maintain the correct flow rate. However, this could be eliminated if the soxhlet thimble or filter is changed before pressure drops below 100 millimetres of mercury Lippmann[39] stated that another limitation of the eleutriator type sampler is that it must be operated in a fixed horizontal position, and the vacuum pump is too heavy to carry around. It is also essential to clean out the captured dust on the eleutriator plates periodically in order to prevent the contamination of the collected respirable size dust by the reentrained non-respirable dust. These are some disadvantages of the Hexhlet eleutriator but they are not limitations, as indicated by Lippmann, if patience and care are exercised, and handled properly, useful results could be obtained.

According to Roach[7], chrysotile asbestos dust sampling results of the UNICO respirable dust sampler and the Hexhlet correlate very well. The interesting aspect of these results is that, as it was indicated by Ashford and Jones[41] earlier, UNICO sampler oversamples the respirable fraction of asbestos dust. Findings of Rendall et al.[3], Rendall[44], Timbrell[45], and Balzer[46] corroborate the findings of Roach that cyclones oversamples the respirable size chrysotile fibres in comparison to Hexhlet.

Wagner and Skidmore[42] indicated that horizontal eleutriators are efficient in collecting the respirable size airborne chrysotile asbestos dust but they do not take into consideration the interception of respirable long fibres by the upper respiratory tract, and therefore overestimate the respirable fraction of the airborne chrysotile fibres which penetrate into the alveolar region. On the same subject Timbrell and Skidmore[43] stated that the horizontal eleutriator is not complete as a selector of respirable fibrous dust. Because their experimental work with rats indicated that the airborne respirable fibrous dust counts of the inhalation chamber did not correspond very well with the retained dust in the lungs of rats which were exposed to the same concentration. However, in discussing the paper D.C.F. Muir [43] indicated that respiratory airways of the rats are much smaller than humans and long fibres which may penetrate into the alveolar regions of human's lungs cannot penetrate into the alveolar sections of the rat's lungs and in

upper respiratory tract. Moreover, the clearance of dust is more efficient. This argument was supported by J.L. Balber [43] stating that in his observations at autopsies of asbestos workers, it is not uncommon to find random fibres 100 or almost 200 micrometres in length in the alveolar region. During the same discussion J.D. Brain [43] indicated that curly fibres cannot penetrate into the deeper portions of the rat's lungs; therefore, they settle in the bronchial tree where muco-cilliary action is efficient. Those fibres which penetrated into the deeper parts of the lung may exist there for a short or extended period of time, and this existence is dependent on their solubility; thus, the size distribution of fibres found in the rat's lung is critically dependent on the time interval between exposure and sacrifice of the animal. Therefore, as described in Chapter V, these discussions also indicated that inhalation, retention, and clearance of dust are complicated problems and the experimental results are not well understood and are scattered and varied. Thus, the collection efficiency of Hexhlet should not be doubted on the basis of this type of experimental results.

Rendall et al. [3] and Rendall [44] indicated that UNICO 18 is not a good respiarble size dust sampler for asbestos dust smpling, because it samples non-respirable fibres which have fibre diameters larger than 3 micrometres. They also indicated that the best instrument for gravimetric respirable asbestos dust sampling is the Hexhlet horizontal eleutriator as compared to thermal precipi-

tators, midget impinger, cyclone and konimetres[3]. However, Rendall et al.[3] also stated that the wire mesh protector, which is in front of the Hexhlet eleutriator, collected a heavy deposit of fibre during sampling, and since this could affect the action of eleutriator recommend that it should be removed. In practice, if the eleutriator is cleaned after every sample is taken, and when the dust concentrations are not above the recommended threshold limit values this problem does not occur. Balzer[46] showed that the aerodynamic behaviours of asbestos fibres such as chrysotile and amosite, when sampled by Hexhlet eleutriator, is the same as suggested by Timbrell's work[47] that an effective equivalent fibre diameter could be obtained by multiplying the chrysotile fibre diameter by a factor of 2.5 and amosite by 3.5. Tomb and Corn[48] have used a horizontal eleutriator to calibrate the cyclone sampler for sampling equivalent aerodynamic diameters of coal, limestone and mica dust. The factors of multiplication for limestone and coal dust were approximately one but for mica particles which were close to oblate ellipsoid shape it was 1.3. This is another indication that the settling velocity of the elongated particles, are dependent on their equivalent aerodynamic diameters. Also it is generally accepted by researchers that when it is desired to subject experiment animals to only respirable size asbestos dust, the generated airborne dust is eleutriated and then animals are subjected to it[42][49]. Therefore, it can be concluded that the Hexhlet horizontal eleutriator is an adequate instru-

ment for the use of airborne respirable asbestos dust sampling for industrial hygiene research work.

6.2.7.2 Other Gravimetric Samplers with Cyclone Size Selector Attachment:

Cyclones have been used in the mineral industry for years as dust separators and collectors. Over the last 20 years miniature designs have been used as respirable size dust selectors for gravimetric dust sampling instruments[30]. The basic principle of cyclonic separation of dust from air is that, dust laden air enters the cylindrical section of the cyclone tangentially and follows a spiral path. As the air approaches to the axis of the cyclones the velocity of the air increases and large particles, due to centrifugal force, are removed from the air stream, and collected at the lower conical chamber of the cyclone. Respirable sized particles are trapped and collected by a membrane filter as the air escapes through and is exhausted by the axial outlet tube of the cyclone (see Fig. 6.4). The following empirical formula indicates the relationship between the diameter D, of particles which are collected by the cyclone with 50 percent efficiency and the velocity of the air, $\nu$, the diameter or width of the cyclone inlet, $B_c$, the effective number of turns made by the air stream in the cyclone, $N_t$, the average inlet velocity, $V_c$, density of the particle $\rho_p$, and the density of the air, $\rho_a$[36]:

$$D = \frac{9\nu B_c}{2\Pi N_t V_c(\rho_p - \rho_a)}$$

As stated above, unlike eleutriators, the performance of cyclones cannot be calculated precisely as they are empirical devices. However, their advantage over eleutriators is that they are small and during sampling their orientation is not critical. However, with cyclones, in order to prevent contamination of respirable size dust fraction by the non-respirable fraction, care must be taken not to tip them over or carry them upside down. The cut off curves of cyclones are not as sharp as eleutriators but are gradual (see Fig. 6.2 and 6.5). During recent years, because of their small size and light weight cyclones have received a better acceptance for their use in the mining industry of North America and West Germany as "personal dust samplers" in comparison to horizontal eleutriators such as MRE Gravimetric Dust Sampler Type 113A(30).

The APM (Ambient Pollution Monitor) is a gravimetric sampler, which utilizes two sampling channels simultaneously. One channel is fitted with a 10 millimetre cyclone which samples respirable size airborne dust and the second channel samples the total airborne dust(1). APM was designed to measure the airborne dust concentrations automatically by using the β radiation attenuation principle. The principle is explained by Trudeau(1) in detail. Because of the instrument's practicality, sensitivity and sturdiness, it is extensively used in Quebec asbestos mills to monitor the returned air quality.

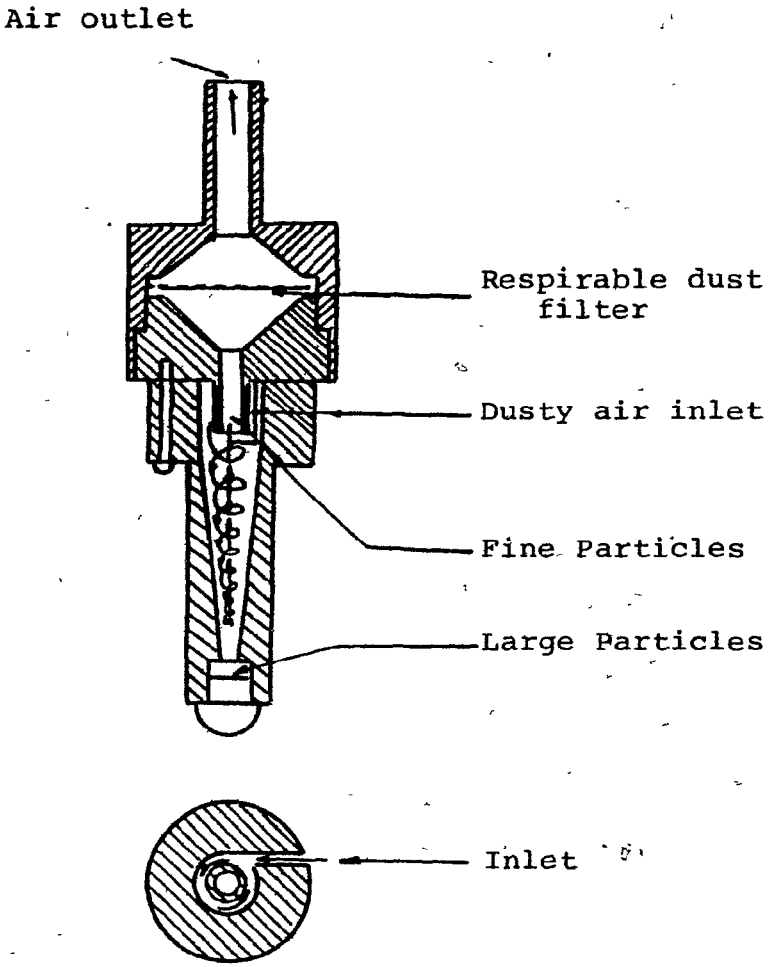


Fig. 6.4 - Diagram of a Cyclone Sampler[30]

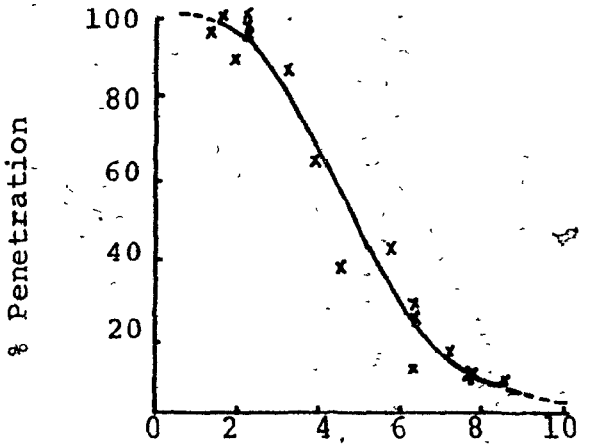


Fig. 6.5 - Selection curve for Cyclone Sampler[30]

Respirable Dust Monitor (RDM 101-4) is another gravimetric sampler which again uses a 10 millimetre cyclone to collect only the respirable size dust at 2 litres per minute and the gravimetric evaluation is done automatically, again based on β radiation principle. The difference between the RDM 101-4 and the APM is that RDM 101-4 has only one channel and when the cyclone is not fitted it can give the total airborne dust concentration of the air. The automatic dust sampling and evaluation cycle of RDM 101-4 is 4 minutes while the APM dust sampling time varies between 70 minutes and two hours. It is a light weight and practical instrument for spot-checking of the respirable and total airborne dust concentrations of the air and commonly used in asbestos mines and mills of Quebec. According to Knight[27][29] and Trudeau[1] when the membrane filter count results are compared with RDM 101-4 there is no direct relationship (see Fig. 6.6). Knight[29] states that the ratio of fibre to rock in various parts of the mill is not constant and the chrysotile fibre size distribution does vary with time, within the mill, thus, the respirable mass to fibre count ratio is not constant and will vary as well[29]. Therefore the biggest disadvantage of APM and RDM 101-4 is that they do not differentiate between the fibre fraction of the airborne asbestos dust and the other airborne particles which are rock dust and other air pollutants, and it is difficult to correlate these results with membrane filter dust count results.

6.2.8 Royco and Airborne Asbestos Dust Sampling:

During the last two decades, the Royco Particle Counter has been accepted as one of the most efficient laboratory instruments for sampling and counting the dust particles of sizes ranging from 0.3 to over 10 micrometres in fifteen separate size ranges. The air sampling rate can be varied from 0.01 to 0.1 cubic feet per minute.

Royco operates on the light-scattering principle and as the dusty air is passing through a photoelectric cell, each individual dust particle generates an electrical pulse. These electrical pulses are amplified by a photo-multiplier which feeds an electronic digital counting system. This system, by differentiating the pulse heights, classifies the particles according to their diameters. Addingly[6] and Roach[7] tested the Royco to determine its suitability for sampling asbestos dust, and compared the Royco results with other dust sampling instruments. Their findings indicate that the Royco is effective and efficient. However, like other automatic devices, (described above), it only indicates the total respirable size dust and does not differentiate the asbestos dust from others. The other disadvantage of Royco is that, it is a very heavy, non-portable, and sensitive instrument and therefore it is not suitable to be used in the atmospheric conditions that exist in mines and mills even as a "fixed station sampling" instrument.

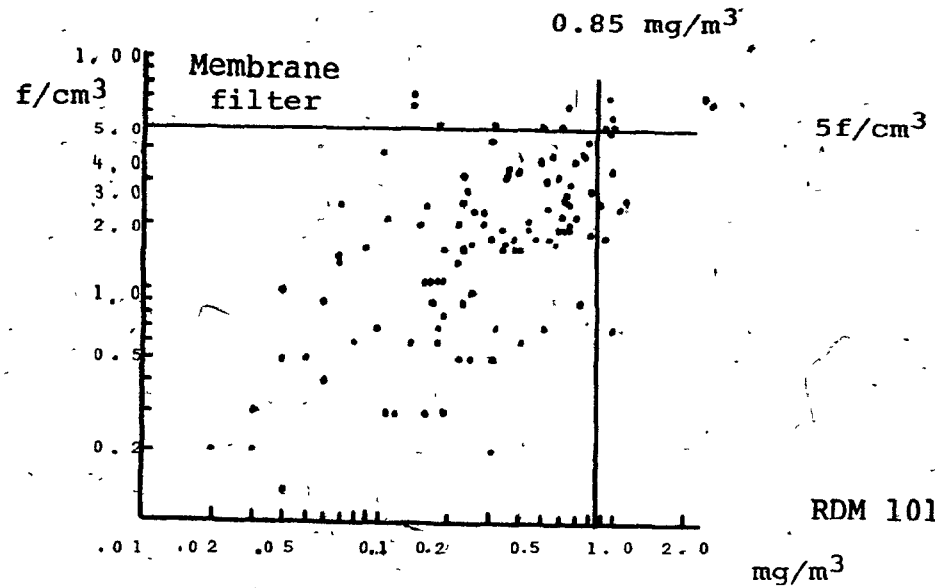


Fig. 6.6 (1) (27) Determination of equivalent dust concentrations

## 6.3 Chrysotile Asbestos Dust Indentification and Measurements By Electron Microscopy and Microprobe Analysis:

The ability to see fibres of diameters smaller than 0.3 or 0.2 micrometres with an optical microscope is limited(1)(52). Furthermore with optical methods, positive identification of different types of asbestos fibres of diameters 0.5 micrometres and smaller is practically impossible(52)(53).

Recent developments in electron microprobe chemical analysis have proven that the identification of particles smaller than 10 nanometres (100 Angstroms) with a scanning electron microscope (SEM), and smaller than 5 nanometres (50 Angstroms) with Transmission electron microscope (TEM) is possible(53)(54)(55)(56)(57). Also, with TEM, selected area electron difraction analysis is possible which provides the observer the opportunity of double checking on the identification of asbestos fibres.

### 6.3.1 Scanning Electron Microscopy and Fibre Identification:

Ordinarily, the Scanning Electron Microscope (SEM) image is not a static image, and the observed three dimensional view or topographic depth of the particles are persistant images which are displayed on the cathode ray tube. These images are renewed, usually twice per second, in the same way as a radar image system(52)(56)(57). Basically, SEM is an instrument which scans a finely focussed or a narrow beam of medium energy electrons

(5 to 50 kilo electron volts) across a sample. Because of their interaction with the sample they generate or produce secondary electron emissions, backscattered electrons and X-rays (see Fig. 6.7) from the sample. Each one of these signals can be detected, amplified and displayed on the cahtode-ray tube screen (52)(57). Usually, the secondary electron mode is used to detect the three dimensional topography of the particles and this is dependent on the contrast produced by the particles with different thicknesses. However, as the particle's third dimension, height or thickness, get smaller, the contrast of the image against the supporting surface gets also smaller. Therefore, the claimed resolution of 5 to 10 nanometres (50 to 100 Angstroms), by the manufacturers, loses its effectiveness(52). In order to overcome this problem and improve the contrast, it is suggested that backscattered electrons should be used to develop the image(57). It is explained that, in this mode, the generation of backscattered electrons, and therefore the obtained contrast, is dependent on the mean atomic number of the particle chemistry, and not on the particle thickness. However, experimental work has shown that again the contrast of small particles would approach the contrast of the supporting surface and the resolution would suffer(52).

For X-ray analysis, the scanning electron beam is stopped and a stationary beam is positioned on the desired particle

or fibre. The X-rays emmitted from the particle are detected by the X-ray detector and each emmitted X-ray is sorted out according to the intensity of their energies. In order to identify the observed particle or fibre, the obtained energy dispersive X-ray spectrum is related to the predetermined X-ray spectrum of pure minerals which have known chemistry; and this type of microprobe analyser is called "Energy Dispersive Analyser" (EDXA) (52) (56) (57).

In summary, fibre identification with SEM, as explained above, is dependent on the observed morphology of the fibre and the chemical composition as measured with EDXA microprobe. However, the chemical compositions of the amphibole group asbestos minerals and fibres are very similar to each other and most of the time it is too difficult to differentiate, chemically or visually, the very fine fibres of this group. Furthermore, when the diameter of the microbeam is larger than the observed fibre diameter, the chemistry of the background material interferes with the fibre X-ray analysis result.

6.3.2 Transmission Electron Microscopy and Fibre Identification: The transmission electron microscope uses an electron gun and electron lenses to produce a beam of electrons which is focused on to a sample. The electrons which are scattered by the specimen are treated by the electronic equipment and set of lenses to produce the magnified electron image

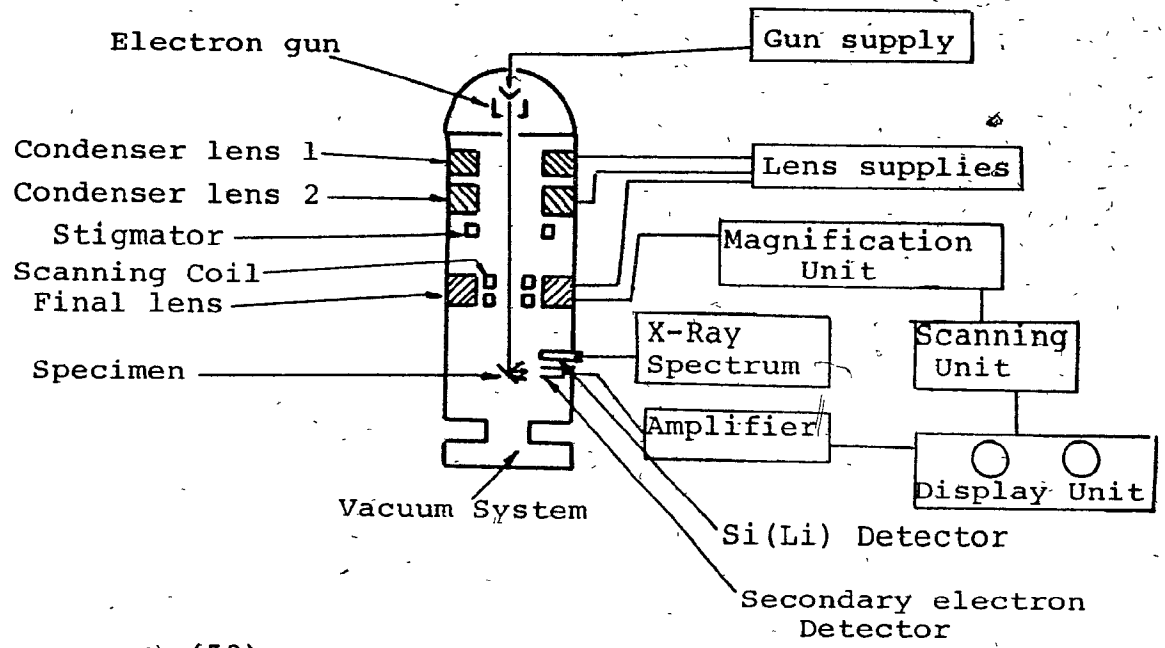


(52)

Fig. 6.7 - Schematic diagram of a scanning electron microscope with energy dispersive X-ray analyser

of the specimen[52][54][55] (see Fig. 6.8). Also an optical microscope is fitted to the TEM, for examining and positioning the specimen on a stage which can be, manually or automatically, moved or rotated.

Since the resolution of TEM is in the order of 5 to 10 angstroms[52][54][55], it is superior to the SEM, and is a more suitable instrument for energy dispersive X-ray analysis. The size of the microbeam is as small as 40 angstroms and because of better resolution ability, precise spotting of the beam on the desired particle or fibre is possible. The X-ray spectrum analysis and measurements are done by the same type of X-ray spectroscope attachement as explained for SEM. Pooley[54][55] has showed that chemical analysis of fibres less than 0.1 micrometre diameter with energy dispersive X-ray analyser (EDXA) is possible. Chatfield[52] stated that when the TEM's selected area electron diffraction (SAED) analysis ability is combined with the EDXA chemical analysis, the identification of the most difficult minerals and distinguishing them from each other, such as submicronic amphibole group asbestos fibres, is possible.

In SAED mode operation of TEM, since different minerals have different crystal structures, a particular mineral specimen would scatter the electrons from a point at a particular angle which are focussed at a single point in the image plane. The combination of these points would establish an electron diffraction pattern of the observed

mineral or fibre[52] (see Fig. 6.8). With a modern TEM it is possible to rotate or tilt the sample so that the crystalline fibre may be examined along its principal cystallographic directions. However, Seshan[58] has showed that the electron diffraction patterns of single amphibole UICC asbestos fibres are insensitive to tilts of ± 20° along and perpendicular to the fibre axis. But it should be also remembered that, it may not be possible to obtain an electron diffraction pattern from all of the observed fibres. The reason being that either some fibres are too thick and absorb the electron beam totally or they might be too thin to scatter the electron beam sufficiently to obtain a visible diffraction pattern..

The identification of submicroscopic chrysotile asbestos fibres with TEM is somewhat easier. Usually, single chrysotile asbestos fibres have hollow cores or tubular appearance; although it is known that halloysite has similar tubular appearance, with SAED and EDXA analysis the chrysotile fibre can be distinguished, very easily, from the halloysite[59][60]. Pooley[54] has shown that with EDXA analysis, trace minerals which are within the asbestos fibre structure can be successfully detected. Furthermore, trace minerals such as iron oxides can be easily distinguished from the contaminating mineral Magnetite, because the dispersive energy X-ray spectrum of magnetite is much stronger than the other iron oxides.

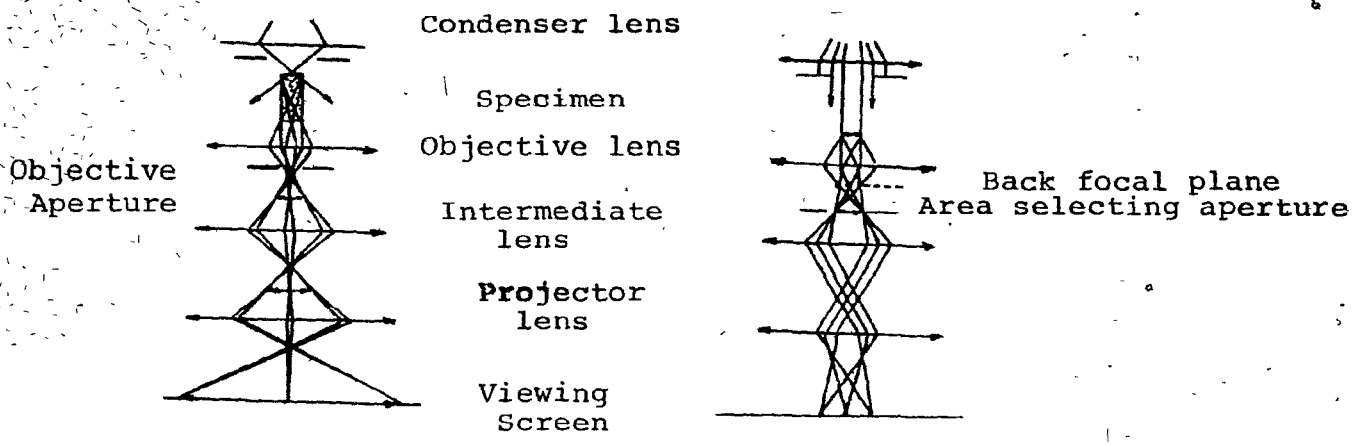


Fig. 6.8 Ray diagram[52] showing operation of transmission electron microscope in both microscopy and selected area electron diffraction modes

Pooley[60] has also shown that inhaled chrysotile asbestos fibres can be identified in human tissue due to their tubular appearance and more positively from their diffraction patterns. Langer and Pooley[61], Langer et al[62][63][64] and Pontefract et al[65] stated that, electron diffraction patterns can be obtained from suspect fibres in human tissue and positive identification can usually be made. Asbestos fibres however, particularly chrysotile, can lose magnesium in the biological environment, thus altering their structure and diffraction pattern. Positive identification of chrysotile asbestos fibrils, with a minimum aspect ration of 3 to 1, is then best made by TEM and EDXA[52].

The only drawback of TEM in comparison to SEM is the time consuming sample preparation and transfer of fibres and particulates collected on membrane filters to electron microscope (EM) grids for TEM studies. Spurney et al[66] suggested that since the surface of the Nuclepore filters are flat and uniform, the observation of fibres on carbon coated Nuclepore filter surfaces is not obstructed by

the surface texture of the filter. However, Ortiz and Isom[67] and later Hwang et al.[68] have shown that fibres and particles which are collected on membrane filters can be successfully transfered on to 400 mesh copper grids, without any loss or a maximum loss of 3% of the collected fibres, for TEM study. With this method, first filters are taped onto glass slides and exposed to acetone vapours in order to fuse and collapse the porous membrane filter and create a smooth surface for microscopic observation. Later, the dust laden filter is coated with gold-palladium and carbon in a vacuum evaporator equipped with a rotary stage. After the coating is completed, squares smaller than EM grids are cut out from the coated filter and placed on the grids which are already on a polyurethane sponge, and 90% of the sponge is immersed in an acetone bath. Eventually, the membrane filter dissolves and the coated specimen is completely transfered onto the EM grid.

At present, a TEM equipped with EDXA and SAED is the most powerful analytical tool available for the identification of airborne asbestos fibres.

6.4 Analytical Methods to Determine Chemical or Elemental Composition of Chrysotile Asbestos Dust:

Two of the commonly used analytical methods for the determination of chemical or elemental composition of chrysotile asbestos dust are X-ray diffraction and atomic absorption spectroscopy.

According to Keenan and Lynch[53] the results of both methods correspond within ± 10 to 15 percent.

The advantages of the X-ray diffraction method are: (a) the sample is not consumed during the analysis and therefore further tests or studies can be pursued with the same sample, (b) qualitative as well as quantitative analysis of the sample is possible. (c) it is quick. Once the existence of the asbestos in the sample is qualitatively proven then the more time consuming quantitative analysis results are sought[69]. The disadvantages of the X-ray diffraction method are: (a) the total weight of the sample should be larger than 1 milligram and the maximum length of the fibres should be smaller than 5 micrometres. Nenadic and Crable [69] stated that when the length of the fibres are between 1 and 20 micrometres, the error of analysis is 12 percent. (b) if and when the chrysotile fibre's crystalline structure is altered or they are contaminated with other unwanted or unimportant minerals the diffraction patterns cannot be easily identified, and errors could be made (c) the chrysotile fibres cannot be differentiated from the non-fibrous serpentine dust and results contain both minerals[53]. Atomic absorbtion spectroscopy is a more sensitive analytical tool than the X-ray diffraction method.

Atomic absorption spectroscopy is a method for the elemental analysis of samples in solution in an aqueous solvent. Ordinarily, the sample is dissolved in hydrochloric

and nitric acid, and diluted with distilled water and then the diluted solution is tested. When analysing the elements of chrysotile and its contaminating minerals, especially magnetite ($Fe_3O_4$), the sample is dissolved in hydrofluoric acid, because magnetite is a very difficult mineral to dissolve completely in other acids.

The summary of the atomic absorption analysis is as follows: A certain portion of the prepared solution is aspirated into the flame of the instrument, (see Fig. 6.9) and the atoms of the vaporized sample are irradiated by a hollow-cathode lamp which is made from the analysis element. The atomic vapour of the elements absorb the resonance-line radiation emitted by the same element in the hallow-cathode lamp, which decreases the light intensity passing through the instrument's monocromator to the photodetector. The amount which is absorbed by the atom vapour is a measure of the concentration of the element in the sample(53). The advantages of the atomic absorption spectroscopy is that it is a very sensitive and accurate method for anlysing very minute amounts of elements in bulk samples or in airborne dust samples. The accuracy of this method is indicative by the expected error which is smaller than $\pm$ 5 percent in determining 0.5 micro-grams of iron(53). The only disadvantage of this method when analysing for chrysotile asbestos is, it does not differentiate the fibrous chrysotile mineral from

the non-fibrous serpentine which has the same chemical composition but not the same structure. Therefore, the analytical result may contain both of these minerals when they are co-existing in the work environment.

Recently, Barbeau[70] has been developing a chemical method which utilizes titration by hydrochloric acid and magnesium determination in solvent for evaluation of chrysotile asbestos when it is present in the sample to more than 10 percent. He has shown that with this method the chrysotile asbestos would be differentiated from the other serpentine minerals. However he has also stated that at this stage, his results are serving to show the possibilities and difficulties rather than to prove the accuracy and precision of a chemical method of chrysotile determination.

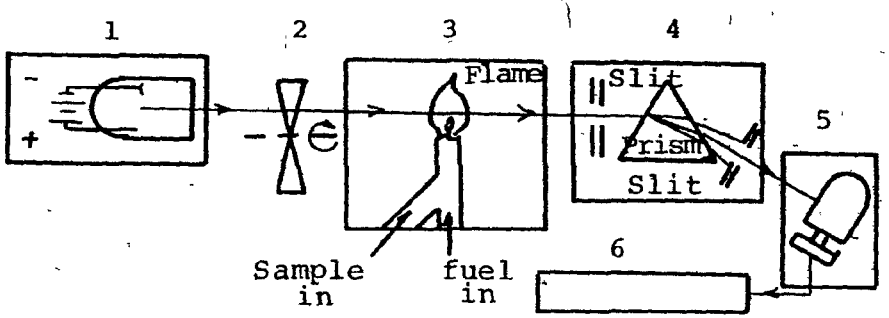


1. Hollow-cathode lamp
2. Rotating chopper
3. Vaporizing system
4. Monochromator
5. Photodetector
6. Electronics and readout

(53)
Fig. 6.9 - Atomic absorption spectrometer light path

## 6.2 Conclusion:

The detailed study of chrysotile asbestos dust sampling instrumentation has shown that the Hexhlet horizontal eleutriator is the best suited, and is a practical and reliable instrument, for gravimetric sampling of respirable size asbestos dust, as defined by BMRC, in large quantities for industrial hygiene research purposes, where the hazards and concentration standards are based entirely on the respirable fraction.

Cyclones are most commonly used as the first stage of the gravimetric size selective dust sampling instruments in Northern America. Although its selection curve of respirable size dust is better matched with the theoretical alveolar deposition curve, it does not have a sharp cut off, thus cyclones over sample the respirable size chrysotile asbestos fibres in comparison to Hexhlet.

The existing respirable size dust sampling instruments have the disadvantage that cannot differentiate the harmful chrysotile asbestos fibre fraction from the inert fraction of the dust. In order to identify and quantify the chrysotile asbestos fraction of the sample, cumbersom, time consuming and expensive transmission electron microscopy and EDXA and SAED microprobe analysis are necessary. Although more practical, chemical and analytical tools such as atomic absorption spectroscopy and X-ray diffraction methods could provide accurate chemical and elemental analysis of the sample, they cannot differentiate the fibrous chrysotile asbestos

from other serpentine minerals, and therefore a better and simpler method of quantification of chrysotile asbestos dust is necessary.

## LIST OF REFERENCES FOR CHAPTER VI


1. Trudeau, M., "Methods For the Evaluation of Asbestos Dust Concentration At The Workplace", In: Short Course in Mineralogical Techniques of Asbestos Determination, Editor: R.L. Ledoux, Mineralogical Association of Canada, Quebec, May 1979, pp. 213-252.

2. Rajhans, G.S., "Fibrous Dust - Its Measurement and Dust Control". C.I.M. Bulletin, Aug. 1970.

3. Rendall, R.E.G. and Van Sittert, G.C.H., "The Stability of Conventional Dust Instruments", In: International Conference on Pneumoconiosis, Department of Mines Republic of South Africa, Johannesburg, Apr./May 1969, pp. 35-39.

4. Holmes, S., "Development in Dust Sampling and Counting, Techniques In the Asbestos Industry", In: Annals of the New York Academy of Sciences, Ed. H.E. Whipple, Vol. 132, Art. 1, Dec. 1965, pp. 228-297.

5. Ayer, H.E., Lynch, J.R., and Fanney, J.H., "A Comparison of Impinger and Membrane Filter Techniques for Evaluating Air Samples In Asbestos Plants", In: Annals of the New York Academy of Sciences, Ed. H.E. Wipple, Vol. 132, Art. 1, Dec. 1965, pp. 274-287.

6. Addingley, C.G., "Dust Measurement and Monitoring in the Asbestos Industry", In: Annals of The New York Academy of Sciences, Ed. H.E. Wipple, Vol. 132, Art. 1, Dec. 1965, pp. 298-305.

7. Roach, S.A., "Measurement of Airborne Asbestos Dust by Instruments Measuring Different Parameters", In: Annals of The New York Academy of Sciences, Ed. H.E. Wipple, Vol. 132, Art. 1, Dec. 1965, pp. 306-315.

8. Renshaw, F.M., Bachman, J.M., and Pierce, J.O., "The Use of Midget Impingers and Membrane Filters for Determining Particle Counts", American Industrial Hygiene Association Journal, Mar./Apr. 1969, pp. 113-116.

9. Jacobson, M., and Tomb., T.F., "Relationship Between Gravimetric Respirable Dust Concentration and Midget Impinger Number Concentration". American Industrial Hygiene Association Journal, Nov./Dec. 1967, pp. 554-556.

10. Bardswick, W.A., and White, F.T.M., "Trends in the Instrumental Assessment of Industrial Dustiness", CIM Annual Conference, Montreal, April 1969.

11. Sub-Committee on Asbestosis of The Permanent Commission and International Association on Occupational Health., "Evaluation of Asbestos Exposures in the Working Environment", Institute of Occupational Health, Helsinki, Finland, Work Environment - Health, Vol. 8, No. 3, 1971, pp. 71-73.

12. Joint AIHA-ACGIH Aerosol Hazards Evaluation Committee, "Recommended Procedures for Sampling and Counting Asbestos Fibres", American Industrial Hygiene Association Journal, Feb. 1975, Vol. 36, pp. 83-90.

13. Joint AIHA-ACGIH Aerosol Hazards Evaluation Committee, "Background Documentation on Evaluation of Occupational Exposure to Airborne Asbestos", American Industrial Hygiene Association Journal, Feb. 1975, Vol. 36, pp. 91-103.

14. Harness, I., "Airborne Asbestos Dust Evaluation", Annals Occupational Hygiene, Pergamon Press, 1973, Great Britain, Vol. 16, pp. 397-404.

15. Addingly, C.G., "Asbestos Dust and Its Measurements", Annals Occupational Hygiene, Pergamon Press, 1966, Great Britain, Vol. 9, pp. 73-82.

16. Ortiz, L.W., Ettinger, H.J., and Fairchild, C.I., "Calibration Standards for Counting Asbestos", American Industrial Hygiene Association Journal, Feb. 1975, Vol. 36, pp. 104-112.

17. Leidel, N.A., Bayer, S.G., and Zumwalde, R.D., "USPHS/NIOSH Membrane Filter Method for Evaluating Airborne Asbestos Fibres", NIOSH Publication, Nov. 1973, pp. 1-11.

18. National Health and Medical Research Council, Australian Department of Health, "Membrane Filter Method For Estimating Airborne Asbestos Dust", F.D. Atkinson Government Printer, Camberra, Oct. 1976, pp. 1-52.

19. Regulation Codes and Protocole Report EPS 1-AP-75-1, "Standard Reference Methods for Source Testing: Measurement of Emissions of Asbestos Mining and Milling Operations", Air Pollution Directorate, Environmental Protection Service, Dec. 1976, pp. 1-31.

20. Doran, G.V., "Measurement of Airborne Asbestos Dust at Cassiar", Cassiar Asbestos Corporation Ltd., Cassiar, B.C., 1977, pp. 1-65.

21. Knight, G., "Overlap Problems in Counting Fibres", American Industrial Hygiene Association Journal, Feb. 1975, Vol. 36, pp. 113-114.

22. Gibbs, G.W., "Comments" to Methods Used in the Measurement of Asbestos-Dust Exposures, by R.S.J. DuToit. Proceedings of Asbestos Symposium, Johannesburg, Oct. Published by National Institute of Metallurgy, Randburg, 1978, pp. 19-36.

23. Gibbs, G.W., Baron, P., Becket, S., Dillen, R., duToit, R., Koponen, M., and Robock, K., "A Summary of Asbestos Fibre Counting Experience in Seven Countries". Annals of Occupational Hygiene, 1977, Vol. 20, No. 4, pp. 321-332.

24. Walton, W.H., Attfield, M.D., and Becket, S.T., "An International Comparison of Airborne Asbestos Fibres Sampled on Membrane Filters", Annals of Occupational Hygiene, 1976, Vol. 19, pp. 215-224.

25. Gibbs, G.W., and DuToit, R.S.J., "Environmental Considerations in Surveillance of Asbestos Miners and Millers", Conference Paper in Proceedings of Asbestos Symposium, Johannesburg, Oct. 1978, pp. 1-17.

26. Dust Measurement Advisory Panel, Asbestos International Association, "Draft Proposal of a Reference Method for the Determination of Fibre Concentration at Work Places in the Asbestos Industry by Optical Microscopy". Washington, D.C., 1978.

27. Knight, G., "Factors Affecting the Response of Airborne Dust Samplers and the Comparisons Between them", Q.A.M.A. Technical Report - TM77-7, Nov. 1977, pp. 1-17.

28. Knight, G., "One Study on Reproducibility of Chrysotile Asbestos Fibre Counting". Q.A.M.A. Technical Report - TM78-5, Feb. 1978, pp. 1-24.

29. Knight, G., "Gravimetric Sampling in Asbestos Mines and Mills", Q.A.M.A. Technical Report - TM77-9, Nov. 1977, pp. 1-33.

30. Walton, W.H., and Hamilton, R.J., "The Measurement of Airborne Dust", In: Medicine In the Mining Industries, Edited by: J.M. Rogan, F.A. Davis Company, Philadelphia, 1972, pp. 145-165.

31. Brown, J.H., Cook, K.M., Ney, F.G., and Hatch, T., "Influence of Particle Size Upon the Retention of Particulate Matter in the Lung", American Journal Public Health, 1950, Vol. 40, p. 450.

32. Wright, B.M., "A Size-Selecting Sampler for Airborne Dust", British Journal of Industrial Medicine, 1954, Vol. 11, pp. 284-288.

33. C.F. Casella and Co. Ltd., "Hexhlet", Leaflet 930/4/AR.

34. Walton, W.H., "The Theory of Size Classification of Airborne Dust Clouds by Elutriation", British Journal of Applied Physics, 1954, Supplement No. 3, p. 29.

35. Hamilton, R.J., and Walton, W.H., "The Selective Sampling of Respirable Dust", In: Inhaled Particles and Vapours, Editor: C.N. Davies, Pergamon Press, Oxford, 1961, p. 465.

36. Green, H.L., and Lane, W.R., "Health Hazards: Estimation of Mass Concentration", In: Particulate clouds: Dust, Smokes, and Mists, E. and F.N. Spond Ltd., London, Second Edition, 1964, pp. 361-364.

37. Lippmann, M., and Harris, W.B., "Size-Selecting Samplers for Estimating Respirable Dust Concentrations", Health Physics, 1962, Vol. 8, p. 155.

38. Morrow, P.E., "Aerosol Characterization and Deposition", American Review of Respirable Disease, Dec. 1974, Vol. 110, pp. 88-89.

39. Lippmann, M., "Respirable Dust Sampling", American Industrial Hygiene Association Journal, 1970, Vol. 31, pp. 138-159.

40. Davies, C.N., "Deposition and Retention of Dust In the Human Respiratory Tract", Annals of Occupational Hygiene, April 1964, Vol. 7, p. 169.

41. Ashford, J.R., and Jones, C.O., "Field Trials with the Hexhlet and Conicycle Airborne Dust Samplers and the Standard and Long Running Thermal Precipitators", Annals of Occupational Hygiene, April 1964, Vol. 7, p. 85.

42. Wagner, J.C., and Skidmore, J.W., "Asbestos Dust Deposition and Retention in Rats", In: Annals of the New York Academy of Sciences, Ed. H.E. Wipple, Vol. 132, Art. 1, Dec. 1965, pp. 77-88.

43. Timbrell, V., and Skidmore, J.W., "The Effect of Shape on Particle Penetration and Retention in Animal Lungs", In: Inhaled Particles III, W.H. Walton, Unwin Bros., Ltd., Surrey, U.K. 1970, pp. 49-56.

44. Rendall, R.E.G., "The Data Sheets on the Chemical and Physical Properties of the U.I.C.C. Standard Reference Samples", In: International Conference on Pneumoconiosis, Department of Mines Republic of South Africa, Johannesburg, Apr/May 1969, p. 14.

45. Timbrell, V., "Characteristics of the International Union Against Cancer, Standard Reference Samples of Asbestos", In: International Conference on Pneumoconiosis, Department of Mines Republic of South Africa, Johannesburg, Apr./May 1969, pp. 21-33.

46. Balzer, J.L., "Aerodynamics Properties of Fibrous Aerosols", Non-published Data, Environmental Health Sciences School of Public Health, University of California, Berkely.

47. Timbrell, V., "Inhalation of Fibrous Dust", In: Annals of the New York Academy of Sciences, Ed. H.E. Wipple, Vol. 132, Art. 1, Dec. 1965, pp. 255-273.

48. Tomb, T.F., and Corn, M., "Comparison of Equivalent Spherical Volume and Aerodynamic Diameters for Irregularly Shaped Particles", American Industrial Hygiene Association Journal, Jan. 1973, pp. 13-24.

49. Evans, J.C., Evans, R.J., Holmes, A., Hounam, R.F., Jones, D.M., Morgan, A., and Walsh, M., "Studies in the Deposition of Inhaled Fibrous Material in the Respiratory Tract of the Rat and Its Subsequent Clearance Using Radioactive Tracer Technique", Environmental Research, 1973, Vol. 8, pp. 180-201.

50. Stevens, D.C., and Stephenson, J., "A Size Selective Dust Sampler Which Conforms to the Lung Model Proposed by the I.C.R.P. Task Group on Lung Dynamics", United Kingdom Atomic Energy Authority, Research Group Report, Health Physics and Medical Division, Harwell, Berkshire, 1971, pp. 1-8.

51. Lippmann, M., and Hydonieus, A., "A Multi-Stage Aerosol Sampler For Extended Sampling Intervals", American Industrial Hygiene Association Journal, Nov./Dec. 1970, pp. 730-737.

52. Chatfield, E.J., "Measurement of Asbestos Fibres In the Work Place and in the General Environment", In: Short Course in Mineralogical Techniques of Asbestos Determination, Editor: R.L. Ledoux, Mineralogical Association of Canada, Quebec, May 1979, pp. 111-163.

53. Keenan, R.G., and Lynch, J.R., "Techniques for the Detection, Identification and Analysis of Fibres", American Industrial Hygiene Association Journal, Sept./Oct. 1970, pp. 587-593.

54. Pooley, F.D., "The Identification of Asbestos Dust With An Electron Microscope Microprobe Analyser", Annals of Occupational Hygiene, Pergamon Press, 1975, Vol. 18, pp. 181-186.

55. Pooley, F.D., "The Electron Microprobe Analysis of Fine Mineral Particles", Department of Mineral Exploitation, University College Cardiff, (Non published paper).

56. Beckett, S.T., "The Evaluation of Airborne Asbestos Fibres Using a Scanning Electron Microscope", Annals of Occupational Hygiene, Pergamon Press, 1973, Vol. 16, pp. 405-408.

57. DeNee, P.B., "Mine Dust Characterization Using the Scanning Electron Microscope", American Industrial Hygiene Association Journal, Oct. 1972, pp. 654-660.

58. Seshan, K., "Explanation for the Insensitivity of Tilts of the Electron Defraction Paterns of Amphibole Asbestos Fibres", Environmental Research, 1977, Vol. 14, pp. 46-58.

59. Samudra, A.V., Bock, F.C., Harwood, C.F., and Stochman, J.D., "Evaluating and Optimizing Electron Microscope Methods for Characterizing Airborne Asbestos", Environmental Sciences Research Laboratories, EPA 600/2-78-037, June 1978, pp. 1-49.

60. Pooley, F.D., "Electron Microscope Characteristics of Inhaled Chrysotile Asbestos Fibre", British Journal of Industrial Medicine, 1972, Vol. 29, pp. 146-153.

61. Langer, A.M., and Pooley, F.D., "Identification of Single Asbestos Fibres in Human Tissue", In: Proceedings of the International Conference on the Biological Effects of Asbestos, Lyon, France, 2-6 Oct., 1972, Paper No. 19, p. 119.

62. Langer, A.M., Rubin, I.B., Selikoff, I.J., and Pooley, F.D., "Chemical Characterization of Uncoated Asbestos Fibres From The Lungs of Asbestos Workers by Electron Microprobe Analysis", The Journal of Histochemistry and cytochemistry, 1972, Vol. 20, pp. 735-740.

63. Langer, A.M., Rubin, I.B., and Selikoff, I.J., "Chemical Characterization of Asbestos Body Cores By Electron Microprobe Analysis", The Journal of Histochemistry and Cytochemistry, 1972, Vol. 20, pp. 723-734.

64. Langer, A.M., Ashley, R., Baden, V., Berkley, C., Hammond, E.C., Mackler, A.D., Magiore, C.J., Nicholson, W.J., Rohl, A.N., Rubin, I.B., Sastre, A., Selikoff, I.J., "Indentification of Asbestos in Human Tissues", Journal of Occupational Medicine, March 1973, Vol. 15, No. 3, pp. 287-295.

65. Pontefract, R.D., Bolohan, R., and Kraetz, W., "An Energy Dispersive X-Ray Analysis System Combined with a Transmission Electron Microscope, Their Application to Asbestos Fibre Analysis, Siemens Analytical Application Note No. 107, 1-3.

66. Spurney, R.K., Stober, W., Ackerman, E.R., Lodge, Jr. J.P., Spurney, Jr. K., "The Sampling and Electron Microscopy of Asbestos Aerosol in Ambient Air By Means of Nuclepore Filters", Journal of the Pollution Control Association, May 1976, Vol. 26, pp. 496-498.

67. Ortiz, L.W., and Isom, B.L., "Transfer Technique for Electron Microscopy of Membrane Filter Samples", American Industrial Hygiene Association Journal, July 1974, pp. 423-425.

68. Hwang, C.Y., Corsillo, A., and Mansel, J., "Electron Microscope Studies of Asbestos Fibres", Microscopical Society of Canada, 1976, Vol. 3, pp. 64-65.

69. Nenadic, C.M., and Crable, J.V., "Application of X-ray Defraction to Analytical Problems of Occupational Health", American Industrial Hygiene Association Journal, Aug. 1971, pp. 529-538.

70. Barbeau, C., "Evaluation of Chrysotile By Chemical Methods", In: Short Course in Mineralogical Techniques of Asbestos Determination, Editor: R.L. Ledoux, Mineralogical Techniques of Asbestos Determination, Editor: R.L. Ledoux, Mineralogical Association of Canada, Quebec, May 1979, pp. 197-212.

71. ACGIH, "Threshold Limit Values for Chemical Substances and Physical Agents in the Work Room Environment with Intended Changes for 1978, Cincinnati, OH, 45201, p. 2.

# CHAPTER VII

# MAGNETISM AND MAGNETIC PROPERTIES OF MAGNETITE AND CHRYSOTILE ASBESTOS

## 7.1 GENERAL:

The susceptibility of chrysotile asbestos at room temperature in a strong magnetic field, in excess of 5000 Oersteds, is positive and constant. Therefore chrysotile asbestos is paramagnetic [1] [2]. Chrysotile asbestos, however, has magnetite particles intimately associated with it [1] [2] [3] [6] [7] and the remanent magnetic field of these magnetite particles, can be measured using a fluxgate or other magnetometers [8] [9].

The earlier study of Dr. Cohen [12] has indicated that there is a relationship between the mass and the remanent magnetic field of this associated magnetite. It is important, therefore, to understand the magnetic properties of fine magnetite and chrysotile asbestos dust in order to utilize such a relationship, between the mass and remanent magnetic field, in determining the mass concentrations of airborne chrysotile.

## 7.2 Basic Principles of Magnetism and Magnetic Properties of Magnetite:

The textbook definition of the magnetic field is: "a vector field produced in space by an electrical current, or by magnetic material, or by both [4] [5] [14] [15] [16] [17] [18]".

A material is called magnetic if it produces a new magnetic field in response to an external magnetic field applied to it; or when it possesses such property by nature without the existence of an external magnetic field (4) (5). When such a material is placed in a magnetic field it is magnetized and the intensity of magnetization is measured in units of induced magnetic moment per unit volume of the material. The density of magnetic flux "B" in the material is given by the relation:

$$B = H + 4 \P J$$

Where "J" is the induced magnetic moment per unit volume of the material, and "H" is the applied external magnetic field.

In "cgs emu" units the intensity of a magnetic field is measured in Oersteds and the strength of magnetic induction is measured in Gauss. The dimensions of H and B are the same (4). However, in order to identify and distinguish the intensity of a magnetic field from the strength of magnetic induction, two separate unit names of Oersted and Gauss are used. Commonly used magnetic units are presented in table 7.1.

The magnetic lines of force through a substance depend on its permeability "μ" which is defined as:

$$\mu = \frac{B}{H}$$

The magnetic susceptibility is a measure of the increase in magnetic moment caused by the application of a field, and is

defined by:

$$k = \frac{J}{H}$$

When $k < 0$ diamagnetic, $k > 0$ paramagnetic. For most of the diamagnetic and paramagnetic substances, k is constant even for fairly high magnetic fields in the order of $10^4$ Oersteds. For ferromagnetic substances like iron, nickel, cobalt and magnetite, volume susceptibility could vary between 10 (for large fields) and $10^5$ emu/cm$^3$ (for low fields). These substances, with the exception of magnetite, are known as ferromagnetic. Magnetite is ferrimagnetic but it shows characteristics similar to those of ferromagnetism (5).

The magnetic moment of substances is due to the orbital motion of electrons within the atoms. The smallest element of the magnetic moment of the orbital motion of an electron is expressed as follows and called Bohr magneton (4) (5):-

$$\mu_B = \frac{eh_p}{4 M_o C} = 0.9274 \times 10^{-20} \text{ emu}$$

where: e = The charge of the electron

$h_p$ = Planck's constant

$M_o$ = Statical mass of the electron, and

C = Velocity of light

With ferromagnetic materials, the magnetic moments of all neighbouring atoms are parallel to each other, and act against

the disturbing forces associated with thermal agitation(4)(5)(17).

According to Nagata (4), all magnetic moment vectors in a ferromagnetic crystal are in the same direction (see Fig. 7.2a). However, there are some materials that are antiferromagnetic. In these cases the neighbouring atom's magnetic moments are antiparallel, or in opposite direction to each other, owing to a negative exchange interaction. Because of this characteristic, these materials are named as antiferromagnetic (see Fig. 7.2b).

Ferrimagnetism is a special case, in which the magnetic moments of metallic ions in two different crystallographic sites are coupled antiferromagnetically. The opposing magnetic moment vectors, however, are not equal to each other (see Fig. 7.2c). The difference in these magnetic moments, therefore, creates the ferrimagnetic state and results in a spontaneous magnetization, similar to that for ferromagnetic materials.

The magnetic structure of ferrimagnetic materials is often a spinel form, however, magnetite has an inverse spinel structure (see Fig. 7.3). Magnetite has a strong spontaneous magnetization and is observed to be 4.08 emu/cc. Since, in most respects, ferrites, especially magnetite, have magnetic properties which are very similar to those of ordinary

Table 7.1 - MAGNETIC UNITS

| QUANTITY | INTERNATIONAL SYSTEMS OF UNITS | CGS UNITS emu | CGS GAUSSIAN UNITS |
|---|---|---|---|
| Magnetic Flux | Weber = Wb | $10^8$ Maxwells | |
| Magnetic Flux Density "B" | Tesla = T | $10^4$ Gauss<br>$10^{-5}$ Gauss = 1$\gamma$ | |
| Magnetic Field Strength "H" | $\frac{1000}{4\pi}$ $\frac{\text{Ampère}}{\text{meter}}$ | [Oersted] | Oersted = 1Oe = $\frac{1 \text{ dyne}}{1 \text{ mpu}}$ |
| Permeability $\mu = \frac{B}{H}$ | $4\pi\ 10^{-7}$ $\frac{\text{Henry}}{\text{m}}$ | 1 (unity) | 1 (unity) |

Note: Weber = Volt.Second  Tesla = Weber/$m^2$
Henry = Weber/A

$$\varepsilon_o \mu_o = \frac{1}{c^2}$$

$\varepsilon_o$ = Permittivity = $\frac{1}{36\pi}$ $10^{-9}$ Farrad/m

$\mu_o$ = Permeability = $4\pi\ 10^{-7}$ Henry/m

$c$ = Velocity of Light = $3 \times 10^8$ m/sec

} SI unit

ferromagnetic materials, the term "ferromagnetic material" will hereafter include "ferrimagnetic material" and magnetite.

7.2.1 Induction of Magnetization, Hysteresis of Ferromagnetic Materials, and the Demagnetization Process:

In the process of magnetizing a steel rod, the flux density through the steel rod does not increase linearly with increasing magnetizing field. The relationship which exists between the flux density "B" of the steel rod and the magnetizing field "H" is shown as line "OM" in figure 7.4. If, after reaching the saturated magnetization value "M" on the curve, the magnetizing field is slowly decreased, the flux density of the steel rod does not return along the curve described with increasing "H" but lags and follows the path M to R. At the point "R", although the magnetizing field is equal to zero, the steel rod still retains some magnetization. The magnitude of magnetization "OR", which is retained by the steel rod, is called residual magnetism or the remanent magnetic field. The property of retaining a greater or lesser degree of a magnetization is called the retentivity of the substance. In order to reduce the remanent magnetic field to zero a magnetizing field in the opposite direction must be applied to the specimen. The value of "-H" at which "B" is reduced to zero is called the coercive force. This is measured by the magnitude of "OC". Increasing the

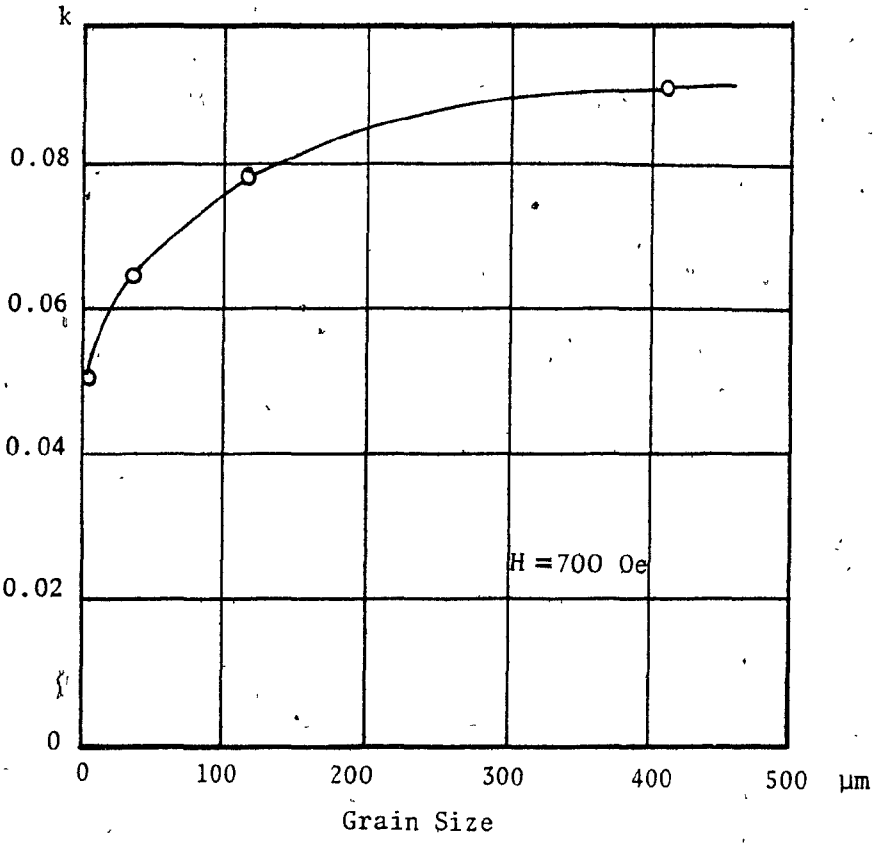


Fig. 7.1 Specific Susceptibility of Natural Magnetite as Dependent on Grain Size.[4]

magnetizing field in the same direction as "OC" carries the curve to "M'". This point corresponds to "M" on the other limb of the curve. In an exactly analogous process the curve expressing the relation between "B" and "H" may be carried from "M'" to "M", as was employed in going from "M" to "M'". "OR'" gives the value of the remanent magnetic field as did "OR" and, correspondingly, "OC'" measures the coercive force(14)(15)(18). The curve "OM" is called a "normal induction curve" and the loop "MRCM'R'C'M" is known as a "hysteresis loop". This property of magnetic materials makes it possible to have permanent magnets. In order to have high magnetic permanence the coercive force of such material should be very large(14)(15)(18). By studying the magnetization curves of various alloys, and in particular the effects on these curves when special heat treatments are applied to the metals, it has been possible to find alloys which will give certain specified magnetic properties(4)(15). For example, the magnetic field shielding material permalloy possesses a very high permeability for small magnetizing forces after it has been subjected to heat treatment.

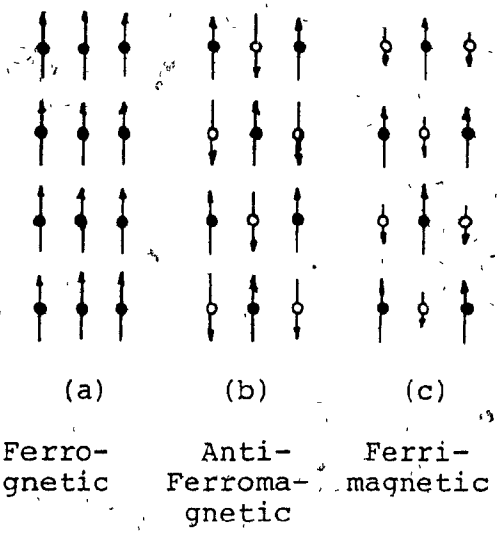


Fig. 7.2 [4] Schematic illustration of distribution of magnetization vectors in crystals

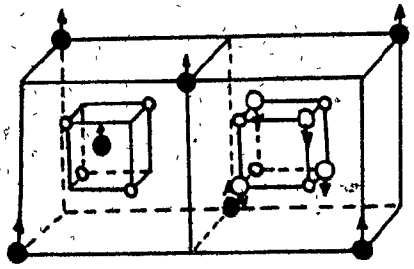

● 8a - position

○ 16d - position

Fig. 7.3 [4] Inverse spinel structure (magnetite). The arrows indicate the spin magnetic moment.

The cyclic process shown in figure 7.5 explains a process called demagnetization. If a piece of metal which has been magnetized is subjected to a progressively diminishing alternating field, the metal will eventually be demagnetized. It is observed that the normal induction curve of the metal is the locus of the peaks of the gradually decreasing hysteresis loops. Therefore, if the final loop is infinitely small, the normal induction curve will be at the point H = o, B = o, which is defined as the neutral point, and the metal would be demagnetized (15) (18).

7.2.2 Magnetization Curves of Magnetite and Magnetocrystalline Anisotropy:

Magnetite is a mineral which has a cubic crystal structure and a number of atoms composing a regular crystal lattice. As is seen in figure 7.6 the characteristic magnetization curves of a single crystal of magnetite are dependent on the crystallographic orientation (4)(5). Although the Weiss' theory assumed the special case of isotropic material, in reality ferromagnetic crystals, as well as the magnetite crystals, have an axis of easiest magnetization and one of most difficult magnetization. This anisotropic characteristic of magnetization is called magnetocrystalline anisotropy (4)(5). According to figure 7.6 the axis of easiest magnetization of magnetite is [111] and the axis of most difficult magnetization is [100], and the difference in magnetization energy between these two axes is defined as the

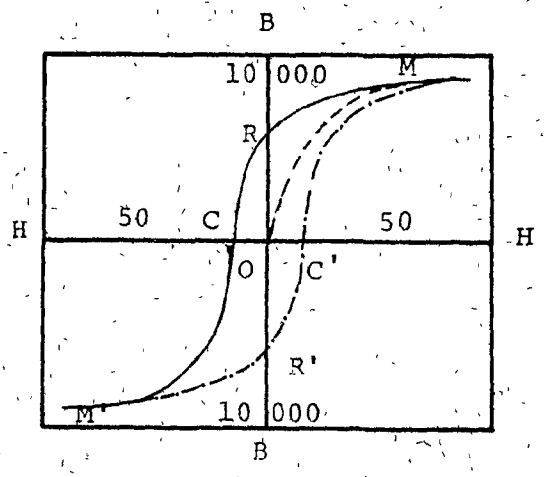


(15)

Fig. 7.4 - Induction and hysteresis curve for a ferromagnetic body

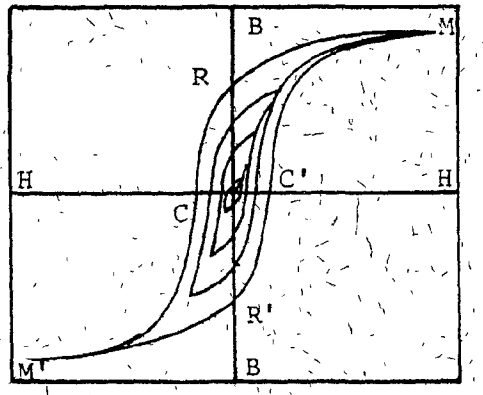


(15)

Fig. 7.5 - Graded cyclic magnetization of iron. The normal induction curve lies along the peaks of the gradually decreasing hysteresis loops

magnetocrystalline anisotropy energy. Although it is shown in figure 7.6 that a single magnetite crystal exhibits anisotropy in a field of 450 Oersteds, Bozorth (5), indicates that magnetocrystalline anisotropy remains even in magnetic fields of 5000 Oersteds. Therefore, depending on the orientation of a magnetite crystal in magnetizing fields, the measured induced magnetization will be varied.

7.2.3 Magnetostriction of Magnetite:

Another important factor which affects the magnetization of magnetite is magnetostriction. This is caused by mechanical deformation in the direction of the three major crystal axes, due to magnetization along the respective axes (4). Therefore, magnetostriction can be interpreted as strain in the crystal structure due to magnetic interaction among the atoms composing the crystal lattice (5). Furthermore, if there are some impurities associated with the magnetite crystal, some internal stresses are caused by these impurities and, therefore, the lattice of the crystal is deformed and the total magnetic energy of the crystal is changed, causing alterations in the magnetization curves (4) (5). The induced magnetization of magnetite is thus strongly dependent on stress distribution within the crystal structure.

7.2.4 Magnetic Domains of Magnetite:

Nagata (4) stated that even a single ferromagnetic or magnetite crystal is composed of a number of domains called

magnetic domains. According to Weiss' theory each magnetic domain has a spontaneous magnetization, but the total sum of the magnetization of these domains may be cancelled out at the well demagnetized stage. These domains are separated from each other by the domain walls which have a finite width (4).

The existence of more than one domain in a ferromagnetic crystal is an indication that the interaction of the magnetic moments of the neighbouring atoms are not only due to exchange energy but also to other forces which resist the formation of large domains (4) (5). Therefore, the remanent magnetization and coercive force of magnetite are the results of established equilibrium among these forces. The energies that play a role in the formation of domains are: (a) exchange energy, (b) magnetocrystalline energy, (c) magnetostatic energy, and (d) magnetoelastic energy.

7.2.5 Magnetization Processes of Fine Magnetite Particles and Their Magnetic Behaviour:

The internal stresses have a dominating effect on magnetization of fine magnetite particles. If in the crystal structure of a magnetite particle, it is assumed that the direction of the stresses are random, the magnetization of domains in this particle, after demagnetization, is also random when the external magnetic field is around zero (4) (5). Because of the domain structure of magnetite when the external magnetic field is applied the magnetization curve is

due to either the displacement of walls of domains or the rotation of domains in the direction of magnetization and towards the applied magnetic field (4). The different states of distribution of magnetization vectors in polycrystals are shown in figure 7.7.

The size of the magnetite particles also has an important effect on the domain structure of the particles. Since the domain walls have finite width, as the particle size gets smaller the number of the domain walls decreases and, at some stage, the particle contains a single domain. When the size of a magnetite crystal approaches the critical size of a single domain, any one of the four types of domain structures could be encountered, as shown in figure 7.8. Magnetite particles as small as 1 micrometre diameter have shown multidomain structure (4) (5).

The coercive force of fine particles increases and reaches a maximum as the particle size approaches that of a single domain (5). The coercive forces of various sizes of magnetite are shown in Fig. 7.9. The coercive force of magnetite particles larger than 100 micrometres is very low. The coercive force is approximately proportional to the inverse of particle size. Due to high coercivity the fine particles have persisting uniform remanent magnetization. In a single domain particle, changes in magnetization can occur only in the rotation process of the total magnetic moment of the particle,

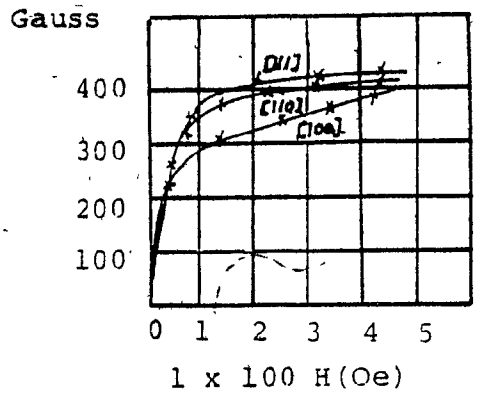


Fig. 7.6 [4] - Magnetization curves of a single magnetite crystal (After Weiss)

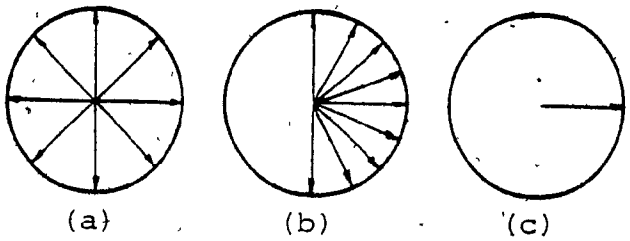


(a) Demagnetized state

(b) Remanent magnetization

(c) Saturated magnetization

Fig. 7.7 [4] - Distribution of magnetization vectors in polycrystals

and the internal magnetization energy depends only on the orientation of the magnetic moment with respect to certain axes fixed in the particle (4). When the induced saturation magnetization, $J_S$, (obtained at magnetic field "H" > "$H_O$" the critical field of rotation) is kept stable until the magnetizing field, H, decreases to the negative critical field of rotation, $-H_O$, and that when H goes beyond $-H_O$, the $J_S$ suddenly changes its direction and becomes $-J_S$. In this case the hysteresis is rectangular and the remanent magnetic field is very high and uniform. However, if the particles are very small, i.e. $\lesssim$ 25 Å, thermal fluctuation of their magnetic moment can play an important role on the magnetic behaviour of these particles. The system then behaves as a paramagnetic system in which the moments are very large. This is called superparamagnetism. In this case if the value of H exceeds $H_O$ in any direction, the induced magnetization J is always $+J_S$ or $-J_S$. Thus, there is no hysteresis at all, J being reversible with respect to H, and the remanent magnetic field is zero (4) (45).

For an assemblage of independent particles of single domain the remanent magnetization is equal to half of the saturation magnetization, and the coercive force is about half the maximun critical field of rotation of individual particles (4).

Although the coercive force of ferromagnetic and magnetite particles decreases as the particle size increases, the specific susceptibility increases with the increased particle size (see Fig. 7.1). Therefore, the remanence increases very rapidly with increasing volume (4) (46).

According to Nagata (4), magnetite particles in the size range of 0.01 to 5 μm have remanent magnetic field in the order of 2 x $10^{-5}$ to 10 x $10^{-5}$ emu/gram. Therefore, since the remanent magnetic field of airborne respirable size magnetite particles is dependent on their particle size, and interaction between the particles, this remanent magnetic field can be different for two different samples of equal mass. In other words, the variations in particle size distribution, and the distribution of the magnetic material in the sample, can affect the remanent magnetic field readings of two different airborne respirable magnetite samples of similar mass.

During this research work, the size distribution and sample geometry were kept identical by standardizing the airborne pure magnetite and chrysotile dust sampling technique with a Hexhlet horizontal eleutriator described in chapter VIII in detail.

According to Parasnis (47) the magnetic anomaly "B" of a homogeneously magnetized spherical particle, at a distance "r"

from its centre, along a line parallel to the magnetization is:

$$B = \frac{2JV}{r^3}$$

Where, "J", is the net intensity of magnetization and, "V", the volume of the sphere. However $J = J_i + J_r$ depending upon whether the induced intensity, "$J_i$", in response to the earths magnetic field has the same or the opposite direction as the remanent intensity, "$J_r$". In order to minimize the effect of the earths magnetic field on the measurements, magnetic shielding was used as described in chapter VIII. Furthermore, during all of the magnetic measurements of the standard and unknown samples, the sample orientation was kept the same.

It should be also remembered that the magnetic field of a particle, which has a dipole characteristic, decreases as the inverse cube of the distance. Therefore, the distance from the magnetic field measuring probe should not be varied from sample to sample, otherwise discrepancies due to field readings will occur. As explained in chapter VIII, this distance was always kept at 1 mm with a vernier control.

During this work, the remanent magnetic fields measured with a fluxgate magnetometer comprise the vertical Z component of the samples' total field (representing a magnetic dipole).

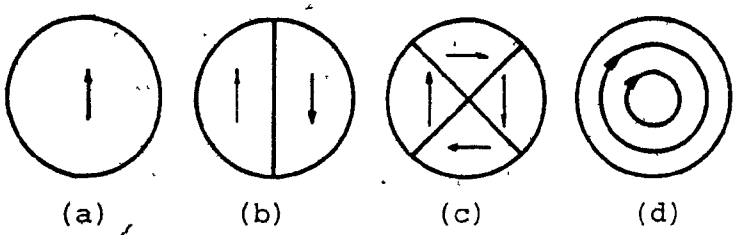


Fig. 7.8 [4] - Types of simple domain arrangements in a small sphere: (a) applies for single domain structure, (b) for high anisotropy in a uniaxial crystal, (c) for high anisotropy in a cubic crystal, and (d) for low anisotropy.

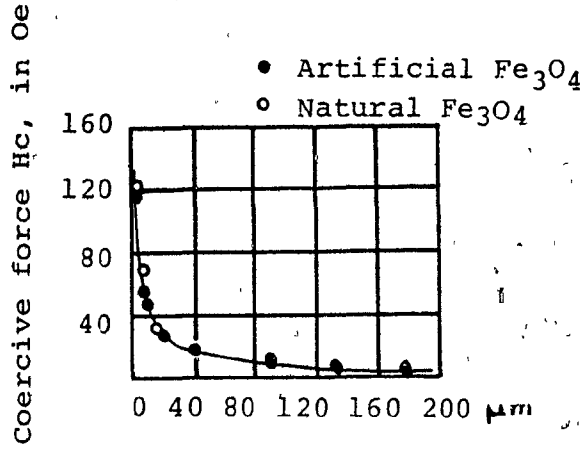


Fig. 7.9 [4] - Coercive force of magnetite as dependent on particle size. (After Gottschalk)

## 7.3 Detection of The Distribution of Ferromagnetic and Magnetite Particles in Human Lungs by Remanent Magnetic Field Measurements:

Since 1963 Baule and McFee[19][20] and, later, Cohen[21] and Cohen et al.[22][23] have been working on detection of the magnetic field of the heart (which is called magnetocardiogram) and have shown that the magnetic field of the heart is in the range of $10^{-7}$ and $10^{-8}$ gauss. Similarly, Cohen et al.[24] and Cohen[12][25][26][31] have successfully detected the magnetic fields around the human body produced by skeletal muscles, magnetic material in the lungs and the brain's electrical activity using a SQUID magnetometer.

According to Cohen[12], there are two types of mechanisms that produce magnetic fields in the body. (a) Magnetic field production by naturally occuring electric currents in the body and (b) remanent magnetic field production by magnetic materials in the body. Our main interest is the remanent magnetic fields of magnetite particles.

Cohen[9][12][26] has shown that the distribution of inhaled magnetite particles in human lungs can be determined by simple gradiometric measurements with a fluxgate magnetometer.

The fluxgate magnetometer is simple to operate; it is inexpensive and it is possible to detect fields less than $10 \times 10^{-7}$ gauss when the fluxgate is used as a gradiometer.

During 1973-74, a preliminary study of Quebec asbestos miners and millers by Dr. C. Cohen of MIT, demonstrated that measurements of the remanent magnetic field intensities of the chest of these workers were capable of distinguishing between groups of workers with high and low total accumulated dust exposure indices[12][30][34] (see Fig. 7.10).

Although chrysotile asbestos fibres are not themselves ferromagnetic, they are commonly associated with magnetite. Magnetite is a contaminating mineral and it is a by-product of serpentinization. Magnetite is in granular form throughout the serpentine fillings and partings in asbestos veins, and also occurs as fibrous intergrowths with, and among, the chrysotile fibres and bundles[1][2]. The intergrowths are very difficult to separate from the chrysotile fibres and impart a grey colour to them. Pundsack[41], with his "Stuffed Tube Hypothesis", tries to explain the co-existence of the magnetite with chrysotile as follows. Each bunch of chrysotile fibres has two types of pores. The first type of pores is in between the individual fibres. The pores are thought to be partly filled with serpentine-like material which did not form completely into the cylindrical structure; and the second type of pores inside each individual fibre[41]. Since magnetite is also a by-product of serpentinization, the particles inside these pores might well contain magnetite[41].

Therefore, it is potentially possible to measure the actual dust dose for men working with chrysotile asbestos, and to develop a rapid method for monitoring airborne chrysotile asbestos fibre concentrations when magnetile is associated with the fibres.

Kalliomaki[28] and Kalliomaki et al.[27][29] showed that the magnetic determination of pulmonary contamination, based on remanent magnetization of ferromagnetic contaminating particles, is possible. The magnetizing field used was 200 gauss. They state that the radiological findings of the lungs of shipyard arc welders correlated well with the amounts of welding fume contaminants measured with the magnetic method.
Cohen et al.[30][34] have also showed that the remanent magnetic fields of a welder's lungs are a hundred times larger than the remanent magnetic fields of Quebec asbestos mine and mill workers (see Fig. 7.10). Since the magnetite content of the asbestos used in asbestos manufacturing plants is low, the magnetic chest scans showed lower magnetic fields than the asbestos mine and mill workers.
For foundry workers, who because of their work, inhale large quantities of magnetite, the magnetic readings of the lungs are the highest (30) (see Fig. 7.10).

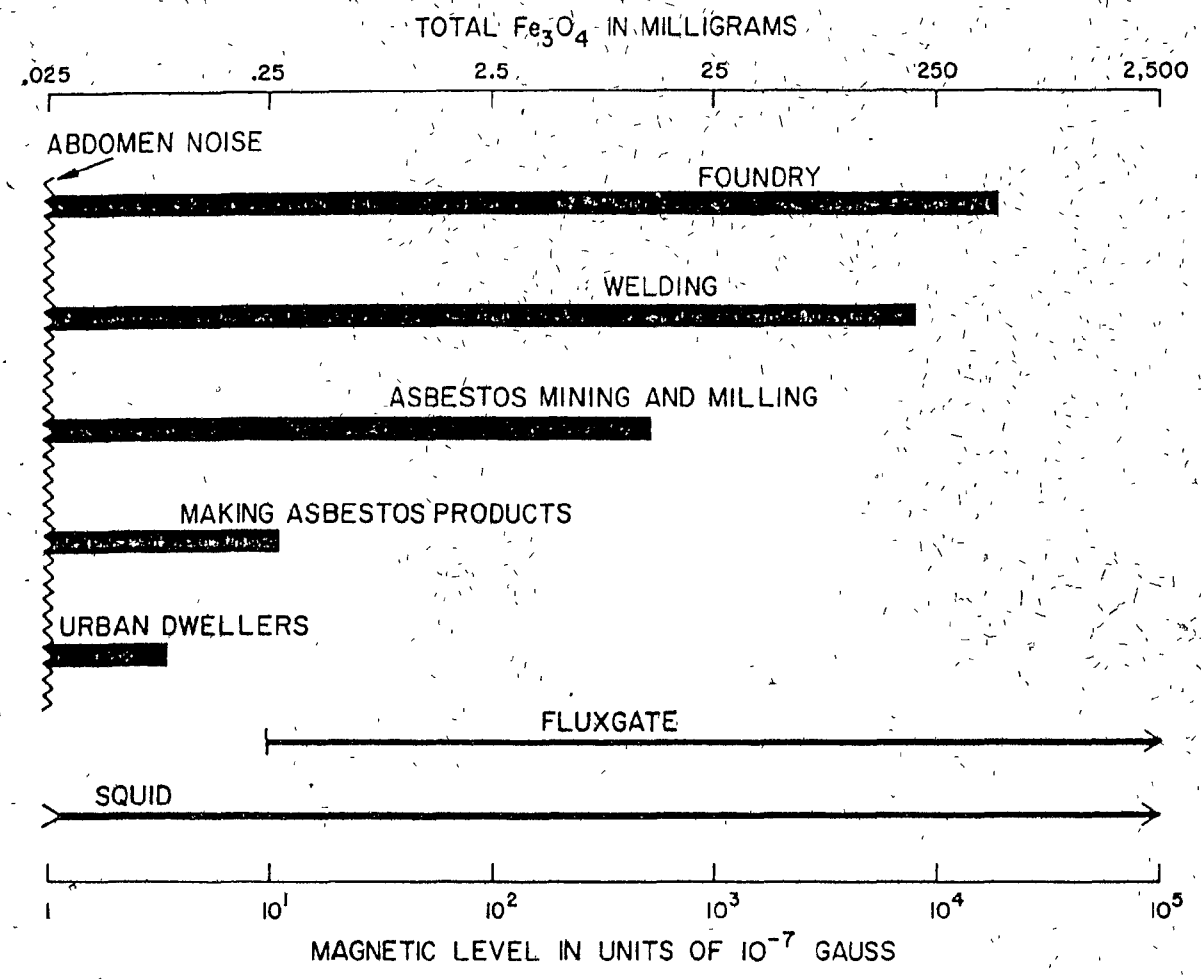


*Fig. 7.10 The range of magnetic field at the chest, due to $Fe_3O_4$ in the lung, of persons in various groups. A magnetizing field of 300 gauss is assumed, and no significant decrease due to magnetic relaxation. Not included here are granite (quarry) workers and coal miners. For comparison, the range of sensitivity is shown for the two detectors which can be used for this type of work, the fluxgate and the SQUID. The SQUID can readily measure the steady field due to all cases presented here, including that due to normal ion currents in the abdomen; a good commercial fluxgate gradiometer can measure lung levels somewhat lower than $10 \times 10^{-7}$ gauss. For large-scale monitoring, it is seen that the convenient fluxgate can only be used in the primary asbestos mining and milling industry, but not for asbestos manufacturing plants.*(30)

Freedman et al.[32] have shown that since magnetite and pyrrhotite are commonly found with and/or within coal, it is possible to measure the remanent magnetic fields of the lungs of coal workers, and the distribution patterns of dust in the lung. Similarly, Freedman et al.[32] and Stroink et al.[43][44] were successful in measuring the dust distributions in the lungs of asbestos insulation workers and miners by the magnetic method. Also, they concluded that the magnetic data correlates with reported distributions of lung dust determined by radioaerosol and pathological methods, and magnetopneumography may be an effective non-invasive method for studying patterns of lung dust clearance[32][43][44].

7.4 Biological Effects of Magnetic Fields:

In order to measure the remanent magnetic fields of the magnetite content of human lungs, the subject is magnetized either with a hand held alnico bar magnet or in a uniform field produced by two air-core Helmoltz coils[30]. Although magnetite particles are saturated in a field of 1000 Oersteds (and therefore the best magnetizing field to use is in the range of 1000 to 1500 Oersteds), because of the difficulty in attaining such high magnetizing fields with practical hand held magnets or coils, the researchers have elected to work within the range of 200 to 700 Oersteds[27][28][30][32]. However, the findings of Cohen[21][25][26][30][31] that the human body and the important organs of the body,

such as the brain and heart, have their own magnetic field activities introduces an important question; is the human exposure to stationary magnetic fields in the order of 200 to 1500 Oersted dangerous to health? This question has been a concern of other scientists and Barnothy[35] has brought together in one volume the present-day knowledge in all the active fields of biomagnetic research. The effects of high magnetic field intensities of 1200 Oersteds on the growth rate of barley seedlings were apparent, and reported growth rate of seedlings in the magnetic field were significantly greater than those of control samples[35]. However, the plants did not suffer from any ill effect. Similarly, young mice have been subjected to 4200 Oersted magnetic fields and their growth rate have been studied for 20 days. The inhibition of the growth rate was found to be insignificant [35]. However, the shock, or after effect, of the high magnetic field, 4 days after removal from the field, have indicated a weight loss in all mice[35]. The life span of the study group did not suffer from high magnetic field[35]. However, it is reported that in rats, wound healing and tissue generation slows down in 3000 to 4000 Oersted magnetic fields[35]. Mice exposed to very high, 100,000 to 120,000 Oersted, magnetic fields for 1 hour duration have survived with no ill effect[35].

Reiter[36] reported that alternating electric fields may cause some biological changes in man, such as changes in blood pressure, respiration and heart frequency, skin and rectal temperature, changes of electrocardiogram and blood count. However, the stationary magnetic fields did not yield any ill effect on mammals or man[36]. Ketchen et al.[37] have reviewed the biological effects of the interaction of stationary magnetic fields with man and animals and recommended that whole body or head exposure for extended period of times should be limited to maximum 200 Oersteds stationary magnetic fields. The biological effects of magnetic fields on man are summarised in Table 7.2. The Directors of the Stanford Linear Accelerator Group for Stanford, California have recommended exposure limits to stationary magnetic fields as shown in Table 7.3[37].

Although present experimental work[35][36][37] in exposure of the body to stationary magnetic fields, and Cohen's[30] findings, have indicated that magnetite dust inhalation and its magnetization is not harmful to health, Sterling[33] stated that magnetized particles could form clusters in lungs and these clusters could be a potential health hazard. Therefore, he suggests that until health hazards related to this type of work are investigated, it should be avoided[33].

7.5 Low Magnetic Field Measuring Device: The Fluxgate Magnetometer (Model MF-5000) and the Principle of Its Operation:

For the measurements of magnetic fields of low intensity, a compact, fully transistorized fluxgate magnetometer, Model MF-5000, of Automation Industries was used. Ordinarily, this precision instrument has the measuring range from 1000 milligauss to 1 milligauss full scale value. However, after the alterations explained in chapter VIII, its sensitivity has been increased from $2 \times 10^{-5}$ to $6 \times 10^{-7}$ gauss in gradiometric mode.

The probe (Model MF-F-100 Field and Gradient Probe) of the fluxgate magnetometer consists of a core of magnetic material, such as mu-metal or permalloy, which has very high permeability at low magnetic fields. Each of these cores are wound with primary and secondary coils. The two primary windings are connected in series and energized by 20KHz. current, produced by a constant current source, (see Fig. 7.11). This current is sufficient to magnetize the cores to saturation, in opposite polarity, twice each cycle. The secondary coils, which consist of many turns of fine wire, are connected to the inputs of a differential amplifier; that is an amplifier whose output is proportional to the difference between two input signals. In the

Table 7.2 -- Biological Effects of Magnetic Fields on Man[37]

| Field (Oe) | Time of Exposure | Effect |
|---|---|---|
| 2,500 | Unknown | No sensation, no change in pulse rate or respiration |
| 15,000 | Unknown | Taste sensation in mouth |
| 20,000 | 15 minutes | Slight sensation of pain in filled teeth |
| Unknown* | Unknown | Irritability, fatigue, occasional dizziness, altered appetite, headache; both bradycardia and tachycardia, decrease in arterial blood pressure; itching, burning, numbness, and marbling pattern in hands; change in electroencephalogram. |
| 100,000 | Short | Bitter coldness, aching bones, and feeling of ants moving on the hands. |
| 5,000 | 3 days/man year | No effect noted. |

* Soviet workers engaged in fabrication of permanent magnets.

Table 7.3 - Recommended Exposure Limits to Stationary Magnetic Fields[37]

| Period | Body Area | Field Strength (Oe) |
|---|---|---|
| Extended Periods, hours: | Whole body or head | 200 |
| | Arms and hands | 2,000 |
| Short Periods, minutes: | Whole body or head | 2,000 |
| | Arms and hands | 20,000 |

Note: It is recommended that people not linger unnecessarily in magnetic fields, regardless of intensity.

Exposure above 20,000 Oersteds for arms and hands and, 2,000 Oersteds for whole body and head should be avoided.

absence of an external d.c. magnetic field, the saturation of cores is symmetrical and of opposite sign near the peak of each half-cycle. As a result, the outputs from the two secondary windings cancel.

The presence of an external field parallel to the cores causes saturation to occur earlier for one half-cycle than the other. This produces an unbalance, because the core fluxes do not cancel. Since the differential output voltage from the secondary winding is proportional to dB/dt, a series of voltage pulses are fed into the amplifier. Before the total signal of 40KHz from the probes is fed into the amplifier, it feeds the coupling transformer and is shaped to an essentially perfect sine wave. After the signal is amplified, filters and transformer coupling are used to tune the circuits carrying the signal. On the other side, a portion of the 40KHz produced by the oscilator is fed to a phase sensitive detector with a 90° phase shift as a reference voltage.

The 40KHz signal voltage is matched with the reference voltage and a dc output signal is produced whose polarity is plus or minus depending on whether the signal voltage is 180° in or out of phase with the reference voltage. The final signal is integrated and 60 cycle noise is filtered by a low pass filter and fed to a chart recorder.

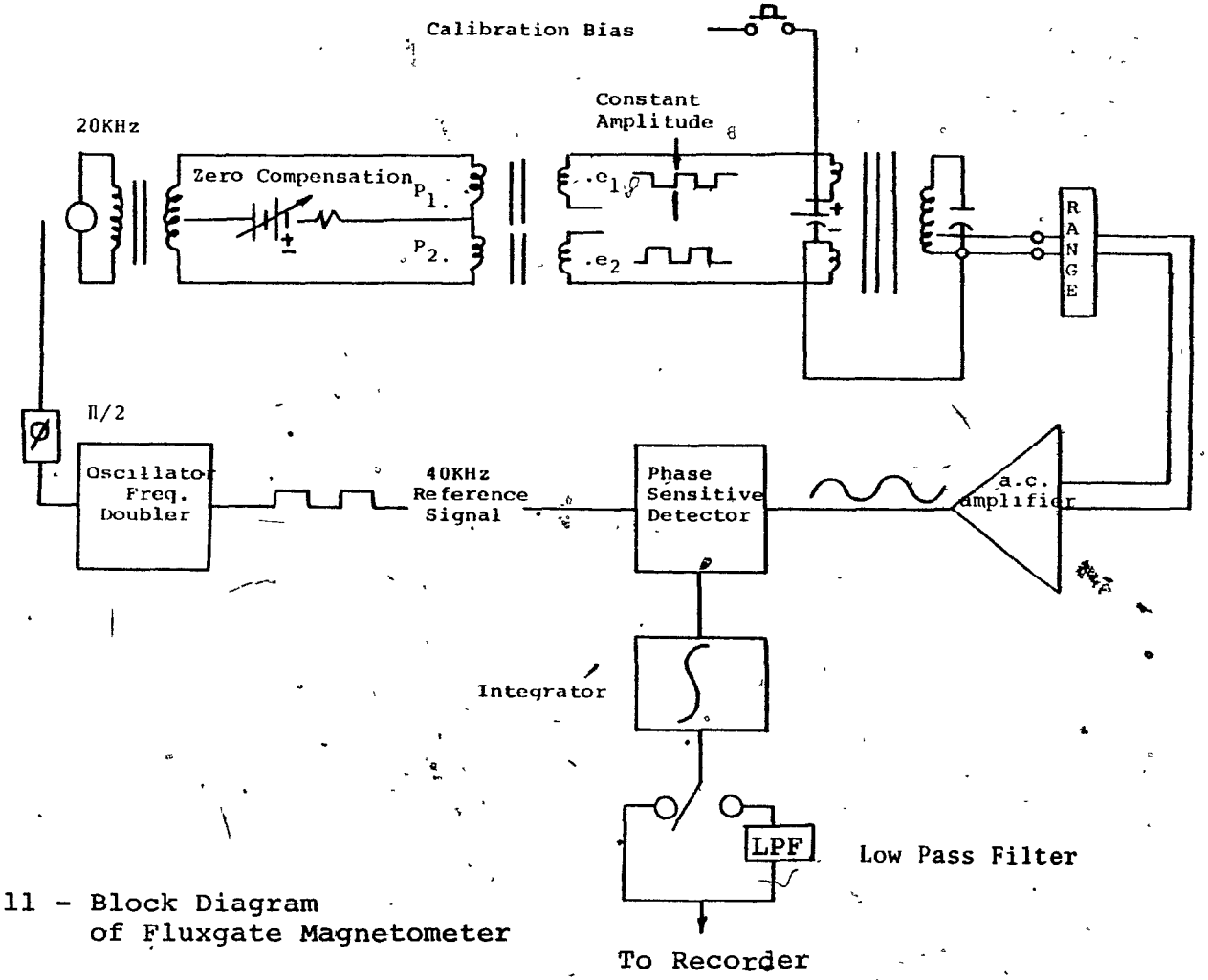


Fig. 7.11 - Block Diagram of Fluxgate Magnetometer

## 7.6 High Magnetic Field Measuring Device: Gaussmeter (Model D-855) and the Principle of Its Operation:

For the measurements of high magnetic fields, generated by electromagnets, coils and alnico hand held magnets, a gaussmeter, Model D-855 of Dyna-Empire, Inc., was used. It is a fully transistorized instrument, designed to measure either AC (RMS) or DC magnetic fields having flux densities from 10 gauss to 30,000 gauss.

The basic principle of magnetic flux measurements used may be described as a flux-modulated carrier - amplifier system. A locally generated AC carrier signal is fed as an exciting current to the Hall element (see Fig. 7.12). The flux to be measured at the probe modulates the AC carrier within the Hall sensor, producing an AC output voltage which is accurately proportional to flux density. The flux modulated AC carrier output is amplified by the carrier amplifier, then restored to a flux proportional voltage by the Synchronous Demodulator, without loss of polarity (field direction) information. The demodulator drives the panel meter and output jacks. Also, a separate AC detector is connected to the synchronous demodulator output to produce a DC meter reading for AC fields.

## 7.7 New Developments in The Field of Instrumentation for Measurement of Magnetic Lung Contaminants, Airborne Asbestos Fibres and Other Magnetic Materials:

During 1979 the Outokumpu Oy Company of Finland, in collaboration with Kalliomaki (28), designed and manufactured a unique system for measurement of magnetic lung contaminants. The instrument is called "LUNGCO" and is fully automatic and computerized. The subject's chest is magnetized by a pair of coils. The probe of a sensitive fluxgate magnetometer scans the chest of the subject and maps the magnetic contaminant distribution of the lung. The remanent magnetic field readings are automatically fed to a micro-computer and the results are displayed on a video terminal and/or a printer. The microcomputer can also be programmed to calculate and display other relevant data. The reproducibility of the method is $\pm$ 5 percent.

Again, Outokumpu Oy Company of Finland manufactured, in 1975, a magnetic balance which is called "Satmagan". It uses the principle of magnetizing the material up to saturation in high magnetic fields and then, by measuring the remanent magnetic field, the mass of the magnetic material content of the sample is determined with an accuracy of $\pm$ 0.2 percent for total sample weights between 1 and 7 grams.

Recently (in 1980), LKAB International AB Company

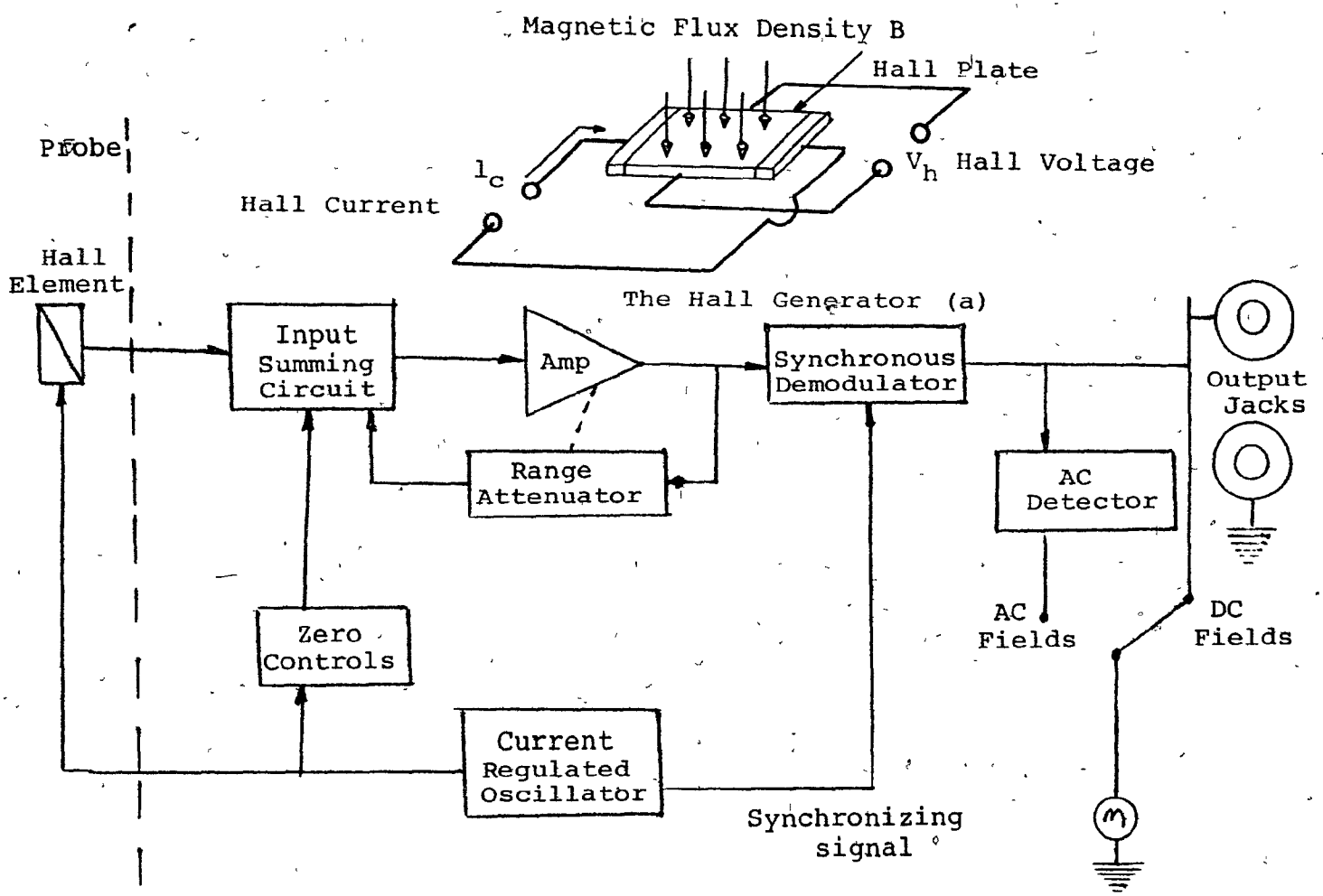


(a) Haul Generator of the Gaussmeter

Fig. 7.1 2(b) Block Diagram of the Gaussmeter

of Sweden, developed an instrument called an "Iron Content Meter." The instrument consists of a magnet coil (measuring ring), a remanent magnetic field measuring probe and a meter. This instrument is used to determine the iron content and ore grades of magnetite ore. The ore is magnetized for five minutes by the coil. After five minutes the magnetizing field is turned off automatically and the remanent magnetic field is read by the instrument and the iron content is shown by a meter with an accuracy of ± 5 percent.

Timbrell[38] and Vickers Instruments, with collaboration of Timbrell[39], have developed a new technique which utilizes the magnetic properties of asbestos fibres to align them on membrane filters either parallel or normal to an applied magnetic field*. With this technique the aligned asbestos fibres are observed under a microscope and, with the aid of distinctive light-scattering patterns when illuminated by a laser beam, the quantity of asbestos fibres present are assessed. Subsequently, the magnetically aligned fibres, are again observed while being illuminated by a laser beam, and being rotated 360°. The individual fibres with varying length and width give different intensities of scattered light patterns and peaks. A microprocessor sums the areas under the peaks, correcting automatically for

* Riis and Chatfield[48] have reported a similar technique for the detection of asbestos fibres in water samples by aligning the fibres in a magnetic field of 1.0 Tesla. Subsequently fibres are illuminated by a normal incidence laser beam. The scattered light intensity is measured as a function of the angular position of the original magnetic field direction, and the peaks which occur allow the concentration of aligned fibres to be deduced.

background, and determines the size, surface area and number of airborne asbestos fibres in the samples[39]. The instrument is capable of detecting automatically the range of 50 to 5000 fibres per square millimetre of membrane surface, and functions well for concentrations in the range 0.1 to 10 fibres per millilitre of air sampled.

The "Fibrous Aerosol Monitor" (FAM) manufactured by GCA Corporation, Technology Division, can determine the number of airborne chrysotile fibres according to prespecified fibre characteristics, that is counting particles with an aspect ratio of 3:1 and longer than 5 micrometres in length[40]. Air, driven by a diaphram pump, enters the "FAM" at a rate of 2 litres per minute and passes through a chamber in which laminar air flow is developed. Then air, with airborne particles, is subjected to a rotating electric field. This field induces a dipole charge separation on the fibres and aligns them with the applied rotating field. This gives the fibres a motion of several hundred oscillations per second. Then, the light scattering signature associated with these fibres is detected while they are illuminated by a monochromatic light beam from a laser. Because longer fibres produce narrower pulses than shorter ones, the "FAM" is able to discriminate between fibres of different lengths by sensing the sharpness of individual pulses.

## 7.8 CONCLUSION:

Although chrysotile asbestos fibres are paramagnetic, the associated magnetite imparts ferromagnetic characteristics to the fibre samples. It is also observed that there can be a relationship between the remanent magnetic field and the mass of magnetite. Since the start of this research work several manufacturers have developed instruments which utilize this relationship and measure the magnetite and/or iron content of lung contaminants, airborne dust and iron ore grades by directly measuring the remanent magnetic fields. Therefore, it can be concluded that if the association of magnetite with airborne chrysotile asbestos is based on a constant ratio, the direct remanent magnetic field measurements may indicate the fibre content by mass and number in the airborne samples.

## LIST OF REFERENCES FOR CHAPTER VII


1. Schwarz, E.J., Winer, A.A., "Magnetic Properties of Asbestos, with Special Reference to the Determination of Absolute Magnetite Contents", CIM Bulletin, Dec. 1971, pp. 55-59.

2. Winer, A.A., Schwarz, E.J., "Magnetic Content of Asbestos Concentrates", Unpublished report of EMR, Mines Branch & Geological Survey of Canada.

3. Cossette, M., Delvaux, P., "Technical Evaluation of Chrysotile Asbestos Orebodies", In: Short Course in Mineralogical Techniques of Asbestos Determination, Editor: R.L. Ledoux, Mineraological Association of Canada, May 1979, p. 102.

4. Nagata, T., "Rock Magnetism", Maruzen Company Ltd., Tokyo, 1961, pp. 1-39, 80-81, 222-245.

5. Bozorth, R.M. "Ferromagnetism", D. Van Nostrand Company, Inc., Princeton, New Jersey, Toronto, London and Melbourne, Revised Edition, Sept. 1968, pp. 1-13, 243-246, 502-513, 649, 681 and 769.

6. Gibbs, G.W., "Qualitative Aspects of Dust Exposure in the Quebec Asbestos Mining and Milling", In: Inhaled Particles III. Editor W.H. Walton, Unwin Bros., Ltd., Surrey, England, 1971, pp. 783-799.

7. Wicks, F.J., "Mineralogy, Chemistry and Chrystallography of Chrysotile Asbestos", In: Short Course in Mineralogical Techniques of Asbestos Determination, Editor: R.L. Ledoux, Mineralogical Association of Canada, May 1979, p. 68.

8. Cohen, D., "Ferromagnetic Contamination In The Lungs and Other Organs of the Human Body", Science, May 1972, Vol. 180, p. 745.

9. Lax, B., "Annual Report, Francis Bitter National Magnet Laboratory", MIT, Cambridge, Mass. August 1973, pp. 100-102.

10. Assad, J.R., "Comite d'Etude Sur La Solubrite Dans l'Industrie de l'Amiante, Beudry Commission, Oct. 1976, Document # 1.

11. Heidermans, G., "Determination of Asbestos Fine Dust According to Mass Concentration", In: Short Course in Mineralogical Techniques of Asbestos Determination, Editor: R.L. Ledoux, Quebec, May 1979, pp. 165-196.

12. Cohen, D., "Magnetic Fields of Human Body", Physics Today, August 1975, pp. 34-43.

13. Gibbs, G.W., "Techniques of Asbestos Determination - Research Perspective", In: Short - Course in Mineralogical Techniques of Asbestos Determination, Editor: R.L. Ledoux, Quebec, May 1979, p. 264.

14. Stevenson, R., Moore, R.B., "Theory of Physics", W.B. Saunders Company, Philadelphia and London, 1967, pp. 471-593.

15. Williams, S.R., "Magnetic Phenomena", McGraw-Hill Book Company Inc., New York, London, 1931.

16. Pohl, R.W., "Physical Principles of Electricity and Magnetism", 1930, pp. 86-139.

17. Zijlstra, H., "Experimental Methods in Magnetism", In: Selected Topics in Solid State Physics, Editor: E.P. Wohlfarth, Vol. IX, John Wiley & Sons, Inc., New York, pp. 126-133.

18. Lee, E.W., "Magnetism", Penguin Books, 1963, pp. 49-65, 83-128, 192-204.

19. Baule, G.M., McFee, R., "Detection of the Magnetic Field of the Heart", American Heart Journal, 1963, Vol. 66, p. 95.

20. Baule, G.M., McFee, R., "Theory of Magnetic Detection of the Heart's Electrical Activity", Journal of Applied Physics, 1965, Vol. 36, p. 2066.

21. Cohen, D., "Magnetic Fields Around The Torso: Production by Electrical Activity of Human Heart", Science, 1967, Vol. 156, p. 652.

22. Cohen, D., Chandler, L., "Measurements and a Simplified Interpretation of Magnetocardiograms from Humans", MIT Circulation, 1969, Vol. 39, pp. 395-402.

23. Cohen, D., McCaughan, D., "Magnetocardiograms and Their Variation Over the Chest In Normal Subjects", American Journal of Cardiology, 1972, Vol. 29, pp. 678-685.

24. Cohen, D., Givler, E., "Magnetomyography: Magnetic Fields Around The Human Body Produced by Skeletal Muscles", Applied Physics Letters, 1972, Vol. 21, pp. 114.

25. Cohen, D., "Magnetoencephalography: Detection of the Brain's Electrical Activity with a Superconducting Magnetometer", Science, 1972, Vol. 175, pp. 664-666.

26. Cohen, D., "Magnetic Fields Produced by Steady Currents in Human and Animal Bodies", MIT, Francis Bitter National Magnet Laboratory, Semi-Annual Progress Report, 1973, pp. 1-24.

27. Kalliomaki, P.L., Karp, P.J., Katila, T., Makipaa, P., Saara, P., and Tossavainen, A., "Magnetic Measurements of Pulmonary Contamination", Scandinavian Journal of Work Environment and Health, 1976, No. 4, pp. 232-239.

28. Kalliomaki, P.L., "Measurement of Magnetic Lung Contamination in VIVO", Evaluation of the Method and Its Application to Arc Welders, Academic Dissertation. The Medical Faculty of the University of Oulu, 1977, Helsinki.

29. Kalliomaki, P.S., Alanko, K., Korhonen, O., Mattsson, T., Vaaranen, V., and Koponen, M., "Amount and Distribution of Welding Fume Lung Contaminants Among Arc Welders", Scandinavian Journal of Work Environment and Health, 1978, No. 4, pp. 122-130.

30. Cohen, D., "Report of the Low-Field Group: The Magnetic Field of the Lung", Francis Bitter National Magnet Laboratory, MIT, 1978, pp. 1-33.

31. Cohen, D., "Magnetic Field Produced by The Human Body: Some New Findings", Proceedings of Intermag Conference, 1978.

32. Freedman, A.P., Green, F.H.Y., and Rudnitzky, J., "Magnetopneumographic Scanning For Non-Invasive Regional Determination of Occupationally Acquired Lung Dust Distribution". Journal of Occupational Medicine, 1980,Vol.22,p.613

33. Sterling, T.D., "Possible Risk to Human Lungs From Magnetometric Dust Clearence Experiments", Journal of Applied Physics, 1981, Vol. 52, No. 3, pp. 2575-2577.

34. Cohen, D., Crowther, T.S., Gibbs, G.W., and Becklace, M.R., "Magnetic Lung Measurements in Relation to Occupational Exposure in Asbestos Miners and Millers of Quebec", Environmental Research, 1981, Vol. 26, pp. 535-550.

35. Barnothy, M.F., "Biological Effects of Magnetic Fields", Plenum Press, New York, 1964.

36. Reiter, R., "Biological Effects of Electric, Magnetic, and Electromagnetic Fields", Circular, Institute For Atmospheric Environmental Research, D-8100 Garmisch-Partenkirchen, Kreuzeckbahn-strasse 19, Nov. 1976.

37. Ketchen, E.E., Porter, W.E., and Bolton, N.E., "The Biological Effects of Magnetic Fields on Man", American Industrial Hygiene Association Journal, Jan. 1978, Vol. 39, pp. 1-11.

38. Timbrell, V., "Alignment of Respirable Asbestos Fibres by Magnetic Fields", Annals of Occupational Hygiene, Pergamon Press 1975, Vol. 18, pp. 299-311.

39. Technical Report: "Automatic Detection and Counting of Asbestos Fibres", American Industrial Hygiene Association Journal, July 1979, Vol. 40, pp. A.50-A.53.

40. Page, S.J., "Correlation of the Fibrous Aerosol Monitor With the Optical Membrane Filter Counter Technique", U.S. Bureau of Mines Report of Investigations, RI8467, United States Department of Interior, 1980, pp. 1-21.

41. Pundsack, F.L., "The Pore Structure of Asbestos", Journal of Physical Chemistry, 1961, Vol. 65, pp. 30-33.

42. Chatfield, E.J., "Measurement of Asbestos Fibres in the Work Place and in the General Environment," In: Short Course in Mineralogical Techniques of Asbestos Determination, Editor: R.L. Ledoux, Mineralogical Association of Canada, Quebec, May 1979, pp. 111-163.

43. Stroink, G. Dahn, D. and Holland, J., "Magnetopneumographic Estimation of Lung Dust Loads and Distribution in Asbestos Miners and Millers", Am. Rev. of Resp. Disease, 1981, Vol. 123 No. 4, p. 144.

44. Stroink, G., Dahn, D. and Brauer, F., "A Lung Model to Study the Magnetic Field of Lungs of Miners (to be published).

45. Chikazumia, S., "Physics of Magnetism", John Wilev and Sons (1964), pp. 411-417.

46. Berkowitz, A.E., and Kneller, E., "Magnetism and Metallurgy", Academic Press, N.Y., 1969, Vo. I, pp. 377-393 and 427-431.

47. Parasnis, D.S., "Mining Geophysics", Method in Geochemistry and Geophysics, Elesevier Publishing Company, Amsterdam, London, New York, 1966, pp. 326-327.

48. Riis, P., and Chatfield, E.J., "Development of a Rapid Survey Technique for the Detection of Asbestos Fibres", Paper Presented at Asbestos Standards Workshop, National Bureau of Standards, Washington, D.C., Oct. 1980, pp. 1-25.

## CHAPTER VIII

## RESEARCH WORK: DETERMINATION OF THE RELATIONSHIP BETWEEN FERROMAGNETIC PARTICLES AND AIRBORNE CHRYSOTILE FIBRES IN THE ASBESTOS MINES AND MILLS OF QUEBEC

### 8.1 General Purpose

Airborne concentrations of chrysotile asbestos in Canadian mines and mills are currently measured using membrane filters for sampling and phase contrast microscopy for fibre counting. As explained earlier, this is a slow and tedious procedure and, the reproducibility of results from one person to another is low. The accuracy and reproducibility can probably be improved by automating the counting procedure. As stated earlier, since the start of this research work, Timbrell[1], with the financial backing of Vickers Instruments, has studied and utilized the magnetic properties of asbestos fibres and developed "The Timbrell-Vickers Automatic Fibre Evaluation System."[2]

Assad[3] and Heidermans[4] have suggested that automated mass measuring methods may provide rapid results for continuous monitoring of the asbestos in work environments and stated that a mass measuring method, based on Beta absorption, has already been adopted in West Germany. Nevertheless, there is still a need for a rapid and easy method of monitoring airborne asbestos dust for engineering and industrial hygiene purposes.

In the previous chapter it was explained that the ferro-

magnetic characteristic of chrysotile asbestos is due to its association with ferromagnetic particles, and the presence of these particles can be detected by measuring their remanent magnetic field with a fluxgate magnetometer. The measurement of the remanent magnetic field intensities, associated with respirable chrysotile asbestos dust, using a fluxgate magnetometer, is relatively simple. Similarly, Dr. Cohen of MIT was able to detect and quantify the remanent magnetic field intesities and magnetite content of the lungs of living persons working in the Quebec chrysotile mining industry[5] [6] [7] [12]. Such measurements of airborne dust and magnetic chest scans of workers would provide a basis for developing a rapid method for monitoring airborne asbestos fibre concentrations in work places and the dose of exposure of asbestos workers. In order to develop such methods, it is necessary to determine the relationships between the remanent magnetic field intensities; the mass of magnetite and their association with the airborne respirable chrysotile fibres.

Therefore, a critical issue is to determine whether or not airborne magnetite particles are intimately attached to fibres and whether or not the associated remanent magnetic field intensities are related to measured mass and/or number concentrations of airborne respirable asbestos fibres.

8.2 Materials and Methods:

In order to conduct the laboratory investigations under controlled conditions and maintain repeatability, the following experimental design and set-up was standardized and used for all measurements:

(a) Filtering Media and Dust Distributions:

It is noted in chapter 7 that, because of the sensitivity of the magnetic measurements to size, size distribution and shape of the samples, all of the airborne magnetite and chrysotile dust samples were collected on 41 mm diameter Millipore membrane filters with a size selective sampler, Hexhlet horizontal eleutriator. The effects on measurements of thickness variations of the samples being in the 1 to 3 micrometre range, could not be detected by the fluxgate magnetometer used for these experiments. Therefore, the measured results were not affected by the sample thickness variations.

As discussed in chapter 5 the airborne particles have log normal size distribution and the majority of the particles are smaller than 2 μm. Similarly the magnetite particles co-existing with the chrysotile are within the intersticies of fibres which themselves are smaller than 3 μm. Any major effect of particle size was reduced by using only the fraction of airborne magnetilte passing the horizontal eleutriator; i.e. the McGill magnetite dust and the airborne magnetite in the mines, mills and laboratory were size selected using the same method.

(b) Magnetic Field Measurements:

Since the magnetic readings are sensitive and proportional to the inverse cube of the distance between the filter samples and the probe, all magnetic measurements were carried out exactly 1 mm away from the face of the probe.

The probe used was Model MF-F-100 Field and Gradient Probe (see Fig. 8.12A). The effective magnetic core length of the probe pair is 32 mm. The probe pair are housed in 2 separate plastic housings with dimensions 10 x 10 x 70 mm, and each probe has a cable about 10 feet long terminating in a 10 pin Bendix connector. The closest distance between both probe cores is 20 mm. The axes of the probe cores are parallel to the plastic housings longitudinal axes within $\pm 1^{\circ}$. If both probes are placed immediately next to one another, interaction may affect the calibration by about 1%. However, during this research work both probes were placed in the provided plastic holder 20 mm apart in the gradiometric mode.

The results given in this thesis apply only to the geometry and instruments used and the results have no meaning if any of these is changed.

All of the fluxgate magnetometer readings in this thesis are for the vertical Z component of the total remanent magnetic field of the samples which represents magnetic dipoles. The scale in gauss has no relevance to the total remanent magnetic field since the instrument used measures uniform fields or gradients.

8.2.1 Materials:

In order to conduct the laboratory investigations, and establish the existence of a relationship between the remanent magnetic field intensities and the mass of airborne respirable magnetite particles and their association with chrysotile fibres, the following materials were collected from different sources:

(a) Pure Magnetite: The pure magnetite was supplied by the Department of Metallurgical Engineering of McGill University. The purity of the magnetite was 99.95 percent and the particle size minus 400 Tyler mesh (-38μm).

(b) Bulk Chrysotile: For the purpose of chrysotile asbestos dust generation, the bulk chrysotile asbestos of commercial grades #6 and 7, and tailings, were provided from nine different mills of Quebec. Accordingly, each bulk chrysotile asbestos sample was marked with a Roman number and they were identified by these numbers from I to IX.

(c) UICC Standard Reference Samples of Rhodesian Chrysotile: The standard "Union Internationale Contre Le Cancer" reference samples of Rhodesian chrysotile were provided by Mr. R. Rendall, previously of MRC Pneumoconiosis Research Unit of Johannesburg, South Africa. The respirable size standard reference samples, of specific asbestos types, were produced from commercial grades of as-

bestos by blending and grinding them[21]. Timbrell et. al[21] stated that, during the production of the standard reference samples of asbestos, it was important that the materials should not be ground more than necessary in order to: (i) minimize changes in the crystalline structures, (ii) preserve the fibrous nature of the particles, which is thought to be related to the biological effects of asbestos, and (iii) have the size distributions of dust clouds generated from the reference samples to resemble those occurring in asbestos mines, mills, and factories.

(d) Airborne Chrysotile Asbestos Samples: In order to relate the laboratory investigation results of dust clouds, generated from the bulk chrysotile samples, to those occurring in asbestos mines and mills, two of the Quebec asbestos mills were visited and airborne respirable and nonrespirable chrysotile asbestos samples were collected for further microscopic, magnetic, and chemical investigations.

(e) Lung Specimens: The lung specimens obtained from the autopsies of chrysotile asbestos workers were provided by the Epidemiology Department of McGill and collected by Drs. A. D. McDonald, N. Rowlands, and G. W. Gibbs for magnetic measurements and dust counts.

### 8.2.2 Methodology and Instrumentation:

#### 8.2.2.1 Environmental Chamber:

For the laboratory experiments, chrysotile asbestos was

rendered airborne in an existing environmental chamber. The chamber is constructed of plexiglass and has the geometric shape of a regular pentagonal bi-pyramid (see Fig. 8.1). The sides of the pentagon are 3.5 feet wide and 2.9 feet high and the equal pyramidal section sides of the chamber have 3.5 feet triangular sides and are 1.7 feet high. The total volume of the environmental chamber is 90 cubic feet, with the middle containing a volume of approximately 60 cubic feet and pyramidal sections containing 15 cubic feet each.

On one side of the chamber, an air tight access door is fitted. In order to handle the instrumentation inside the chamber, without interrupting the operation by opening the door, three pairs of 31 inches long rubber gloves were fitted at three adjacent sides.

Air pressure in the chamber is positive and a constant airflow is maintained and recirculated by an eight inch diameter centrifugal fan. The fan has radial blades and is pulley driven by a 1/4 horse power motor. It has a capacity for delivering 350 cubic feet of air at a static pressure of 1/8 inches of water gauge. The air is introduced by a 5 inch diameter duct at the bottom end of the pyramidal section of the chamber and exhausted through the top end. Since the air is introduced through the pyramidal shaped sections of the chamber, the airflow within the chamber is reasonably uni-

form. The airflow distribution was checked by a smoke tube and the air velocity profile accross the chamber was measured by a "low velocity, hot-wire anemometer." The average air velocity was found to be 19 feet per minute and in the centre section of the chamber it reached a maximum velocity of 24 feet per minute. Air velocities at the side walls were in the vicinity of 17 feet per minute. At the corners of the chamber, slight turbulance was noticed. However, this did not create any problem in maintaining the uniformity of the flow in the other parts of the chamber. Therefore, it was concluded that the measured velocity profile of the chamber is representative of existing airflow patterns in general work areas of plants and underground mines and that the chamber has a suitable design for dust cloud generation.

8.2.2.2 Chrysotile Asbestos Dust Cloud Generation:

Dust clouds were generated by a modified Timbrell dust cloud generator, patterned after the dust cloud generator described by Timbrell et al. (8). The Dust cloud generator consisted of two components: (a) a dust feeding mechanism, and (b) a dust dispersing chamber.

(a) Dust Feed Mechanism:

The asbestos fibres are packed and contained in a plastic cylinder, from where a fibre plug is pushed into a dispersing chamber by a piston. The piston is driven by a synchronous motor at a constant speed of 3 r.p.m. The intensity of the dust cloud is controlled through a set of interchange-

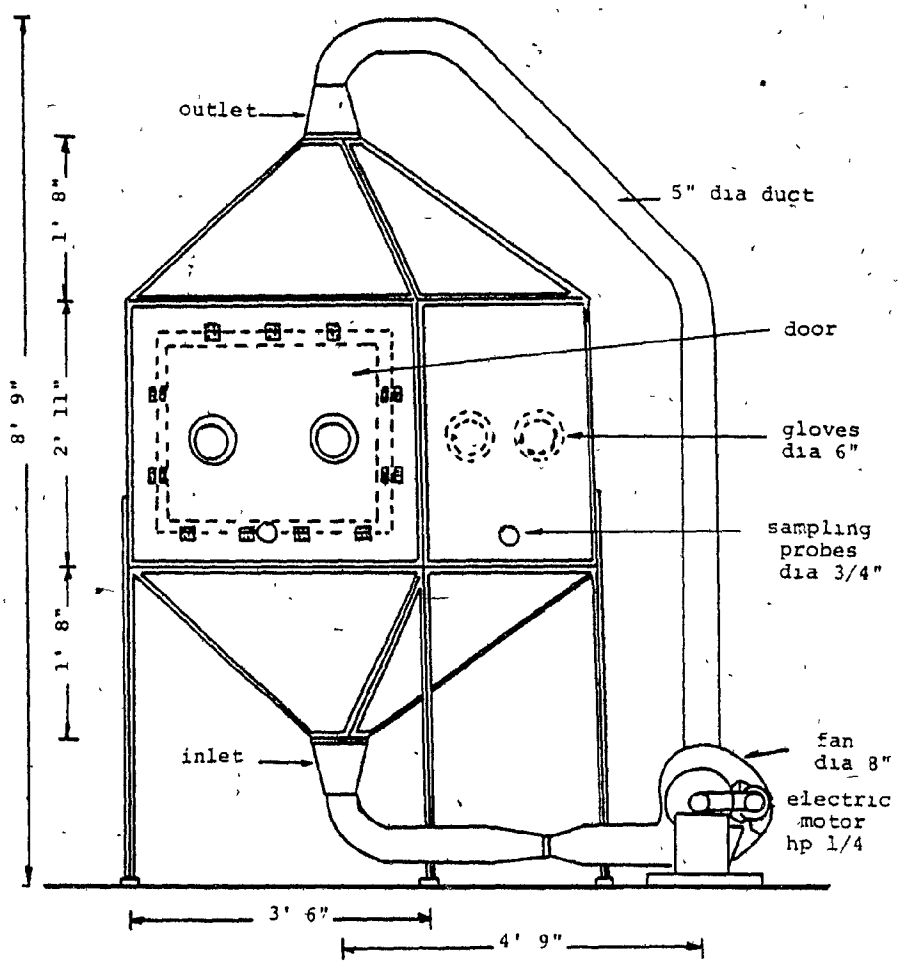


Fig. 8.1 - Environmental Chamber

able gears, which varies the speed of advancement of the piston within the plastic cylinder (see Fig. 8.2). For this research work, the smallest gear ratio of 30:1 was used, which gave a 1 millimetre horizontal advance to the piston for every 30 revolutions.

(b) Dust Dispersing Chamber

The dust feed mechanism is connected to the dust dispersing chamber through the plastic cylinder. This unit comprises a steel bowl with rotating vanes (see Fig. 8.3). The vanes are powered by a small electric motor rotating at 1,725 r.p.m. The rotor is fabricated from 3/64 inch thick steel plate and has an appropriate clearance between the base and walls of the bowl to prevent asbestos fibres being caught between the blade and the bowl and being rolled into balls or bundles of fibres. Furthermore, in order to prevent the asbestos plug from following the circular rotation of the vanes, and to aid the fibre bundles in separating from each other and dispersing, compressed air is supplied at a rate of 15 litres per minute at 20 p.s.i. pressure. The compressed airline has a 6/32 inch internal diameter and is connected to the side of the steel bowl at a 45 degree angle. Prior to releasing the compressed air into the dispersing chamber, it is filtered from all contaminants (such as oil mist) and dried. The dispersed asbestos fibres are exhausted from the dust dispersing chamber via 1/4 inch diameter copper tube and connected to the main air

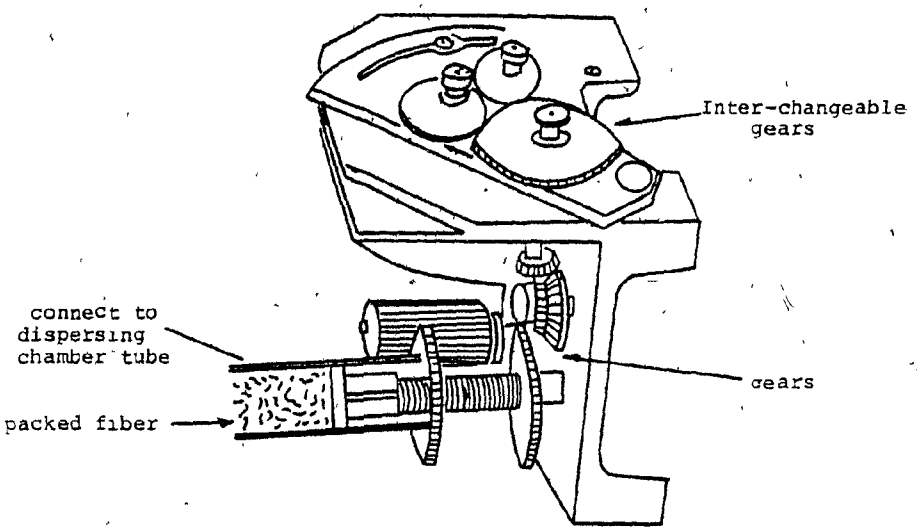


Fig. 8.2 - Dust Feed Mechanism

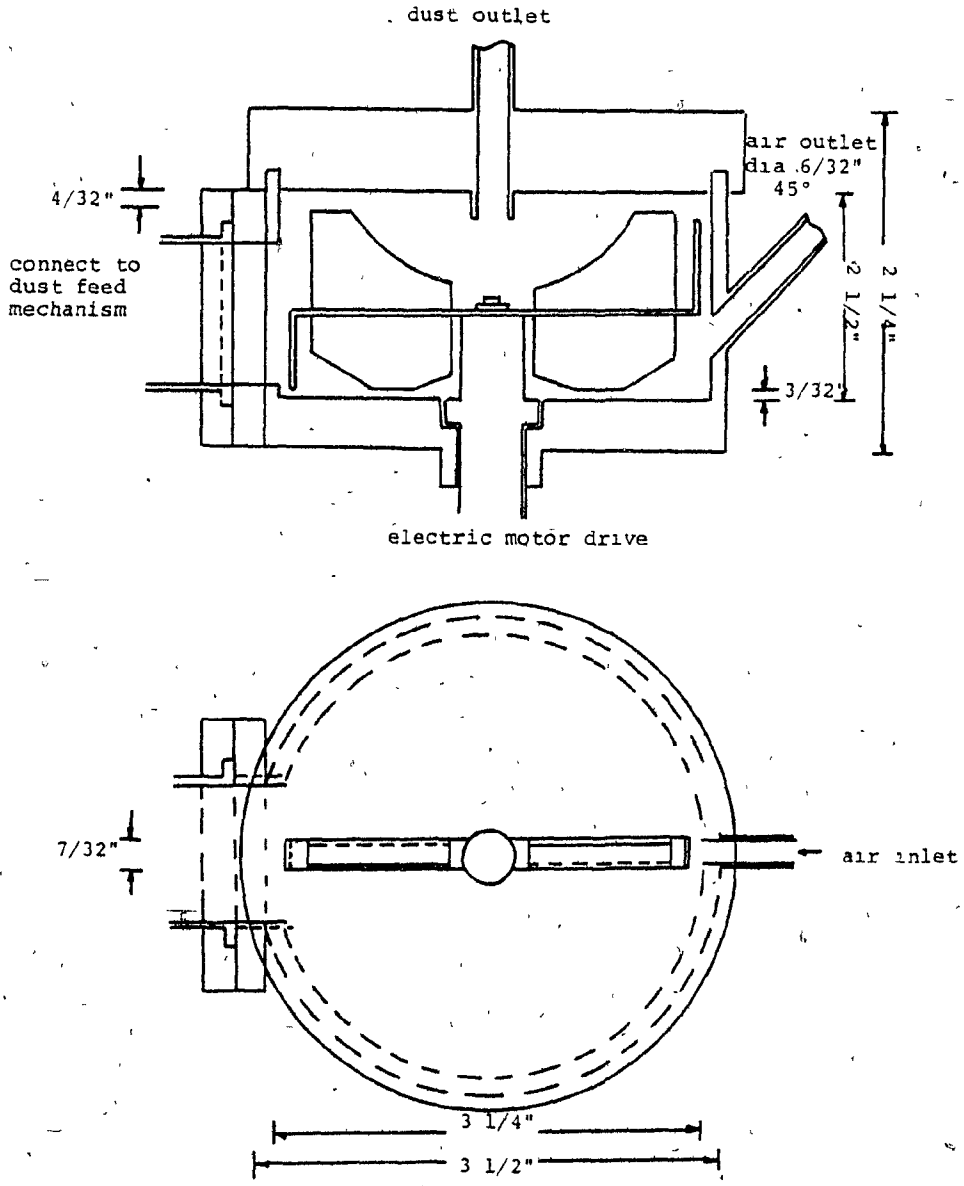


Fig. 8.3 - Fiber Dust Dispersing Chamber

streamline at the throat of a venturi. At the throat of the venturi, the static pressure of the flowing air being negative, and the velocity pressure being highest, the fibres are drawn out from the copper tube at high velocities thus, eliminating plugging of the exhaust. From here the asbestos fibres follow the 5 inch diameter air duct into the environmental chamber and are rendered airborne. It was observed in this work, and also, by Timbrell et al.[8], that complete disintegration of all flocks of chrysotile is difficult and that some appear as large fibre bundles in the dust clouds generated by the dispenser. However, this condition did not cause any problem during the dust sampling operation because their large-mass, macroscopic fibre bundles settle very rapidly and do not reach the heights where sampling instruments were placed. Also the respirable size selection characteristics of the Hexhlet horizontal eleutriator prevented these macroscopic bundles from being collected. The only disadvantage is that the fibre consumption of the dispenser does increase and frequent refilling of the plastic container becomes necessary if too many of these flocks of chrysotile fibres are released. However, Beckett[9] has stated that by modifying the dispenser this problem could be eliminated. Beckett[9] had modified the dispenser by adding an additional air jet through the top of the dispenser bowl and blowing compressed air at the asbestos-plug entry point through a needle, at pressures up to 40 pounds per square inch. Spurny et al.[10] have shown that a vibrat-

ing fluidized bed would produce a better and uniform supply of airborne dust clouds from fibrous or non-fibrous powders. However, since these generated dust clouds were not for the use of inhalation chambers, and the presence of flocks of fibres did not cause any sampling problems, Timbrell's modified dust cloud dispenser was accepted as a suitable fibrous dust cloud generating device for this type of research work.

8.2.2.3 Chrysotile Dust Sampling, Equipment and Methodology:

At the early stages of the experiment, it was realized that, due to static electricity within the chamber, excess quantities of fine dust particles and fibres have been attracted to, and accumulated at, the plexiglass walls of the chamber. The major cause of the static electricity was friction, created by the flow of the dry air (humidity content of the air was measured to be 25 percent) against the plexiglass walls of the chamber. However, this problem was eliminated by spraying the inside walls of the chamber with a mixture of one part "Cynamid-Catanac, SN" antistatic agent and 20 parts of water.

The generated chrysotile dust cloud was monitored by filtering the air through a membrane filter at a sampling rate of 2 litres per minute. The membrane filters used were 37 millimetres in diameter, Millipore Type AA, white, with a pore size of 0.8 micrometres. The air suction was provided by a

small battery operated MSA air pump. Although the dust feed mechanism was working at its lowest speed, the generated fibre concentrations were too high; and therefore, continuous monitoring was impossible. Therefore, samples were taken at the beginning, in the middle, and at the end of each experiment. Duration of the sampling time was kept below ten minutes. In the beginning of the experiments, longer sampling periods were tried. However, the membrane filters were found to be too crowded with fibres and, therefore, microscopic evaluation and counting of the fibre content of the filters, were impossible. Thus, sampling time was reduced to less than ten minutes.

For respirable size gravimetric chrysotile dust sampling the Hexhlet horizontal eleutriator was used. As explained in chapter VI, air was drawn through the horizontal eleutriator, by direct coupling of a vacuum pump, at a rate of 50 litres per minute. The vacuum pump used was a type RB1-61 with an AC motor delivering 1,725 r.p.m. The respirable size chrysotile dust and fibres were collected by membrane filters. These filters were 41 millimetres in diameter, Millipore Type AA, white, with a pore size of 0.8 microns. A constant air volume of 50 litres per minute was maintained by a critical orifice, irrespective of progressive dust loading of the filter media, as long as the pressure difference across the critical orifice was maintained above 100 millimetres of mercury. In order to collect gravimetric samples or airborne respirable size chrysotile with varying

ranges of mass, the sampling time was randomly varied from 10 seconds up to 15 minutes. This time variation has provided the required mass distribution of samples from minimum 0.1 milligram to maximum 5 milligrams. In deciding on the required minimum number of samples for representing the dust cloud population properly, the following statistical condition was considered. According to statistical tables of Fisher and Yates[11], beyond the 40 degrees of freedom (or when $n > 42$), there is a high probability (90%) that the sample average will be close to the population mean[11]. Thus the minimum sample size was decided to be much larger than 42, and from each source of chrysotile dust clouds, at least 60 samples were taken. When the membrane filters were visually studied, it was observed that the collected fibres were mainly concentrated in the centre portion of the filters, and the smaller portion of the collected fibres were randomly and less densely scattered in the remaining area of the filters. In order to measure the effect of the variation in distribution of magnetic particles associated with fibres on the remanent magnetic field measurements, smaller size 25 mm cyclones were used and a limited number of respirable size samples of chrysotile fibres from the sources of # VI and VII, and of pure magnetite, were collected (see Figs. 9.4, 9.5, 9.7, 9.8, 9.10 and 9.11).

In order to eliminate the possibility of contamination of the chrysotile samples, the environmental chamber; dust dispenser; and sampling equipment were carefully vacuumed;

wiped off with a damp cloth and dried at the end of each experiment. Furthermore, magnetite dust clouds were never generated in the same chamber as the chrysotile dust clouds.

8.2.2.4 Mass Determination of the Gravimetric Samples:

Millipore membrane filters were used as filtering media for mass determination. Millipore membrane filters are very sensitive to variations of humidity within the air and precautions should be taken to avoid errors attributable to changes in the moisture content of the collecting filter during gravimetric sampling. In order to eliminate the effect of humidity, all of the Millipore membrane filters were dried in an oven at a temperature of 75° C for two hours, and desiccated for 48 hours. At the end of 48 hours, blank membrane filters were weighed and, for each sampling filter, a blank control filter was alloted. After each experiment, both filters were returned to the desiccator for 48 hours and later demagnetised and weighed. For demagnetization of filters, an ordinary magnetic tape erasing coil was used. The difference in weight of the control filter caused by humidity, plus or minus, was subtracted from or added to the weight of the sampling filter. When the humidity of the air was less than 30 percent, this difference was zero. In the majority of the cases, the humidity of the air was constantly 25 percent and the correction factor was zero. However, the dryness of the air has caused electrostatic charges and created a considerable problem during the weighing of

samples. This problem was eliminated by placing a radioactive ionizing unit under the weighing pan. The radioactive substance of the unit, ionized the air in the balance chamber and, therefore, the conductivity of the air was substantially increased causing the sample to lose its electrostatic charge rapidly.

A Sartorius balance was used, which had a maximum capacity of 2.5 grams and precision of ± 0.1 milligram. Therefore, variations of this magnitude could cause large errors for small mass determinations, especially when the mass is less than 1 milligram. In order to avoid the weighing errors in chemical analyses, all the atomic absorption analyses were based on sample weights larger than 3 milligrams. A such weights the weighing error is ± 3.3 percent. Similarly, the slope of the line which determines the relationship between the magnetic field and the mass is more sensitive to large mass changes. Therefore, errors in small masses would not affect the results substantially. However, to minimize the errors of weighing each filter paper was weighed 3 times before and after sampling and the average of the 3 was taken as the correct sample weight. However, in determining the calibration curves for pure magnetite, more sensitive mass determination was necessary because the average magnetite content of the chrysotile samples was 3 percent, and those chrysotile samples weighing less than 3 milligrams would have a magnetite content weighing less than 0.1 milligrams. Therefore, the measurement

of the corresponding mass of pure magnetite with the existing balance was not possible. In order to achieve this, a series of 10 milligrams of respirable size pure magnetite was weighed and evenly dispersed in 10 millilitre of OT solution by an ultrasonic vibrator. Ten equal parts of each mixture were then taken and diluted again. This dilution and ultrasonic mixing was continued until a range of magnetite samples from 0.001 to 0.04 milligrams was obtained.

8.2.2.5 Sample Analysis By Fibre Counting With Phase Contrast Optical Microscopy:

Millipore membrane filters are thin porous membranes of cellulose esters and have an open sponge structure. Therefore, during filtration, the separation of fibres from air occurs almost exclusively at the upper surface of the filter media. Thus, fibre counting under the phase contrast optical microscope becomes easier, since fibres are resting directly on the filter surface, and depth of focus problems are minimized.

Filters containing the chrysotile fibre samples were prepared and mounted on microscope slides in the following manner: A few drops of Triacetin (glycerol triacetate) were dropped on a clean 7.5 x 2.5 cm microscope slide. Then, using tweezers, the filter was carefully removed from the filter-holder, and placed on a hard surface. With a sharp scalpel a wedge shaped section was cut out and placed on top of the

Triacetin on the microscope slide, dust side uppermost. The sample was then covered with a 22 x 22 millimetre square cover slip, making sure that no air bubbles were trapped underneath its surface. A period of thirty minutes was usually sufficient to completely clear the filter. It was wise to mark the location of the wedge with a wax pencil to facilitate finding the fibres under the microscope.

The refractive index of the cleared or transparent membrane filter, being very close to that of chrysotile under bright field illumination, may make fibres be almost invisible. The refractive index of transparent filters is 1.5 and for chrysotile fibre is 1.55. Therefore, a phase contrast microscope is used to increase the visibility of the chrysotile. Phase contrast illumination, which utilizes the interference patterns produced by the combination of two out of phase columns of light; is capable of revealing objects imbedded in media with an index of refraction only slightly different from that of the object.

The microscope used was a Carl Zeiss Photomicroscope, fitted with a Ph2 Neofluar 25/0.60 objective, optovar 1.6 and 12.5 x eye pieces. The Millipore membrane filters were studied under a magnification of 500 X, and the resolution was coded by the manufacturer to be 0.3 micrometres. The eye piece had a Patterson-Cawood graticule to estimate fibre widths and diameters by visual comparison. The graticule

was calibrated against a stage micrometer and fibre size ranges were established as shown in tables 8.1 and 8.2 and in figures 8.4 and 8.5.

In order to minimize bias in counting, and eliminate counting errors due to overlaping of the randomly selected microscopic fields, the Australian membrane filter method was used[13]. In Canada there is no established standard membrane filter method. According to Schneider[22] some of the fibre counting rules overestimate the number of fibres because of bias in the counting method. However, he has indicated that in the case of the Australian membrane filter method, counting fibres by optical microscopy, the overestimation is not serious[22].

According to the Australian method, at least a total of 100 fibres were counted in a minimum number of 20 fields[13]. All fibres which cross either the left or bottom side only, or left and bottom sides, or left and top sides, or top and bottom sides were counted[13]. Those fibres which cross either the right or top side only, or right and top sides, or right and bottom sides, or left and right sides were not counted[13].

All single fibres, split fibres and grouped fibres were counted as one fibre when they conform to the basic requirements of fibre definition, (see chapter six for fibre definition), at its greatest thickness and longest length.

Similarly, all fibres with other particles attached were counted as one if the particle width was not more than 3 micrometres.

The fibre concentrations were calculated according to the following formula[13] [14]:

$$C_f = \frac{A}{a} \cdot \frac{N}{n} \cdot \frac{1}{r} \cdot \frac{1}{t}$$

Where $C_f$ = Concentrations of fibres in fibres/cubic centimetre of air.

N = Total number of fibres counted

n = Number of graticule areas counted

A = Effective filter area in square millimetres

a = Graticule area in square millimetres

r = Flow rate of air through filter in cubic centimetres/minute

t = Sampling time in minutes

When several consecutive samples were taken, time weighted averages were calculated from single values[13] [14]:

$$C_f = \frac{\Sigma \; Ci.ti}{ti} \triangleq \frac{C_1 t_1 + C_2 t_2 + \ldots + C_k t_k}{t_1 + t_2 + \ldots + t_k}$$

Where: $C_f$ = Time weighted average value

Ci = Single value of concentration

ti = Time for which Ci is representative

k = Total number of samples

Table 8.1 - Average Diameters of Chrysotile Dust Clouds in Environmental Chamber, In Terms of Equivalent Unit Density Spheres and Actual Fibre Diameters: **

| | Mode of Diameter | Median of Diameters | Arithmetic Mean of Diameters | Geometric Mean of Diameters | Geometric Mean of Deviation |
|---|---|---|---|---|---|
| Equivalent Unit Density Sphere | 1.25μm | 1.35μm | 1.77μm | 2.5μm | ± 0.46 |
| Actual fibre* Diameters | 0.5μm | 0.54μm | 0.71μm | 1μm | ± 0.18 |

* Actual Fibre Diameter = Equivalent Unit Density Sphere Diameter ÷ 2.5

** Optical Observations

Table 8.2 - Chrysotile Asbestos Fibre Length Distribution of Chrysotile Dust Clouds in Environmental Chamber: (Optical Observations)

| Fibre Length in μ | Frequency Distribution in % | Cumulative Frequency Distribution |
|---|---|---|
| 50 - 100 | 0.5 | 0.5 |
| 20 - 50 | 2.3 | 2.8 |
| 10 - 20 | 4.2 | 7.0 |
| 5 - 10 | 5.8 | 12.8 |
| 2.5 - 5 | 36.7 | 49.5 |
| 0.5 - 2.5 | 50.3 | 99.8 |

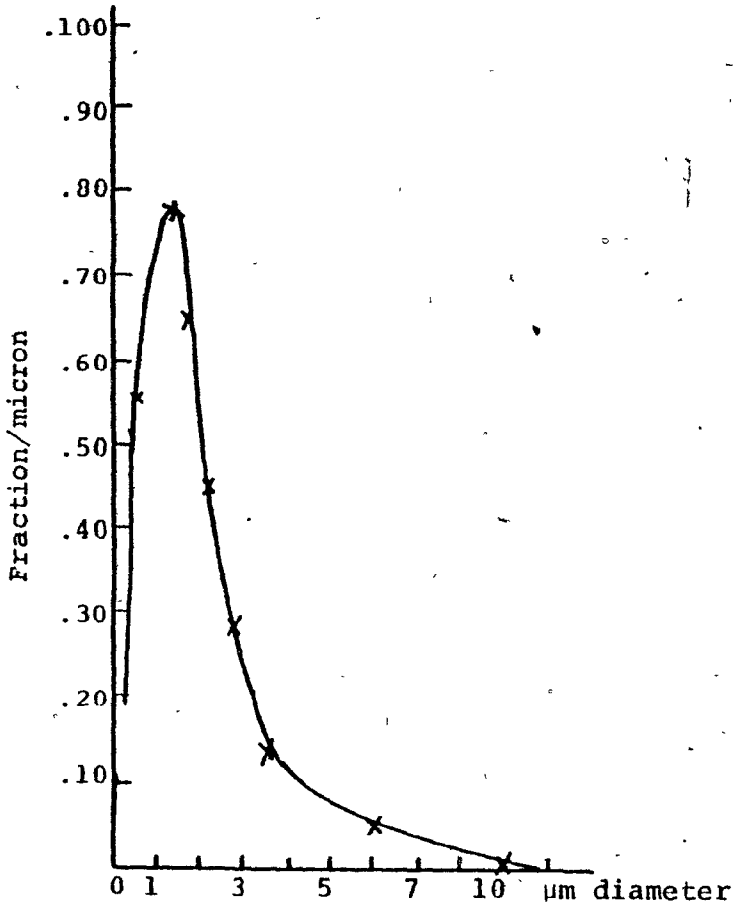


Fig. 8.4 - Fibre Diameter Distribution of Chrysotile Dust Clouds in Environmental Chamber In Terms of Unit Density Spheres *
(* Unit Density Sphere = Fibre diameter x 2.5)
Note: Optical observation

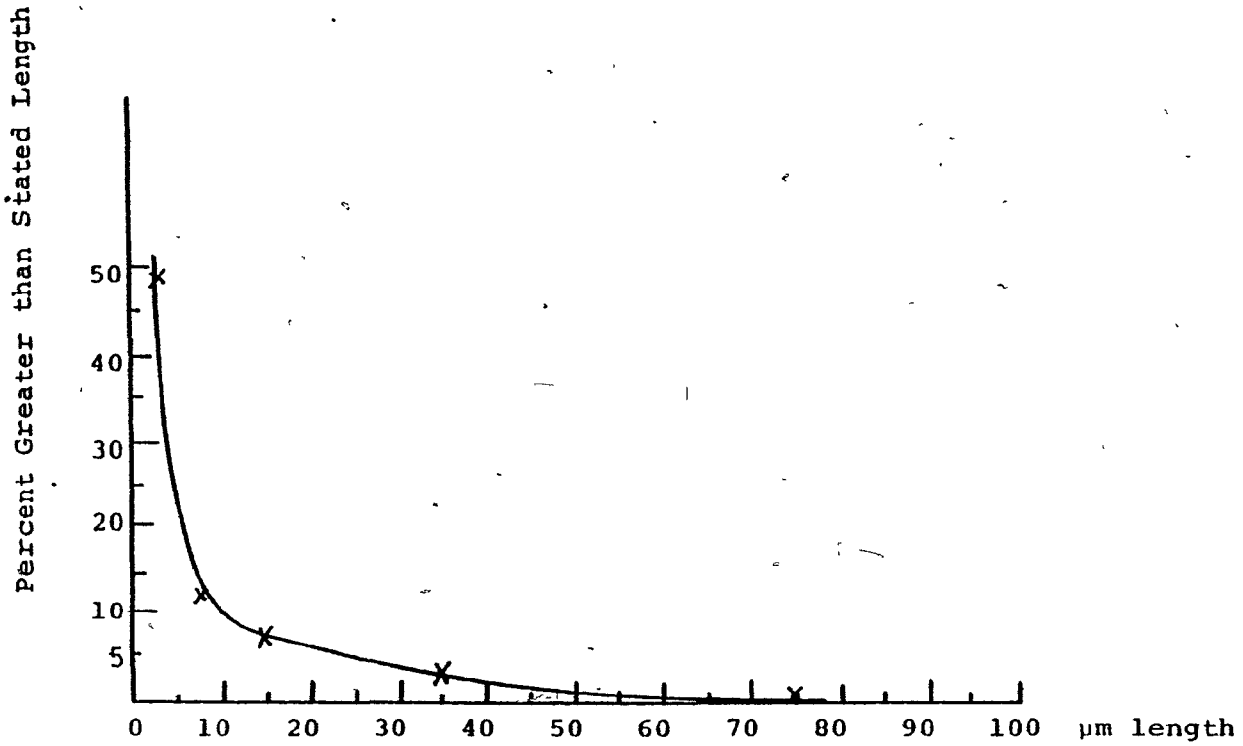


Fig. 8.5 - Length Distribution of Chrysotile Fibres in Dust Clouds in Environmental Chamber

During the optical microscopic studies, more than four thousand fibres were counted and sized. Figure 8.4 shows the asbestos fibre size distribution of chrysotile dust clouds, in terms of unit density spheres, as existed in the environmental chamber. The mode, median, arithmetic and geometric means, and geometric standard deviation of the diameters of airborne fibres are shown in table 8.1. Figure 8.5 and table 8.2 show the asbestos fibre length distribution of chrysotile dust clouds in the environmental chamber. It is observed that more than 40 percent of the airborne chrysotile fibres are longer than 5 micrometres and only 7 percent are longer than 15 micrometres.

In order to check the reproducibility of the fibre counting and sizing, 20 percent of the millipore membrane filter samples were recounted and sized by the same person. Results of both counts checked within ± 5%. Similar random recheck counts were conducted by the author and the discrepancy was found to be only ± 15 to 20 percent.

8.2.2.6 Sample Analysis By Using Transmission and Scanning Electron Microscope:

The electron microscope used was a JEOL 100 CX (TEM-SCAN) and had the following attachments and analytical capabilities: EDXA (energy dispersive analyser of X-rays); scanning; scanning-transmission; SAED (Selected area diffraction patterns) and micro-diffraction patterns via STEM mode.

The purpose of analysing the airborne chrysotile samples under the electron microscope was to identify the magnetic particles from other opaque particles such as antigorite, brucite and talc, which co-exist with chrysotile fibres in the airborne dust. Furthermore, to determine how intimately magnetite particles are attached to the fibres and what percent of the opaque particles are magnetite. Although, with atomic absorption analysis the iron content of the samples can be determined, it is not known what portion of the determined iron is magnetite and what portion is existing as iron oxide in the chemical structure of chrysotile, as a contaminating mineral.

Three of the airborne samples of Mill # V were mounted on 3 mm diameter copper grids, as described in chapter VI, and on each sample 21 random fields were studied under 10,000× magnification. All observed opaque particles were counted and their chemical compositions were determined by EDXA. In the first sample, a total of 53 particles were counted and analysed. Out of a total 161 analysed particles, only 5 were found to be magnetite. The other particles were either antigorite or brucite.

Later, two grids from the first sample and another two grids from the second sample were prepared and named as sample # 1 grids "A" and "B", and sample # 2 grids "C" and "D". Thirteen squares of the grid represents 0.126% of

the total grid screen area. With a magnification of 10,000x(9697 to be exact), nine fields have to be counted in order to represent one square of a grid. For each sample, 21 squares of a grid were observed and all fibres and particles were counted. The counted fibres and particles in twenty-one squares represents 0.2% of the total number of fibres and particles. According to classical counting techniques on the electron microscope, this percentage would give a representative count of the sample randomly distributed on the grid.

In order to calculate the actual magnetite content of the samples, the following measurements were carried out From grids A and B, six fields and from grids C and D, four fields were chosen and photographed. The dimensions of the chrysotile fibres, as well as all other particles, were measured and the total surface areas were calculated. For each sample the ratio of the area of opaque particles to the area of chrysotile fibres was determined. The average ratios of the surface areas of particles to chrysotile, and calculated magnetite content, are shown in table 8.3. For samples # 1 and 2, the magnetite content varies between 4.9 and 5.8 percent and the average is 5.4 percent. In order to check the reliability of these results, the iron content of samples 1 and 2 were determined by atomic absorption analysis and found to be 3.6 and 3.8 percent respectively. Therefore, the average percent of iron by weight in magne-

tite for sample # 1 is:

$$\frac{3.6}{\frac{(3.765 \times 1.26) + (4.09 \times 1.28)}{2}} \times 100 = 72\%$$

and for sample # 2 is:

$$\frac{3.8}{\frac{(4.41 \times 1.3 + (4.54 \times 1.25)}{2}} \times 100 = 67\%$$

In reality, pure magnetite contains 73 percent iron. The difference between the experimental and actual value for sample # 1 is 1 percent, for an error of 1.4 percent and for sample # 2 is 6 percent, for an error of 8.2 percent. The magnitude of these errors are acceptable, if one considers that the value of 73% is an idealized value which could vary from sample to sample due to impurities. Also some chrysotile and magnetite were lost when the small portion of samples was taken for further observations under the transmission electron microscope. Furthermore, errors in counting and sizing of fibres and particles could easily affect the end result by 15 to 20 percent. These results indicate that the magnetite content of a sample of airborne respirable size chrysotile asbestos dust, stays relatively constant from sample to sample. It is realized that with such a small number of samples, no statistical evidence can be established.

Table 8.3 - The average Ratios of the Surface Areas of Magnetite* to Chrysotile** and Calculated Magnetite Content:

| Sample and Grid No. | Average Ratio of Surface Areas Opaque Particles/ Chrysotile | Estimated Number of Magnetite Particles Multiplied by Specific Weight of Magnetite*** | Calculated % Magnetite |
|---|---|---|---|
| 1 A | 3.8 | 1.3 | 4.9 |
| 1 B | 4.1 | 1.3 | 5.3 |
| 1 C | 4.4 | 1.3 | 5.7 |
| 1 D | 4.5 | 1.3 | 5.8 |
| | Total Average 4.2 | Total Average 1.3 | Average 5.4 % |

* Assuming spherical geometry using the average of three diameters per particle.

** Assuming cylindrical geometry with actual measured lengths and diameter enclosing the fibre irregularities.

*** On the bases of 3 percent of observed opaque particles being magnetite, as determined by EDXA analysis of the same samples.

8.2.3 Calibration of The Dust Sampling Instruments:

8.2.3.1 Calibration of the Battery Operated MSA Pumps:

The calibration of the battery operated MSA pumps, was carried out with a "Frictionless Soap Bubble Meter." Although, at the research laboratory, a "Wet-Test Meter" was also available, it was rejected for use in calibrating the MSA pumps. The reason is that Wet-Test Meters are not portable instruments and are not available at the visited mines and mills. However, it is important and necessary to calibrate the pumps one half hour after they are fully charged and just before they are being used for dust surveys[14] [15]. As the research laboratory is at least two and a half hours away from the nearest asbestos mill of Quebec, this condition would have not been met if the pumps were calibrated with a Wet-Test Meter at the laboratory before departure. Furthermore, in most instances, two or three days stay at the mill site was necessary. The other potential errors of Wet-Test Meters are; the moving parts are subjected to corrosion and damage from misuse or transportation; there is friction in the bearings and the mechanical counter and the inertia must be overcome at low flow rates[15].

Also, it is important to keep the Wet-Test Meter levelled for accurate calibration measurements and, occasionally, the wet test meter itself must be calibrated. However, when the Wet-Test Meter is in good order, the accuracy is ± 1 percent.

The Soap Bubble Meter utilizes a volumetric laboratory burette. The interior surface of the burette is wetted with a detergent solution. A soap film bubble is introduced at one end and the suction is applied by the pump to be calibrated at the other end. The flowrate, or the volumetric displacement of the bubble per unit time can be determined by measuring the time required for the bubble to pass through the two scale markings, which enclose a known volume, with a stopwatch. Accordingly, by adjusting the pump suction rate, by twisting the calibration valve of the pump with a screw driver, the required flow rate is attained.

As the Soap Bubble Meter is a simple instrument, and has no moving parts, it is reliable and does not need to be calibrated or levelled.

8.2.3.2 Calibration of the Hexhlet Horizontal Eleutriators:

As explained in chapter VI, Hexhlet Horizontal Eleutriators were originally designed to collect spherical respirable size particles according to a prescribed theoretical size selection curve. Although it was shown by Timbrell[17] that

fibres do settle according to their diameters and that their lengths do not play an important role, it was felt necessary to investigate the suitability of the Hexhlet Horizontal Eleutriators in collecting the respirable size airborne fibres, because all of the airborne respirable size chrysotile fibre samples of this research work were collected by a Hexhlet Horizontal Eleutriator.

In order to evaluate what size and quantity of airborne fibres were captured by the horizontal plates of the eleutriator, 2.5 cm. wide strips of Millipore membrane filters, of 0.8 micrometre pore size, were mounted along the full length of the plates. These strips of filters were divided into 10 equal parts and at the end of the sampling period, the first part, middle, and last part of each strip was cut out and prepared for phase contrast optical microscopic analysis. The fibres were counted, sized, and classified (see Figs., 8.6 to 8.9). Also, chrysotile fibres which penetrated to the back filter were studied in a similar manner. Comparison of the theoretical selection curve of the Hexhlet Horizontal Eleutriator for respirable spherical particles and the selection curve for actual chrysotile fibres, as determined by this experiment, are shown in table 8.4 and figure 8.10 in terms of equivalent unit density spheres. The results of this investigation indicate that the Hexhlet Horizontal Eleutriator is over sampling the airborne respirable size chrysotile fibres by only 9.8 percent.

This result is in agreement with Lippman's[16] statement that the Hexhlet Horizontal Eleutriator over samples the respirable size chrysotile fibres by 10 percent. Therefore, the Hexhlet Horizontal Eleutriator is an adequate respirable size selective instrument for chrysotile fibres as well.

According to the stated specifications, the flow rate of the Hexhlet is 50 litres per minute. This flow rate was checked with a Dry-Gas Meter and found to be very accurate, fluctuating only between 50 to 52 litres per minute. When the back filter was relatively clear of high level concentrations, the flow rate was maintained at 52 litres per minute but after 15 minutes of sampling, and 4.5 milligrams of fibre accumulation, the flow rate had dropped to 50 litres per minute. The mass of 98 percent of the collected chrysotile fibres in the laboratory dust chambers was less than 4.5 milligrams. Therefore, even under these heavy dusty conditions, the Hexhlet flow rate is accurate. In the Asbestos Milling Industry, this level of heavy dust loading conditions was never reached.

### 8.2.4 Remanent Magnetic Field Measurements, Magnetic Shielding and Magnetometers:

#### 8.2.4.1 Magnetization of the Samples:

After the airborne, respirable-size pure magnetite and chrysotile samples were weighed, they were subjected to

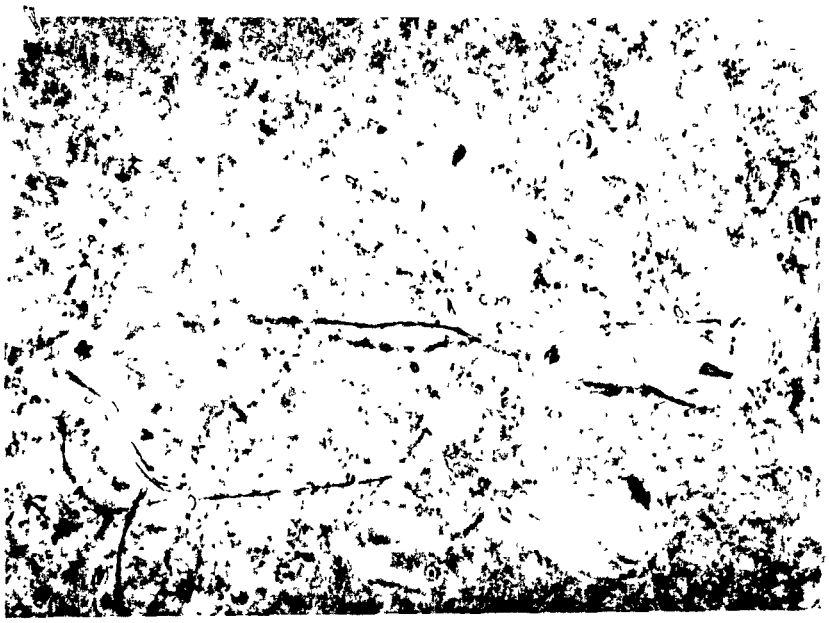

(a)

(b)

Scale: ⟷ = 10 μm

Fig. 8.6 (a)(b) - Picture (a): Settled Nonrespirable Fibres and Dust at The Entrance of the Hexhlet's Eleutriator Plate. Picture (b): Settled Dust Particle and Fibres in the Middle of the Hexhlet s Eleutriator Plate (Test # I).

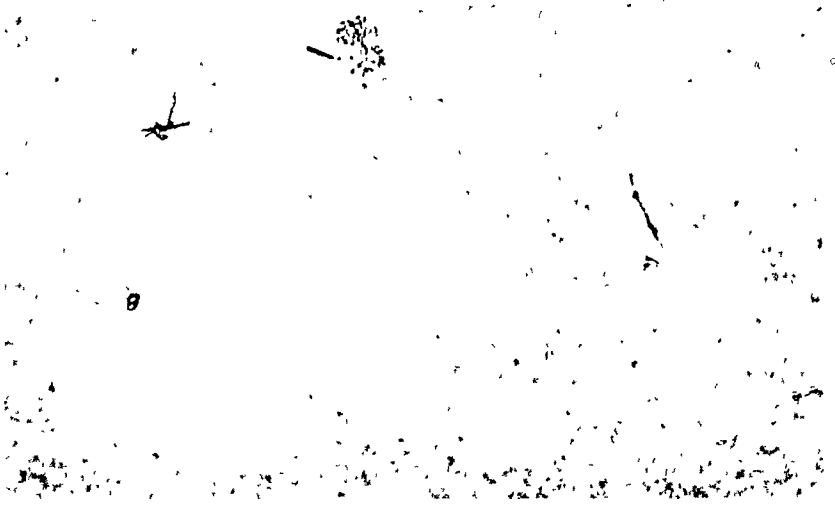

(a)

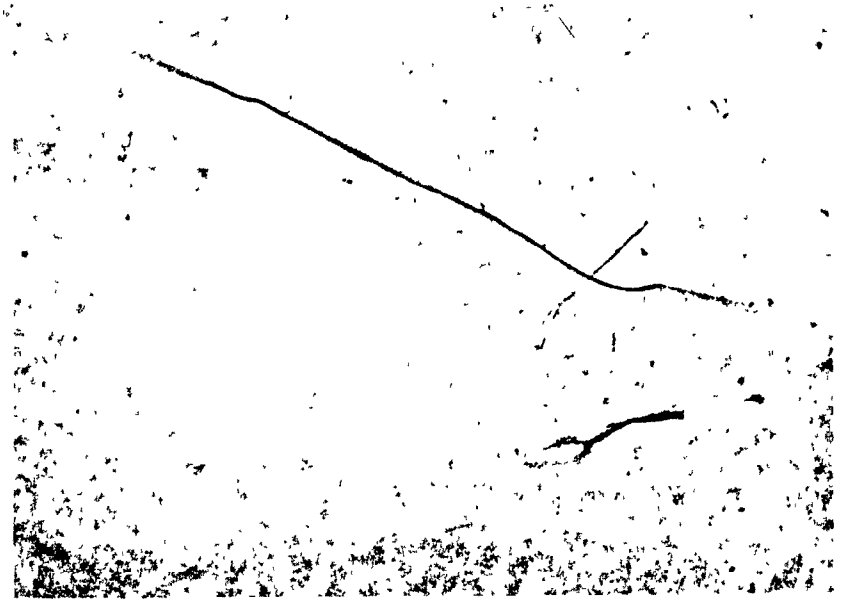

(b)

Scale: ⟷ = 10 μm

Fig. 8.6 (c)(d) - Picture (c): Settled Nonrespirable Dust and Fibre at the End of the Hexhlet's Eleutriator Plate.
Picture (d): Settled Fibres at the End of the Hexhlet's Eleutriator Plate (Test # I).

(a)

(b)

Scale: ⟷ = 10 μm.

Fig. 8.7 (a)(b) - Picture (a): Settled Nonrespirable Dust and Fibres at the Entrance of the Hexhlet's Eleutriator Plate.
Picture (b): Settled Nonrespirable Particle in the Middle of the Hexhlet's Eleutriator Plate (Test #II).

(c)

(d)

Scale: ⟼ = 10 µm

Fig. 8.7 (c)(d) - Picture (c): Nonrespirable Fibres in the Middle of the Hexhlet's Eleutriator Plate. Picture (d): Settled Nonrespirable Fibres at the End of the Hexhlet's Eleutriator Plate (Test # II).

(e)

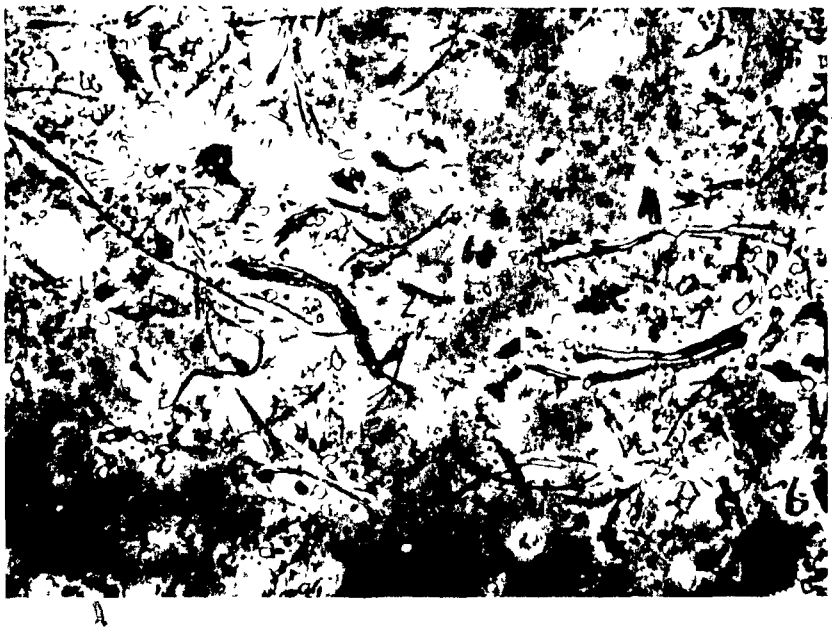

(f)

Scale: ⟷ = 10 µm

Fig. 8.7 (e)(f) - Picture (e): Particles and Fibres at the End of the Hexhlet's Eleutriator Plate. Picture (f): Fibres and Particles in the Hexhlet's Back Filter (Test #II).

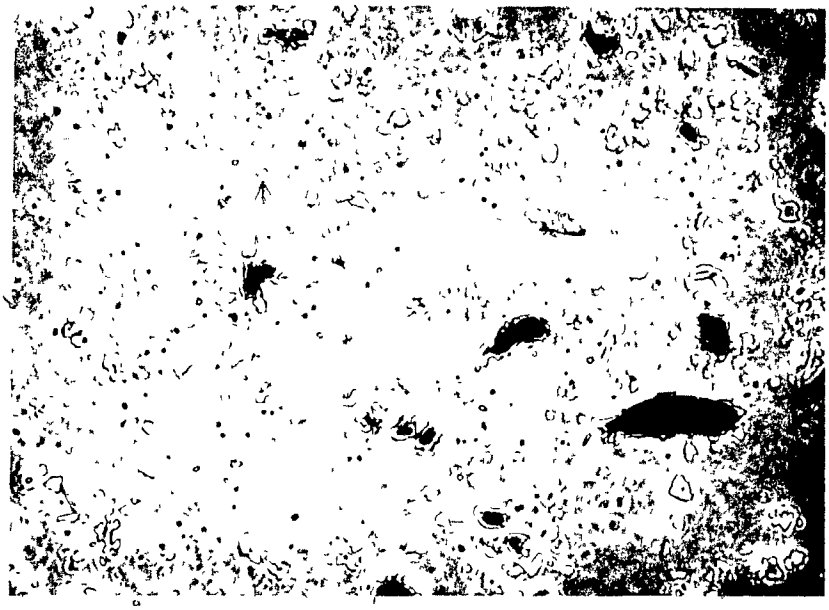

(a)

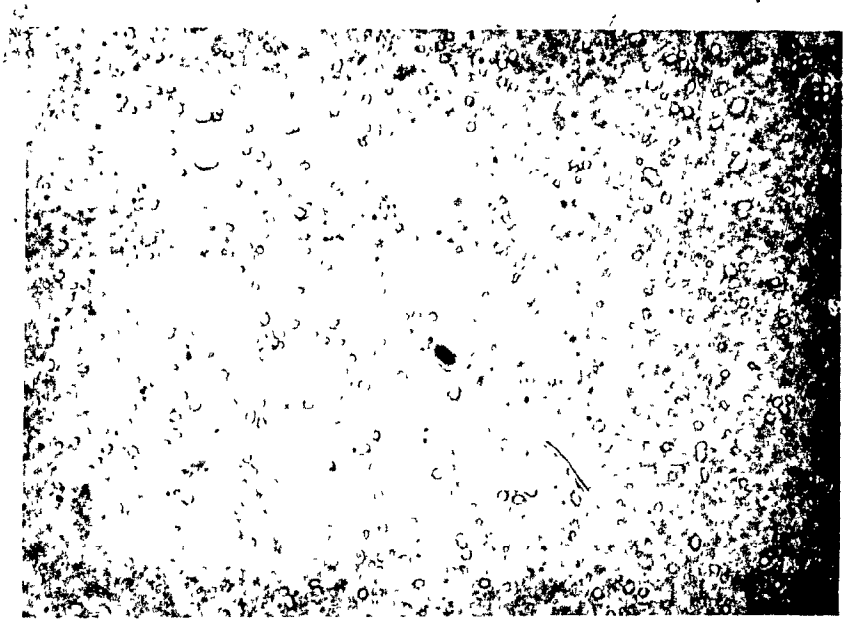

(b)

Scale: ⟷ = 10 μm

Fig. 8.8 (a)(b) - Picture (a): Total Airborne Silica Dust. Picture (b): Silica Dust After Being Eleutriated by the Hexhlet Eleutriator (Back Filter).

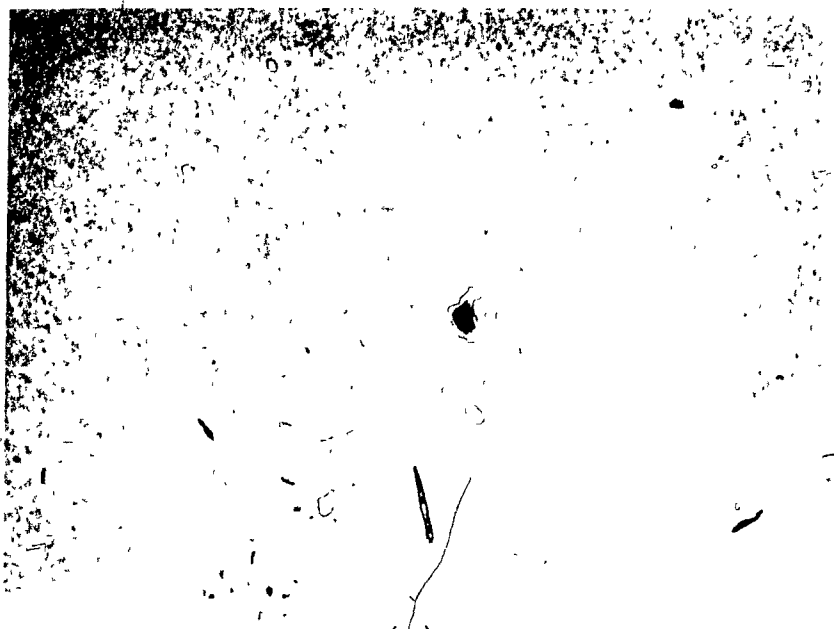

(c)

Fig. 8.8 (c) - Silica Dust as Settled in the Middle Part of the Hexhlet Eleutriator Plate.

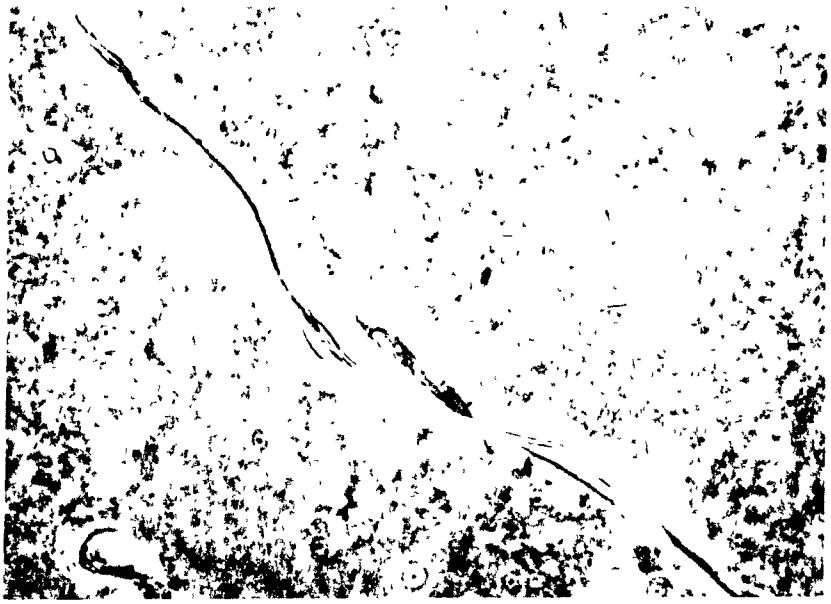

Scale: ⟷ = 10 µm

Fig. 8.9 - Respirable and Nonrespirable Fibres and Particles in the Air Monitor Filter (Test #III).

Table 8.4 - Size Selection Curve of Hexhlet Horizontal Eleutriator for Respirable Chrysotile Asbestos Dust in Terms of Equivalent Unit Density Spheres:

| Diameter in µm | % Captured by The Eleutriator Plates | % Retained by/or Penetrated to Back Filter | % Theoretical Penetration | Deviation From Theoretical | % Error |
|---|---|---|---|---|---|
| 0.0 - 1 | 10 | 90 | 100 | -10 | -2.13 |
| 1 - 2 | 1 | 99 | 97 | + 2 | +0.43 |
| 2 - 3 | 18 | 82 | 86 | - 4 | -0.85 |
| 3 - 4 | 5 | 95 | 74 | +21 | +4.47 |
| 4 - 5 | 20 | 80 | 58 | +22 | +4.68 |
| 5 - 6 | 49 | 51 | 39 | +12 | +2.55 |
| 6 - 7 | 89 | 11 | 16 | - 5 | -1.06 |
| 7 - 8 | 95 | 5 | | + 5 | +1.06 |
| 8 - 9 | 97 | 3 | | + 3 | +0.64 |
| | | 516 | 470 | +46 | +9.79 |

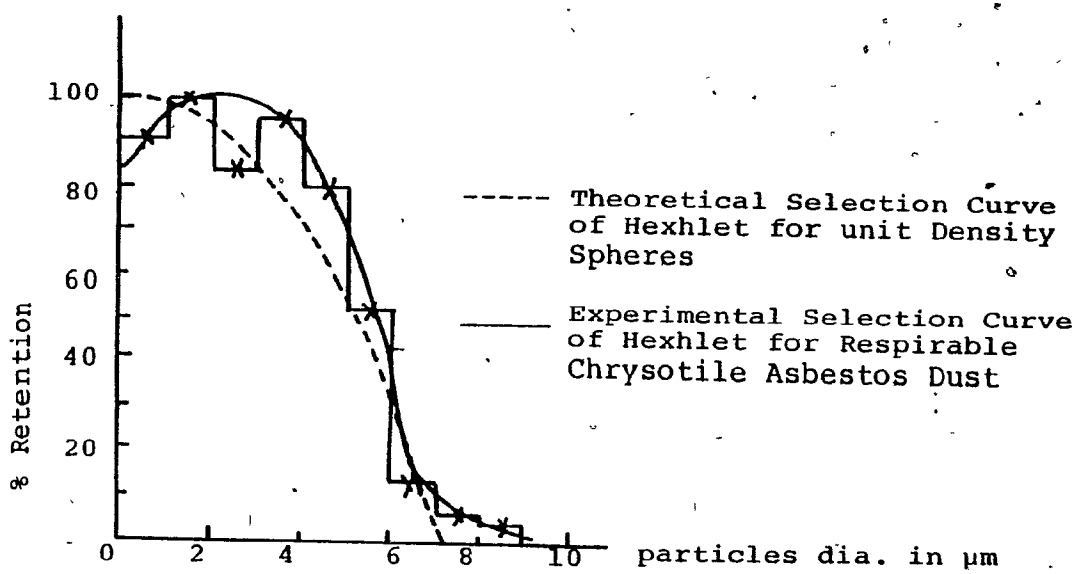


Fig.8.10 - Selection Curve of Hexhlet for respirable chrysotile Asbestos Dust*Compared with Theoretical Unit Density Spheres
(*Unit Density Spheres = Fibre Diameter x 2.5)

2000 Oersteds of inducing magnetic field for 10 seconds. The inducing magnetic field was produced by two opposing 10 centimetre diameter dipole electromagnets. The electromagnets were powered by a 12 volt car battery and were drawing 2.5 Amperes of DC current. The diameter of the centre poles were 5 centimetre wide (see figure 8.11). The gap between the two dipoles was arranged in such a manner that it would allow a 1.7 cm thick petry dish, which contained the Millipore membrane filters with dust samples, to be tightly placed between the two centre poles.

Before deciding on the use of Millipore membrane filters for sampling, the magnetic characteristics of blank membrane filters were tested. Each blank membrane filter was subjected to 2000 Oersteds of inducing magnetic field and their remanent magnetic fields were then measured. The magnetic fields of the blank membrane filters were not detectable.

The 2000 Oersted magnetic field intensity, produced between the gap of the two dipoles was measured by a Type D-855 Gaussmeter with an accuracy of ± 0.5 to 2%, and found to be uniformly distributed without any fluctuation. The Model D-855 Gaussmeter is a fully transistorized instrument, designed to measure either AC (RMS) or DC magnetic fields having flux densities from 10 gauss to 30,000 gauss.

This span is covered in seven ranges with full scale readings of 30, 100, 300, 1000, 3000, 10,000 and 30,000 gauss. The operating principle of the equipment is based on the Hall Effect and was described in chapter VII.

8.2.4.2 Magnetic Shielding:

The induced, or remanent, magnetic field of the samples was measured in a magnetic shielding box, by a sensitive fluxgate Model MF-5000 magnetometer. Although the measured magnetic fields were much smaller than the earth's magnetic field of 0.5 gauss, the magnetic shielding may not be necessary if the gradient probe system of the Fluxgate magnetometer is used to measure the field produced by the sample gradiometrically*. However, it was felt that shielding against the other changing or varying background AC and DC magnetic fields or noises was necessary. These background magnetic noises may be produced by electric motors, elevator systems in the building; moving cars in the adjacent street or parking lot; electric wiring and neon lights of the building, static electricity and metal objects carried by the person who is doing the low-field measurements.

According to Cohen[17], the magnetic shielding can be developed by utilizing three phenomena of shielding without using expensive superconductive materials. These phenomena are:

(a) Ferromagnetism: ferromagnetic shells can be developed

* This statement is correct since all the sample orientations were kept the same for all measurements.

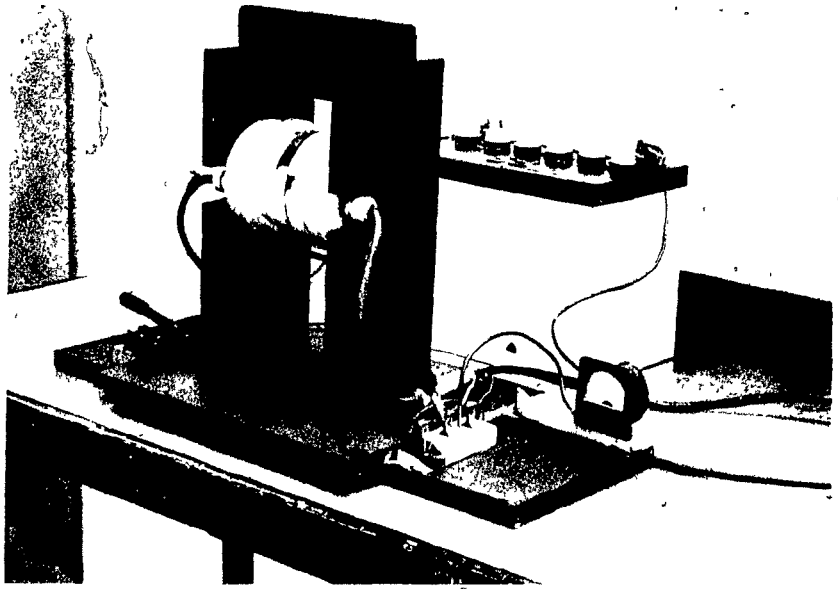

(a)

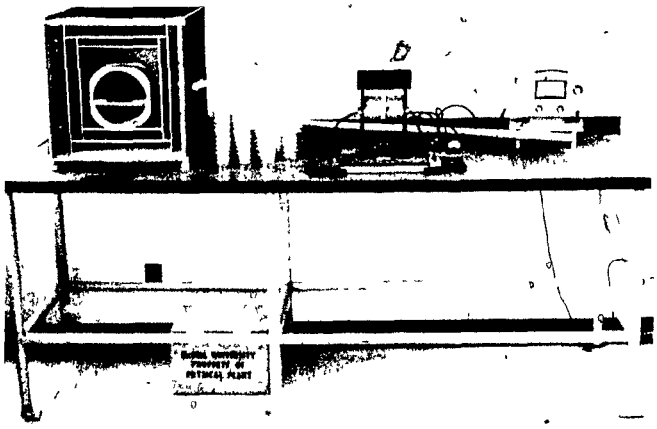

(b)

Fig. 8.11 - Picture (a): Electromagnets Powered by 12 Volts Car Battery and a Millipore Filter in a Petry Dish in the Gap of the Electromagnets Being Magnetized.
Picture (b): A General View of the Magnetic Shielding Box at Far Left, Some Samples and Electromagnets in the Middle and the Fluxgate Magnetometer at Far Right.

from permalloys. These types of shells are good for shielding the frequency range from DC to 1 mega Hertz.

(b) Induced eddy currents: this type of shell is made of a good conductor, such as aluminum, and the created shielding acts only on AC magnetic fields.

(c) Active Shielding: This is created by the production of magnetic fields from artificial currents. In this case the magnetic field produced opposes or counterbalances the outside field[17].

The shielding factor "S" for phenomena (a) can be calculated as follows:[17] One spherical shell:

$$S = \frac{1.3\ \mu t}{d}$$

where: $\mu$ = permeability

$t$ = thickness

$d$ = diameter

Two spherical shells: $S = \frac{1.3\ \mu t}{dav}^{2} \left(1 - \frac{di^3}{do^3}\right)$

where: dav = average diameter

di = inner diameter

do = outer diameter

Note: For cubical shells replace 1.3 by 0.7

At McGill University, a cube shaped magnetic shielding box was designed by the author of this thesis. The basic

design criteria was based on the MIT shielding room of the Francis Bitter National Magnet Laboratory of Massachusetts Institute of Technology[17], and is made of three various layers of shielding shells, as shown in figure 8.12. The shielding box was designed in such a manner that the useful volume of the inner-most shell is 1 cubic foot or 0.027 cubic metre. The first layer is made of 0.16 centimetre thick moly-permalloy mounted on a sheet of 1.88 centimetre thick plywood. The second layer is composed of a sheet of 0.63 centimetre aluminum on which a plate of 0.16 centimetre moly-permalloy is mounted. The third and final layer of moly-permalloy of 0.16 centimetre thick is mounted on the inside portion of a 0.63 centimetre thick plate of aluminum, which composed the inner walls of the third cubical shell. The outer shell was wound with 99 turns of 0.11 centimetre diameter copper wire.

The moly-permalloy is made of 70 percent nickel, 4 percent molybdenum and 16 percent iron. Moly-permalloy, even at a zero induction field and room temperature, has a permeability of 35,000[18]. The moly-permalloy sheets were assembled by screwing them together with aluminum bolts and nuts. In order to have a uniform strain distribution and to maintain the high permeability of the moly-permalloy sheets, the required sizes of sheets were cut, and holes for bolting were drilled at the manufacturers plant according to the design specifications of the shielding

box. Subsequently, in order to normalize the created uneven stress and strain distributions, due to cutting and drilling, and to maintain the high permeability at 35,000, the moly-permalloy sheets were subjected to heat treatment at the plant. Furthermore, all of the joining side edges and corners were wrapped together with moly-permalloy foil and tightly bolted.

Cohen[17] stated that when the shape of the shielding shells is not spherical, the corners of other shapes reach out and bring in extra flux, and some of this extra flux leaks into the shielded room.

The lower magnetic noise limit in the shielded area is due to the noise generated from the inner walls[17][18]. These noises can be categorized in three groups. The first type of inner wall noise is due to mechanical seismic vibrations of the walls and to movements due to expansion and contraction of the inner walls under the changing temperature. The second type of inner wall noise is named Johnson noise. In the inner layers, the Johnson voltage will create a noise current and this in return will provide a magnetic noise[17][18]. The changing temperature would cause rotation of the magnetic domains and produce changing magnetic noises inside the shielded area[17] [18]. In our case;

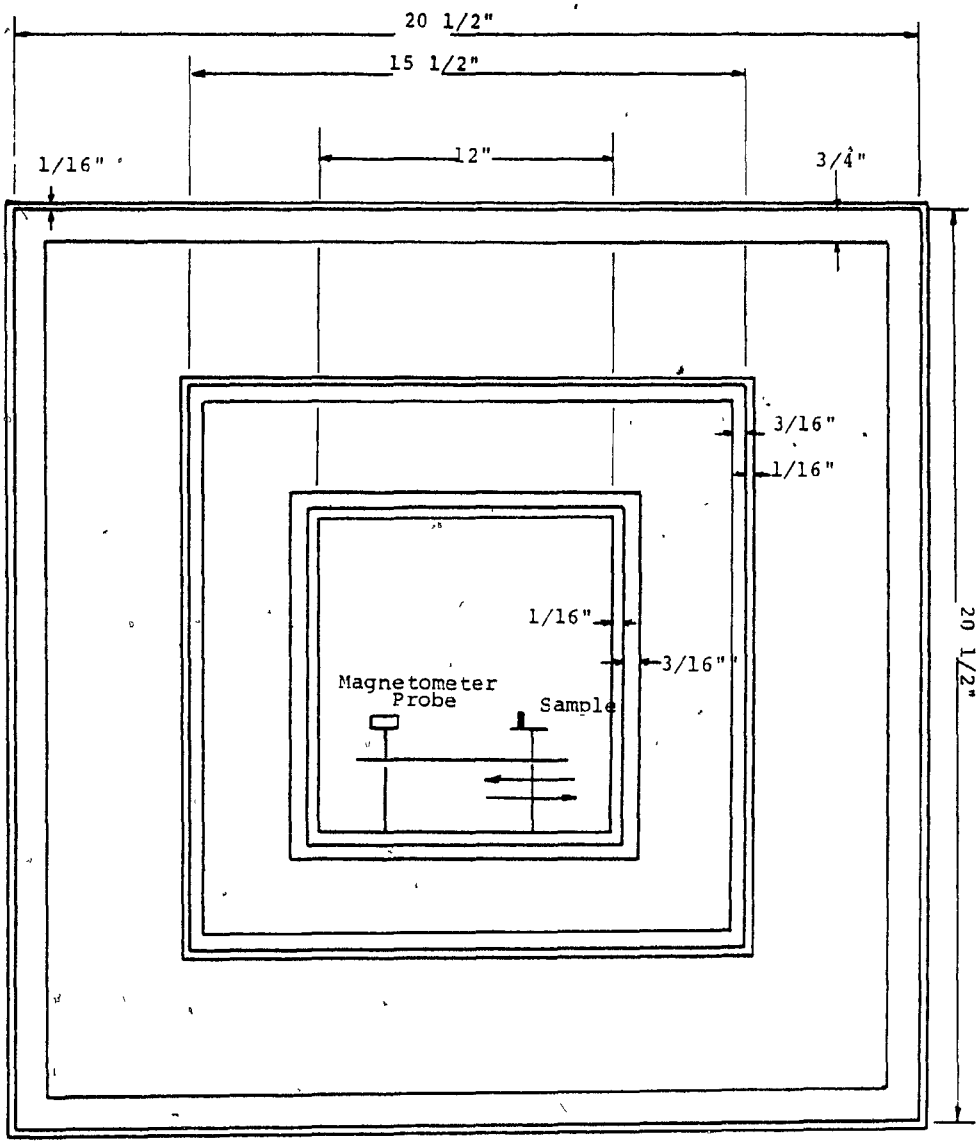


Fig. 8.12 - Section through Magnetic Shielding Box

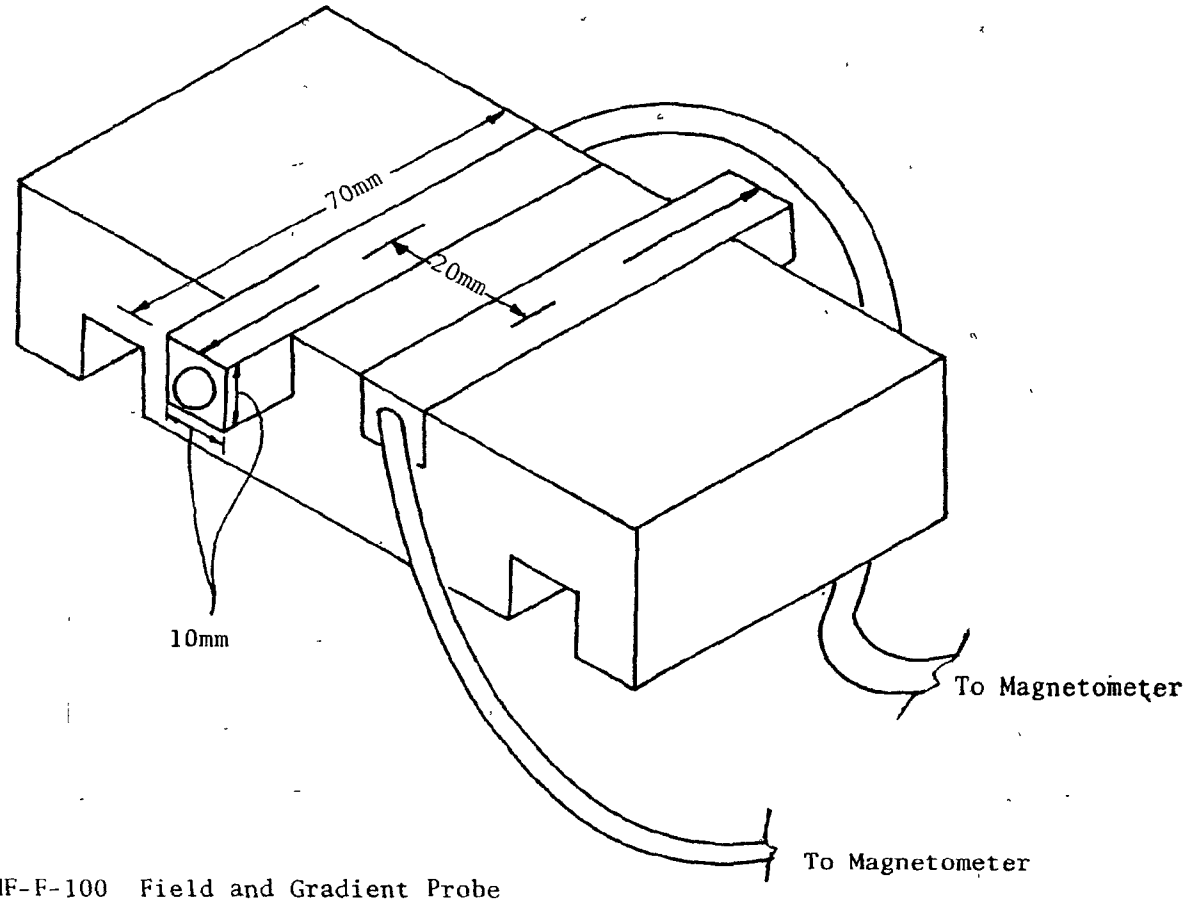


Fig. 8.12A - MF-F-100 Field and Gradient Probe in Gradient Mode

although the shielded volume was very small, the inner wall noise was very low (1 μ gauss in a band width of 0-10 Hz) and its effect on magnetic measurements could be eliminated by the zero adjustment of the fluxgate magnetometer.

The active shielding, created by the 99 turns coil, was in the range of 1200 gauss when 10 amperes of DC current being passed through the coil. According to Bozorth[18], in such an induction field the permeability of the moly-permalloy reaches 70,000 and, at such high permeability, the shielding factor is calculated to be 33,000. However, because of the remoteness of the laboratory location, the background noises were in the range of $10 \times 10^{-6}$ gauss and, inside the shielding box, without the active shielding, their detection was impossible. Therefore, during the remanent magnetic field measurements, active shielding was not necessary and was not used.

8.2.4.3 The Fluxgate Magnetometer, Model MF-5000:

The Fluxgate Model MF-500 magnetometer is a fully transistorized, precision instrument for the measurement of magnetic fields of low intensity, in the range from 1000 milligauss to 1 milligauss full scale. The full scale output voltage of the instrument is 1 volt. The 1 milligauss or $1 \times 10^{-3}$ gauss full scale is further divided into 100 divisions and, when the probes are side by side, the sensitivity of the instrument is $1 \times 10^{-5}$ gauss. However, when the

probes are back to back, facing the opposite directions, or when they are in gradient mode, the sensitivity is $2 \times 10^{-5}$ gauss and the output voltage is one hundreth of a volt, or 10 millivolts. After consultation with Dr. Cohen of MIT, it was decided that by installing a "low-pass-filter" the instrument's residual noise level of 60 cycles could be significantly reduced and by using a chart recorder, which could respond to 0.2 millivolt DC signal, the sensitivity of the instrument could be increased to:

$$\frac{0.2 \text{ mV}}{10 \text{ mV}} \times 2 \times 10^{-5} \text{ gauss} \div 0.68 = 6 \times 10^{-7} \text{ gauss}$$

The value of 0.68 is a correction factor and its determination is shown in the next page and denoted as $C_F$.

In order to calculate the necessary magnitude of noise filtering, the small signal of the 1 milligauss scale of the fluxgate magnetometer was subjected to an AC test and the frequency response for -3db was measured as fluctuating between 1 and 1.5 Kilo Hertz. After the installation of the "low-pass-filter," (See Fig. 7.11) the filtered -3db cut off frecuency of the fluxgate magnetometer can be calculated as follows (See Fig. 8.14):

$$f_{-3db} = \frac{1}{2\P \dfrac{R_1 R_2}{R_1 + R_2} C}$$

where: $R_1$ = 0.47 is the resistance of the low-pass filter in megaohms

$R_2$ = Input resistance of the chart recorder in megaohms

$C$ = 1 μF

The chart recorder which was used, is a one pen type, Omni Scribe recorder and has a one megaohm input resistance. Therefore, the filtered cut off frequency is:

$$f_{3db} = \frac{.47 + 1}{2\P \times .47 \times 1} = 0.50 \text{ Hertz and}$$

the measured residual noise level of 60 cycle with the filter on, is 200 microvolts. The correction factor of the magnetic field read-out can be calculated as follows:

$$C_F = \frac{R_2}{R_1 + R_2} = \frac{1}{1.47} = 0.68$$

This correction factor value was also experimentally tested. While the low-pass-filter was off, the calibration button of the fluxgate magnetometer was depressed and both the magnetometer's meter needle and the chart recorder's pen were deflected the total 100 divisions of the full scale range. After the low-pass-filter was turned on, the procedure repeated. This time, while the magnetometer's meter needle has deflected fully, the chart recorder's pen has deflected only 68 divisions of the 100 divisions of full scale. In this manner both instruments were calibrated by utilizing the internal magnetic source of the fluxgate magnetometer. In order to check the accuracy of the internal calibration, the following external calibration proce-

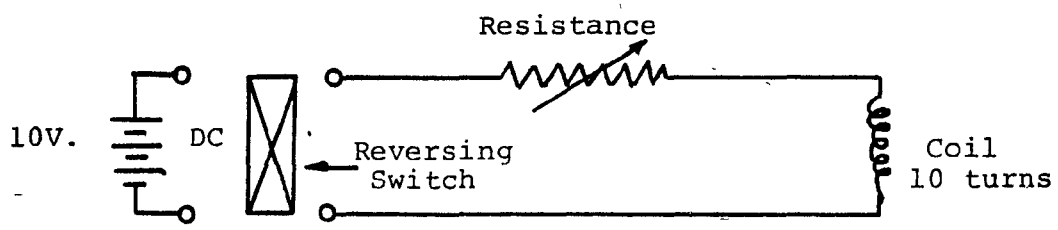


Fig. 8.13 - Tests to Measure the Capacity & the Accuracy of Fluxgate Magnetometer:

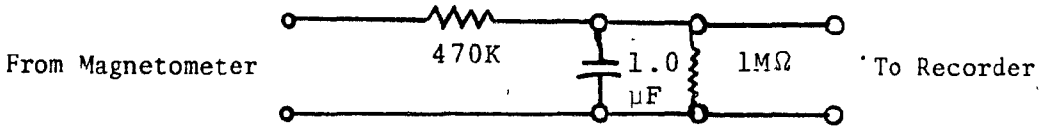


Fig. 8.14 - Low Pass Filter for - 3db cut off

dure was used:

The probes of the Fluxgate magnetometer were placed into a calibrated solenoid side by side and, by orienting the probe and solenoid, the meter of the magnetometer was zeroed. By applying a precise current to the coil, the generated magnetic field can be calculated with the following formula; and the meter needle of the fluxgate magnetometer is adjusted with a screw driver, until the proper field indication on the meter is reached.

$$H = \frac{2\P NI}{10R}$$

where: H = Magnetic field in gauss

N = Number of turns of coil = 10 turns

I = Current in Ampers: varied for different experiments

R = Radius of the Solenoid in centimetres = 10.25 centimetre

The same experiment was conducted for both DC adding, and DC opposing conditions by using a reversing switch (see fig. 8.13). Both types of experiment gave accurate results for currents ranging from 0.1 milliampers up to 100 milliampers. Therefore, it was concluded that the internal calibration device of the instrument was operating accurately and that the fluxgate magnetometer was calibrated properly.

The Omni Scribe chart recorder has five spans of 1, 10, 100 milli volts, and 1 and 10 volt integrator and 12 chart

speeds. For the majority of the gradiometric measurements, while the fluxgate gradiometer was set at the full span of $4 \times 10^{-5}$ gauss, the chart recorder was set at a 10 milli volt span and half an inch per minute chart speed (or 1.25 cm/min.). Therefore, 1 division of the chart span would measure 0.1 milli volt or $4 \times 10^{-7}$ gauss. However, since the low-pass-filter was on, the measured value of $4 \times 10^{-7}$ gauss was corrected with the factor of 0.68. For this type of setting, therefore, the smallest measurable magnetic field is $6 \times 10^{-7}$ gauss. The drift of the chart recorder, for the first 30 minutes warm up time is 1 percent; and thereafter, is 0.1 percent of full scale. In order to eliminate or minimize the errors of drifting, after every magnetic measurement of a sample, the chart recorder was checked. The magnitude of the drifting error is a function of the required time to complete a set of measurements for a sample, and the magnitude of the measured magnetic field. No experimental measurements were carried out during electrical storms.

8.2.3.3 Remanent Magnetic Field Measurements*:

In order to prevent magnetic contamination, all Millipore membrane filter samples were handled with a pair of non magnetic plastic tweezers and after handling each

---

* All of the fluxgate meter readings are the vertical Z component of the total remanent magnetic field of the samples which represent magnetic dipoles.

sample, the tweezers were wiped off with a Kleenex tissue. The remanent magnetic field of each membrane filter sample was measured four times by slowly approaching the probe along the axis of the probe and stopping exactly 1 mm away from the probe with the aid of a vernier and then retracting the sample in a similar manner. Subsequently, these four magnetic readings were averaged. However, it was observed that the distribution of dust on these 41 millimetre membrane filters was not uniform and, therefore, for the purpose of checking the accuracy of these readings, another method of magnetic measurement was applied. With this second method, the cross section of the surface area of each membrane filter sample was scanned across its diameter, 1 millimetre away from the probe. After rotating the sample by 90 degrees, the traverse was repeated. The averages of these magnetic readings were compared with the averages of the first method. In the majority of the cases, the average results of both methods were practically the same. However, when the average results of these two methods did not agree within the limits of $\pm$ 10 percent, measurements for both methods were repeated.

The first few samples were turned over and it was observed that the magnetic signals in both directions were the same. Therefore, it was concluded that due to effective shielding the induced magnetization due to the earth's field could not be detected by the magnetometer.

In chapter VII it was explained that the scatter of the

remanent magnetic field results, for the same mass of magnetite, is due to variation of the particle size of magnetite from one sample to another, the magnetic orientation of these magnetite particles with respect to each other, and the crystal structure orientation of the magnetite particles with respect to the magnetizing field[18]. Therefore, regardless of how uniform the distribution of the magnetite content of the airborne chrysotile fibres is, the remanent magnetic field readings will be scattered for the same mass of different chrysotile samples.

After the completion of all measurements, the remanent magnetic field versus mass of chrysotile was plotted. For the plotted data of each type of chrysotile asbestos, and for pure magnetite, calibration curves were fitted as straight lines.

The reproducibility of the calibration curves was checked. For this purpose all of the samples were demagnetized and then magnetized again and their magnetic fields were measured for a second time. The new data matched with the old data within the limits of $\pm$ 5 percent. Furthermore, from the same type of chrysotile asbestos, new dust clouds were generated and Hexhlet samples were taken. The remanent magnetic fields of these second set of samples corresponded very well with the first-set data and were within the 90 percent

confidence limits of the calibration curves. Similarly the remanent magnetic field measurements were repeated while the samples were 1 centimetre away from the probe. As expected, the magnetic field readings were reduced by the ratio of the cube of the distance.

8.3 Field Studies:

Once the relationship between the remanent magnetic field readings and the airborne respirable size chrysotile fibre concentration was established, calibration curves for the determination of respirable mass and optical microscope fibre counts were developed. In order to measure the usefulness and applicability of this new method, in determination of the airborne respirable chrysotile fibre content of the atmosphere of Quebec asbestos mining industry, mill # VII was visited. Total and respirable size airborne dust samples were collected, side by side, by the membrane filter method and Hexhlet eleutriator respectively. Depending on the grade variation and grade quality of the mined ore, it is expected that the quantity of airborne chrysotile fibres, and therefore, the associated magnetite content and the magnetic field of the total airborne dust, would vary. Similarly, as the chrysotile ore is milled and further processed, the magnetite content of the product would be reduced and, therefore, the measured remanent magnetic fields would also be reduced. In considering the remanent magnetic field of the chrysotile asbestos

ore, it should be noted that other impurities, such as rock and other minerals, dilute the mass of the airborne chrysotile dust. Therefore, the measured remanent magnetic field of chrysotile ore should be lower per unit mass of total airborne dust than that of a unit mass of commercial chrysotile. If a proportionality between remanent magnetic field and chrysotile fibre mass in various mill products is demonstrated, the chrysotile fibre content of the total airborne dust can be determined insitu by measuring the remanent magnetic field of the collected total airborne respirable dust and using the appropriate calibration curve.

In order to test for such proportionality, and to measure the sensitivity of the magnetic method with respect to the variations in the magnetite content of airborne dust at different stages of the milling process of chrysotile asbestos, dust samples were taken at the dry rock storage plant; milling and screening area; and above the bagging machines. Prior to setting up the membrane filter and Hexhlet dust sampling instrumentation at the mill, the log book of the weekly dust surveys of mill #VII were studied and, according to the advice of the mill engineer, the average dust sampling time was determined to be 90 minutes. In order to eliminate the possibility of not having enough dust, or of having too much, with crowded filters to count, the sampling time of different MSA pumps was varied from 75 minutes to 120 minutes. The Hexhlet horizontal

eleutriator sampling time was varied from 15 to 45 minutes and various weights of dust samples were collected. Fifteen MSA pumps were available for Millipore membrane filter sampling and, therefore, at least 30 membrane filter samples could be collected during a work shift. However, the number of the Hexhlet eleutriators were only two; and therefore, for the same duration of time only 6 to 10 samples could be collected.

During the sampling period, the sampling rates of all MSA pumps were checked and adjusted to the original calibrated rate of 1.8 litres per minute whenever necessary. Hexhlet horizontal eleutriators were always set up hotizontally and after each sample was taken, the front grills were wiped off with a clean cloth to eliminate any possible fibre accumulation. The collected samples were kept in petry dishes and, after returning to the research laboratory of McGill University, they were transferred to desiccators and kept for 48 hours.

As explained earlier, all samples were demagnetized, weighed, magnetized again and the remanent magnetic fields measured. Subsequently, the chrysotile fibre and magnetite contents of the samples were determined by using the optical phase contrast microscope, and the transmission and scanning electron microscopes respectively, as explained earlier (see Table 8.5). In order to double check, and to show that the observed samples

were mainly chrysotile, and/or serpentine, the magnesium and iron content of the randomly selected Millipore membrane filter samples were determined by using atomic absorption analysis, as explained chapter VI (see table 8.6). In order to investigate, and determine, whether or not the magnetite content of the airborne chrysotile and bulk chrysotile samples is uniform, atomic absorption analysis for iron was, similarly, conducted and the iron content of airborne respirable size chrysotile, as well as that of bulk chrysotile, was determined. In table 8.7 and figures 8.15 and 8.16 the iron content and magnetic readings of nonrespirable bulk chrysotile samples, as well as those of airborne respirable chrysotile samples, are shown. Table 8.8 shows the chrysotile and iron content of the provided chrysotile asbestos of Quebec and Rhodesian UICC samples, analyzed by atomic absorption spectroscopy. In order to demonstrate the extent of attachment of the magnetite particles to the chrysotile fibres of airborne respirable samples, the dust specimens were diluted in a solution of dioctyl sodium sulphosuccinate and subjected to ultrasonic vibratory cleaning for two hours. In this experiment an attempt was made to separate the particles of magnetite from the chrysotile fibres. The particles of magnetite, being denser, were expected to be separated from the fibres and settle faster, according to Stoke's law, in the settling tube. At predetermined intervals (20, 40, 60, and 120 seconds) samples were taken at the bottom of the

Table 8.5 - Magnetite Content as Determined by Electron Microscope Observations:

| Name of the Mill | AA Analysis: Iron Content in % | Calculated % Magnetite* | Magnetite % As Determined By EM | Average % Magnetite |
|---|---|---|---|---|
| # VI | 2.6 | 3.56 | 3.81 | 3.28 |
| # VI | 2.1 | 2.88 | 2.75 | |
| #VII | 1.1 | 1.51 | 1.43 | |
| #VII | 0.9 | 1.23 | 1.18 | 1.27 |
| #VII | 1.0 | 1.37 | 1.46 | |

* All of the iron content of the sample is assumed to be magnetite.

settling tube. Optical and electron microscopy studies of these samples, however, have shown that magnetite did not separate from the chrysotile fibres and they continued to co-exist.

After completion of the required analysis of samples, and being encouraged by the relatively positive results, as a next step, Mill #VI was visited. At this mill also the same sampling strategies were followed and microscopic, chemical, and magnetic field tests were carried out (see figures 9.24 to 9.29). In order to test the reproducibility of these results, Mill #VI was revisited six months later and more samples were collected. The results of both surveys were compared. With this investigation it was shown that, although the magnetite content of the milled chrysotile ore may change from time to time, for the same ore body, it is relatively uniform and, if the appropriate calibration curves are used, the mass and the number concentration of chrysotile fibres in the airborne respirable dust can be determined by simply measuring the remanent magnetic field of the sample. Furthermore, by using the remanent magnetic field measurements, the iron content of the samples in question can also be determined. Fig. 8.16 indicates that there is a definite relationship between the remanent magnetic readings and the total iron content of the chrysotile samples of Quebec. Therefore in all discussions in chapter 9, the iron content of all chrysotile dust samples was assumed to be due to magnetite content of the sample and the remanent field arises from the magnetite present. This is a reasonable assumption, because as discussed in chapter 1 of this thesis, and according to other researchers (Harrington, Reimchussel, Speil and Leineweber and Stroink) the non magnetite iron in the lattice of the chrysotile crystals is at most 1.5%.

Table 8.6 - Total Chrysotile and/or Serpentine and Iron Content of Airborne Chrysotile Samples from Mills # VI and VII*

| Designated Name of the Mill | Location at the Mill | Percent Magnesium Content | Determined Percent Chrysotile and/or Serpentine | Respirable Dust Percent Iron Content | Average Percent Iron in Respirable Dust | Average Percent Iron in Total Dust |
|---|---|---|---|---|---|---|
| VI | Dry Rock Storage | 26.48<br>26.81<br>27.22<br>24.07 | 87.5<br>88.6<br>90.0<br>79.6 | 5.67<br>5.60<br>5.44<br>5.50 | 5.4 | 5.7 |
| VI | Milling & Screening | 26.65<br>26.39<br>27.78<br>27.95 | 88.1<br>87.2<br>91.8<br>92.4 | 4.31<br>5.71<br>5.06<br>4.83 | 4.95 | 5.3 |
| VI | Above Bagging Machine | 29.83<br>28.96<br>28.24<br>29.15 | 98.6<br>95.7<br>93.4<br>96.4 | 1.45<br>1.55<br>1.83<br>1.57 | 1.6 | 2.0 |
| VII | Dry Rock Storage | 28.00<br>27.85<br>29.08<br>27.92 | 92.6<br>92.1<br>96.1<br>92.3 | 2.13<br>1.95<br>1.80<br>1.72 | 1.90 | 2.00 |
| VII | Milling & Screening | 28.76<br>29.59<br>28.83<br>29.06 | 95.1<br>97.8<br>95.3<br>96.1 | 1.20<br>1.25<br>1.46<br>1.13 | 1.26 | 1.3 |
| VII | Above Bagging Machine | 29.25<br>29.56<br>29.74<br>28.18 | 96.7<br>97.7<br>98.3<br>93.2 | 0.86<br>0.92<br>0.97<br>1.03 | 0.95 | 1.1 |

*Four samples per location.

Table 8.7 - Iron Content of Quebec Chrysotile Asbestos

| Weight for Sample in mg. | Iron Content of Bulk Nonrespirable Chrysotile | | Iron Content of Respirable Chrysotile | | Magnetic Readings in $10^{-5}$ Gauss | |
|---|---|---|---|---|---|---|
| | %Fe | mg.Fe | %Fe | mg.Fe | Nonrespirable | Respirable |
| 5 | 4.8 | 0.24 | 2.6 | 0.13 | 15 | 10 |
| 5 | 5.0 | 0.25 | 3.2 | 0.16 | 15 | 5 |
| 5 | 4.8 | 0.24 | 3.2 | 0.16 | 15 | 5 |
| 5 | 5.0 | 0.25 | 3.6 | 0.18 | 10 | 10 |
| 5 | 4.0 | 0.20 | 3.2 | 0.16 | 10 | 5 |
| 10 | 5.1 | 0.51 | 3.0 | 0.30 | 25 | 10 |
| 10 | 5.0 | 0.50 | 3.2 | 0.32 | 25 | 15 |
| 10 | 5.1 | 0.51 | 3.0 | 0.30 | 25 | 10 |
| 10 | 4.9 | 0.49 | 3.3 | 0.33 | 20 | 15 |
| 10 | 4.9 | 0.49 | 3.3 | 0.33 | 20 | 15 |
| 15 | 5.2 | 0.78 | 3.1 | 0.47 | 40 | 20 |
| 15 | 5.3 | 0.80 | 2.9 | 0.44 | 40 | 20 |
| 15 | 5.0 | 0.75 | 3.4 | 0.51 | 40 | 20 |
| 15 | 4.8 | 0.72 | 3.1 | 0.47 | 40 | 20 |
| 15 | 4.9 | 0.74 | 3.0 | 0.45 | 35 | 20 |
| 20 | 4.9 | 0.98 | 3.3 | 0.66 | 50 | 30 |
| 20 | 4.9 | 0.98 | 3.2 | 0.64 | 50 | 25 |
| 20 | 4.9 | 0.98 | 3.2 | 0.64 | 50 | 30 |
| 20 | 5.1 | 1.02 | 3.3 | 0.66 | 50 | 25 |
| 20 | 5.2 | 1.04 | 3.2 | 0.64 | 50 | 30 |
| 25 | 4.8 | 1.20 | 3.2 | 0.80 | 60 | 40 |
| 25 | 5.0 | 1.25 | 3.3 | 0.83 | 60 | 40 |
| 25 | 4.7 | 1.18 | 3.1 | 0.78 | 60 | 35 |
| 25 | 4.6 | 1.15 | 3.3 | 0.88 | 55 | 40 |
| 25 | 4.9 | 1.23 | 3.3 | 0.83 | 60 | 35 |

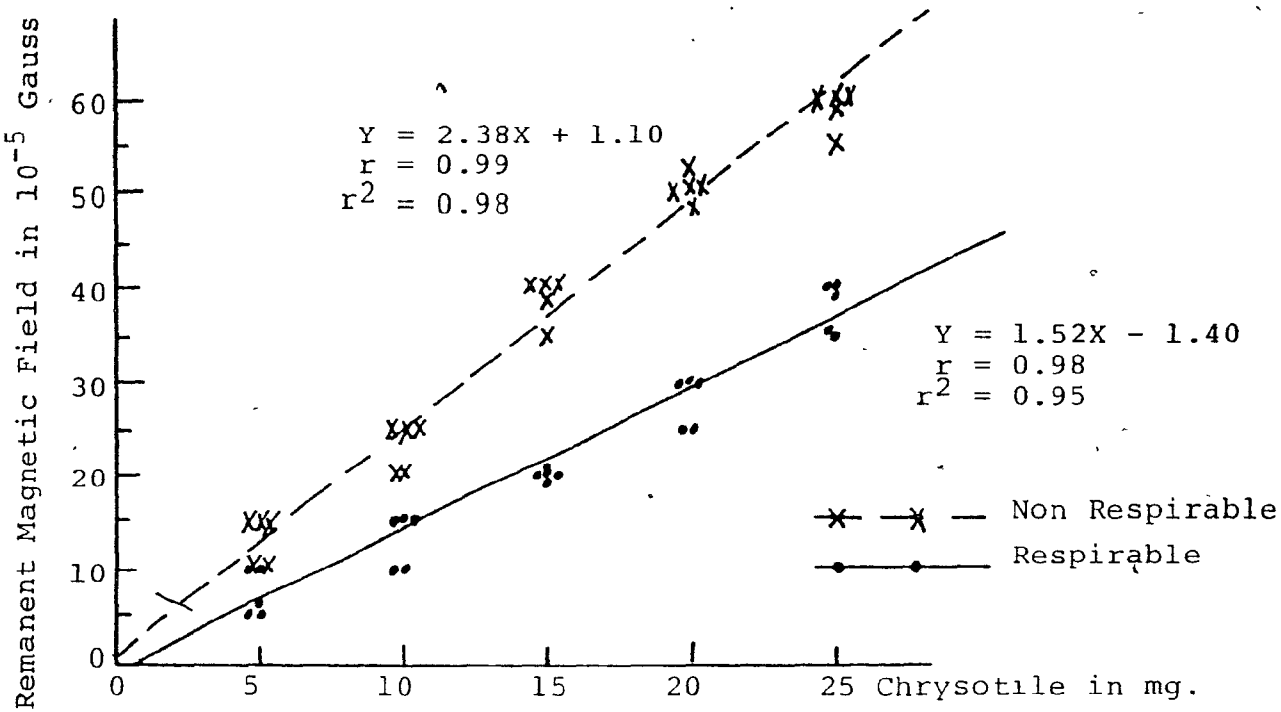


Fig. 8.15- Linear Relationship Between Magnetic Field Readings and Mass of Chrysotile

Note: Each point representing a separate sample.

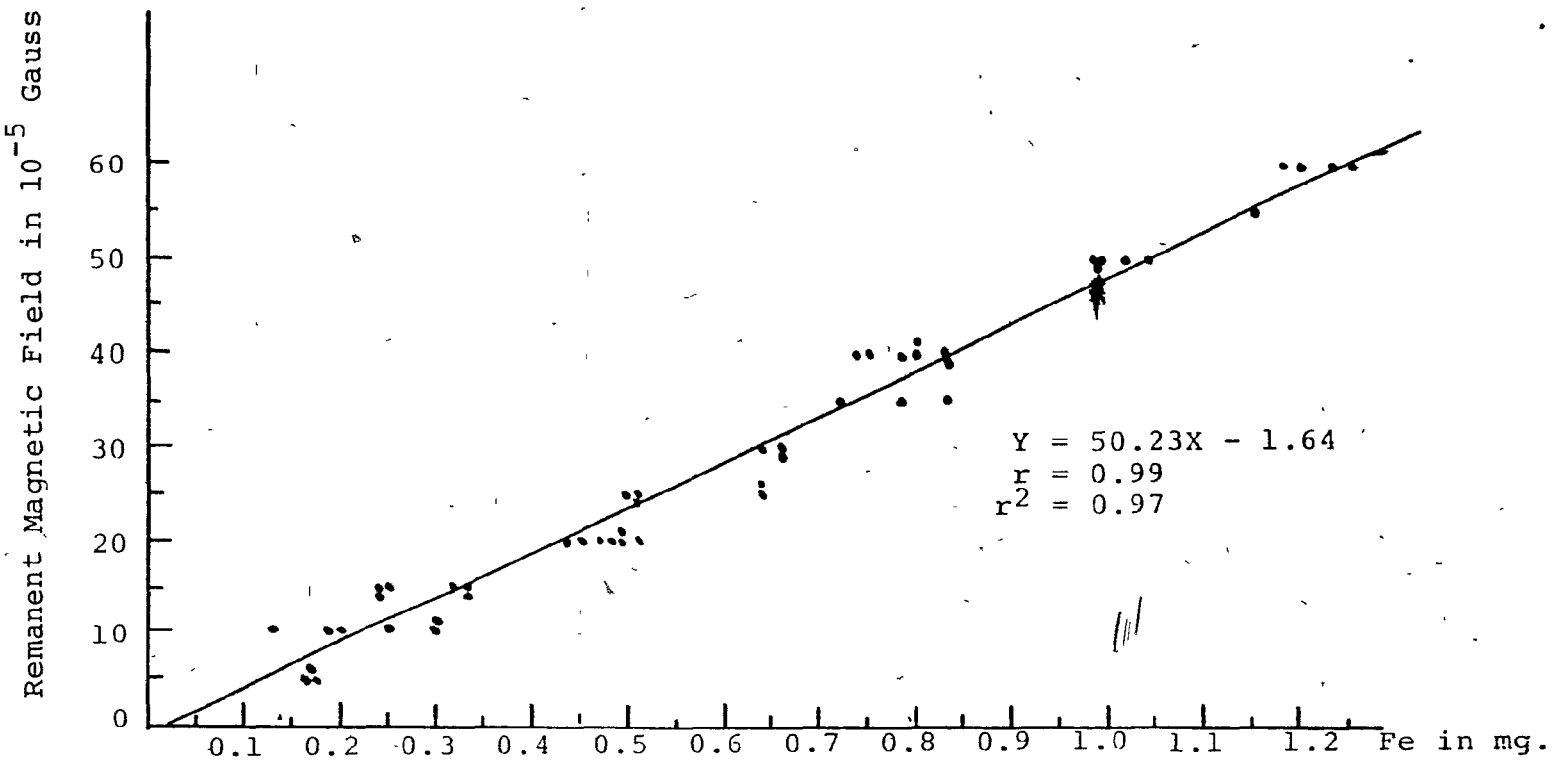


Fig.8.16 - Linear Relationship Between Magnetic Field Readings and Mass of Total Iron Present in Quebec Chrysotile.

Table 8.8 - Chrysotile Content* of Grade # 6 Asbestos of Quebec, Determined by Magnesium Analysis with Atomic Absorption Method, and Iron Content

| Designated Name of the Mill | Percent Magnesium | Determined Percent Chrysotile | Percent Iron | Average Percent Iron | Total Percent |
|---|---|---|---|---|---|
| I | 29.15 | 96.4 | 2.1 | | 98.5 |
| | 29.44 | 97.3 | 1.8 | 1.85 | 99.1 |
| | 29.23 | 96.6 | 1.6 | | 98.2 |
| | 29.30 | 96.9 | 1.9 | | 98.8 |
| II | 29.45 | 97.4 | 1.8 | | 99.2 |
| | 29.45 | 97.4 | 1.7 | 1.75 | 99.1 |
| | 29.62 | 97.9 | 1.5 | | 99.4 |
| | 29.14 | 96.3 | 2.0 | | 98.3 |
| III | 29.24 | 96.8 | 1.4 | | 98.2 |
| | 29.58 | 97.8 | 0.8 | 1.15 | 98.6 |
| | 29.69 | 98.1 | 0.9 | | 99.0 |
| | 29.23 | 96.6 | 1.5 | | 98.1 |
| IV | 29.05 | 96.0 | 1.7 | | 97.7 |
| | 28.63 | 94.6 | 3.5 | 2.70 | 98.1 |
| | 28.78 | 95.1 | 3.4 | | 98.5 |
| | 29.24 | 96.7 | 2.2 | | 98.9 |
| V | 29.08 | 96.1 | 2.6 | | 98.7 |
| | 28.66 | 94.7 | 3.6 | 3.30 | 98.3 |
| | 28.90 | 95.6 | 3.3 | | 98.9 |
| | 28.65 | 94.7 | 3.8 | | 98.5 |
| VI | 29.09 | 96.2 | 1.8 | | 98.0 |
| | 29.20 | 96.5 | 2.5 | | 99.0 |
| | 29.58 | 97.8 | 1.6 | 1.56 | 99.4 |
| | 28.90 | 95.5 | 1.2 | | 96.7 |
| | 29.36 | 97.1 | 1.1 | | 98.2 |
| | 28.89 | 95.1 | 1.3 | | 96.8 |
| | 29.58 | 97.8 | 1.5 | | 99.3 |
| | 29.23 | 96.6 | 1.6 | | 98.2 |
| | 29.42 | 97.3 | 1.8 | | 99.1 |
| | 29.04 | 96.0 | 1.2 | | 97.2 |
| VII | 29.68 | 98.1 | 1.1 | | 99.2 |
| | 29.70 | 98.2 | 1.1 | | 99.3 |
| | 29.65 | 98.0 | 1.1 | | 99.1 |
| | 29.65 | 98.0 | 1.0 | | 99.0 |
| | 29.52 | 97.6 | 1.2 | 1.05 | 98.8 |
| | 29.80 | 98.5 | 0.9 | | 99.4 |
| | 29.65 | 98.0 | 1.1 | | 99.1 |
| | 29.77 | 98.4 | 0.9 | | 99.3 |
| | 29.68 | 98.1 | 1.0 | | 99.1 |
| | 29.68 | 98.1 | 1.1 | | 99.2 |
| VIII | 29.03 | 96.0 | 2.7 | | 98.7 |
| | 29.06 | 96.1 | 3.1 | 3.10 | 99.2 |
| | 28.90 | 95.5 | 3.3 | | 98.8 |
| | 28.98 | 95.8 | 3.3 | | 99.1 |
| IX | 29.28 | 96.8 | 1.7 | | 98.5 |
| | 29.30 | 96.9 | 1.8 | 1.55 | 98.7 |
| | 29.51 | 97.6 | 1.4 | | 99.0 |
| | 29.52 | 97.6 | 1.3 | | 98.9 |
| Rhodesian | 29.45 | 97.4 | 1.4 | | 98.8 |
| UICC | 29.40 | 97.2 | 1.2 | 1.63** | 98.4 |
| Chrysotile | 29.25 | 96.7 | 2.0 | | 98.7 |
| | 29.14 | 96.3 | 1.9 | | 98.2 |

* It is assumed that all of the magnesium is part of the chrysotile chemistry.

** Iron Content of the UICC samples was indicated to be 1.7%.

## LIST OF REFERENCES FOR CHAPTER VIII


1. Timbrell, V. "Alignment of Respirable Asbestos Fibres By Magnetic Fields," Annals of Occupational Hygiene, Pergamon Press, 1975, Vol. 18, pp. 299-311.

2. Technical Report "Automatic Detection and Counting of Asbestos Fibres," American Industrial Hygiene Association Journal, July 1979, pp. 50-23.

3. Assad, J.R. "Comite d'etude Sur La Salubrite Dans L' Industrie de L'amiante Beudry Commission, Oct. 1976, Document # 1.

4. Heidermans, G. "Determination of Asbestos Fine Dust According to Mass Concentration," In: Short Course in Mineralogical Techniques of Asbestos Determination, Editor: R.L. Ledoux, Quebec, May 1979, pp. 165-196.

5. Cohen, D. "Magnetic Fields of Human Body" Physics Today, August 1975, pp. 34-43.

6. Gibbs, G. W. "Techniques of Asbestos Determination-Research Perspective," In: Short Course in Mineralogical Techniques of Asbestos Determination, Editor: R. L. Ledoux, Quebec, May 1979, p. 264.

7. Cohen, D. "Ferromagnetic Contamination In The Lungs And Other Organs Of The Human Body," Science, May 1972, Vol. 180, p. 745.

8. Timbrell, V., Hyett, A.W., and Skidmore, J.W. "A Simple Dispenser For Generating Dust Clouds From Standard Reference Samples of Asbestos," Annals of Occupational Hygiene, Pergamon Press, 1968, Vol. 11, pp. 273-281.

9. Becket, S. T. "The Generation and Evaluation of UICC Asbestos Clouds in Animal Exposure Chambers," Annals of Occupational Hygiene, Pergamon Press, 1975, Vol. 18, pp. 187-199.

10. Spurney, K. R., Boose, C., Horchrainer, D., Monig, F. J. "A Note On the Dispersing of Fibrous Powders," Annals of Occupational Hygiene, Pergamon Press, 1976, Vol. 19, pp. 85-87

11. Neter, J., Wasserman, W., and Whitmore, G.A. "Statistical Tables of Fisher and Yates," In: Fundamental Statistics for Business and Economics, Allyn and Bacon, Inc., Boston, London, Sydney, 1975, pp. 200-745.

12. Cohen, D., Crowthers, T. S., Gibbs, G. W., and Becklake, M. R. "Magnetic Lung Measurements in RElation to Occupational Exposure in Asbestos Miners and Millers of Quebec," Environmental Research, Vol. 26, pp. 535-550, 1981.

13. National Health and Medical Research Council, Australian Department of Health "Membrane Filter Method For Estimating Airborne Asbestos Dust," F.D. Atkinson Government Printer, Camberra, Oct. 1976, pp. 1-52.

14. Trudeau, M. "Method For the Evaluation of Asbestos Dust Concentration at the Workplace," In: Short Course in Mineralogical Techniques of Asbestos Determination, Ed.: R.L. Ledoux, Mineralogical Association of Canada, Quebec, May 1979, pp. 213-252.

15. Drew, R.T., Lippmann, M. "Calibration of Air Sampling Instruments," Section I. pp. I-5-I-6.

16. Lippmann, M. "Respirable Dust Sampling," American Industrial Hygiene Association Journal, 1979, Vol. 31, pp. 138-159.

17. Cohen, D. "Large Colume Conventional Magnetic Schields," Revue de Physique Appliquee, Feb. 1970, Vol. 5, pp. 53-58.

18. Bozorth, R.M. "Ferromagnetism," D. Van Nostrand Company Inc.," Princeton, New Jersey, Toronto, London, Melbourne, 1968, pp. 138-141.

19. Cohen, D. "Enhancement of Ferromagnetic Shielding Against Low-Frequency Magnetic Fields," Applied Physics Letters, Feb. 1967, Vol. 10, #3, pp. 67-69.

20. Kennedy, J.B. and Neville, A.M.: "Basic Statistical Methods for Engineers and Scientists," 2nd. Edition, IEP a Dun-Donnelly Publisher, New York, 1976, pp. 178-180.

21. Timbrell, V. and Rendall, R.E.E.: "Preparation of the UICC Standard Reference Samples of Asbestos," Powder Technology, Elsevier Sequoia, S.A., Lousanne, 1971/72, Vol. 5, pp. 279-287.

22. Schneider, T.: "The Influence of Counting Rules On The Number and On The Size Distribution of Fibres," Annals of Occupational Hygiene, Pergamon Press, 1979, Vol. 21, pp. 341-350

## CHAPTER IX

## STATISTICAL ANALYSIS AND INTERPRETATION OF RESULTS

9.1 General:

In this section, the term calibration line is applicable only to the correlation results pertaining to the standardized techniques previously described in this work and can not be used as calibration lines for any other technique. The correlations of these lines with the measured data will be statistically analyzed. Their reliability will be determined and the remanent magnetic field survey results of chrysotile dust will be interpreted. In order to systematically carry out these objectives, the findings are grouped as follows:

(a) Calibration Curves for mass determination of the airborne, respirable size pure magnetite.

(b) Calibration curves for mass determination of the airborne, respirable size chrysotile asbestos for various Quebec mills.

(c) Calibration curves for number determination of the Chrysotile fibre content of airborne respirable size dust for various mills of Quebec, and establishment of the relationship between magnetite and chrysotile fibres by electron microscopy.

(d) Correlation of the remanent magnetic fields with the mass and number of airborne fibres in various locations of the visited mills and interpretation of the measured remanent magnetic field results in terms of mass and number of airborne respirable chrysotile fibres.

(e) Correlation of the remanent magnetic field measurements of asbestos workers' lung specimens (obtained from autopsies) with the determined mass and dust counts.

(f) Recommendations for further research.

(g) Conclusion.

9.2 Calibration Curves for Mass Determination of Airborne, Respirable Size Pure Magnetite:

Figures 9.1 to 9.5 show the calibration curves for mass determination of airborne, respirable, pure magnetite, for various sampling instruments. As stated earlier, the measured remanent magnetic field is the vector sum of the fields from all particles existing in the same sample[1]. Therefore, when the two magnetite samples have the same mass but two different particle distribution patterns, the vector sum of the magnetic fields of all particles would give different remanent magnetic field results. As expected, the distribution patterns of pure magnetite on Hexhlet samples of 41 millimetre diameter Millipore filters differ from the distribution patterns on Cyclone samples of 25 millimetre diameter Millipore filters. Therefore, the measured remanent magnetic fields of the magnetite samples of these two samplers are different, although both samples have the same mass. The remanent magnetic field measurements for the cyclone samples were greater than those for the Hexhlet samples, due to the greater

particle population density on 25 millimetre membrane filters than on the 41 millimetre Hexhlet filters. However, for the same sampling method, the particle distribution pattern from one sample to another does not vary very much. The remanent magnetic field results of these samples are repeatable and correlations between the mass and remanent fields are good (see table 9.1).

The coefficient of determination of the calibration line for the Hexhlet samples of pure magnetite is 92.6% and, therefore, the regression line fits the observed data very well (see Fig. 9.1)*. The coefficient of correlation is 96.2 percent. Both the T-test and the F-test indicate that the null hypothesis, of all true partial regression coefficients being equal to zero, is rejected at the significance levels of 0.1 percent and 1 percent respectively. In other words the line is not horizontal, Y is a function of X and there is a correlation between the X and Y values. According to Nair's method[2], the values of extreme deviates were tested for rejection as outliers. In all cases, the outliers were not rejected at the level of 5 percent significance, or, in other words, although there is a 5 percent probability that an outlier does not belong to the population, it is not rejected. When the

---

* All numbers, as they appear behind the equation "Y" in most graphs in chapter 9 should be multiplied by $10^{-7}$.

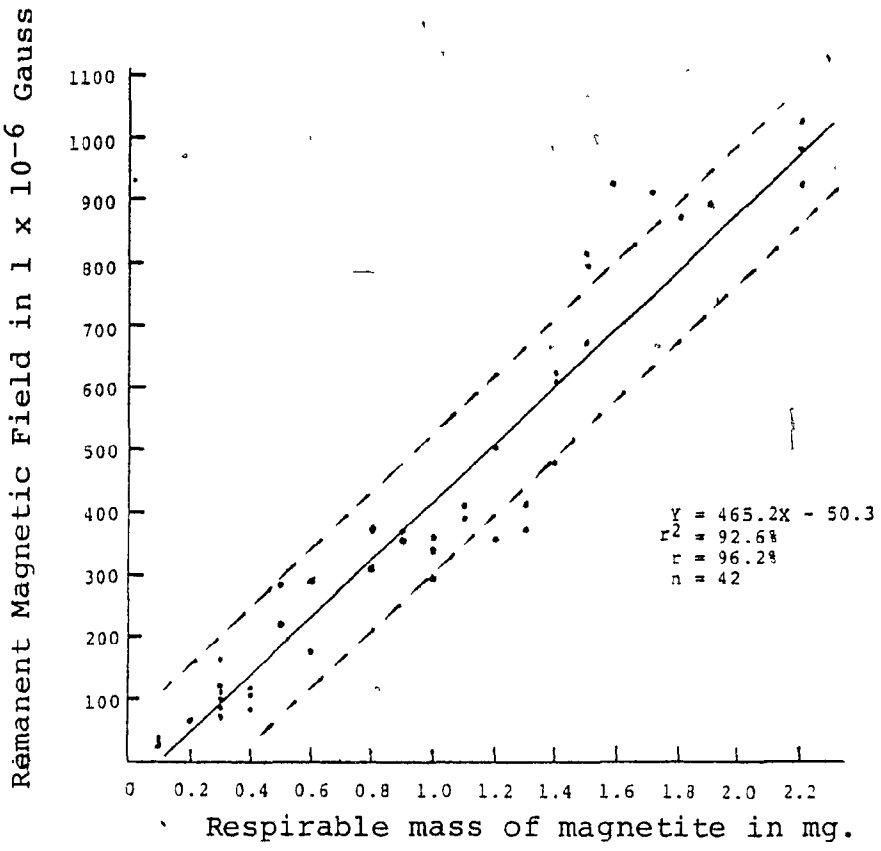


Fig. 9.1 - Correlation of the Remanent Magnetic Field with the Mass of Pure Magnetite Hexhlet Samples. Dotted Line Represents the Confidence Limit of 90%. Magnetic measurements were made while the samples were at the probe (Diameter of Membrane filter was 41 mm)

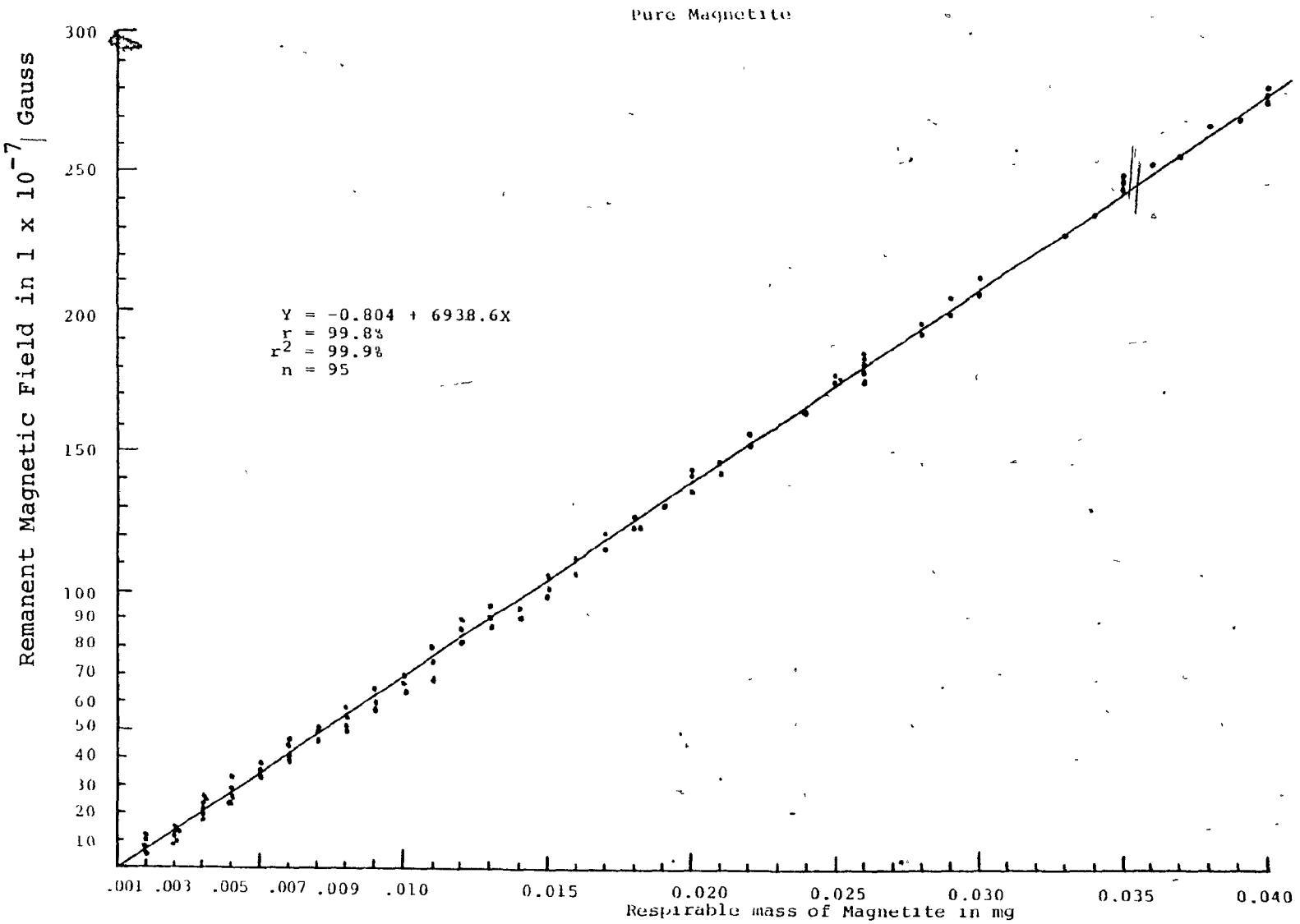


Fig. 9.2 - Calibration Line for Pure Magnetite Mass Determination Airborne Samples were collected using Hexhlet Horizontal Eueltriator. Magnetic measurements were made while the samples were at the probe.

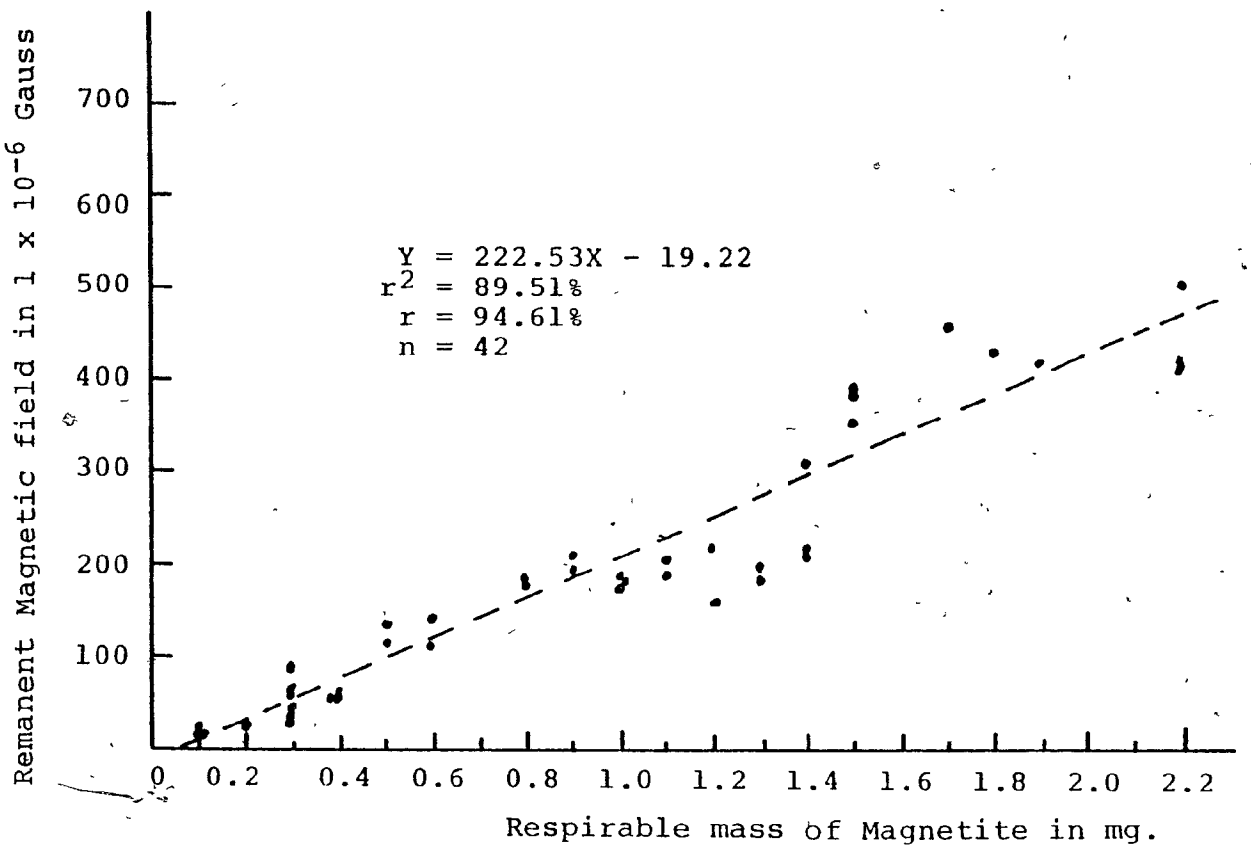


Fig. 9.3 - Correlation of the Remanent Magnetic Field with the Mass of Pure Magnetite Hexhlet Samples. Magnetic measurements were made while the samples were 1 cm. away from the probe.

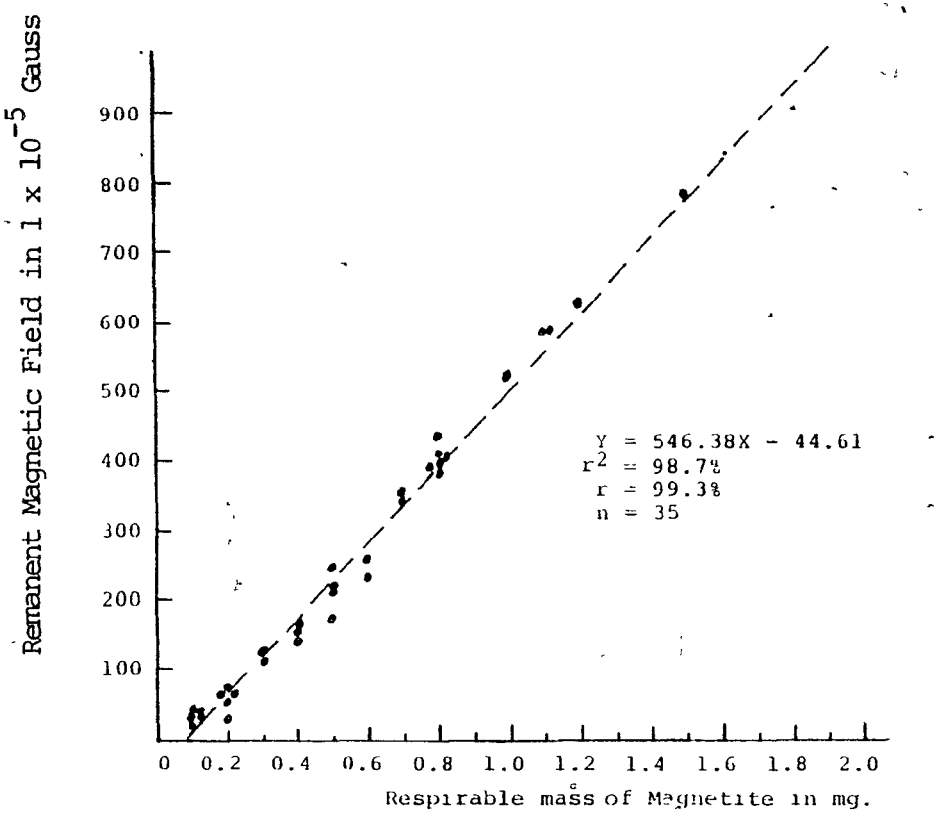


Fig. 9.4 - Correlation of the Remanent Magnetic Field with the Mass of Pure Magnetic Cyclone Samples. Magnetic Measurements were made while the samples were at the probe.. (Diameter of Membrane Filter was 25 mm)

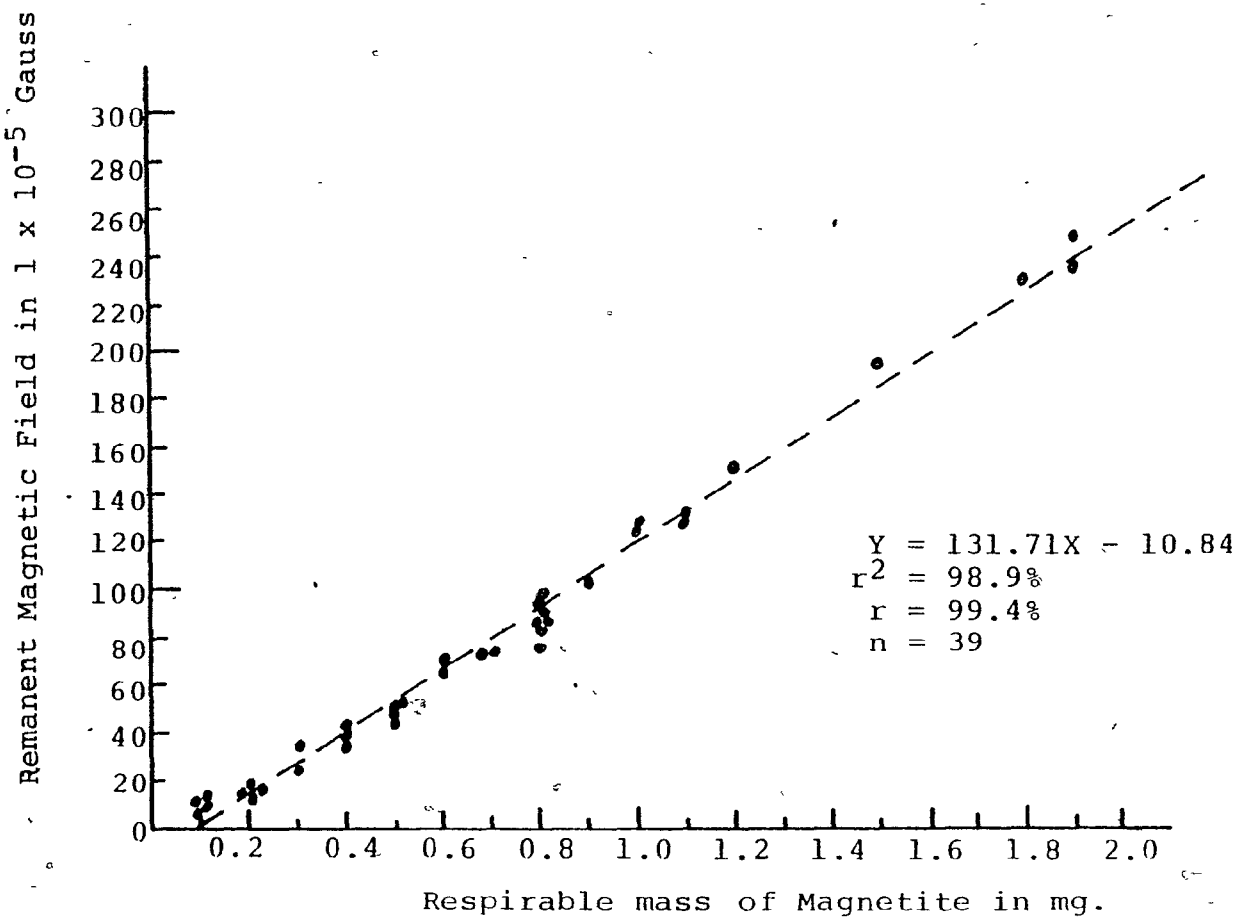


Fig. 9.5 - Correlation of the Remanent Magnetic Field with the mass of Pure Magnetite Cyclone Samples. Magnetic Measurements were made while the samples were 1 cm. away from the probe

Chauvenet's criterion [2] was used, the test results again indicated that all of the outliers belong to the population. Since both criteria results did indicate acceptance, and remanent magnetic field fluctuations are common and dependent on the particle distribution patterns, neither of the outliers were rejected. This calibration line can be used to determine the iron content of samples of chrysotile which have masses larger than 10 milligrams. The reason is that, if a 10 milligram chrysotile sample contains 2 percent iron, the weight of the magnetite content will be:

$$\text{Magnetite Content} = \frac{10 \text{ milligrams} \times 2\%}{73\% \text{ iron in magnetite}} = 0.27 \text{ milligrams}$$

The value of 0.27 milligrams is at the lower determination limit of the calibration line, as seen in figure 9.1. At such low values the error of estimating the mass for 90 percent confidence is as high as $\pm$ 40 percent. However, this error for higher values, such as 3 milligrams magnetite, drops to ±7 percent. The calibration line, which is seen in figure 9.2, has a 99.8 percent coefficient of determination and 99.9 percent coefficient of correlation. This calibration line is developed for determining the mass of magnetite for very small quantities of chrysotile, such as 0.1 milligrams, and vice-versa. If a 0.1 milligram chrysotile

Table 9.1 - Statistical Data for Hexhlet Samples of Pure Magnetite:

| Name of the Coordinates | Mean | Standard Deviations |
|---|---|---|
| X = Respirable Mass in mg. | 0.95 | 0.62 |
| Y = Magnetic Field in $10^{-6}$ Gauss | 392.68 | 298.67 |

| | Standard Error | The Calculated Value of T for T-Test for Corrolation |
|---|---|---|
| $a_o$ = - 5034 | 23.19 | - 2.17 |
| $a_1$ = 465.17 | 20.49 | 22.70 |

$r^2$ = 92.6% (Coefficient of Determination)

r = 96.2% (Coefficient of Correlation)

Standard Error of the Estimate: 81.15

Calculated F value for F-Test: 515.45

sample contains 1 percent iron, the weight of the magnetite content is $1.4 \times 10^{-3}$ milligrams. At this low value the error of estimating the mass is $\pm$ 30 percent. However, for middle range values, such as 2.5 milligrams of chrysotile, the error of estimating the mass of iron content is as low as $\pm$ 5 percent.

Correlation of the calibration line, with the data of cyclone samples for pure magnetite, is much better than the Hexhlet samples' correlation. The reason is that the particle distribution of cyclone samples on the 25 millimetre diameter millipore filter is much more uniform and is denser in comparison with the sample distribution on Hexhlet filters. As the filter diameter of cyclone samples are much smaller than the filter diameters of Hexhlet samples, the gradiometric probe of the fluxgate magnetometer can also detect the influence of magnetic fields of the out-lying particles.

## 9.3 Calibration Curves for Mass Determination of the Airborne, Respirable Size Chrysotile Asbestos for Various Mills of Quebec:

The statistical data for determining the accuracy of the calibration curves for mass determination of the airborne, respirable size, chrysotile fibres are listed in tables 9.2 to 9.5. The coefficient of determination of the calibration line for the Hexhlet samples of Mill # VI is 96.8 percent (see Fig. 9.6 and table 9.2), and indicates that the regression line

fits the observed data very well*. The coefficient of correlation is 98.4 percent. Both the T-test and the F-test indicate that the null hypothesis, of having all the true partial regression coefficients equal to zero, is not true and should be rejected at the significance levels of 0.1 percent and 1 percent respectively. Again the Nair's and Chauvenet's tests indicated that all of the outliers belong to the sample population at the level of significance of 5 percent and 12.5 percent respectively. In this case, the accuracy of determining the mass of airborne chrysotile also increases as the weight of the sample increases. When the mass of the Hexlet sample is small, the error of determining the mass for 90 percent confidence limits is as high as $\pm$ 7 percent. Calibration lines for the cyclone samples of Mill # VI chrysotile are seen in figures 9.7 and 9.8. The coefficient of determination of the line in Fig. 9.8 is 95.1% and is similar to the value of the coefficient of determination for Hexhlet samples. When the samples were at the probe, the remanent magnetic fields were somewhat more uniform and the coefficients of determination and correlation were improved (see Fig. 9.7).

---

*It is noted that, because of the sensitivity of measurements to size and shape of samples, distance between filter and probe, magnetite purity and particle size, etc., the coefficients of these calibration curves are specific to the technique and materials used in this work.

Table 9.2 - Statistical Data for Hexhlet Samples of Grade # 6 Chrysotile from Mill # VI:

| Name of the Coordinates | Mean | Standard Deviation | Formula of the Line | Standard Error | Calculated Value of T for Correlation |
|---|---|---|---|---|---|
| X = Respirable Mass in mgs. | 1.30 | 1.0 | $a_o$ = - 33.69 | 5.69 | - 5.92 |
| Y = Magnetic field in $10^{-7}$ Gauss | 160.20 | 152.3 | $a_1$ = 149.33 | 3.48 | 42.96 |

$r^2$ = 96.8% coefficient of Determination

r = 98.4% coefficient of Correlation

Standard Error of the Estimate: 27.25

Calculated F value for F-Test: 486.80

Degree of Freedom: 60

Table 9.3 - Statistical Data for Hexhlet Samples of Grade # 6 Chrysotile from Mill # VII:

| Name of the Coordinates | Mean | Standard Deviation | Formula of the Line | Standard Error | Calculated Value of T for Correlation |
|---|---|---|---|---|---|
| X = Respirable Mass in mgs. | 2.11 | 1.17 | $a_o$ = - 26.49 | 8.29 | - 3.20 |
| Y = Magnetic field in $10^{-7}$ Gauss | 195.73 | 127.27 | $a_1$ = 105.31 | 3.45 | 30.52 |

$r^2$ = 91.5% Coefficient of Determination

r = 95.6% Coefficient of Correlation

Standard Error of the Estimate: 37.21

Calculated F Value for F-Test: 931.55

Degree of Freedom: 86

Table 9.4 - Statistical Data for Hexhlet Samples of Rhodesian Chrysotile U.I.C.C. Samples:

| Name of the Coordinates | Mean | Standard Deviation | Formula of the line | Standard Error | Calculated Value of T for Correlation |
|---|---|---|---|---|---|
| X = Respirable Mass in mgs. | 1.95 | 1.81 | $a_o$ = - 11.43 | 9.70 | - 1.18 |
| Y = Magnetic field in $10^{-7}$ Gauss | 196.41 | 206.35 | $a_1$ = 106.67 | 3.66 | 29.15 |

$r^2$ = 87.0% Coefficient of Determination

r = 93.3% Coefficient of Correlation

Standard Error of Estimate: 74.45

Calculated F Value for F-Test: 849.56

Degree of Freedom: 126

Table 9.5 - Statistical Data for Hexhlet Samples, Chrysotile From Various Mills

| | Mill I | Mill II | Mill III | Mill IV | Mill V | Mill VIII | Mill IX |
|---|---|---|---|---|---|---|---|
| X = Respirable Mass in Mg. | | | | | | | |
| Mean of Mass | 2.33 | 1.99 | 1.63 | 2.33 | 2.48 | 2.15 | 2.09 |
| Standard Dev. of Mass | 1.06 | 1.08 | 1.16 | 1.18 | 1.51 | 0.68 | 0.90 |
| Y = Magnetic field in $10^{-7}$ Gauss | | | | | | | |
| Mean of Field | 348 | 206.15 | 61.72 | 292.69 | 128.06 | 419.14 | 210.77 |
| Standard Dev. of Field | 171.31 | 133.75 | 65.62 | 125.50 | 63.73 | 129.72 | 121.12 |
| $a_o$ | -13.97 | 41.99 | -4.74 | 71.57 | 56.16 | 62.69 | -36.10 |
| $a_1$ | 155.63 | 82.69 | 40.72 | 94.87 | 29.00 | 166.01 | 122.26 |
| Standard Error of $a_o$ | 15.62 | 24.43 | 6.22 | 14.45 | 10.54 | 37.22 | 14.52 |
| Standard Error of $a_1$ | 6.13 | 10.83 | 3.12 | 5.54 | 3.64 | 16.56 | 6.57 |
| Calculated Value of T for $a_o$ | -9.90 | 1.72 | -0.76 | 4.95 | 5.33 | 1.68 | -2.49 |
| Calculated Value of T for $a_1$ | 25.42 | 7.63 | 13.07 | 17.12 | 7.97 | 10.03 | 18.60 |
| $r^2$ | 91.9% | 43.6% | 71.7% | 79.1% | 46.5% | 74.0% | 82.7% |
| r | 95.9% | 66.1% | 84.7% | 88.9% | 68.2% | 86.0% | 91.0% |
| Standard Error of Estimate | 48.82 | 100.42 | 29.58 | 57.32 | 46.62 | 66.16 | 50.34 |
| Calculated F | 645.91 | 58.28 | 170.81 | 293.11 | 63.55 | 100.55 | 345.92 |
| Degree of Freedom | 56 | 73 | 66 | 76 | 71 | 34 | 71 |

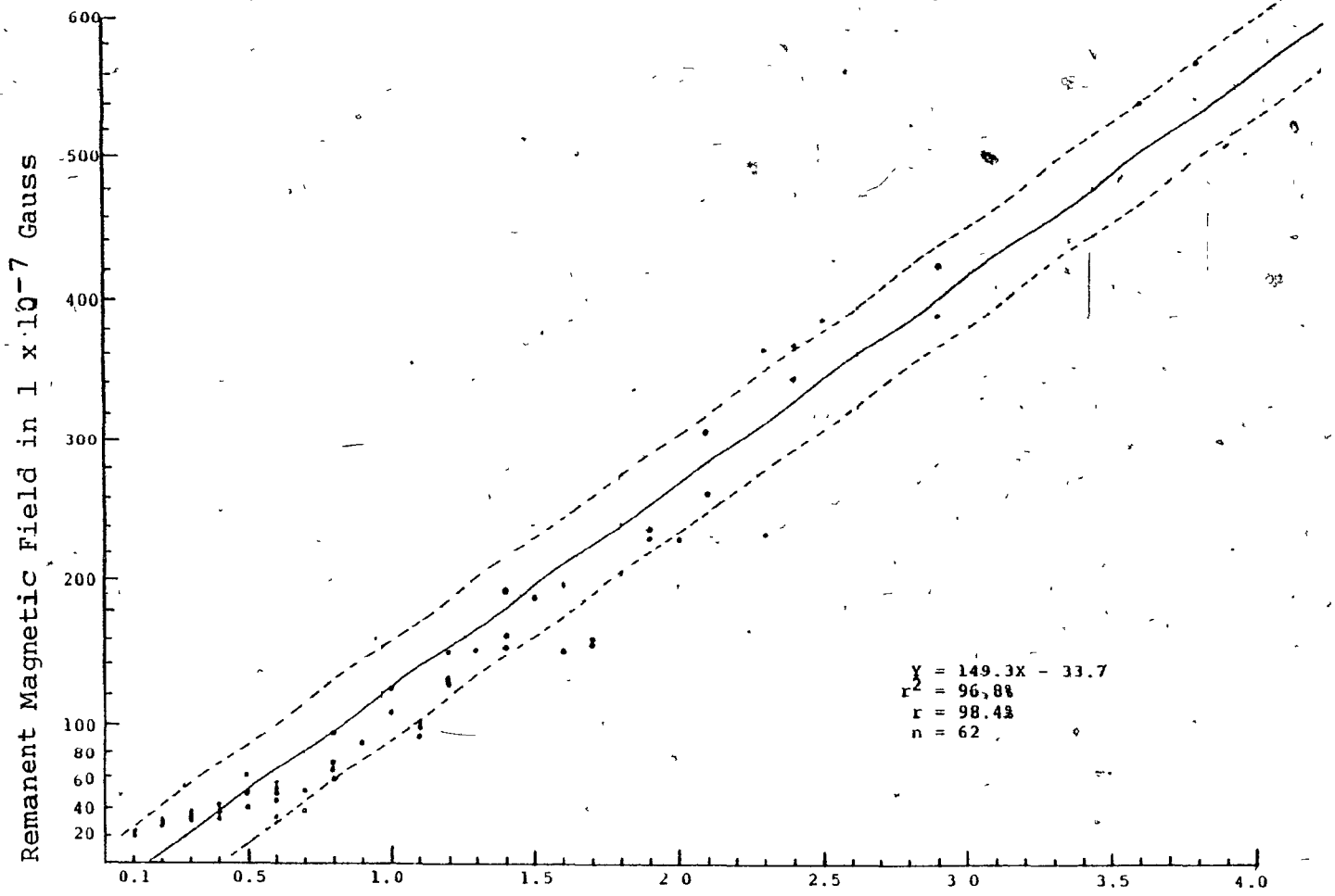


Fig. 9.6 - Calibration Line for Mill # VI Chrysotile Mass Determination. Airborne Samples were collected using Hexhlet Horizontal Eleutriator. Dotted line represents the confidence limit of 90% Magnetic measurements were made while the samples were at the probe

The calibration lines of Hexhlet and cyclone samples for Mill # VII chrysotile asbestos are seen in figures 9.9 and 9.10. The coefficient of determination of the calibration line for Hexhlet samples is 91.5 percent and the correlation coefficient is 95.6 percent. The other statistical data are shown in table 9.3. The F test and T test results were all favourable at a level of significance of 1 and 0.1 percent respectively and, therefore, these statistical analyses indicate that, statistically, there is a significant relationship between the remanent magnetic field readings and the measured mass. Furthermore, all of the outliers have been shown to belong to the population of the samples at a level of significance of 5 and 12.5 percent, for Nair's and Chauvenet's tests respectively. When the correlation coefficient of 87.9 percent, for Mill # VII chrysotile cyclone data, is compared with the correlation coefficients of the Hexhlet and cyclone samples of pure magnetite and Mill # VI, it will be observed that this correlation figure is low, relative to the others. However, statistically, the correlation coefficient of 87.9 percent is substantially higher than the theoretical critical correlation coefficient value of 49.6 percent for two variables and a sample population with 24 degrees of freedom at a 1 percent level of significance. The reason for such a decrease in the correlation coefficient is the small number of cyclone samples and the low iron content of the Mill # VII chrysotile

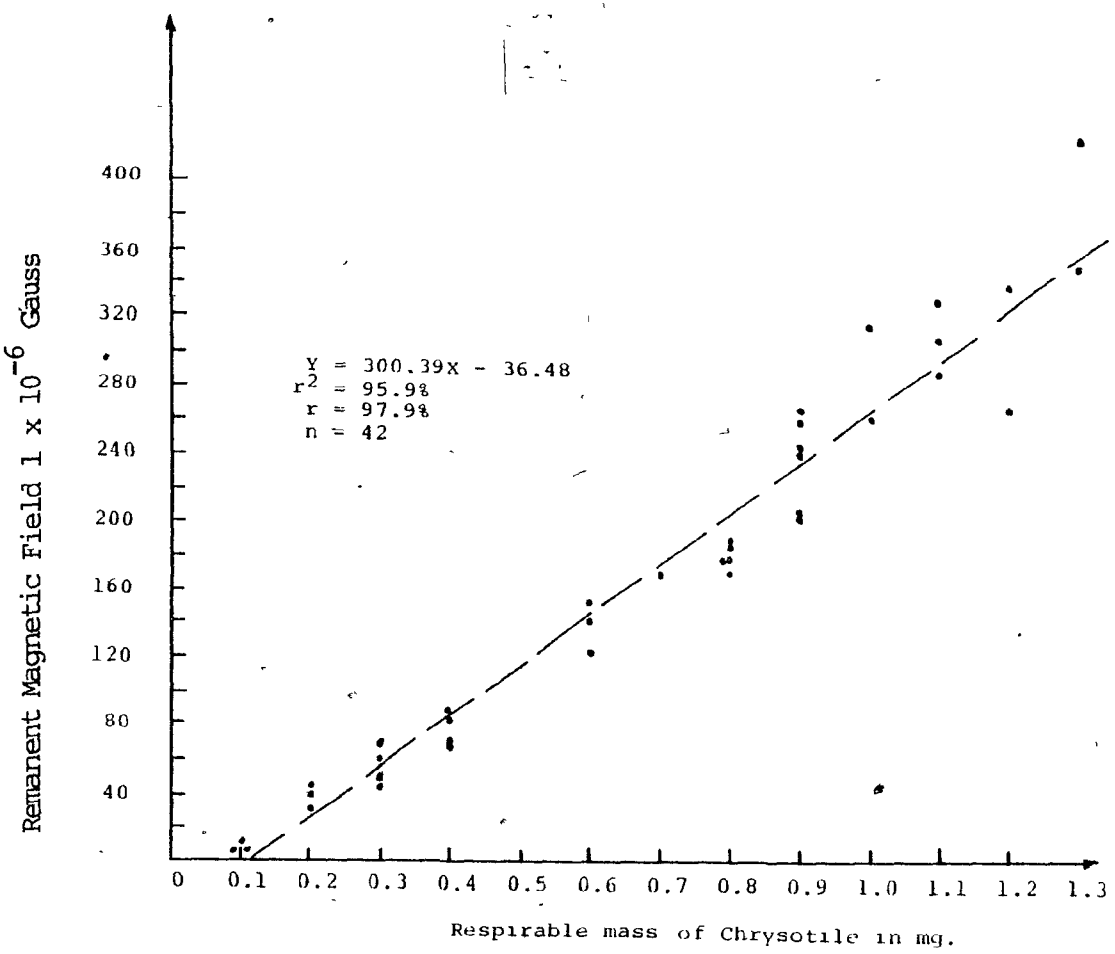


Fig. 9.7 - Correlation of the Remanent Magnetic Field with the Mass of Mill # VI Chrysotile Cyclone Samples, Magnetic Measurements were made while the samples were at the probe.

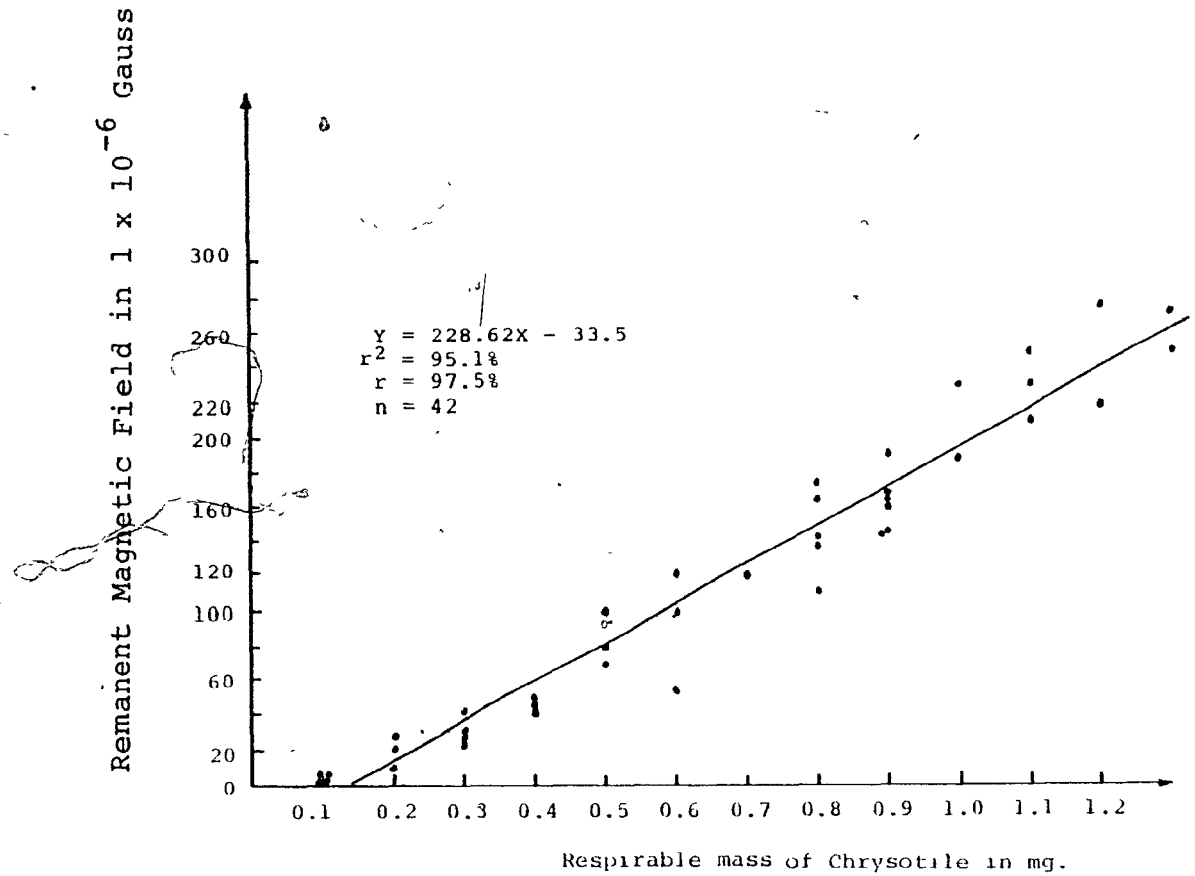


Fig. 9.8 - Correlation of the Remanent Magnetic Field with the Mass of Mill # VI Chrysotile Cyclone Samples. Magnetic Measurements were made while the samples were 1 cm away from the Probe.

(1.05 percent iron) in comparison with the chrysotile of Mill # VI and with pure magnetite. It is observed that when the iron content of chrysotile is lower than 1.5 percent, the distribution of magnetite within the sample is not very uniform, thus producing scatter in the data of remanent magnetic field readings. Similarly, the iron content of Mill # III chrysotile is only 1.15 percent and the magnetic readings for Hexhlet samples show considerable scatter (see Appendix B), with the coefficient of determination at 77.7 percent and coefficient of correlation at 84.7 percent.

Among the nine calibration curves, the two which have the lowest coefficient of determination values are Mill # II and Mill # V (see table 9.5 and Appendix B). The chrysotile from Mill # II is grade # 7 and, other than chrysotile, it contains some antigorite and brucite. The chrysotile from Mill # V is slip fibre and, with this type of fibre, uniform and homogeneous dust cloud generation was practically impossible. During the dust cloud generation, because of the harshness of this type of chrysotile, the blade of the dust generator was broken on two occasions. Although the coefficient of determination for the calibration line of Mill # II is only 43.6 percent, and for Mill # V it is 46.5 percent, in both cases the data are statistically sound at the level of significance of 1 percent. Both F and T test results have indicated that, between the remanent magnetic field readings and the measured mass, there is a

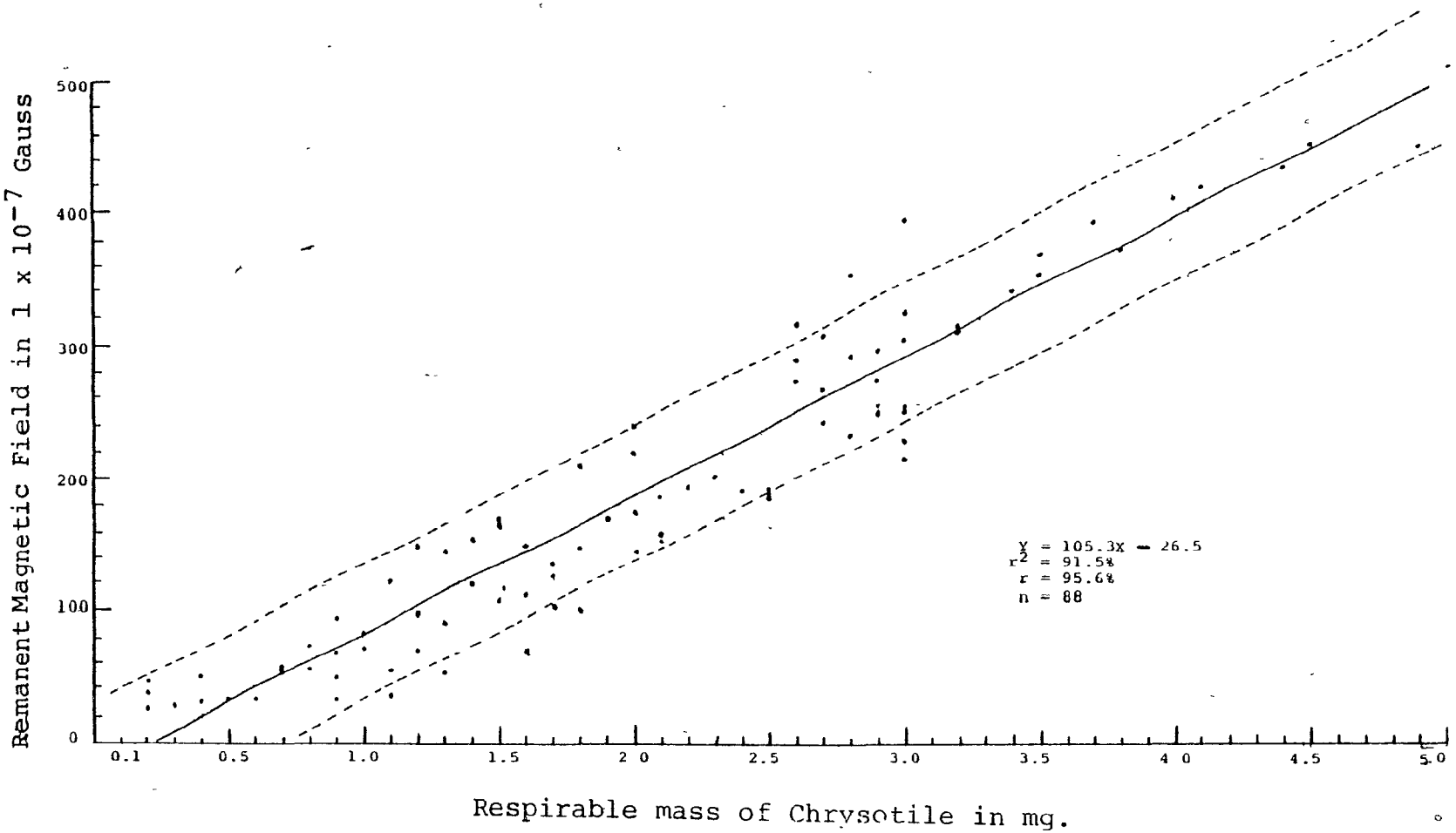


Fig. 9.9 - Calibration Line for Mill # VII Chrysotile Mass Determination. Airborne Samples were collected using Hexhlet Horizontal Eleutriator. Dotted line represents the confidence limit of 90%. Magnetic measurements were made while the samples were at the probe.

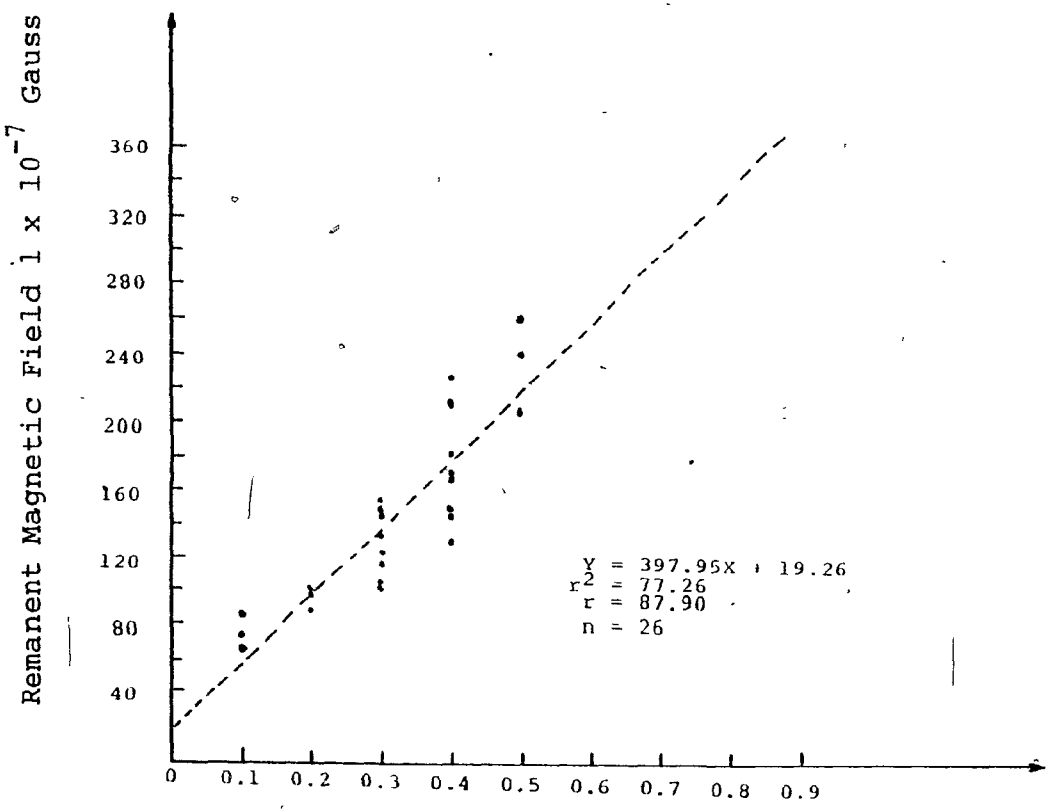


Fig. 9.10 - Correlation of the Remanent Magnetic Field with the Mass of Mill # VII Chrysotile Cyclone Samples. Magnetic measurements were made while the samples were at the probe.

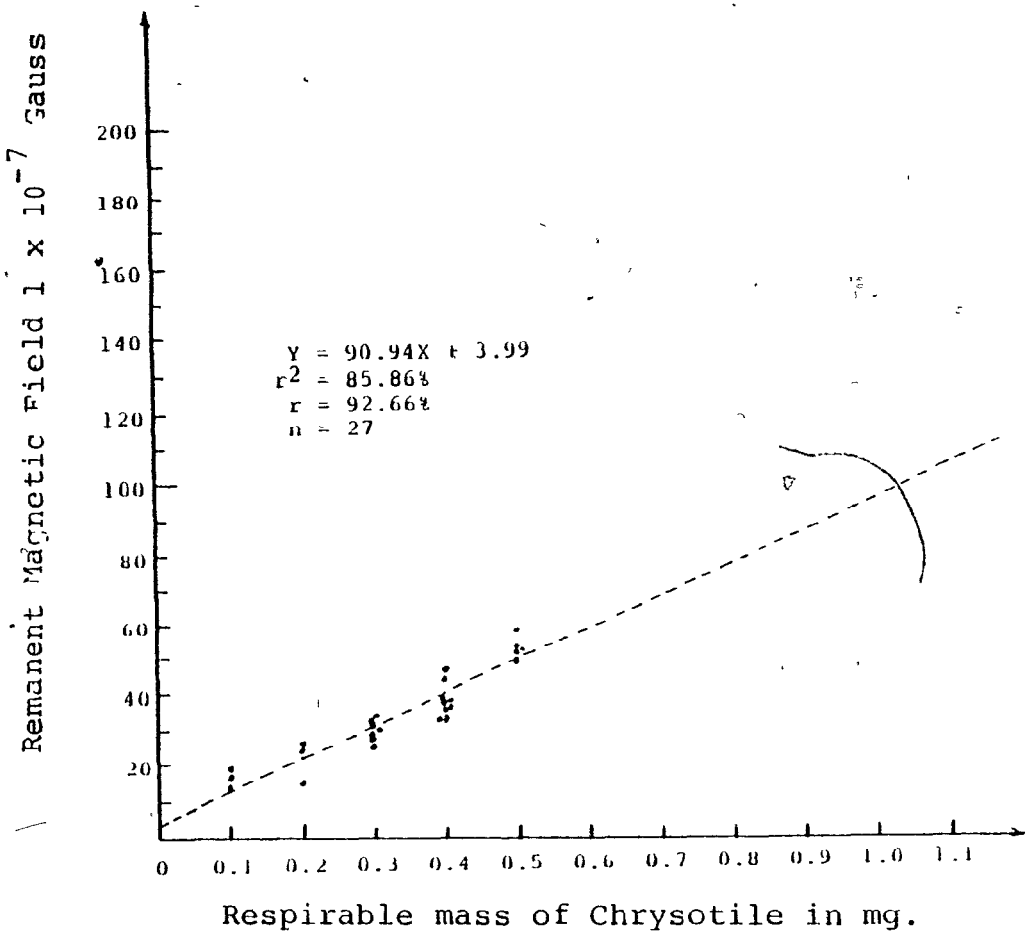


Fig. 9.11 - Correlation of the Remanent Magnetic Field with the mass of Mill # VII Chrysotile Cyclone Samples. Magnetic measurements were made while the Samples were 1 cm. away from the probe.

relationship at the 1 and 0.1 percent levels of significance, respectively.

The coefficient of determination of the calibration line for the Rhodesian Chrysotile U.I.C.C. samples is 87.0 percent and the coefficient of correlation is 93.3 percent (see table 9.4 and appendix B). Although the total number of samples of the Rhodesian chrysotile is higher than that for the other types of chrysotile, and has a degree of freedom of 126, the correlation result is lower in comparison to correlations for Mills # I, VI, and VII. The reason is that during the preparation of the U,I.C.C. samples [3], in order to produce respirable size chrysotile dust, the chrysotile asbestos was ground for a long period of time and, therefore, some of the contained magnetite was separated from the chrysotile fibres. When the U.I.C.C. samples were rendered airborne in the dust chamber, since the separated magnetite particles have different aerodynamic behavior than the fibres, the collected Hexhlet samples did not have a uniform magnetite distribution and this affected the correlation results. However, in all cases, the drawn calibration lines are statistically significant and there is a consistent relationship between the remanent magnetic field readings and the mass of chrysotile fibres. In this research work, although, by using electron microscope and EDXA techniques it was shown that practically all of the iron was in the form of magnetite, in order to further investigate this, the measured remanent

magnetic fields of pure magnetite versus the remanent magnetic fields of chrysotile from Mill # VI, VII, and VIII, with equivalent magnetite mass, are compared in figures 9.12, 9.13 and 9.124, respectively. Measurements for these figures used the pure magnetite samples from McGill as a reference and the same sampler, measuring geometry, and size distribution for both magnetite and chrysotile samples. The 45° theoretical line also implies that all iron measured in the chrysotile sample is due to magnetite*. The remanent magnetic fields of chrysotile from Mill # VI is practically the same as the pure magnetite's and the determined line is parallel to the theoretical 45° line. In the other two cases, the lines representing the results had slopes different from 45°.

9.4 Calibration Curves for Number Determination of Chrysotile Fibre Content of the Airborne Respirable Size Dust for Various Mills of Quebec:

Calibration lines for number determination of the chrysotile fibre content of airborne respirable size dust, in terms of chrysotile fibres per microscopic field, are shown in figures 9.15 to 9.23. In all cases the coefficient of determination and correlation for the calibration lines are good and vary between 88 and 97.7 percent. Variations in the slopes of the lines are indicative of the variations in magnetite content of each type of chrysotile. The slopes of the calibration lines of chrysotile from Mills I, II, VI, and IX are 0.84, 0.68, 0.77, and 0.65 respectively,

---

* Stroink et al.([7]), by using Mössbauer technique, have indicated that up to 1.5% of the iron could be found as impurities in the crystal latice of the UICC chrysotile reference samples.

varying as the atomic absorption iron content analysis results of these chrysotile samples are varying, at 1.85 1.75, 1.56, and 1.55 percent iron respectively. Therefore, this is another indication that the magnetite particles, which are producing the remanent magnetic field of chrysotile fibres, are intimately attached to, or associated with, the chrysotile fibres and that variations in the measured remanent magnetic fields are due to variations in magnetite content of the chrysotile fibres.

Results of the optical microscope measurements of the airborne dust samples of two Quebec chrysotile mills have indicated that the percentage of the airborne fibres, which are equal to or longer than the 5 micrometers, varies between the 1.5 and 10 percent. This variation depends on the location from which the sample is taken and the number of fibres, which are equal to or longer than 5 micrometers, increases from dry rock storage to bagging areas of the mills. These fibre length distribution results agree very well with the findings of Gibbs and Dutoit[4]. However, results of the optical microscope measurements of 143 environmental chamber samples have indicated that 24 to 45 percent of the generated dust cloud population is equal to, or longer than, 5 micrometers. All the other fibres which did not meet the index concentration criterion (which defines the fibre as "particles with at least 3 to 1 length to diameter aspect ratio, and are longer than 5 micrometers,

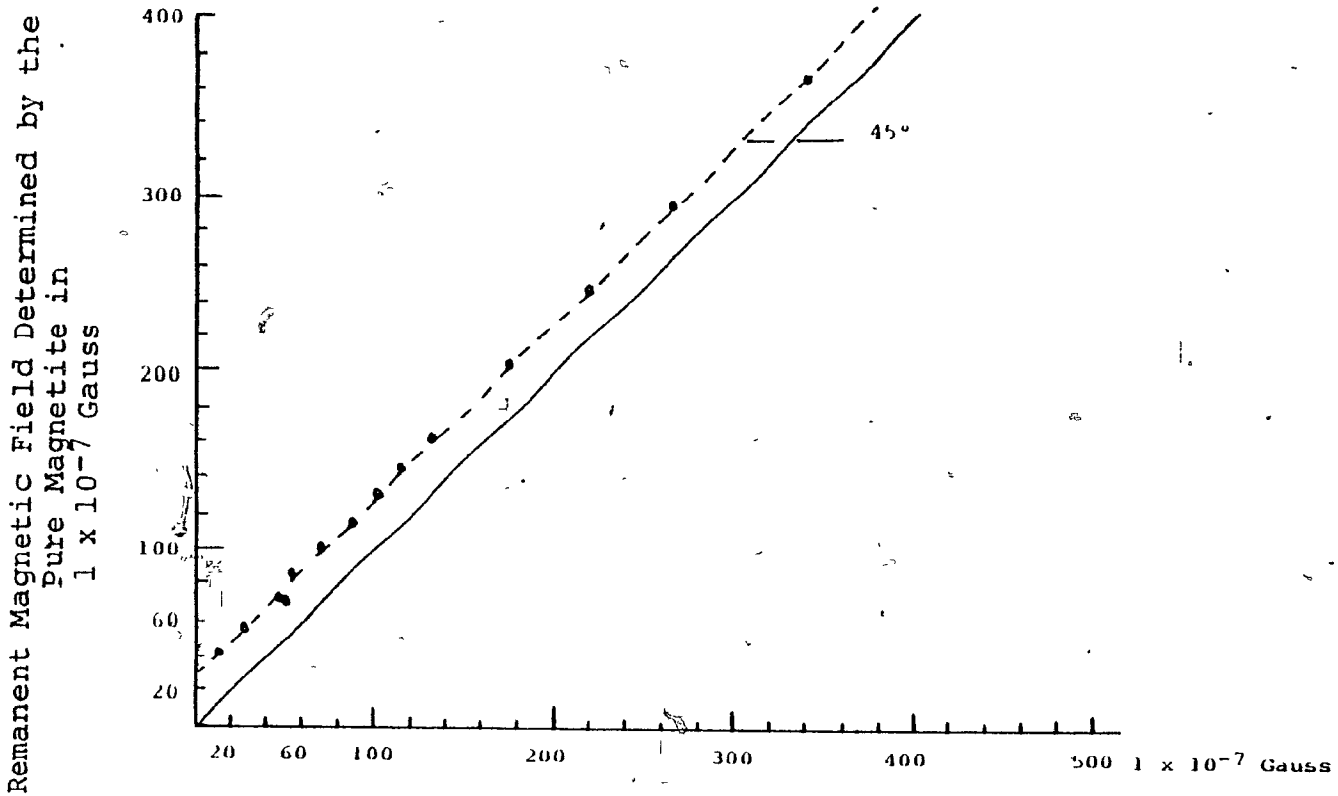


Fig. 9.12 - Correlation of Magnetic Fields. Correlation of the Magnetic Fields of Pure Magnetite and Magnetite Content of Chrysotile Samples of Mill # VI, for Equivalent Magnetite Masses, Sampling and Measurement Techniques.

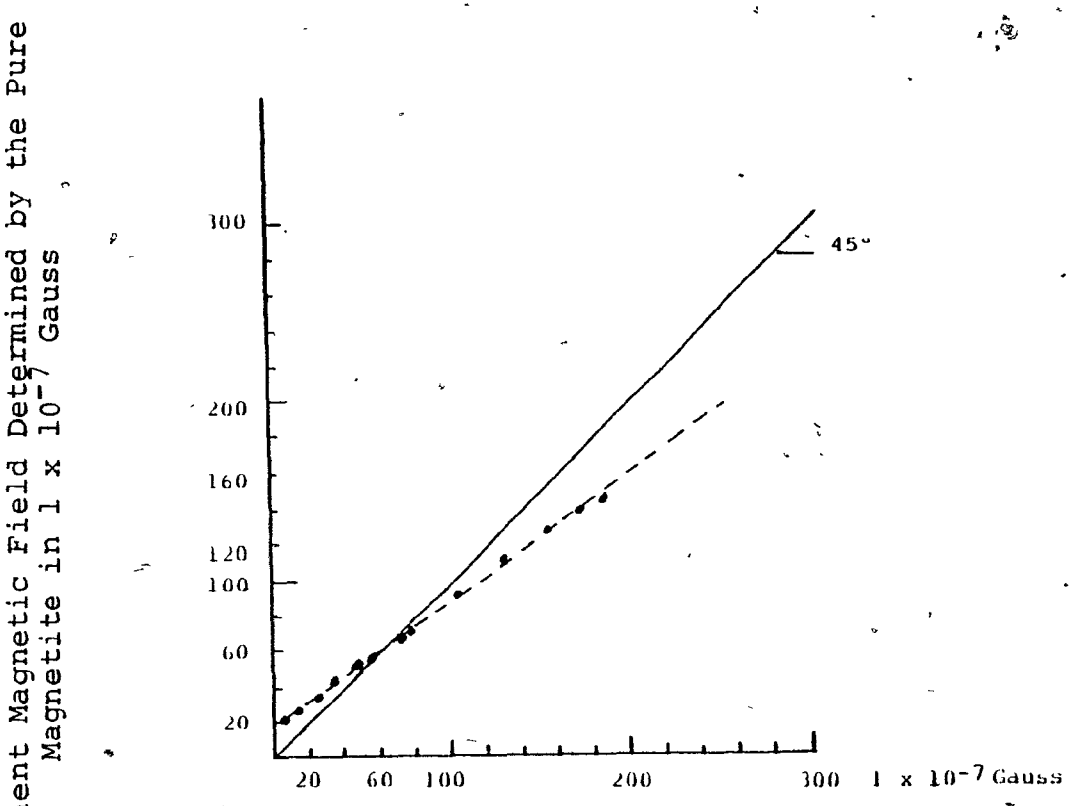


Remanent Magnetic Field Determined by the Magnetite Content of Chrysotile of Mill # VII in 1 x $10^{-7}$ Gauss.

Fig. 9.13 - Correlation of Magnetic Fields of Pure Magnetite and Magnetite Content of Chrysotile Samples of Mill # VII, for Equivalent Magnetite Masses, Sampling and Measurement Techniques.

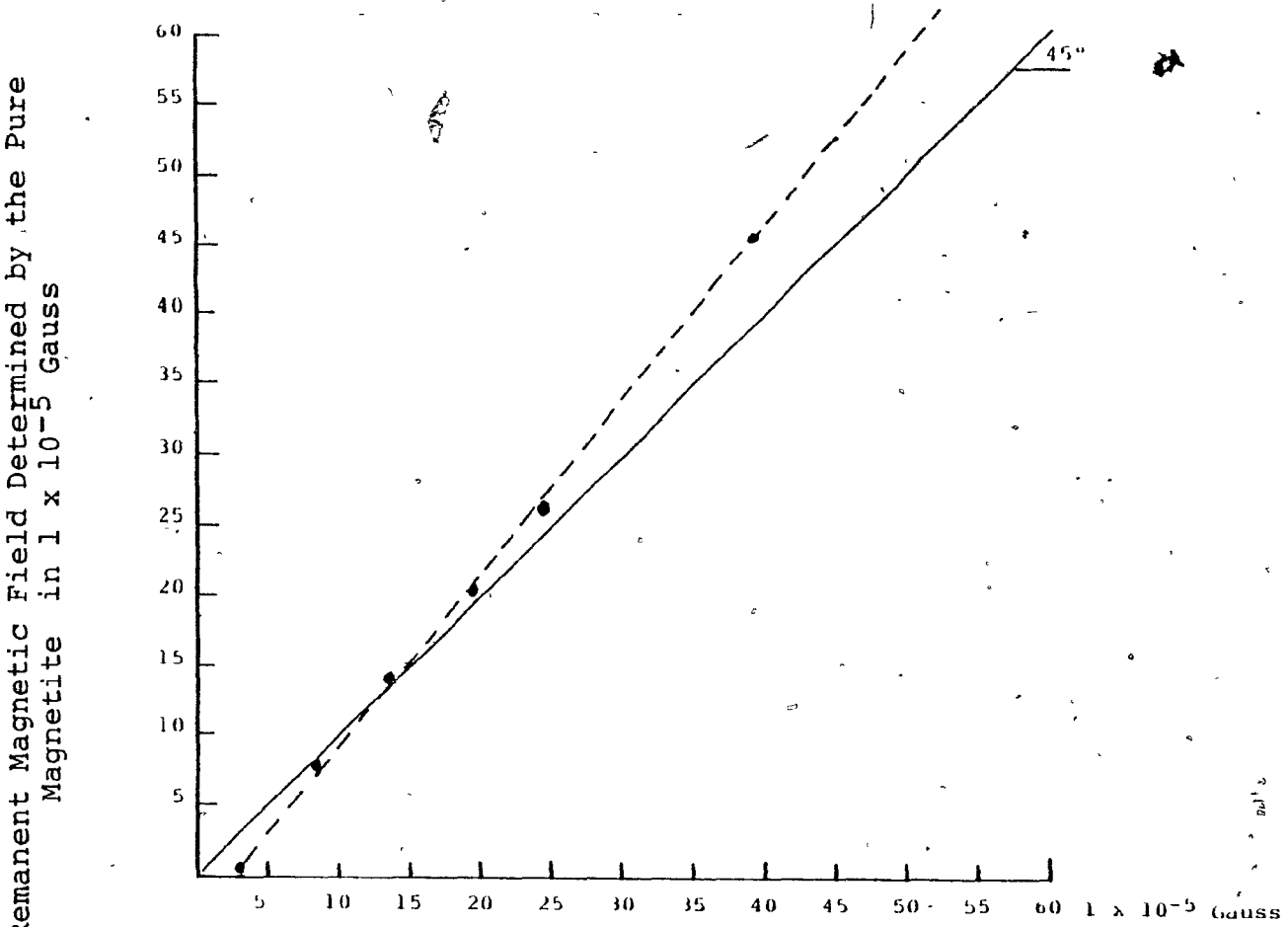


Fig. 9.14 - Correlation of the Magnetic Fields of Pure Magnetite and Magnetite Content of Bulk Chrysotile Samples of Mill # VIII for Equivalent Masses, Sampling and Measurement Techniques. Bulk Chrysotile Sample Masses were Varying Between 5 and 25 mg.

and whose diameter is limited by the respirability of the fibres at maximum 3 micrometers") are counted as particles. The interesting observation is that there is no signigicant correlation between the remanent magnetic field and the total dust count. This is another indication that magnetite particles are not associated with dust particles but associated with chrysotile fibres. Thus, high fibre concentrations in the airborne laboratory samples causes the slopes of the calibration lines to be steeper than the correlation lines of the field samples. When these samples were studied with an electron microscope, it was observed that some of these particles were short chrysotile fibres or bundles and few of them were associated with magnetite (see Fig. 9.24 a, b, c, and d). Among other particles, there were few magnetite particles which were not attached to fibres (see Fig. 9.25 a, b, and 9.26 a). Although the separate magnetite particles, and short fibres with magnetite particles attached, contribute to the total remanent magnetic field of the sample, they are not included in the total fibre count and, therefore, the plotted data are somewhat scattered. This scatter is more obvious when the samples are from dry rock storage areas, at which places chrysotile is not refined. As an example, Fig. 9.27-a shows a large antigorite particle containing iron and surrounded by few chrysotile fibres. The magnetic field contribution of this particle to the total field would be substantial.

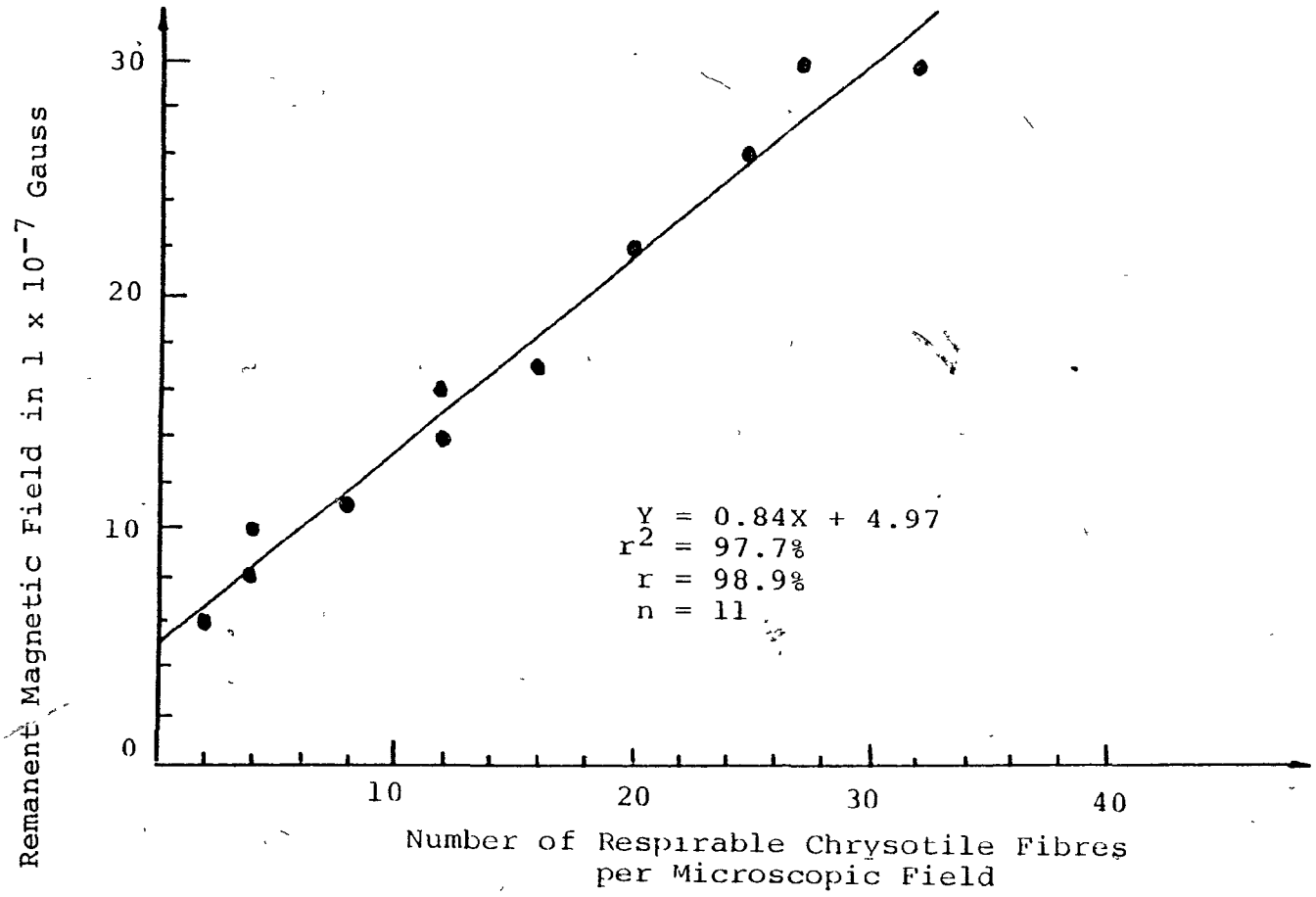


Fig. 9.15 - Calibration Line For Fibre Number Determination for Mill # 1 Chrysotile

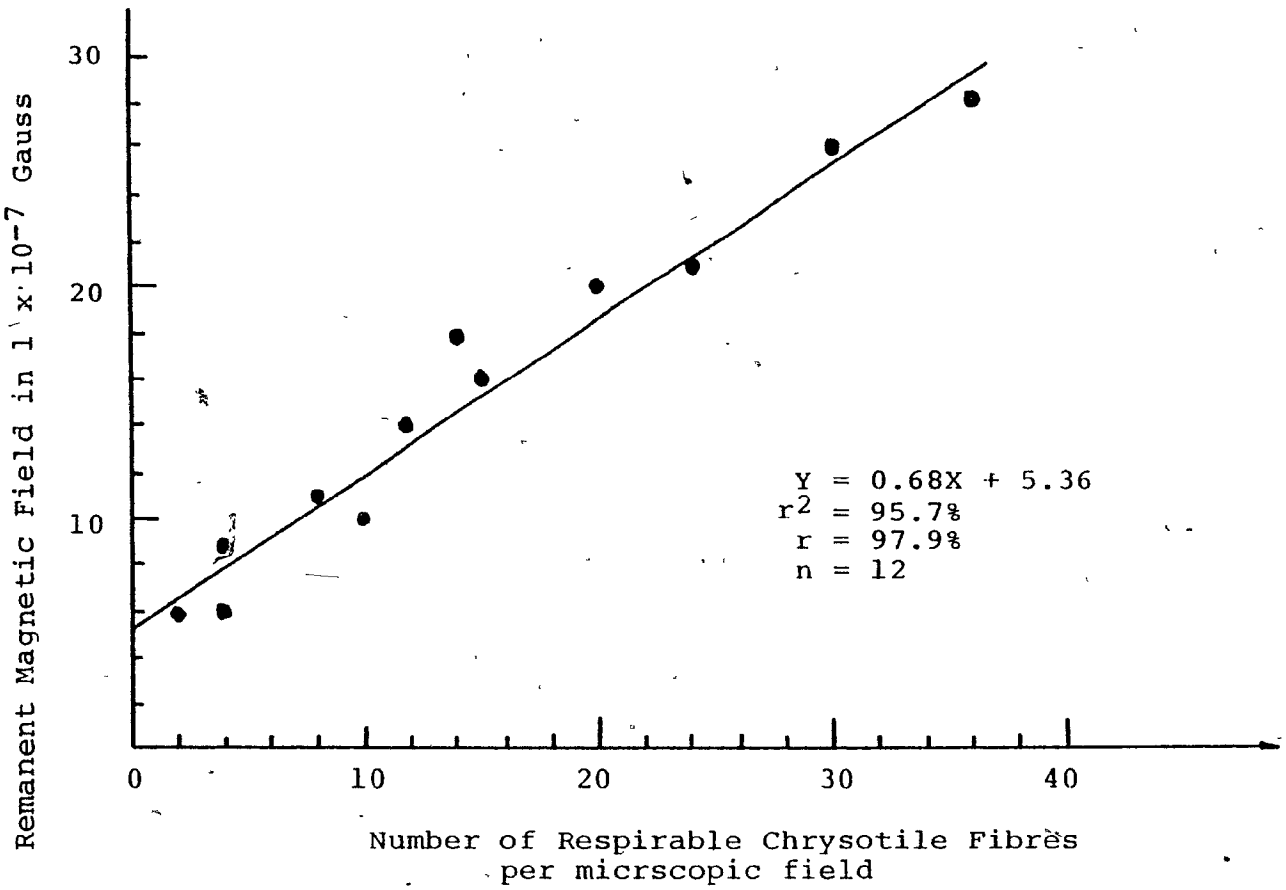


Fig. 9.16 - Calibration Line For Fibre Number Determination For Mill # II Chrysotile

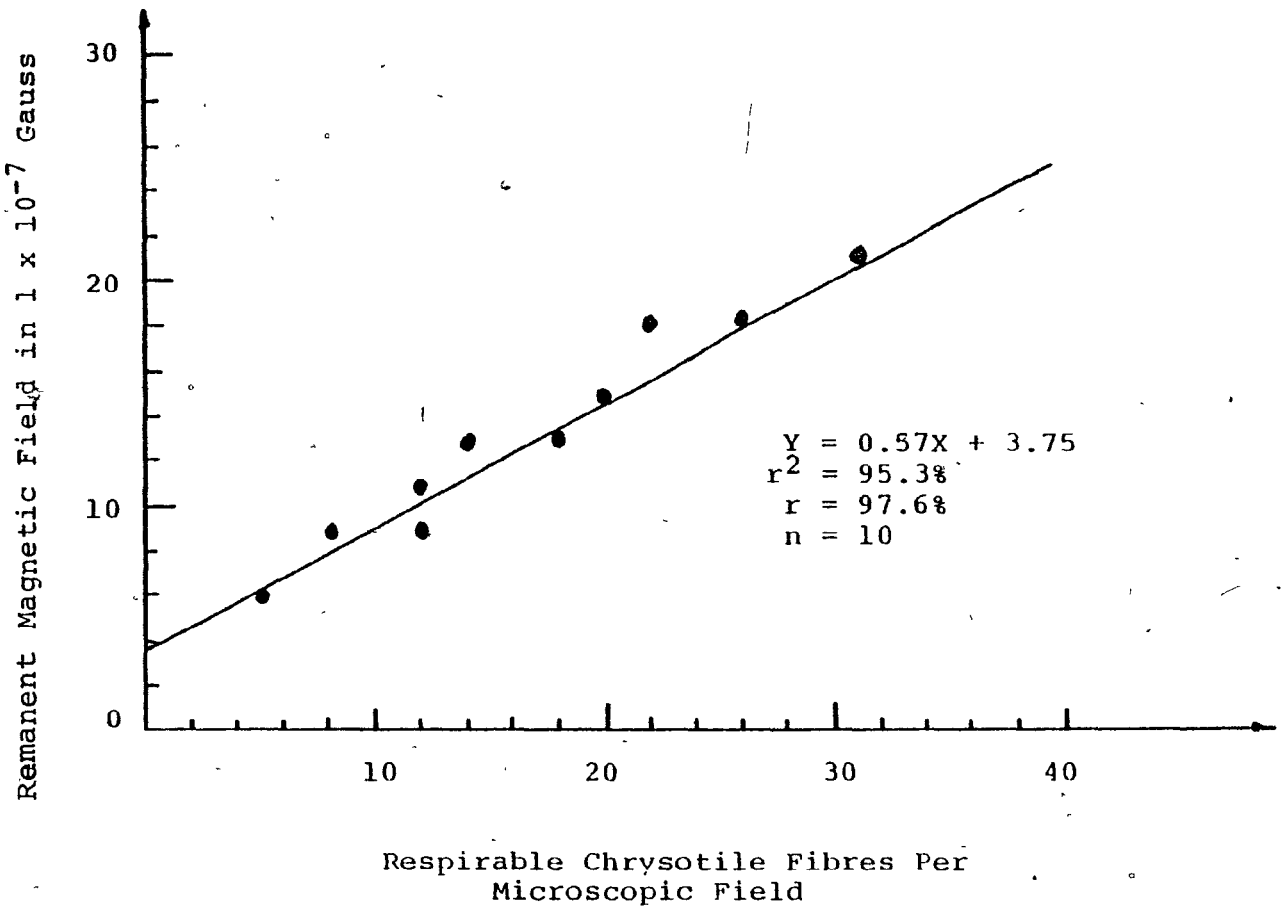


Fig. 9.17 - Calibration Line For Fibre Number Determination For Mill # IV Chrysotile

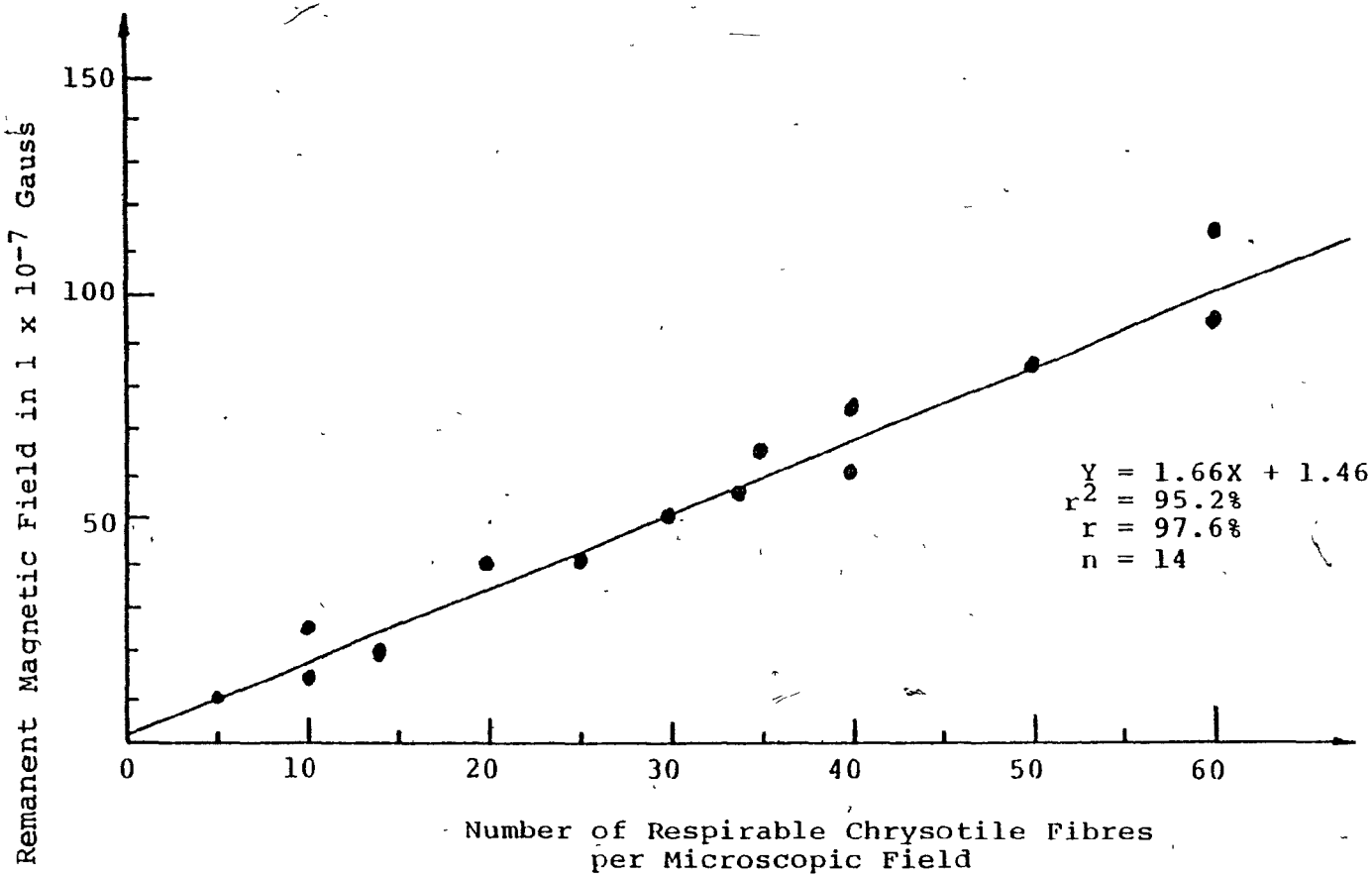


Fig. 9.18 - Calibration Line For Fibre Number Determination For Mill # V Chrysotile

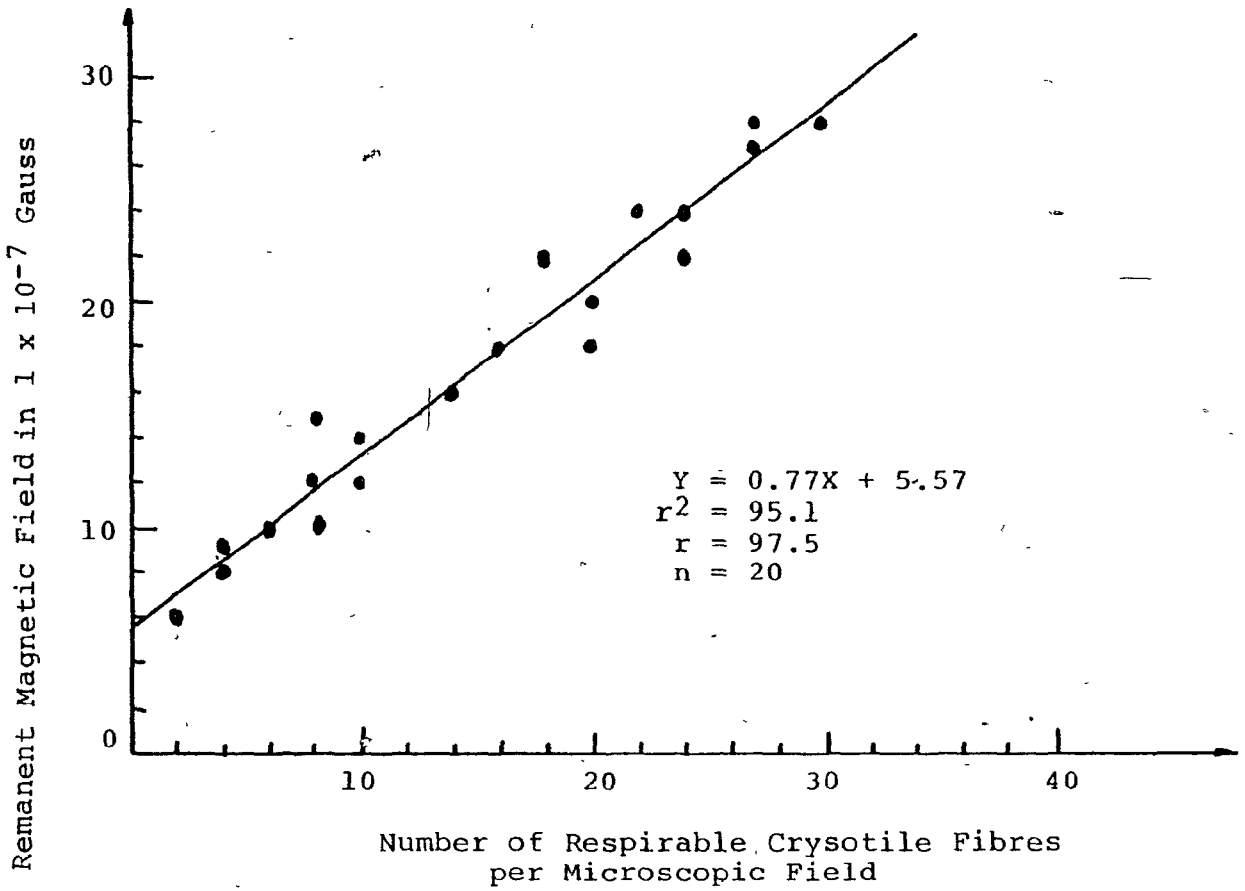


Fig. 9.19 - Calibration Line For Fibre Number Determination for Mill # VI Chrysotile

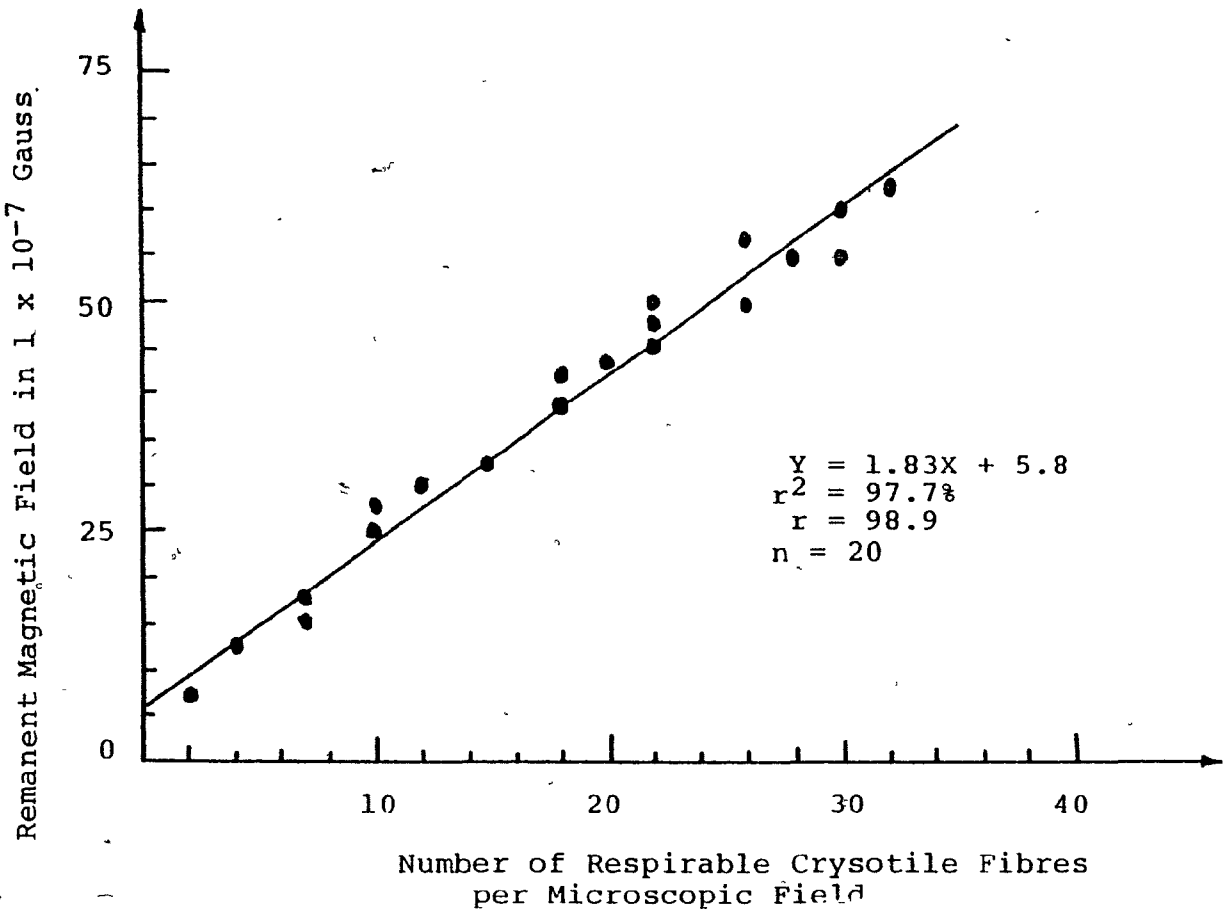


Fig. 9.20 - Calibration Line For Fibre Number Determination for Mill # VII Chrysotile

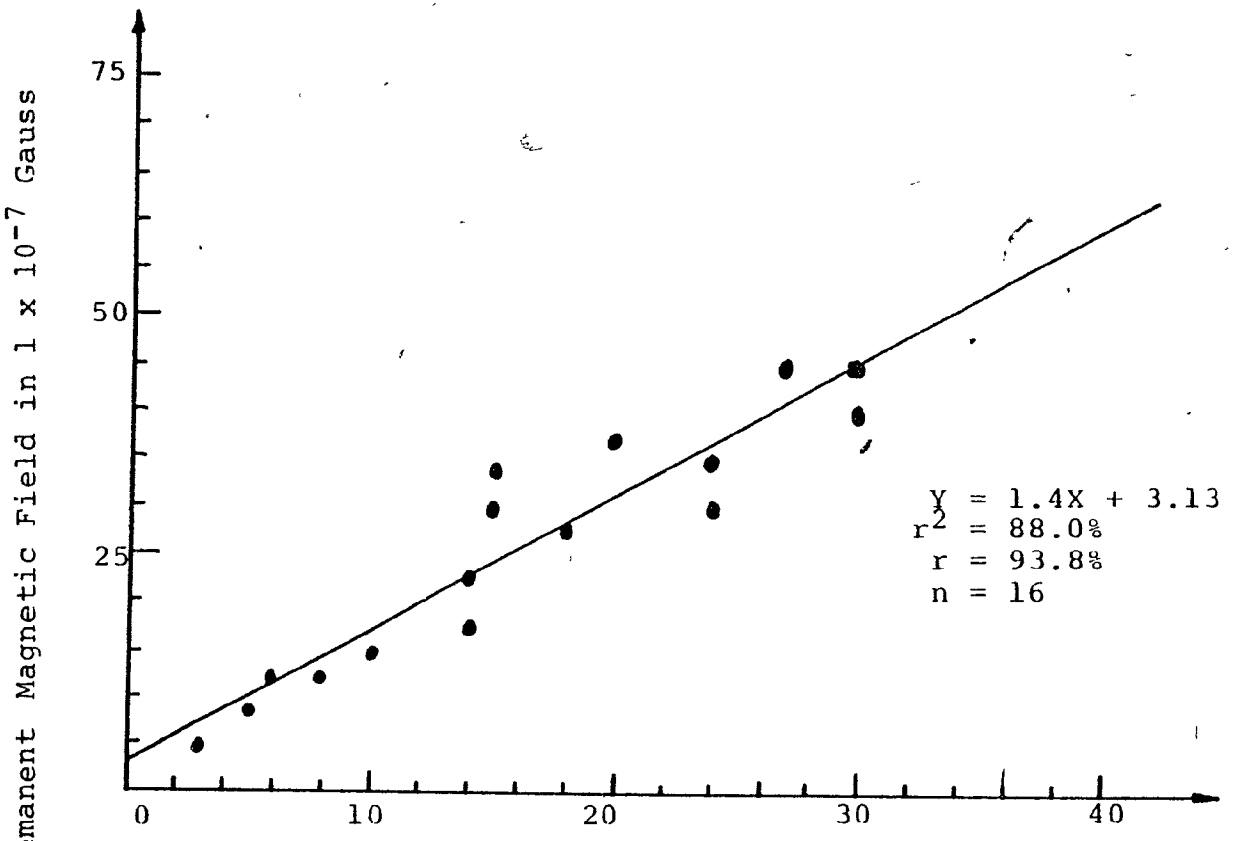


Fig. 9.21 - Calibration Line For Fibre Number Determination for Mill # VIII Chrysotile

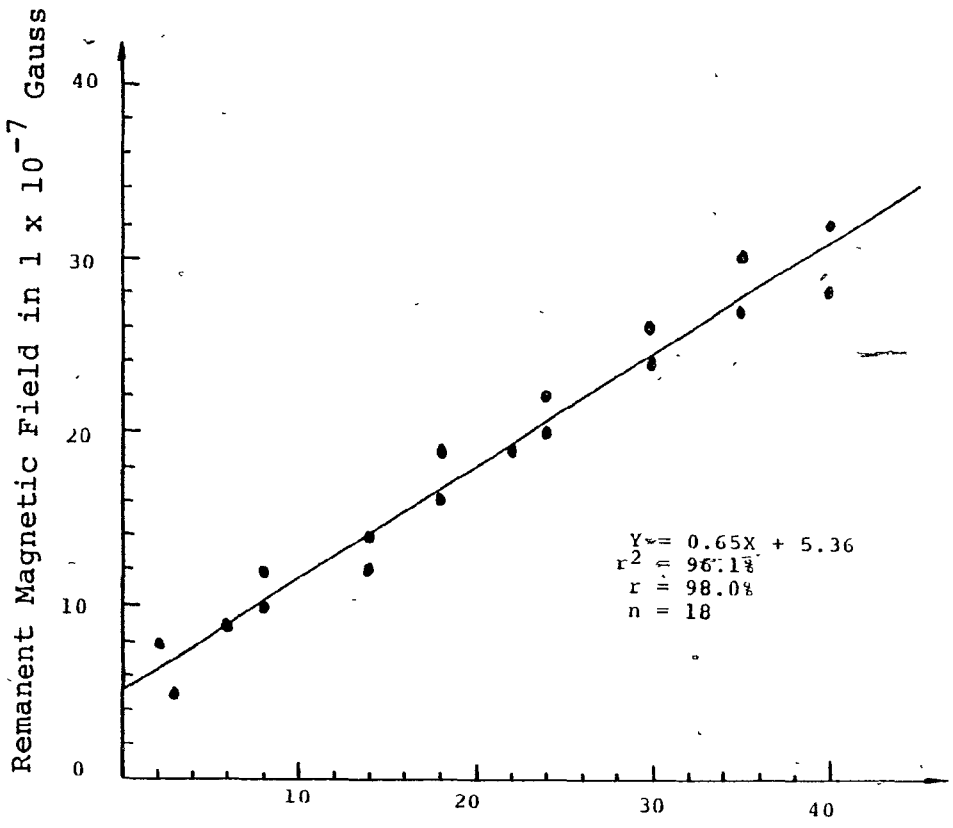


Fig. 9.22 - Calibration Line For Fibre Number Determination For Mill IX Chrysotile

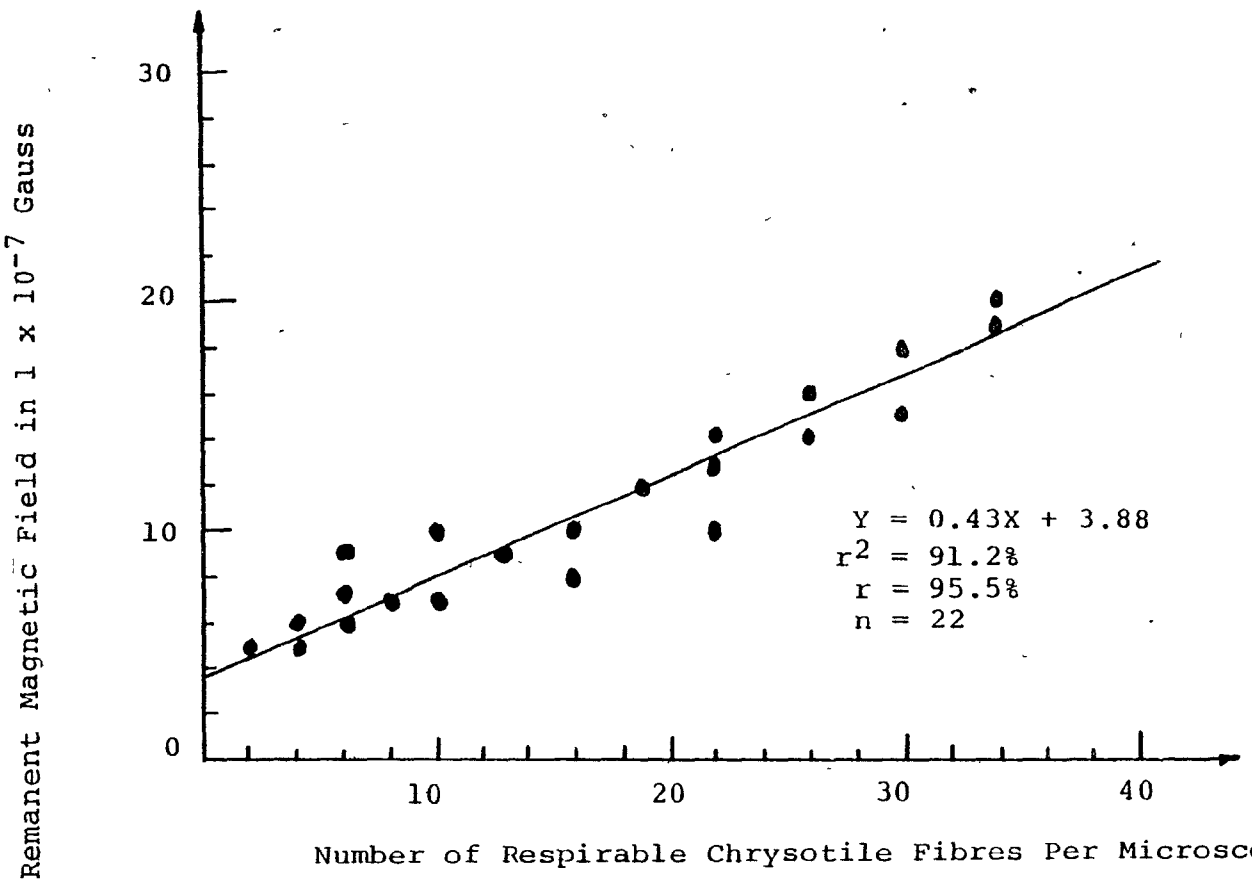


Fig. 9.23 - Calibration Line For Fibre Number Determination For Rhodesian Chrysotile U.I.C.C. Samples

The airborne samples from the bagging area show a more uniform iron distribution among the fibre bundles in figures 9-28-a, b, c, and d. During the electron microscopic studies, more than 100 single chrysotile fibres were analysed and it was concluded that iron or magnetite particles do not exist in the hollow cores of the chrysotile fibres, but that they are intimately attached to the fibres (see Fig. 9.29) and occur among the fibres in the fibre bundles (see Figs. 9.24, 9.28). The EDXA and SAED analysis results did not indicate any iron or other metal contamination from the milling process of the chrysotile ore. All of the observed iron or magnetite particles were either associated with antigorite and brucite particles or with chrysotile fibres.

## 9.5 Correlation of the Remanent Magnetic Fields With the Mass and Number of the Airborne Fibres in Various Locations of the Visited Mills and Their Interpretation:

Figures 9.30 to 9.32 show the correlation of the remanent magnetic field with the mass of respirable and total airborne dust, Figures 9.33 to 9.35 show the correlation between the remanent magnetic field and the number of airborne chrysotile fibres per microscopic field at various locations of Mill # VII.

Samples from the dry rock storage area indicate that the iron content of samples from this area is higher than that for other areas of the mill and, therefore, the slope

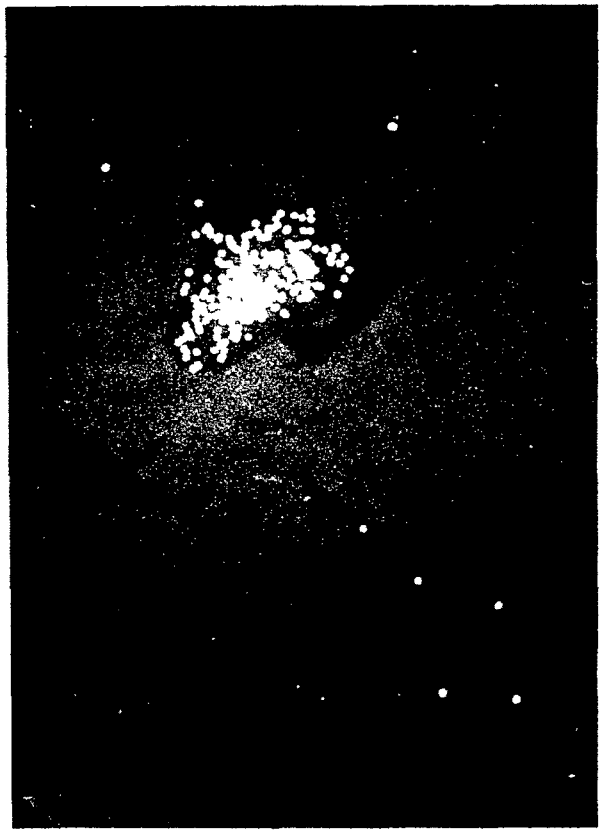

Scale: 0.5 cm = 1 μm (x5K)
(a)

Scale: 1.5 cm = 1 μm (x15K)
(b)

Fig. 9.24 Picture (a) shows a magnetite particle associated with short fibres.
Picture (b) shows a magnetite particle associated with submicroscopic fibres.
Magnetite identified by X-ray elemental mapping.

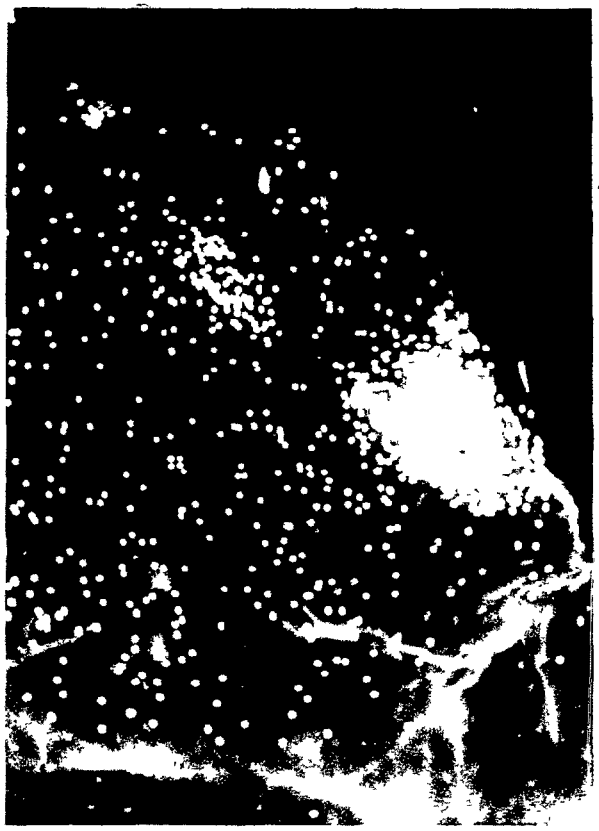

Scale: 3 cm = 1 μm (x30K)
(c)

Scale: 3 cm = 1 μm (x30K)
(d)

Fig. 9.24 Picture (c) shows a magnetite particle and some iron associated with a small fibre bundle.
Picture (d) shows magnetite associated with submicroscopic chrysotile fibres.

Scale: 0.5 cm = 1 μm (x5K)
(a)

Scale: 1.5 cm = 1 μm (x15K)
(b)

Fig. 9.25 Magnetic Particle associated with antigorite (at the bottom of picture "a" and in picture (b) magnified 15,000 times). Magnetite identified by X-ray elemental mapping.

Scale: 1 cm = 1 μm (x10K)
(a)

Fig. 9.26 Picture (a) shows a brucite particle.

Scale: 1·cm = 1 μm (x10K)
(a)

Fig. 9.27 Picture (a) shows a large antigorite particle surrounded by chrysotile fibres.

Scale: 0.5 cm = 1 μm (x5K)

(a)

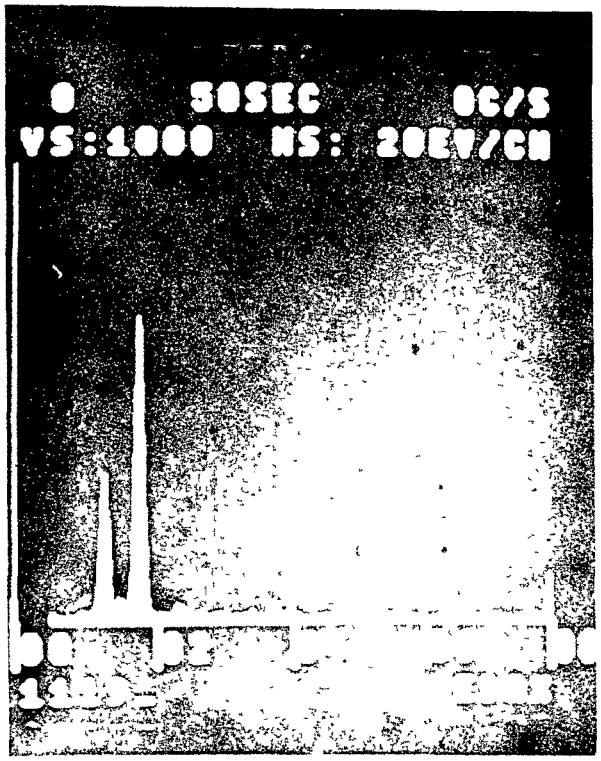


(b)

Fig. 9.28 Picture (a) shows a typical chrysotile fibre bundle and microdifraction patterns indicating iron content.
Picture (b) shows the EDXA analysis of the bundle.

Scale: 1 cm = 1 µm (x10K)
(c)

Scale: 5 cm = 1 µm (x50K)
(d)

Fig. 9.28 Picture (c) show the same chrysotile fibre bundle magnified 10,000 times and (d) fibre bundle magnified 50,000 times and showing a minute magnetite particle surrounded by fibres in the centre of the picture.

Scale: 3 cm = 1 μm (x30K)
(a)

Scale: 3 cm = 1 μm (x30K)
(b)

Fig. 9.29 Pictures (a) and (b) show a magnetite particle intimately attached to the chrysotile fibre.
Picture (b) shows the identification of the magnetite particle with X-ray elemental mapping.

of the correlation line is steeper. However, in all three areas of the mill, the iron content of the respirable and total airborne dust is practically the same (see Figs. 9.30 to 9.32). Although the remanent magnetic field is correlated very well with the mass of the collected samples, the indicated mass of the samples includes the mass of non fibrous dust, or other than chrysotile mass. In order to determine the chrysotile content of the total airborne respirable mass, the calibration line for Mill # VII should be used (see Fig. 9.9). However, if the iron content of the sample is not the same as the iron content of the chrysotile sample which is used to produce the calibration line, and since the measured remanent magnetic field is dependent on the mass and iron content of the chrysotile sample, determination of the sample mass should incorporate corrections for the iron content of field and calibration samples. As an example, if 3 milligrams of dust sample from the above bagging area of Mill VII were taken, Fig. 9.32 indicates a remanent magnetic field of $77.6 \times 10^{-7}$ gauss. The average iron content of samples in this area is 0.95 percent and the iron content of the chrysotile samples, which had produced the calibration line, is 1.05 percent. Rearranging the regression equation from Fig. 9.9 to estimate chrysotile mass from the measured remanent magnetic field and prorating the field and calibration sample iron contents, gives:

$$\frac{(77.6+26.5)\ 10^{-7}}{105.3 \times 10^{-7}} \times \frac{1.05}{0.95} = 1.08 \text{ mg. chrysotile. Therefore,}$$

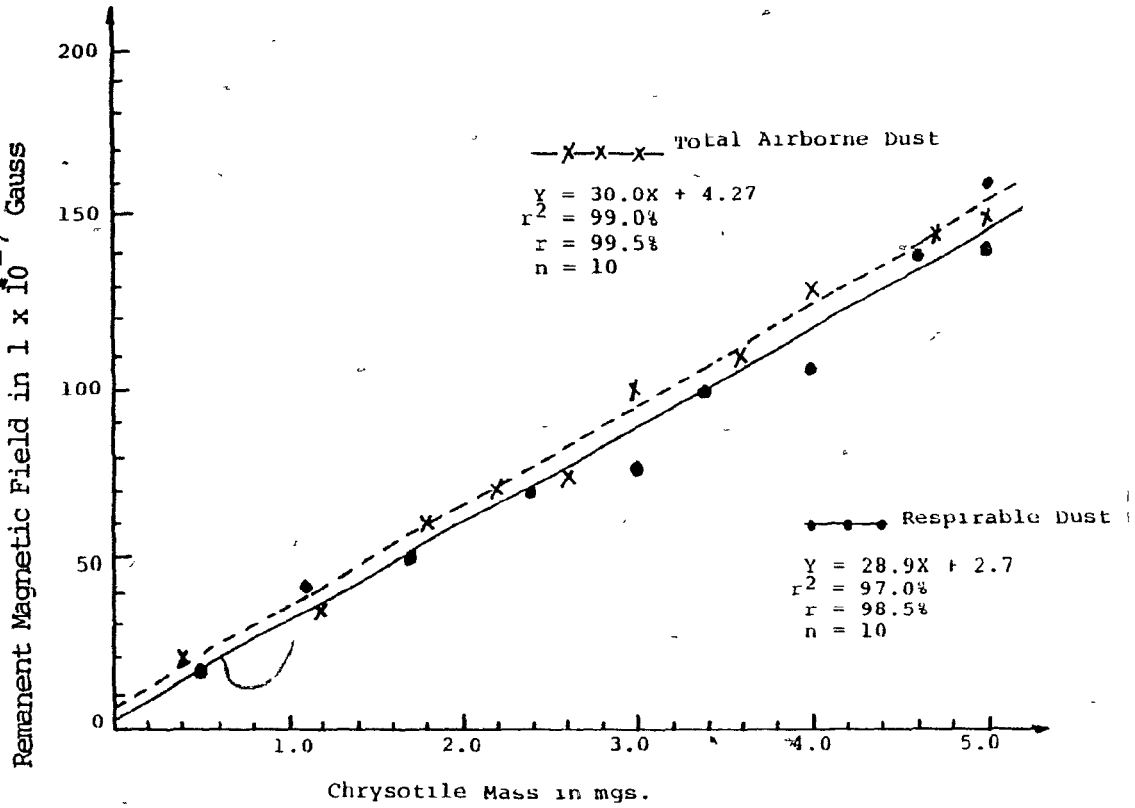


Fig. 9.30 - Correlation of the Remanent Magnetic Field with the Mass of Airborne Dust at Dry Rock Storage Area of Chrysotile Mill # VII.

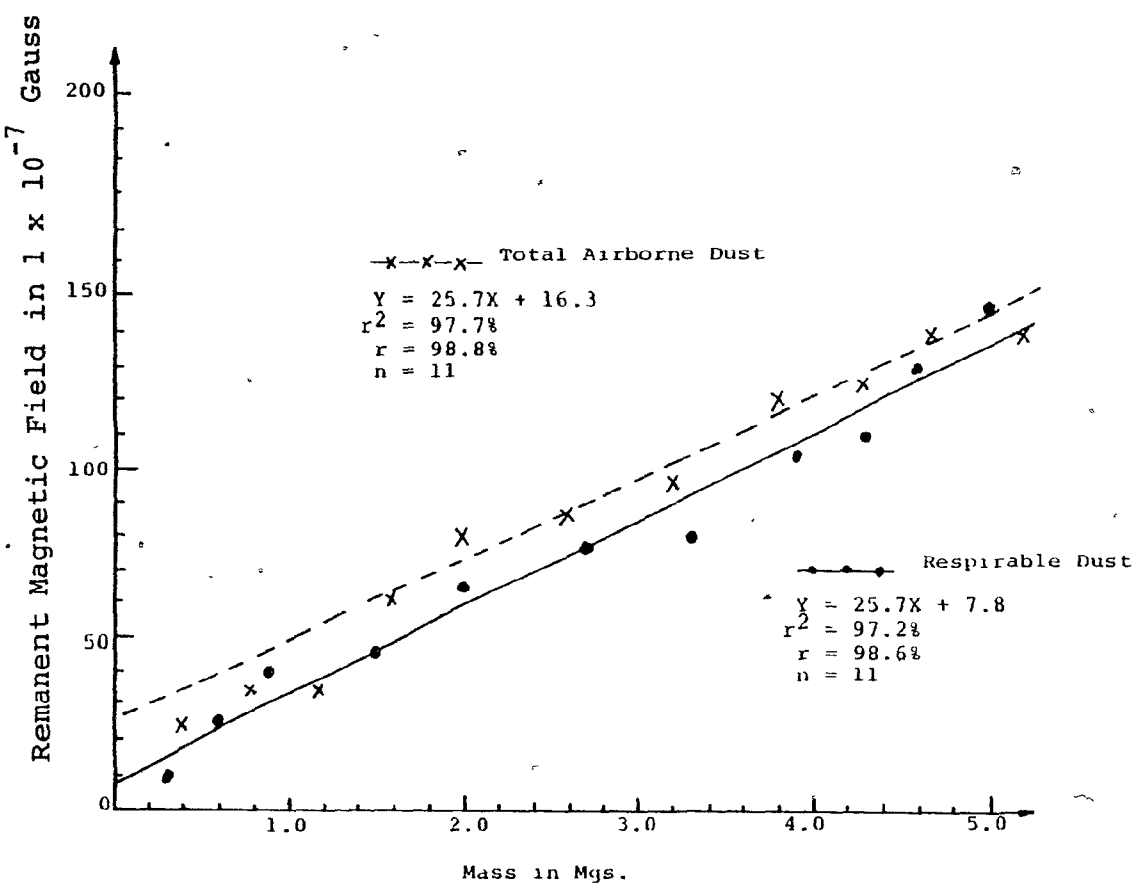


Fig. 9.31 - Correlation of the Remanent Magnetic Field with the Mass of Airborne Dust at Milling and Screening Area of Chrysotile Mill # VII.

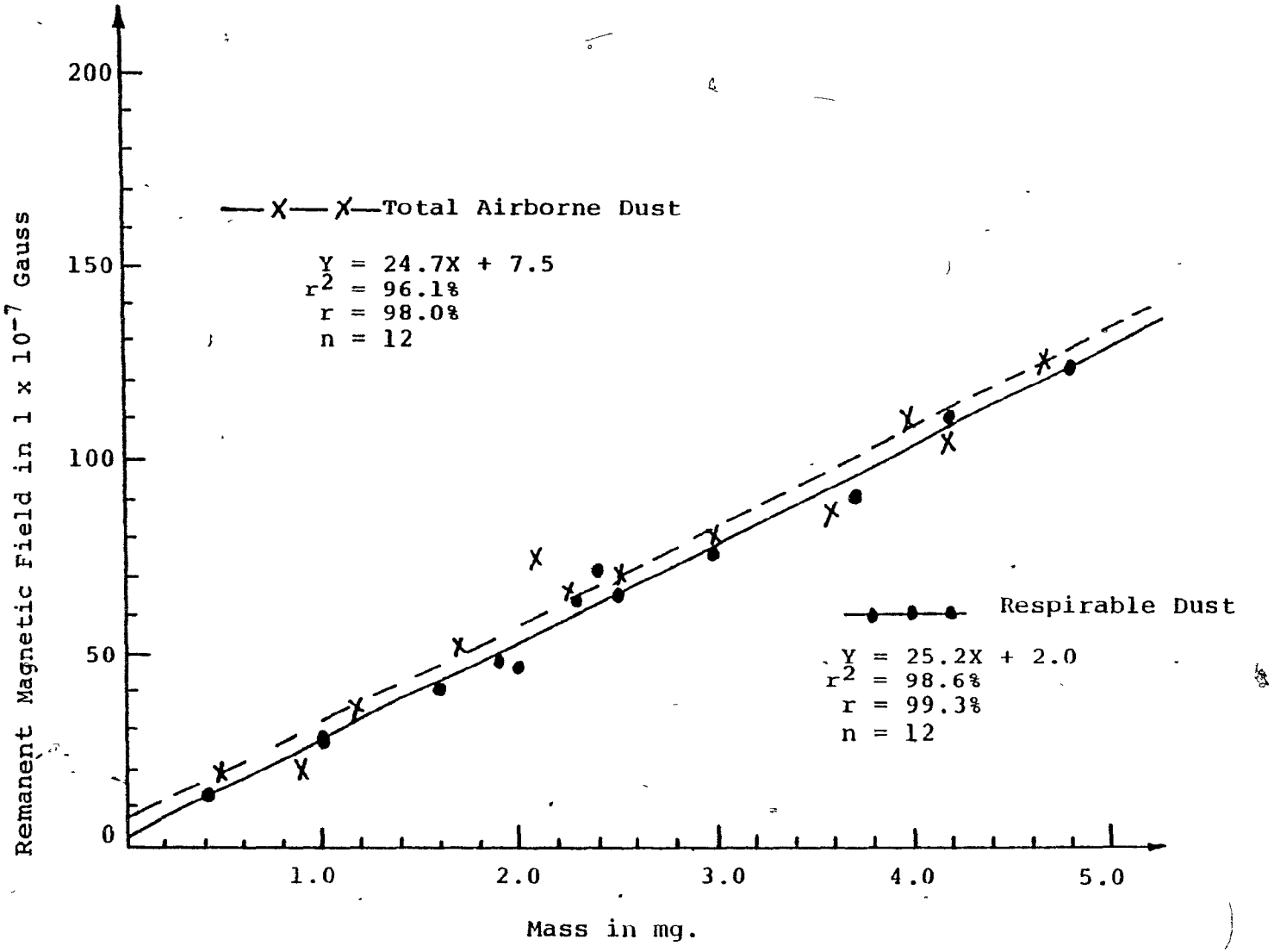


Fig. 9.32 - Correlation of the Remanent Magnetic Field with the Mass of Airborne Dust at Above Bagging Area of Chrysotile Mill # VII

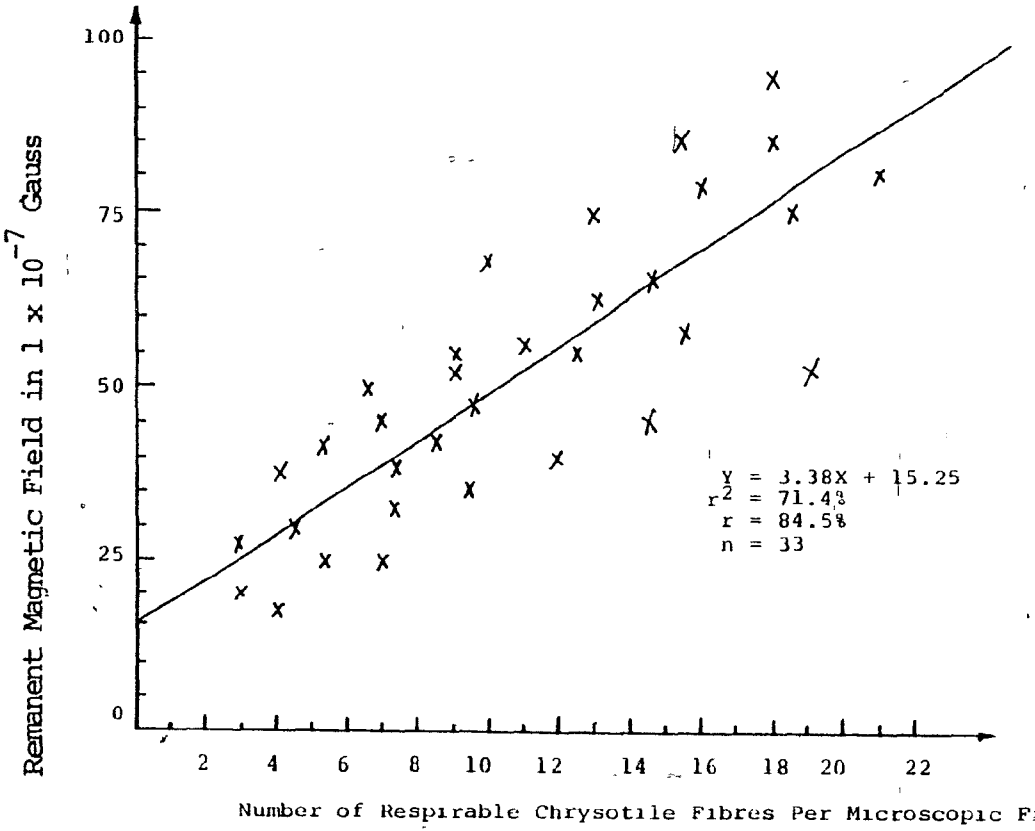


Fig. 9.33 - Correlation of the Remanent Magnetic Field with the Number of Airborne Respirable Chrysotile Fibre per Microscopic Field at Dry Rock Storage, Mill # VII

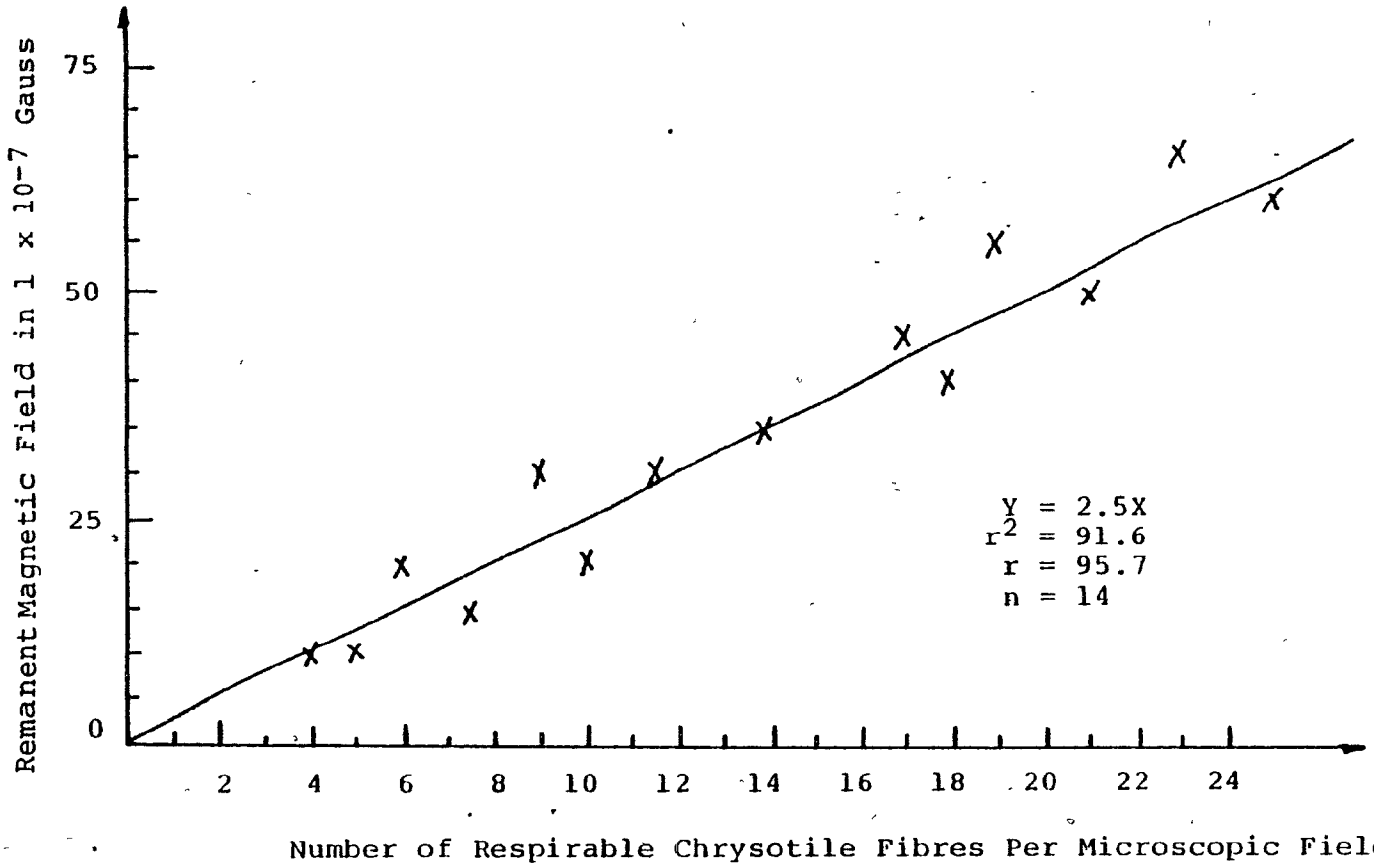


Fig. 9.34 - Correlation of the Remanent Magnetic Field with the Number of Airborne Respirable Chrysotile Fibres Per Microscopic Field at Milling and Screening Area, Mill # VII

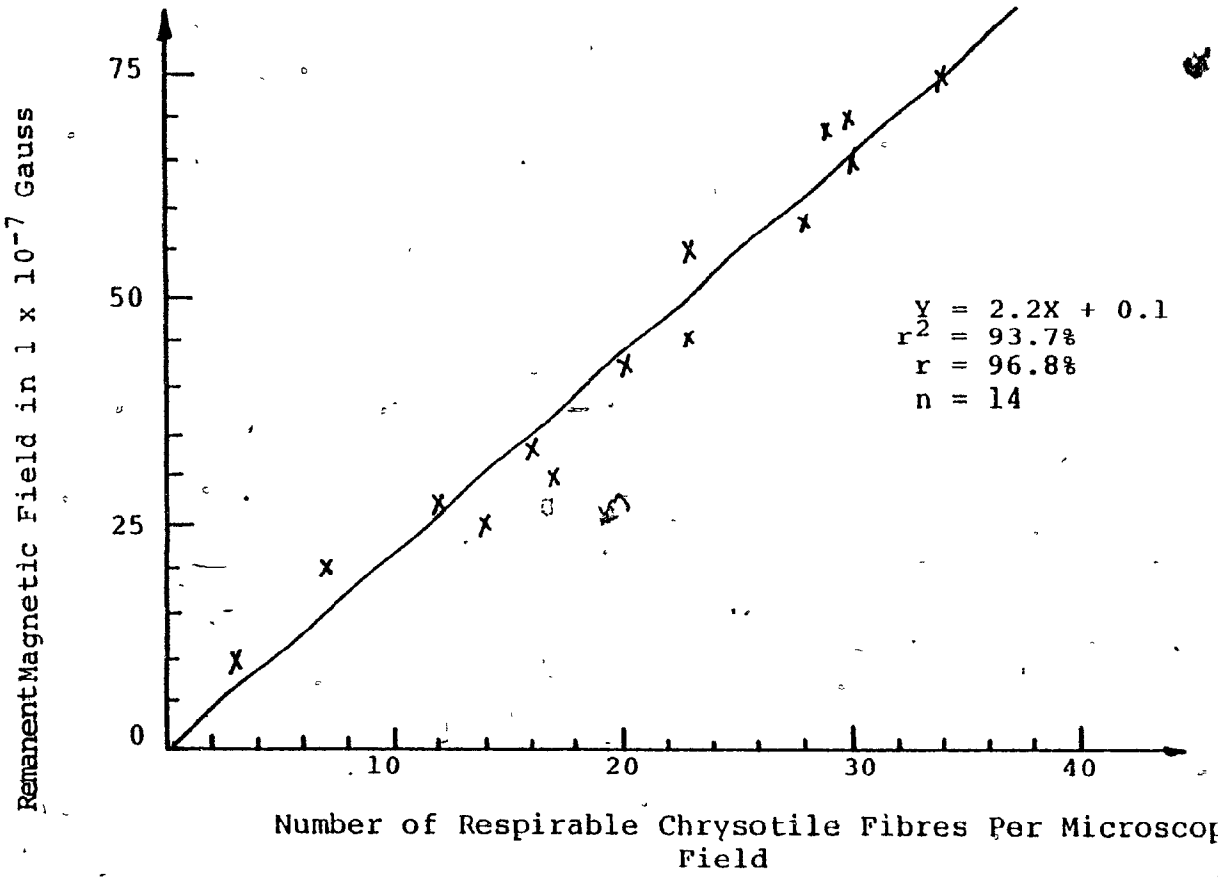


Fig. 9.35 - Correlation of the Remanent Magnetic Field With the Number of Airborne Respirable Chrysotile Fibre Per Microscopic Field at Above Bagging Area, Mill # VII

above the bagging area, the chrysotile content of the airborne dust sample is 35 percent. Similarly, the chrysotile content of the dust samples from the dry rock storage area, and from the milling and screening area are 24 and 31 percent respectively. From the mining engineers point of view, the additional finding is that the grade of the chrysotile ore can be determined by measuring the remanent magnetic field of the ore.

In considering the fibre count of the airborne dust at the dry rock storage area, the coefficient of correlation of the remanent magnetic field with the number of airborne respirable chrysotile fibres per microscopic field is 84.5 percent (see Fig. 9.33), lower than the coefficients of correlation for the milling and screening area, and for the bagging areas, which are 95.7 and 96.8 percent respectively. The reason for this being that, as the chrysotile ore is refined in different milling stages, iron-bearing rock and gangue minerals are separated from the chrysotile fibre samples. This causes the iron content of the ore to drop as the chrysotile is refined. Therefore, the measured remanent magnetic field of the end product is more indicative of the fibre count and the mass of chrysotile. However, since the associated remanent magnetic field is due to the iron content of the chrysotile sample, a relationship between the fibre counts of the field surveys and the calibration line for the fibre counts of Grade # 6

chrysotile can be established as follows. If the remanent magnetic field of a dry rock storage area sample is 90 x $10^{-7}$ gauss, with an iron content 2.02 percent, the estimated fibre count, according to calibration line in Fig. 9.20, would be:

$$\text{Fibre* Count} = \frac{(90-5.8)\ 10^{-7}}{1.83 \times 10^{-7}} \times \frac{1.05}{2.02} = 23.9 \text{ Fibres,}$$

which compares well with the actual count of 22 fibres per microscopic field.

*The iron content of the Grade "6" chrysotile is 1.05 and the formula of the calibration line is: Y=1.83X+5.8. In this calculation the 9 percent error is acceptable when compared with the ± 15 percent error due to human error in the microscopic counting technique. If the sampling time was 120 minutes and the sampling rate was 1.8 litres per minute, then the airborne respirable chrysotile content per cubic centimetre of air is:

$$\frac{1.075 \times 10^9\ \mu m^2 \text{ (total area of a 37 mm dia. millipore filter)}}{3440\ \mu m^2 \text{ (area of a microscopic field under 500 x)}} =$$

= 312561 number of fields per 37 mm diameter millipore filter.

$$\frac{312561 \text{ total No. of fields} \times 23.9 \text{ fibres/field}}{120 \text{ minutes} \times 1.8 \text{ litres/min.} \times 1000 \text{ cc/lt.}} =$$

= 34.6 fibres/cc of air

Note: Face masks were always used in this area during the actual mill survey.

However, for small number of fibres per microscopic

field, this error could reach as high as ± 50 percent. This is due to inconsistent iron contents of the airborne dust samples. In order to keep the error within acceptable limits, it is suggested that sampling times should be kept equal to or longer than two hours.

Similar observations can be made for Mill # VI airborne dust surveys (see Figs. 9.36 to 9.41). However, in this case, the repeatability of the results was investigated and the same mill was revisited 6 months after the first visit. As is seen in figures 9.36 to 9.41, dust survey correlation results from both visits are practically the same and chemical results indicated no change in the iron content of airborne samples. However, the remanent magnetic field difference between the smallest and largest sample being small (for example in figures 9.38 and 9.41 it is between $6 \times 10^{-7}$ gauss and $18 \times 10^{-7}$ gauss) the error of determination could be significantly large. In other words, the correlation lines are close to horizontal. Therefore, in order to minimize the error of determination, larger samples could be collected and the sampling time should be lengthened beyond two hours.

## 9.6 Correlation of the Remanent Magnetic Field Measurements of Lung Sepcimens from Autopsy of Asbestos Workers with the Determined Mass and Counts of Chrysotile.

The dry lung tissues provided by the Epidemiology Department at McGill were irregular in size and shape and differed from

the pure magnetite reference samples in the way that the magnetite was distributed over the sample area. The author had no control over possible iron contamination during disection.

Therefore, since the shapes of the lung tissues are different from each other and different from that of "the pure magnetite reference samples", the estimates of the magnetite and chrysotile content of the lung tissues may not indicate the true values. However, these estimates were calculated to observe if there was any rational relationship between the measured magnetic fields and the actual counts of fibres in the lung tissue specimens.

Magnetic measurements on these tissues were made at a sample-probe separation of 1 mm. The magnetite concentration, determined by remanent magnetic field measurements of dry lung tissue samples of asbestos workers, showed determination and correlation coefficients of 83.7 and 91.5 percent, respectively, when correlated with chrysotile concentrations in Fig. 9.42, and of 98.6 and 99.3 percent respectively, when correlated with fibre concentration in Fig. 9.44. However, there was no significant correlation between magnetite content per gram of dry lung tissue (see Fig. 9.43). Furthermore, the number of chrysotile fibres estimated by the magnetic method are approximately 20 to 25 times larger than the

actually counted number of chrysotile fibres. This discrepancy between the two results may be both attributed to the effective clearance mechanism of the lungs as explained in chapter V, section 5.4.4 of this thesis and the difference of the magnetite distribution between the lung specimens and the reference samples due to different geometry. Dr. Rowlands, who had counted the fibre content of the dry lung specimens, has stated that the counted total number of fibres are much lower than expected. It is believed that inhaled and deposited chrysotile asbestos fibres break down into submicroscopic fibrels, and because of their high rate of solubility in lungs, chrysotile fibres may be ingested and disappear from the lung tissue completely ([1]). Therefore, the observation of a small number of chrysotile fibres in the dry lung tissues of asbestos workers is not surprising.

However, the remanent magnetic field measurements of the dry lung tissues have indicated the existence of a magnetite content and since magnetite is, in the majority of the

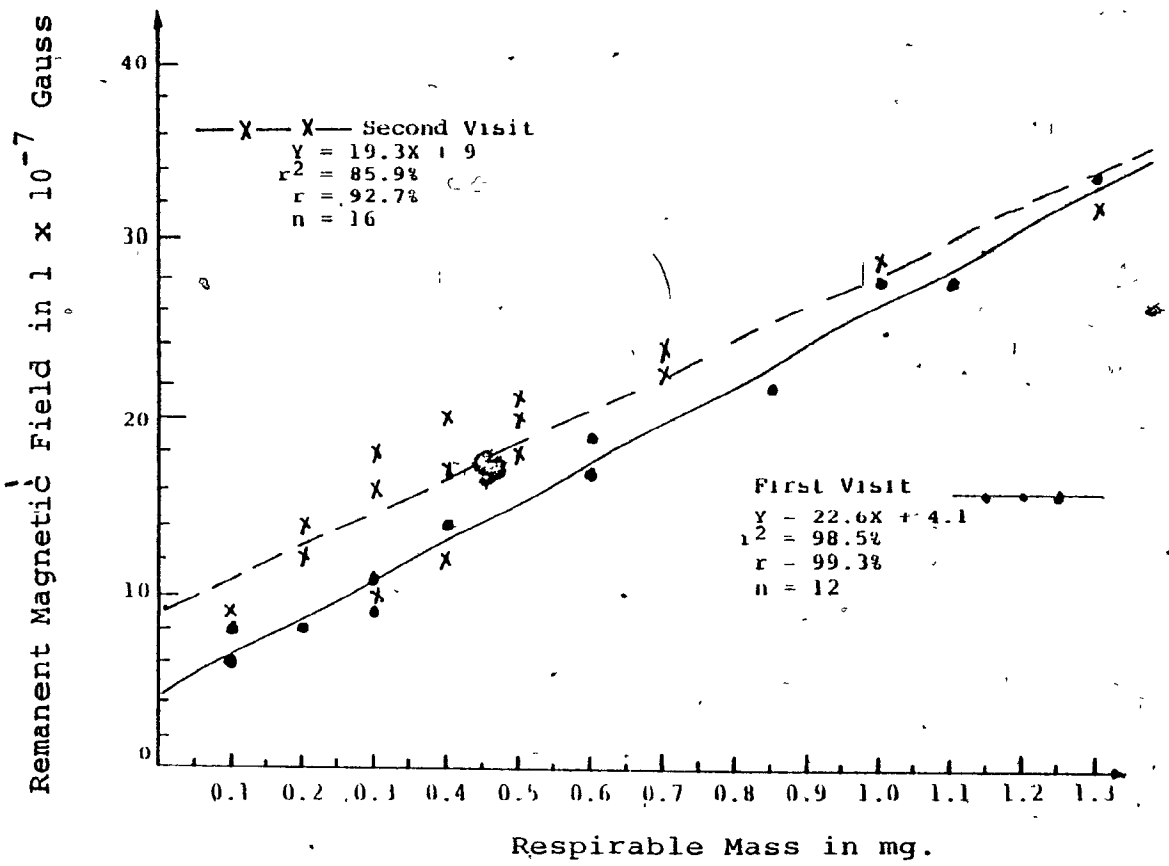


Fig. 9.36 - Airborne Respirable Dust at Dry Rock Storage Area of Mill # VI and its correlation with Remanent Magnetic Field.

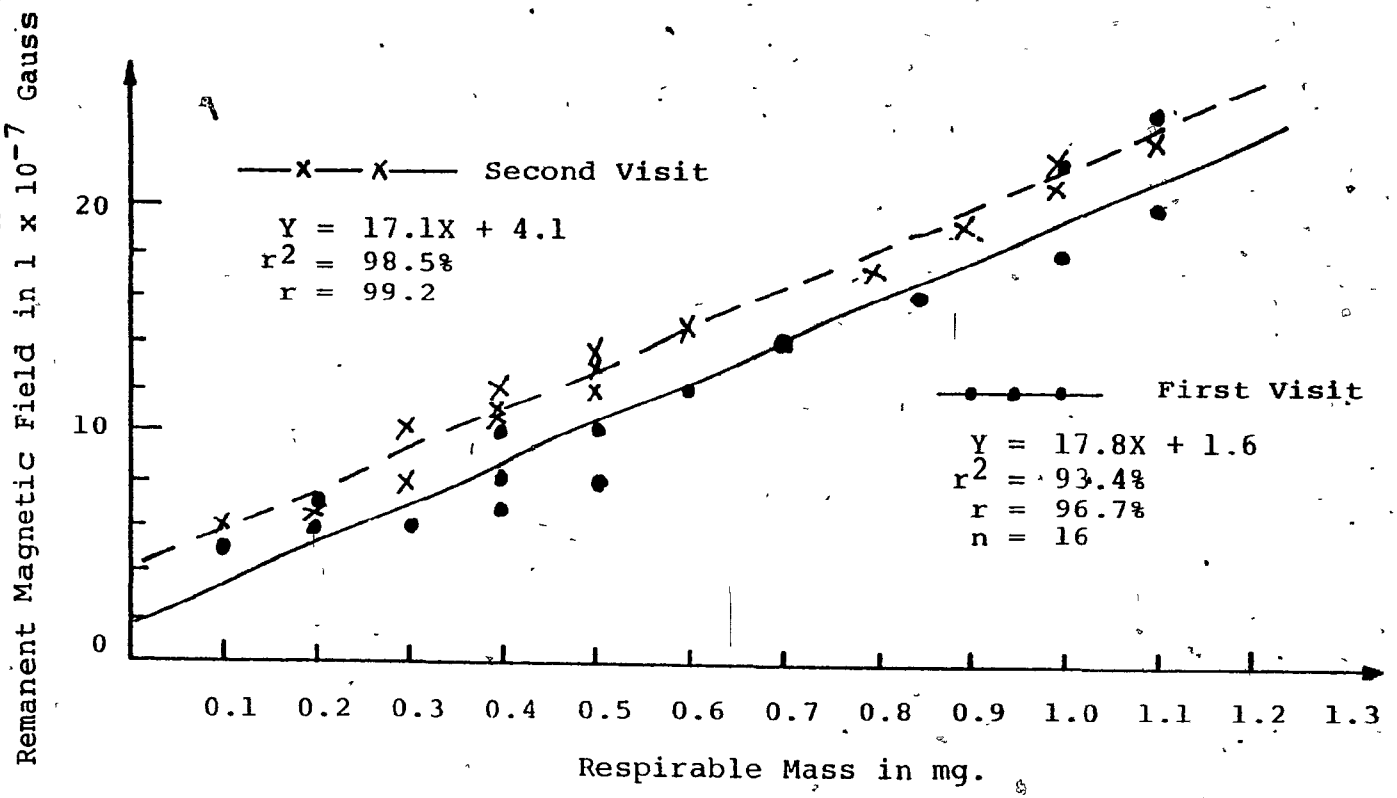


Fig. 9.37 - Airborne Respirable Dust At Milling and Screening Area of Mill # VI and it's correlation with Remanent Magnetic field

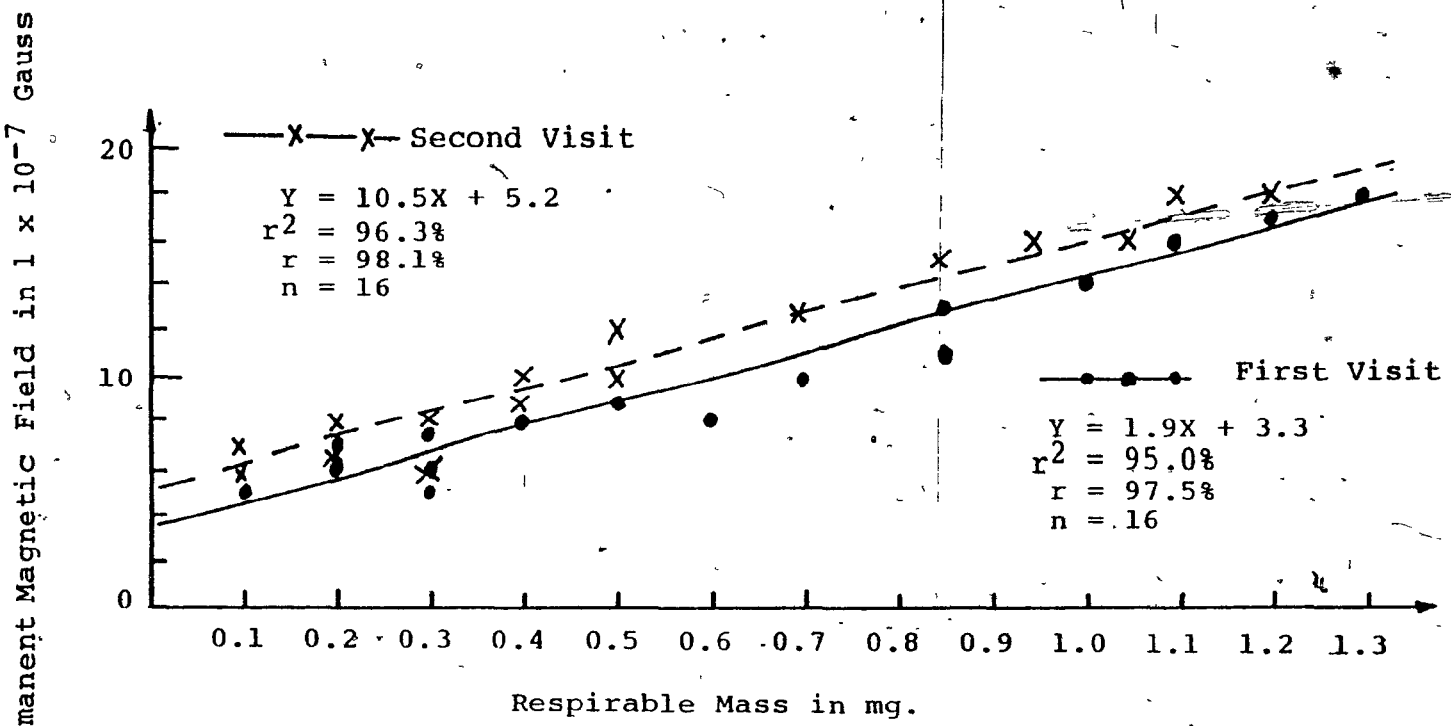


Fig. 9.38 Airborne Respirable Dust at Above Bagging Area of Mill # VI and it's correlation with Remanent Magnetic field

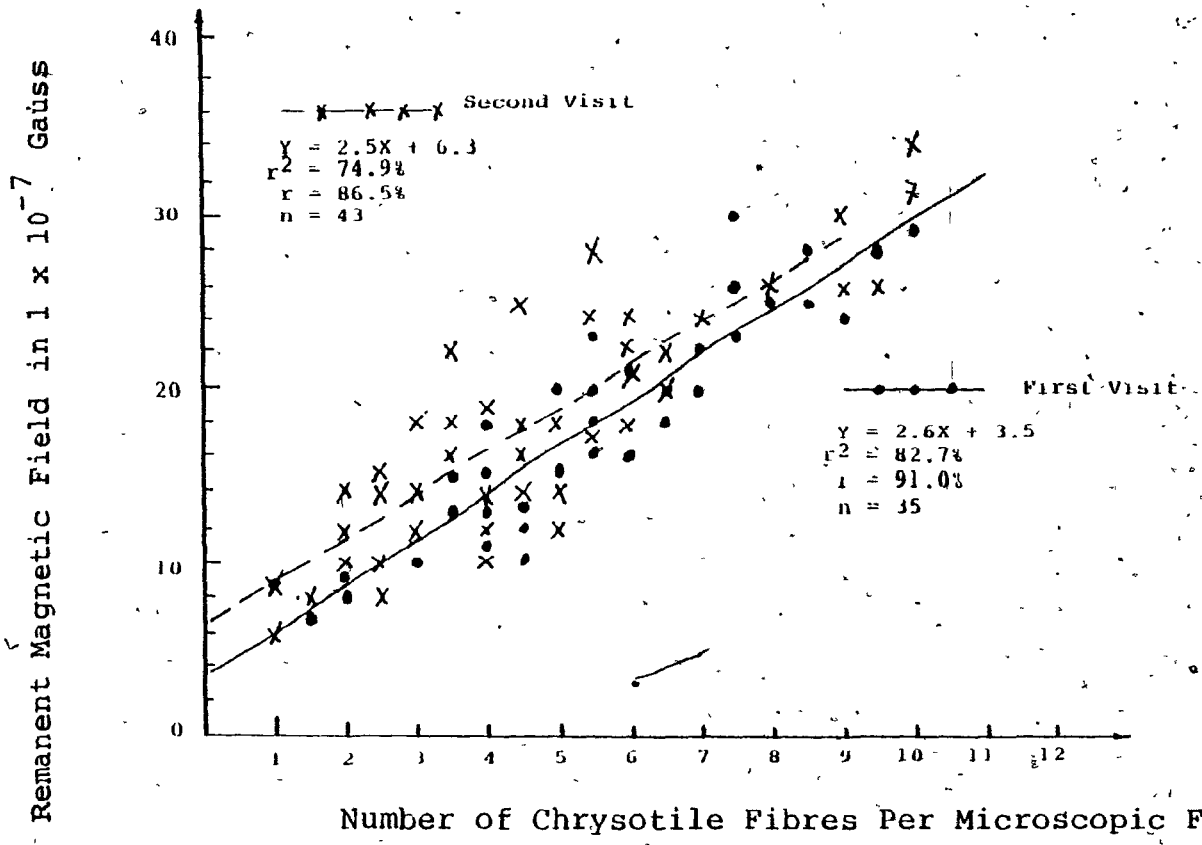


Fig. 9.39 - Correlation of the Remanent Magnetic Field with the Number of Airborne Respirable Chrysotile Fibre Per Microscopic Field at Dry Rock Storage Area of Mill # VI.

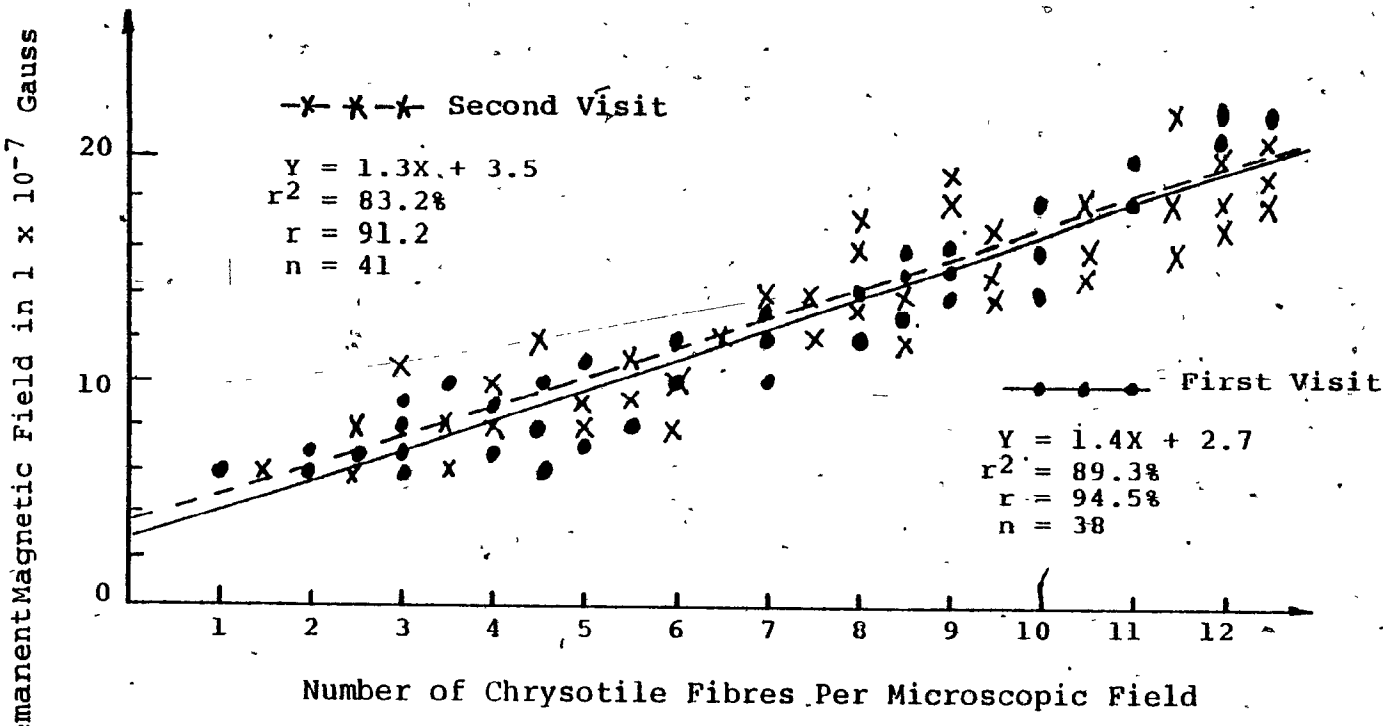


Fig. 9.40 - Correlation of the Remanent Magnetic Field With the Number of Airborne Respirable Chrysotile Fibres Per Microscopic Field At Milling & Screening Area of Mill # VI

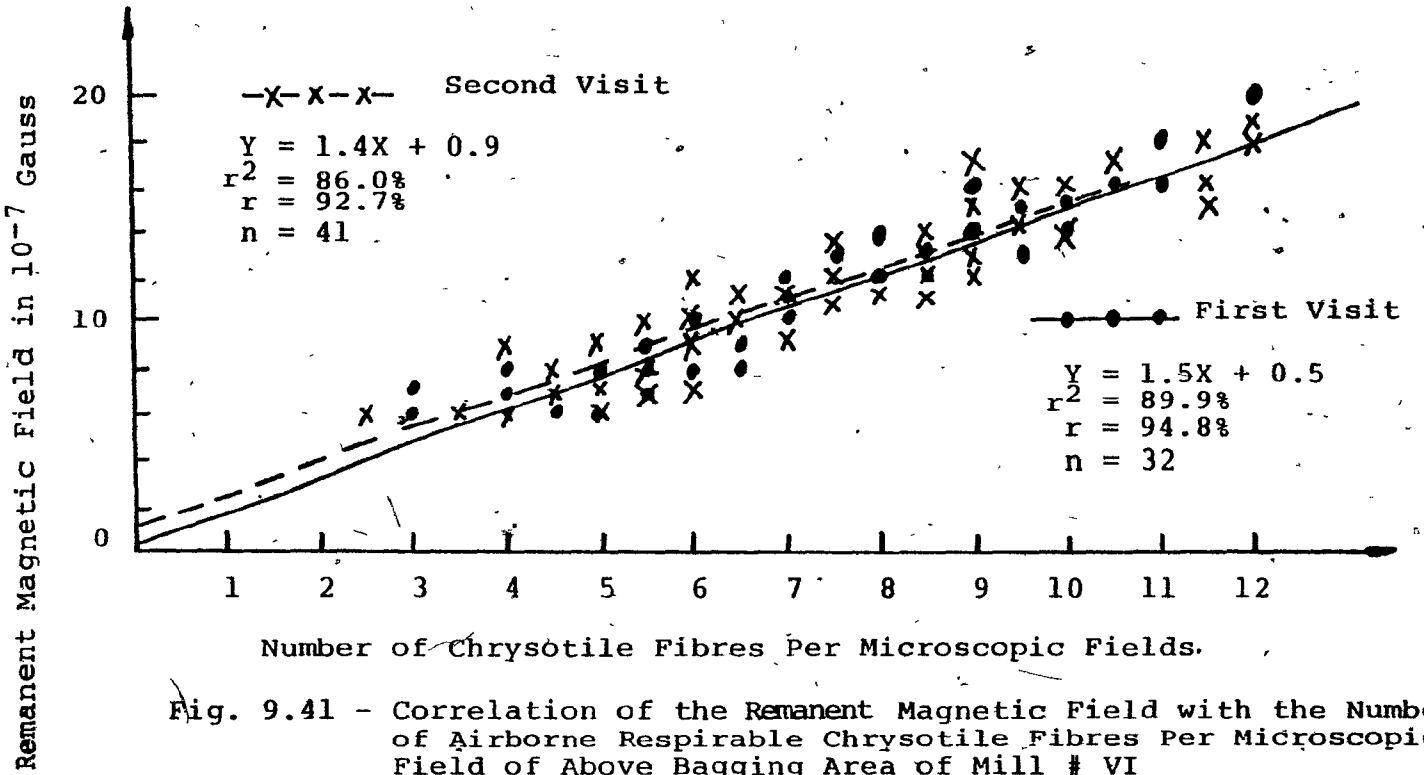


Fig. 9.41 - Correlation of the Remanent Magnetic Field with the Number of Airborne Respirable Chrysotile Fibres Per Microscopic Field of Above Bagging Area of Mill # VI

cases, attached to, and associated with, airborne chrysotile, the co-existence of both minerals in the lungs may not be an unexpected occurrence.

The encouraging aspect of this experimental research is that where no chrysotile fibre count was reported, there was either no detectable remanent magnetic field associated with that particular lung specimen or it was significantly lower than that for lung specimens which were reported to contain chrysotile (see table 9.6 specimens # B22 to B44). Similarly as the measured magnetic field intensity has increased, the reported actual chrysotile fibre counts have also increased. Cohen et al's[1] research in "Magnetic lung measurements in relation to occupational exposure in asbestos miners and millers of Quebec" have also indicated that the magnetic method, in principle, is sensitive to the individual differences in deposition and clearance and may not indicate the exact fibre content of the lungs. However, it might be useful in the primary industries to detect

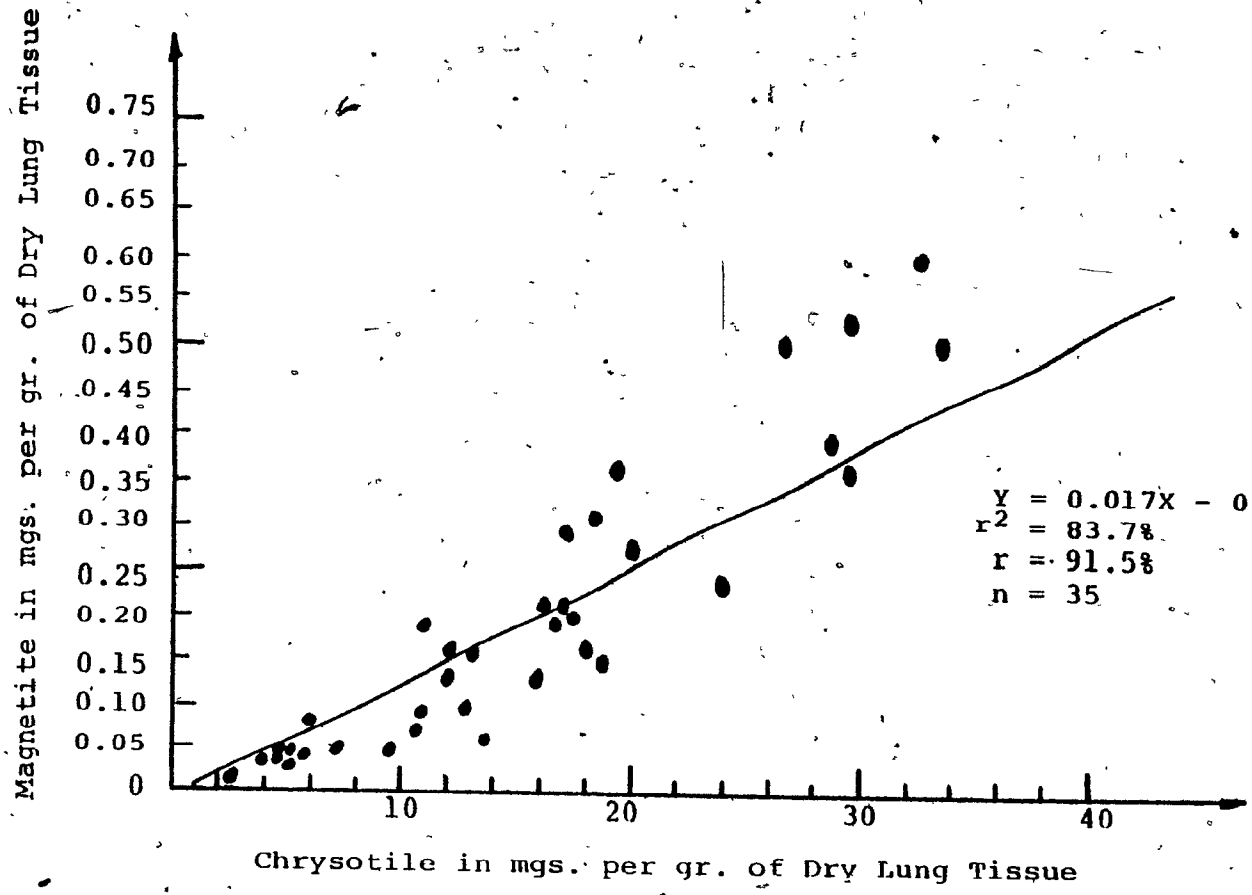


Fig. 9. 42- Determination of the mass of Chrysotile Content of the Dry Lung Tissue by Magnetic Measurements

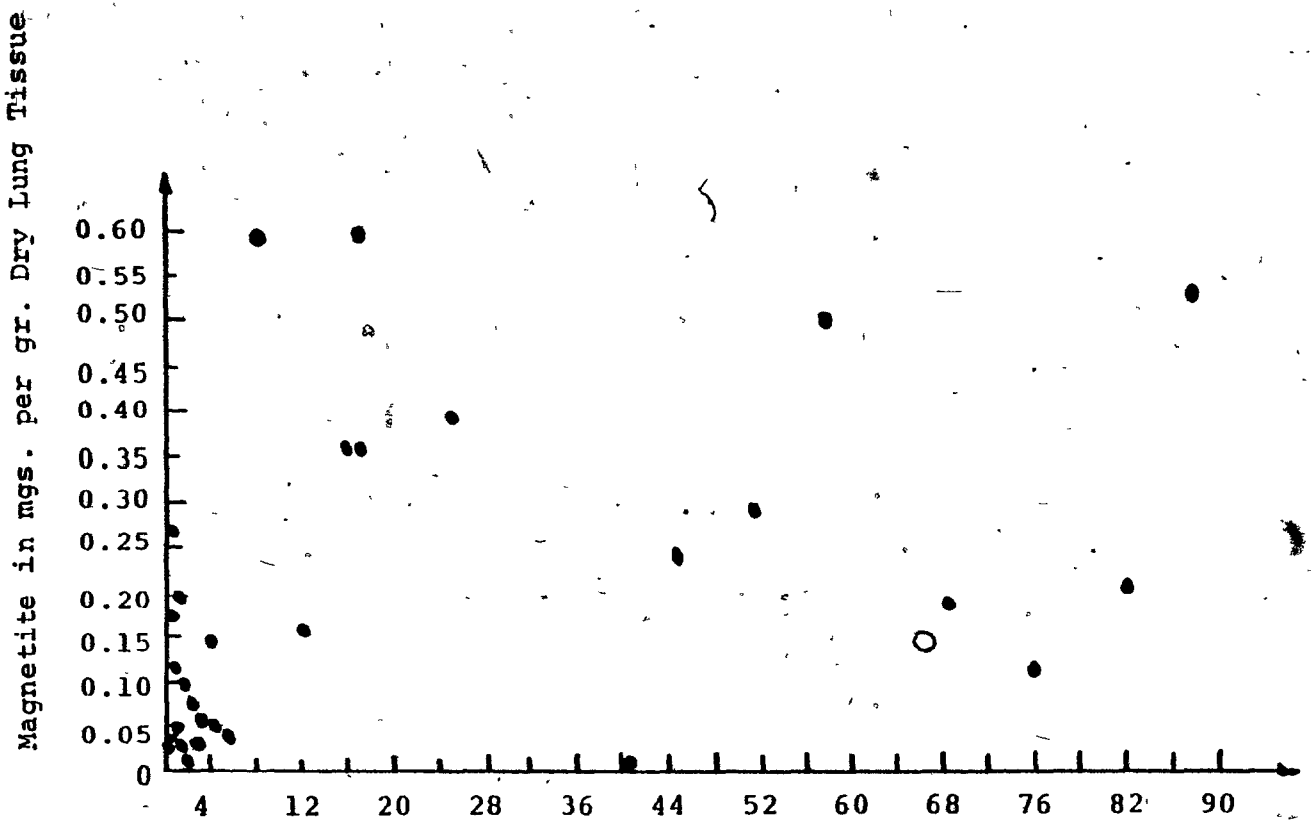


Fig. 9.43 - Plot of Chrysotile Fibre and $Fe_3O_4$ Contents of Dry Lung Tissues.

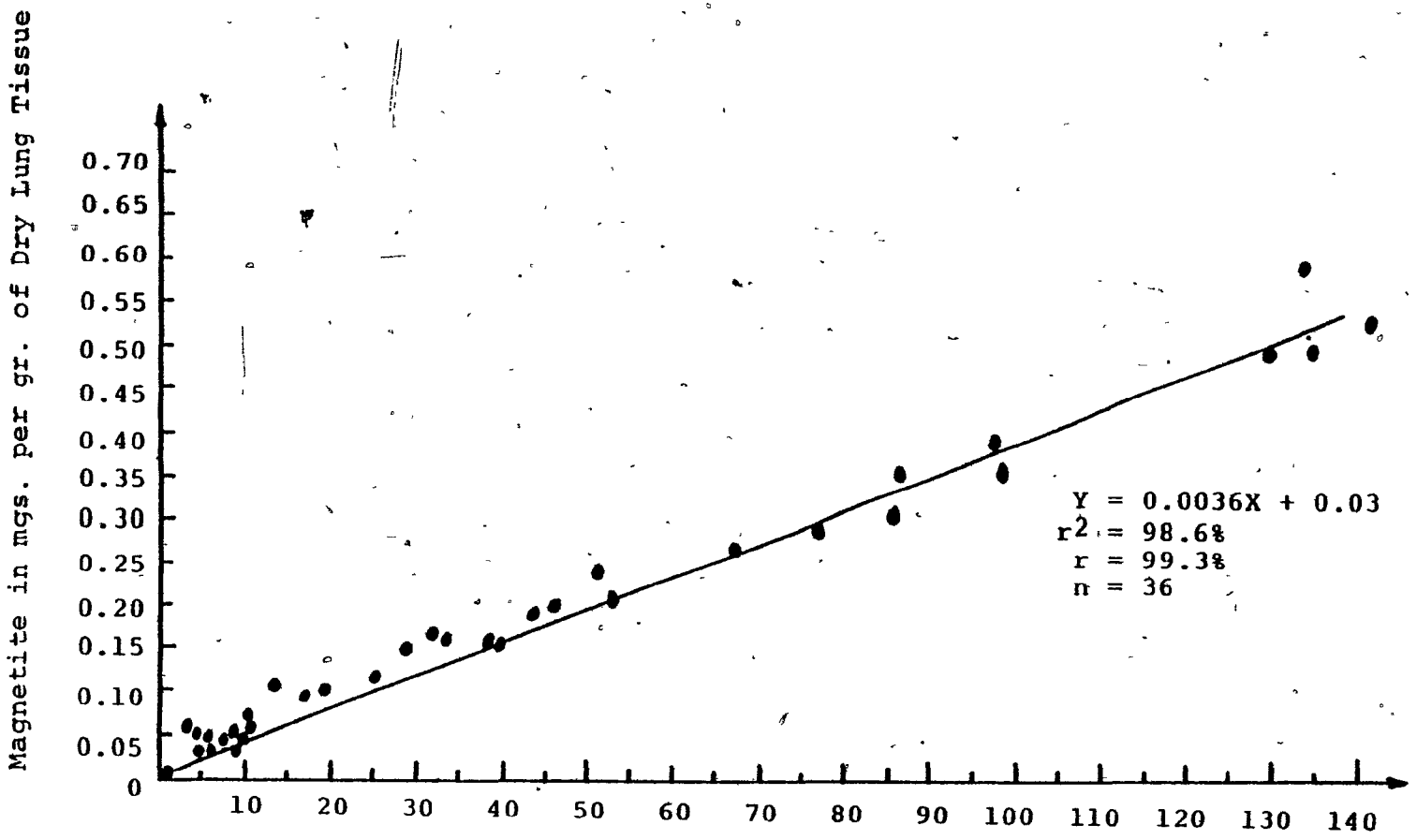


Fig. 9.44 - Correlation of the Number of Chrysotile Fibre Content of the Dry Lung Tissue with $Fe_3O_4$ content as Determined by Remanent Magnetic Field Measurement Method

workers with impaired clearance by measuring comparably higher magnetic fields than is normal[1].

Therefore, although the association of magnetite particles with chrysotile fibres permits estimation of the mass and concentration of chrysotile in airborne dust, via the remanent magnetic field, different clearance rates from the lungs for each mineral may change the magnetite to chrysotile ratio in lung tissue samples. However, whilst the magnetic lung measurements may not indicate the exact amount and concentration of chrysotile in the lung, the persisting remanent magnetic fields of the asbestos worker's lungs may indicate the dose of chrysotile to which a worker may have been exposed.

9.7 Recommendations for Further Research:

Although it has been shown that, with remanent magnetic field measurements, the mass and number of airborne respirable fibres of chrysotile can be determined, the application of the magnetic measurements to human lungs and determination of the chrysotile content or the dose of exposure to the asbestos dust needs to be investigated further. Specifically, the question of "possible risk to human lungs from magnetometric dust clearance experiments", raised by Sterling[5], has to be answered.

Table 9.6 - Actual Dust Counts and Magnetically Determined Magnetite and Chrysotile Content of the Dry Lung Tissues of Asbestos Workers:

| Survey No. | Weight of the Dry Lung Tissue in mgs. | Number of Fibres per gram of Dry Lung Tissue $1 \times 10^6$ | Number of Chrysotile Fibres per gram of Dry Lung Tissue $1 \times 10^6$ | % Chrysotile of the Total Fibre Count | Magnetic Reading in $1 \times 10^{-7}$ Gauss | Magnetite Per gram of Dry Lung Tissue in mgs. | Magnetically Determined Chrysotile per gram dry Lung Tissue in mgs. | Magnetically Determined Number of Chrysotile Fibres per gram of Dry Lung Tissue $1 \times 10^7$ |
|---|---|---|---|---|---|---|---|---|
| A8 | 17.5 | 76 | 15.2 | 20 | 43 | 0.36 | 29.36 | 86.8 |
| A9 | 51.0 | 42 | 15.1 | 36 | 213 | 0.60 | 32.40 | 165 |
| A16 | 79.0 | 37 | 14.8 | 40 | 197 | 0.36 | 19.56 | 98.4 |
| A17 | 69.0 | 4 | | | 14 | 0.03 | 4.63 | 5.0 |
| A18 | 21.0 | 43 | 12.0 | 28 | 23 | 0.16 | 18.08 | 33.7 |
| A20 | 25.8 | 26 | 1.0 | 4 | 35 | 0.20 | 17.84 | 46.3 |
| A15 | 35.0 | 409 | 81.8 | 20 | 51 | 0.21 | 16.21 | 52.7 |
| A25 | 28.9 | 9 | 0.4 | 4 | 53 | 0.27 | 20.09 | 66.6 |
| A29 | 42.3 | 231 | 87.8 | 38 | 154 | 0.53 | 29.72 | 142.4 |
| B1 | 16.9 | 100 | 45.0 | 45 | 27 | 0.24 | 24.06 | 51.5 |
| B6 | 22.0 | 145 | 58.0 | 40 | 76 | 0.50 | 33.40 | 130.0 |
| B7 | 18.8 | 40 | 4.0 | 10 | 19 | 0.15 | 18.78 | 29.0 |
| B12 | 81.4 | 28 | 5.6 | 20 | 21 | 0.04 | 4.50 | 7.7 |
| B14 | 86.9 | 3 | | | 17 | 0.03 | 3.91 | 5.3 |
| B17 | 28.0 | 16 | (impossible to analyse) | | 23 | 0.12 | 13.56 | 25.3 |
| B19 | 95.0 | 8 | | | 29 | 0.045 | 4.42 | 10.0 |
| B20 | 61.0 | 36 | 4.3 | 12 | 209 | 0.50 | 26.65 | 133.4 |
| B21 | 20.6 | 115 | 25.3 | 22 | 55 | 0.30 | 28.84 | 97.4 |
| B22 | 5.6 | 50 | | | NIL | NIL | NIL | NIL |
| B28 | 16.0 | 127 | 76.2 | 60 | 11 | 0.11 | 18.71 | 13.8 |
| B30 | 10.0 | 51 | 40.8 | 80 | NIL | NIL | NIL | NIL |
| B31 | 16.8 | 15 | | | 19 | 0.17 | 21.01 | 32.5 |
| B38 | 14.1 | 6 | | | NIL | NIL | NIL | NIL |
| B41 | 12.0 | 8 | | | NIL | NIL | NIL | NIL |
| B44 | 62.3 | 24 | | | NIL | NIL | NIL | NIL |
| B16 | 67.0 | 7 | | | NIL | NIL | NIL | NIL |
| B49 | 41.0 | 35 | 3.5 | 10 | 16 | 0.06 | 8.12 | 10.3 |
| B58 | 8.0 | 72 | 8.6 | 12 | 32 | 0.59 | 55.01 | 134.1 |
| B60 | 98.1 | 26 | 2.1 | 8 | 8 | 0.013 | 2.85 | 1.0 |
| B63 | 65.7 | 21 | | | 20 | 0.047 | 5.47 | 8.9 |
| B67 | 56.7 | 96 | 51.8 | 54 | 113 | 0.20 | 17.33 | 76.9 |
| B55 | 14.5 | 125 | 20 | 16 | 307 | 3.06 | 157.38 | |
| B71 | 27.2 | 573 | 68.8 | 12 | 35 | 0.19 | 16.92 | 43.9 |
| B75 | 60.0 | 13 | 2.6 | 20 | 130 | 0.31 | 18.27 | 86.2 |
| B11 | 27.8 | 32 | 1.6 | 5 | 19 | 0.10 | 12.70 | 19.6 |

Table 9.6 (continued)

| Survey No. | Weight of the Dry Lung Tissue in mgs. | Number of Fibres per gram of Dry Lung Tissue $1 \times 10^6$ | Number of Chrysotile Fibres per gram of Dry Lung Tissue $1 \times 10^6$ | % Chrysotile of the Total Fibre Count | Magnetic Reading in $1 \times 10^{-7}$ Gauss | Magnetite Per gram of Dry Lung Tissue in mgs. | Magnetically Determined Chrysotile per gram Dry Lung Tissue in mgs. | Magnetically Determined Number of Chrysotile Fibres per gram of Dry Lung Tissue $1 \times 10^7$ |
|---|---|---|---|---|---|---|---|---|
| B25 | 28.9 | 8 | 0.3 | 4 | 13 | 0.07 | 10.82 | 10.4 |
| A5 | 31.7 | 11 | (impossible to analyse) | | NIL | NIL | NIL | NIL |
| A4 | 19.7 | 5 | (impossible to analyse) | | 7 | 0.06 | 13.84 | 3.0 |
| A12 | 56.2 | 7 | (impossible to analyse) | | 14 | 0.04 | 5.68 | 6.1 |
| B26 | 40.0 | 5 | (impossible to analyse) | | 44 | 0.16 | 13.01 | 39.0 |
| B45 | 49.0 | 4 | (impossible to analyse) | | 54 | 0.16 | 11.99 | 40.1 |
| B66 | 32.4 | 27 | (impossible to analyse) | | 19 | 0.09 | 10.90 | 16.8 |
| B68 | 44.1 | 6 | (impossible to analyse) | | 15 | 0.05 | 7.40 | 8.7 |
| B74 | 29.8 | 4 | (impossible to analyse) | | 9 | 0.05 | 9.60 | 4.7 |

On the basis of his literature review, Sterling states that,"when the lung content is magnetized, the ferromagnetic particles migrate within the viscous media of the lungs and form clusters of particles." Since the cluster of particles cannot be cleared from the lungs easily, it could create a potential risk to the health of human lungs[5]. However, it is known that human lungs contain viscous mucus and that the tissues are very elastic. It is probable, therefore, that the formation of clusters introduces an elastic distortion of the tissues and, if the field is not maintained too long, relaxation of the tissues and the action of viscous fluids may redisperse the clusters, thus accounting for Cohen's observed reduction in field intensity with time[6]. However, experimentally, the extent of the risk of causing any harm to the lungs should be investigated and, if it is proven not to be harmful, the research in magnetic lung surveys of humans should only then progress.

In order to test further the use of the magnetic method in determining the magnetite or iron content of the dry lung tissues, it is recommended that the iron content of dry lung tissues should be determined using another analytical method and results of both methods should be compared.

Furthermore, in determining the dose of chrysotile dust exposure using the magnetic method, it is necessary to calculate the dust exposure index accurately and to analytically understand the clearance mechanism of the lungs. Otherwise the magnetically estimated dust exposure results will not correlate with the calculated dust exposure index.

It is also recommended that more sensitive balances and megnetometers be used in order to improve the sensitivity of mass and fibre number determination.

As this current research was carried out under laboratory conditions, some field tests, to determine the extent of interference due to magnetic noise in the mine environment, would be needed.

In view of Dr. Cohen's experience [1] where it was possible to measure magnetic fields associated with magnetite in human subjects in the Thetford mines area it is likely that such magnetic noise would not be a serious problem.

## CONCLUSIONS

With the experimental arrangements used in this research it was found that:

1. Experimental data have shown that there is a linear relationship between the mass and the remanent magnetic field of pure magnetite. Therefore, by measurement of the remanent magnetic field of a sample of pure magnetite with a gradiometric fluxgate magnetometer the mass of magnetite in the sample can be determined directly after quantitative definition of the relationship relative to a standard pure magnetite sample.

2. Extensive microscopic investigations and chemical analyses have shown that the mass ratio of chrysotile to magnetite is constant for each specific commercial grade of chrysotile produced in a specific Quebec Chrysotile mill. This mass ratio varies from mill to mill.

3. The agreement between theoretical and experimentally determined sizes of fibres collected as a respirable fraction utilizing horizontal eleutriation to remove nonrespirable fibres and dust were good. Therefore, Hexhlet horizontal eleutriator would seem to be a suitable instrument for the determination of the respirable fraction of airborne dust in Quebec Chrysotile mills.

4. When bulk samples of chrysotile asbestos are rendered airborne the mass ratio of magnetite to chrysotile (as

measured by magnesium content) in the airborne respirable size fraction of dust is constant and similar to that in the bulk product.

5. The remanent magnetic fields of airborne pure magnetite and of the magnetite associated with chrysotile asbestos are similar to within ± 10 percent. Therefore, it is concluded that the measured magnetic fields of airborne chrysotile fibres are essentially due to magnetite particles which are intimately associated with fibres. This relationship was investigated further and it was found that the measured remanent magnetic fields were correlated with microscopic fibre counts but not with total particle counts, which is another indication that magnetite particles are mainly associated with the chrysotile fibres.

6. It has been established that magnetite is intimately associated with chrysotile fibres in a constant proportion for a given grade of chrysotile, and that a linear relationship exists between the remanent magnetic field and mass of magnetite in the sample. Thus, the remanent magnetic field also indicates the mass of chrysotile for a specific grade.

7. It was shown that airborne chrysotile fibre concentrations are also linearly related to measured remanent

magnetic fields. Based on this linear relationship, for each Quebec asbestos mill, curves were developed to predict both mass and number of fibres in airborne dust samples using magnetic field measurements.

8. At present there are very limited number of methods to differentiate and determine the mass of chrysotile from serpentine in airborne dust samples. The relationship obtained suggests that magnetic measurements might be applicable to the determination of chrysotile dust in Quebec chrysotile mine and mill environments. An advantage is that it is a rapid and practical method and training in the use of the fluxgate magnetometer is very easy. Each measurement is repeatable with an error ± 5 per cent.

9. In view of the documented relatively low proportion of non - magnetic iron associated with chrysotile and the reasonably good relationships between the measured magnetic field and iron content of the various grades of commercial chrysotile it is possible that, from a mining engineers point of view, these relationships might have the potential for the evaluation of the grade and iron content of the chrysotile ore.

10. The remanent magnetic field measurements of dry lung tissues obtained at autopsies did not correlate well with the actual fibre counts. Thus it appeared on the limited series studied that magnetic lung measurements do not give exact fibre contents of lung tissue. It is probable that the size, shape and other lung tissue variables as well as differences in the lung clearance rates for magnetite and chrysotile are responsible for such lack of correlation.

## REFERENCES FOR CHAPTER IX


1. Cohen, D., Crowther, T.S., Gibbs, G.W., Becklake, M.R. "Magnetic Lung Measurements in Relation to Occupational Exposure in Asbestos Miners and Millers of Quebec," Environmental Research, 1981, Vol. 26, pp. 535-550.

2. Kennedy, J.B., and Neville, A.M. "Basic Statistical Methods for Engineers and Scientists," 2nd Edition, IEP a Dun-Donnelley Publisher, New York, 1976, pp. 178-180, 218-219, 264-271, 298-301, 310-313, 452-454, 457, 460-463.

3. Timbrell, V., Rendal, R.E.G. "Preparation of the U.I.C.C. Standard Reference Samples of Asbestos," Powder Technology, Elsevier Sequoia S.A. Lausanne, Netherland, 1971/72, Vol. 5, pp. 279-287.

4. Gibbs, G.W., and DuToit, R.S.J. "Environmental Data In Mining," Biological Effects of Asbestos, Lyon, International Agency for Research on Cancer, 1973, pp. 138-144.

5. Sterling, T.D. "Possible Risk to Human Lungs from Magnetometric Dust Clearance Experiments," Journal of Applied Physics, March 1981, Vol. 52 # 3, pp. 2575-2577.

6. Cohen, D., "Report of the Low-Field Group: The Magnetic Field of the Lung," Francis Bitter National Magnet Laboratory, MIT, pp. 1-33.

7. Stroink, G., Blaauw, C., White, C.G. and Leiper, W., "Mössbauer Characteristics of UICC Standard Reference Asbestos Samples", Canadian Meineralogist, 198, Vol. 18, pp. 285-290.

APPENDIX "A"

# APPENDIX A

## A.1 Carey-Canadian Mine, Quebec:

### A.1.1 Mining:

Mining at Carey-Canadian is carried out by open pit methods in two pits, "B" and "C". An average of 5,000 tons of ore per day is hauled to the wet rock storage, and 11,500 tons of waste is stripped daily. The overall waste-to-ore ratio would be two-to-one once the two deposits are mined out.

Mining equipment consists of:

1- 12 cu. yd. rubber-mounted front-end loader

1- 6 cu. yd. rubber-mounted front-end loader

1- 6 cu. yd. electric shovel

1- 4 1/2 cu. yd. electric shovel

6- 50 ton diesel trucks

6- 35 ton diesel trucks

2- track-mounted bulldozers
1- rubber-mounted bulldozer
1- road grader
3- track-mounted self-propelled drills

Throughout the operation, a 45 foot bench height and a 10% haulage road grade are maintained.

Primary blastholes are 4 inches in diameter. Secondary drilling is done with two jack-hammer drills, drilling 1 inch diameter holes.

Blasting is done with special asbestos paper-wrapped explosives in the ore, and bulk slurries in waste stripping.

Two semi-mobile electrically-driven compressors of 900 and 750 cfm capacity, and one mobile 900 cfm diesel-driven compressors supply air for primary drilling. The air for secondary drilling is supplied by a mobile 125 cfm compressor.

Two electrically driven pumps of a capacity of 2000 Usgpm mounted on floating platforms, two 1500 Usgpm submersible pumps, and one 2000 USgpm diesel pump are used for dewatering purposes.

A.1.2 Ore Processing:

The ore is crushed in a 48 by 60 inch primary jaw crusher, set at 6 inches, then in a 5 foot standard secondary

cone crusher set at 2 1/2 inches. It then proceeds to a wet rock surge bin of 5000 tons capacity. Vibrating screens remove undersize in front of each crusher.

The ore is subsequently dried in three louvre-type rotary dryers using on the average 90 tph of oil per dryer. The dry ore is stored in different sections of a 24,000 ton capacity dry rock storage bin according to fibre characteristics. Marginal ore is up-graded in a beneficiation circuit in the dryer and crusher building.

Milling operations are carried out 24 hours a day, six days a week, treating an average of 5,000 tons of ore per day.

Vibrating feeders feed the ore from the dry rock storage onto a belt conveyor. There are twelve feeders available for blending of different types of ore.

On the way to the mill, the ore passes through a 5 foot shorthead cone crusher, set at 3/4 inches, in closed circuit with a vibrating screen. The circuit has a maximum capcity of 300 tph.

In the mill, the ore is automatically fed to six parallel rock lines where the fibre is relased from rock in vertical hammer mills and aspirated from standard shaking screens, aspirating drums and gyrating

screens. The cleaning is handled in standard graders and gyrating screens, while the grading is achieved in gyrating screens and sifters. Whizzer-type separators and specific gravity separators control the grit content.

Finished fibre is fed into bins for blending, and then pressure packed in paper, jute, polyethylene, woven, or valve-type paper or jute bags.

## A.2 National Asbestos Mines Limited, Quebec:

### A.2.1 Mining:

Mining is carried out using open pit methods. The mine operates 16 hours daily, 5 days a week. The daily tonnage is 4,600 tons of ore and 6,000 tons of waste, for a waste-to-ore ratio of 1.3 to 1.

The mine equipment consists of:

| | | |
|---|---|---|
| Shovels | 1 | Bucyrus Erie 4 1/2 cu. yd. electric model 110B |
| Tractors | 2 | Cat D-7 |
| Loader | 1 | Caterpillar 988 front-end loader, 6 cu. yd. bucket |
| Crane | 1 | Model 655 P&H with 55 foot boom and 9,400 lb dropball |
| Trucks | 5 | Euclid R-45, 45 ton, haulage |
| | 1 | Euclid B-ITD, 22 ton, haulage |
| | 1 | 3 ton Fargo for servicing |
| | 1 | Sudenga, for mixing and loading of holes with ammonium nitrate |
| Drills | 1 | Gardner-Denver PR-143, drilling 5 inches |
| | 2 | Gardner-Denver Air-Tracks (123) |
| Road Grader | 1 | Champion model D-565 |

In the pit, benches are 45 foot. Blasting is done in

multiple rows using 5 inch diameter, 75 degrees holes. Secondary breaking is done with the crane-mounted heavy dropball.

A.2.2 Ore Processing:

Primary crushing is done at the millsite in a 48 by 60 inch Allis-Chalmers jaw crusher, then in a 5 1/2 foot Symons cone secondary crusher in a closed circuit.

The ore is dried in two Ruggles-Cole rotary dryers, 60 foot by 80 inch, fired with bunker "C" oil. A dryer by-pass circuit and an ore-concentrating circuit are used when required. Normal crushing and drying rate is 290 tph.

The dried ore is transported by a conveyor system to a 10,000 tons capacity dry rock storage building. A Hewitt-Robins belt tripper is used with reclaim operated by remote control.

The mill is designed for 160 tph, for a milling rate of 3,840 tons per day, in 24 operating hours.

Mill equipment includes one tertiary Symons short-head cone crusher, fiberizers, gyrating screens, trommel screens, sifters, air classifiers, and separators. The air system handles 450,000 cfm, with a Wheelabrator bag filter system.

The product is pressure packed in paper, polyethylene, or jute bags.

## A.3 Bell Asbestos Mine, Quebec

### A.3.1 Mining:

The production at this mine comes from two underground operations. The daily production is 3,000 tons of ore. The mine operates on two eight-hour shifts, five days a week. The details of current operations could not be found. However, a short description of the plans made in 1967 for the second underground development, currently in operation, was found in October 1967 issue of mining in Canada.

> "The Company has begun a project which will develop its second underground level for the production of ore by the caving method.
>
> Involved is the sinking of a new shaft to a depth of 1,450 feet...with a complete new surface plant.
>
> In order to produce fibre in the best possible condition, and to avoid long orepasses and large underground openings in relatively soft serpentine rock, it was determined to use a car-in-cage hoisting system with the primary crusher on surface.
>
> The cage will have two decks... and will carry a mine car with a seven-ton payload on each deck.
>
> The cars will be loaded onto the cage by pneumatic rams underground and on the surface, and will be circulated through a tippler on the surface by a system of traversers, creepers, and pneumatic rams.

> The ore from the tippler will pass through a 42 inch by 48 inch jaw crusher... then will be taken to the existing mill by a series of 36 inch conveyor belts.
>
> Ventilation will be downcast in the new shaft, and will be actuated by two surface fans supplying 100,000 cfm of heated air. The present production shaft will bring the returned air to the surface, and there will be booster fans underground.
>
> The ore production will be by the caving method with a column height of about 400 feet. Haulage from the orebody to the new shaft will be by 10-ton trolley locomotives pulling trains of 14 cars".

A.3.2 Ore Processing:

The ore from the jaw crusher passes over a rod deck screen. The fines go to the dryer, and the coarse are hand sorted, then sent to a 4 1/2 foot Symons standard secondary crusher.

The fines are dried in vertical tower dryers, with bituminous coal as fuel. The fine and coarse fractions are stored and fed to the mill separately. Primary and secondary crushing and drying is done two shifts per day, five days per week.

Milling is carried out three shifts per day, five days per week, with a daily tonnage of approximately 3,000.

Fine and coarse ore are fed automatically to the mill by vibrating feeders controlled by conveyor scales.

Free fibre is aspirated, and the remaining ore fractions are blended. Further fibre is released by two stages of 4 foot short-head cone crushers, on stage of Nordberg gyradiscs, one stage of impact crushers, and one stage of Jumbo fiberizers. Gyrating screens with aspiration follow each stage of crushing. The fibre concentrates are then cleaned, dedusted, classified and blended.

500,000 cfm of air are used and filtered in the milling process.

## A.4 King-Beaver, Quebec:

### A.4.1 Mining:

67% of production at King-Beaver comes from the open pit, and 33% from the two underground operations. The daily tonnage is 12,000 tons of ore.

The two underground mines are connected underground. The No. 3 shaft (King) is 1,500 feet deep with levels at 855, 900, 1,100, and 1,300 feet. The No. 4 shaft (Johnson) is 1,275 feet deep, with levels at 950 and 1,100 feet. Most of the underground production comes from the No. 4 shaft.

Underground mining is carried out by the block caving methods. Originally, rhombic blocks, with sides of 160 feet in plan view, were laid out, each block served

by four grizzly drifts with six grizzlies per drift, drawing from the undercut level. Ore was scraped into chute raises which led to the level 45 feet below. Some of the production comes from the 50 hp slusher system. Drifts are spaced on 50 foot centers 100 feet long, with six to eight drawpoints per drift. Slushing is done directly into cars.

In 1972, production also started from a small isolated pocket of ore. Here, five-yard front-end loaders muck directly from drawpoints spaced on 50 foot centers.

Ventilation of both operations is provided by a fan situated on the 900 foot level between the two shafts. It draws 60,000 cfm at 3 inches wg, down No. 3 shaft, and exhausts through No. 4 shaft. Propane heaters at No. 3 shaft provide up to 6,000,000 Btu per hour in winter to heat the air.

The Beaver open pit is scheudled to produce 3,200 tons of rock per day, on three shifts, six days per week. Ore production accounts for 8,000 to 10,000 tons.

Blast holes are from 4 inch to 5 inch in diameter and are drilled inclined at 70 degrees. Pneumatic or hydraulic crawler-mounted drills are used.

Blasting is carried out with slurry-type explosives, which are purchased in bulk and pumped directly into

the blastholes by the manufacturers. Wherever areas are dry enough, A.N.F.O. is used.

Loading is done using electric shovels and diesel front-end loaders. There are four shovels, each with a 6 cu. yd. bucket, and two front-end loaders, one with an 8, and the other with a 10 cu. yd. bucket. Two electric shovels with 3 cu. yd. buckets are kept on stand-by.

Hauling is done in 45 ton rear-dump trucks.

A.4.2 Ore Processing:

Underground ore is crushed underground in a 42 inch by 48 inch jaw crusher set at 5 1/2 inches. It is then hoisted to an ore bin in the head frame. It is screened into plus 3 inch and minus 3 inch fractions on a 5 foot by 10 foot vibrating screen. The plus 3 inch product is crushed in a 5 1/2 foot cone crusher, set at 13/16 ich. The cone crusher product and the minus 3 inch primary crusher product are conveyed to tower dryers. The ore falls approximately 55 feet through a network of closely-spaced bars against an upward current of heated air. The moisture content is brought from 7% down to 1 1/2%. The dried ore is conveyed to a 20,000 ton rock storage bin. From there it is loaded into 70 ton capacity semi-trailer bottom dump trucks and transported 1-1/3 miles to a 12,000 ton capacity storage bin at the

Beaver Ore Preparation and Storage Plant, where it is blended with dried open pit ore in the Beaver OPS bin.

Open pit ore is dumped by haulage trucks into a 120 ton capacity jaw crusher sluice. A 5 foot by 22 foot apron feeder conveys the ore into a 48 by 60 inch jaw crusher set at 6 1/2 inches. The discharge is screened on 6 by 12 foot vibrating screens into four products: plus and minus 3 inches, and plus and minus 1 1/2 inches. The plus 3 inch ore is crushed in a 5 1/2 foot cone crusher, set at 1 1/2 inches, in closed circuit with the rock screens, dividing ore into minus 3 inches plus 1 1/2 inches, and minus 1 1/2 inches. The minus 3 inches plus 1 1/2 inches fraction is dried in horizontal rotary driers or bypasses to the storage bin. The minus 1 1/2 inch fraction is dried in tower dryers.

The dried ore is conveyed to the Beaver OPS 12,000 ton capacity rock storage bin, where it is blended with the dried underground ore, and the mixture is drawn from the bin for milling operations.

In the mill fibre separation is achieved using reciprocating screens, cyclone separators, and vertical hammer mills. Cleaning and grading of the fibre concentrate is accomplished using screens, horizontal trommel graders, and vertical and horizontal dusters. The degree of fiberization is controlled in hammer mills or opposed-

faced emery grinders, attrition mills or pulverizers.

The finished fibre is pressure or semi-pressure packed, or bagged loosely in either paper, jute, jute-laminated, or polyethylene containers.

## A.5 British-Canadian Mine, Quebec:

### A.5.1 Mining:

Mining is carried out by open pit methods. In 1972, the pit was over a mile long, and half a mile wide.

The mine operates 24 hours a day, six days a week. Approximately 8,000 tons of ore and 52,000 tons of waste are mined daily.

The major equipment used is as follows:

| | |
|---|---|
| 5- | 6 yd. 4,000 volt electric shovels |
| 4- | 5 yd. 4,000 volt electric shovels |
| 2- | 4 yd. 4,000 volt electric shovels |
| 30- | 45 ton haulage trucks |
| 2- | track-mounted bulldozers |
| 3- | rubber-tired payloaders |
| 1- | road grader |
| 2- | 6 inch down-the-hole self-contained drills |
| 4- | vertical single drill units, 4 inch holes |
| 2- | horizontal twin drill units, 3 inch holes |
| 1- | horizontal single drill unit, 3 inch holes |
| 4- | stationary compressors, 10,000 cfm |
| 2- | portable compressors, 1,200 cfm |

The normal mining bench height is 55 feet. Hole spacing varies with the type of drill used. A variety of explosives, principally of the slurry type. The slurry is delivered to the blasting site in special tank trucks

that mix and inject the proper mixture into the hole. All secondary breaking is done by hand-held pluggers or mudcapping.

To optimize efficiency, all shovel foremen's vehicles are equipped with intercom radios. All haulage trucks are equipped with two-way radios and are controlled by a central dispatcher located in a cabin on the side of the pit, where maximum visibility of the pit operations is possible.

A.5.2 Ore Processing:

The ore preparation and storage department No. 1 operates 24 hours a day, six days a week, with an average throughout of 360 tons per hour.

Ore from the trucks is fed into a 48 by 60 inch jaw crusher set at 5 1/2 inches, then screened into plus and minus 5 inch fractions. The plus 5 inch is hand sorted. Between 1,000 and 1,200 tons per day are discarded as barren rock. Secondary crushing then reduces all oversize material to minus 1 1/4 inch.

The crushed ore is then dried in vertical tower dryers. The dry ore is stored in a 25,000 ton capacity bin.

Mill No. 1 operates 24 hours a day, six days a week, treating 6,600 tons of ore daily. No further pertinent detail about mill No. 1 could be obtained.

The ore preparation and storage department No. 2 handles an average throughput of 360 tph.

Ore from the pit is fed to a 48 by 60 inch jaw crusher set at 5 inches. It is then fed to a cone crusher and reduced to minus 1 3/4 inches. The plus 1 inch material is sent to four magnetic beneficiators. The rejects are sent to the dump, and the "concentrate" goes to two oil-fired rotary furnaces. The minus 1 inch material is dried separately in two rotary dryers. Both dried products are stored in a 24,000 ton dry storage bin before being drawn to the mill.

Mill No. 2 treats 6,000 tons of ore daily. Ore is drawn from the main dry storage bin into a 200 ton surge bin at the head of the mill. From the surge bin, the ore is fed to four identical rock circuits, consisting of screens, crushers and fiberizers with aspiration after each stage. A final stage of fiberizing is done by air-swept ball mills. The fibre is then given a primary cleaning on gyrating screens. The finished fibre is pressure packed into jute, paper, or polyethylene bags.

## A.6 Lake Asbestos of Quebec Limited:

### A.6.1 Mining:

This is an open pit operation. Mining is carried out 24 hours a day, six days a week. On the average,

15,000 tons of ore and 30,000 tons of barren rock and overburden are mined daily.

The pit has been designed with vertical bench heights of 40 feet, for a final back slope in rock of 45 degrees. Haulage roads are 50 feet wide with a maximum grade of 8%. In 1967, average length of haul was 10,000 feet for waste at a 550 foot lift, and 6,200 feet for ore at a 400 foot lift.

Major mining equipment consists of two 4 cu. yd. and four 5 cu. yd. electric shovels, supplemented by two loaders of 9 cu. yd. and 6 cu. yd. capacity respectively, a 2 1/2 cu. yd. diesel shovel, six 35-ton, five 40-ton and seventeen 50-ton capacity rear-dump diesel trucks.

Primary drilling is done by three Ingersoll-Rand Model 325-A down-the-hole drills, equipped with automatic feed and lubrication, making 6 1/2 inch diameter holes. Gardner-Denver "Air Tracs" drilling 3 inch holes are used for pioneering new benches and some secondary work. The greater part of secondary work, which consists of breaking large blocks, is done by a Travel Drill, a self-contained drilling unit mounted on a rubber-tired chassis and equipped with a 230 cfm diesel-powered compressor.

A.6.2 Ore Processing:

The ore is crushed in a 48 by 60 inch jaw crusher, with a N-500 Hazemag as stand-by, then in a 7 foot cone crusher

operating in closed circuit with shaker screens. The crushed ore is stored in an open area of about 125,000 tons capacity. It is then dried in either vertical or rotary dryers, and stored in a 20,000 ton capacity dry ore storage bin located between the drying plant and the mill.

The mill has a rated capacity of 9,000 tons per day. Crushing is done in gyrating crushers, air-swept Hazemag crushers, and in air-swept Torreys and fiberizers. Cleaning and grading of fibre is performed on shaking screens, gyrating screens, standard graders, dusters, and classifiers.

Finished fibre is pressure packed in jute, paper, or polyethylene bags.

A.7 Normandie Mine, Quebec:

A.7.1 Mining:

So far, all production has come from the open pit operation. Mining is carried out 24 hours a day, 5 days a week. An average of 8,800 tons of ore and 4,620 tons of barren rock are handled daily.

Major mining equipment consists of:

3- 5 cu. yd. 2,200 volt electric shovels
1- 3 1/2 cu. yd. diesel shovel
7- 35 ton diesel trucks
7- 45 ton diesel trucks

1- track-mounted bulldozer
1- rubber-tired bulldozer
2- 5 cu. yd. rubber-tired payloaders
1- 10 cu. yd. rubber-tired payloaders
1- road grader
2- track-mounted down-the-hole-rock drills for 6 1/4 inch diameter down holes
1- track-mounted percussion drill for 4 inch diameter holes
1- track-mounted percussion drill for 3 inch diameter toe holes
1- 1,200 cfm portable compressor
1- 900 cfm portable compressor
1- 175 cfm portable compressor
1- self-propelled drillhole blowing apparatus
1- self-contained truck-mounted bulk handling apparatus for controlled mixing and loading of A.N.F.O. into drillholes

Mining method is the standard open-cut benching system, maintained by haulageways of a maximum 10% slope. Above the 575 foot elevation, 50 foot high benches are established, while 40 foot high benches are standard below this elevation. This will result in a pit with an overall slope of 45 degrees, 750 feet deep, and with a rim diameter of about half a mile.

A.7.2 Ore Processing:

The crushing and drying plant is operated three shifts per day, 5 days a week, and handles an average of 610 tons per hour.

Primary crushing is done in two 48 by 60 inch jaw crushers set at 6 1/4 inches. A 30 inch conveyor, 1,700 feet in length coveys the ore to the secondary crushers and dryers. Secondary crushing is done in

5 1/2 foot cone crushers which reduce the ore to minus 3/4 inch. At this stage, 2,400 tons per day of barren rock are removed by hand sorting.

Minus 1 1/4 inch ore is dried in three tower dryers, and the plus 1 1/4 inch ore in two rotary dryers. The dried ore is stored in a 30,000 ton capacity dry rock storable bin, from which it is fed to the mill.

The mill is operated six days a week, and treats an average of 7,400 tons of rock per day. A fibre concentrate is removed from the fines of the minus 3/4 inch feed before the feed is delivered to the coarse and fine rock bins of the six Aerofall Mills. The Aerofall Mills contain an 18,000 lb. ball charge and are air-swept by 90,000 cfm per mill. The crushed rock from the Aerofall Mills is delivered to two batteries of rock screens with suction; the lifts from these screens plus the initial fibre concentrate make up the feed to the long and short fibre concentrate bins located at the head of the fibre treating mill. Three batteries of fiberizers are used to extract fibre remaining in the rock, with screening and lifts after each stage of fiberizing. Grading and cleaning of the fibre is done on gyrating and shaking screens, and in standard graders and dusters.

The finished fibre is either pressure-packed or

loose-packed in paper, jute, or plastic containers.

A. 8 The Jeffrey Mine, Quebec :

A.8.1 Mining:

Presently all production comes from the open pit operation.

In 1970, a $75 million development program was begun, based on a completely computerized study, which calls for an annual rate of 40 million tons of material removed, ensuring the production of more than 600,000 tons of fibre per year. The skipway system was removed in early 1973 to permit major expansion of the open pit.

The open pit dimensions in 1974 were 3,500 feet North-South, 5,500 feet East-West, and 850 feet deep.

In the present benching system in the pit, mining of overburden is being done almost continuously along the network of haulage roads. The sand and clay overburden, ranging in depth from 30 feet to 300 feet, consists of earth and the several varieties of rock surrounding the orebody. Much of this is drilled and blasted. Rotary drills are used, and shots vary in size depending on conditions. Usually two to four 15 cu. yd. electric shovels are being used, loading to 100 ton and 200 ton diesel-electric end-dump trucks. These haul the 65,000

tons per day of overburden and rock waste from 6,000 to 8,000 feet out of the pit to the dumping areas. This dump now covers about 250 acres.

All loading is handled by a fleet of 15 electric shovels including:

4- Bucyrus Erie 6 cu. yd. and 10 cu. yd.
9- Harnischfeger 6 cu. yd., 10 cu. yd., and 15 cu. yd.
2- Marion 15 cu. yd.

Usually 10 shovels are in use per shift. The larger shovels (15 and 10 cu. yd.) are used primarily to strip overburden and waste rock. The 6 cu. yd. shovels and some of the 10 cu. yd. units are used to load ore.

The haulage fleet at the Jeffrey Mine is gradually being converted to the larger units, which have been found to be more efficient and economical. There are about 70 haulage trucks.

These include:

22- Dart SL35 (40 ton) trucks
31- Lectra Haul M-100's (100 ton)
13- Wabco Haulpak 120 A's and B's (120 ton)
4- Lectra Haul M200's (200 ton) with 1,650 hp plants

The 200-ton trucks are being used almost exclusively for hauling overburden, along with some of the 120-ton units. All of the big trucks are diesel-electric using either generators or alternator-rectifiers.

The 40 and 100 ton trucks, and some of the 120 ton units haul the ore and waste rock. The waste rock is hauled about 3 miles to a waste dump in another area. Up to 20 trucks haul ore from the pit to the plant. This is a haul of about 1 1/2 miles, with the maximum haul out being about 2 miles up grades of up to 12%. The ore is usually dumped to the primary crusher, but stockpile is also maintained at ground level, from which the crusher can be fed by 15 cu. yd. front-end loaders while blasts are in progress, and during shift changes.

Mining the ore is usually carried on simultaneously at 4 to 5 locations in the pit, including the bottom level. Faces average 35 feet in height, and 7 1/2 inch and 9 inch rotary drills are used in a three shift operation. Drills now in use include:

3- Bucyrus Erie BE40R
2- Gardner-Denver RDC 30
2- Gardner-Denver PR143 percussion drills on crawlers
2- modified crawler-mounted Travel Drills for secondary work

Shots are made with several rows, averaging about 50,000 tons. Explosive used is DuPont "Tovex" 20E premixed explosive, provided by pumper trucks from a slurry plant operated on the premises by the manufacturer. Nonmetallized slurry is used to avoid possible fibre contamination. Millisecond delays, 50-gain

Primacord, and boosters are used.

All blasting is done at 4 pm on the dayshift, and the larger blasts are monitored with a seismograph. A laser transit is used to monitor pit slopes.

A.8.2 Ore Processing:

At the plant, on ground level, the trucks dump the ore at the primary crusher building, to manganese-steel-lined dump pockets on both sides, capable of receiving simultaneously the loads of two 100 ton trucks. The Fuller-Traylor 91GATX gyratory primary crusher with a hydraulic setting adjustment, has a 72 inch feed opening, and is rated at 3,000 tph crushing from maximum 72 inch size to minus 7 inches. The crushed ore is discharged into a 300 ton live surge bin feeding onto an 84 inch conveyor. A metal detector stops the conveyor if tramp metal is present in the ore.

The primary fibre separation is done in the new mill No. 6, and the cleaning and grading in the old mill No. 5.

A 60 inch wide, 1,000 wide long belt conveyor carries the ore from the primary crusher to mill No. 6. An Eriz suspended magnet over the head pulley of the conveyor protects against metal. The conveyor discharges into a 300 ton distribution bin at the top of the mill.

Three apron feeders discharge from the bin to three identical secondary crushing flows of 1,000 tph each. In each flow, conveyors feed to a 6 by 16 foot Simplicity vibrating grizzly screen. 700 tph of plus 3 inch oversize go to an 84 inch Allis-Chalmers Hydrocone reducing to a minus 3 inch. The minus 3 inch thrus go to a 7 by 16 foot Simplicity rod-deck screens that separate a 3/4 inches the fractions that are to be fed to the dryer and concentrator plants.

Conveyors feed the minus 3/4 inch fraction to seven 225 ton storage bins, which discharge through screw feeders to seven FMC/Link-Belt Fluid Flow single-bed dryers. These can dry 150 tph each from 10% to 1% moisture content. Cyclones collect the fine fibre, and this, with the asbestos rock is carried on belt conveyors to the 30,000 ton capacity dry rock storage building. Fine dust goes to a 700,000 cfm Wheelabrator bag filter.

In the concentrator section, the oversize ore is further reduced in size to free the remaining fibre. The fibre is removed by aspiration, and the barren rock is rejected. The ore is first discharged from the conveyors to a 3,000 ton storage bin, then fed to seven Hazemag APK60 primary impactors. These handle 250 tph each, and discharge by gravity on seven 6 by 12 foot Simplicity

DD rod-deck screens. The minus 3/8 inch ore goes by conveyor to dry rock storage. The oversize is conveyed to a 1,000 ton storage bin.

Ore from this bin is separated to identical flows beginning with 11 Hazemag APK50 secondary impactors, then 11 Nordgerg Symons 6 by 10 foot SD screens with 1/4 inch openings. The oversize rock goes to tailing disposal. The minus 1/4 inch material is fed to 11 gyrating screens with fibre aspirators. The remaining fibre goes to 11 hammer-mill-type fiberizers. These handle 35 tph each. The fibre is then separated from the rock by the 22 final fibre aspirating screens. The waste rock all goes to the tailing disposal area.

All the concentrate, along with material from the dryers goes to the 30,000 ton dry rock storage building. From here the concentrate is fed to mill No. 5 for final grading and cleaning.

Mill No. 5 has a yearly capacity of 600,000 tons of fibre. On the 12th floor of the mill are bag filters from which air can be exhausted or recirculated to reheat the mill. On the 11th floor are the primary rock bin and the cyclones that precede the filters. On the 10th floor are feeders from the bin to fibre screens. A large conveyor passing through the 9th

floor brings rock from the first floor on the primary side of the mill to the bin on the secondary side of the 11th floor. On the 8th floor are the primary rock screens, where the first separation of the fibre from the rock is made. The aspirated fibre goes to the collectors on the 11th floor. On the 7th floor are graders, which separate the long and short fibres. On the 6th floor are the storage bins for the cements and floats section of the mill. On the 5th floor is weighing and batching equipment to blend cements and floats. On the 4th floor are 2 1/2 or 5 ton mixers for the various grades of fibre. On the 3rd floor is located the fibre development section of the mill, where equipment and product tests are made. On the 2nd floor are the fibre distribution and the automatic weighing hoppers, which weigh out 100 lb. batches of fibre to the pressure packing machines.

The tailings from the plant are hauled to waste piles over the tailings section of the company's 23 mile railroad.

APPENDIX "B"

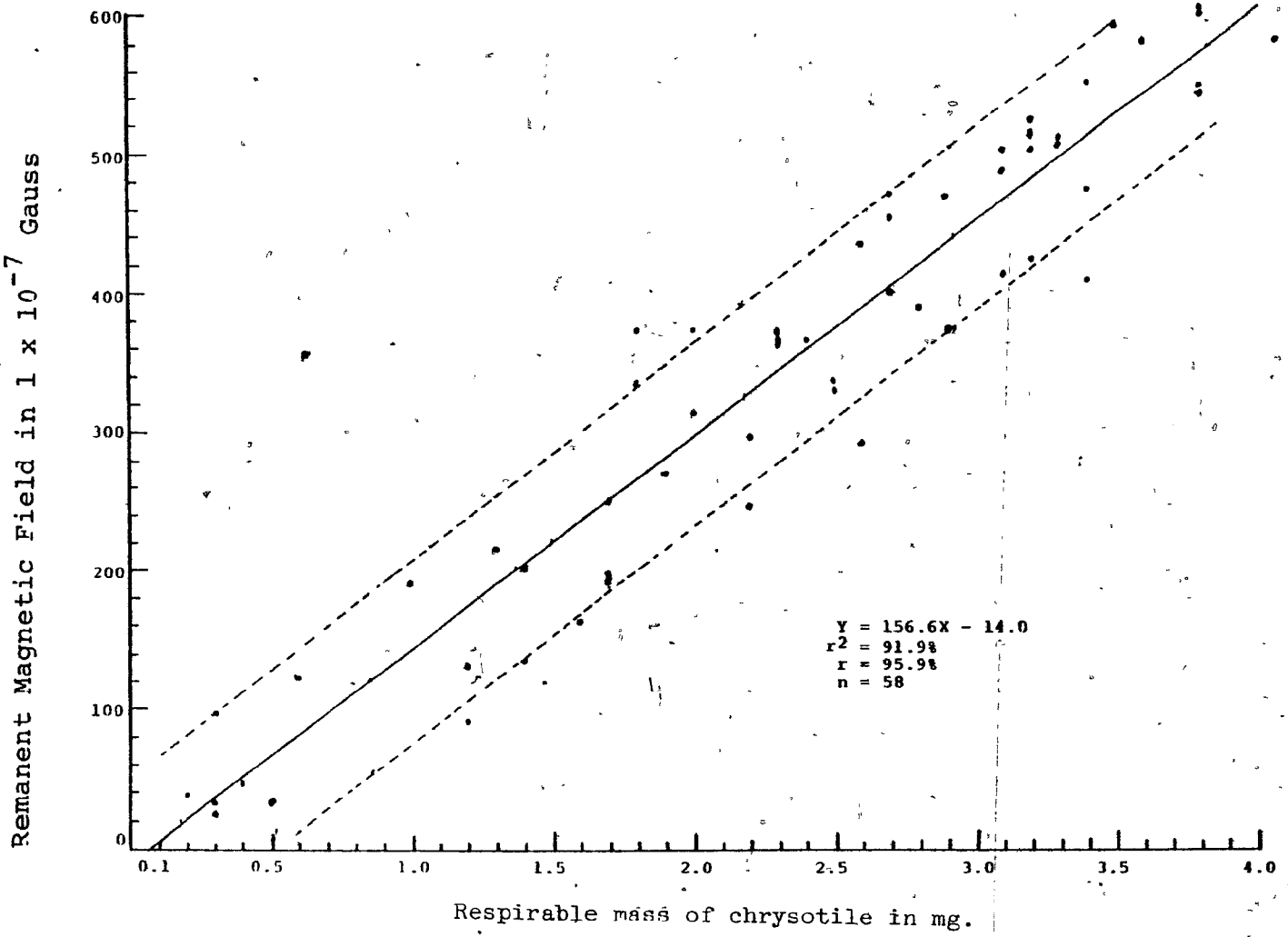


Fig. B.1 - Calibration Line for Mill # I Chrysotile Mass Determination with Confidence Limits of 90% (dotted lines).

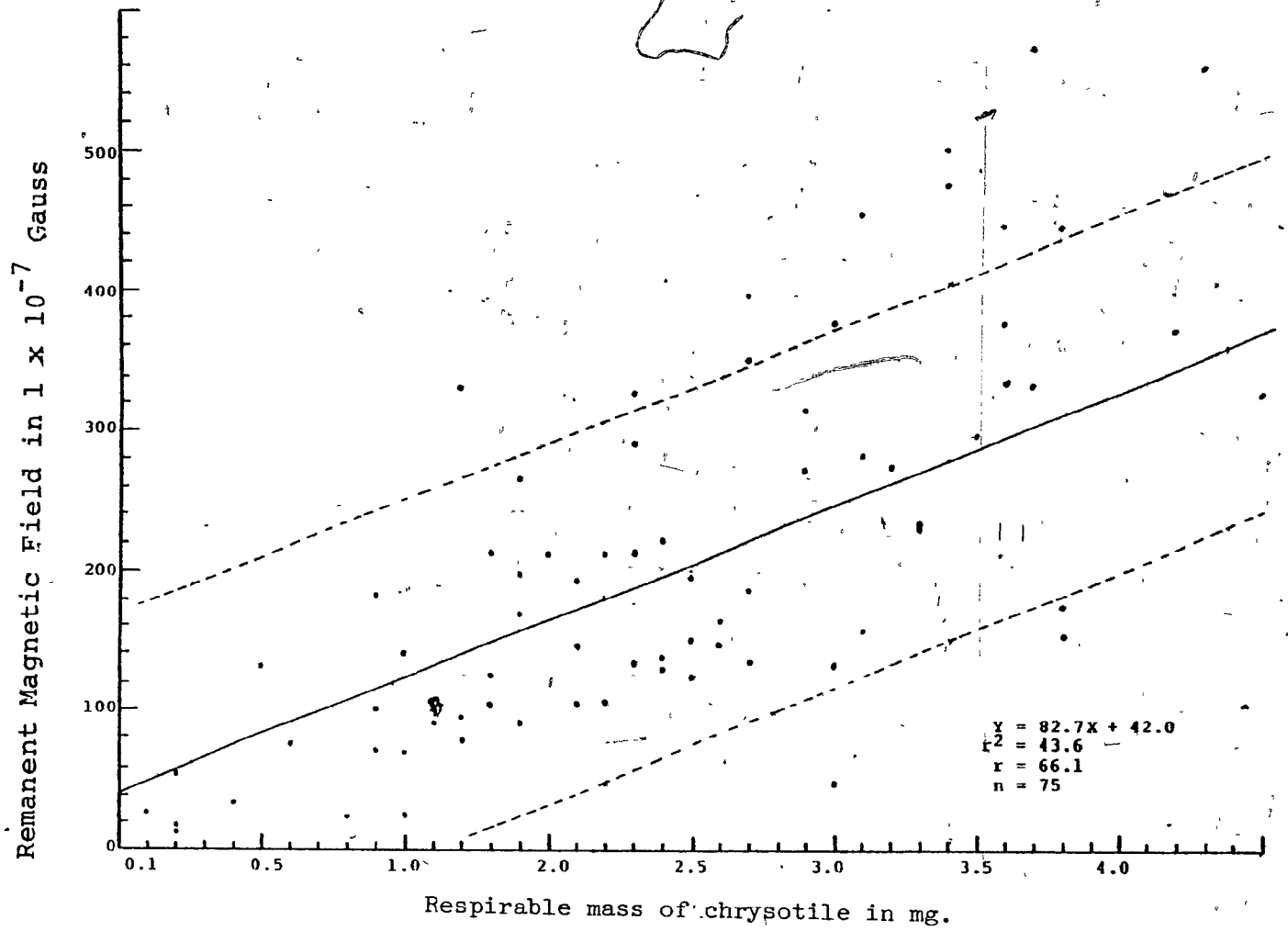


Fig. B.2 - Calibration Line for Mill # II Chrysotile Mass Determination with Confidence Limits of 90% (dotted lines).

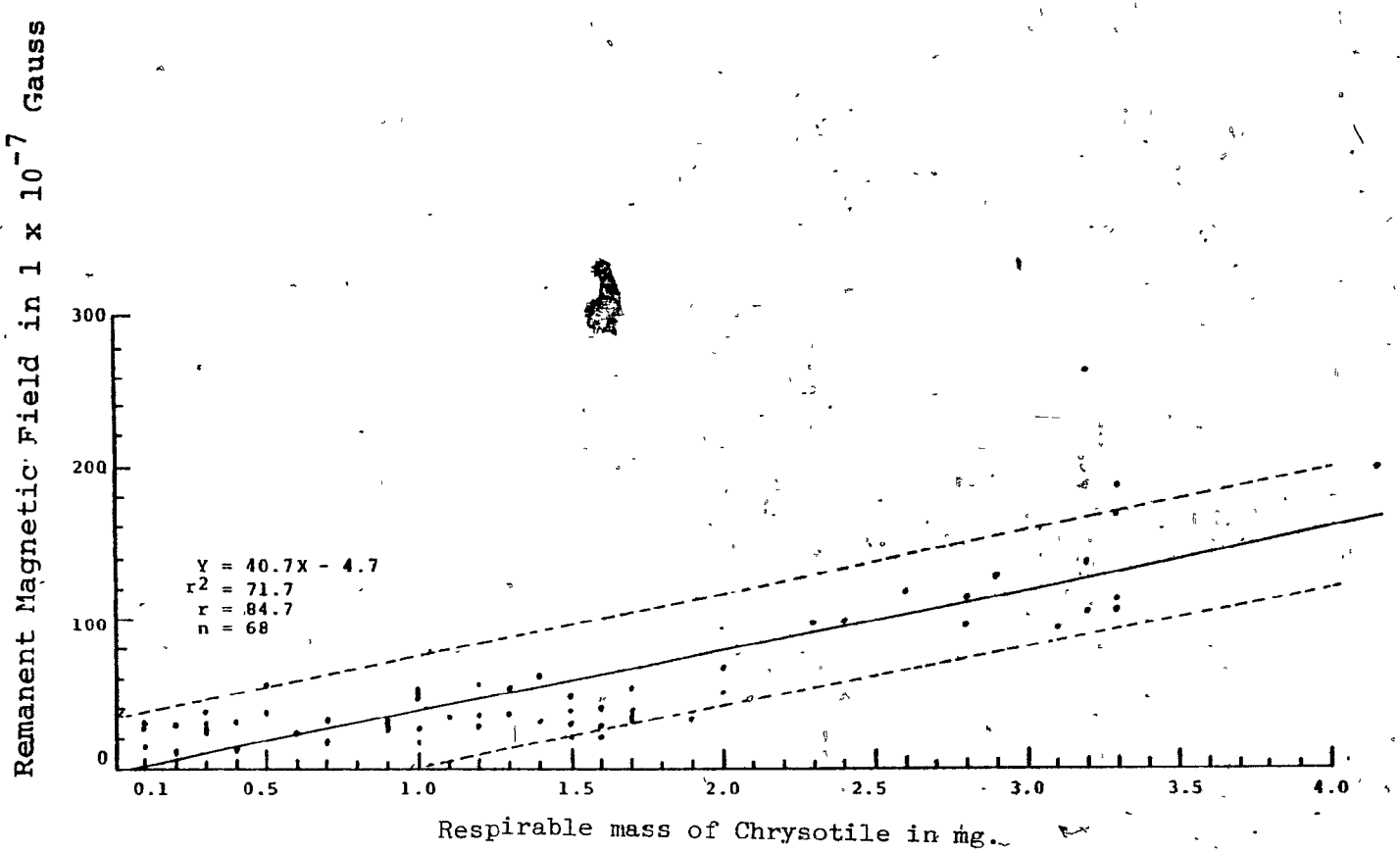


Fig. B.3 - Calibration Line for Mill # III Chrysotile Mass Determination with Confidence Limits of 90% (dotted lines).

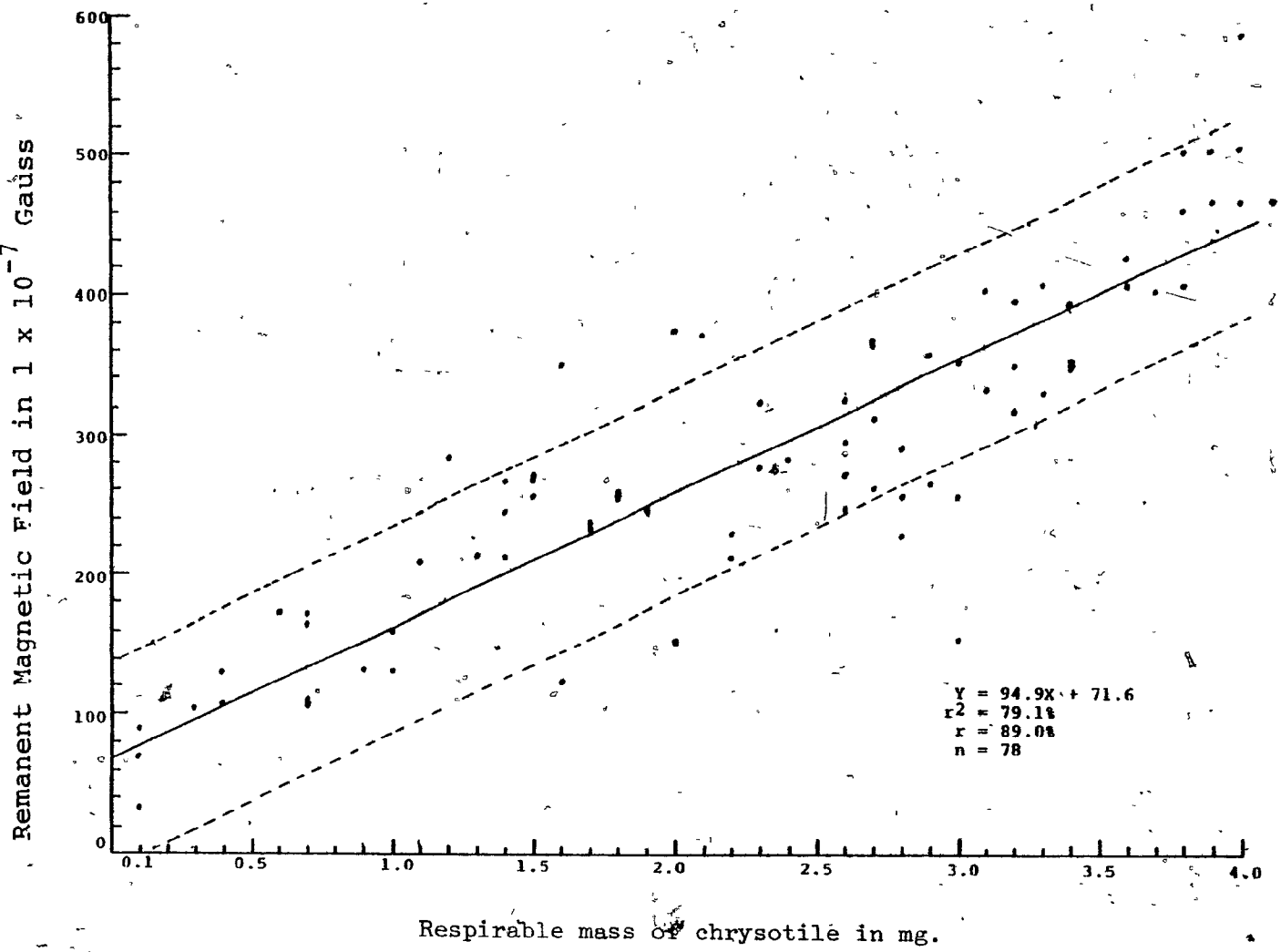


Fig. B.4 - Calibration Line for Mill # IV Chrysotile Mass Determination with Confidence Limits of 90% (dotted lines).

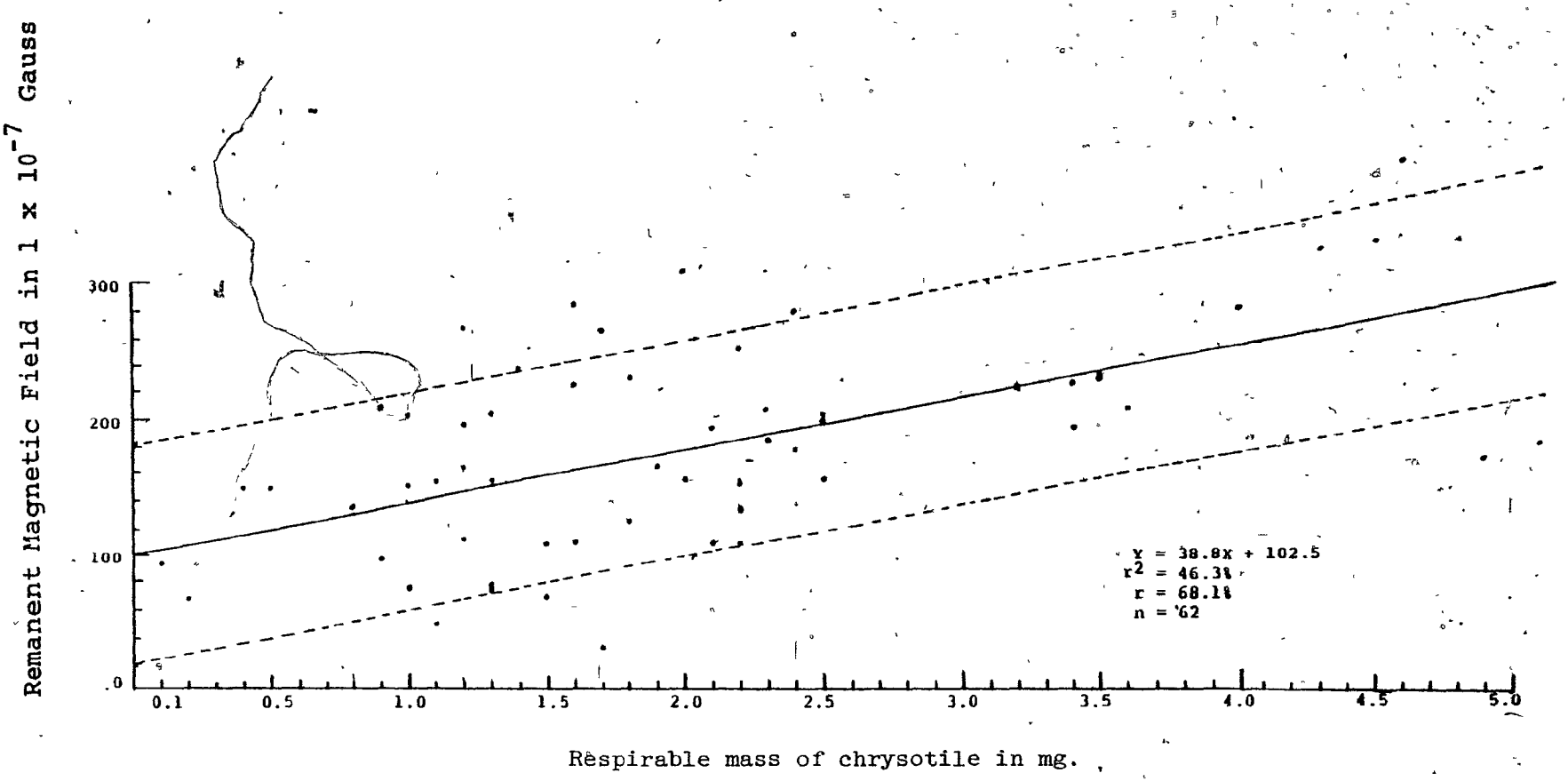


Fig. B.5 - Calibration Line for Mill # V Chrysotile Mass Determination with Confidence Limits of 90% (doted lines).

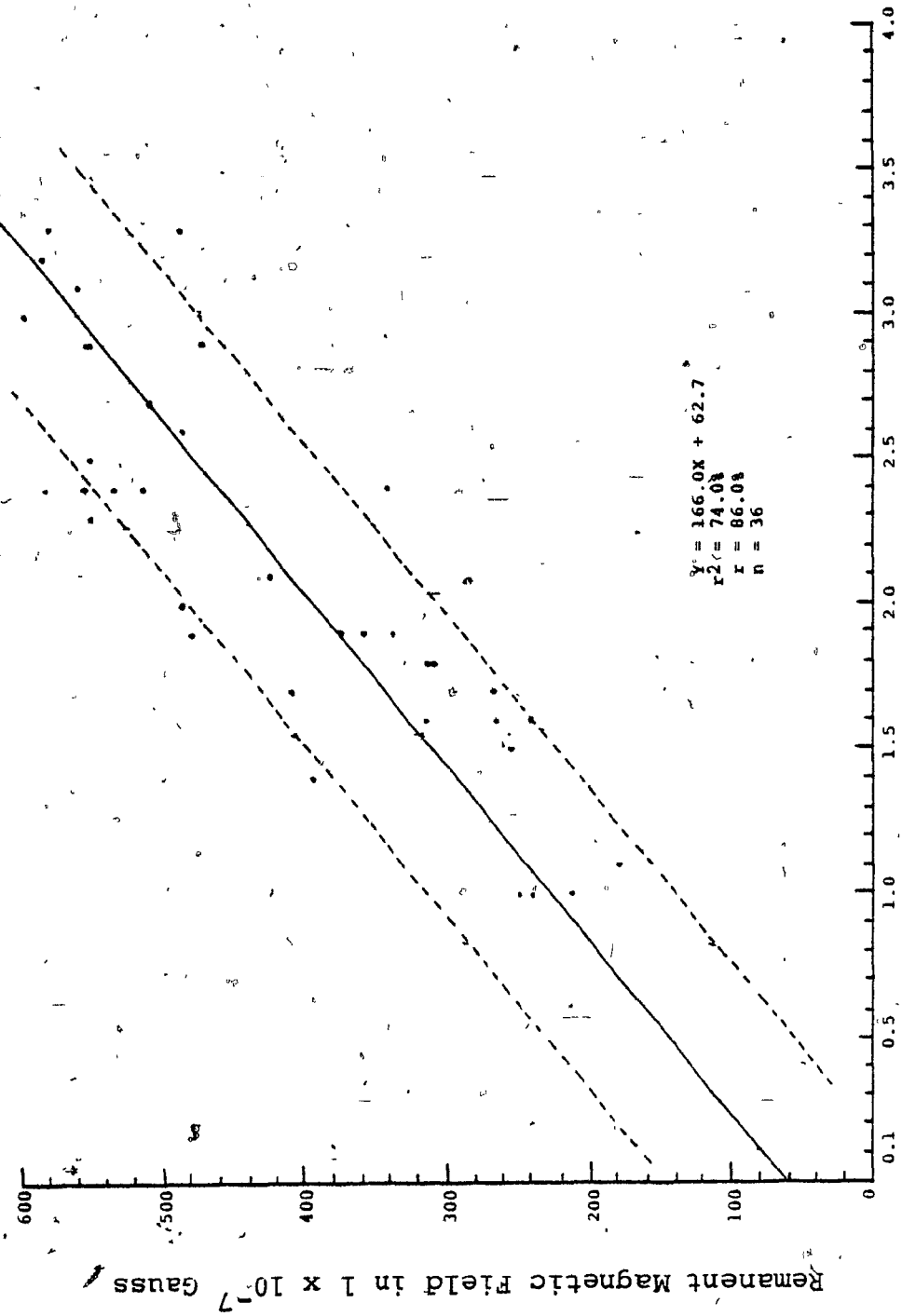


Fig. B.6 - Calibration Line for Mill VIII Chrysotile Mass Determination with Confidence Limits of 90% (dotted lines).

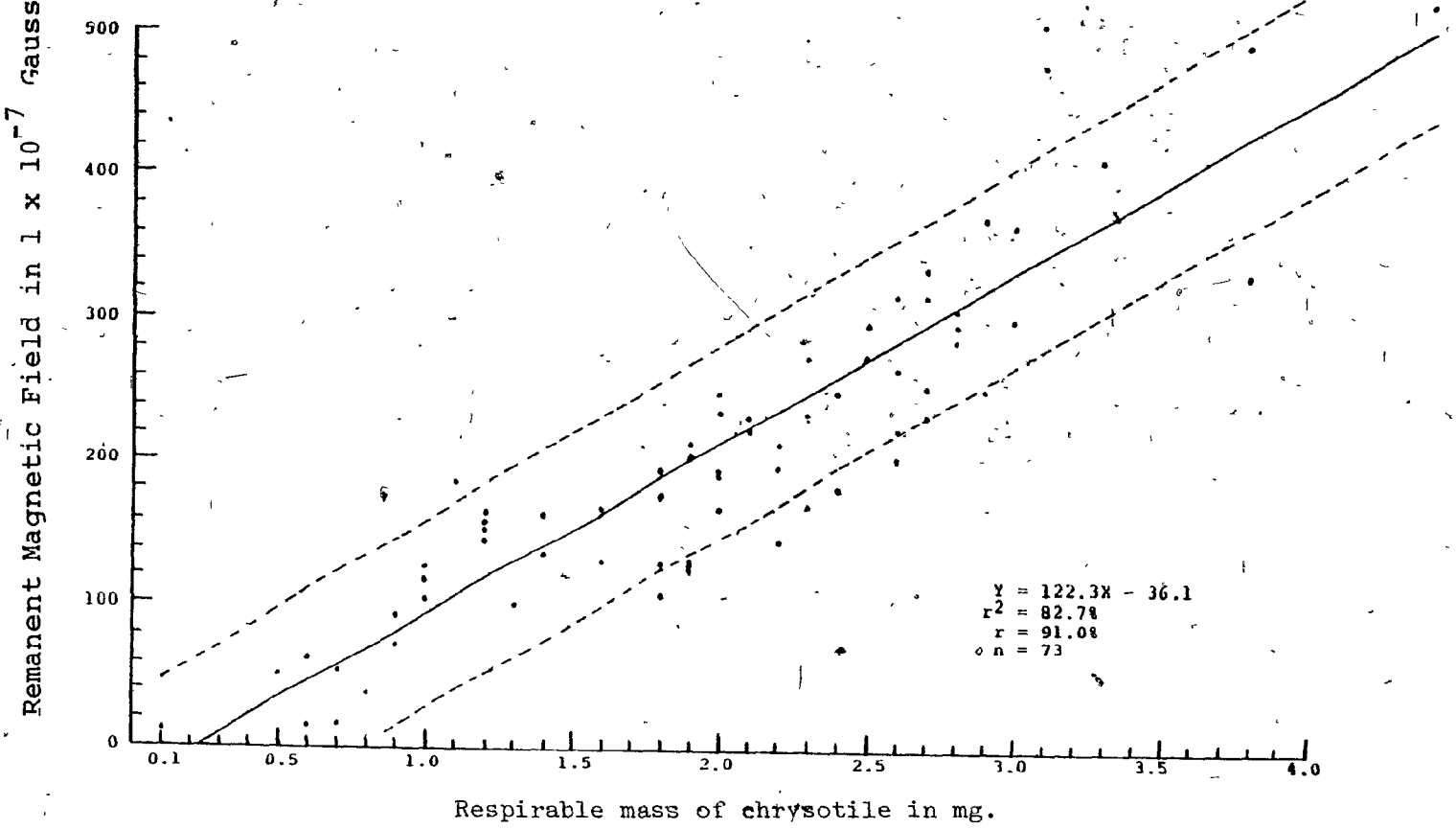


Fig. B.7 - Calibration Line for Mill # IX Chrysotile Mass Determination with Confidence Limits of 90% (dotted lines).

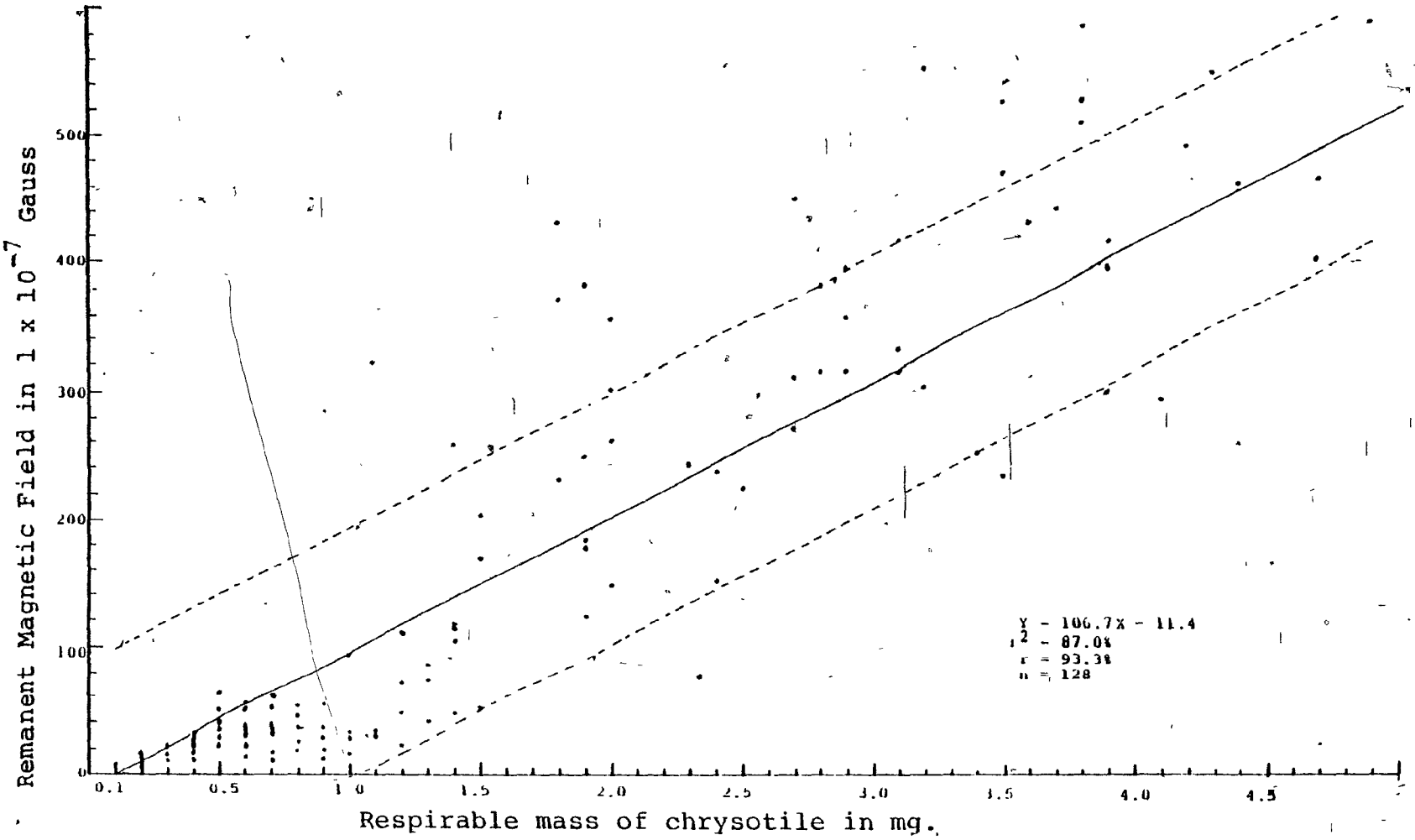


Fig. B.8 - Calibration Line for Rhodesian UICC Chrysotile Mass Determination with Confidence Limits of 90% (dotted lines).

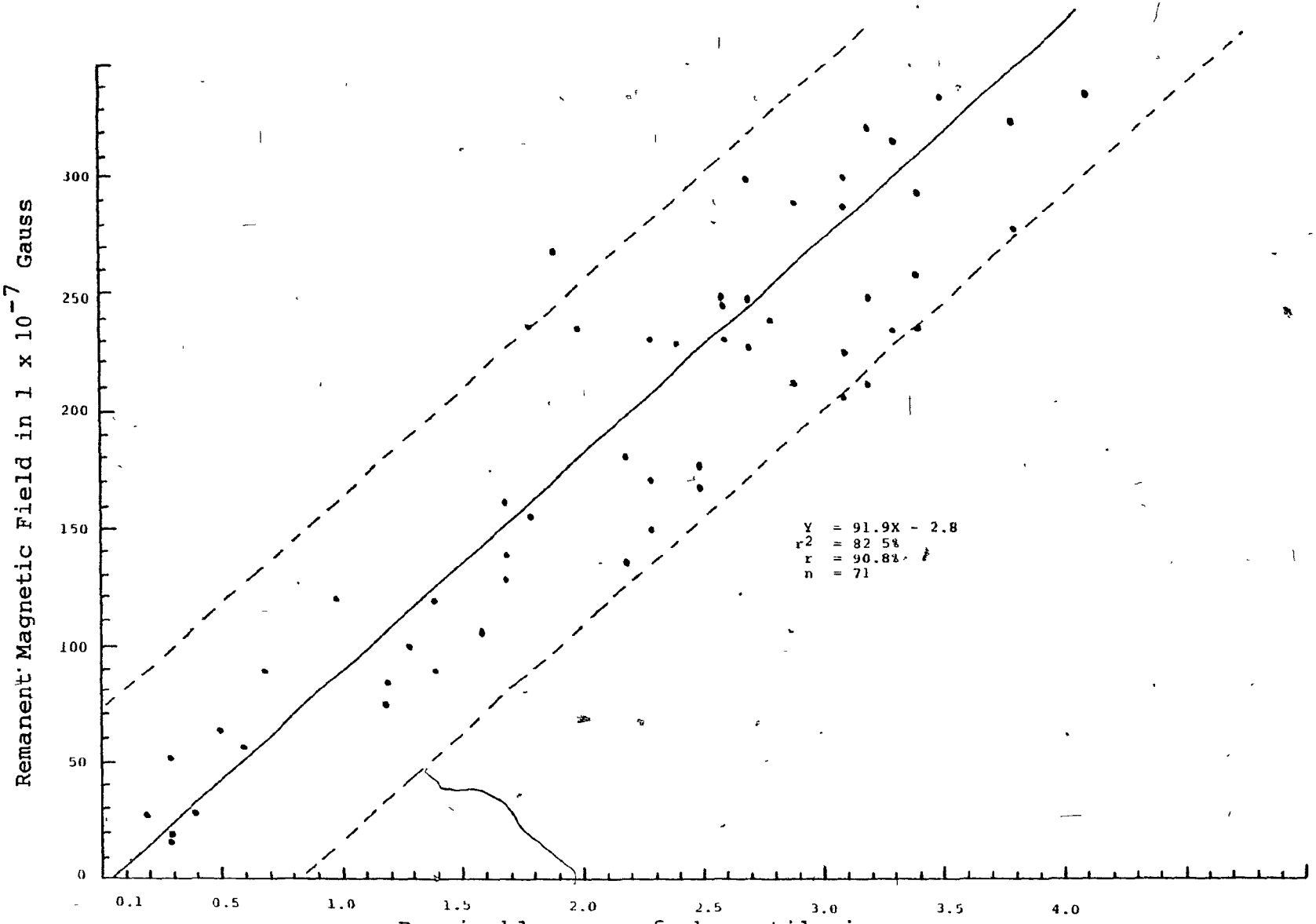


Fig. B.9 - Correlation of the Remanent Magnetic Field with the Mass of Mill # 1 Chrysotile. (Sample 1 cm. Away From the Probe)

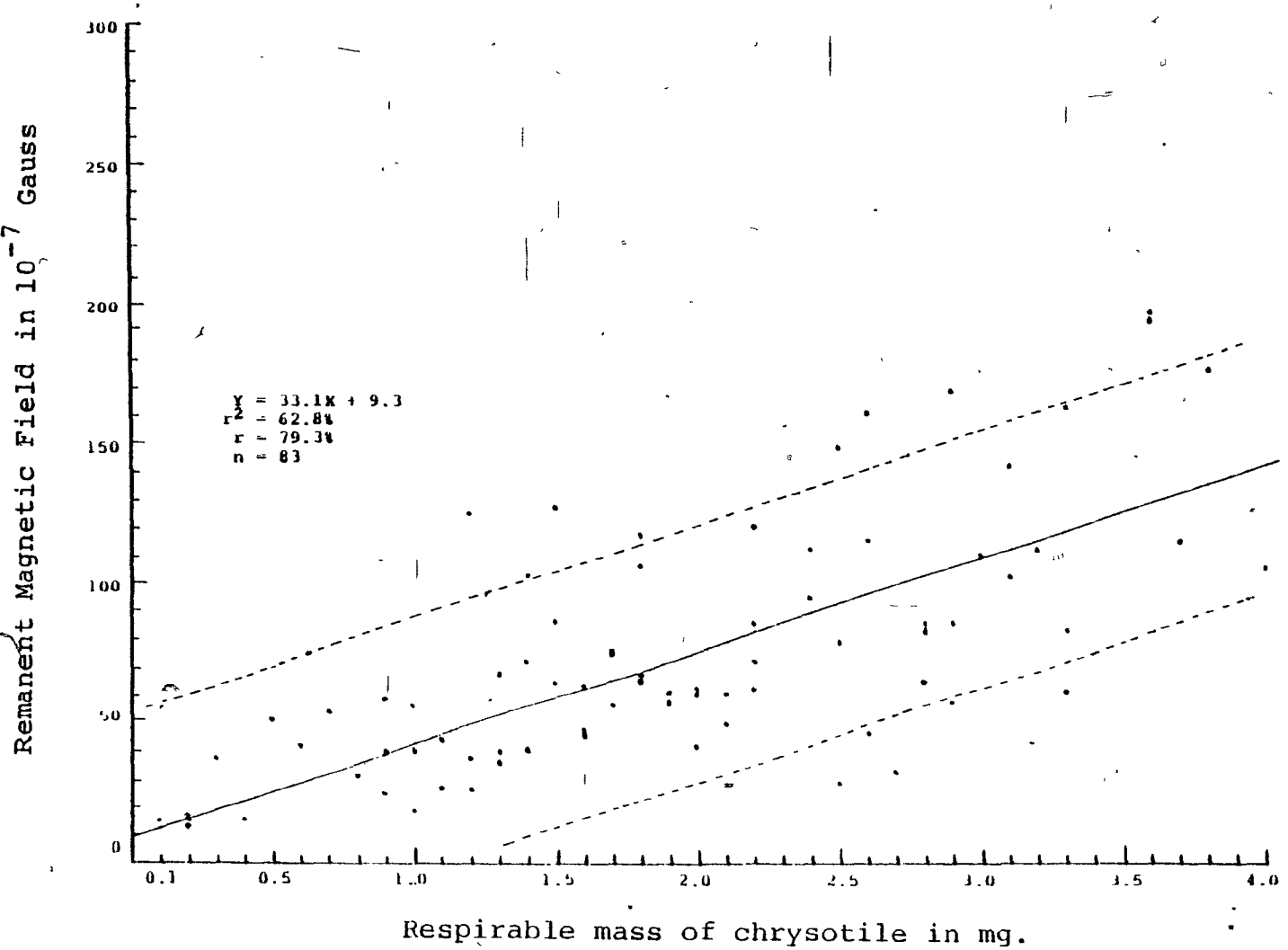


Fig. B.10 - Correlation of the Remanent Magnetic Field with the Mass of Mill # II Chrysotile. (Sample 1 cm Away From The Probe).

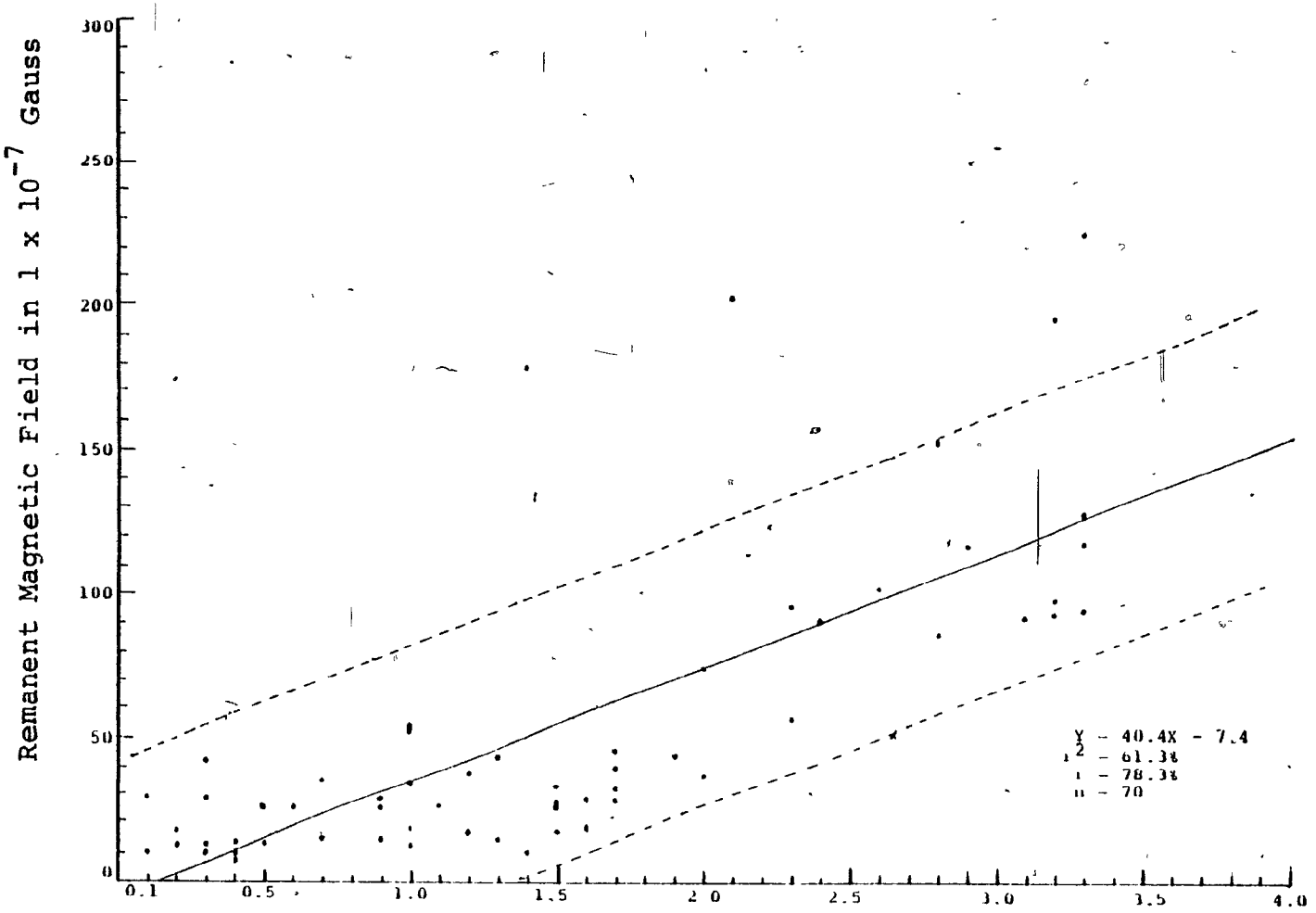


Respirable mass of chrysotile in mg.

Fig. B.11 - Correlation of the Remanent Magnetic Field with the Mass of Mill # III Chrysotile (Sample 1 cm Away From The Probe).

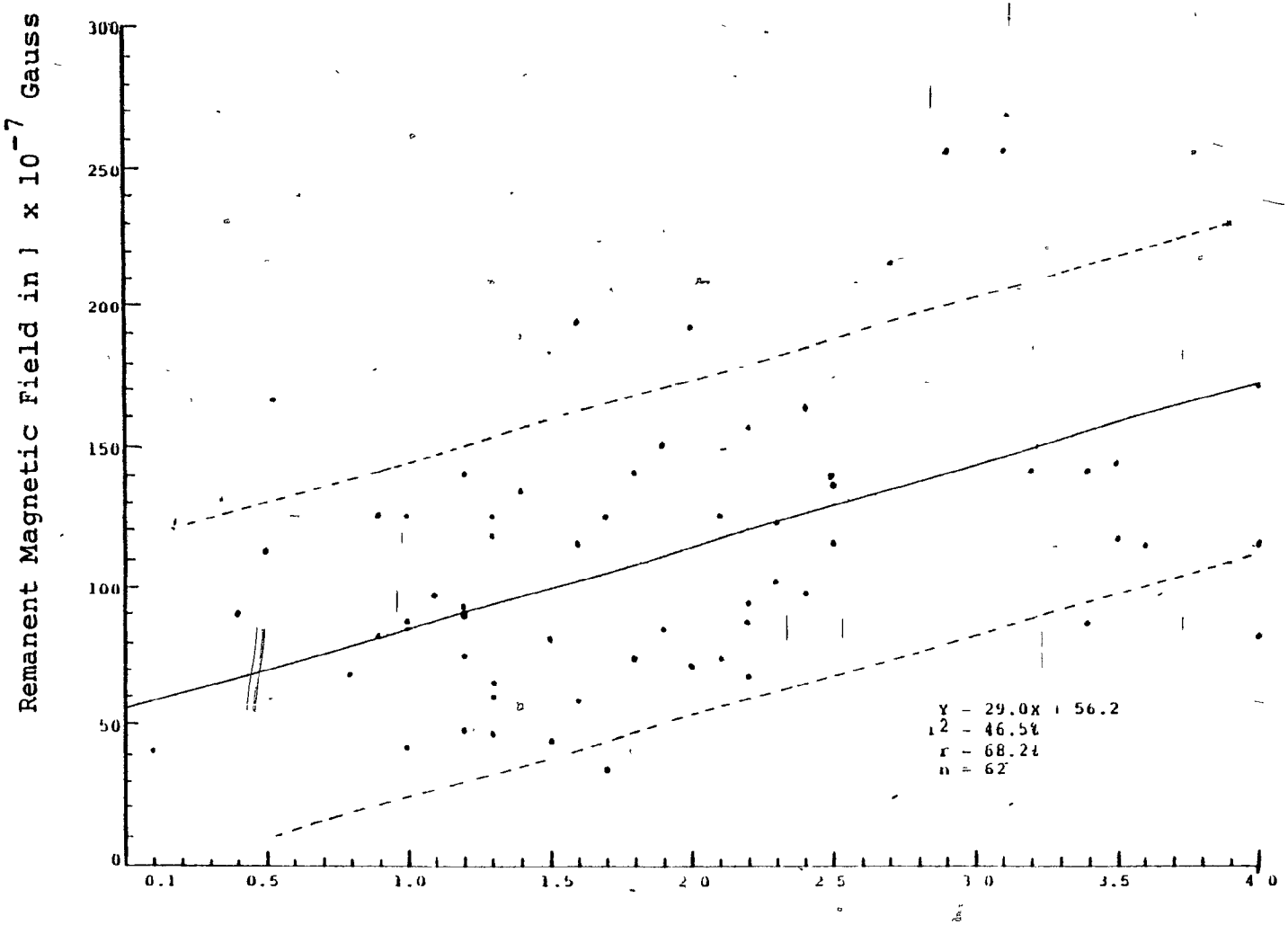


Fig. B.12 - Correlation of the Remanent Magnetic Field with the Mass of Mill # V Chrysotile (Sample 1 cm Away From The Probe).

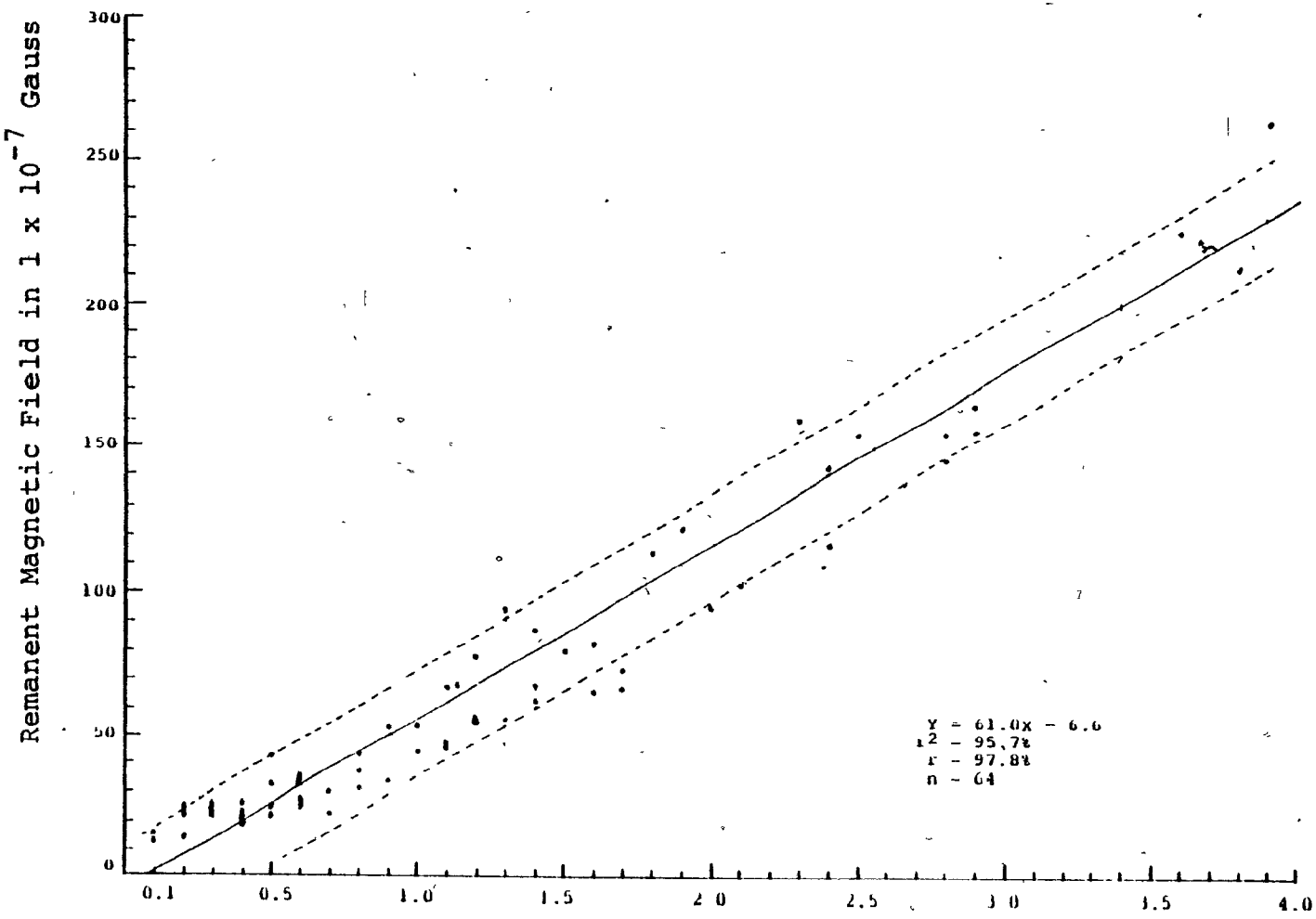


Fig. B.13 - Correlation of the Remanent Magnetic Field with the Mass of Mill # VI Chrysotile (Sample 1 cm Away From The Probe).

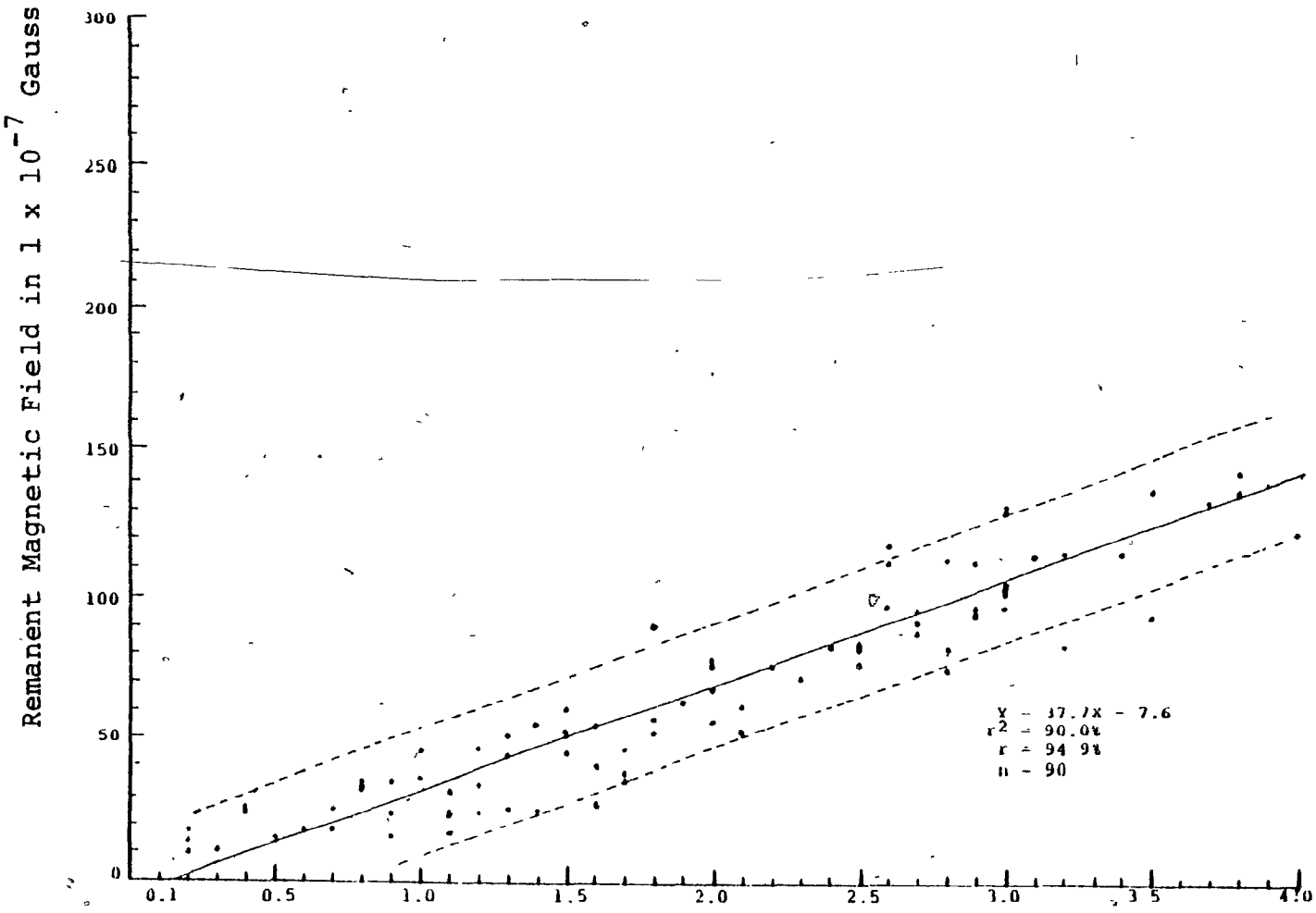


Fig. B.13 - Correlation of the Remanent Magnetic Field with the Mass of Mill # VI Chrysotile (Sample 1 cm Away From The Probe).

## BIBLIOGRAPHY


1. Addingly, C.G., (1965), "Dust Measurement and Monitoring in the Asbestos Industry", In: Annals of The New York Academy of Sciences, Ed. H.E. Wipple, Vol. 132, Art. 1, Dec., pp. 298-305.

2. Addingly, C.G., (1966), "Asbestos Dust and Its Measurements", Annals Occupational Hygiene, Pergamon Press, Great Britain, Vol. 9, pp. 73-82.

3. Allen, C.C., Gill, J.S., Koski, J.S. et al., (1957), "The Jeffrey Mine of Canadian Johns- Manville Co. Ltd.", 6th Commonwealth Mining and Metallurgical Congress.

4. Allen, M.P. and Smith, R.W., (1975), "Dissolution of Asbestos Minerals In Acid and Buffered Salt Solutions", In: Third International Conference on the Physics and Chemistry of Asbestos Minerals, Aug., p.2.

5. Argal, Jr. G.O., (1980), "World Production Leaders", World Mining Yearbook, July, pp. 118-119.

6. Ashford, J.R. and Jones, C.O., (1964), "Field Trials with the Hexlet and Conicycle Airborne Dust Samplers and the Standard and Long Running Thermal Precipitators", Annals of Occupational Hygiene, Apr., Vol. 7, p. 85.

7. Assad, J.R., (1976), "Comite d'etude sur la salubrite dans l'industrie de l'amiante", Beudry Commission, Oct., Document #1.

8. Assad, J.R., et Associes, (1976), "Etude mineralogique de l'amiante au Quebec en relation avec son exploitation. extraction et utilisation", Comite d'etude sur la salubrite dans l'industrie de l'amiante. Document 1, Universite Laval, Quebec.

9. Ayer, H.E., Lynch, J.R., Fanney, J.H., "A Comparison of Impnger and Membrane Filter Techniques for Evaluating Air Samples In Asbestos Plants", In: Annals of the New York Academy of Sciences, Ed. H.E. Wipple, Vol. 132. Art. 1, Dec., pp. 274-287.

10. Badollet, M.S., (1951), "Asbestos a Mineral of Unparalleled Properties", Transactions CIMM, Vol. 54, pp. 151-161.

11. Badollet, M.S.,(1975), "Asbestos" A Remarkable Mineral Fiber, pp. 1-4.

12. Balzer, J.L., "Aerodynamics Properties of Fibrous Aerosols", Non-published Data, Environmental Health, University of California, Berkely.

13. Barbeau, C., (1979), "Evaluation of Chrysotile By Chemical Methods", In: Short Course in Mineralogical Techniques of Asbestos Determination, Editor: R.L. Ledoux, Mineralogical Association of Canada, Quebec, May, pp. 197-212.

14. Bardswick, W.A., and White, F.T.M., (1969), "Trends in the Instrumental Assessment of Industrial Dustiness", CIM Annual Conference, Montreal, April.

15. Barnothy, M.F., (1964), "Biological Effects of Magnetic Fields", Plenum Press, New York.

16. Bates, T.F. Sands, L.B., Mink, J.F., (1950), Tubular Crystals of Crysotile Asbestos, Science, Vol. III, pp. 512-514.

17. Baule, G.M., McFee, R., (1963), "Detection of the Magnetic Field of the Heart", American Heart Journal, Vol. 66, p. 95.

18. Baule G.M., McFee, R., (1965), "Theory of Magnetic Detection of the Heart's Electrical Activity", Journal of Applied Physics, Vol. 36, p. 2066.

19. Bayliss, D.L.,Dement, J.M., Wagoner, J.K., Blejer, H.P., (1975), "Mortality Patterns Among Fibrous Glass Production Workers", Annals New York Academy of Sciences, pp. 324-335.

20. Beakmans, J.M., (1970), "The Deposition of Asbestos Particles in the Human Respiratory Tract", International Journal of Environmental Studies, Gordon and Breach Science Publishers Ltd., Exeter, England, Vol. 1, pp. 31-34.

21. Beckett, S.T., (1973), "The Evaluation of Airborne Asbestos Fibers Using A Scanning Electron Microscope", Annals of Occupational Hygiene, Pergamon Press, Vol. 16, pp. 405-408.

22. Beckett, S.T., (1975), "The Generation and Evaluation of UICC Asbestos Clouds in Animal Exposure Chambers", Annals of Occupational Hygiene, Pergamon Press, Vol. 18, pp. 187-199.

23. Becklake, M.R., (1976), State of Art: "Asbestos-Related Diseases of the Lung and Other organs: Their Epidemiology and Implications for Clinical Practice", American Review of Respiratory Disease, Vol. 114, pp. 187-227.

24. Becklake, M.R., (1979), "environmental Exposure to Asbestos", Chest, Sept., Vol. 76, pp. 245-247.

25. Becklake, M.R., Liddell, F.D.K., Manfreda, J. and McDonald, J.C., (1979), "Radiological Changes after Withdrawal from Asbestos Exposure, British Journal of Industrial Medicine, Vol. 36, pp. 23-28.

26. Beeckman, J.M., (1970), "Deposition of Ellipsoidal Particles in the Human Respiratory Tract", Assessment of Airborne Particles, Editors: T.T.Mercer, P. Morrow, W. Stober, Charles and Thomas Publishers, Spring Field, Ill., Chap. 17, pp. 361-370.

27. Berger H., (1963), Asbestos Fundamentals, Chemical Publishing Co. New York.

28. Berry, L.G., Mason, B., (1959), Mineralogy, Freeman and Co.,Sanfransisco.

29. Boucher, M.A., (1971), "Asbestos", Canadian Minerals Yearbook 1971, Editor: V. Donnelly, Energy, Mines and Resources, Canada, pp. 30-38.

30. Bowden, D.H., (1976), "The Pulmonary Mocrophage", Environ. Health Presp., Vol. 16, pp. 55-60.

31. Bozorth, R.M., (1968), "Ferromagnetism", D.Van Nostrand Company, Inc., Princeton, New Jersey, Toronto, London and Melbourne, Revised edition Sept., pp. 1-13, 138-141, 243-246, 502-513, 649, 681 and 769.

32. Brain, J.D., Sorokin, S.P., and Godleski, J.J., "Quantification, Origin, and Fate of Pulmonary Macrophages", In: Respiratory Defense Mechanism, Part I, Editors: Brian, Proctor and Reid, Vol. 5, pp. 849-892.

33. Brian, J.D., Valberg, P.A., (1974), "Models of Lung Retention Based on ICRP Task Group Report", Arch. Environ. Health, Vol. 28, Jan., pp. 1-11.

34. Brown, J.H., Cook, K.M., Ney, F.G. and Hatch, T., (1950), "influence of Particle Size Upon the Retention of Particulate Matter in the Human Lung", American Journal of Public Health, Vol. 40, April, pp. 450-458.

35. Cadle, R.D., (1965), "Particle Size", Theory and Industrial Application. Reinhold Publishing Corp., New York, pp. 65-94.

36. Camner, P., Hollstrom, P.A., Lundborg, M., Philipson, K., (1977), "Lung Clearance of 4 μm Particles Coated with Silver, Carbon or Beryllium", Arch., Environ. Health, Vol., 32, pp. 58-61.

37. Camner, P. and Philipson, K., (1971), "Intra-Individual Studies of Tracheobronchial Clearance in Man Using Fluorocarbon Resin Particles Tagged with 18F and 99TC, In: Inhaled Particles III, Editor: W.H. Walton, Unwin Bros., Ltd., Surrey, England, Vol. 1, pp. 157-163.

38. C.F. Casella and Co. Ltd., "Hexhlet", Leaflet 930/4/AR.

39. Chatfield, E,J,, (1979), "Measurement of Asbestos Fibres in the Work Place and in the General Environment", In: Short Course in Mineralogical Techniques of Asbestos Determination, Editor: R.L. Ledoux, Mineralogical Association of Canada, Quebec, May, pp. 111-163.

40. Choi, I. and Smith, R.W., (1975), "Identification of the Transition Elements Associated with Asbestos Minerals and their Behaviour in Aqueous Solution", In: Third International Conference on the Physics and Chemistry of Asbestos Minerals, Aug., p. 2-3.

41. Clifton, R.A., (1977), "Asbestos", Mineral Commodity Profiles, Bureau of Mines, United States Department of the Interior, MCP-6, Sept., Washington, D.C., pp. 1-17.

42. Clifton, R.A., (1979), "Asbestos", Mineral Commodity Profiles, Bureau of Mines, United States Department of the Interior, July, Washington D.C., pp. 1-19.

43. Clifton, R.A., (1980), "Asbestos", U.S. Mineral Commodity Summaries for 1979, Jan., pp. 14-15.

44. Clifton, R.A., (1981), "Asbestos", U.S. Mineral Commodity Summaries for 1980, Jan., pp. 12-13.

45. Cohen, D., (1967), "Magnetic Field Around The Torso: Production by Electrical Activity of Human Heart", Science, Vol.156, p. 652.

46. Cohen, D., (1967), "Enhancement of Ferromagnetic Shielding Against Low-Frequency Magnetic Fields", Applied Physics Letters, Feb., Vol. 10, #3, pp. 67-69.

47. Cohen, D., (1970), "Large Volume Conventional Magnetic Shields", Revue de Physique Appliquee, Feb., Vol. 5, pp. 53-58.

48. Cohen, D., (1972), "Magnetoencephalography: Detection of the Brain's Electrical Activity with a Super-conducting magnetometer", Science, Vol. 175, pp. 664-666.

49. Cohen, D., (1972), "Ferromagnetic Contamination in the Lungs and Other Organs of the Human Body", Science, May, Vol. 180, p. 745.

50. Cohen, D., (1973), "Magnetic Fields Produced by Steady Currents in Human and Animal Bodies", MIT, Francis Bitter National Magnet Laboratory, Semi-Annual Progress Report, pp. 1-24.

51. Cohen, D., (1975), "Magnetic Fields of Human Body", Physics Today, August, pp. 34-43.

52. Cohen, D., (1978), "Report of the Low-Field Group: The Magnetic Field of the Lung", Francis Bitter National Magnet Laboratory, MIT, PP. 1-33.

53. Cohen, D., (1978), "Magnetic Field Produced by the Human Body: Some New Findings", Proceedings of Intermag Conference.

54. Cohen, D., (1969), "Measurements and a Simplified Interpretation of Magnetocardiograms from Humans", MIT Circulation, Vol. 39, pp. 395-402.

55. Cohen, D., Crowthers, T.S., Gibbs, G.W., and Becklake, M.R., (1981), "Magnetic Lung Measurements in Relation to Occupational Exposure in Asbestos Miners and Millers of Quebec", Environmental Research, Vol. 26, pp. 535-550.

56. Cohen, D., Givler, E., (1972), "Magnetomyography: Magnetic Fields Around the Human Body Produced by Skeletal Muscles", Applied Physics Letters, Vol. 21, pp. 114.

57. Cohen, D., McCaughan, D., (1972), "Magnetocardiograms and Their Variation Over the Chest In Normal Subjects", American Journal of Cardiology, Vol., 29, pp. 678-685.

58. Commins, B.T., Gibbs, G.W., (1969), "Contaminating Organic Material in Asbestos", British Journal of Cancer 23, pp. 358-362.

59. Cosette, M., Delvaux, P., (1979), "Technical Evaluation of Chrysotile Asbestos Orebodies", In: Short Course in Mineralogical Techniques of Asbestos Determination, Editor: R.L. Ledoux, Mineralogical Association of Canada, May, p. 102.

60. The Committee on Environmental Health, American College of Chest Physicians, (1976), "The Pulmonary Response to Fiberglass Dust", Chest, Feb., Vol. 69, pp. 216-219.

61. Comroe, J.H., Foster, R.E., Dubois, A.B., Briscoe, W.A., Carlsen, E., (1971), "The Lung", Clinical Physiology and Pulmonary Function Tests, second edition, Yearbook Medical Publishers Inc., Chicago, pp. 1-9, 72-73, 112-114.

62. Crally, L.J., Keenan, R.G., Kupel, R.E., Kinser, R.E. and Lynch, J.R., (1968), "Characterization and Solubility of Metals Associated with Asbestos Fibers", American Industrial Hygiene Conference, May 13-17.

63. Currens, W.W., (1912-13), Asbestos Mines and Minerals, Pub. Scranton, Pa. Vol. 33, pp. 229-230.

64. Davies, C.N., (1949), "Inhalation Risk and Particle Size in Dust and Mist", British Journal of Industrial Medicine, June, Vol. 6, pp. 245-253.

65. Davies, C.N., (1964), "Deposition and Retention of Dust in the Human Respiratory Tract", Annals of Occupational Hygiene, Apr., Vol. 7, p. 169.

66. Davies, C.N., (1974), "Deposition of Inhaled Particles in Man", Chemistry and Industry, June, pp. 441-444.

67. Davis, J.M.G., and Gross, P., (1971), "Are Ferruginous Bodies and Indication of Atmospheric Pollution by Asbestos", Archives of Pathology, Vol. 90, pp.238-242.

68. DeNee, P.B., (1972), "Mine Dust Characterization Using the Scanning Electron Microscope", American Industrial Hygiene Association Journal, Oct., pp. 654-660.

69. Doran, G.V., (1977), "Measurement of Airborne Asbestos Dust at Cassiar", Cassiar Asbestos Corporation Ltd., Cassiar, B.C., pp. 1-65.

70. Drew, R.T., Lippmann, M., "Calibration of Air Sampling Instruments, Section I, pp. I-5-I-6.

71. Dust Measurement Advisory Panel, Asbestos International Association, (1978), "Draft Proposal of a Reference Method for the Determination of Fiber Concentration at Work places in the Asbestos Industry by Optical Microscopy", Washington, D.C.

72. Dyson, E.D., and Beach, S.A., (1968), "The Movement of Inhaled Material From the Respiratory Tract to Blood. An Analogue Investigation of the New Lung Model", Health Physics, Pergamon Press, Northern Ireland, Vol. 15, pp. 385-397.

73. Elmes, P.C., Simpson, M.J.C., (1977), "Insulation Workers in Belfast; A Further Study of Mortality Due to Asbestos Exposure (1940-75)", British Journal of Industrial Medicine, Vol.34, pp. 174-180.

74. Evans, J.C., Evans, R.J., Holmes, A., Hounam, R.F., Jones, D.M., Morgan, A., and Walsh, M., (1973), "Studies on the Deposition of Inhaled Fibrous Material in the Respiratory Tract of theRat and its Subsequent Clearance Using Radioactive Tracer Techniques, 1. UICC Crosidolite Asbestos", Environmental Research 6, Academic Press Inc., pp. 180-201.

75. Freedman, A.P., Green, F.H.Y., and Rudnitzky, J.,(1980) "Magnetopneumographic Scanning For Non-Invasive Regonal Determination of Occupationally Acquired Lung Dust Distribution". J. Occ. Med., Vol.22, p.613.

76. Gaze, R., (1965), "The Physical and Molecular Structure of Asbestos", Annals of the New York Academy of Sciences, Vol. 132, Art. 1. pp. 23-30, New York.

77. Gibbs, G.W., (1970), "The Organic Geochemistry of Chrysotile Asbestos from the Eastern Townships, Quebec", Geochemica et Cosmochimica Aeta, Vol. 35, pp. 485-502, Pergamon Press, Northern Ireland, Dec.

78. Gibbs, G.W., (1971), "Qualitative Aspects oust Exposure in the Quebec Asbestos Mining and Milling", In: Inhaled Particles III. Editor W.H. Walton, Unwin Bros. Ltd., Surrey, England, pp. 783-799.

79. Gibbs, G.W., (1978), "Comments" to Methods Used in the Measurement of Asbestos-Dust Exposures, by R.S.J. DuToit. Proceedings of Asbestos Symposium, Johannesburg, Oct. Published by National Institute of Metallurgy, Randburg, pp. 19-36.

80. Gibbs, G.W., (1979), "Etiology of Pleural Calcification: A Study of Quebec Chrysotile Asbestos Miners and Millers", Archives of Environmental Health, Mar/Apr., pp. 76-83.

81. Gibbs, G.W., (1979), "Techniques of Asbestos Determination-Research Perspective", IN: Short Course in Mineralogical Techniques of Asbestos Determination, Editor: R.L.Ledoux, Quebec, May, p. 264.

82. Gibbs, G.W., Baron, P., Becket, S., Dillen, R., DuToit, R., Koponen, M., and Robock, K., (1977), "A Summary of Asbestos Fiber Counting Experience in Seven Countries", Annals of Occupational Hygiene, Vol. 20, #4, pp. 321-332.

83. Gibbs, G.W., Hui, H.Y., (1971), "The Organic Content of Canadian Chrysotile", American Industrial Hygiene Association Journal, Aug.

84. Gibbs, G.W., and DuToit, R.S.J., (1973), "Environmental Data in Mining", Biological Effects of Asbestos, Lyon, International Agency for Research on Cancer, pp. 138-144.

85. Gibbs, G.W., and DuToit, R.S.J., (1978), "Environmental Considerations in Surveillance of Asbestos Miners and Millers", Conference Paper in Proceedings of Asbestos Sumposium, Johannesburg, Oct., pp. 1-17.

86. Goldstein, B., Rendal, R.E.G., (1969), "Ferruginous Bodies", In: International Conference on Pneumoconiosis, Johannesburg, Apr/May, pp. 40-46.

87. Gormley, P.G. and Kennedy. M, (1949), Proc. Roy. Irish Academy, 52A, p. 163.

88. Green, G.M., (1973), "Alveolobronchiolar Transport Mechanisms", Arch. Intern. Med., Vol. 131, p. 109.

89. Green, H.L. and Lane, W.R., (1964), "Particulate Clouds: Dusts, Smokes and Mists", Their Physics and Physical Chemistry and Industrial and Environmental Aspects, Second Edition, E & F.N. Spon Ltd., London, pp. 63-75.

90. Green, H.L., and Lane, W.R., (1964), "Health Hazards: Estimation of Mass Concentration", In: Particulate Clouds: Dust, Smokes, and Mists, E and F.N. Spond Ltd., London, Second Edition, pp. 361-364.

91. Gross, P., (1976), "The Biologic Categorization of Inhaled Fiber Glass Dust", Archives of Environmental Health, Mar./Apr., pp. 101-106.

92. Gross, P., Charleston, S.C., (1974), "Is Short-Fibered Asbestos Dust a Biological Hazard?", Arch. Environ. Health, Aug., Vol.29, pp. 115-117.

93. Gross, P., Pfeitzer, A.E., and Ha-ch, T.F., (1966), "Alveolar Clearance: Its Relation to Lesions of the Respiratory Bronchiole", Amer. Rev. Resp. Dis., Vol. 94, pp. 10-19.

94. Hahn-Weinheimer, P., and Hirner, A., (1975), "Major and Trace Elements in Canadian Asbestos Ore Bodies - Analytical Results and Statistical Interpretation", In: Third International Conference on the Physics and Chemistry of Asbestos Minerals, Aug., p. 2.

95. Haley, T.J., (1975), "Asbestosis: A Reassesment of the Overall Problem", Journal of Pharmaceutical Sciences, Sept., Vol. 64, pp. 1435-1447.

96. Hamilton, R.J., and Walton, W.H., (1961), "The Selective Sampling of Respirable Dust", In: Inhaled Particles and Vapours, Editor: C.N. Davies, Pergamon Press, Oxford, p. 465.

97. Hanes, F.E., (1974), "Asbestos", Canadian Minerals Yearbook 1974, Editor: G.H. Meldrum, Energy, Mines and Resources, Canada, pp. 47-55.

98. Harrington, J.S., (1965), "Chemical Studies of Asbestos", Annals of the New York Academy of Sciences, Vol. 132, Art. L, pp. 31-47, New York.

99. Harrington, J.S., Allison, A.C., and Badami, D.V., (1975), "Mineral Fibers: Chemical, PHYsicochemical and Biological Properties", pp. 291-402.

100. Harrington, J.S., Roe, F.J.C., (1965), "Studies of Carcinogenesis of Asbestos Fibers and their Natural Oils", Annals of the New York Academy of Sciences, Vol. 132, Art. 1, pp. 439-450, New York.

101. Haris, Jr, R.L. Fraser, D.A., (1976), "A Model for Deposition of Fibers in the Human Respiratory System", American Industrial Hygiene Association Journal, Feb., pp. 73-89.

102. Haris, Jr. R.L., Timbrell, V., (1976), "The Influence of Fiber Shape in Lung Deposition-Mathematical Estimates", Inhaled Particles IV, pp. 75-89.

103. Harness, I., (1973), "Airborne Asbestos Dust Evaluation", Annals Occupational Hygiene, Pergamon Press, Great Britain, Vol. 16, pp. 397-404.

104. Heidermans, G., (1979), "Determination of Asbestos Fine Dust According to Mass Concentration", In: Short Course in Mineralogical Techniques of Asbestos Determination, Editor: R.L. Ledoux, Quebec, May, pp. 165-196.

105. Heyder, J., Gebhart, J., Heigwer, G., Roth, C., Stahlhofen, W., (1973), "Experimental Studies of the Total Deposition of Aerosol Particles in the Human Respiratory Tract", Aerosol Science, Pergamon Press, Vol. 4, pp. 191-208.

106. Heyder, J., Gebhart, J., and Stahlhofen, W., (1974), "Diameters of Airborne Particles", Water, Air and Soil Pollution 3, D. REIDEL Publishing Company, Dordrecht, Holland, pp. 567-572.

107. Hill, J.W., (1978), "Man-made Mineral Fres", J. Soc. Occup. Med., Great Britain, Vol. 28, pp. 134-141.

108. Hodgson, A.A., (1965), "Fibrous Silicates", Royal Institute of Chem., Lecture Series, No. 4.

109. Holmes, A., Morgan, A., Sandalls, F.J., (1968), "Determination of Chromium, Cobalt, Iron, Nickel and Scandium in the Intenational Union Against Cancer (UICC) Asbestos Reference Samples by Newton-Activation", AERE-R591), Harwell, Berkshire.

110. Holmes,S., (1965), "Development in Dust Sampling and Counting, Techniques in the Asbestoe Industry", In: Annals of the New York Academy Of Sciences, Ed. H.E. Whipple, Vol. 132, Art. 1, Dec., pp. 228-297.

111. Hounam, R.F., Block, A., Walsh, M., (1971), "The Deposition of Aerosol Particles in the Nasopharyngeal Region of the Human Respiratory Tract", Aerosol Science, Pergamon Press, Vol. 2, pp. 47-61.

112. Hwang, C.Y., Corsillo, A., and Mansel, J., (1976), "Electron Microscope Studies of Asbestos Fibers", Microscopical Society of Canada, Vol. 3, pp. 64-65.

113. Hounam, R.F., Morgan, A., "Particle Deposition", Respiratory Defense Mechanism part I, Lung Biology in Health and Disease, Editors: Brian, Proctor, Reid, Vol. 5, pp. 125-156.

114. Jacobson, M. and Tomb, T.F., (1967), "Relationship Between Gravimetric Respirable Dust Concentration and Midget Impinger Number Concentration", American Industrial Hygiene Association Journal, Nov.-Dec., pp. 554-556.

115. Jeffery, W.G., (1968), "Asbestos" Canadian Minerals Yearbook 1968, Editor: G.E. Thompson, Energy, Mines and Resources, Canada, pp. 99-107.

116. Jeffery, W.G., (1969), "Asbestos" Canadian Minerals Yearbook 1969, Editor: G.E. Thompson, Energy, Mines and Resources, Vanada, pp. 107-114.

117. Joint AIHA-ACGIH Aerosol Hazards Evaluation Committee, (1975), "Background Documation on Evaluation of Occupational Exposure to Airborne Asbestos", American Industrial Hygiene Association Journal, Feb., Vol. 36, pp. 91-103.

118. Joint AIHA-ACGIH Aerosol Hazards Evaluation Committee, (1975), "Recommended Procedures for Sampling and Counting Asbestos Fibers", American Industrial Hygiene Association Journal, Feb., Vol.36, pp. 83-90.

119. Kalliomaki, P.L. (1977), "Measurement of Magnetic Lung Contamination in VIVO", Evaluation of the Method and Its Application to Arc Welders, Academic Dissertation. The Medical Faculty of the University of Oulu, Helsinki.

120. Kalliomaki, P.S, Alanko, K., Korhonen, O., Mattsson, T., Vaaranen, V., Koponen, M., (1978), "Amount and Distribution of Welding Fume Lung Contaminants Among Arc Welders", Scandinavian Journal of Work Environment and Health, No. 4, pp. 122-130.

121. Kalliomaki, P.L., Karp, P.J., Katila, T., Makipaa, P., Saara, P., and Tossavainen, A., (1976), "Magnetic Measurements of Pulmonary Contamination", Scandinavian Journal of Work Environment and Health, No. 4, pp. 232-239.

122. Keenan, R.G., and Lynch, J.R., (1970), "Techniques for the Detection, Identification and Analysis of Fibers", American Industrial Hygiene Association Journal, Sept.-Oct., pp. 587-593.

123. Kennedy, J.B., and Neville, A.M., (1976), "Basic Statistical Methods for Engineers and Scientists", 2nd Edition, IEP a Dun-Donnelley Publisher, New York, pp. 178-180, 218-219, 264-271, 298-301, 310-313, 452-454, 457, 460-463.

124. Ketchen, E.E., Porter, W.E., and Bolton, N.E., (1978), "The Biological Effects of Magnetic Fields on Man", American Industrial Hygiene Association Journal, Jan. Vol. 39, pp. 1-11.

125. Killin, A.F., (1970), "Asbestos", Canadian Minerals Yearbook 1970, Editor: G.E. Thompson, Energy, Mines and Resources, Canada, pp. 109-116.

126. Knight, G., (1975), "Overlap Problems in Counting Fibers", American Industrial Hygiene Association Journal, Feb., Vol. 36, pp. 113-114.

127. Knight, G., (1977), "Factors Affecting the Response of Airborne Dust Samplers and the Comparisons Between Them", Q.A.M.A. Technical Report - TM77-7, Nov., pp 1-17.

128. Knight, G., (1977), "Gravimetric Sampling in Asbestos Mines and Mills", Q.A.M.A. Technical Report - TM77-9, Nov., pp. 1-33.

129 Knight, G., (1978), "One Study on Reproducibility of Chrysotile Asbestos Fiber Counting", Q.A.M.A. Technical Report - TM78-5, Feb., pp. 1-24.

130. LaBelle, C.W., and Brieger, H., (1961), "Patterns and Mechanisms in the Elimination of Dust From the Lung", In: Inhaled Particles and Vapours, Editor: C.N.Davies, Pergamon Press, London, Vol. I, pp. 356-368.

131. Lamarche, R.Y. and Wicks, F.J., (1975), "Where to Look for New Asbestos Deposits", In: Third International Conference on the Physics and Chemistry of Asbestos Minerals Aug., pp. 1-2, 5-6.

132. Landahl, H.D., (1950), "On the Removal of Airborne Droplets by the Human Respiratory Tract: I. The Lung", Bulletin Math. Biophys., Vol. 12, p. 43.

133. Langer, A.M., Ashley, R., Baden, V., Berkley,C., Hammond, E.C., Mackler, A.D., Magiore, C.J., Nicholson, W.J., Rohl, A.N., Rubin, I.B., Sastre, A., Selikoff, I.J., (1973), "Identification of Asbestos in Human Tissues", Journal of Occupational Medicine, Mar., Vol. 15, No. 3, pp. 287-295.

134. Langer, A.M., and Pooley, F.D., (1972), "Identification of Single Asbestos Fibers in Human Tissue", In: Proceedings of the International Conference on the Biological Effects of Asbestos, Lyon, France, 2-6 Oct., Paper No. 19, p. 119.

135. Langer,A.M., Rubin, I. and Selikoff, I.J., (1969), "Electron Microprobe Analysis of Asbestos Bodies", In: Pneumoconiosis. Proceedings of the International Conference Johannesburg, Editor: H.A. Shapiro, Oxford University Press, Cape Town, 1969, pp. 57-69.

136. Langer, A.M., Rubin, I.B., and Selikoff, I.J., (1972), "Chemical Characterization of Asbestos Body Cores by Electron Microprobe Analysis", The Journal of Histochemistry, Vol. 20, pp. 723-734.

137. Langer, A.M., Rubin, I.B., Selikoff, I.J., and Pooley, F. d., (1972), "Chemical Characterization of Uncoated Asbestos Fibers From the Lungs of Asbestos Workers by Electron Microprobe Analysis", The Journal of Histochemistry and Cytochemistry, Vol. 20, pp. 735-740.

138. Laurent, R., (1975), "Petrology of the Asbestos Serpentinites of South Quebec", In: ThirdInternational Conference on the Physics and Chemistry of Asbestos Minerals, Aug., pp. 5-12.

139. Lax, B., (1973), "Annual Report, Francis Bitter National Magnet Laboratory", MIT, Cambridge, Mass. August, pp. 100-102.

140. Lee, E.W., (1963), "Magnetism", Penguin Books, pp. 49-65, 83-128, 192-204.

141. Leidel, N.A., Bayer, S.G., and Zumwalde, R.D., (1973), "USPHS/NIOSH Membrane Filter Method for Evaluating Airborne Asbestos Fibers", NIOSH Publication, Nov., pp. 1-11.

142. Liddel, D., Eyssen, G., Thomas, D. and McDonald, C., (1977), "Radiological Changes Over 20 Years in Relation to Chrysotile Exposure in Quebec", Inhaled Particles IV, Edited by W.H. Walton, Pergamon Press, Oxford & New York, pp. 799-811.

143. Lippmann, M., (1979), "Respirable Dust Sampling", American Industrial Hygiene Association Journal, Vol. 31, pp. 138-;59.

144. Lippmann, M., Albert, R.E., (1969), "The Effect of Particle Size on the Regional Deposition of Inhaled Aerosols in the Human Respiratory Tract", American Industrial Hygiene Association Journal, May-June, pp. 257-275.

145. Lippmann, M., Albert, R.E., Peterson, Jr. H.T., (1970), "The Regional Deposition of Inhaled Aerosols in Man", In: Inhaled Particles III, Editor: W.H. Walton, Unwin Bros. Ltd., Surrey,i: 105-122.

146. Lippmann, M., and Harris, W.B., (1962), "Size-Selecting Samplers for Estimating Respirable Dust Concentrations", Health Physics, Vol. 8, p. 155.

147, Lippmann, M., and Hydonieus, A.,(1970), "A Multi-Stage Aerosol Sampler for Etended Sampling Intervals", American Industrial Hygiene Association Journal, Nov.-Dec., pp. 730-737.

148. Lockwood, T.H., (1974), "The Analysis of Asbestos for Trace Metals", American Industrial Hygiene Association Journal, Vol. 35, No. 5, May.

149. Martin, D., and Jacobi, W., (1972), "Diffusion Deposition of Small Sized Particles in the Bronchial Tree", Health Physics, Pergamon Press Northern Ireland, July, Vol. 23, pp. 23-29.

150. Maltoni, G.G., Melardi, C., Prodi, V., Tarroni, G., (1972), "Deposition Efficiency of Monodisperse Particles in Human Respiratory Tract", American Industrial Hygiene Association Journal, Sept. pp. 603-610.

151. McDonald, J.C., (1973), "Cancer in Chrysotile Mines and Mills", Biological Effects of Asbestos, International Agency for Research on Cancer, Lyon, pp. 189-194.

152. McDonald, J.C., (1977), "Asbestosis in Chrysotile Mines and Mills", In: Biological Effects of Asbestos, Switzerland, pp. 155-159.

153. McDonald, J.C., "Asbestos and Public Health", for Discussion by CMA Sub-Committee on Environmental Air Pollution and Health (Not Published).

154. McDonald, J.C., Becklake, M-R., Gibbs, G.W., McDonald, A.D., and Rossiter, C.E., (1974), "The Health of Chrysotile Asbestos Mine and Mill Workers of Quebec", Archives of Environmental Health, Feb., Vol.28, pp. 61-68.

155. McDonald, J.C., and Becklake, M.P., (1975), "Asbestos Related Diseases in Canada", Hefte zur Unfallheilkunde, Heft 126, pp. 521-535.

156. McDonald, A.D., Harper, A., El Attar, O.A., and McDonald, J.C., (1970), "Epidemiology of Primary Malignant Mesothelial Tumors in Canada", Cancer, Oct., Vol. 26. No. 4, pp. 914-919.

157. McDonald, J.C., Liddell, F.D.K., Gibbs, G.W., Eyssen, G.E. and McDonald, A.D., (1980), "Dust Exposure and Mortality in Chrysotile Mining 1910-75", British Journal of Industrial Medicine, Vol. 37, pp. 11-24.

158. McDonald, A.D., Magner, D., and AYSSEN, G., (1973), "Primary Malignant Mesothelial Tumors in Canada, 1960-1968", Cancer, Apr., Vol. 31, No. 4, pp. 869-876.

159. McDonald, J.C., and McDonald, A.D., (1977), "Epidemiology of Mesothelioma From Estimated Incidence", Prevention. Medicine, Vol. 6, pp. 426-446.

160. McDonald, A.D. and McDonald, J.C., (1973), "Epidemiologic Surveillance of Mesothelioma in Canada", CMA Journal, Sept., Vol. 109, pp. 359-362.

161. McDonald, J.C., McDonald, R.D., Gibbs, G.W., Siemiatycki, J., Rossiter, C.E., (1971), "Mortality in the Chrysotile Asbestos Mines and Mills of Quebec", Archives of Environmental Health, June, Vol. 22, pp. 677-686.

162. Mc Donald, J.C., Rossiter, C.E., Eyssen, G., McDonald, A.D., (1973), "Mortality in the Chrysotile Producing Industry of Quebec: A Progress Report, IVth. International Pneumoconiosis Conference, Apimodia Publishing House, Bucharest, Romania, pp. 232-237.

163. Mercer, T.T., (1967), "On the Role of Particle Size in the Dissolution of Lung Burdens", Health Physics, Pergamon Press, Northern Ireland, Vol. 13, pp. 1211-1221.

164. Mercer, T., (1975), "The Deposition Model of the Task Group on Lung Dynamics: A Comparison with Recent Experimental Data", Health Physics, Pergamon Press, Northern Ireland, Nov., Vol. 29, pp. 673-680.

165. Merrill, R.J., (1957), "The Carey-Canadian Asbestos Deposit", 6th Commonwealth Mining and Metallurgical Congress.

166. Miller, K., and Harrington, J.S., (1972), "Some Biochemical Effects of Asbestos on Macrophages", Br. J. Exp. Path., Vol. 53, pp. 397-405.

167. Mining Association of Canada, (1980), Facts & Figures, Mining in Canada, pp. 9, 32-35.

168. Monkman, L.J., (1975), "Mineralogical and Chemical Contaminants in Graded Milled Chrysotile". Third International Conference on Asbestos, University Laval, Quebec, Aug. 17-21.

169. Moorhouse, W.W. (1959), "The Study of Rocks in Thin Section", Harper & Row, Publishers, New York and Evanston, p. 313.

170. Morgan, A., Evans, J.C., Evans, R.J., Hounam, R.F., Holms, A., and Doyle, S.G., (1975), "Studies on the Deposition of Inhaled Fibrous Material in the Respiratory Tract of the Rat and Its Subsequent Clearance Using Radioactive Tracer Techniques, II. Deposition of the UICC Standard Reference Samples of Asbestos", Environmental research 10, Academic Press Inc., pp. 196-207.

171. Morgan, A., Lally, A.E., and Holmes, A., (1972), "Some Observation on the Distribution of Trace Metals in Chrysotile Asbestos", AERE-R7188, Harwell, Berkshire.

172. Morrow, P.E., (1972), "Clearance Kinetics of Inhaled Particles", In: Respiratory Defense Mechanism Part I, Editors: Brian, Proctor, Reid, Vol. 5, pp. 489-543.

173. Morrow, P.E., (1973), "Alveolar Clearance of Aerosols", Arch. Intern. Med., Jan., Vol.131, pp. 101-108.

174. Morrow, P.E., (1974), "Aerosol Characterization and Deposition" American Review of Respiratory Disease, Vol. 110 (b), Dec., pp. 88-99.

175. Moss, O.R., (1971), "Shape Factors for Airborne Particles", American Industrial Hygiene Association Journal, April, pp. 221-229.

176. Muir, D.C.F., (1972), "Medicine in the Mining Industries", Editor: J.M. Rogan, F.A. Davis Company, Philadelphia, pp. 56-69.

177. Nagata, T., (1961), "Rock Magnetism", Maruzen Company Ltd., Tokyo, pp. 1-39, 80-81, 222-245.

178. Nasr, A.N.M., (1967), "Pulmonary Hazard From Exposure to Glass Fibers", Journal Occup. Med., Vol. 9, pp. 345-348.

179. National Health and Medical Research Council Australian Department of Health, (1976), "Membrane Filter Method for Estimating Airborne Asbestos Dust", F.D. Atkinson Government Printer, Camberra, Oct. pp. 1-52.

180. Nenadic, C.M., Crable, J.V., (1971), "Application of X-Ray Defraction to Analytical Problems of Occupational Health", American Industrial Hygiene Association Journal, Aug., pp. 529-538.

181. Neter, J., Wasserman, W., and Whitmore, G.A., (1975), "Statistical Tables of Fisher and Yates", In: Fundamental Statistics for Business and Economics, Allyn and Bacon, Inc., Boston, London, Sydney, pp. 200-745.

182. Newball, H.H., and Brahim, S.A., (1976), "Respiratory Response to Domestic Fibrous Glass Exposure", Environmental Research, Vol. 12, pp. 201-207.

183. Ortiz, L.W., Ettinger, H.J., and Fairchild, C.I., (1975), "Calibration Standards for Counting Asbestos", American Industrial Hygiene Association Journal, Feb., Vol. 36, pp. 104-112.

184. Ortiz, L.W., and Isom, B.L., (1974), "Transfer Technique for Electron Microscopy of Membrane Filter Samples", American Industrial Hygiene Association Journal, July, pp. 423-425.

185. Osha, (1971), "Emergency Standard for Exposure to Asbestos Dust", Federal Digest, U.S. Department of Labour, May 29, Washington, D.C., Vol. 36, No. 105, Part II.

186. Ostiguy, G., (1976), "Health Hazards of Asbestos Exposure", Hotel Dieu de Montreal, Faculte de Medecine, Universite de Montreal, Aug.

187. Page, S.J., (1980), "Correlation of the Fibrous Aerosol Monitor with the Optical Membrane Filter Counter Technique", U.S. Bureau of Mines Report of Investigations, RI8467, United States Department of Interior, pp. 1-21.

188. Parkes, W.R., (1974), "Occupational Lung Disorders", Butterworth & Co., (Canada) Ltd., Toronto, pp. 4-14, 71-73, 276-323.

189. Pelnar, P.V., (1969), "Diagnosis Evaluation of Working Capability and Compensation in Asbestosis and Its Complications", XVI. International Congress on Occupational Health, Sept., Tokyo, pp. 199-202.

190. Pelnar, P.V., (1972), "Asbestos inQuebec Mining Industry", Lecture notes.

191. Peto, J., Doll, R., Howard, S.V., Kinlen, L.J., and Lewinsohn, H.C., (1977), "A Mortality Study Among Workers in an English Asbestos Factory", British Journal of Industrial Medicine, Vol. 34, pp. 169-173.

192. Polo, Marco, (1903), Travels, Book 1, Chapter XLII of the Province of Chingintalas, John Murry 3rd Edition, London, pp. 212-213.

193. Pohl, R.W., (1930), "Physical Principles of Electricity and Magnetism", pp. 86-139.

194. Pontefract, R.D., Bolohan, R., and Kraetz, W., "An Energy Dispersive X-Ray Analysis System Combined with a Transmission Electron Microscope, Their Application to Asbestos Fibre Analysis", Siemens Analytical Application Note No. 107, pp. 1-3.

195. Pooley, F.D., (1972), "Electron Microscope Characteristics of Inhaled Chrysotile Asbestos Fibre", British Journal of Ind. Medicine, Vol. 29, pp. 146-153.

196. Pooley, F.D., (1975), "The Identification of Asbestos Dust With an Electron Microscope Microprobe Analyser", Annals of Occupational Hygiene, Pergamon Press, Vol. 18, pp. 181-186.

197. Pooley, F.D., "The Electron Microprobe Analysis of Fine Mineral Particles", Department of Mineral Exploitation, University College Cardiff, (Non published paper).

198. Pott, F., Huth, F., and Friederichs, K.H., (1974), "Tumorigenic Effect of Fibrous Dusts in Experimental Animals", Environmental Health Perspectives, Vol. 9, pp. 313- 315.

199. Pundsack, F.L., (1961), "The Pore Structure of Asbestos", Journal of Physical Chemistry, Vol. 65, pp. 30-33.

200. Rajhans, H.S., (1970), "Fibrous Dust - Its Measurement and Dust Control". C.I.M. Bulletin, Aug.

201. Regulation Codes and Protocole Report EPS 1-AP-75-1, (1976), "Standard Reference Methods for Source Testing: Measurement of Emissions of Asbestos Mining and Milling Operations", Air Pollution Directorate, Environmental Protection Service, Dec., pp. 1-31.

202. Reimschussel, G., (1975), "The Association of Trace Minerals with Chrysotile Asbestos", Third International Conference on Asbestos, University Laval, Quebec, Aug. 17-21.

203. Reiter, R., (1976), "Biological Effects of Electric, Magnetic, and Electromagnetic Fields", Circular, Institute for Atmospheric Environmental Research, D-8100 Garmisch-Partenkirchen, Kreuzeckbahnstrasse 19, Nov.

204. Rendall, R.E.G., (1969), "The Data Sheets on the Chemical and Physical Properties of the U.I.C.C. Standard Reference Samples", In: International Conference on Pneumoconiosis, Department of Mines Republic of South Africa, Johannesburg, Apr.-May, p. 14.

205. Rendall, R.E.G. and Van Sittert, G.C.H., (1969), "The Stability of Conventional Dust Instruments", In: International Conference on Pneumoconiosis, Department of Mines Republic of South Africa, Johannesburg, Apr./ May, pp. 35-39.

206. Renshaw, F.M., Bachman, J.M., and Pierce, J.O., (1969), "The Use of Midget Impingers and Membrane Filters for Determining Particle Counts", American Industrial Hygiene Association Journal, Mar.-Apr., pp. 113-116.

207. Report No. ARB-TDA-01-75, (1975), Asbestos as a Hazardous Contaminant II, Ministry of the Environment, Air Resources Branch, Toronto, Ont., January, pp. 9-10.

208. Riordon, P.H., (1957), "The Asbestos Belt of Southeastern Quebec". The Geology of Canadian Industrial Mineral Deposits, 6th Commonwealth Mining and Metallurgical Congress.

209. Riordon, P.H., (1957), "The Asbestos Deposits of Thedford Mines, Quebec", 6th Commonwealth Mining and Metallurgical Congress.

210. Riordon, P.H., (1957), "The British-Canadian Mine", 6th Commonwealth Mining and Metallurgical Congress.

211. Riordon, P.H., (1957), "Normandie and Vimy Ridge Mines", 6th Commonwealth Mining and Metallurgical Congress.

212. Roy, J.C., Barbeau, C., and Dupuis, M., (1975), "Characterization of Chrysotile and Asbestos Ore by Substitution Ions", Third International Conference on Asbestos, University Laval, Quebec, Aug. 17-21.

213. Roach, S.A., (1965), "Measurement of Airborne Asbestos Dust by Instruments Measuring Different Parameters", In: Annals of the New York Academy of Sciences, Ed. H.E. Wipple, Vol. 132, Art. 1, Dec., pp. 306-315.

214. Samudra, A.V., Bock, F.C., Harwood, C.F., and Stocham, J.D., (1978), "Evaluating and Optimizing Electron Microscope Methods for Characterizing Airborne Asbestos", Environmental Sciences Research Laboratories, EPA 600/2-78-037, June, pp. 1-49.

215. Schlesinger, R.B., Lippman, M. (1972), "Particle Deposition is Costs of the Human Upper Tracheobronchial Tree", American Industrial Hygiene Association Joutnal, April, pp. 237-251.

216. Schneider, T., (1979), "The Influence of Counting Rules on the Number and on the Size Distribution of Fibres", Annals of Occupational Hygiene, Pergamon Press Ltd., Vol. 21, pp. 341-350.

217. Schwarz, E.J., Winer, A.A., (1971), "Magnetic Properties of Asbestos with Special Reference to the Determination of Absolute Magnetite Vontents", CIM Bulletin, Dec., pp. 55-59.

218. Seaton, A., (1975), "Asbestosis" in Occupational Lung Diseases, Editors: W.M.K.C. Morgan and A. Seaton, W.B. Saunders Company, Toromto, pp. 124-148.

219. Selikoff, I.J., Hummond, E.C., (1969), "Asbestos Bodies in The New York City Population in Two Periods Of Time", In: International Conference on Pneumoconiosis, Johannesburg, Apr/May, pp. 47-53.

220. Selikoff, I.J., Hummond, E.C., Churg, J., (1969), "Mortality Experience of Asbestos Insulation Workers", In: International Conference on Pneumoconiosis, Johannesburg, Apr/May, pp. 97-103.

221. Selikoff, I.J., Nicholson, W.J., and Langer, A.M., (1972), "Asbestos Air Pollution", Archives Environmental Health, July, Vol. 25, pp. 1-13.

222. Seshan, K., (1977), "Explanation for the Insensitivity of Tilts if the Electron Defraction Patterns of Amphibole Asbestos Fibres", Environmental Research, Vol. 14, pp. 46-58.

223. Shetigra, P.T., Morgan, R.W., (1975), "Asbestos, Smoking and Laryngeol Carcinoma", Archives of Environmental Health, Vol. 30, pp. 317-519.

224. Silverman, L. and Billings, C.E., (1961), "Pattern of Airflow in the Respiratory Tract", In: Inhaled Particles and Vapours, Editor: C.N. Davies, Pergamon Press, London, p. 9.

225. Sinclair, W.E., (1959), Asbestos, Its Origin, Production and Utilization, Mining Publications Ltd., Second Edition.

226. Smith, B.A., and Davies, M.G., "The Association of Phagocytosed Asbestos Dust with Lysosome Enzymes", The Journal of Pathology, Vol. 105 #3, pp. 153-157.

227. Speil, S. and Leinweber, J. P., (1969), Asbestos Minerals in Modern Technology Environmental Technology, Volume 2, No. 3, April. Reprint Academic Press, Inc., pp. 2-29.

228. Spurney, K.R., Boose, C., Horchrainer, D., Monig, F.J., (1976), "A Note on the Dispersing of Fibrous Powders", Annals of Occupational Hygiene, Pergamon Press, Vol. 19, pp. 85-87.

229. Spurney, K.R., Stober, W., Ackerman, E.R., Lodge, Jr., J.P., Spurney, Jr. K., (1976), "The Sampling and Electron Microscopy of Asbestos Aerosol in Ambient Air by Means of Nuclepore Filters", Journal of the Pollution Control Association, May, Vol. 26, pp. 496-498.

230. Standard Industrial Classification Manual, (1970), Asbestos Mines S.I.C. 071, Catalogue 12-501. Revised each year. Energy and Minerals Section of the Manufacturing and Primary Industries Division, Ottawa, Canada.

231. Stanton, M.F., (1972), "Some Aetiologic Considerations of Fibre Carcinogenesis", Biological Effects of Asbestos, Lyon, Oct., paper 43A, pp. 43A-L-14.

232. Stanton, M.F., and Wrench, C. (1972), "Mechanism of Mesothelioma Induction with Asbestos and Fibrous Glass", Journal of National Cancer Institute, Vol. 48, pp. 297-321.

233. Sterling, T.D., (1981), "Possible Risk to Human Lungs from Magnetometric Dust Clearance Experiments", Journal of Applied Physics, March, Vol. 52, #3, pp. 2575-2577

234. Stevens, D.C., and Stephenson, J., (1971), "A Size Selective Dust Sampler Which Conforms to the Lung Model Proposed by the I.C.R.P. Task Group on Lung Dynamics", United Kingdom Atomic Energy Authority, Research Group Report, Health Physics and Medical Division, Harwell, Berkshire, pp. 1-8.

235. Stevenson, R., Moore, R.B., (1967), "Theory of Physics", W.B. Saunders Company, Philadelphia and London, pp. 471-593.

235A Stroink, G. Dahn, D. and Holland, J., (1981), "Magnetopneumographic Estimation of Lung Dust Loads and Distribution in Asbestos Miners and Millers", Am. Rev. of Resp. Disease, Vol. 123, No. 4, p. 144.

235B Stroink, G., Dahn, D. and Brauer, F., "A Lung Model to Study the Magnetic Field of Lungs of Miners (to be published).

236. Stuart, B., (1976), "Deposition and Clearance of Inhaled Particles", Environmental Health Perspectives, Aug., Vol. 16, pp. 41-53.

237. Stuart, B.O., Wash, R., (1973), "Deposition of Inhaled Aerosols", Arch. Intern. Med., Vol. 131, Jan., pp. 60-73,

238. Sub-Committee on Asbestosis of the Permanent Commission and International Association on Occupational Health, (1971), "Evaluation of Asbestos Exposures in the Working Environment", Institute of Occupational Health, Helsinki, Finland, Work Environment - Health, Vol, 8 #3, pp. 71-73.

239. Task Group on Lung Dynamics, (1966), "Deposition and Retention Models for Internal Dosimetry of the Human Respiratory Tract", Health Physics, Pergamon Press, Northern Ireland, Vol. 12, pp. 173-207.

240. Taskinen, E., Ahlman, K., and Wiikeri, M., (1973), "A Current Hypothesis of the Lymphatic Transport of Inspired Dust to the Parietal Pleura", Chest, Aug., Vol. 64, #2, pp. 193-196.

241. Taulbee, D.B., and Yu, C.P., (1975), "A Theory of Aerosol Deposition in the Human Respiratory Tract", Journal of Applied Physiology, Vol. 38, No. 1, January, pp. 77-85.

242. Technical Report, (1979), "Automatic Detection and Counting of Asbestos Fibres", American Industrial Hygiene Association Journal, July, Vol. 40, pp. A.50-A.53.

243. Thomas, R.G., (1968), "Transport of Relatively Insoluable Materials From Lung to Lymph Nodes", Health Physics, Pergamon Press, Northern Ireland, Vol. 14, pp. 111-117.

244. Thomson, M.L., and Pavia, D., (1974), "Particle Penetration and Clearance in the Human Lung", Arch. Environ. Health, Oct., Vol. 29, pp. 214-219.

245. Thomson, M.L., Short, M.D., (1969), "Mucocilliary Function in Health, Chronic Obstructive Airway Disease and Asbestos", Journal of Applied Physiology, Vol. 26, p. 535.

246. Timbrell, V., (1965), "The Inhalation of Fibrous Dust", Annals of the New York Academy of Sciences, Vol. 132, Art. 1, New York, pp. 255-273.

247. Timbrell, V., (1969), "Characteristics of the International Union Against Cancer, Standard Reference Samples of Asbestos", In: International Conference on Pneumoconiosis, Department of Mines Republic of South Africa, Johannesburg, Apr.-May, pp. 21-23.

248. Timbrell, V., (1970), "The Inhalation of Fibres", In: Pneumoconiosis, Editor: H.A. Shapiro, Proceedings of the International Conference 1969, Johannesburg, Cope Town, Oxford University Press, pp. 3-9.

249. Timbrell, V., (1975), "Alignment of Respirable Asbestos Fibres by Magnetic Fields", Annals of Occupational Hygiene, Pergamon Press, Vol. 18, pp. 299-311.

250. Timbrell, V., Hyett, A.W., and Skidmore, J.W., (1968), "A Simple Dispenser for Generating Dust Clouds From Standard Reference Samples of Asbestos", Annals of Occupational Hygiene, Pergamon Press, Vol. 11, pp. 273-281.

251. Timbrell, V., Pooley, F., Wagner, J.C., (1969), "Characteristics of Respirable Asbestos Fibres", In: International Conference on Pneumoconiosis, Dept. of Mines, Republic of South Africa, pp. 120-125.

252. Timbrell, V., Rendal, R.E.G., (1971-72), "Preparation of the U.I.C.C. Standard Reference Samples of Asbestos", Powder Technology, Elsevier Sequoia, S.A. Lausanne, Netherland, Vol. 5, pp. 279-287.

253. Timbrell, V., Skidmore, J.W., (1970), "The Effect of Shape on Particle Penetration and Retention in Animal Lungs", In: Inhaled Particles III, W.H. Walton, Unwin Bros. Ltd., Surrey, U.K., pp. 49-56.

254. Tomb, T.F., and Corn, M., (1973), "Comparison of Equivalent Spherial Volume and Aerodynamic Diameters for Irregularly Shaped Particles", American Industrial Hygiene Association Journal, Jan., pp. 13-24.

255. Trauffer, W.E., (1974), "Canadian Johns-Manville's Jeffrey Mine at Asbestos, Quebec". Pit & Quary, pp. 58-64.

256. Trudeau, M., (1979), "Methods for the Evaluation of Asbestos Dust Concentration at the Workplace", In: Short Course in Mineralogical Techniques of Asbestos Determination, Editor: R.L. Ledoux, Mineralogical Association of Canada, Quebec, May, pp. 213-252.

257. Turkevitch, J., Hiller, J., (1949), Electron Microscopy of Collodial Systems, Analytical Chemistry, Vol. 21, pp. 475-485.

258. U.N. Statistical Yearbook (1978), "Asbestos", Mining and Quarrying, New York, N.Y., pp. 216-217.

259. Vagt, G.O., (1972), "Asbestos", Canadian Minerals Yearbook 1972, Editor: G.H. Meldrum, Energy, Mines and Resources, Canada, pp. 39-45.

260. Vagt, G.O., (1975), "Asbestos", Canadian Minerals Yearbook 1975, Editor: G.H. Meldrum, Energy, Mines, and Resources, Canada, pp. 49-58.

261. Vagt, G.O., (1976), "Asbestos", Canadian Minerals Yearbook 1976, Editor: R.B. Abbott, Energy, Mines and Resources, Canada, pp. 51-60.

262. Vagt, G.O., (1977), "Asbestos", Canadian Minerals Yearbook 1977, Editor: R.B. Abbott, Energy, Mines and Resources, Canada, pp. 25-34.

263. Vagt, G.O., (1978), "Asbestos", Canadian Minerals Yearbook 1978, Editor: R.B. Abbott, Energy Mines and Resources, Canada, pp. 1-9.

264. Vagt, G.O., (1979), "Asbestos" Preprint from Canadian Minerals Yearbook 1979, Energy, Mines and Resources, Canada, pp. 1-11.

265. Vagt, G.O., (1981), "Asbestos", Canadian Mining Journal, Vol. 102, No. 2, February, pp. 129-130.

266. Van As, A., (1977), "Pulmonary Airway Clearance Mechanisms: a Reappraisal", Amer. Rev. Resp. Dis., Vol. 115, pp. 721-726.

267. VanDers, I., Kerr, P.F., (1967), Mineral Recognition, John Wiley & Sons Inc., New York.

268. Wagner, J.C., and Skidmore, J.W., (1965), "Asbestos Dust Deposition and Retention in Rats", In: Annals of the New York Academy of Sciences, Vol. 132, Art. 1, New York, pp. 77-86.

269. Walton, W.H., (1954), "The Theory of Size Classification of Airborne Dust Clouds by Elutriation", British Journal of Applied PHysics, Supplement No. 3, p. 29.

270. Walton, W.H., Attfield, M.D., and Becket, S.T., (1976), "An International Comparison of Airborne Asbestos Fibres Sampled on Membrane Filters", Annals of Occupational Hygiene, Vol. 19, pp. 215-224.

271. Walton, W.H., and Hamilton, R.J., (1972), "The Measurement of Airborne Dust", In: Medicine in the Mining Industries, Edited by: J.M. Rogan, F.A. Davis Company, Philadelphia, pp. 145-165.

272. Whittaker, E.J.W., (1979), Mineralogical Association of Canada, "Short Course in Mineralogical Techniques of Asbestos Determination", Quebec, May, pp. 1-34.

273. Whittaker, E.J.W., (1967), Oxford Conference on the Physics and Chemistry of Asbestos Minerals, Paper No. 1-1.

274. Wicks, F.J., (1979), "Mineralogy, Chemistry and Chrystallography of Chrysotile Asbsestos", In: Short Course in Mineralogical Techniques of Asbestos Determination, Editor: R.L. Ledoux, Mineralogical Association of Canada, May, pp. 35-72.

275. Williams, S.R., 91931), "Magnetic PHenomena", McGraw-Hill Book Company Inc., New York, London.

276. Winer, A.A., Schwarz, E.J., "Magnetic Content of Asbestos Concentrates", Unpublished Report of EMR, Mines Branch & Geological Survey of Canada.

277. Winston, F.R., Bayliss, L.E., (1962), "Human Physiology" Fifth Edition, J.A. Churchill Ltd., London.

278. Wright, B.M., (1954), "A Size-Selecting Sampler for Airborne Dust", British Journal of I-dustrial Medicine, Vol. 11, pp. 284-288.

279. Yada, K., (1967), Study of Chrysotile Asbestos by High Resolution Electron Microscopy, Acta Crystallographica, Vol. 23, pp. 703-708.

280. Zijlstra, H., "Experimental Methods in Magnetism", In: Selected Topics in Solid State Physics, Editor: E.P. Wohlfarth, Vol. IX, New York, pp. 126-133.

281. Zukowski, R., and Gaze, R., (1959), "Tensile Strength of Asbestos", Nature 183, 35 london.

282. Zussman, J., Brindley, G.W., (1957), Electron Diffraction Studies of Serpentine Minerals, American Mineralogist, Vol. 42, pp. 133-157.